

Publication No. FHWA-RD-94-042
September 1994



2B97-208490

A Simplified Field Method for Capacity Evaluation of Driven Piles



U.S. Department of Transportation
Federal Highway Administration

Research and Development
Turner-Fairbank Highway Research Center
6300 Georgetown Pike
McLean, Virginia 22101-2296

REPRODUCED BY: **NTIS**
U.S. Department of Commerce
National Technical Information Service
Springfield, Virginia 22161

FOREWORD

This report presents the results of a study on a simplified field method for the capacity evaluation of driven piles based on dynamic measurements during driving. The simplified method, entitled the Energy Approach is proposed as an alternative to other dynamic analyses that are based on one-dimensional wave equation solutions. Based on the analysis of a large data set of over 120 piles load test to failure with corresponding dynamic measurements, and an additional 403 PDA monitored piles, the authors found the Energy Approach method provided excellent evaluations of pile capacity.




Charles J. Nemmers, P.E.
Director, Office of Engineering and
Highway Operations Research and
Development

NOTICE

This document is disseminated under the sponsorship of the Department of Transportation in the interest of information exchange. The United States Government assumes no liability for its contents or use thereof. The contents of this report reflect the views of the contractor, who is responsible for the accuracy of the data presented herein. The contents do not necessarily reflect the official policy of the Department of Transportation. This report does not constitute a standard, specification, or regulation.

The United States Government does not endorse products or manufacturers. Trade or manufacturers' names appear herein only because they are considered essential to the object of this document.

1. Report No. FHWA-RD-94-042		2.  PB97-208490		3. Recipient's Catalog No.	
4. Title and Subtitle A SIMPLIFIED FIELD METHOD FOR CAPACITY EVALUATION OF DRIVEN PILES				5. Report Date September 1994	
7. Author(s) Samuel G. Paikowsky, John E. Regan, and John J. McDonnell				6. Performing Organization Code	
				8. Performing Organization Report No.	
9. Performing Organization Name and Address University of Massachusetts Lowell Department of Civil Engineering 1 University Avenue Lowell, Massachusetts 01854				10. Work Unit No. (TRAIS) 3E3A-0922	
12. Sponsoring Agency Name and Address Office of Engineering and Highway Operations R&D 6300 Georgetown Pike McLean, Virginia 22101-2296				11. Contract or Grant No. DTFH61-92-C-00038	
				13. Type of Report and Period Covered Final Report May 1992 - June 1993	
15. Supplementary Notes Contracting Officer's Technical Representative (COTR) - Carl Ealy, HNR-30				14. Sponsoring Agency Code	
16. Abstract A simplified method based on energy balance between the total energy delivered to the pile and the work done by the pile/soil systems is proposed. This method, entitled the Energy Approach, assumes elasto-plastic load displacement pile-soil relations. Calculated transferred energy and maximum pile displacement from the measured data, together with the field blow count, are used as input parameters. This method does not consider the propagation process and is aimed at providing a real-time pile-capacity prediction in the field. Two large data sets were gathered at the University of Massachusetts at Lowell. One, PD/LT, contains 208 dynamic measurement cases on 120 piles monitored during driving, followed by a static load test to failure. The data were obtained from various sources and reflect variable combinations of soil-pile-driving systems. The other, PD, contains data on 403 piles monitored during driving and was provided by Pile Dynamics Inc. of Cleveland, Ohio. All cases were examined and analyzed. The Energy Approach method was found to provide excellent evaluations of pile capacity under all conditions. The method is, therefore, proposed to be used in the field for instantaneous capacity determination. The predictions of this method were found on the average to provide more accurate evaluations than the sophisticated office methods, especially for records obtained at the end of initial driving. The Energy Approach is, therefore, also proposed to be used as an independent tool to evaluate the office methods.					
17. Key Words Driven piles, dynamic analysis of piles, Energy Approach, CAPWAP, TEPWAP, driven-pile capacity.			18. Distribution Statement No restrictions. This document is available to the public through the National Technical Information Service, Springfield, Virginia 22161.		
19. Security Classif. (of this report) Unclassified		20. Security Classif. (of this page) Unclassified		21. No. of Pages 313	22. Price

PREFACE

This research study presents a simplified field method for the capacity evaluation of driven piles based on dynamic measurements during driving.

Dynamic analyses of piles are methods aimed at the prediction of pile behavior under static loads based on the pile response during installation. These methods are based upon the concept that pile penetration under each blow induces failure of the soil, hence, an instantaneous load test is performed.

The reliability of these analyses is enhanced through data obtained by dynamic measurements during driving. Two methods are currently employed for the analysis of the measured data. Both methods are based on the solution of the one-dimensional wave equation for the stress wave traveling through the pile following the hammer's impact. One, an office analysis, utilizes a numerical solution of a mathematical model for the pile-soil system under measured boundary conditions (e.g., the computer codes CAPWAP or TEPWAP). The other, a field analysis known as the "Case Method," which is based on a simplified closed-form solution and empirical correlations, provides an instantaneous evaluation of the pile capacity following each hammer blow.

Substantial experience suggests the existence of major limitations to the field method. In addition, no large-scale evaluation has been carried out for the office methods since their development.

A simplified method based on energy balance is proposed as an alternative field method. This method, entitled the Energy Approach, assumes elasto-plastic load displacement pile-soil relations. Calculated transferred energy and maximum pile displacement from the measured data, together with the field blow count, are used as input parameters for the Energy Approach.

Two large data sets were gathered at the University of Massachusetts at Lowell. One, PD/LT, contains 208 dynamic measurement cases on 120 piles monitored during driving, followed by a static load test to failure. The data were obtained from various sources and reflect variable combinations of soil-pile-driving systems. The other, PD, contains data on 403 piles monitored during driving and was provided by Pile Dynamics, Inc. of Cleveland, Ohio. All cases were examined and analyzed.

The results of the presented study invalidate the concept of a unique recommended correlation between the viscous damping parameters and soil type in both wave-based analyses. It is shown that energy losses should be attributed more to soil inertia rather than soil damping. As such, energy losses are mostly pile-shape-dependent in addition to the soil type and driving resistance influences.

The Energy Approach method was found to provide excellent evaluations of pile capacity. Therefore, the method is proposed to be used in the field for instantaneous capacity determination. The predictions of this method were found, on the average, to provide more accurate evaluations than the sophisticated office methods, especially for records obtained at the end of initial driving. The Energy Approach is, therefore, also proposed to be used as an independent tool to evaluate the office methods.

Through evaluation of the current dynamic analyses, pointing out their sources of deficiencies and offering an alternative method, this study contributed to the increase in safety and decrease in cost of driven-pile foundation systems.

SI* (MODERN METRIC) CONVERSION FACTORS

APPROXIMATE CONVERSIONS TO SI UNITS

Symbol	When You Know	Multiply By	To Find	Symbol	When You Know	Multiply By	To Find	Symbol
LENGTH								
in	inches	25.4	millimeters	mm	millimeters	0.039	inches	in
ft	feet	0.305	meters	m	meters	3.28	feet	ft
yd	yards	0.914	meters	m	meters	1.09	yards	yd
mi	miles	1.61	kilometers	km	kilometers	0.621	miles	mi
AREA								
in ²	square inches	645.2	square millimeters	mm ²	square millimeters	0.0016	square inches	in ²
ft ²	square feet	0.093	square meters	m ²	square meters	10.764	square feet	ft ²
yd ²	square yards	0.836	square meters	m ²	square meters	1.195	square yards	yd ²
ac	acres	0.405	hectares	ha	hectares	2.47	acres	ac
mi ²	square miles	2.59	square kilometers	km ²	square kilometers	0.386	square miles	mi ²
VOLUME								
fl oz	fluid ounces	29.57	milliliters	mL	milliliters	0.034	fluid ounces	fl oz
gal	gallons	3.785	liters	L	liters	0.264	gallons	gal
ft ³	cubic feet	0.028	cubic meters	m ³	cubic meters	35.71	cubic feet	ft ³
yd ³	cubic yards	0.765	cubic meters	m ³	cubic meters	1.307	cubic yards	yd ³
NOTE: Volumes greater than 1000 l shall be shown in m ³ .								
MASS								
oz	ounces	28.35	grams	g	grams	0.035	ounces	oz
lb	pounds	0.454	kilograms	kg	kilograms	2.202	pounds	lb
T	short tons (2000 lb)	0.907	megagrams (or "metric ton")	Mg (or "t")	megagrams (or "metric ton")	1.103	short tons (2000 lb)	T
TEMPERATURE (exact)								
°F	Fahrenheit temperature	5(F-32)/9 or (F-32)/1.8	Celsius temperature	°C	Celsius temperature	1.8C + 32	Fahrenheit temperature	°F
ILLUMINATION								
fc	foot-candles	10.76	lux	lx	lux	0.0929	foot-candles	fc
fl	foot-Lamberts	3.426	candela/m ²	cd/m ²	candela/m ²	0.2919	foot-Lamberts	fl
FORCE and PRESSURE or STRESS								
lbf	pound-force	4.45	newtons	N	newtons	0.225	pound-force	lbf
lbf/in ²	pound-force per square inch	6.89	kilopascals	kPa	kilopascals	0.145	pound-force per square inch	lbf/in ²

(Revised September 1993)

* SI is the symbol for the International System of Units. Appropriate rounding should be made to comply with Section 4 of ASTM E380.

TABLE OF CONTENTS

1 - INTRODUCTION.....	1
1.1 OVERVIEW.....	1
1.2 THE PRESENT RESEARCH STUDY.....	2
1.3 CONTRIBUTIONS.....	3
1.4 MANUSCRIPT LAYOUT.....	3
2 - BACKGROUND.....	7
2.1 GENERAL.....	7
2.2 STATIC ANALYSIS.....	7
2.3 STATIC LOAD TESTS.....	8
3 - DYNAMIC ANALYSIS OF PILES.....	9
3.1 GENERAL.....	9
3.2 DYNAMIC EQUATIONS.....	9
3.2.1 Review.....	9
3.2.2 The Basic Principle.....	10
3.2.3 Energy Transfer.....	10
3.3 THE WAVE EQUATION.....	12
3.3.1 Formulation and Principles.....	12
3.3.2 Pre-Driving Analysis.....	16
3.3.3 Post-Driving Analysis - CAPWAP/TEPWAP.....	16
3.3.4 Wave Equation Analysis - Discussion.....	16
3.4 FIELD ANALYSIS AND THE PILE-DRIVING ANALYZER.....	19
3.5 THE CASE METHOD.....	19
3.5.1 General.....	19
3.5.2 The Case Method Equation.....	19
3.5.3 Case Damping Coefficient.....	20
3.5.4 Case Method Variations.....	23
(a) The Damping Factor Method, RSP.....	23
(b) The Maximum Resistance Method, RMX.....	23
(c) The Minimum Resistance Method, RMN.....	24
(d) The Unloading Method, RSU.....	24
(e) The Automatic Method, RAU.....	24
3.5.5 Evaluation.....	25
(a) Critical Discussion.....	25
(b) Review of Existing Experience.....	25
3.5.6 Capacity Predictions.....	28
3.5.7 Summary.....	29
4 - THE ENERGY APPROACH.....	31
4.1 BACKGROUND.....	31

4.2 UNDERLYING CONCEPT.....	32
4.3 THE ENERGY EQUATION.....	32
4.4 ENERGY LOSSES AND SOIL INERTIA.....	34
4.4.1 General Considerations.....	34
4.4.2 Soil Displacement.....	34
4.4.3 Soil Acceleration.....	36
4.4.4 Expected Performance.....	37
5 - DATA BASE BUILDUP.....	39
5.1 GENERAL.....	39
5.2 DATA SET PD/LT.....	39
5.2.1 Static Load Test Analysis.....	39
(a) Davisson's Criteria.....	41
(b) The Shape-of-Curve Method.....	41
(c) The Limited Total Settlement Methods.....	43
(d) DeBeer's log-log Method.....	43
(e) The Representative Static Capacity.....	43
5.2.2 Dynamic Measurements Analysis.....	43
(a) GROUP 1 - Complete CAPWAP Analyses.....	45
(b) GROUP 2 - Incomplete CAPWAP Analyses.....	47
(c) GROUP 3 - TEPWAP Analyses.....	50
5.3 DATA SET PD.....	55
6 - DATA SET PD/LT.....	57
6.1 GENERAL.....	57
6.2 SITE AND PILE INFORMATION - TABLE 20.....	57
(a) Columns 1-4.....	57
(b) Columns 5-8.....	57
(b) Columns 9 and 10.....	58
6.3 PILE DRIVING AND DYNAMIC MEASUREMENTS - TABLE 21.....	58
(a) Columns 1 and 2.....	58
(b) Columns 3-5.....	58
(c) Column 6.....	59
(d) Columns 7-10.....	59
6.4 PARAMETERS OF DYNAMIC ANALYSES - TABLE 22.....	60
(a) Columns 1 and 2.....	60
(b) Column 3.....	60
(c) Columns 4 and 5.....	60
(d) Columns 6-9.....	60
6.5 PILE CAPACITY: STATIC LOAD TEST AND	
DYNAMIC ANALYSES - TABLE 23.....	60
(a) Columns 1-3.....	60
(b) Columns 4-8.....	61
(c) Column 9.....	61

(d) Columns 10-12.....	61
7 - DATA SET PD.....	63
7.1 PILE/SOIL AND DYNAMIC MEASUREMENTS OF DATA SET	
PD - TABLE 24.....	63
(a) Columns 1 and 2.....	63
(b) Columns 3 and 4.....	63
(c) Columns 5-9.....	63
(d) Columns 10-14.....	63
(e) Columns 15 and 16.....	63
7.2 SIDE/TIP QUAKE AND DAMPING PARAMETERS OF DATA	
SET PD - TABLE 25.....	64
(a) Columns 6 and 7.....	64
(b) Columns 8 and 9.....	64
8 - ANALYSIS OF DATA SET PD/LT.....	65
8.1 OVERVIEW.....	65
8.1.1 Purpose.....	65
8.1.2 Outline.....	65
(a) Damping Parameters-Soil Type Correlations.....	65
(b) Prediction Methods-Load Test Capacity.....	65
(c) Office Method/Field Method Predictions.....	66
8.2 DAMPING PARAMETERS AND SOIL TYPE	
GRAPHICAL CORRELATIONS.....	66
8.2.1 Case Method Damping.....	66
8.2.2 Smith Damping.....	67
8.3 DYNAMIC PREDICTIONS-STATIC CAPACITY GRAPHICAL	
CORRELATIONS.....	67
8.3.1 Correlations Breakdown.....	67
8.3.2 Pile Type Correlations.....	69
(a) All Piles.....	69
(b) Large Displacement Piles.....	73
(c) Small Displacement Piles.....	74
(d) Intermediate Conclusions.....	75
8.3.3 Pile-Soil Type Correlations.....	76
(a) Sand and Silt.....	76
(b) Clay and Till.....	76
(c) Rock.....	77
(d) Intermediate Conclusions.....	77
8.3.4 Correlations of Pile and Soil Type for Different Driving Time	78
(a) All Piles - EOD.....	79
(b) All Piles - BOR.....	80
(c) Large Displacement Piles - EOD.....	80
(d) Large Displacement Piles - BOR.....	81

(e) Small Displacement Piles - EOD.....	81
(f) Small Displacement Piles - BOR.....	82
(g) Intermediate Conclusions.....	82
8.4 STATISTICAL ANALYSIS OF DATA SET PD/LT.....	83
8.4.1 Linear-Regression Analysis.....	84
8.4.2 Actual Distributions of the K Coefficients and their Probabilistic Models.....	85
8.4.3 Mean and Standard Deviation Analysis.....	87
8.5 INTERPRETATION OF THE CONTROLLING PARAMETERS.....	88
8.5.1 Overview.....	88
8.5.2 Dynamic Predictions - Pile Area Ratio Graphical Correlations.....	88
8.5.3 Dynamic Predictions - Driving Resistance Graphical Correlations.....	88
8.5.4 Dynamic Predictions - Driving Resistance and Time of Driving Graphical Correlations.....	92
(a) All Piles at EOD.....	92
(b) All Piles at BOR.....	93
8.5.5 Dynamic Predictions - Driving Resistance and Pile-Type Graphical Correlations.....	93
(a) Small Displacement Piles.....	93
(b) Large Displacement Piles.....	94
8.5.6 The Effect of the Combined Major Controlling Parameters on the Accuracy of the Dynamic Predictions.....	95
(a) Breakdown of Combinations.....	95
(b) Combinations of Pile Type and Driving Resistance.....	95
(c) Combinations of Pile Type, Driving Resistance, and Time of Driving.....	97
9 - ANALYSIS OF DATA SET PD.....	181
9.1 INTRODUCTION.....	181
9.1.1 Purpose.....	181
9.1.2 Overview.....	181
(a) Damping Parameters - Soil-Type Correlations.....	181
(b) Office Method - Field Method Predictions.....	181
9.2 SMITH DAMPING PARAMETERS AND SOIL-TYPE CORRELATIONS.....	181
9.3 CAPWAP AND THE ENERGY APPROACH CORRELATIONS.....	182
9.3.1 All Piles - All Soils.....	182
9.3.2 Large Displacement Piles.....	182
(a) All Cases.....	182
(b) Sand and Silt.....	182
(c) Clay and Till.....	183
(d) Rock.....	183

(e) Unknown Soil Type.....	183
(f) Intermediate Conclusions.....	183
9.3.3 Small Displacement Piles.....	183
(a) All Cases.....	183
(b) Sand and Silt.....	184
(c) Clay and Till.....	184
(d) Rock.....	184
(e) Intermediate Conclusions.....	184
9.3.4 Miscellaneous Piles.....	184
(a) All Cases.....	185
(b) Sand and Silt.....	185
(c) Clay and Till.....	185
(d) Rock.....	185
(e) Unknown Soil Type.....	185
9.4 STATISTICAL ANALYSIS OF DATA SET PD.....	185
9.4.1 Linear Regression Analysis.....	187
9.4.2 Mean and Standard Deviation Analysis.....	187
9.5 SUMMARY AND CONCLUSIONS.....	187
10 - SUMMARY, CONCLUSIONS, AND RECOMMENDATIONS.....	209
10.1 SUMMARY.....	209
10.2 CONCLUSIONS.....	211
10.3 RECOMMENDATIONS.....	215
10.3.1 General.....	215
10.3.2 The Performance of the Office Methods (CAPWAP/TEPWAP).....	216
10.3.3 The Performance of the Energy Approach.....	216
10.3.4 The Correlation Between the Office Methods and the Energy Approach.....	217
10.3.5 Factors of Safety and Risk Analysis.....	217
(a) General.....	217
(b) Absolute Safety Based on Data Set PD/LT.....	218
(c) Factor of Safety and the Associated Risk Based on the Actual Data.....	223
(d) Factor of Safety and the Associated Risk Based on the Probability Distribution Function.....	224
10.3.6 Recommendations for Implementation.....	225
APPENDIX A - DATA SET PD/LT.....	235
APPENDIX B - DATA SET PD.....	263
REFERENCES.....	285

LIST OF FIGURES

<u>FIGURE</u>		<u>PAGE</u>
1	Resistance vs. displacement at the top of the pile.....	11
2	Smith's model simulating the hammer-pile-soil system for use with the one-dimensional wave equation (Smith, 1960).....	14
3	Soil-pile model (left) and the corresponding elasto-plastic soil resistance-displacement relationship (after Smith, 1960).....	15
4	Notations used for model of pile and soil in TEPWAP analysis (Paikowsky, 1982).....	17
5	Flow chart describing the analysis process using TEPWAP (Paikowsky, 1982).....	18
6	Force and velocity traces showing two impact peaks indicative of driving in soils capable of large deformations.....	21
7	Case damping (J_c) values for capacity prediction of offshore piles in the range of ± 20 percent from load test results (after Paikowsky, 1982)....	27
8	The proposed way of obtaining the combined quake, Q (soil and pile).....	35
9	Load-settlement curve of pile-case 95 with the elastic compression line inclined at 20 degrees.....	40
10	Load-settlement curve of pile-case 95 with a scale that does not consider the elastic compression of the pile (following Vesic, 1977).....	40
11	Load-settlement curve for pile-case 50 with the elastic compression line inclined at approximately 20 degrees.....	42
12	Load-settlement data plotted on a logarithmic graph for pile-case 50 to determine the failure load according to DeBeer's method.....	44
13	Force and velocity ($V \cdot EA/C$) traces of pile-case 1, a steel HP12x74 that needed a force correction (not to scale).....	46

14	Digitized force and velocity multiplied by the impedance (EA/C) traces for pile-case 192 used for input into INTEGRATE.....	48
15	INTEGRATE output of pile-case 192 showing the back-calculated Case J_c value and the Energy Approach prediction.....	49
16	Example of the pile identification information of pile-case 191 used as input for the TEPWAP analysis.....	51
17	Example of the soil and pile properties used along the pile elements of pile-case 191 as input for the TEPWAP analysis.....	52
18	Measured force and velocity multiplied by the impedance (EA/C) traces of pile-case 191 used by the TEPWAP analysis.....	53
19	Comparison between measured force near the top of pile-case 191 and the calculated force from TEPWAP analysis.....	53
20	Summary of the final results from TEPWAP analysis performed on pile-case 191.....	54
21	Tip soil conditions vs. calculated case damping coefficient (J_c) based on static load test results for 208 PD/LT pile-cases.....	99
22	Side soil conditions vs. Smith side damping coefficient based on CAPWAP/TEPWAP results.....	100
23	Tip soil conditions vs. Smith tip damping coefficient based on CAPWAP/TEPWAP results.....	101
24	Static load test results vs. CAPWAP or TEPWAP predictions for 204 PD/LT pile-cases in all type of soil (AAA).....	102
25	Static load test results vs. Energy Approach predictions for 202 PD/LT pile-cases in all types of soil (AAA).....	103
26	CAPWAP or TEPWAP predictions vs. Energy Approach predictions for 201 PD/LT pile-cases in all types of soil (AAA).....	104
27	K_{sw} vs. CAPWAP/TEPWAP predictions for 206 PD/LT pile-cases in all types of soil (AAA).....	105
28	K_{sp} vs. Energy Approach predictions for 208 PD/LT pile-cases in all types of soil (AAA).....	106

29	Static load test results vs. CAPWAP or TEPWAP predictions for 162 large displacement PD/LT pile-cases in all types of soil (LAA).....	107
30	Static load test results vs. Energy Approach predictions for 163 large displacement PD/LT pile-cases in all types of soil (LAA).....	108
31	CAPWAP or TEPWAP predictions vs. Energy Approach predictions for 161 large displacement PD/LT pile-cases in all types of soil (LAA).....	109
32	Static load test results vs. CAPWAP or TEPWAP predictions for 42 small displacement PD/LT pile-cases in all types of soil (SAA).....	110
33	Static load test results vs. Energy Approach predictions for 40 small displacement PD/LT pile-cases in all types of soil (SAA).....	111
34	CAPWAP or TEPWAP predictions vs. Energy Approach predictions for 38 small displacement PD/LT pile-cases in all types of soil (SAA).....	112
35	Static load test results vs. CAPWAP or TEPWAP predictions for 139 PD/LT pile-cases in sand and silt (AAS).....	113
36	Static load test results vs. Energy Approach predictions for 136 PD/LT pile-cases in sand and silt (AAS).....	114
37	CAPWAP or TEPWAP predictions vs. Energy Approach predictions for 136 PD/LT pile-cases in sand and silt (AAS).....	115
38	Static load test results vs. CAPWAP or TEPWAP predictions for 51 PD/LT pile-cases in clay and till (AAC).....	116
39	Static load test results vs. Energy Approach predictions for 53 PD/LT pile-cases in clay and till (AAC).....	117
40	CAPWAP or TEPWAP predictions vs. Energy Approach predictions for 51 PD/LT pile-cases in clay and till (AAC).....	118
41	Static load test results vs. CAPWAP or TEPWAP predictions for 14 PD/LT pile-cases in rock (AAR).....	119
42	Static load test results vs. Energy Approach predictions for 14 PD/LT pile-cases in rock (AAR).....	120
43	CAPWAP or TEPWAP predictions vs. Energy Approach predictions for 14 PD/LT pile-cases in rock (AAR).....	121

44	Static load test results vs. CAPWAP or TEPWAP predictions for 96 PD/LT pile-cases in all types of soil at EOD (AEA).....	122
45	Static load test results vs. Energy Approach predictions for 94 PD/LT pile-cases in all types of soil at EOD (AEA).....	123
46	K_{sw} vs. CAPWAP/TEPWAP predictions for 97 PD/LT pile-cases at EOD in all types of soil (AEA).....	124
47	K_{sp} vs. Energy Approach predictions for 98 PD/LT pile-cases at EOD in all types of soil (AEA).....	125
48	CAPWAP or TEPWAP predictions vs. Energy Approach predictions for 94 PD/LT pile-cases in all types of soil at EOD (AEA).....	126
49	Static load test results vs. CAPWAP or TEPWAP predictions for 108 PD/LT pile-cases in all types of soil at BOR (ABA).....	127
50	Static load test results vs. Energy Approach predictions for 108 PD/LT pile-cases in all types of soil at BOR (ABA).....	128
51	CAPWAP or TEPWAP predictions vs. Energy Approach predictions for 108 PD/LT pile-cases in all types of soil at BOR (ABA)....	129
52	Static load test results vs. CAPWAP or TEPWAP predictions for 68 large displacement PD/LT pile-cases in all types of soil at EOD (LEA)....	130
53	Static load test results vs. Energy Approach predictions for 69 large displacement PD/LT pile-cases in all types of soil at EOD (LEA).....	131
54	CAPWAP or TEPWAP predictions vs. Energy Approach predictions for 68 large displacement PD/LT pile-cases in all types of soil at EOD (LEA).....	132
55	Static load test results vs. CAPWAP or TEPWAP predictions for 94 large displacement PD/LT pile-cases in all types of soil at BOR (LBA).....	133
56	Static load test results vs. Energy Approach predictions for 94 large displacement PD/LT pile-cases in all types of soil at BOR (LBA).....	134

57	CAPWAP or TEPWAP predictions vs. Energy Approach predictions for 93 large displacement PD/LT pile-cases in all types of soil at BOR (LBA).....	135
58	Static load test results vs. CAPWAP or TEPWAP predictions for 22 small displacement PD/LT pile-cases in all types of soil at EOD (SEA)....	136
59	Static load test results vs. Energy Approach predictions for 20 small displacement PD/LT pile-cases in all types of soil at EOD (SEA).....	137
60	CAPWAP or TEPWAP predictions vs. Energy Approach predictions for 20 small displacement PD/LT pile-cases in all types of soil at EOD (SEA).....	138
61	Static load test results vs. CAPWAP or TEPWAP predictions for 12 small displacement PD/LT pile-cases in all types of soil at BOR (SBA).....	139
62	Static load test results vs. Energy Approach predictions for 12 small displacement PD/LT pile-cases in all types of soil at BOR (SBA).....	140
63	CAPWAP or TEPWAP predictions vs. Energy Approach predictions for 12 small displacement PD/LT pile-cases in all types of soil at BOR (SBA).....	141
64	Histogram and frequency distribution of K_{sw} for 206 PD/LT pile-cases in all types of soil (AAA).....	142
65	Cumulative frequency distribution of K_{sw} for 206 PD/LT pile-cases in all types of soil (AAA).....	143
66	Histogram and frequency distribution of K_{sp} for 208 PD/LT pile-cases in all types of soil (AAA).....	144
67	Cumulative frequency distribution of K_{sp} for 208 PD/LT pile-cases in all types of soil (AAA).....	145
68	Histogram and frequency distribution of K_{cw} for 206 PD/LT pile-cases in all types of soil (AAA).....	146
69	K_{sw} vs. the pile area ratio (A_R) for 201 PD/LT pile-cases in all types of soil.....	147

70	K_{sw} vs. the pile area ratio (A_R) for 201 PD/LT pile-cases in all types of soil (logarithmic scale).....	148
71	K_{sp} vs. the pile area ratio (A_R) for 203 PD/LT pile-cases in all types of soil.....	149
72	K_{sp} vs. the pile area ratio (A_R) for 203 PD/LT pile-cases in all types of soil (logarithmic scale).....	150
73	K_{sw} vs. blow count (BPI) for 206 PD/LT pile-cases in all types of soil (AAA).....	151
74	K_{sp} vs. blow count (BPI) for 208 PD/LT pile-cases in all types of soil (AAA).....	152
75	K_{sw} vs. blow count (BPI) for 95 PD/LT pile-cases in all types of soil at EOD (AEA).....	153
76	K_{sp} vs. blow count (BPI) for 96 PD/LT pile-cases in all types of soil at EOD (AEA).....	154
77	K_{sw} vs. blow count (BPI) for 109 PD/LT pile-cases in all types of soil at BOR (ABA).....	155
78	K_{sp} vs. blow count (BPI) for 110 PD/LT pile-cases in all types of soil at BOR (ABA).....	156
79	K_{sw} vs. blow count (BPI) for 57 PD/LT pile-cases with pile area ratios >350 in all types of soil.....	157
80	K_{sp} vs. blow count (BPI) for 57 PD/LT pile-cases with pile area ratios >350 in all types of soil.....	158
81	K_{sw} vs. blow count (BPI) for 144 PD/LT pile-cases with pile area ratios <350 in all types of soil.....	159
82	K_{sp} vs. blow count (BPI) for 146 PD/LT pile-cases with pile area ratios <350 in all types of soil.....	160
83	K_{sw} vs. blow count (BPI) for 16 PD/LT pile-cases with pile area ratios >350 and blow counts <6 BPI (0.24 blows/mm) in all types of soil.....	161

84	K_{sp} vs. blow count (BPI) for 16 PD/LT pile-cases with pile area ratios >350 and blow counts <6 BPI (0.24 blows/mm) in all types of soil.....	162
85	K_{sw} vs. blow count (BPI) for 41 PD/LT pile-cases with pile area ratios >350 and blow counts >6 BPI (0.24 blows/mm) in all types of soil.....	163
86	K_{sp} vs. blow count (BPI) for 41 PD/LT pile-cases with pile area ratios >350 and blow counts >6 BPI (0.24 blows/mm) in all types of soil.....	164
87	K_{sw} vs. blow count (BPI) for 64 PD/LT pile-cases with pile area ratios <350 and blow counts <6 BPI (0.24 blows/mm) in all types of soil.....	165
88	K_{sp} vs. blow count (BPI) for 64 PD/LT pile-cases with pile area ratios <350 and blow counts <6 BPI (0.24 blows/mm) in all types of soil.....	166
89	K_{sw} vs. blow count (BPI) for 80 PD/LT pile-cases with pile area ratios <350 and blow counts >6 BPI (0.24 blows/mm) in all types of soil.....	167
90	K_{sp} vs. blow count (BPI) for 82 PD/LT pile-cases with pile area ratios <350 and blow counts >6 BPI (0.24 blows/mm) in all types of soil.....	168
91	K_{sw} vs. blow count (BPI) for 12 PD/LT pile-cases at EOD with pile area ratios >350 and blow counts <6 BPI (0.24 blows/mm).....	169
92	K_{sp} vs. blow count (BPI) for 12 PD/LT pile-cases at EOD with pile area ratios >350 and blow counts <6 BPI (0.24 blows/mm).....	170
93	K_{sw} vs. blow count (BPI) for 27 PD/LT pile-cases at EOD with pile area ratios >350 and blow counts >6 BPI (0.24 blows/mm).....	171
94	K_{sp} vs. blow count (BPI) for 27 PD/LT pile-cases at EOD with pile area ratios >350 and blow counts >6 BPI (0.24 blows/mm).....	172
95	K_{sw} vs. blow count (BPI) for 36 PD/LT pile-cases at EOD with pile area ratios <350 and blow counts <6 BPI (0.24 blows/mm).....	173

96	K_{sp} vs. blow count (BPI) for 36 PD/LT pile-cases at EOD with pile area ratios <350 and blow counts <6 BPI (0.24 blows/mm).....	174
97	K_{sw} vs. blow count (BPI) for 20 PD/LT pile-cases at EOD with pile area ratios <350 and blow counts >6 BPI (0.24 blows/mm).....	175
98	K_{sp} vs. blow count (BPI) for 21 PD/LT pile-cases at EOD with pile area ratios <350 and blow counts >6 BPI (0.24 blows/mm).....	176
99	K_{sw} vs. blow count (BPI) for 18 PD/LT pile-cases at BOR with pile area ratios >350 and all blow counts.....	177
100	K_{sp} vs. blow count (BPI) for 18 PD/LT pile-cases at BOR with pile area ratios >350 and all blow counts.....	178
101	K_{sw} vs. blow count (BPI) for 88 PD/LT pile-cases at BOR with pile area ratios <350 and all blow counts.....	179
102	K_{sp} vs. blow count (BPI) for 89 PD/LT pile-cases at BOR with pile area ratios <350 and all blow counts.....	180
103	Side soil conditions vs. Smith side damping based on CAPWAP results for 372 PD pile-cases.....	191
104	Tip soil conditions vs. Smith tip damping based on CAPWAP results for 377 PD pile-cases.....	192
105	CAPWAP predictions vs. Energy Approach predictions for 398 PD pile-cases in all types of soil.....	193
106	CAPWAP predictions vs. Energy Approach predictions for 238 large displacement PD pile-cases in all types of soil.....	194
107	CAPWAP predictions vs. Energy Approach predictions for 89 large displacement PD pile-cases in sand and silt.....	195
108	CAPWAP predictions vs. Energy Approach predictions for 50 large displacement PD pile-cases in clay and till.....	196
109	CAPWAP predictions vs. Energy Approach predictions for 76 large displacement PD pile-cases in rock.....	197
110	CAPWAP predictions vs. Energy Approach predictions for 22 large displacement PD pile-cases in unknown soil types.....	198

111	CAPWAP predictions vs. Energy Approach predictions for 76 small displacement PD pile-cases in all types of soil.....	199
112	CAPWAP predictions vs. Energy Approach predictions for 26 small displacement PD pile-cases in sand and silt.....	200
113	CAPWAP predictions vs. Energy Approach predictions for 21 small displacement PD pile-cases in clay and till.....	201
114	CAPWAP predictions vs. Energy Approach predictions for 29 small displacement PD pile-cases in rock.....	202
115	CAPWAP predictions vs. Energy Approach predictions for 85 miscellaneous PD pile-cases in all types of soil.....	203
116	CAPWAP predictions vs. Energy Approach predictions for 40 miscellaneous PD pile-cases in sand and silt.....	204
117	CAPWAP predictions vs. Energy Approach predictions for 21 miscellaneous PD pile-cases in clay and till.....	205
118	CAPWAP predictions vs. Energy Approach predictions for 19 miscellaneous PD pile-cases in rock.....	206
119	CAPWAP predictions vs. Energy Approach predictions for five miscellaneous PD pile-cases in unknown soil types.....	207
120	Side soil conditions vs. Smith side damping based on CAPWAP/TEPWAP results for 581 pile-cases.....	212
121	Tip soil conditions vs. Smith tip damping based on CAPWAP/TEPWAP results for 581 pile-cases.....	213
122	Risk analysis of CAPWAP/TEPWAP predictions for 206 PD/LT pile-cases in all types of soil.....	228
123	Risk analysis of Energy Approach predictions for 208 PD/LT pile-cases in all types of soil.....	229
124	Risk analysis of CAPWAP/TEPWAP predictions for 95 PD/LT pile-cases in all types of soil at EOD.....	230
125	Risk analysis of Energy Approach predictions for 96 PD/LT pile-cases in all types of soil at EOD.....	231

126 Risk analysis of CAPWAP/TEPWAP predictions for 39
small displacement ($A_R > 350$) PD/LT pile-cases in all
types of soil at EOD..... 232

127 Risk analysis of Energy Approach predictions for 39
small displacement ($A_R > 350$) PD/LT pile-cases in all
types of soil at EOD..... 233

LIST OF TABLES

TABLE

1	Data set PD/LT contributors.....	5
2	Recommended J_c values according to the soil type at the pile tip....	22
3	Subgrouping of the piles in data set PD (indicating the number of piles in each group).....	56
4	Breakdown of all PD/LT categories.....	68
5	Linear-regression analysis of K_{sw} for selected PD/LT pile-cases.....	70
6	Linear-regression analysis of K_{sp} for selected PD/LT pile-cases.....	71
7	Linear-regression analysis of K_{cw} for selected PD/LT pile-cases.....	72
8	Statistical analysis of K coefficients for all PD/LT pile-cases.....	89
9	Statistical analysis of the area ratio, resistance, and time of driving combination.....	96
10	Linear-regression analysis of K_{cw} for PD pile-cases.....	186
11	Statistical analysis of K_{cw} for PD pile-cases.....	188
12	Linear regression summary of selected PD/LT and PD subgroups.....	189
13	Statistical analysis summary of selected PD/LT and PD subgroups.....	190
14	Linear regression and statistical analysis of Ksw for selected PD/LT pile-cases.....	219
15	Linear regression and statistical analysis of Ksp for selected PD/LT pile-cases.....	220

16	Linear regression and statistical analysis of Kew for selected PD/LT and PD pile-cases.....	221
17	Linear regression and statistical analysis of Kew for selected PD/LT pile-cases.....	222
18	Absolute factor of safety based on data set PD/LT.....	223
19	Factor of safety and associated risk.....	227
20	Site and pile information for PD/LT.....	235
21	Pile driving and dynamic measurements for PD/LT.....	242
22	Parameters of dynamic analysis for PD/LT.....	249
23	Pile capacity based on static load test and dynamic analysis for PD/LT.....	256
24	Pile/soil and dynamic measurements of data set PD.....	263
25	Side/tip quake and damping parameters of data set PD.....	275

CHAPTER 1 - INTRODUCTION

1.1 OVERVIEW

The study of driven-pile foundations and their behavior under dynamic and static loads dates back to the late 19th century. Until that time, the design of driven piles was mainly based on experience. Dynamic equations were the first attempt at a theoretical assessment of the static capacity of driven piles. The "general" dynamic equation was developed based on the assumption that the pile and the hammer are two rigid bodies and that the calculated resistance is equal to the static capacity of the pile (Poulos and Davis, 1980).

The dynamic analyses are attractive as they attempt to predict the static capacity based on the pile behavior during driving. As such, they utilize data that is readily available during the construction operation. Moreover, they enable "real-time" capacity assessment during installation.

Hence, recent centuries have seen an increasing demand on the foundation engineer to further improve the dynamic methods of analysis. As a result, more research was performed in this area and it was realized that pile driving was not accurately represented by rigid-body mechanics (Newtonian impact), (Cummings, 1940). This realization led to the development of analyses based on wave theory utilizing the one-dimensional wave equation (Smith, 1960).

Stress-wave analyses consider the fact that each hammer blow produces an elastic stress wave that moves down the length of the pile at the speed of sound. This indicates that the entire pile is not stressed simultaneously (rigid-body mechanics), which is one of the basic assumptions of the dynamic equations.

A major improvement was gained with the direct measurement of the pile response under each hammer blow. Early large-scale studies (e.g., Michigan State Highway Commission, 1965; Texas Highway Department, 1973; and Ohio Department of Transportation, 1975) led to the development of an effective and reliable commercial system (Goble *et al.*, 1970, 1975). This system, known as the PDA (Pile-Driving Analyzer), enables complete and relatively easy acquisition of dynamic measurements and their analysis during driving. Similar systems were later developed outside the United States (FPDS-3-TNO, 1993; Reiding *et al.*, 1988; and Iwanowski, 1987).

The obtained dynamic measurements are used in two ways. One is a field analysis known as the Case Method (Goble *et al.*, 1970 and Rausche *et al.*, 1975). This analysis is based on a simplified solution of the wave equation and provides a "real-time" capacity

assessment during driving. The other is an office analysis that is based on the wave equation solution utilizing the force and velocity signals at the point of measurement. Several existing codes are based on this principle, for example, CAse Pile Wave Analysis Program, CAPWAP, (Goble *et al.*, 1970); TEchnion Pile Wave Analysis Program, TEPWAP, (Paikowsky, 1982 and Paikowsky and Whitman, 1989); and TNO (Middendorp and van Weel, 1986).

These analyses enable evaluation of a variety of parameters in addition to the static capacity. These evaluations include extreme stresses, pile-damage assessment, and load-settlement relations to name a few. These advantages are offset, however, by the time required to produce the results and the cost incurred during this time.

A large-scale assessment (100 or more piles) of the analyses utilizing dynamic measurements has not been carried out since their initiation. Limited studies suggest substantial limitations to the Case Method (e.g., Trow Report, 1978; Paikowsky, 1982; and Thompson and Goble, 1988). Mixed experiences were reported for the office methods. These reports ranged from excellent predictions for very large offshore open-pipe piles in sand (Paikowsky, 1982) to poor performance of concrete piles in clay and till (Trow Report, 1978).

Based on the existing experiences, it was clearly evident that in order to improve the state of the art it is necessary: (1) to develop an alternative method for capacity evaluation in the field and (2) to assess the performance of the different dynamic analyses and their underlying assumptions based on accumulating a large data set. Both needs are addressed by the present research.

1.2 THE PRESENT RESEARCH STUDY

The present research study is based on the aforementioned needs and consists of three major parts. The first part (chapter 4) presents an alternative field method known as the Energy Approach. This method combines the basic principle of the energy balance together with data provided through dynamic measurements. The method was first proposed by Paikowsky (1982) based on experience gained during the construction of a large offshore facility. The method was further examined on a limited scale in the Boston area (Paikowsky, 1984, 1990). Preliminary evaluations were carried out by McDonnell (1991) and Paikowsky and Chernauskas (1992).

The second part (chapters 5, 6, and 7) presents the buildup of two large-scale data sets. One data set, PD/LT (Pile Dynamic/Load Test), comprises 208 dynamic measurements on 120 piles monitored during driving, followed by a static load test to failure. All the cases were monitored using the PDA (Pile-Driving Analyzer) and the various data sources are outlined in the following section. The second data set, PD (Pile Dynamic),

contains data on 403 piles monitored during driving. This data set was provided exclusively by Pile Dynamics, Inc. of Cleveland, Ohio and was originally presented by McDonnell (1991).

The third part (chapters 8, 9, and 10) presents the analysis and interpretation of the data sets. The field and office methods are examined and analyzed. Possible mechanisms underlying the different methods are suggested and the obtained results are evaluated in light of these proposed mechanisms.

1.3 CONTRIBUTIONS

Advances in geotechnical engineering in general, and foundation engineering in particular, may take place only through ultimate full-scale evaluations. Full-scale observations are difficult to obtain and require collaboration and understanding between the owner (the "client"), the designer, the contractor, and the researcher. In the presented case, such understanding could have taken place through: (1) the vision of the Federal Highway Administration, which realized the need to support and carry out research; (2) the cooperative and research-oriented nature of GRL, Inc. and Pile Dynamics, Inc. of Cleveland, Ohio; and (3) the many contributors outlined below that realized the advantage of sharing their information for the benefit of all. Table 1 outlines the contributors to data set PD/LT. As previously noted, data set PD was provided exclusively by Pile Dynamics, Inc. of Cleveland, Ohio.

As these data sets have been and will continue to be useful to several research areas, the researchers at the University of Massachusetts at Lowell thank all of the contributors for their cooperation in providing their data.

1.4 MANUSCRIPT LAYOUT

The following are short descriptions for each of the following chapters:

Chapter 2 — Provides a brief background of static analyses and static load tests.

Chapter 3 — Details the various dynamic analyses currently employed, including dynamic equations, the Case Method, and CAPWAP/TEPWAP.

Chapter 4 — Develops the proposed Energy Approach.

Chapter 5 — Outlines the buildup and analysis of data sets PD/LT and PD.

- Chapter 6 — Outlines the tables presented in appendix A containing data set PD/LT.
- Chapter 7 — Outlines the tables presented in appendix B containing data set PD.
- Chapter 8 — Discusses and presents the graphical and statistical results obtained from analyzing data set PD/LT.
- Chapter 9 — Discusses and presents the graphical and statistical results obtained from analyzing data set PD.
- Chapter 10 — Provides summary, conclusions, and recommendations.
- Appendix A — Presents data set PD/LT, including pile geometry, subsurface conditions, dynamic measurements, dynamic parameters, static load test results, CAPWAP/TEPWAP capacity predictions, and the Energy Approach predictions.
- Appendix B — Presents data set PD, including pile geometry, skin and toe soil, dynamic measurements, and CAPWAP and Energy Approach predictions.

Table 1. Data set PD/LT contributors.

Organization	Persons in charge and/or contact people	Number of cases	Reference
U.S. Federal Highway Administration	Richard Cheney, Jerry DiMaggio, Albert DiMillio, Chris Dumas, and Carl Ealy	126	FHWA Dynamic Monitoring and Pile-Load Test Reports-Project 56: Colorado (1987), Iowa (1988), Kentucky (1993), Louisiana (1990), Maine (1990), Minnesota (1991), Missouri (1988), Nebraska (1989), Oklahoma (1988), Oregon (1987), Pennsylvania (1991), Vermont (1991), Washington (1984).
Pile Dynamics, Inc. and GRL, Inc.	George Goble, Garland Likins, Frank Rausche, and Mark Svinkin	47	Abe, Likins, and Morgano (1990). Inhouse Reports.
Ontario Ministry of Transportation	Betty Bennet, Murty Devata, John Pertruzziello, and Mark Vasavithisaan	14	Pile-Load Capacity Evaluation HWY 404 Structures-Site 33 (1978), Foundation Evaluation and Design Report-Site 35 Ontario MOT (1983), Thompson and Devata (1980).
The Trow Group Limited	Shaheen Ahmad, Steven Cheng, Tony Maini, and David Thompson	35	The Trow Report (1978), Cheng and Ahmed (1988), Thompson and Devata (1980), Inhouse Reports, Foundation Evaluation and Design Report-Site 35 Ontario MOT (1983).
GZA GeoEnvironmental	William Beloff and Steve Roy	15	Inhouse Reports
Gannet and Flemming	James Langer and John Masland	10	Inhouse Reports
Law Engineering	Kevin Kett	6	Inhouse Reports
STS Consultants	Patrick Hannigan	4	Inhouse Reports
Wagstaff Piling	David Klingberg and Julian Siedel	4	Inhouse Reports
Haley and Aldrich Inc.	Christopher Snow, David Thompson, and James Weaver	6	Inhouse Reports
Florida DOT	William "Bubba" Knight	59	Inhouse Reports
Oklahoma DOT	Steve Jacobi	7	Inhouse Reports
Washington DOT	Ralph Henning	4	Inhouse Reports
Iowa DOT	Curtis Monk	4	Inhouse Reports
Oregon DOT	Glen Thommen	2	Inhouse Reports
Louisiana DOT	Mark Morvant	3	Inhouse Reports
Anna GeoDynamics, Inc.	Bengt Fellenius	2	Edde and Fellenius (1990)

Note: The total number does not add up to 208 pile cases as different sources may have contributed information for the same pile case.

CHAPTER 2 - BACKGROUND

2.1 GENERAL

The use of driven piles for foundation support for a variety of structures, such as bridges, buildings, towers, and dams, is a practice that dates back to prehistoric times.¹ Piles are used to transfer superstructure loads through soft soil layers and/or water. Pile resistance is developed through the soil, as in the case of friction piles, or from competent underlying soil or rock strata, as in the case of end-bearing piles. Most piles incorporate a combination of both frictional resistance and end-bearing resistance.

In this chapter, the main difficulty with using piles as foundation systems is addressed. Engineers have limited ability to predict the capacity and integrity of driven piles. As a result, high factors of safety are used when designing deep foundations, which add significant costs to projects. Pile capacity may be estimated using static or dynamic analyses and may be confirmed by static load tests. The following includes a brief discussion of static analyses and static load tests. The alternative methods, namely dynamic analyses, are outlined in chapter 3.

2.2 STATIC ANALYSIS

The initial design of pile foundations requires the evaluation of pile capacity via static analysis. The Federal Highway Administration (FHWA) incorporates static formulas (Tomlinson and Nordlund methods) for the analysis of driven piles in their pile analysis program, *SPILE* (DiMaggio, 1991). Static formulas estimate driven-pile capacities on the basis of soil-strength parameters obtained from subsurface exploration programs and from pile-soil interaction relations. The predictions are simply a summation of the estimated point and skin resistance of the pile. For a description of various methods, see, for example, Bowles, 1988. There is, however, a great deal of uncertainty in these analyses and their accuracy is highly questionable.

Briaud *et al.* (1988) examined the capacity predictions from 12 static analyses applied to 100 piles that were statically load tested to failure. They concluded that all methods produced unsatisfactory results, especially in layered soil strata. Similar conclusions were drawn when the best methods were averaged and used to predict the capacity of piles

¹The Neolithic inhabitants of Switzerland supported their homes 12,000 years ago on wooden poles driven in shallow lakes. The ancient Egyptians depicted manpower pile-driving operations and failures. The Romans supported many of their bridges over the Rhine River with driven-timber piles.

driven in varying soil layers.

Unfortunately, the inaccuracy of static analysis results in the use of very high safety factors leading to higher construction costs.

2.3 STATIC LOAD TESTS

Static load testing is the only method available to determine the actual static capacity of piles. This method involves physically loading a pile at specified time intervals (see, for example, ASTM D-1143) and monitoring the settlement of the pile top until failure. The results of these tests are then plotted (load vs. settlement) and the failure load is interpreted using various methods (outlined in chapter 5). These tests are expensive, time-consuming, and, as a result, are not commonly performed.

Static testing is typically carried out as a "proof test" on piles to determine the pile's performance in supporting a service load, usually twice the design load (e.g., Massachusetts Highway Dept. (1989), Virginia DOT (1987), and Alabama State Highway Dept. (1985) State highway codes). It is important to note that the proof test does not provide the ultimate pile capacity and, therefore, does not contribute to the effort of increasing accuracy and reducing foundation costs. Although the test is typically carried out to twice the design load, the actual employed factor of safety may be much higher as the actual pile capacity is unknown. Proof testing is less expensive than loading a pile to failure and is therefore more frequently performed.

In spite of the difficulties in carrying out a load test to failure and the possible inaccuracies of the data (see Fellenius, 1989), it remains as the only means to examine actual pile capacity.

Data set PD/LT, which is presented in chapter 6, contains cases of 120 piles load tested to failure. The interpretation of the test results was carried out using a variety of methods as outlined in section 5.2.1.

CHAPTER 3 - DYNAMIC ANALYSIS OF PILES

3.1 GENERAL

Dynamic analyses of piles are methods that predict pile capacity based on the behavior of the hammer-pile-soil system during driving. Such methods are based on the idea that the driving operation induces failure in the pile-soil system. In other words, pile driving is analogous to a very fast load test under each hammer blow. The pile must, however, experience a minimum permanent displacement, or set (approximately 0.1 inch [2.5 mm]), during each hammer blow to fully mobilize the resistance of the pile-soil system. If there is very little or no permanent downward displacement of the pile tip, then the pile-soil system experiences mostly elastic deformation. As a result, capacity predictions based on measurements taken at this time would not be indicative of the full resistance of the pile-soil system.

There are basically two methods of estimating the capacity of driven piles based on dynamic driving resistance: pile-driving formulas (i.e., dynamic equations) and wave-equation analysis.

3.2 DYNAMIC EQUATIONS

3.2.1 Review

For centuries (Cummings, 1940), quantitative analyses of pile capacity have been performed using dynamic equations. These equations can be categorized into three groups: theoretical equations, empirical equations, and those that consist of a combination of the two. It is important to mention that 45 of the State highway departments in the United States include a dynamic formula in their foundation specifications for the determination of bearing value for single-acting steam/air hammers. Of these 45 States, 30 use the Engineering News Record (ENR) formula and 9 States use other variations of the rational pile formula. In general, all the pile formulas, with the exception of the Gates formula, are derived from the rational pile formula (Bowles, 1988). A reference will be made here only to theoretical equations because:

- Empirical and semi-empirical equations are restricted to the conditions and assumptions of their original data set.
- State highway building codes utilize theoretical equations.

3.2.2 The Basic Principle

The theoretical equations have been formulated around analyses that evaluate the total resistance of the pile, based on the work done by the pile during penetration. Observations of the hammer's ram stroke and the pile set are used in determining this work done by the hammer and the pile. These theoretical equation formulations assume elasto-plastic force-displacement relations (see figure 1). The total work is computed as:

$$W = R_u \left(S + \frac{Q}{2} \right) \quad (1)$$

where

R_u	=	yield resistance
S	=	pile set, denoting the permanent displacement (plastic deformation) of the pile under each hammer blow
Q	=	quake, denoting the elastic deformation of the pile-soil system.

In general, dynamic equations are inaccurate (see for example Housel, 1965, 1966; Flaate, 1964; and Olsen and Flaate, 1967) and a high factor of safety (F.S.) is therefore required when using their estimated capacity (e.g., F.S.=6 for the ENR equation). Dynamic equations are largely inaccurate because:

- Their parameters, such as the efficiency of energy transfer and the pile/soil quake, are crudely approximated.
- Some of the theoretical developments of the rational pile formula, especially those relating the energy transfer mechanism to a Newtonian analysis of ram-pile impact, are theoretically invalid (see, for example, Cummings, 1940 and Taylor, 1948).
- There is no differentiation between static and dynamic soil resistances where it is known that such differences exist, especially in cohesive soils (Taylor, 1948).

3.2.3 Energy Transfer

The theory of energy transfer analysis in many of the dynamic equations assumes that the hammer-pile impact is consistent with Sir Isaac Newton's third law, Conservation of Momentum. Newton's relationship applies to the impact of two free rigid bodies. In the case of dynamic equations, these rigid bodies are considered to be the hammer and the pile. This law of motion states that if no external forces are acting on the two rigid bodies, then the total momentum of the system is conserved. The impulsive forces acting during the impact are actually internal and, therefore, do not affect the total momentum

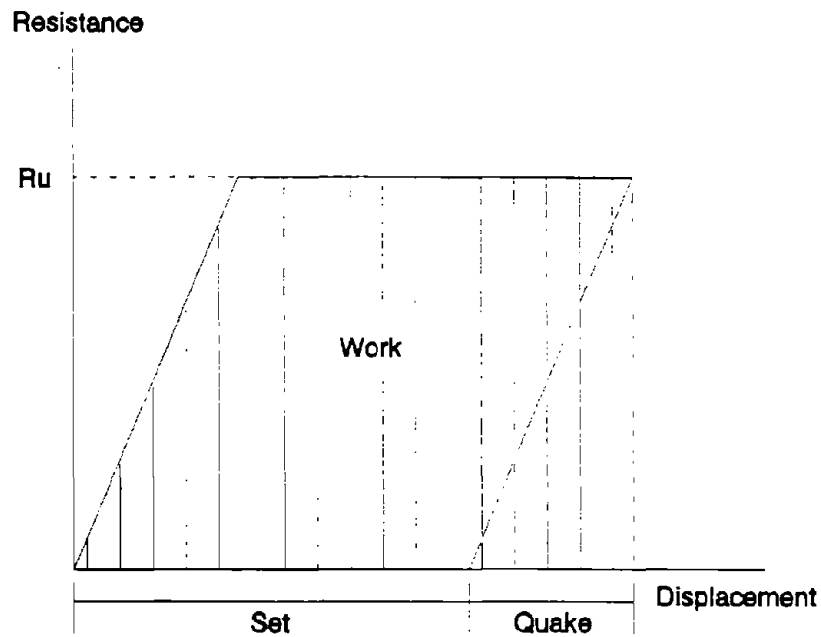


Figure 1. Resistance vs. displacement at the top of the pile.

of the system (see Cummings, 1940). This is clearly not the case for driven piles, which are elastic rather than rigid and experience end bearing as well as frictional resistance. Newton is reported to have stated that his expression for the impact of two massive bodies did not apply for "bodies ... which suffer some such extension as occurs under the strokes of a hammer" (see Taylor, 1948).

The ENR formula, published in 1888, was originally developed for use with timber piles and a drop hammer (Bowles, 1988). This formula further simplifies the assumptions made by the rational pile formula by equating the efficiency of the ram-pile impact to 1. This oversimplification does not consider three factors:

- Energy losses that occur in the pile-driving system during impact.
- Work used in the elastic compression of the pile and soil.
- Varying efficiencies of the wide range of hammers used today.

These simplifications in the development and use of the ENR formula result in a

necessary safety factor of 6 (Taylor, 1948). Briaud and Tucker (1988) checked the prediction accuracy of the ENR equation in 68 pile cases. The static capacity was determined based on a reference settlement equal to one-tenth of the pile diameter plus the elastic compression of the pile. The mean of the ratio predicted over measured load was 0.82 with a standard deviation of 0.38. Further reference to these results is made in chapter 10. Overall, the low reliability of dynamic equations requires very high factors of safety that make their use extremely uneconomical.

3.3 THE WAVE EQUATION

3.3.1 Formulation and Principles

Issacs (1931) concluded that many pile-driving formulas were incorrectly based on Newtonian mechanics for the pile/hammer impact and he became the first person to suggest the use of an analysis based on the one-dimensional wave equation instead. This proposed solution assumed that the toe of the pile was fixed and that no side resistance existed (Lowery *et al.*, 1969). Fox (1932) proposed an exact solution to Issacs formulation; however, without the aid of computers, many simplified assumptions were necessary because of the complexity of his solution (Smith, 1960).

Stress-wave propagation in a pile during driving can be described by the following one-dimensional wave equation (after Paikowsky and Whitman, 1990) modified to include frictional resistance along the pile:

$$E_p \frac{\partial^2 u}{\partial x^2} - \frac{S_p}{A_p} f_s = \rho_p \frac{\partial^2 u}{\partial t^2} \quad (2)$$

where E_p , ρ_p = modulus of elasticity and unit density of the pile material
 $u(x,t)$ = longitudinal displacement of infinitesimal segment
 f_s = frictional stress along the pile
 A_p , S_p = pile area and circumference, respectively.

The displacement (u) causes strains in each pile element that can be used to calculate pile stresses as well as the resistance developed in the soil. This displacement can be determined with respect to time and location. The friction stresses (f_s) are generated by the movement of the pile. When the pile is subjected to free-wave motion ($f_s=0$), the stress propagation equation becomes the familiar one-dimensional wave equation:

$$c^2 \frac{\partial^2 u}{\partial x^2} = \frac{\partial^2 u}{\partial t^2} \quad (3)$$

where

$$c = \sqrt{\frac{E_p}{\rho_p}} \quad (4)$$

c = wavespeed of the pile material
 E_p = modulus of elasticity of the pile
 ρ_p = density of the pile material.

Among the assumptions implicit in the development of the one-dimensional wave equation are prismatic shape and homogeneity. Also, it is assumed that under loading, plane parallel cross sections remain plane and parallel and that a uniform distribution of stress exists across each plane. The assumption of uniaxial stress does not include uniaxial strain and, therefore, lateral expansions and contractions (Poisson's effect) arise from the axial stresses associated with lateral inertia (Graff, 1975). The additional friction term (after Paikowsky and Whitman, 1990) was included under the assumption that the soil is stationary (having no inertia effects), and the action of the friction forces does not violate any of the previous assumptions.

The so-called "wave equation methods" are based on a numerical solution of the one-dimensional wave equation. The numerical solution utilizes mathematical models for the pile and the pile-soil system. When the one-dimensional wave equation numerical solution is used for pre-driving analysis, the driving system is also modeled.

In 1960, Smith developed a numerical model to simulate the dynamic behavior of the hammer-pile-soil system during driving. This model is represented by a series of discrete masses and springs used for solving the one-dimensional wave equation (see figure 2). The soil resistance is modeled via a spring, slider, and dashpot, which represent the static and dynamic soil resistances (see figure 3). The elasto-plastic soil model is employed for the static soil resistance in Smith's solution. The distance traveled by the pile toe during the elastic deformation of the soil is represented by the soil quake (Smith, 1960). As the elastic limit of the soil is reached (represented by the slider in sequence with the spring), plastic deformation takes place. The plastic deformation, or irreversible compression of the soil, is denoted by the permanent set of the soil (see figure 3).

According to this model, point A represents the ground resistance buildup to the ultimate resistance, R_u . Plastic failure occurs as the ground resistance has reached its maximum and the adjacent pile segment displaces, plastically, to point B. Unloading the soil at point B produces an elastic rebound, equal to the quake, to point C. The

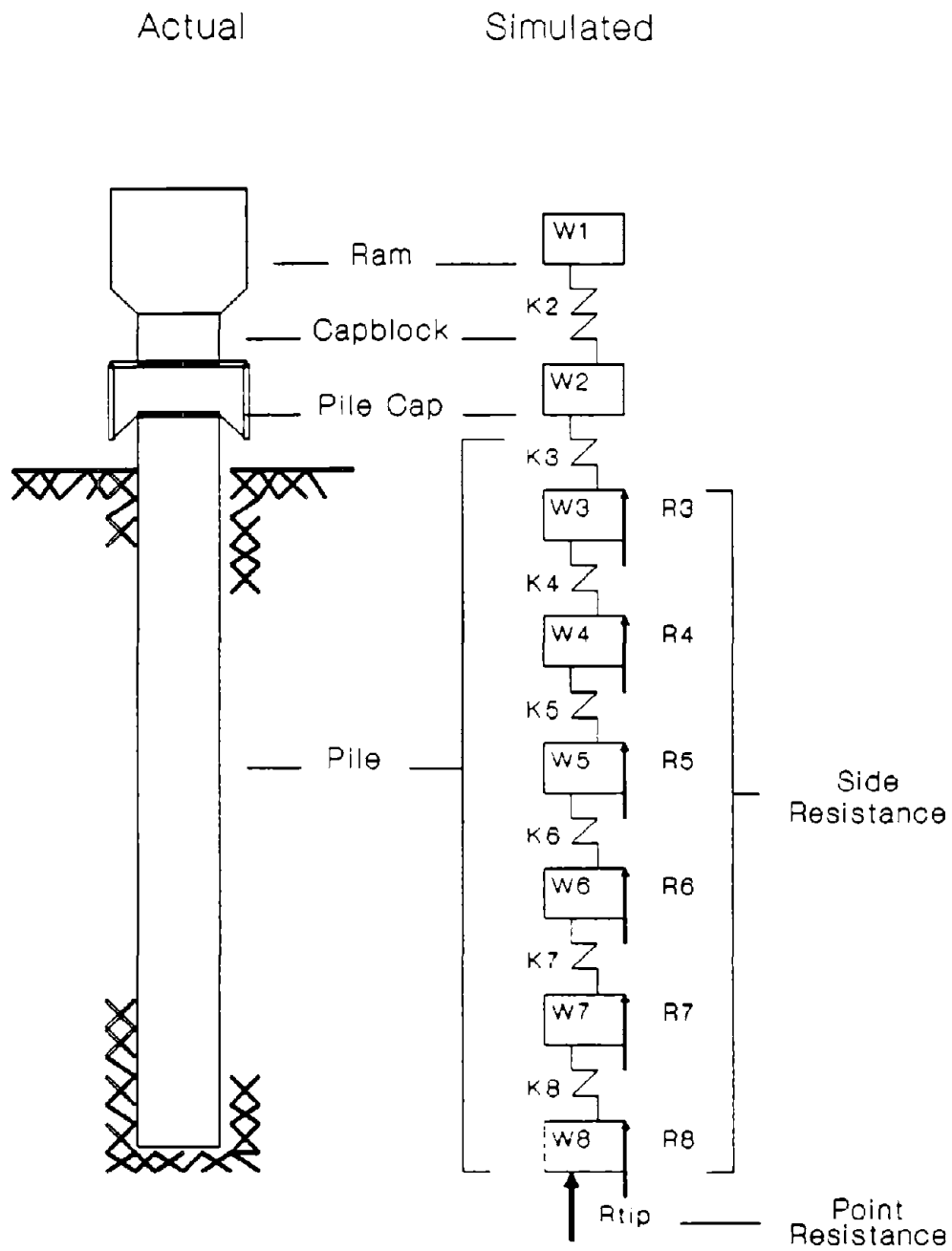


Figure 2. Smith's model simulating the hammer-pile-soil system for use with the one-dimensional wave equation (Smith, 1960).

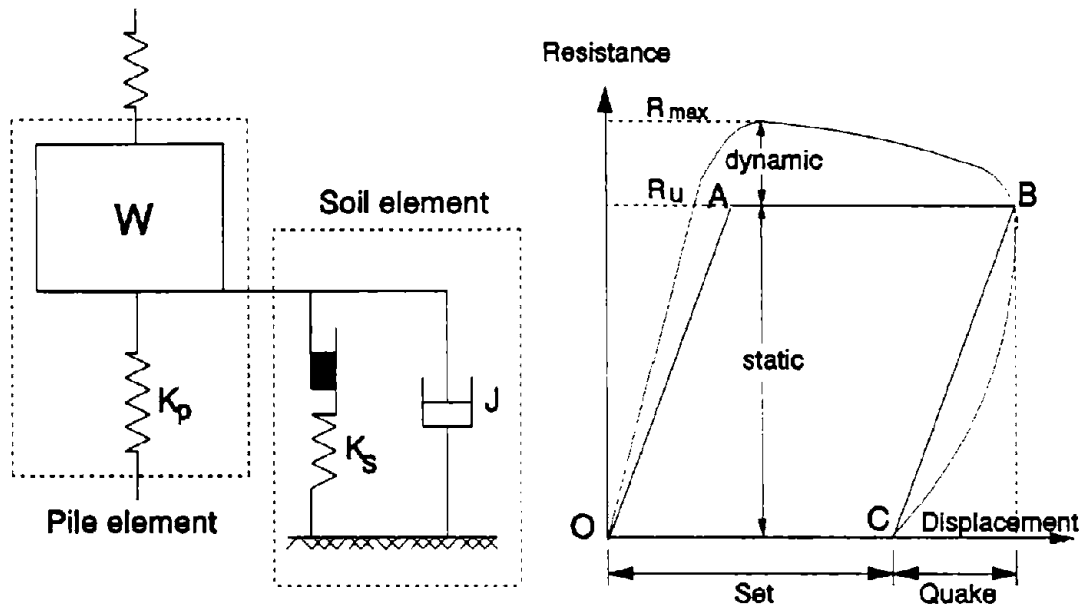


Figure 3. Soil-pile model (left) and the corresponding elasto-plastic soil resistance-displacement relationship (after Smith, 1960).

permanent set is, therefore, equal to the distance OC, which, in turn, is equal to distance AB (Smith, 1960). The static soil resistance-displacement relationship, as presented by Smith (1960), is modeled by a spring (K_s) and a slider, where W represents the mass of the pile element.

The dynamic component of the soil's resistance is assumed to be viscous (soil-type related) and is, therefore, velocity-dependent. This dynamic resistance is modeled by a dashpot (J) parallel to the spring (see figure 3). The resisting soil force (R_{max}) developed under each hammer blow is a combination of the static and dynamic soil resistances:

$$R_{max} = R_s + R_d \quad (5)$$

where R_{max} = total resistance

$$\begin{aligned}
 R_s &= \text{static resistance} \\
 R_d &= \text{dynamic resistance.}
 \end{aligned}$$

The wave equation formulation is used in two general ways: pre-driving analysis and post-driving analysis.

3.3.2 Pre-Driving Analysis

The so-called "wave equation analysis" utilizes the one-dimensional wave equation to predict dynamic pile behavior before construction and models the pile-soil system and the driving system (i.e., the hammer, cushion, and capblock), as suggested by Smith (1960). This computerized solution is used for the evaluation of the penetration resistance (i.e., blow count) and the driving stresses in the modeled pile under given conditions. The static capacity is then determined by relating the computed static capacity-penetration resistance relationship for a certain energy rating to observed dynamic resistances during driving. Such analyses enable engineers to determine a suitable pile-site-equipment combination.

3.3.3 Post-Driving Analysis - CAPWAP/TEPWAP

Post-driving analyses utilize the measured force signal (calculated from strain readings) and the measured velocity signal (integrated from acceleration readings) obtained near the pile top during driving. These analyses model the pile-soil system as shown in figure 4 with the element denoted as number 3 representing the point of measurement. The velocity signal is used as a boundary condition at that point while varying the parameters describing the soil resistance in order to match the calculated and measured force signals. These parameters include the side and tip quake, side and tip damping, the pile shaft resistance, and the pile tip resistance. Additional parameters may be used to describe soil resistance and rebound ratio for unloading different from that of loading. The process is described in the form of a flow chart in figure 5. The subscripts msd. and cal. denote measured and calculated values, respectively. Iterations are performed by changing the soil-model variables for each pile element in contact with the soil until the best match between the force signals is obtained. The results of these analyses are assumed to represent the actual distribution of the ultimate static capacity of the pile.

This procedure was first suggested by Goble, Likins, and Rausche (1970), utilizing the computer program CAPWAP. Similar analyses were developed by others (see Paikowsky, 1982 and Paikowsky and Whitman, 1989) utilizing the program code TEPWAP.

3.3.4 Wave Equation Analysis - Discussion

Post-driving analyses utilize the measured force and velocity waves, hence, the energy delivered to the pile in these models is exact. The models can consider the "damping" at

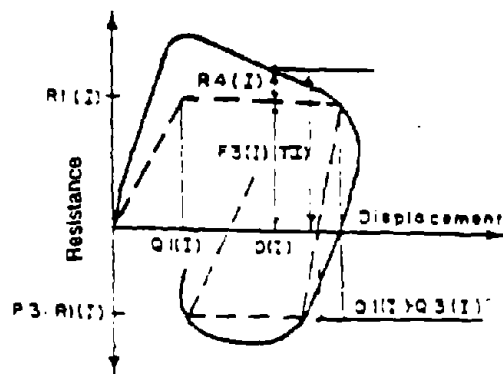
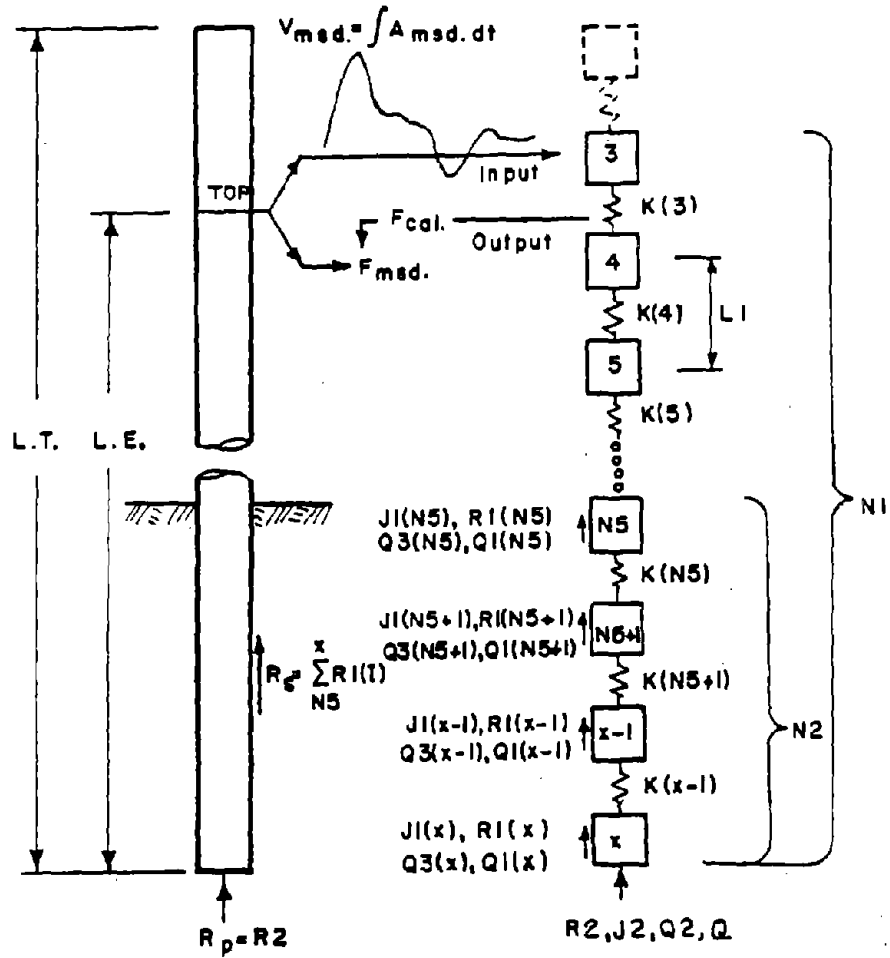


Figure 4. Notations used for model of pile and soil in TEPWAP analysis (Paikowsky, 1982).

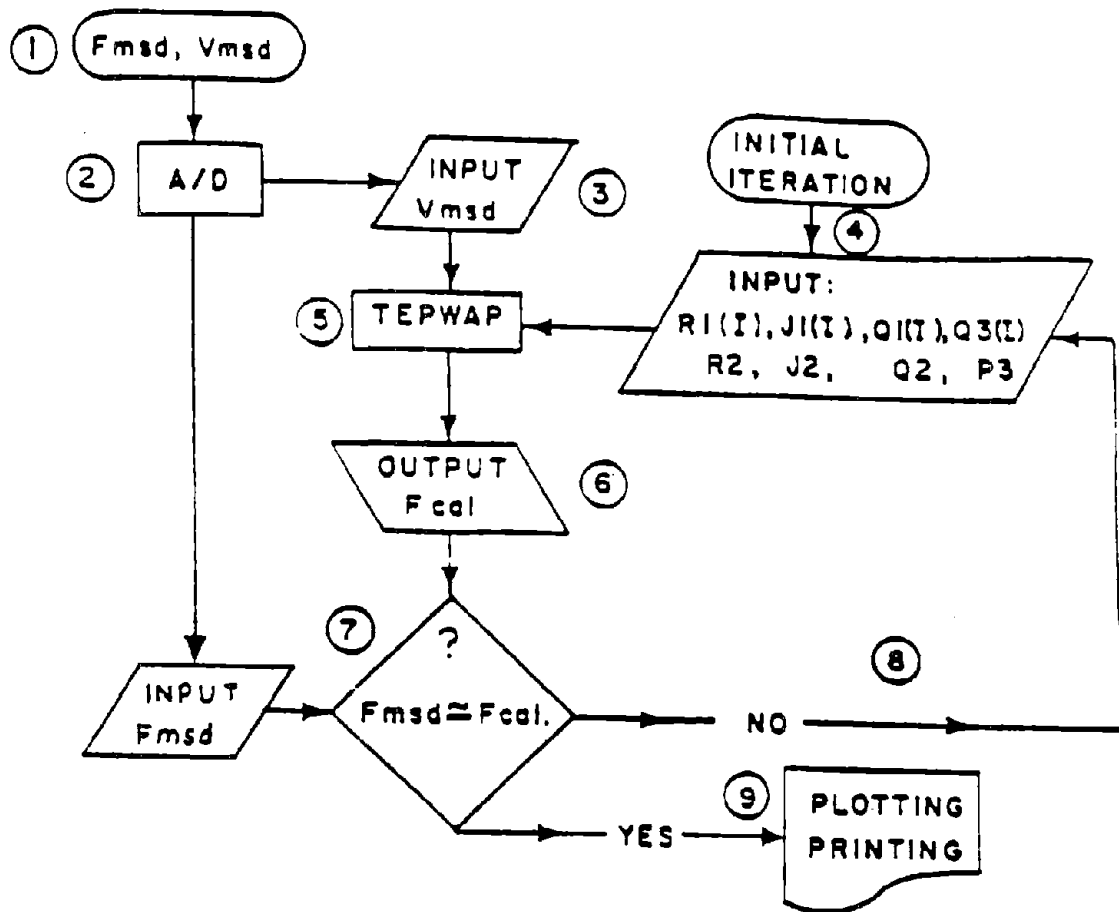


Figure 5. Flow chart describing the analysis process using TEPWAP (Paikowsky, 1982).

each depth by utilizing different damping parameters for each of the discrete units and, therefore, account, to some degree, for different energy losses in the surrounding soils and the various pile-type effects. Such analyses may result in a force distribution along the pile that differs from the actual one, but by keeping the energy balanced, the calculated total resistance may be accurate (a case study of large instrumented piles that showed such results was presented by Paikowsky, 1982). A method that presents a simplified solution for the wave propagation phenomenon (i.e., the Case method, see section 3.5), with the attempt to correlate the energy losses to the soil type at the tip, does not capture the actual phenomena and does not necessarily keep a balance of energy. The resulting factor (J_c) is difficult (if not impossible) to correlate to the soil type at the pile tip. A simple field method that predicts pile capacities in "real-time" remains attractive, however, because of its ability to monitor pile capacity during driving.

3.4 FIELD ANALYSIS AND THE PILE-DRIVING ANALYZER

Capacity evaluation in the field is attractive because of the potential to increase quality control and to improve construction efficiency of deep foundation systems. The procedure of monitoring pile driving by dynamic measurements is well established. Early large-scale studies (e.g., Michigan State Highway Commission, 1965; Texas Highway Department, 1973; and Ohio Department of Transportation, 1975; see also Highway Research Record, 1967 and Goble *et al.*, 1970) led to the development of commercial systems that enable complete and relatively easy acquisition of dynamic measurements and analysis during driving. These dynamic measurements include acceleration and strain readings recorded at the pile top under each hammer blow. The most popular acquisition and analysis system in the United States is the pile-driving analyzer (PDA) (see Pile Dynamics Inc., 1990).

The PDA calculates a number of different physical quantities, including force (from strain readings), velocity and displacement (from acceleration readings), maximum delivered energy (to the pile top), and tension and compression stresses. These results are used to predict the pile capacity, as well as to examine the hammer performance, stresses in the pile, and pile integrity. The PDA predicts pile capacities in the field by utilizing a simplified evaluation method, known as the Case method.

3.5 THE CASE METHOD

3.5.1 General

The Case method (see Goble *et al.*, 1970 and Rausche *et al.*, 1975), is a simple field procedure used by the PDA to estimate pile capacities. Analysis by the Case method is based on the assumptions of a uniform elastic pile, ideal plastic soil behavior, and a simplified wave propagation formulation. Employed are force and velocity measurements taken at the pile top and a correlation between the soil at the pile tip to a damping parameter.

3.5.2 The Case Method Equation

The Case method calculates the total soil resistance (RTL) active during pile-driving, using the following equation:

$$RTL = \frac{[F(T1) + F(T1 + \frac{2L}{C})]}{2} + [v(T1) - v(T1 + \frac{2L}{C})] * \frac{MC}{2L} \quad (6)$$

where

F(T1)	=	measured force at the time T1
F(T1+2L/C)	=	measured force at the time T1 plus 2L/C
v(T1)	=	measured velocity at the time T1
v(T1+2L/C)	=	measured velocity at the time T1 plus 2L/C
L, M	=	length and mass of the pile, respectively
C	=	speed of wave propagation in the pile.

Different variations of the Case method have been developed taking T1 as the time of impact or modified to include a time delay constant allowing higher RTL values to be obtained. The time T1 is defined, in equation form, as:

$$T1 = TP + \delta \quad (7)$$

where

TP	=	time of the impact peak
δ	=	time delay.

The time delay is required in soils capable of large deformations before achieving full resistance (see figure 6). A time delay is also used in situations where the hammer impact is uneven (PDA Manual, 1990).

The total resistance calculated is a combination of the static resistance (S) which is displacement-dependent, and the dynamic resistance (D) which is velocity-dependent. Therefore, the total resistance (Goble *et al.*, 1975) is:

$$RTL = S + D \quad (8)$$

Several factors that influence the pile-soil system must be considered when the total predicted resistance is evaluated. These factors include the damping coefficient, time-dependent soil strength changes, and refusal driving when the soil's resistance is not fully mobilized under a single hammer blow.

3.5.3 Case Damping Coefficient

The dynamic resistance D is considered to be viscous in nature, hence, a function of the velocity at the pile toe (V_{toe}) and a damping constant (J) where:

$$D = J * V_{toe} \quad (9)$$

By applying the wave propagation theory, the pile toe velocity can be calculated as a

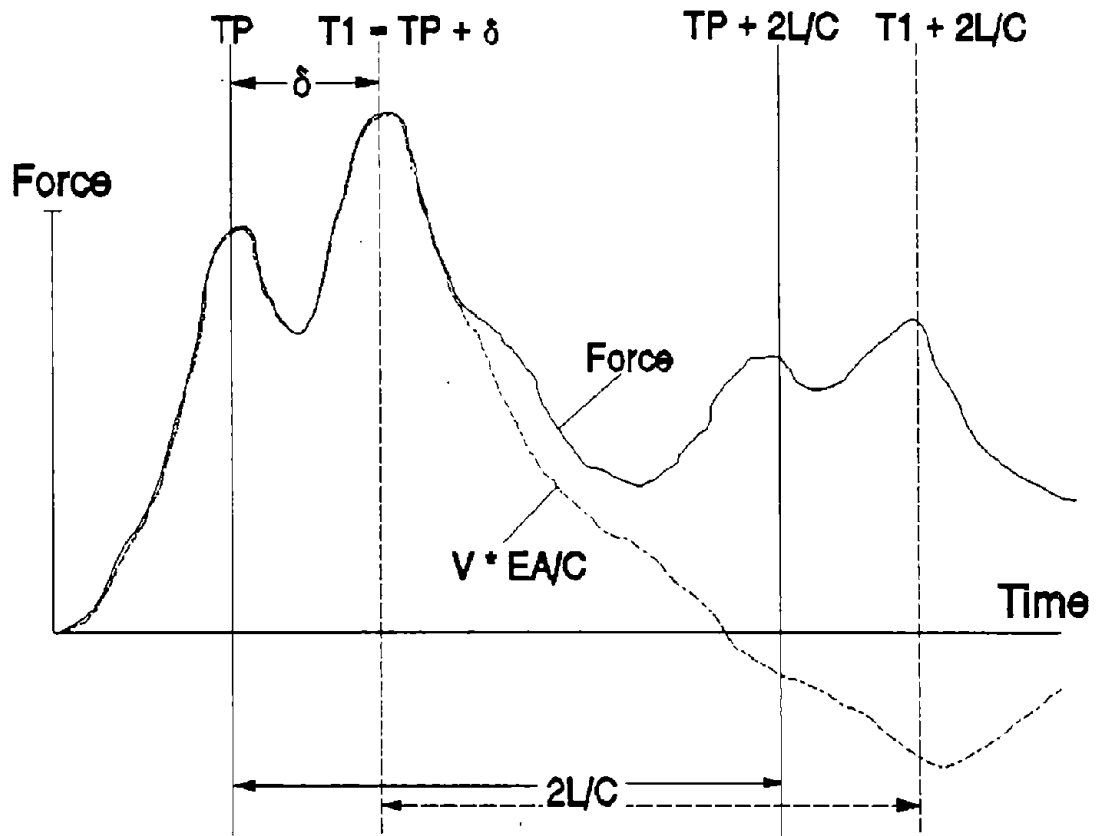


Figure 6. Force and velocity traces showing two impact peaks indicative of driving in soils capable of large deformations.

function of the velocity at the pile top (Goble *et al.*, 1975):

$$V_{toe} = 2V_{top} - \frac{L}{MC}RTL \quad (10)$$

where

L	=	pile length
M	=	pile mass
C	=	wave speed of the pile material
R	=	total resistance
V_{top}	=	velocity at pile top.

V_{top} is taken as the pile top velocity at the time T1.

According to Goble *et al.* (1975), remolding effects cause the majority of the damping resistance to be concentrated near the pile tip. Consequently, the damping constant is determined according to the soil type at the pile tip. In most cases, the damping constant (J) is proportional to the pile properties (EA/C) and, therefore, is represented by a dimensionless coefficient (J_c) using the following equation:

$$J = J_c \frac{EA}{C} \quad (11)$$

where J_c = dimensionless Case damping coefficient
 E = elastic modulus of the pile material
 A = pile cross-sectional area
 C = wave speed of the pile material.

The recommended values for J_c have changed since the initial estimates made by Goble *et al.* (1975) as a result of improvements to the PDA and continued research in this area. In 1975, Goble *et al.* (1975) published recommended J_c values for various soil types. These recommendations have been revised in PDA Manual-Model GCPC (1990). Both sets of recommended J_c values are given in the following table:

Table 2. Recommended J_c values according to the soil type at the pile tip.

Soil Type at Pile Tip	Goble et al., 1975	PDA Manual, 1990
clean sand	0.05	0.10 to 0.15
silty sand	0.15	0.15 to 0.25
sandy silt	0.2	-
silt	0.3	0.25 to 0.40
silty clay / clayey silt	0.55	-
silty clay	-	0.40 to 0.70
clay	1.1	0.70 to 1.00

It is suggested that J_c values less than 0.10 are unlikely. Large J_c values result in more conservative capacity predictions, and the range of $J_c = 0.5$ to 1.0 can cause large capacity differences (PDA Manual, 1990). J_c can be back-calculated from static load test results and applied to other piles nearby, provided they are driven in similar soil strata. Negative damping coefficients are physically meaningless and are set to zero should they occur. If load testing to failure is not conducted at a particular site, subsurface

investigation of the underlying soil strata must be carried out to provide the necessary information needed to estimate J_c .

3.5.4 Case Method Variations

Several variations of the Case method have evolved for the analysis of different driving situations and soil types. The variations are similar in that they all begin with the initial total resistance prediction (RTL) of equation (6). Five distinct methods are used to employ the predicted RTL: Damping Factor Method, the Maximum Resistance Method, the Minimum Resistance Method, the Unloading Method, and the Automatic Method. A brief review of each of these methods follow (for details, see the 1990 PDA Manual).

(a) The Damping Factor Method, RSP

The Damping Factor Method uses the velocity at the toe of the pile (V_{toe}) of equation (10), which may be rewritten as:

$$V_{toe} = V_{top} + \frac{[F(T1) - RTL]}{\frac{MC}{L}} \quad (12)$$

and the Case damping constant (J_c) is nondimensionalized by the pile impedance (MC/L), to determine the static capacity (RSP) (PDA Manual, 1990). The equation, which was discussed in the last section, utilizes damping constants empirically derived from static load tests where:

$$RSP = RTL - J \frac{MC}{L} * V_{toe} \quad (13)$$

This expression is the standard Case method equation used for normal driving conditions.

(b) The Maximum Resistance Method, RMX

The Maximum Resistance Method uses the RSP equation with $2L/C$ as a fixed quantity. The time $T1$ used in the RSP equation is varied between the impact time (TP) and $TP + 30$ ms to find the corresponding maximum RSP value, denoted as RMX (see figure 6).

Originally (Goble *et al.*, 1967), it was proposed to choose the time $T1$ as the time when the pile top velocity becomes zero (referred to (e), the automatic method, RAU). Time delay methods were then developed (Goble *et al.*, 1975). The most familiar one is $T1 = TP$, the time of maximum velocity. This was then modified to $T1 = TP + \delta$, where δ is a time-delay constant required to enable full resistance to be developed. The maximum resistance method (RMX) is a variation of this approach, where $T1$ will result in the maximum static resistance (R_s). This $T1$ is not necessarily the same one that will produce the maximum total resistance RTL. RMX can be used in cases of large soil

quakes or short rise times where the full resistance is not mobilized by the time the stress wave reaches the pile toe. This method is advantageous for large displacement piles with substantial end-bearing. The RMX resistance may not, however, develop until unacceptably large displacements occur. Caution should be taken when using RMX in silts and clays with high damping factors because over-predictions may result.

(c) The Minimum Resistance Method, RMN

Tension cracks, splices, and changes in cross-sectional area may vary the wave speed along a single pile. To compensate for these changes, the Minimum Resistance Method uses the first or second peak as the impact time (T1) in the capacity equation. The tip reflection time, T2 or (T1+2L/C), is varied through the 2L/C "window," which is centered around T2 and is ±20 percent of 2L/C. The minimum capacity (RMN) is determined using the tip reflection time. This method can be used with confidence if the blow count is less than 40 blows per foot (131 blows per meter) (PDA Manual, 1990).

(d) The Unloading Method, RSU

For long piles with high frictional resistance, the measured velocity can become negative before a reflection from the tip is observed at time T2. Under such conditions, the upper portion of the pile experiences decreasing displacement or rebounding. This results in an unloading of the upper soil layers resistance and the computed capacities are under-predicted. The Unloading Method compensates for this by calculating the total friction in the upper unloading layers from the force velocity difference. This friction is then divided by two thus yielding the correction. The unloading resistance (RSU) then is:

$$RSU = RTL + K - J[F(T1) + v(T1) * \frac{MC}{L} - RTL - K] \quad (14)$$

where K = the unloading correction coefficient.

The correction coefficient is calculated from:

$$K = \frac{[F(T3) - V(T3)(\frac{MC}{L}) - F(TP) + V(TP)(\frac{MC}{L})]}{2} \quad (15)$$

where T3 = 2TP + 2l/C - T0 and T0 is the time of zero velocity (before 2L/C) (PDA Manual, 1990).

(e) The Automatic Method, RAU

The Automatic Method computes the capacity (RAU) for the first time where the computed pile toe velocity (V_{toe}) is zero. This method, originally proposed by Goble *et al.* (1967), does not select a damping coefficient because damping must be zero when V_{toe} is zero; therefore, the resistance at this time is completely static. This method

provides an exact solution for the end-bearing for piles with no skin friction and is recommended for use on piles with very little frictional resistance. Another variation of this method attempts to convert any skin friction into end-bearing resistance. This is proposed for piles having moderate skin friction, but are unaffected by J (PDA Manual, 1990).

3.5.5 Evaluation

(a) Critical Discussion

Two fundamental questions should be addressed regarding the Case Method approach:

- What is the time (T_1) that should be used to calculate the total resistance (RTL)?
- What is the meaning and reliability of the Case damping factor?

Based on the various methods described in section 3.5.4, the Case method produces a range of results according to the way in which it is employed. The "right" way and the "correct" T_1 are questionable, and depend on the driving system and soil and pile conditions.

The Case damping coefficient J_c is based on viscous damping in a dimensionless form. Thus, the dynamic resistance is correlated to the calculated velocity at the tip of the pile, and J_c is assumed to be related to the soil type at the pile's tip. To find the J_c to be used for different soils, the damping coefficient was calculated to fit failure loads obtained from static load tests. These damping coefficients were calculated for a range of ± 20 percent of the load test results, resulting in ranges of the J_c coefficient that were then ascribed to each soil type (Goble *et al.*, 1975).

The correlation between J_c and soil type is questionable and may or may not be feasible. The following section evaluates the use of J_c and demonstrates that the pile's dynamic resistance is influenced by several additional factors that cannot be appropriately considered through the use of the Case damping factor. A detailed examination of the J_c parameter is presented in section 8.2.1.

(b) Review of Existing Experience

The Case method has been the subject of different comparison studies attempting to evaluate its reliability. When static load testing is conducted on a pile, the corresponding Case damping coefficient can be obtained through back-calculating. This coefficient can then be compared to typical J_c values recommended to be used with the given soil conditions. Such information enables the determination of the reliability of the Case method for individual testing sites. Comparisons between the Case method and CAPWAP analysis results (in place of static load testing) have also been conducted (see, for example, Thompson and Goble (1988) or Riker and Fellenius (1988)).

The Trow Company (1978) examined 226 piles and 40 static load tests at 21 different sites. Their report concluded that the Case Method was shown to be in closer agreement with static load tests than dynamic formulas. For end-bearing piles, the range of the applicable damping factor is narrow, and the use of J_c values between 0 and 0.3 led to predictions within ± 25 percent of the load test results (excluding piles in till at one site). However, for friction piles, the choice of damping values was critical for the correct prediction of the capacity, and the tested pile's capacity was about twice the predicted one.

Four full-scale static load tests were conducted offshore and analyzed by Paikowsky (1979-1982). Open-ended pipe piles (48 in and 60 in [1219 mm and 1524 mm] diameters) were dynamically monitored during driving in a predominantly calcareous sand soil profile. The Case damping coefficient values (J_c) for capacity predictions in the range of ± 20 percent from the load test results are presented in figure 7. In order to be consistent with the data analysis of chapter 6, the J_c values of figure 7 are based on the same data used for CAPWAP and TEPWAP analyses that were somehow different from the one observed in the field. These values varied between $J_c = 0.06$ to 0.37, fitting the load tests, and in different ranges for each of the individual cases (e.g., $0.18 \leq J_c \leq 0.52$ for T-2/A and $-0.20 \leq J_c \leq 0.31$ for T-2/B).

Despite the Case method being used in only one of its forms, a significant scatter exists in the "recommended" damping coefficient field values that are considered more accurate than values from a general data set (see table 2).

A pile-testing study that began in 1980 was conducted in Milwaukee, WI, to establish foundation design criteria, such as the most suitable pile type and driving depth (see Riker and Fellenius, 1988). This project was undertaken because of the extensive pile installation program required for the construction of a wastewater plant (3,000 to 4,000 driven piles). The test piles consisted of steel H-piles and closed-ended pipe piles, with varying thicknesses, and were founded in glacial soil deposits. Approximately 40 piles were monitored during initial driving and/or during restriking, using a pile driving analyzer (PDA). All of these piles were analyzed using CAPWAP, and from these results, a J_c value was back-calculated for each pile. This analysis allowed engineers to correlate J_c values for the remaining piles at the site, provided they are founded in similar soils. Similarly, the Case method was performed on each test pile and capacity predictions were obtained using the calibrated J_c factors determined from the CAPWAP analyses. The results of this comparison show that when using pile-site-calibrated J_c factors for thick-walled steel pipe piles, the Case method predictions were within 20 percent of the CAPWAP results. Riker and Fellenius concluded that in light of the consistency of the J_c values at this site, the reliability of the Case method for rapid field predictions was demonstrated. They also cautioned, however, that additional CAPWAP analyses are necessary if other pile types are to be used at this site.

A comparison study between static load tests to failure and the Case method was carried

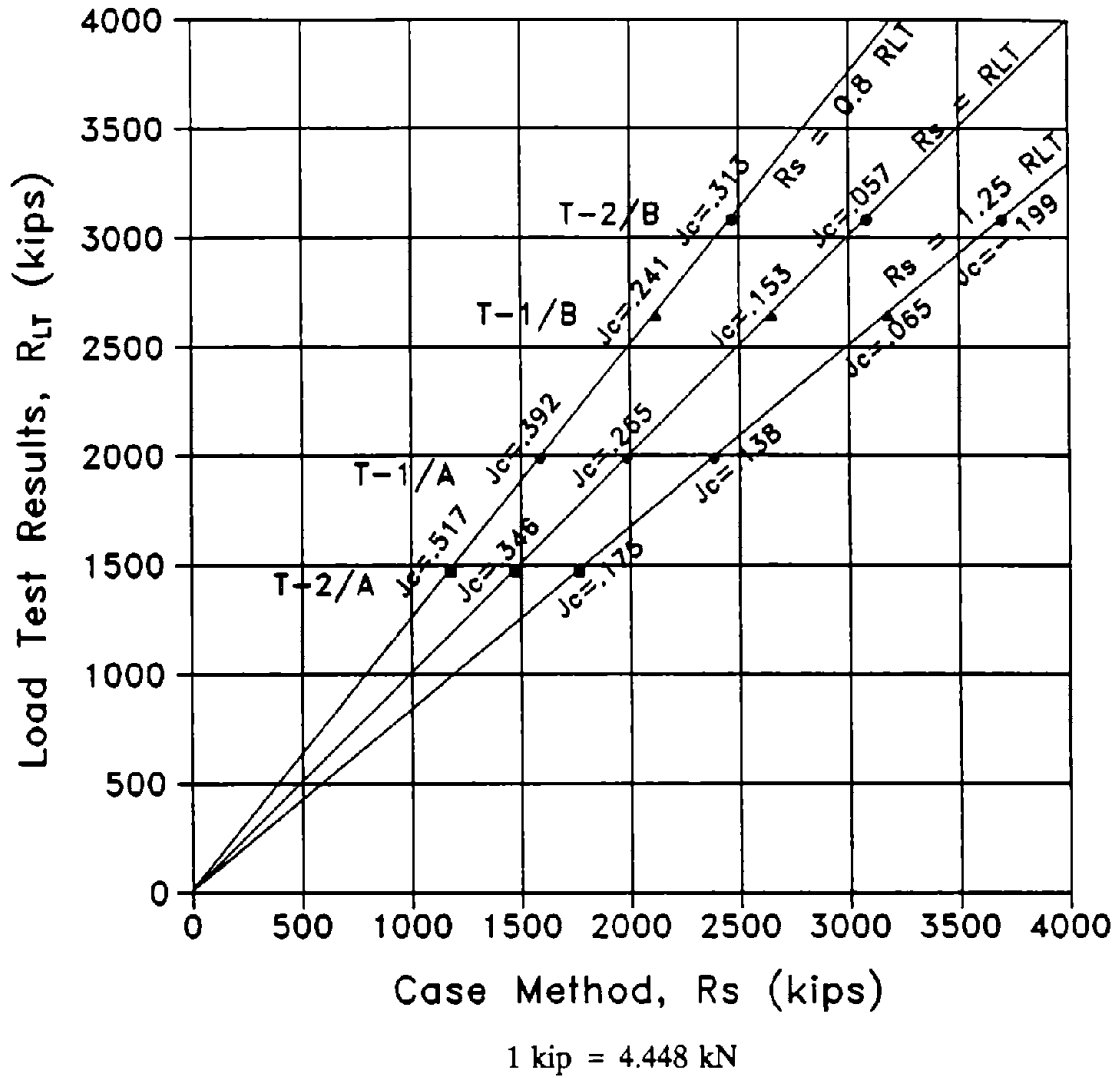


Figure 7. Case damping (J_c) values for capacity prediction of offshore piles in the range of ± 20 percent from load test results (after Paikowsky, 1982).

out in Europe by Bustamante and Weber in 1983 (Bustamante and Weber, 1988). This study consisted of dynamically monitoring six different shaped-steel H-piles using a PDA and load testing them to failure. The piles were tested at two different sites, and the general soil profiles consisted of sandy and clayey soils, respectively. The study results indicated that the predictions made by the Case method and CAPWAP were in agreement with capacities determined by static load testing. However, the Case damping

coefficients for the sandy site required calibration from CAPWAP results or static load test results.

Thompson and Goble (1988) tested 25 piles at 9 different sites across the eastern regions of Canada and the United States. All of the piles were founded in granular soils and were dynamically monitored using the PDA. CAPWAP analyses had been performed at the beginning of restriking (BOR). The results confirmed that the Case damping constants required to match CAPWAP capacities were high compared to recommended values. These high damping constants varied from 0.24 to 0.70 in the same soil on the same site and from 0.24 to 0.85 for all nine sites. These values are in sharp contrast to the $J_c = 0.05$ that was recommended to be used in sand by Goble *et al.* (1975) and $J_c = 0.10$ to 0.15 recommended by the PDA Manual (1990). Higher damping constants than expected will result in capacity over-predictions by the Case method. Thompson and Goble pointed out that their wide-range data set eliminated the possibility of treating these results as consequence of localized geographic or geologic conditions, and suggested that since they could not find an explanation for these high values, every project involving piles driven in sand should be calibrated for the correct J_c value.

Paikowsky and Chernauskas (1992) examined nine piles that were monitored during driving at the end of driving and/or at the beginning of restrike and were driven into soils ranging from sandy-silt to rock and till. Their study included static load tests to failure, whereby the failure loads were then employed to back-calculate Case damping factors. The results indicated that there is no specific correlation between the damping coefficient and the soil type. Thompson and Goble (1988) further concluded that it may be necessary at some projects to incorporate CAPWAP analyses with every pile to confirm the predictions by the Case method.

3.5.6 Capacity Predictions

The static resistance of the pile is predicted by subtracting the dynamic resistance from the total resistance (equation 8). As the static resistance may be time-dependent, it is often necessary to restrike piles and conduct dynamic analyses sometime after the end of initial driving (EOD). Setup may cause the static capacity to increase, while relaxation may cause the static capacity to decrease. Setup most often occurs in cohesive soils due to either (1) dissipation of excess pore pressure in the vicinity of the pile after driving or (2) thixotropy (an increase in strength with time without changing the water content) and a variety of reasons not always well-understood that may be referred to as "aging" (Schmertmann, 1991).

Soil relaxation most often occurs when piles are driven into dense fine sand or silts, shearing the soil beyond its peak resistance to residual strength. This results in smaller long-term frictional resistance. Although relaxation occurs less frequently than setup, its determination may be crucial. Restriking can lead to a more economical foundation system in the event of setup, and can prevent major structural problems in the event of

relaxation (Likins *et al.*, 1990).

When driving reaches refusal (e.g., a set of 0.1 in [2.5 mm] or less, most often regarded as 12 blows per inch [0.47 blows per millimeter]), the Case method may under-predict the static capacity of the pile. This is consistent with the concept that the driving operation must induce failure in the pile-soil system. If the pile experiences a small permanent set, or none at all, then the soil resistance is not fully mobilized (which indicates that the pile-soil system is mostly within the elastic range). Under such conditions, the predicted static capacity relates to the mobilized value only, often resulting in an under-prediction (PDA Manual, 1990).

3.5.7 Summary

The dynamic analysis of pile driving is based on the one-dimensional wave equation that describes the stress propagation through a slender elastic body. An additional term that accounts for the external forces acting on that body is added to the equation in order to consider the soil resistance. Traditionally, this resistance is considered to consist of static and dynamic components, as previously described. Practically, however, the dynamic component (even though represented by viscous damping) accounts for other energy losses, such as radiation, soil inertia, true damping, and more (Paikowsky and Whitman, 1989). These factors are determined by the pile shape, the acceleration at the pile toe, and the surrounding soil and, hence, cannot be correlated only to the soil type at the pile tip, as suggested by the Case method. The wave equation type of solutions (including CAPWAP) can consider the damping at each depth of pile penetration and, therefore, account for the different surrounding soils and pile type. The Case method simplified solution is not capable of this damping consideration. The correlation of the energy losses to the pile tip velocity and the soil type at the tip oversimplifies the complex phenomena; the resulting damping factor is difficult to correlate, leading to unreliable predictions. The accuracy of the Case method as a means of analyzing driven piles in the field will be further examined in chapter 8, based on the analysis of data set PD/LT in appendix A.

CHAPTER 4 - THE ENERGY APPROACH

4.1 BACKGROUND

While the static soil resistance is represented relatively adequately by the elasto-plastic soil model (see figure 3), the viscous damping accounts practically for various energy losses such as radiation, soil inertia (at the pile tip in particular), true damping, and viscosity in cohesive soils. As such, the model parameters (i.e., damping coefficients) cannot be calibrated on the basis of soil type alone. If such a calibration was possible, there would be no need to use different damping coefficients for the same soil next to the toe or the skin.

This observation has three major implications:

1. The success of the soil model in correctly representing the physical phenomena next to the pile is really controlled by its ability to account for the energy losses (in particular, those due to dynamic actions).
2. Calibration of the soil model parameters cannot be done on the basis of soil type alone. The calibration requires consideration of the combination of the pile and soil types (mainly small vs. large displacement piles), driving resistance, and, in addition, awareness of the installation details during construction (e.g., the use of jetting or preaugering).
3. A byproduct of 1 and 2 can explain why one method of analysis fails while the other succeeds (e.g., the Case method and CAPWAP).

The prediction of static capacity from pile driving, either by dynamic equations or by the one-dimensional wave equation, requires a balance of energy (i.e., the total energy that is transferred to the pile through the driving system is equal to the work done by the resisting forces during penetration).

Even though most of the theoretical and semi-empirical dynamic formulas were based on the energy principle, their reliability is very low, for the following reasons (see section 3.2 for discussion):

- Their analysis of Newtonian impact between the ram and the cushion/capblock system is theoretically invalid and, therefore, it led

to incorrect predictions of the amount of energy transferred to the pile.

- The elastic soil-pile rebound (quake) was estimated or calculated based on a static approach.

Analyses such as CAPWAP, on the other hand, utilize dynamic measurements and, therefore, the transferred energy is known. With the appropriate pile and soil modeling, the number of unknowns is limited and the different energy losses can be accounted for indirectly through dynamic resisting forces based on viscous dampers, as previously discussed.

4.2 UNDERLYING CONCEPT

The concept of the "Energy Approach," in which basic energy relations are used in conjunction with dynamic measurements, was presented by Paikowsky (1982). Limited additional studies were carried out by Paikowsky (1984), McDonnell (1991), and Paikowsky and Chernauskas (1992). The underlying concept of this approach is the energy balance that is developed between the total energy delivered to the pile and the work done by the pile/soil system. The required "real-time" prediction in the field calls for a simplified solution and, therefore, does not consider the propagation process, while distinguishing between:

- Energy loss from elastic soil/pile deformations.
- Work done by the static resistance on plastic soil deformations.
- Energy loss due to various combined factors associated with the pile penetration (i.e., damping, radiation, inertia, etc.).

4.3 THE ENERGY EQUATION

The energy delivered to the pile is:

$$E_n = \int V(t)F(t)dt \quad (16)$$

where $V(t)$ = velocity signal at the pile top for the analyzed blow
 $F(t)$ = force signal at the pile top for the analyzed blow.

The velocity signals are obtained by measurements of acceleration, $a_{cc}(t)$, where:

$$V(t) = \int a_{cc}(t) dt \quad (17)$$

The force signals are obtained by processing the measurements of strain, $\epsilon(t)$, whereby:

$$F(t) = \epsilon(t)EA \quad (18)$$

where E = modulus of elasticity of the pile material
 A = cross-sectional area of the pile.

These measurements and calculations are immediately processed by the data acquisition system after each hammer blow.

The force/displacement relations of the pile/soil system are assumed to be elasto-plastic, which is consistent with the basic dynamic equations and static resistance of soil models in the wave equation analyses.

The total work done by such a system (elastic and plastic), therefore, will be (referring to figure 1):

$$W = R_u(S + \frac{Q}{2}) \quad (19)$$

where R_u = yield resistance
 Q = quake denoting the combined elastic deformation of the pile and soil
 S = set denoting the plastic deformation.

The quake is determined by finding the maximum displacement reduced by the plastic deformation (permanent set) under each hammer blow, such that:

$$Q = D_{max} - S \quad (20)$$

where D_{max} = maximum value of $\int V(t)dt$.

The permanent set can theoretically be determined by D_{fin} = final value of $\int V(t)dt$. However, the displacement is the second integration of the measured acceleration. Any offset in the acceleration measurement (e.g., due to DC voltage in the accelerometers) will have a relatively small effect on D_{max} , but a much greater effect on D_{fin} (for further discussion, see experimental work by Bernardes, 1989). It is more practical to use the field blow count, such that $S = Set = 1/BPI$ (blows per inch) (see figure 8).

The maximum resistance under the above assumptions is obtained from $E_n = W$, and becomes the proposed Energy Approach (uncorrected):

$$R_u = \frac{E_n}{Set + \frac{(D_{max} - Set)}{2}} \quad (21)$$

This resistance can be taken as the maximum possible resistance and can be correlated to the predicted static capacity (P_u) by a correlation factor, such that:

$$P_u = K_{sp} * R_u \quad (22)$$

where K_{sp} = "static pile" correlation factor accounting for all dynamic energy losses.

The K_{sp} factor is correlated to pile type (small vs. large displacement), soil type (mainly granular vs. cohesive), and driving resistance.

4.4 ENERGY LOSSES AND SOIL INERTIA

4.4.1 General Considerations

Soil inertia is a major factor contributing to the energy loss during driving. As such, a substantial portion of the dynamic resistance should be a function of two parameters:

- Mass/volume of the displaced soil that is a function of the pile geometry, namely, small vs. large displacement piles.
- Acceleration of the displaced soil, especially at the tip that conveniently can be examined as a function of the driving resistance.

4.4.2 Soil Displacement

The volume of the displaced soil is identical to the volume of the penetrating pile, excluding the cases in which pile plugging takes place (Paikowsky and Whitman, 1990). The piles, therefore, can be classified as small (e.g., H and open pipe) and large (e.g., closed pipe and concrete) piles. Additional classification of open-pipe piles can take place according to a tip-area ratio similar to that used for soil samplers (Paikowsky *et al.*, 1989).

As most of the soil displacement takes place at the tip area, the classification of piles can

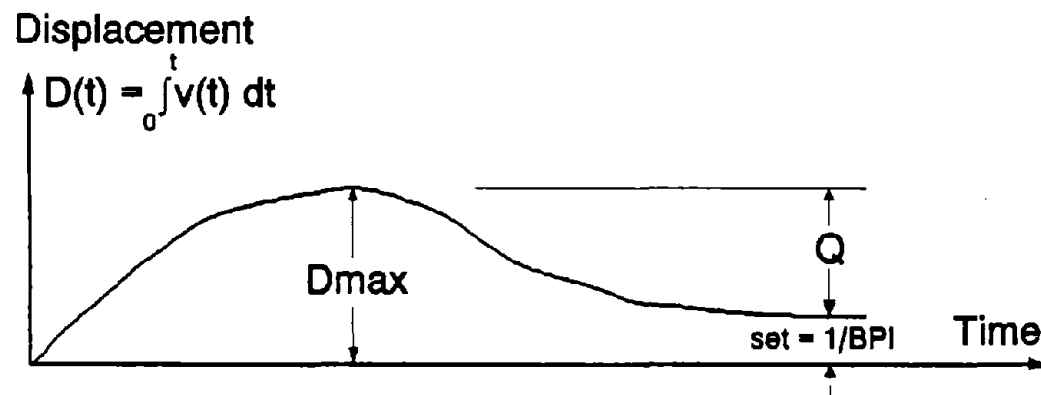
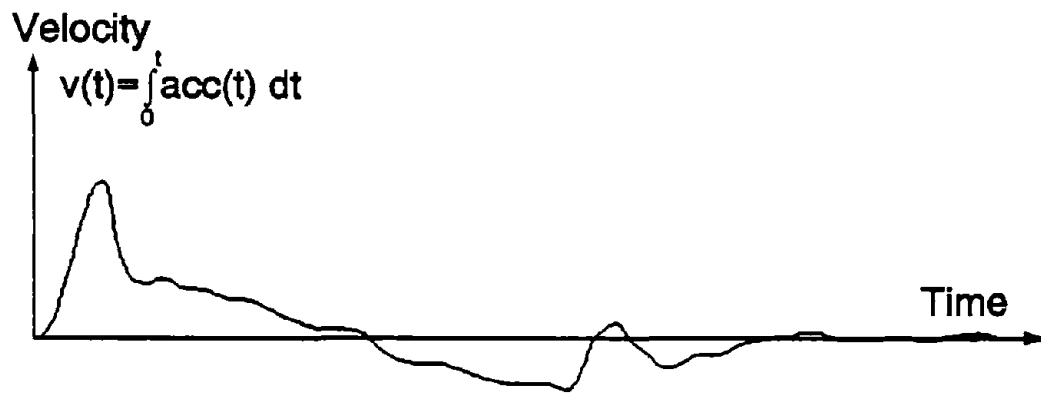
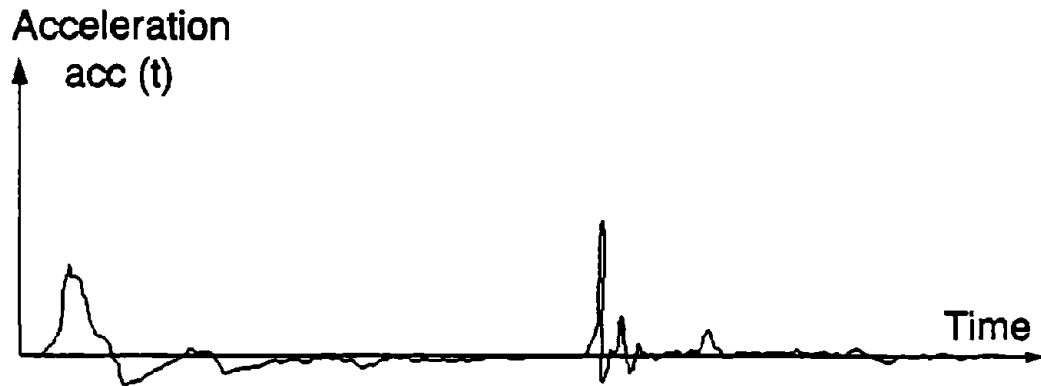


Figure 8. The proposed way of obtaining the combined quake, Q (soil and pile). [Not to scale.]

be better served by looking at the ratio between the piles embedded surface area and the area of the pile tip:

$$A_R = \frac{A_{skin}}{A_{tip}} \quad (23)$$

where A_R = pile area ratio
 A_{skin} = pile's surface area in contact with soil
 A_{tip} = area of the pile tip.

According to this ratio, a pile that is traditionally referred to as a "large displacement" pile can behave like a small displacement pile if it is driven deep enough. Because the frictional resistance of a pile increases as the pile skin area in contact with soil increases, the effect of the soil mobilized at the tip decreases. As the pile's embedded surface area and the skin friction increases, the energy losses resulting from the mobilization of the soil mass at the pile tip will decrease relative to the energy losses along the side of the pile. For example, the area ratio for cylindrical (closed-end) piles is:

$$A_R = \frac{2\pi R * D}{\pi R^2} = \frac{2D}{R} \quad (24)$$

in which D = penetration depth
 R = pile radius.

For the same pile diameter, this area ratio increases linearly with depth, e.g., a 14-in (356-mm) diameter pile will have an area ratio of 69 at the depth of 20 ft (6.1 m) and an area ratio of 360 at the depth of 105 ft (32 m). It is clear that the effect of soil inertia at the tip in the second case will be substantially smaller than that in the first case and the pile may be classified as a "small displacement pile." A quantitative boundary between "small" and "large" displacement piles on the basis of the area ratio is presented in section 8.5.

4.4.3 Soil Acceleration

The energy loss through the work performed by the inertia forces at the displacement of the soil mass at the tip is directly related to the acceleration of this mass. The direct evaluation of these accelerations are beyond the scope of the present research. The indirect evaluation of these accelerations can be performed through the driving resistance, which is the measure of the pile's displacement under each hammer blow. With low driving resistance there is high velocity (i.e., free-end analogy) and high acceleration at the pile tip, hence, high inertia of the tip soil mass. This results in a soil inertia "force" that, when multiplied by the pile displacement at the tip, produces a large loss of energy. In the case of high driving resistance (hard driving), there is little, if any, mobilization of the tip soil mass and the acceleration at the tip is very low. Therefore,

the corresponding energy loss is small.

4.4.4 Expected Performance

In summation, according to the above hypothesis, the largest loss of "unknown" energy occurs when large displacement piles experience easy driving (large tip displacement). The smallest loss of "unknown" energy occurs with small displacement piles driven under high blow counts (hard driving).

Considering the preceding criteria, the Energy Approach should theoretically produce two distinct trends:

- In the case of high "unknown" energy losses, i.e., in easy driving of piles with small area ratios, the Energy Approach predictions should yield a tendency of over-prediction. Hence, R_u is expected to be higher than the actual resistance as the large energy losses were not considered. As a result, K_{sp} is expected to be smaller than unity ($K_{sp} < 1.0$).
- In the case of small "unknown" energy losses, i.e., hard driving of piles with large area ratios, the Energy Approach predictions should yield a tendency of under-prediction. Hence, R_u is expected to be smaller than the actual resistance as there are only small energy losses and the full capacity may not have been developed. As a result, K_{sp} is expected to be higher than unity ($K_{sp} > 1.0$).

CHAPTER 5 - DATA BASE BUILDUP

5.1 GENERAL

In order to examine the dynamic analyses and calibrate the Energy Approach method, extensive case study data was assembled. The information was divided into two major categories describing two data sets: set PD/LT and set PD. Data set PD/LT contains data for piles on which dynamic measurements, office analyses (CAPWAP or TEPWAP), and a static load test to failure have been conducted. Data set PD contains data for piles that were monitored by dynamic measurements during driving, followed by office analyses and occasionally a static proof test (not to failure). Section 1.3 outlines the source and/or reference of the obtained data. The following chapter describes the procedures used for analyzing the case studies comprising the data sets.

5.2 DATA SET PD/LT

The piles of data set PD/LT were analyzed in two stages: a static load test analysis followed by a dynamic measurements analysis. The static load test analysis was intended to produce a representative static resistance (denoted by R_s) for each pile, using several load test interpretation methods. The dynamic measurements analyses involved several different methods, including the application of computer programs specifically developed for the analysis of dynamic measurements taken during driving.

5.2.1 Static Load Test Analysis

A universal criterion capable of establishing the ultimate capacity of a pile is essential in improving the accuracy of static load test interpretations. Various ultimate load criteria have been proposed and used by researchers and design organizations (see, for example, Vesic, 1977 and Fellenius, 1989). Significant disagreements remain among these methods as they are based on different principles and produce different values under varying pile types and sizes, load test procedures, and surrounding soils.

Vesic (1972) pointed out that interpreting a pile's ultimate load based solely on a visual examination of its load-settlement curve (i.e., shape of the curve) may be misleading and can result in different pile capacities depending on the scale used to plot the curve. Figures 9 and 10 demonstrate this point by presenting the same load-settlement relations using two different scales. Figure 9 shows a load-settlement curve indicating a pile capacity of approximately 140 kips (623 kN) whereas the curve in figure 10 suggests that the pile's displacement at 140 kips (623 kN) may still be based on the elastic compression of the pile and that the pile capacity is approximately 170 kips (756 kN).

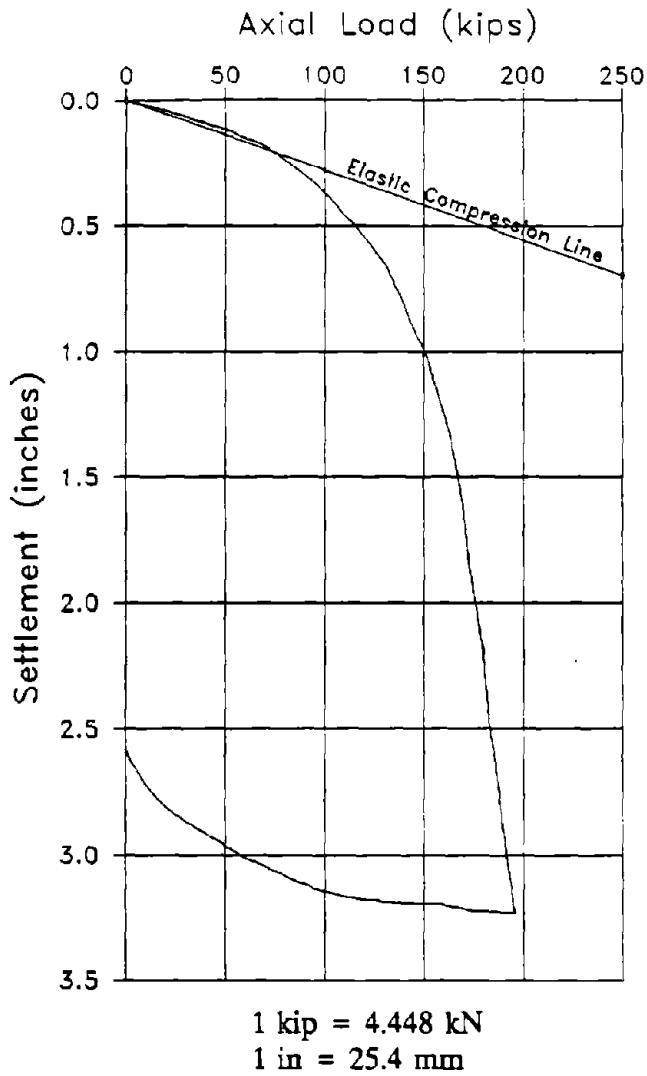


Figure 9. Load-settlement curve of pile-case 95 with the elastic compression line inclined at 20 degrees.

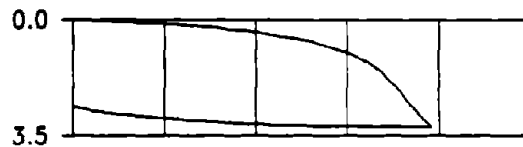


Figure 10. Load-settlement curve of pile-case 95 with a scale that does not consider the elastic compression of the pile (following Vesic, 1977).

One solution to this problem is to implement a common scale, based on the pile's elastic deformation. When plotting load-settlement curves, the elastic deformation of a fixed end, frictionless pile is expressed as:

$$\delta = \frac{PL}{EA} \quad (25)$$

where δ = calculated elastic deformation of the pile
 P = applied load
 L = pile length
 E = elastic modulus of the pile material
 A = cross-sectional area of the pile.

The elastic compression line obtained by equation 25 is based on the assumption that all of the load applied to the pile top is transferred to the pile toe. To implement a scale proportional to all load settlement curves, the elastic compression line should be inclined at an angle of about 20 degrees to the load axis (see figure 11).

In order to facilitate this scale, all of the load-settlement curves in set PD/LT were digitized using the program DIGITIZE, developed at University of Massachusetts-Lowell by Chernauskas and Paikowsky. These curves were then replotted, using the graphics software GRAPHER, to produce curves that were proportional to each pile's elastic compression line inclined at 20 degrees.

After replotting, each load-settlement curve was analyzed using five different failure load interpretation procedures: Davisson's Criteria, the Shape of Curve method, Limited Total Settlement methods ($\Delta = 1$ in [25.4 mm] and $\Delta = 0.1B$), and DeBeer's method.

(a) **Davisson's Criteria** (Davisson, 1972), or offset limit, defines the failure load of a pile as the load corresponding to the settlement that exceeds the elastic compression of the pile (δ) by an offset (X) equal to 0.15 in (3.8 mm) plus a factor equal to the diameter of the pile divided by 120. The offset is simply:

$$X = 0.15 + \frac{B}{120} \quad (26)$$

where B = diameter of the pile in inches.

The Davisson's Criteria line is parallel to the elastic compression line and predicts the failure load at its intersection with the load-settlement curve. Figure 11 illustrates the use of Davisson's failure criteria for load-settlement relations of pile-case 50, yielding a capacity of 817 kips (3634 kN).

(b) **The Shape-of-Curve Method** is a failure load approximation that usually yields a

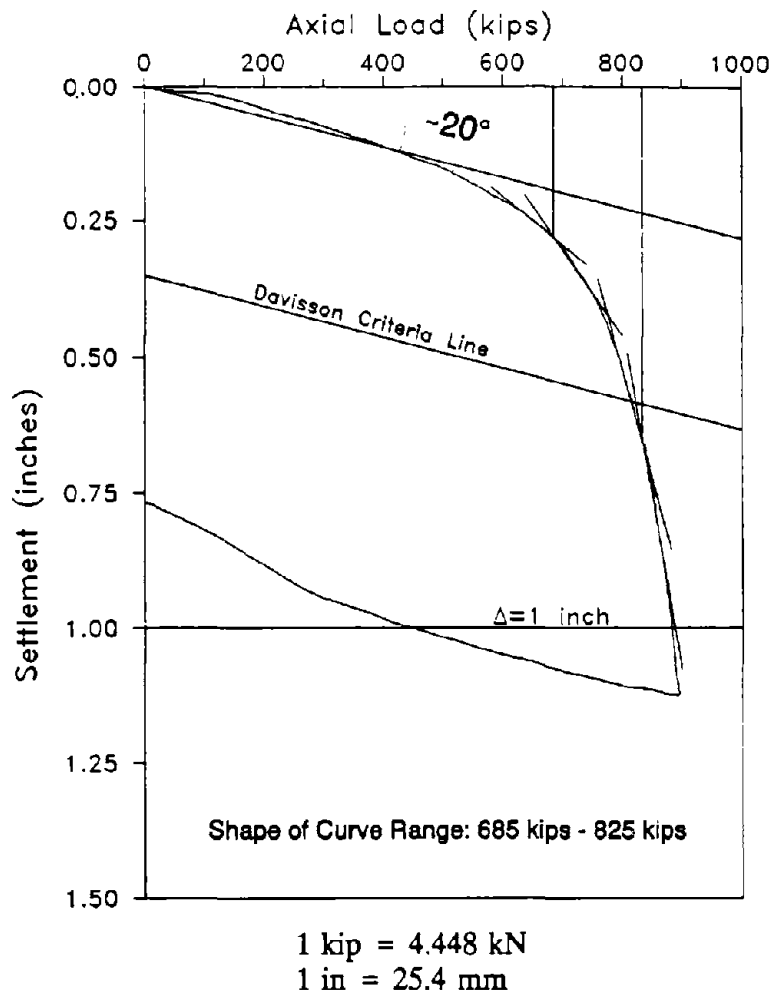


Figure 11. Load-settlement curve for pile-case 50 with the elastic compression line inclined at approximately 20 degrees.

range of values over which the pile is considered at or near failure. The boundaries of this range can be determined by examining the minimum curvature in the load-settlement curve through lines drawn tangent to the load-settlement curve (similar to the method proposed by Butler and Hoy (1977)). The failure range is relatively easy to define for load-settlement curves that exhibit general failure or plunging failure (rapid settlement with slightly increased loads) (see figure 11 for example). Piles that experience local failure, or non-plunging failure, are difficult to analyze using the shape-of-curve method because of the uniform changes in slope of lines drawn tangent to the curve. Figure 11 illustrates the use of the shape-of-curve procedure, yielding an

estimated capacity range of between 685 kips and 825 kips (3047 kN and 3670 kN) with a representative average of 755 kips (3358 kN).

(c) **The Limited Total Settlement Methods**, $\Delta = 1$ in (25.4 mm) and $\Delta = 0.1B$ (Terzaghi, 1942), define the failure load as the load corresponding to settlements of 1 in and 0.1B, respectively, where B is the diameter of the pile. These methods are not applicable in many cases. For example, the elastic compression for a very long steel pile often exceeds 1 in (25.4 mm) and/or 0.1B without inducing any plastic deformation in the soil. Figure 11 shows as an example, a load-settlement curve for pile-case 50, a 24-in (610-mm) square concrete pile that experiences a plunging failure well before a displacement of 1 in (25.4 mm). Also, it is obvious that a settlement of 0.1B, or 2.4 in (61 mm) in this case, does not represent the failure load of this pile and, therefore, is not applicable.

(d) **DeBeer's log-log Method** (DeBeer, 1970) defines the failure load as the load corresponding to the intersection of two distinct slopes created by the load-settlement data plotted using logarithmic scales. Figure 12 illustrates the use of DeBeer's criteria for the load-settlement curve of pile-case 50, leading to an estimated capacity of 748 kips (3327 kN). The two slopes are especially visible for piles that experience plunging failures, yet when using DeBeer's method piles that undergo local failures, the result may be a range of values. As mentioned earlier, each load-settlement curve was digitized from the standard linear plots that they were presented on and the data was stored. This data was later plotted in logarithmic scales to utilize DeBeer's method.

(e) **The Representative Static Capacity:** The capacity results for each method were reviewed independently, based on the load-settlement curves for each pile. After considering the pile type, soil type, size of each pile, and the load test procedure, unrealistic results were eliminated, and the acceptable values were averaged, yielding a final static capacity (R_s). For example, for pile-case 50, presented in figures 11 and 12, the considered criteria were: Davisson's = 817 kips (3634 kN), shape of curve = 685-825 kips (3047-3670 kN), 1.0-in settlement = 887 kips (3945 kN), 0.1B settlement = NA, and DeBeer's = 748 kips (3327 kN). Excluding the 0.1B settlement method, which is not applicable, and 1.0-in (25.4 mm) settlement, which is clearly beyond the failure, the average of all the criteria led to a final static resistance assessment of $R_s = 773$ kips (3438 kN).

5.2.2 Dynamic Measurements Analysis

The analyses performed on piles in data set PD/LT employed office analysis (i.e., CAPWAP or TEPWAP) as well as several computer programs developed to process and manage force and velocity signals, including DIGITIZE, PDAP, INTEGRATE, and FILECHNG.

The dynamic analyses were performed in different ways depending on the completeness of each pile case. In all cases, the pile geometry (i.e., type, material, length of

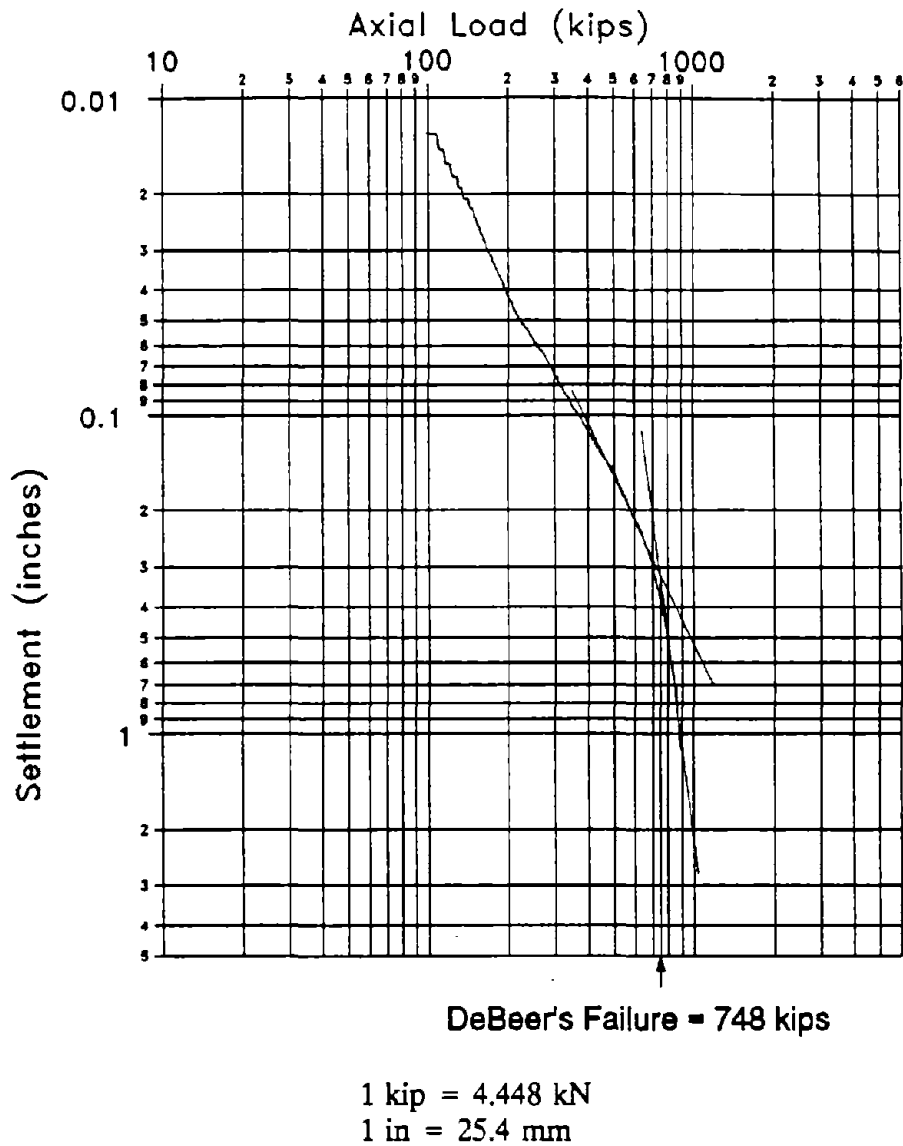


Figure 12. Load-settlement data plotted on a logarithmic graph for pile-case 50 to determine the failure load according to DeBeer's method.

penetration, the soil at the pile's tip and side, and the blow count) was known before any type of analysis was initiated. The individual cases were divided into three distinct groups:

- (a) Group 1 — pile cases with complete CAPWAP summaries, including E_{max} , D_{max} , F1, and V1.

(b) Group 2 — pile cases with incomplete CAPWAP summaries, such as those missing E_{max} , D_{max} , $F1$, and/or $V1$.

(c) Group 3 — pile cases that were analyzed using TEPWAP.

(a) GROUP 1 - Complete CAPWAP Analyses

Pile group 1 contains the complete cases available in data set PD/LT. The most common adjustment necessary for the pile cases in this group was a ratio correction between the force at impact ($F1$) and the velocity at impact ($V1$). Theoretically, the force and velocity multiplied by the pile impedance are identical under a passing disturbance, as long as no other external forces act. The ratio between these values is:

$$\frac{V1 \left(\frac{EA}{C} \right)}{F1} \quad (27)$$

where E = modulus of elasticity of the pile material
 A = cross-sectional area of the pile
 C = wave speed of the pile

and should be equal to unity. An acceptable ratio was considered to be 1.0 ± 0.1 . Beyond this ratio, a linear multiplier was applied to either or both parameters (force, velocity, or both) and to their byproducts, e.g., displacement and energy. The ratio between force and velocity may also be influenced by the precompression of a diesel hammer and hammer misalignment.

Precompression in a diesel hammer occurs as the air-fuel mixture is compressed by the ram just prior to combustion. This results in a force that is applied to the pile top. However, as the force is applied relatively slowly and before the actual impact between the ram and the pile top, there is not a corresponding velocity wave. This scenario results in a discrepancy between the impact force ($F1$) and the impact velocity ($V1(EA/C)$), as shown in figure 13. The force and velocity traces of pile-case 1, driven with a Delmag 30 diesel hammer, are shown in figure 13. The observed relations indicate the need for a force reduction (Δ_{total}), which is equal to the difference between Δ_{pk} and Δ_{ps} . Prior to a correction, the ratio ($V1(EA/C)/F1$) for pile-case 1 was 0.874. The factor (Δ_{total}) represents the number of units by which the force must be reduced in order to produce an acceptable ratio according to equation 28. The magnitude of Δ_{total} and the reduction of $F1$ are performed as follows:

$$\Delta_{total} = \Delta_{pk} - \Delta_{ps} = 2 \text{ units} = \frac{2 \text{ units}}{38.5 \text{ units}} \times 250 \text{ kips} = 13 \text{ kips (58 kN)} \quad (28)$$

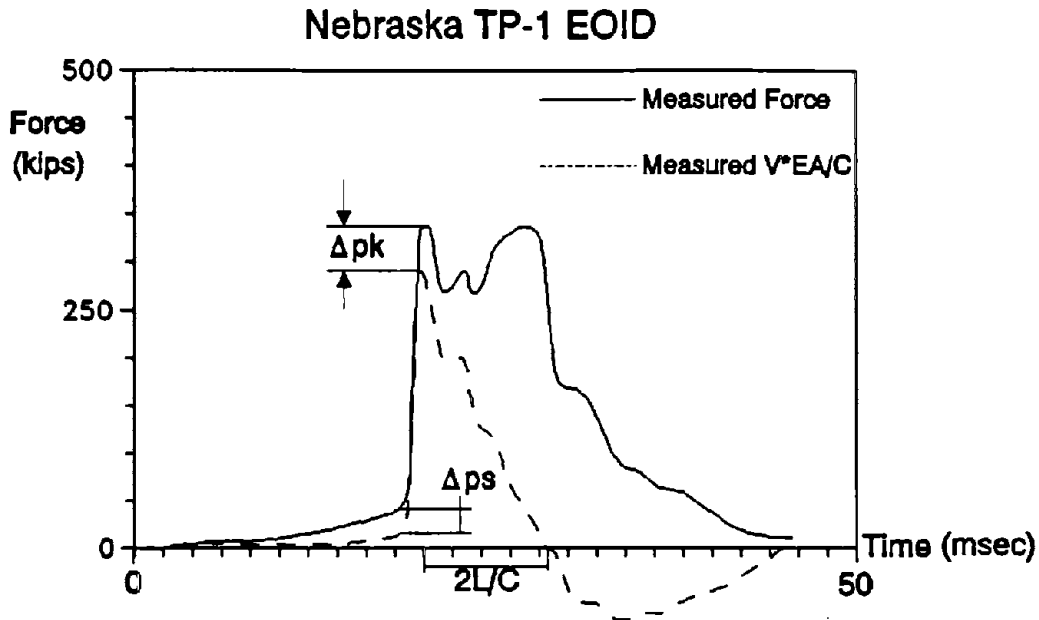


Figure 13. Force and velocity ($V \cdot EA/C$) traces of pile-case 1, a steel HP12x74 that needed a force correction (not to scale).

$$F1 = F1_{\text{uncorrected}} - \Delta_{\text{total}} = 335.4 \text{ kips} - 13 \text{ kips} = F1_{\text{corrected}} = 322.4 \text{ kips} \quad (1434 \text{ kN}) \quad (29)$$

The corrected F1 yields a new $V1(EA/C)/F1$ ratio, an adjusted E_{max} , and a corresponding uncorrected Energy Approach prediction (R_u) as follows:

$$\frac{V1\left(\frac{EA}{C}\right)}{F1_{\text{corrected}}} = 0.909 \quad (30)$$

$$E_{\text{max}} = 18 \text{ kip-ft} \times \frac{322.4 \text{ kips}}{335.4 \text{ kips}} = 17.3 \text{ kip-ft} \Rightarrow R_u = 362 \text{ kips} \quad (1610 \text{ kN}) \quad (31)$$

The procedure for correcting F1 is also performed in a similar manner for adjusting V1 and the corresponding D_{max} , where $D_{\text{max}} = \int V(t) dt$. This is sometimes necessary when

either there is a significant hammer-pile misalignment that creates disturbance in the force and velocity measurements or there is a discrepancy in the measurement itself. The correction procedure for decreasing $V1(EA/C)$ also uses the factor Δ_{total} as determined by the discrepancy in the $F1$ and $V1(EA/C)$ measurements where Δ_{total} is converted to units of force. Similarly, $V1(EA/C)$ is decreased by:

$$V1\left(\frac{EA}{C}\right)_{corrected} = V1\left(\frac{EA}{C}\right)_{uncorrected} - \Delta_{total} \quad (32)$$

producing a corrected ratio:

$$\frac{\left(V1\frac{EA}{C}\right)_{corrected}}{F1} \quad (33)$$

and an adjusted D_{max} :

$$D_{max\ corrected} = \int V1_{corrected} dt \quad (34)$$

The corresponding uncorrected Energy Approach prediction is calculated using the adjusted D_{max} as follows:

$$Ru = \frac{E_{max}}{Set + \frac{D_{max\ corrected} - Set}{2}} \quad (35)$$

(see chapter 4 for Energy Approach details). It should be noted that it is sometimes necessary to correct both the force and the velocity measurements given the proper circumstances. In general, very few pile-cases required correction, the majority of which needed very small adjustments. These corrections usually had an insignificant effect on the obtained J_c and Ru values.

After the static load test analysis and the dynamic analysis were completed, the Case damping coefficient (J_c) was back-calculated using equation 6 as outlined by Goble *et al.* (1980).

(b) GROUP 2 - Incomplete CAPWAP Analyses

The pile cases categorized in group 2 include piles from data set PD/LT that were analyzed via CAPWAP. Difficulties associated with retrieving and accumulating complete pile data cause pile cases to require more analysis in order to produce missing information essential for the study. Typical information missing from pile cases included E_{max} (the maximum energy delivered to the pile top) and D_{max} (the maximum displacement of the pile top). A typical pile case in group 2 includes a static load test plot, subsurface site information, blow count records, and CAPWAP predictions at EOD,

BOR, and/or EOR, excluding the CAPWAP summary tables. The CAPWAP summary tables include pile characteristics, Case method predictions and crucial dynamic measurements (V_{max} , V_{fin} , $V1*Z$, $F1$, F_{max} , D_{max} , D_{fin} , E_{max} , and E_{fin}). In order to determine these missing dynamic parameters, a program was developed at UMASS-Lowell called INTEGRATE (written by L. Chernauskas). This program was specifically developed to calculate the uncorrected Energy Approach and the Case method similar to a more extensive and versatile program called PDAP (Pile Driving Analysis Program), which was developed by Paikowsky (1984). The program PDAP uses recorded field data from the PDA, enables it's manipulation and correction, and produces an Energy Approach prediction and a range of Case method predictions based on all the different variations for different J_c values.

INTEGRATE processes digitized force and velocity ($V*EA/C$) traces (see figure 14 for example) and, using the pile parameters as given by the user, produces the dynamic measurements listed above. INTEGRATE also calculates the uncorrected Energy Approach prediction and back-calculates the Case damping coefficient (J_c) using the following relationship:

$$J_c = \frac{RTL - FINAL R_s}{V1 * \frac{EA}{C} - F1 - RTL} \quad (36)$$

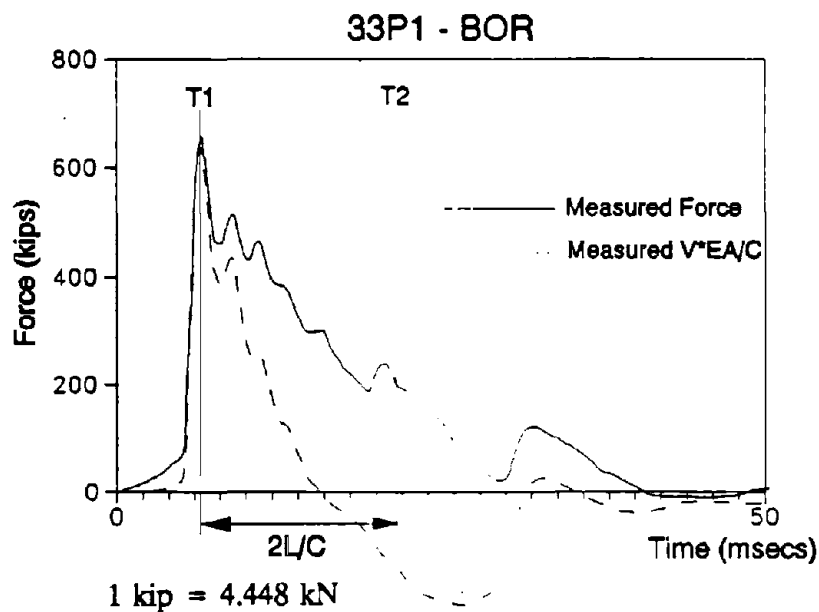


Figure 14. Digitized force and velocity multiplied by the impedance (EA/C) traces for pile-case 192 used for input into INTEGRATE.

**UMASS-LOWELL GEOTECHNICAL ENGINEERING
DYNAMIC PILE TESTING**

SUMMARY OF INPUT PARAMETERS

FILE.....	33P1BOR
PILE LOCATION.....	SITE 33
DATE OF ANALYSIS.....	2-10-92
PILE DESIGNATION.....	33P1-BOR
PILE TYPE.....	HP12x74
HAMMER TYPE.....	B-400
NOMINAL ENERGY OF HAMMER (ft-kips).....	46
PENETRATION DEPTH (ft).....	114.4
2L/C (msecs).....	14.39
TIME INTERVAL (msecs).....	.1
PILE IMPEDANCE - EA/C (kip/sec/ft).....	38.9
FINAL BLOW COUNT (bl/in).....	16
T2 (offset from T1) (msecs).....	14.39

SUMMARY OF OUTPUT PARAMETERS

DMAX.....	0.787
DFIN.....	0.164
HAMMER EFFICIENCY (%).....	69.14
EMAX (kip-ft).....	31.80
EFIN (kip-ft).....	25.55
VMAX (ft/sec).....	15.78
VFIN (ft/sec).....	0.420
FMAX (kips).....	637.38
FFIN (kips).....	42.02
J.....	-0.017
F1 (kips).....	637.38
F2 (kips).....	192.10
V1 (ft/sec).....	15.78
V2 (ft/sec).....	-3.59
(V1*EA/C)/F1.....	0.963

PILE CAPACITY (kips)

DAVISSON'S CRITERIA.....	800
SHAPE OF CURVE.....	800
$\Delta = .1B$	598
$\Delta = 1$ inch.....	522
DEBEERS LOG METHOD.....	800
FINAL R_s	800
CASE RTL.....	792
CAPWAP.....	715
ENERGY APPROACH R_u (uncorrected).....	898

Figure 15. INTEGRATE output of pile-case 192 showing the back-calculated Case J_c value and the Energy Approach prediction.

(Goble *et al.*, 1980). The static load test results are denoted FINAL R_s , and must be supplied by the user. An example of the results of an INTEGRATE analysis of the force and velocity traces shown in figure 14 for pile-case 192 (33P1BOR) is shown in figure 15. After reviewing the force and velocity (EA/C) traces for a given pile case and the $(V1 \cdot EA/C)/F1$ ratio, calculated by INTEGRATE, any necessary corrections and corresponding adjustments to E_{max} and D_{max} can be made, as outlined in section 5.5.2(a); and the uncorrected Energy Approach calculations can be performed.

(c) GROUP 3 - TEPWAP Analyses

Several pile cases in data set PD/LT were lacking the CAPWAP office analysis and, therefore, required wave match analysis to be performed. These pile cases were categorized in group 3 and all of them were analyzed using a computer program called TEPWAP. TEPWAP (Paikowsky, 1982; Paikowsky and Whitman, 1990; and Chernauskas, 1993) utilizes a procedure somewhat similar to the CAPWAP analysis described by Goble *et al.* (1970). This program allows the input of the measured velocity at the pile top as a function of time, solving for a set of parameters describing the soil resistance (dynamic and static) along the pile (see section 3.3.3). Adjustments of the matches are made until the calculated force at the top matches that measured. A good agreement between CAPWAP and TEPWAP analyses was presented by Paikowsky (1982) and further confirmed by Chernauskas (1993).

The pile cases in group 3 were initially analyzed in the same manner as those in group 2, whereby their force and velocity traces were digitized with respect to time using the program DIGITIZE and processed using INTEGRATE. After these steps were successfully completed, three data files were created for each case: an input file, an identification file, and a pile/soil file. An input file for TEPWAP is created using the program DIGPWAPE that processes digitized force and velocity traces and prepares them in the same manner as the PDA. Figures 16 and 17 show the identification file and the pile/soil file for pile-case 191, respectively. These files, along with the digitized force and velocity traces (see figure 18 for example), are necessary for TEPWAP analyses. Iterations are performed, where the user is required to adjust the soil properties (i.e., side and tip damping and quake, and side and tip resistance) until an acceptable force wave match is made. Figure 19 presents the comparison between the calculated force at the top (obtained from the above procedure) to the measured force at the top of pile-case 191.

This particular pile case appears to be exhibiting pile plugging near the tip as indicated by the sudden observed force "jump" near $2L/C$ and again near $4L/C$. Pile plugging is most commonly associated with open-pipe piles or H-piles. It usually refers to the phenomenon that occurs when soil enters the open-pipe pile during driving until the inner-soil cylinder develops sufficient resistance to prevent further soil intrusion (see Paikowsky *et al.*, 1989; Paikowsky and Whitman, 1990). The development of friction along the web of an H-pile can also develop enough resistance to prevent soil intrusion, causing the H-pile to become "plugged." When an H-pile becomes plugged, it then

 UNIVERSITY OF MASSACHUSETTS - LOWELL
 GEOTECHNICAL ENGINEERING
 TEPWAP ANALYSIS

=====
 IDENTIFICATION DATA
 =====

JOB NUMBER.....	TP1EOD
JOB NAME.....	33_P
DATE OF DRIVING.....	10-28-77
PILE DESIGNATION.....	H
TYPE OF PILE.....	HP 12x74
PILE LENGTH (ft.).....	121
TYPE OF HAMMER.....	B-400
NOMINAL ENERGY OF HAMMER (kips*ft).....	46
DEPTH OF PENETRATION (ft.).....	114.4
ELEMENT LENGTH (ft.).....	5.26
DAMPING MODEL.....	SMITH
NUMBER OF BLOWS PER LAST THREE INCHES.....	13, 13, 12
DATE OF ANALYSIS.....	9-16-92
PDA BLOW #.....	2
ITERATION #.....	1
TIME INTERVAL.....	0.200
OPTION NUMBER.....	2

=====
 Figure 16. Example of the pile identification information of pile-case 191 used as input for the TEPWAP analysis.

UNIVERSITY OF MASSACHUSETTS - LOWELL
GEOTECHNICAL ENGINEERING
TEPWAP ANALYSIS

=====

SOIL AND PILE PROPERTIES ALONG PILE ELEMENTS

=====

element no.	dist from gauges (ft)	area (sq.in)	weight (lbs.)	stiffn (k/in)	resist (kips)	sum of resist (kips)	damp (s/ft)	quake (in.)	quake rebind ratio (%)	upward resist ratio (%)
3	5.3	21.8	390.1	10364	0.0	439.0	.000	0.000	0.0	0.0
4	10.5	21.8	390.1	10364	5.0	434.0	.020	0.300	100.0	-50.0
5	15.8	21.8	390.1	10364	5.0	429.0	.020	0.300	100.0	-50.0
6	21.0	21.8	390.1	10364	5.0	424.0	.020	0.300	100.0	-50.0
7	26.3	21.8	390.1	10364	5.0	419.0	.020	0.300	100.0	-50.0
8	31.6	21.8	390.1	10364	5.0	414.0	.020	0.300	100.0	-50.0
9	36.8	21.8	390.1	10364	0.0	414.0	.010	0.300	100.0	-50.0
10	42.1	21.8	390.1	10364	0.0	414.0	.010	0.300	100.0	-50.0
11	47.3	21.8	390.1	10364	0.0	414.0	.010	0.300	100.0	-50.0
12	52.6	21.8	390.1	10364	0.0	414.0	.010	0.300	100.0	-50.0
13	57.9	21.8	390.1	10364	0.0	414.0	.010	0.300	100.0	-50.0
14	63.1	21.8	390.1	10364	5.0	409.0	.010	0.300	100.0	-50.0
15	68.4	21.8	390.1	10364	5.0	404.0	.010	0.300	100.0	-50.0
16	73.6	21.8	390.1	10364	8.0	396.0	.010	0.300	100.0	-50.0
17	78.9	21.8	390.1	10364	8.0	388.0	.010	0.300	100.0	-50.0
18	84.2	21.8	390.1	10364	8.0	380.0	.010	0.300	100.0	-50.0
19	89.4	21.8	390.1	10364	8.0	372.0	.010	0.300	100.0	-50.0
20	94.7	21.8	390.1	10364	8.0	364.0	.010	0.300	100.0	-50.0
21	99.9	21.8	390.1	10364	8.0	356.0	.010	0.300	100.0	-50.0
22	105.2	21.8	390.1	10364	8.0	348.0	.010	0.300	100.0	-50.0
23	110.5	21.8	390.1	10364	8.0	340.0	.010	0.300	100.0	-50.0
24	115.7	21.8	390.1	10364	80.0	280.0	.090	0.150	100.0	-50.0
25	121.0	21.8	390.1	0	100.0	160.0	.080	0.150	100.0	-50.0
tip					160.0	0.0	.080	0.150	100.0	

Figure 17. Example of the soil and pile properties used along the pile elements of pile-case 191 as input for the TEPWAP analysis.

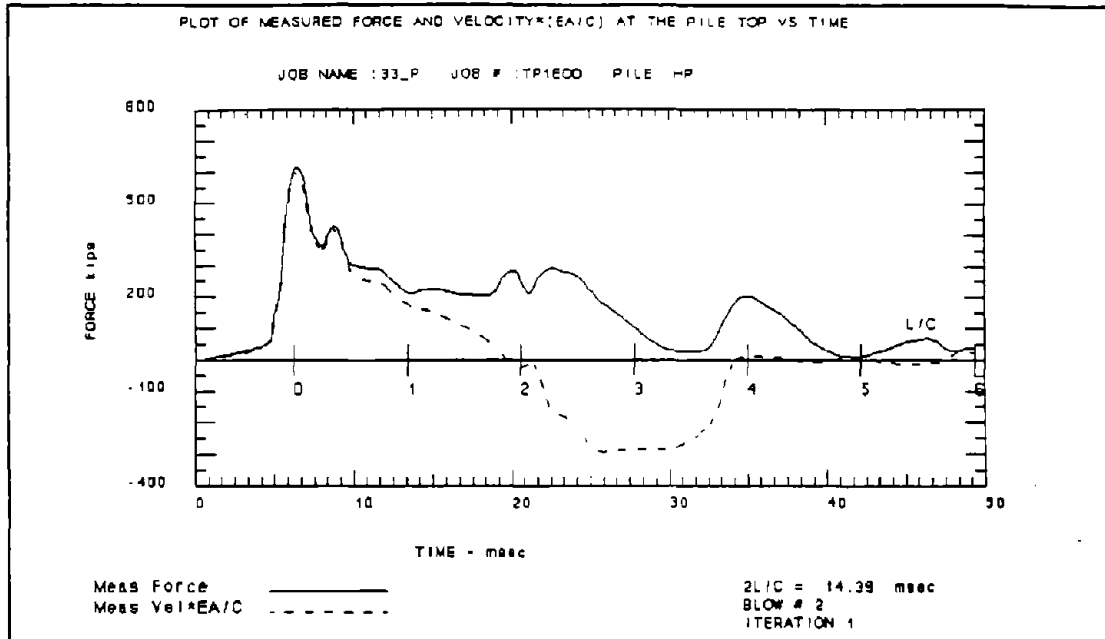


Figure 18. Measured force and velocity multiplied by the impedance (EA/C) traces of pile-case 191 used by the TEPWAP analysis.

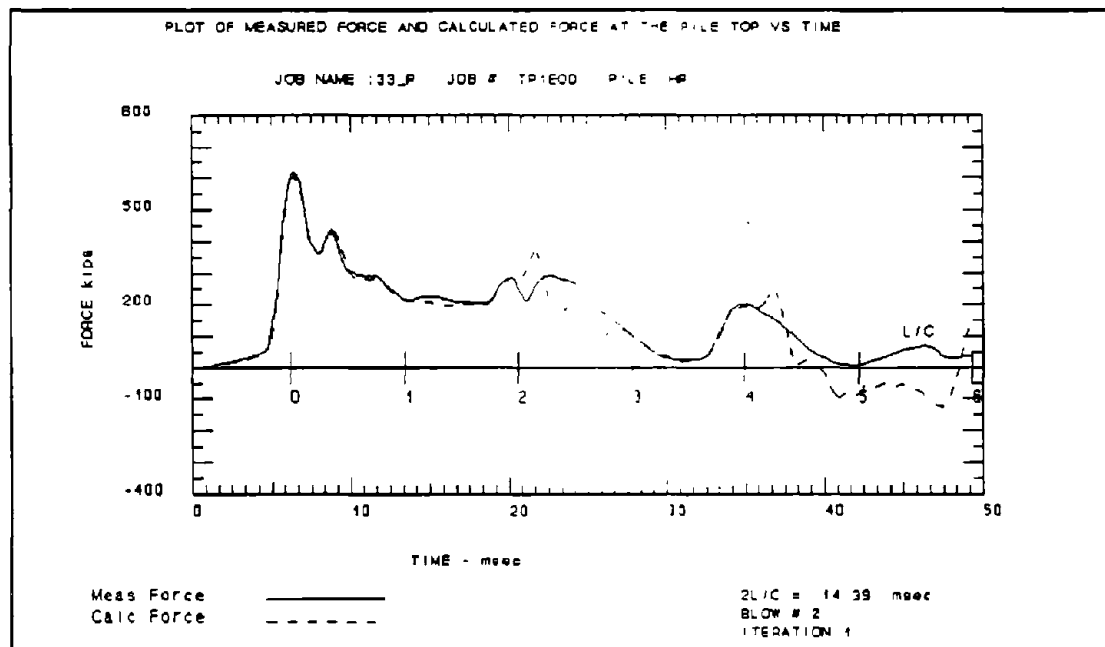


Figure 19. Comparison between measured force near the top of pile-case 191 and the calculated force from TEPWAP analysis.

**UNIVERSITY OF MASSACHUSETTS - LOWELL
 GEOTECHNICAL ENGINEERING
 TEPWAP ANALYSIS**

=====

SUMMARY OF FINAL RESULTS

=====

END RESISTANCE - 160.0 kips
 SIDE FRICTION - 279.0 kips
 TOTAL CAPACITY - 439.0 kips

PERCENT IN FRICTION - 63.6%

TOP QUAKE - 0.79 inches
 SET AT TIP - 0.32 inches

THE SET CORRESPONDS TO 3 Blows Per Inch.

MAXIMUM CALCULATED ENERGY - 32.362 kip*ft
 MAXIMUM MEASURED ENERGY - 32.674 kip*ft

ENERGY DIFFERENCE (CALC - MEAS) - -0.312 kip*ft

MAXIMUM COMPRESSION FORCE IS - 636.49 kips
 IN ELEMENT #3 ON ITERATION 32

MAXIMUM TENSION FORCE IS - -139.18 kips
 IN ELEMENT #19 ON ITERATION 181

THE MAXIMUM STRESS IS - 29.20 kips/sq in.
 THE MINIMUM STRESS IS - -6.38 kips/sq in.

=====

Figure 20. Summary of the final results from TEPWAP analysis performed on pile-case 191.

assumes the penetration characteristics of a large displacement pile (i.e., with a closed rectangular tip). Pile plugging is shown to have the following marked effects: significant contribution to the capacity of piles driven in sand; delay in capacity gain with time for piles driven in clay; and changes in the behavior of piles during installation, causing it to differ from that described by the models commonly used to predict and analyze pile driving (Paikowsky and Whitman, 1990). Further investigation into pile-case 191 shows that the H-pile is embedded over 114 ft (35 m) into silty sand. These conditions are ideal for pile plugging to occur and, therefore, plugging can be attributed to the force match disagreement at $2L/C$ and again at $4L/C$ by TEPWAP as shown in figure 14.

The final summary of results from TEPWAP analyses are produced for each case (see figure 20 for example). These summaries allow the user to investigate the compressive and tensile stresses developed in the pile during driving (e.g., concrete piles) as well as the side and tip resistance and the measured and calculated energy delivered to the pile.

All of the pile cases that were analyzed using TEPWAP are footnoted in the data set tables in chapter 6. The Case damping coefficients for these cases were calculated as part of the INTEGRATE output as previously stated.

5.3 DATA SET PD

Data set PD contains information related to 403 piles; the vast majority were sorted from information related to 428 piles provided by Pile Dynamics, Inc. of Cleveland, Ohio, as part of their support of the Energy Approach method research. Large portions of the PD data set analysis were performed by McDonnell (1991). The data set contains the following information:

- Pile identification, which also refers to the time of measurement, e.g., end of driving (EOD) or beginning of restrike (BOR).
- Soil type on the side and at the tip of the piles.
- Pile type, geometry, material, and modulus of elasticity.
- Hammer type and blow count.
- Resistance obtained by CAPWAP analysis.
- All parameters pertinent to the CAPWAP analysis, e.g., damping factors and quake values.
- Maximum energy, force, velocity, and displacement of the analyzed blow.

- Resistance obtained from different Case method evaluations.

The data set is subgrouped according to pile and soil types, as shown in table 3.

Table 3. Subgrouping of the piles in data set PD (indicating the number of piles in each group).

Pile Type/Soil Type	Sand and Silt	Clay and Till	Rock	N/A*	Total
Small Displacement	26	21	29	-	76
Large Displacement	92	50	78	22	242
Miscellaneous#	40	21	19	5	85
Total	158	92	126	27	403
* - Soil type not available. # - Miscellaneous piles include timber, monotube, pipe with H beams, etc.					

The large size of data set PD provides an excellent basis for the examination of any possible parameter relations. The complete summarized data set is presented in table 24. Correlations between the Energy Approach vs. CAPWAP predictions for the various pile/soil combinations shown in table 3 are presented in chapter 9. The total number of correlations is 15 (see table 3 for number of cases in each category).

CHAPTER 6 - DATA SET PD/LT

6.1 GENERAL

This chapter summarizes the pile cases in data set PD/LT. Four tables are used to group the information into four categories (see appendix A). The groups are as follows: site and pile information (table 20), pile driving and dynamic measurements (table 21), parameters of dynamic analyses (table 22), and pile capacity based on static load test results and dynamic analyses (table 23). The following sections discuss the breakdown of these tables and provide:

- Details of where the information was gathered for each column.
- Methods used to produce the information.
- Definitions of any symbolism used.

For a list of references and contributors to data set PD/LT, see section 1.3.

6.2 SITE AND PILE INFORMATION - TABLE 20

(a) Columns 1-4

The first four columns of table 20 list the case number for each case in data set PD/LT (208 total), the pile-case number, the site reference number, and the site location, respectively. A number is assigned to each pile-case in column 1 for all four tables to provide easier transition from one table to another. The next column lists the pile-case number that corresponds to the pile number as labeled in individual site plans and reports. Included in the pile-case numbers are extensions that designate the time of driving when measurements were taken (e.g., EOD=end of driving, BOR=beginning of restrike, EOR=end of restrike, DD=during driving, and BORL=BOR after load test). A reference number is assigned to each pile-case depending on which project the particular pile was driven and the location column lists the general area where the driving site is located (e.g., county, state, province, or country).

(b) Columns 5-8

The next four columns of table 20 provide pile information, including the pile geometry and the depth to which the pile was driven at the time of analysis. Column 5 briefly lists the pile type according to its material and its cross-sectional dimensions. For example, the notation HP, CEP or CP, and OEP represent a steel H-pile, a steel closed-end pipe pile, and a steel open-end pipe pile, respectively, whereas PSC, VC, and RC represent a pre-stressed concrete pile, voided concrete pile, and simply reinforced-concrete pile. Any

timber piles listed refer to those that were treated prior to driving. Following the pile type notations are the dimensions of the pile. For the closed-end and open-end pipe piles, the wall thickness dimensions can be back-calculated from the piles cross-sectional area listed in column 6. Typically, the pile length below gauges and its penetration depth, shown in columns 7 and 8, were taken from the field driving records (when available) as reported by the field engineer. Many times, the length below gauges is reported as a general value for several piles at one site (e.g., length below gauges = pile length - 3 ft [0.91 m]). There are some cases in which there is no indication as to exact lengths and, instead of assuming the field conditions, the length below gauges according to the CAPWAP results is used.

(c) Columns 9 and 10

The soil type at the side and tip of each pile-case are listed in the final two columns of table 20. This information is obtained from subsurface investigation reports and boring logs and it is considered essential to all pile-cases in data set PD/LT. The soil descriptions listed under side and tip are generalized according to the basic nature of the soil. For example, a pile that is reported to have a sandy silt with traces of clay is listed as sandy-silt. Also, soil types listed in the following manner, cl-sa-silt, for instance, refer to a clayey sandy silt with the most predominant soil listed at the end of the classification. Several abbreviations are used to condense the soil descriptions, these include: sa = sand, si = silt, cl = clay, ti = till, gr = gravel, d. = dense, l. = loose, clcr = calcareous, and carb = carbonious.

6.3 PILE DRIVING AND DYNAMIC MEASUREMENTS - TABLE 21

The pile driving and dynamic measurements information of each pile-case are summarized in table 21.

(a) Columns 1 and 2

In accordance with table 20, the first and second columns in this table list the case number and the pile-case number of each pile-case.

(b) Columns 3-5

The following three columns provide relevant hammer information for each case, such as the hammer type, the rated hammer energy, and the maximum energy delivered to the pile top. The letter abbreviations used denote the manufacturers name, for instance: B = Birmingham, D = Delmag, K = KC = Kobelco, Con = CN = Conmaco, LB = Link Belt, ICE = International Construction Equipment, KB = Kobe, Vul = Vulcan, M = MH = Mitsubishi, and DE = MKT. The abbreviations are followed by the model size (i.e., B-400 refers to a Birmingham 400 diesel hammer). The rated hammer energies are shown according to the manufacturers recommendations. The energy delivered refers to the maximum delivered energy, which is based on the dynamic measurements

and was usually determined from office analyses (i.e., CAPWAP/TEPWAP). It should be noted that often some discrepancy exists between the measured energy in the field as calculated by the PDA to the one reported by CAPWAP. This may be a result of several reasons:

- "Correction" of the waves for better proportionality before carrying out the office analysis.
- Older PDA models require the storage of data in an analog form on magnetic tapes. The data retrieval in those cases always contains some error.
- Field analysis may provide an average value while the office analysis refers to one particular blow. For reasons of consistency, whenever possible, the delivered energy value refers to the one reported by CAPWAP as the maximum energy (E_{max}).

(c) Column 6

The blow count (reported in blows per inch, BPI) is listed in the sixth column of table 21. Several times the blow count records were only in blows per foot and it was, therefore, necessary to convert these values to blows per inch. This conveniently allows the pile set to be derived in units of inches (set = 1/blows per inch). An asterisk follows each blow count that was converted from blows per foot to blows per inch.

(d) Columns 7-10

Following the blow count is the pile impedance, velocity at impact (V_{imp}), force at impact (F_{imp}), the ratio $[(V_{imp} \cdot EA/C)/F_{imp}]$, and the maximum pile displacement (D_{max}). As mentioned in chapter 5, the pile impedance is used to examine the ratio between the velocity and the force waves. The impedance is calculated using:

$$\frac{EA}{C} \tag{37}$$

- where
- E = modulus of elasticity of the pile material at the point of measurement
 - A = cross-sectional area of the pile at the point of measurement
 - C = wave speed of the pile.

The impedance is reported in kips per foot per second. The velocity at impact, V_{imp} (ft/s); the force at impact, F_{imp} (kips); and the maximum displacement of the pile, D_{max} (in), are obtained from dynamic measurements (see chapter 4). These values were typically taken from CAPWAP summaries and/or INTEGRATE results. The ratios between velocity and force $[(V_{imp} \cdot EA/C)/F_{imp}]$, reported in table 21, were those corrected when necessary, as discussed in chapter 5.

6.4 PARAMETERS OF DYNAMIC ANALYSES - TABLE 22

The parameters associated with dynamic analyses (i.e., quake and damping) are listed in table 22.

(a) Columns 1 and 2

The first two columns of table 22 list the case numbers and pile-case reference numbers consistent with tables 20 and 21.

(b) Column 3

The Case damping coefficient (J_c) reported in column 3 was back-calculated using the static load test results (R_s) as the "predicted capacity" for each particular pile and the "standard form" of the Case method utilizing equation 36.

(c) Columns 4 and 5

Columns 4 and 5 present the pile impedance and the calculated $2L/C$, respectively. The magnitude $2L/C$ is the time that it takes for a wave to reach the pile tip and reflect back to the pile top. This term is reported in milliseconds; L represents the pile length below gauges (feet) and C represents the wave speed of the pile material (feet per second).

(d) Columns 6-9

The last four columns list the tip and side quake and the tip and side damping, respectively. These values are used as input into CAPWAP or TEPWAP analyses and were obtained from their summaries. Those values that were used in TEPWAP analyses are denoted with an asterisk. The quake values are reported in inches and the damping is reported in units of seconds/feet.

6.5 PILE CAPACITY: STATIC TESTS AND DYNAMIC ANALYSES - TABLE 23

The static load test results for each pile in data set PD/LT were analyzed using five different failure load interpretation procedures: Davisson's Criteria, Shape-of-Curve method, the Limited Total Settlement methods ($\Delta = 1$ inch and $\Delta = 0.1B$), and DeBeer's method. These procedures are discussed in detail in chapter 5.

(a) Columns 1-3

The case number, pile-case reference number, and load test type are listed in the first three columns. The load test types have been abbreviated: S=standard, Q=quick, SM=slow maintained, LLT=Louisiana load test, FQ=Florida modified quick, and CRP=constant rate of penetration.

(b) Columns 4-8

Following the load test type column are the five load test interpretation methods used (all results are given in kips). The abbreviation NA refers to methods that were not applicable.

(c) Column 9

The static resistance (R_s) represents the average of the resistances given by the five methods (see chapter 5 for discussion).

(d) Columns 10-12

The last three columns report the capacity predictions from CAPWAP or TEPWAP, the Energy Approach, and the Energy Approach correction factor (K_{sp}). The predictions based on TEPWAP analyses are denoted with an asterisk. The CAPWAP/TEPWAP and Energy Approach predictions are reported in kips.

CHAPTER 7 - DATA SET PD

7.1 PILE/SOIL AND DYNAMIC MEASUREMENTS OF DATA SET PD - TABLE 24

The information of data set PD was provided by Pile Dynamics, Inc. of Cleveland, Ohio, as part of their support of the Energy Approach method research. Table 24 in appendix B summarizes the information describing the pile geometry, skin and toe soil, and dynamic measurements of the piles comprising data set PD (403 in all). Initially, this data set consisted of 428 pile-cases, however, 25 cases were removed because they were either duplicates or they were missing information. Table 24 categorizes the PD pile-cases according to pile type and soil type. A summary of these categories is presented in table 3. The correlations between the Energy Approach and CAPWAP are presented in chapter 9.

(a) Columns 1 and 2

The first two columns in table 24 list the reference number and the pile name according to designations made by Pile Dynamics, Inc.

(b) Columns 3 and 4

The side and toe soil are abbreviated in a similar manner to table 20, however, there are several additional soil types included: alluv = alluvial, clayston = claystone, coopermar = coopermarl, limestn = limestone, sastone = sandstone, overburd = overburden, dolom = dolomite, cobbl = cobbles, til = till, tilall = alluvial till, and sigr = silty gravel.

(c) Columns 5-9

The pile type and geometry are given in column 5 and are abbreviated in a similar fashion to table 20. The length below gauges, cross-sectional area, and modulus of elasticity are listed in columns 6, 7, and 8, respectively, and their units are as shown. Hammer type is listed in column 9 and abbreviations are consistent with those in table 20. Additional abbreviations include RAY = Raymond and IHC = IHC Hydrohammer.

(d) Columns 10-14

The dynamic measurements are reported in columns 10 through 13 and are listed as follows: FMX = maximum force at the pile top (kips), EMX = maximum energy delivered to the pile (kip-ft), VMX = maximum velocity at the pile top (ft/s), and DMX = the maximum displacement of the pile top (in). Column 14 contains the blow count for each pile-case reported in blows per inch.

(e) Columns 15 and 16

The last two columns list the CAPWAP predictions (in kips) and the corresponding Energy Approach predictions (in kips) for each pile-case, respectively.

7.2 SIDE/TIP QUAKE AND DAMPING PARAMETERS OF DATA SET PD - TABLE 25

Table 25 in appendix B summarizes the quake and damping parameters used for both the side and tip of each PD pile-case. The first five columns are identical to table 24, however, the pile-cases are listed in ascending order according to the reference numbers in column 1.

(a) Columns 6 and 7

The quake parameters used for the side and tip soil are listed in columns 6 and 7, respectively. These values are reported in inches.

(b) Columns 8 and 9

The last two columns of table 25 list the damping parameters used for the side and tip soil of each pile-case (reported in seconds per foot).

CHAPTER 8 - ANALYSIS OF DATA SET PD/LT

8.1 OVERVIEW

8.1.1 Purpose

The aim of this chapter is to present the analysis of the pile-cases in data set PD/LT in two forms by using:

- Graphical correlations, e.g., between static load test results and dynamic predictions (i.e., CAPWAP/TEPWAP and the Energy Approach), considering different factors such as pile and soil type, time of driving, and driving resistance.
- Statistical analyses in combination with the graphical correlations in order to establish conclusions and recommendations.

8.1.2 Outline

Three different types of correlations were investigated for the pile cases of data set PD/LT. The three categories and their rationales are presented below.

(a) Damping Parameters-Soil Type Correlations

One of the basic concepts presented in this research is that the different damping parameters fulfill the need for absorbing energy rather than truly representing either the soil or the physical phenomena it is subjected to. As such, correlations were built between the different damping parameters (Smith side and tip and the Case damping) and soil type, in order to examine the existence or nonexistence of such relations. The correlations of this category are presented in section 8.2.

(b) Prediction Methods-Load Test Capacity

Three dynamic analysis methods are examined throughout this research: (1) the office analyses (CAPWAP/TEPWAP), the field analysis (the Case method), and the proposed Energy Approach. Correlations were built between the predictions of CAPWAP/TEPWAP analysis and the Energy Approach analysis to the actual capacity based on the load test results. No correlations were built between the Case method predictions and the load test results, due to the following reasons:

- The method has a variety of shapes in which it can be implemented (see section 3.5), hence, no "unique" value would be valid.
- Previous studies (see section 3.5.5) suggested limited accuracy.

- The method is based on the notion of an existing correlation between the J_c damping parameter and the soil type at the tip. This was proven not to exist in the correlations described in group (a) above (see section 8.1.2).

In order to examine the influence of different factors (e.g., pile shape, driving resistance, time of driving, soil type, etc.), these correlations were built from the most generic cases (e.g., CAPWAP vs. load test results for all piles) to the private cases (e.g., CAPWAP predictions vs. load test results for small displacement piles in sand).

The correlations of this category are presented in sections 8.3.2 and 8.3.3 for different pile and soil types and in section 8.3.4 for different driving times. Their statistical analyses and interpretations are presented in section 8.4.

(c) Office Method/Field Method Predictions

Data set PD/LT contains information that is difficult to obtain. In general, very few load tests are carried out and, of those, only a small portion are carried out to failure. A considerably smaller portion is monitored dynamically during driving. As such, a strong correlation between the dynamic methods themselves may prove beneficial where load test data is not available. Correlations between the different predictions can therefore be compared to those obtained for data set PD for which static resistance is not available. These correlations are presented as part of sections 8.3 through 8.6 and are compared to those of data set PD in chapter 9.

8.2 DAMPING PARAMETERS AND SOIL TYPE GRAPHICAL CORRELATIONS

As previously discussed in chapter 4, viscous damping accounts practically for different energy losses, including radiation, soil inertia, and viscosity in cohesive soils. The damping parameters and their calibrations based on soil type have therefore been questioned.

8.2.1 Case Method Damping

The Case damping coefficient (J_c) is based on viscous damping in a dimensionless form, and is assumed to be related to the soil type at the pile's tip. Figure 21 presents the back-calculated Case damping coefficients for data set PD/LT vs. soil type at the pile tip. J_c was calibrated using the static capacity R_s and the "standard" Case method, as outlined by Goble *et al.* (1975) (see equations 6 and 36). It is shown that for the 208 pile-cases reported, no specific correlation exists between the soil type and the damping coefficient. Moreover, the obtained negative damping coefficients have no physical meaning and should be reviewed only for the purpose of illustrating the limitations of the J_c coefficient.

8.2.2 Smith Damping

Figures 22 and 23 compare the Smith damping coefficients (side and tip) used by CAPWAP/TEPWAP to the soil type at the side and tip of the pile, respectively. Corrections were not made to the office analysis, hence, the capacities obtained by the presented analysis reflect the predicted capacity and not the actual static capacity. A large variation of the damping parameter values can be observed for each soil type. Consequently, no specific correlation was made between the damping coefficients and soil type. These relations are further examined for the pile-cases of data set PD in chapter 9 and for all combined cases (581) in chapter 10.

8.3 DYNAMIC PREDICTION-STATIC CAPACITY GRAPHICAL CORRELATIONS

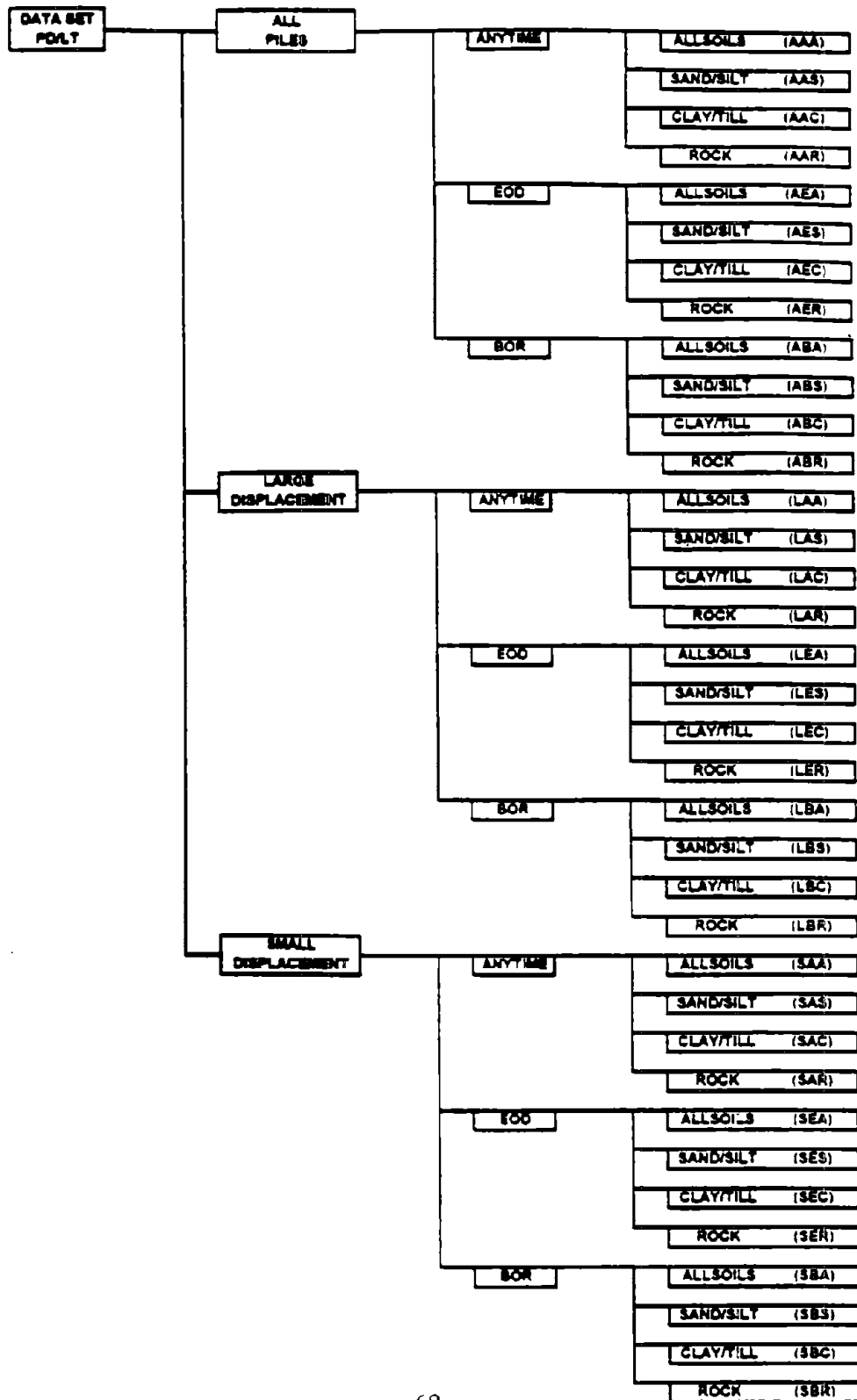
8.3.1 Correlations Breakdown

The graphical relationships between CAPWAP/TEPWAP and the Energy Approach to the static load test results were produced for all PD/LT pile-cases. These relationships are shown in the form of scatter plots (scattergrams). These plots were necessary as no statistical analysis can provide the actual observed information. The scatter plots were further divided into subgroups based on:

- Pile type (i.e., large and small displacement), presented in section 8.3.2.
- Soil type at the pile tip, presented in section 8.3.3.
- Time of driving (i.e., EOD = end of driving, BOR = beginning of restrike), presented in section 8.3.4.

The scatter plots for each different subgroup are shown in a consistent order: (1) static load test vs. CAPWAP/TEPWAP predictions, (2) static load test vs. Energy Approach predictions, and (3) CAPWAP/TEPWAP predictions vs. Energy Approach predictions. A flow chart illustrating the breakdown of all cases is presented as table 4. Each correlation graph includes a first-order best-fit line through zero (shown as the solid line), the corresponding coefficient of determination (r^2), and a set of dashed lines representing the ratio between the actual capacity over the predicted one to allow the assessment of over- and under-predictions. For example, points falling on a dashed line labeled 0.80 designates an over-prediction, where the actual static capacity is 80 percent of the predicted capacity. It should be noted that this ratio is a direct multiplier, hence, the ratio represents the value that when multiplied by the prediction will give the "correct" capacity. This is the inverse to the ratio of the predicted over measured capacity used, for example, by Olson and Dennis (1989) or Briaud *et al.* (1988). The

Table 4. Breakdown of all PD/LT categories.



breakdown of the best-fit line (using linear regression) for all cases is presented in tables 5, 6, and 7.

8.3.2 Pile Type Correlations

(a) All Piles

The following graphs compare static load test results, CAPWAP/TEPWAP, and the Energy Approach, based on the pile type and the soil type at the pile tip.

Figures 24, 25, and 26 present all PD/LT pile-cases in all types of soil. As indicated earlier, all relationships are shown in the following sequence:

- (1) CAPWAP/TEPWAP vs. Static Capacity (figure 24).
- (2) Energy Approach vs. Static Capacity (figure 25).
- (3) CAPWAP/TEPWAP vs. Energy Approach (figure 26).

The information in figure 24 indicates that a large scatter exists when comparing the predicted capacity of the office analyses to the actual static capacity. The predicted capacity ranges from over-predictions of about 0.6 (predicted over actual ≈ 1.7) to a maximum under-prediction of 4.4, with most cases falling within the under-prediction ratio of 2.5 (predicted over actual ≈ 0.4). Overall, the tendency is of under-prediction, with the best-fit line (forced through zero) indicating a ratio of 1.265.

Figure 25 also exhibits a scatter when comparing the Energy Approach predictions to the actual load test results. The predictions range from under-predictions of 1.67 (predicted over actual ≈ 0.6) to over-predictions of 0.45, with most cases falling within the over-prediction ratio of 0.50 (predicted over actual ≈ 2.0). The best-fit line indicates an overall over-prediction with a ratio of 0.839.

It is important to note that the range of under-prediction to over-prediction of the office analyses is about twice that of the Energy Approach. The maximum over-prediction of CAPWAP is 0.57 and the under-prediction is 4.41, compared to the Energy Approach method that ranges between 0.45 and 1.74. These numbers indicate a range of under- to over-prediction of 7.74 for the office analyses, compared to 3.88 for the Energy Approach. This important observation becomes clearer when scattergrams are built as the relationships between the ratio of the actual capacity over the predicted capacity (the slopes in figures 24 and 25) versus the predicted capacity. These relationships are presented in figures 27 and 28 (for the office method and the Energy Approach method, respectively) and clearly demonstrate the large scatter in the prediction ratios in the office methods when compared to that of the Energy Approach. The linear best-fit lines of the data in figures 27 and 28 are:

$$\begin{aligned}K_{sw} &= 1.4867 - 0.00024R_u \\K_{sp} &= 1.0259 - 0.00013Q_u\end{aligned}$$

Table 5. Linear-regression analysis of K_{sw} for selected PD/LT pile-cases.

K _{sw} = Static Load Test Results / CAPWAP or TEPWAP predictions						
Pile-Case Group	Number	Linear Regression				
		Best Fit			Forced through Zero	
		x-coefficient	y-intercept	r squared	x-coefficient	r squared
AAA	206	1.127	97.3	0.707	1.265	0.692
AAS	141	1.128	112.2	0.767	1.272	0.749
AAC	51	1.057	140.7	0.413	1.319	0.383
AAR	14	0.937	-14.0	0.581	0.908	0.580
AEA	97	1.065	151.7	0.779	1.248	0.740
ABA	109	1.344	-36.2	0.616	1.284	0.614
LAA	162	1.315	32.2	0.555	1.372	0.554
LAS	118	1.360	3.6	0.595	1.366	0.595
LAC	43	1.164	118.3	0.411	1.391	0.393
LEA	68	1.450	37.2	0.530	1.529	0.528
LBA	94	1.385	-48.3	0.598	1.307	0.596
SAA	44	1.074	38.8	0.934	1.108	0.932
SAS	23	1.048	138.4	0.968	1.142	0.952
SAC	8	0.854	104.8	0.688	1.021	0.653
SAR	13	0.980	-35.4	0.378	0.908	0.376
SEA	29	1.073	52.2	0.936	1.113	0.933
SBA	15	0.922	76.3	0.812	1.069	0.785

Pile-case legend: XXX

- first letter denotes pile type: A = all piles, L=large displacement, and S=small displacement.
- second letter denotes time of measurement: A=anytime, E=end of driving, and B=beginning of restrike.
- third letter denotes soil type: A=all soils, S=sand and silt, C=clay and till, and R=rock.

Table 6. Linear-regression analysis of K_{sp} for selected PD/LT pile-cases.

Ksp = Static Load Test Results / Energy Approach predictions						
Pile-Case Group	Number	Linear Regression				
		Best Fit			Forced through Zero	
		x-coefficient	y-intercept	r squared	x-coefficient	r squared
AAA	208	0.736	111.5	0.723	0.839	0.703
AAS	141	0.721	130.3	0.725	0.831	0.700
AAC	53	0.789	74.2	0.675	0.872	0.666
AAR	14	0.864	-18.3	0.745	0.830	0.744
AEA	98	0.791	126.6	0.830	0.900	0.804
ABA	110	0.677	111.8	0.597	0.786	0.578
LAA	164	0.668	160.8	0.579	0.832	0.534
LAS	118	0.634	184.2	0.548	0.816	0.489
LAC	45	0.784	88.4	0.669	0.882	0.656
LEA	69	0.787	145.2	0.648	0.966	0.603
LBA	95	0.669	119	0.569	0.780	0.550
SAA	44	0.816	58.2	0.920	0.856	0.916
SAS	23	0.795	129.3	0.930	0.863	0.916
SAC	8	0.767	28.1	0.713	0.804	0.711
SAR	13	0.935	-57.5	0.628	0.829	0.619
SEA	29	0.809	73.2	0.922	0.851	0.917
SBA	15	0.914	-7.1	0.737	0.902	0.737

Pile-case legend:

XXX

- first letter denotes pile type: A = all piles, L=large displacement, and S=small displacement.
- second letter denotes time of measurement: A=anytime E=end of driving, and B=beginning of restrike.
- third letter denotes soil type: A=all soils, S=sand and silt, C=clay and till, and R=rock.

Table 7. Linear-regression analysis of K_{cw} for selected PD/LT pile-cases.

Kew = CAPWAP or TEPWAP predictions / Energy Approach predictions						
Pile-Case Group	Number	Linear Regression				
		Best Fit			Forced through Zero	
		x-coefficient	y-intercept	r squared	x-coefficient	r squared
AAA	206	0.573	73.1	0.782	0.641	0.766
AAS	141	0.592	54.3	0.810	0.637	0.802
AAC	51	0.479	121.8	0.607	0.624	0.539
AAR	14	0.720	96.8	0.783	0.901	0.730
AEA	97	0.675	26.1	0.861	0.698	0.859
ABA	109	0.424	173.6	0.693	0.593	0.553
LAA	162	0.420	163.9	0.701	0.589	0.554
LAS	118	0.415	172.1	0.732	0.586	0.571
LAC	43	0.423	150.3	0.567	0.600	0.446
LEA	68	0.406	158.7	0.611	0.612	0.407
LBA	94	0.411	181	0.670	0.581	0.549
SAA	44	0.742	32.1	0.939	0.764	0.937
SAS	23	0.751	-1.4	0.942	0.750	0.942
SAC	8	0.876	-75.3	0.986	0.779	0.971
SAR	13	0.552	189.4	0.557	0.900	0.329
SEA	29	0.736	35.4	0.940	0.757	0.939
SBA	15	0.971	-80.2	0.871	0.834	0.851

Pile-case legend: **XXX** - first letter denotes pile type: A = all piles, L=large displacement, and S=small displacement.
 - second letter denotes time of measurement: A=anytime E=end of driving, and B=beginning of restrike.
 - third letter denotes soil type: A=all soils, S=sand and silt, C=clay and till, and R=rock.

in which R_u and Q_u are the predicted capacities (in kips) by the office method and the Energy Approach method, respectively. These best-fit linear-regression lines indicate that:

- Predictions are not a function of the load, although both equations indicate a reduction in the ratios (K_{sw} and K_{sp}) with the increase of the load. This increase is very small for both prediction methods.
- Average K_{sp} -value with load is 1.03, where the average K_{sw} with load is 1.49.

A few additional general observations can be made regarding the trends shown in figures 24, 25, 27, and 28:

- No specific correlations seem to exist between accuracy in prediction and soil type.
- Small displacement piles seem to have significantly less scatter than the one observed for the large displacement piles.

The relationship between the predicted capacities of the office methods and the Energy Approach is shown in figure 26. The information demonstrates consistent correlation within the range of 1.00 to 0.40. The best-fit line forced through zero is the ratio of 0.641, which means that the Energy Approach predictions are about 1.56 times those of the office predictions. This ratio is close to: (1) the ratio between the mean prediction ratio of the office methods (1.367) and the Energy Approach (0.925), which leads to 1.48; and (2) the best-fit ratio of the office methods (1.265) and the Energy Approach (0.839), which leads to 1.51.

In observing figure 26, it can also be noted that the scatter of the small displacement piles is much smaller than that of the large displacement piles. Moreover, the ratio of best fit for the small displacement is 0.764 (see figure 34) with a mean value of 0.796 (see table 5). This observation has a special meaning as it indicates that in the cases where small soil inertia takes place, both methods are in much better agreement, with the Energy Approach prediction only about 1.3 times that of the office methods.

(b) Large Displacement Piles

The relationships pertaining to large displacement piles for all soil types are shown in figures 29 through 31.

The relationship between the office analyses and the actual static capacity for large displacement piles shows significant over-predictions. The best-fit line yields an increase from 1.265 — obtained for all piles in figure 24 — to 1.370. The prediction ratios range from 4.41 to 0.57 with most cases in the range of 2.50 to 0.80 (actual over-prediction).

This emphasizes the outlined notion that energy loss takes place mainly due to soil inertia. Hence, the signal matching techniques using viscous damping models can not correctly represent the actual mechanism and, as a result, under-predict the actual pile capacity. It can also be mentioned in this context that the best-fit line ratio for all small displacement piles (to be presented in figure 32) is 1.108.

The information in figure 30 yields similar results to those in figure 25, with a considerable scatter between Energy Approach predictions and actual load test results. No significant changes can be seen from figure 25 through 28 as the best-fit ratio for large displacement piles is consistent at 0.832.

Figure 31 indicates a high correlation between the methods, similar to that presented in figure 26 with the CAPWAP/TEPWAP over Energy Approach ratio ranging from about 1.00 to 0.40. The best-fit line through zero produced a prediction ratio of 0.589 (CAPWAP/TEPWAP over Energy Approach).

(c) Small Displacement Piles

The relationships pertaining to small displacement piles for all soil types are shown in figures 32 through 34.

The correlation between the office method predictions and the actual static capacity for small displacement piles is shown in figure 32. The general trend indicates a relatively good agreement with a best-fit line forced through zero producing a ratio of 1.108, much closer to the desired ratio of 1.0 than that for the large displacement piles. The scatter is substantially smaller than that for the large displacement piles. The prediction ratios range from an over-prediction of about 2.5 to an under-prediction of 0.6 (actual over-prediction) with the majority of data falling between 1.25 and 0.60. While no clear trend can be seen on the basis of soil type, the capacity of all piles driven in rock seem to be over-predicted by the office method. This distinction seems to be more related to driving resistance as all of these cases present high driving resistance of over 10 BPI.

The Energy Approach predictions vs. the actual load test results for small displacement piles are presented in figure 33. The presented relationship indicates a small scatter with ratios ranging from about 1.67 to 0.60, with the majority of the data falling between 1.10 and 0.60. The best-fit line through zero yields a ratio of 0.856, which is only slightly higher than the ratios in figures 25 and 30. It should be noted that the scatter of both methods, the Energy Approach predictions in figure 33 and the office methods in figure 32, are very small when compared to that observed for the large displacement piles, as indicated by the coefficients of determination.

The information in figure 34 indicates that a distinct trend has developed between the two methods of analysis. The data shows very small scatter with ratios ranging between 1.00 and 0.60, with the best-fit ratio through zero equal to 0.764.

(d) Intermediate Conclusions

See tables 5 through 7 for statistical data. Different correlations have been investigated on the basis of pile type.

- A relatively large scatter appears in the predictions of both dynamic methods, the office methods and the Energy Approach, for all cases (AAA). While the office methods under-predict on the average ($K_{sw} = 1.265$), the Energy Approach over-predicts ($K_{sp} = 0.839$). Both scatters are reflected through:
 - (1) Relatively low coefficient of determination for the best-fit line through zero ($r^2 = 0.692$ and 0.703 for the office methods and the Energy Approach, respectively).
 - (2) High intercept for unforced best-fit lines (y-intercept = 97.3 kips and 111.5 kips [432.8 kN and 496 kN] for the office and Energy methods, respectively).
- Much better correlations and a smaller scatter appear for both methods when predicting the capacity of small displacement piles compared to large displacement piles. For the office methods, the best-fit ratios and coefficients of determination are 1.372, $r^2 = 0.554$ and 1.108, $r^2 = 0.932$ for large and small displacement piles, respectively. For the Energy Approach, the best-fit ratios and coefficients of determination are 0.832, $r^2 = 0.534$ and 0.856, $r^2 = 0.916$ for large and small displacement piles, respectively.
- As a result of the above, both methods seem to correlate very well to each other in all cases. A similar ratio is produced for the relationship between the predictions of CAPWAP/TEPWAP and the Energy Approach, regardless of pile type. This ratio varies between 0.641 for all piles to 0.589 for large displacement piles and 0.764 for small displacement piles. The coefficient of determination for the best-fit line through zero, however, is the highest for the small displacement piles ($r^2 = 0.937$), compared to 0.554 for the large displacement piles. This may imply that both methods encounter the same difficulties under the same conditions in spite of the fact that the Energy Approach does not consider any dynamic resistance while the office methods consider dynamic resistance through viscous damping.
- No clear trends in the predictions appear on the basis of soil type at the tip, whereby predictions in all types of soil exist throughout, without any particular order. This conclusion is observational only and requires a quantitative evaluation that is presented in the following section.

8.3.3 Pile-Soil Type Correlations

The PD/LT pile-cases were subgrouped according to the different tip-soil types in an effort to investigate possible trends developing according to end-bearing soils. The correlations follow the sequence outlined in section 8.3.2 for three tip-soil conditions: sand and silt, clay and till, and rock.

(a) Sand and Silt

Figure 35 shows the correlation between the office method predictions and the actual static capacity for a PD/LT pile-case in sand and silt. The results remain consistent with figures 24 and 27 as they continue to under-predict. The best fit through zero shows an under-prediction ratio of 1.272. The scatter is, however, smaller for predictions in sand and silt, with the ratio ranging from 2.5 to 0.80 (load test over-prediction) and the coefficient of determination is 0.749.

The correlation between the Energy Approach predictions and the actual static capacity in sand and silt is shown in figure 36. The scatter is consistent with that of figure 25, with a best fit ratio very similar at 0.831. The ratio range is unchanged and it is difficult to see any different trends based on the sand and silt subgroup. It is noticeable, however, that all predictions pertaining to small displacement piles are contained within a narrow range approximately between 0.80 and 1.60.

The information in figure 27 indicates a good agreement between the office analysis predictions and the Energy Approach predictions for piles driven in sand and silt. The best-fit line forced through zero yields a ratio of 0.639, which is very consistent with the correlations of figures 26 and 31. The range of ratios remains between 1.00 and 0.40, with the majority of the points falling between 1.00 and 0.60. These results suggest that the sand and silt end-bearing soil has little effect on the overall trend of the prediction ratios.

(b) Clay and Till

The relationships in figure 38 between the office analysis predictions and the actual load test results for clay and till result in a similar best-fit line to the one obtained for the relationships in sand and silt. Considering the difference in the number of data points, however, it seems that the 51 cases of piles in clay and till are scattered much more relative to the 139 cases of piles in sand and silt. As a result, the coefficient of determination of the cases in sand and silt is much higher than that of clay and till (0.749 compared to 0.383 for the best-fit line through zero). The best-fit line yielded a ratio of 1.319, which far exceeds the best-fit ratio of figure 24 in which the small displacement piles were included. It is also interesting to note that the best-fit line resulted in a ratio of 1.057 with an intercept of 141 kips (627 kN). Time effects have not been considered in figure 38 and the data represents all states of EOD and BOR. Time effects will be addressed in section 8.3.4.

The relationships between the Energy Approach predictions and the actual static capacity is shown in figure 39. This information indicates a similar scatter (see figures 25, 30, 33, and 36) among the predictions, with the best-fit line remaining nearly unchanged at 0.872 (actual over-prediction). Based on figures 36 and 39, it appears that soil type, alone, has little effect on the overall performance of the Energy Approach.

Figure 40 demonstrates the consistency that has been evident in figures 26, 31, 34, and 37. The correlation between the office analysis predictions and the Energy Approach remain within a range of 1.00 and 0.40, with a distinct trend developing around the 0.80 line. The best-fit ratio (forced through zero) is 0.624 and a comparison with the sand and silt best-fit ratio (figure 37) shows a similar value. The coefficient of determination for the clay and till cases is substantially lower, however, and is approximately 0.539, compared to 0.802 for the best-fit line through zero for the pile cases in sand and silt. This shows that although, on the average, the ratio is unchanged, the agreement between the methods is more scattered for piles in clay.

(c) Rock

The correlation between the office analysis predictions and the actual static capacity for piles end-bearing on rock showed a considerably better prediction ratio with a considerable scatter. The best-fit line in figure 41 yielded an under-prediction ratio of 0.908 with all points falling almost exclusively in the range of 1.25 and 0.60 (actual over-prediction), yielding a poor coefficient of determination of 0.580. These results may be attributable to three reasons: (1) all the piles driven into rock are small displacement piles (except for one), (2) the driving resistance in the majority of cases (13 out of 14) ranges between 10 and 44 blows per inch (0.394 and 1.73 blows per mm), and (3) the presented subset contains only 14 pile-cases.

The information in figure 42 for the correlation between the Energy Approach predictions and the actual static capacity in rock produced very good results, showing excellent agreement that is consistently within a range between 1.00 and 0.60. The best-fit line shows a ratio of 0.823 with a coefficient of determination of 0.744, which is consistent with the other correlations between the Energy Approach and the actual static capacity previously mentioned.

Figure 43 indicates a very good correlation between the office analysis predictions and the Energy Approach predictions. The best-fit line forced through zero yields a ratio of 0.901 and all data points fall within ± 20 percent of the best-fit line.

(d) Intermediate Conclusions

See tables 5, 6, and 7 for statistical data.

Different correlations have been investigated on the basis of soil-type conditions at the tip.

- The office analysis relationships seem to be less scattered for the predictions of piles in sand compared to those in clay. Both best-fit line coefficients indicate a similar ratio for both soil types, 1.272 and 1.319 for sand and clay, respectively. Their coefficients of determination differ substantially however, $r^2=0.749$ and 0.383 for sand and clay, respectively. The "free" trend best-fit line for both cases show an intercept of 112 kips and 141 kips (498 kN and 627 kN) for sand and clay, respectively. The coefficients of determination of these lines are similar, however, to those for the lines forced through zero.
- The relationships of the Energy Approach analyses seem to be consistent for both clay and sand pile-cases. The best-fit ratios through zero and coefficients of determination are 0.831, $r^2=0.700$ and 0.872, $r^2=0.666$ for sand and clay, respectively.
- The relationships between the predicted capacity of piles in rock and the static capacity is different for both methods. The Energy Approach shows consistency in the best-fit coefficient and the coefficient of determination when compared to the sand and clay cases. The office analyses present a much better best-fit line with a relatively high scatter. The presented relationships for rock have been discussed separately and represent a separate case due to the small number of piles and the fact that all of them are small displacement piles driven in a high driving resistance.
- Less scatter appeared for the small displacement piles under all categories of soil types. This is in agreement with the previous section's conclusion that examined the pile-type case.
- A consistent ratio appears between the predictions of both methods and pile types. Higher scatter exists for the predictions in clay compared to sand ($r^2=0.539$ in clay vs. $r^2=0.802$ in sand).

8.3.4 Correlations of Pile and Soil Type for Different Driving Time

Further relationships were developed to examine any trends that may take place as a direct result of the time during driving for which the predictions were made. The subgrouping includes pile type (large displacement and small displacement) and time of driving (EOD = end of driving and BOR = beginning of restrike).

Two comments made in regard to these comparisons are:

- The EOD condition is of great importance as ideally we would like to accurately find the pile capacity at the end of driving state, which also enables us to control driving according to our real-time predictions.

- The BOR records consist of different driving times after the initial EOD. These records were lumped together as one group. As such, the actual setup time and stage in which the driving took place was not considered. For the cases that were examined independently, consistent improvements were observed with each elapse of time since EOD.

(a) All Piles - EOD

Figure 44 presents the relationship between the office analysis predictions and the actual static capacity for all PD/LT piles in all types of soil at the end of driving (AEA). The results show a scatter with the prediction ratio ranging from 4.41 to 0.57, consistent with the best-fit lines produced in figure 24 for predictions at anytime during driving (AAA). The best-fit line forced through zero produced an under-prediction ratio of 1.248, or about +25 percent of the actual static capacity. The coefficient of determination improves somewhat from $r^2=0.692$ for all cases to 0.740 for the EOD conditions. Moreover, it seems that the under-prediction can be mostly attributed to the large displacement piles, whereas the predictions for the small displacement piles seem to concentrate within a zone of lower and more accurate load test over-prediction ratios. With regard to the best-fit line of the relationships in figure 44, it should be noted that the presented best-fit line is the one forced through zero (origin of axis). In most other cases, the slope of the forced best-fit line does not differ much from that of the unforced minimum square best-fit line. For the data presented in figure 44 the situation is different. The unforced best-fit line has a slope of 1.065 (see table 6) with a y-intercept of 152 kips (676 kN). This, again, implies some consistent under-prediction for the office methods in analyzing the EOD records.

The information in figure 45 indicates a prediction range from 1.67 to 0.60 for the correlation between the Energy Approach and the actual static capacity at EOD (AEA). The general scatter is substantially smaller than that of the office methods in figure 44, with a coefficient of determination of $r^2=0.804$. The best-fit prediction ratio increases substantially from the correlation for all cases (figure 25, ratio of 0.839) to 0.901 (prediction over actual ≈ 1.11).

It is important to note that for all the cases where substantial under-predictions took place in the office analyses, reasonable predictions were achieved by the Energy Approach. Observing figure 44, it can be seen that in many cases, the predictions exceed the line denoted by 1.67 (load test 67 percent higher than the prediction) up to a ratio of 4.4. All these cases are within the 1.67 line of the Energy Approach. Although not easily explained, in many cases in which improvement in prediction of the office method was observed with time, more accurate predictions were obtained by the Energy Approach at the EOD.

Figures 46 and 47 present the same data as that presented in figures 44 and 45, in the form of scattergrams of the actual over-prediction ratio versus the predicted capacity.

The aforementioned observations are enhanced by the data presentations of figures 46 and 47, emphasizing the relatively good predictions of the Energy Approach.

Figure 48 presents the correlation between the predictions of the office methods to the Energy Approach. As in previous similar correlations, the scatter between the methods is much smaller than that between the individual methods and the actual static capacity. It is interesting to note that the majority of the small displacement piles concentrate in a narrow band approximately between 0.7 and 1.0. This means that both methods produce very similar results for small displacement piles. From figures 44 and 45, it can also be concluded that both methods produce relatively accurate predictions for the small displacement piles.

(b) All Piles - BOR

The correlation between the actual static capacity and the office analysis predictions based on measurements at the beginning of restrike (ABA) is shown in figure 49. The range of predictions is between 2.5 and 0.80, with a best-fit prediction ratio of 1.284. The majority of the predictions reside within the 1.28 to 0.80 range with a general scatter higher ($r^2=0.614$) than that observed in figure 44, where predictions were based on end-of-driving measurements ($r^2=0.740$).

Figure 50 indicates that a much greater scatter exists for Energy Approach predictions at the beginning of restrike than for predictions made at the end of driving (see figure 45). The tendency is to over-predict more for restrikes with the prediction ratios ranging from 1.25 to 0.40. Consequently, the best-fit prediction ratio (0.786) is lower than that of figure 45 and the coefficient of determination is $r^2=0.578$, compared to 0.804 for EOD conditions.

The results presented in figure 50 are in sharp contrast to those shown in figure 45. While the Energy Approach provided much better predictions for the EOD condition compared to the office methods, it resulted in a larger scatter at the BOR state. In many cases, where improvement was observed with additional restrikes with time for the office methods, no such improvement (or, in many cases, worse predictions) were obtained by the Energy Approach.

Figure 51 exhibits a substantial scatter when compared to figure 48 for EOD predictions. The correlation between the two prediction methods is, however, considerably better than that observed in figures 49 and 50. The scatter exists mainly between 1.00 and 0.40 (CAPWAP/TEPWAP over Energy Approach) with a ratio of 0.593 for the slope of the best fit through zero (CAPWAP/TEPWAP over Energy Approach).

(c) Large Displacement Piles - EOD

Figure 52 shows the correlation of the office analysis predictions and the actual static capacity for large displacement at EOD (LEA). There is a significant scatter ($r^2=0.528$) ranging between 4.41 and 0.74, with most data between 2.50 and 1.00. The best-fit line

prediction ratio is 1.529. The data in figure 52 indicates the difficulties in analyzing records of large displacement piles and the shortcoming of the office methods for the EOD state.

The information in figure 53 indicates relatively good agreement of the Energy Approach and the actual static capacity for large displacement piles at EOD. Although the scatter ranges from 1.67 to 0.60 and the coefficient of determination, $r^2=0.603$, the majority of points lie within ± 20 percent of the actual static capacity, whereby the best-fit line yields a prediction ratio of 0.966. The relative accuracy of the Energy Approach for those cases is surprising and not yet well understood.

The relationship of the prediction methods large displacement piles at EOD is shown in figure 54. In general, the tendency appears to be within the 1.00 and 0.60 range, with a best-fit ratio of 0.612. This ratio meets the substantial under-prediction of the office methods and the relatively high accuracy of the Energy Approach.

(d) Large Displacement Piles - BOR

Figure 55 presents the correlation of the office analysis predictions and the actual static capacity for large displacement piles at BOR (LBA). The correlation demonstrates improved accuracy of the office analyses for BOR compared to the results obtained in figure 52 for EOD. In general, most of the data points fall between 2.0 to 0.80, with the best-fit line as a ratio of 1.307 and a coefficient of determination, $r^2=0.596$. Figure 55 shows improved predictions for large displacement piles relative to the EOD state, but poor predictions relative to those obtained for small displacement piles.

The information in figure 56 indicates a significant scatter for the correlation of the Energy Approach and the actual static capacity for large displacement piles at BOR. This is in contrast to the results obtained in figure 53 for the predictions of large displacement piles at EOD. The prediction ratios range from 1.53 to 0.40, with a best-fit ratio of 0.780 and a coefficient of determination, $r^2=0.550$.

The correlation shown in figure 57, between the prediction methods at BOR, remains consistent with previous findings. The ratios range from 1.00 to 0.40, with very few predictions outside of this range.

(e) Small Displacement Piles - EOD

Figures 58, 59, and 60 present the relationships between the load test results and the office predictions, load test results and the Energy Approach predictions, and the relationships between the prediction methods for small displacement piles at EOD (SEA). Based on previous observations: (1) predictions for small displacement piles (see figures 32, 33, and 34) were much better than those for large displacement piles, and (2) predictions for end of driving (see figures 44, 45, and 46) were better than those at the beginning of restrike, especially for the Energy Approach. Therefore, the combined criteria resulted with very good relationships, as expected.

Figure 58 shows that the office method best-fit line is $K_{sw} = 1.113$ and $r^2 = 0.933$. The relationships have the second best coefficient of determination of all combination cases examined in table 5. The other similarly high correlations and accuracy were obtained for all small displacement piles (SAA) and their subgroup (SAS).

Figure 59 indicates a similar trend for the Energy Approach, yielding a best-fit line with a K_{sp} -ratio of 0.851 and $r^2 = 0.917$. These results are similar to those of all small displacement piles (SAA) and those in sand (SAS).

Figure 60 reflects the outcome of figures 58 and 59, with a best-fit correlation of $K_{sw} = 0.757$ and $r^2 = 0.939$.

(f) Small Displacement Piles - BOR

Figures 61 and 62 present the relationships between the predictions of the dynamic methods and the load test results for a small subgroup (12 cases in the figures and 15 cases in the statistical analysis) of small displacement piles at the beginning of restrike in all soils.

The obtained coefficients are $K_{sw} = 1.069$, $r^2 = 0.785$, and $K_{sp} = 0.902$, $r^2 = 0.737$, which indicate the following:

- The predictions for the BOR state are more scattered than for the EOD state, even for small displacement piles only.
- Out of the entire BOR group, the predictions for the small displacement piles are much better than those for the large displacement piles.

Figure 63 presents the relationships between the two prediction methods for 12 small displacement PD/LT piles in all types of soil at BOR (SBA), indicating a good correlation between them.

(g) Intermediate Conclusions

See tables 5, 6, and 7 for statistical data. Different correlations have been investigated based on the time of driving.

- Based on the data of figures 44 (46), 45 (47), 49, and 50, it is evident that both dynamic methods perform better for the end of driving (EOD) condition than for beginning of restrike (BOR). This is especially true for the Energy Approach method, which shows excellent predictions for all cases of EOD condition (AEA). The conclusions regarding the office method are different. On one hand, there is an improvement for EOD when compared to the overall cases (AAA); on the other hand, the BOR cases, as shown in figure 44, do not reflect correctly the accuracy of the method.

As mentioned earlier, a closer look at the time of driving showed consistent improvement of the office methods with time. The data of figure 49 may, therefore, not correctly represent the accuracy of the method, which may improve when examined, for example, for only the last BOR of each case.

- Based on the data of figures 52, 53, 55, and 56, it is clear that the capacity predictions for large displacement piles are problematic for both dynamic analyses, CAPWAP/TEPWAP, and the Energy Approach. CAPWAP/TEPWAP seem to produce, however, similar results at BOR than at EOD (see figures 44 and 49) subjected to the aforementioned comments. The Energy Approach, on the other hand, produces more accurate results at the end of driving than at the beginning of restrike (see figures 45 and 50). The relationships between the prediction methods, CAPWAP/TEPWAP, and the Energy Approach, show strong correlation between the methods regardless of the time of driving (see figures 43 and 48).
- The above conclusion becomes more clear when comparing the performance of the large displacement piles and small displacement piles for the same driving time. For example, the office method, when comparing AEA (figure 44) to LEA (figure 52) and SEA (figure 58), clearly shows that the predictions for large displacement piles at EOD is very poor compared to that of the small displacement piles at EOD. The same conclusion holds true for beginning of restrike, demonstrating again the importance of the pile type. Similar conclusions are obtained by checking the Energy Approach method for AEA (figure 45), LEA (figure 53), and SEA (figure 59).

8.4 STATISTICAL ANALYSIS OF DATA SET PD/LT

A statistical analysis of the correlations of data set PD/LT was performed in order to quantify the accuracy of both the office analysis and the Energy Approach predictions as well as the correlation between them. The statistical analysis was performed in three stages:

- (I) Determination of the first-order best-fit lines (forced through zero and y-intercept) by linear regression, in combination with the sample coefficient of determination (r^2) to measure the accuracy of the best fit (note that the coefficient of determination is a square of the coefficient of correlation (r)).

- (II) Examination of the fitness of the data to known probability distribution functions (PDF).
- (III) Determination of the mean and the standard deviation of the individual ratios (e.g., load test to Energy Approach) as a measure of variability.

8.4.1 Linear-Regression Analysis

The results of the linear regression analysis performed on selected subgroups of table 4 and the presented graphical relationships of section 8.3 are summarized in tables 5, 6, and 7.

The tables summarize the different subgroups for the ratios between: (1) the static resistance to the office method predictions (K_{sw}) in table 5, (2) the static resistance to the Energy Approach predictions (K_{sp}) in table 6, and (3) the relationship between the predictions of the office methods and those of the Energy Approach in table 7.

The first two columns of each of the tables list the pile-case subgroup and the total number of cases considered in that group. The number of cases shown in the tables may be equal or greater than the numbers shown in the figures for the same correlations. This occurs when some of the data points exceed the dimensions of the plots. Linear regression was performed for each group to determine: (1) the best-fit line ratio, (2) the best-fit line ratio forced through zero, and (3) the coefficient of determination for each analysis. The results are listed in columns 3, 4, and 5 for the best-fit line and 6 and 7 for the best-fit line through zero, in each table. For example, the best-fit line forced through zero for the K_{sp} coefficients calculated for the subgroup AEA (all piles, at EOD, for all soils) was found to have a slope of 0.900 with a coefficient of determination, $r^2=0.804$. The sample coefficient of determination (r^2) for each subgroup was determined to measure the representativeness (accuracy) of the best fit and the best fit through zero.

The coefficient of determination (r^2) represents the proportion of the sum of squares of deviations of the y-values about their mean, and it is a measure of the contribution of "x" in prediction "y". By definition, a scatter at higher x-values will influence this coefficient more than a scatter close to the origin of axes. The coefficient of determination varies between 0 and 1; the first indicating no correlation or contribution and the last ($r^2=1$) is a perfect match where all the points fall on the best-fit, least-squares line. For example, $r^2=0.6$ means that 60 percent of the sum of squares of deviations of the observed y-values about their mean is attributed to the linear relations between y and x. (actual vs. predicted). In other words, 60 percent of the variability in y is explained by the regression equation. According to Ryan (1989), a meaningful correlation is obtained with $r^2 \geq 0.80$, which coincides with $p \leq 0.0011$; p is the probability of obtaining an F-value as or larger than the calculated value. This value of $r^2=0.8$ may be rigorous relative to

correlations in geotechnical engineering. The results, therefore, may be reviewed in the following ranges (Veneziano, 1993):

$r^2 \geq 0.80$	good correlation
$0.60 \leq r^2 < 0.80$	moderate correlation
$r^2 < 0.60$	poor correlation.

Table 5 presents the results of the K_{sw} analysis and the best correlation of all subgroups was found to be for all small displacement piles in all soils (SAA) and in sand and silt (SAS). Reasonable correlation was found for all piles based on the end of driving records, especially for the small displacement piles. Poor correlations were found for all piles at BOR in all soils (ABA) and for all large displacement piles (LAA), both at EOD (LEA) and at BOR (LBA).

The coefficients of table 6 indicate that the Energy Approach presents slightly better correlation overall for all cases (AAA) than that of the office methods, where both methods show moderate correlation according to the above coefficient of determination standards. The Energy Approach method shows very high accuracy for small displacement piles in all soils at all times (SAA), mostly due to its excellent performance in sand and silt (SAS). The Energy Approach prediction shows excellent correlation for all piles at EOD in all soils (AEA), producing a best fit through zero sample coefficient of distribution of 0.804, mostly again due to the high accuracy for the small displacement piles (SEA). Low accuracy was also determined for all piles at BOR in all soils (ABA), similar to that of the office methods.

Table 7 enables the examination of under what conditions both methods predict similarly or differently, indicating that, in general, the correlation between the methods is stronger than the correlation between the individual methods and the actual capacity with especially strong correlations in the cases where both methods predict well, namely small displacement piles and end of driving.

8.4.2 Actual Distributions of the K Coefficients and their Probabilistic Models

The K coefficients are defined as follows:

$$K_{sw} = \frac{\text{Actual static capacity}}{\text{CAPWAP / TEPWAP prediction}} \quad (38)$$

$$K_{\varphi} = \frac{\text{Actual static capacity}}{\text{Energy Approach prediction}} \quad (39)$$

$$K_{sw} = \frac{CAPWAP/TEPWAP\ prediction}{Energy\ Approach\ prediction} \quad (40)$$

These ratios are equivalent to the ratios marked and denoted by the straight lines on the scatter plots of sections 8.3.2, 8.3.3, and 8.3.4.

The distributions of the individual K coefficients for all PD/LT pile-cases are presented in figures 64, 66, and 68 in the form of histograms. The cumulative frequency distribution of K_{sw} and K_{sp} are presented in figures 65 and 67, respectively. The histograms were plotted for K coefficients ranging from 0.0 to >3.0 in 0.1 intervals and include all the available information. The left y-axis shows the total number of K coefficient occurrences, whereas the right y-axis shows the frequency (normalized number of occurrences).

The common parameters most often used to evaluate prediction methods are the mean and standard deviation of the normal distribution. The normal distribution best represents occurrences ranging from $-\infty$ to $+\infty$ with the highest probability at the mean. The ratio between the actual capacity to the predicted one (or its inverse) is limited between 0 to $+\infty$ and, hence, its distribution is not symmetrical. Even though, in many cases where the data is "normally" distributed, the normal distribution will represent it in a reasonable fashion (e.g., see figure 68). In many other cases, the normal distribution is incapable of correctly reflecting the accuracy (represented by the mean) and the precision (represented by the standard deviation) of the predicting method. A better probability distribution function for cases ranging from 0 to $+\infty$ is the log-normal distribution. A simple transformation can be performed from the mean and standard deviation of the normal distribution to the log-normal distribution parameters (see, for example, Benjamin and Cornell, 1970), which allows plotting of the log-normal distribution. Both distributions, normal and the corresponding (transformed) log-normal distributions, were plotted for the ratios between actual capacity to the predictions of the office methods (K_{sw} , figure 64) and the actual capacity to the Energy Approach predictions (K_{sp} , figure 65). In any case, the actual data must be reviewed as scatter graphs (section 8.3.2, 8.3.3, and 8.3.4) and histograms before the establishment of any conclusions.

The information presented in figure 64 for the K_{sw} coefficients (actual capacity over CAPWAP/TEPWAP predictions) indicates a concentration of cases (about 50 percent of all cases) between 0.9 and 1.3, with a significant scatter of the other 50 percent of the cases across a wide range of K values from 0.57 to 4.41. A normal distribution curve was added to the actual data based on the analysis results presented in table 8. The actual data seems to differ from the normal distribution and explains the relatively large standard deviations of the K_{sw} . The "transformed" log-normal distribution seems to better represent the actual data, but yet, falls short of representing it accurately. An

attempt to improve the log-normal distribution representation of the actual data was carried out by decreasing the standard deviation parameter ($\ln\sigma_x$, note: not that of the standard deviation). The results are shown in the form of a log-normal distribution and plotted using dashed lines that seem to represent the peak and over-prediction side better, but do not seem to represent the under-prediction side as well. Figure 65 presents the cumulative frequency distribution of the K_{sw} ratio. Due to the large range of values, a gradual increase in the cumulative frequency distribution takes place for values of K_{sw} greater than 1.3.

Figure 66 shows the distribution of the K_{sp} values for all PD/LT pile-cases and the data fits reasonably well with the normal distribution description. The "transformed" log-normal distribution seems to fit the data even better, allowing good representation of the data skewness. About 75 percent of the cases fall in the range between 0.6 and 1.2, with the mean at 0.925. An attempt to improve the log-normal distribution was carried out by decreasing the standard deviation ($\ln\sigma_x$). The results, again, are better only for part of the data, showing better agreement with the peak and the underestimation, and worse representation for the overestimated capacities. Figure 67 presents the cumulative frequency distribution of the K_{sp} ratio. A moderate increase exists for about 50 cases between 0.4 and 0.7, followed by a sharp increase of about 150 cases between 0.7 and 1.2. The distribution ends with a moderate slope of about 10 cases, up to about 1.7.

The distribution of the K_{ew} coefficients is presented in figure 68. The results of this distribution indicate excellent correlation between the office analysis predictions and the Energy Approach predictions (CAPWAP/TEPWAP over Energy Approach), represented well by the normal distribution.

8.4.3 Mean and Standard Deviation Analysis

Table 8 presents the statistical analysis for all PD/LT correlations listed in table 4 (see chapter 6 and tables 20 through 23 in appendix A for details). The first column of table 8 lists the pile-case group according to the abbreviation system shown in table 4. The table reports the normal distribution mean and standard deviation for each subgroup in a similar sequence mentioned in section 8.3.2. The subcolumns for each K coefficient list the total number of pile-cases analyzed, the mean value determined, and the corresponding standard deviation. It should be emphasized that even for cases in which better representation is given through the log-normal distribution, the mean and the standard deviation remain a powerful tool for the evaluation of the accuracy, through the mean, and for the precision, through the standard deviation.

8.5 INTERPRETATION OF THE CONTROLLING PARAMETERS

8.5.1 Overview

Section 4.4.4 outlined the expected performance of the dynamic analyses based on the hypothesis that the majority of the energy is lost through soil inertia. This hypothesis was partially confirmed by the results presented in the previous sections. A closer examination of the controlling parameters and their influence on the accuracy of the dynamic analyses follows.

8.5.2 Dynamic Predictions - Pile Area Ratio Graphical Correlations

To investigate a possible relationship between the office analysis, the Energy Approach predictions, and pile geometry, K_{sw} and K_{sp} values were correlated with the pile area ratio (see sections 4.4.2 and 4.4.3).

Figures 69 and 70 present the correlation between the K_{sw} -values and the pile area ratio (A_R). The data are presented using two scales (linear and logarithmic) to allow the assessment of the many cases for which A_R varies between approximately 90 to 300, which create a "spot" when presented in a linear scale. For pile area ratios less than 350, a significant scatter can be observed with K_{sw} -values exceeding 2.0. In general, K_{sw} -values closer to unity appear as A_R increases. Some scatter appears, however, at very large A_R ratios that may indicate the influence of additional parameters on the K_{sw} -values (e.g., driving resistance).

Figures 71 and 72 present the correlation between K_{sp} and the pile area ratio. Significantly smaller scatter appears in the K_{sp} -values compared to that of the K_{sw} -values. The general trend is similar to that of figure 69 — most scatter appears within a zone in which the pile area ratio is smaller than 350.

The pile area ratio seems to enable the quantification of the definition of large displacement and small displacement piles. The information from figures 69 through 72 suggest that considerable consistency is developed for pile area ratios > 350 . From these correlations, it was concluded that large displacement piles can be defined as those with pile area ratios < 350 and small displacement piles defined as those with pile area ratios > 350 . The following section examines the relationship between the prediction of the dynamic analyses and the driving resistance, as the complementary factor to the pile type in controlling the soil's inertia (see section 4.4 for background).

8.5.3 Dynamic Predictions - Driving Resistance Graphical Correlations

Figure 73 presents the ratio between the load test results over the office method predictions (K_{sw}) vs. blow count at the time of measurement for all PD/LT pile-cases

Table 8. Statistical analysis of K coefficients for all PD/LT pile-cases.

Pile-Case Group	Ksw			Ksp			Kew		
	No.	Mean	Standard Deviation	No.	Mean	Standard Deviation	No.	Mean	Standard Deviation
AAA	206	1.367	0.5334	208	0.925	0.2932	206	0.712	0.1815
AAS	141	1.385	0.4758	141	0.942	0.3127	141	0.702	0.1771
AAC	51	1.443	0.6760	53	0.906	0.2689	51	0.681	0.1736
AAR	14	0.906	0.1922	14	0.827	0.1402	14	0.925	0.1073
AEA	97	1.478	0.6167	98	1.023	0.3073	97	0.743	0.1844
AES	58	1.534	0.5310	58	1.089	0.3244	58	0.742	0.1766
AEC	28	1.598	0.7576	29	0.971	0.2742	28	0.672	0.1729
AER	11	0.877	0.1957	11	0.810	0.1510	11	0.936	0.1132
ABA	109	1.268	0.4257	110	0.838	0.2509	109	0.684	0.1748
ABS	83	1.282	0.4049	83	0.840	0.2605	83	0.674	0.1731
ABC	23	1.254	0.5160	24	0.827	0.2354	23	0.692	0.1777
ABR	3	1.010	0.1667	3	0.888	0.0816	3	0.887	0.0890

Pile-case legend: **XXX :** - first letter denotes pile type: A=all piles, L=large displacement, S=small displacement.
- second letter denotes time of measurements: A=anytime, E=EOD, B=BOR.
- third letter denotes soil type: A=sand and silt, C=clay and till, and R=rock.

Table 8. Statistical analysis of K coefficients for all PD/LT pile-cases (continued).

Pile-Case Group	Ksw			Ksp			Kew		
	No.	Mean	Standard Deviation	No.	Mean	Standard Deviation	No.	Mean	Standard Deviation
SAA	44	1.250	0.5542	44	0.926	0.2445	44	0.796	0.1798
SAS	23	1.486	0.6127	23	1.021	0.2313	23	0.746	0.2028
SAC	8	1.132	0.4679	8	0.820	0.3172	8	0.738	0.0854
SAR	13	0.906	0.2001	13	0.822	0.1448	13	0.921	0.1104
SEA	29	1.252	0.5616	29	0.935	0.2616	29	0.802	0.1772
SES	14	1.530	0.6013	14	1.029	0.2606	14	0.715	0.1784
SEC	4	1.309	0.6067	4	0.949	0.4120	4	0.738	0.0797
SER	11	0.807	0.1957	11	0.810	0.1510	11	0.936	0.1132
SBA	15	1.247	0.5591	15	0.908	0.2150	15	0.784	0.1904
SBS	9	1.418	0.6604	9	1.009	0.1912	9	0.793	0.2392
SBC	4	0.955	0.2442	4	0.691	0.1436	4	0.737	0.1033
SBR	2	1.064	0.1960	2	0.888	0.1154	2	0.839	0.0461

Pile-case legend: XXX : - first letter denotes pile type: A=all piles, L=large displacement, S=small displacement.
- second letter denotes time of measurements: A=anytime, E=EOD, B=BOR.
- third letter denotes soil type: A=all soils, S=sand and silt, C=clay and till, and R=rock.

(AAA). As indicated in chapter 6, the blow count per inch was often calculated based on records of blows per foot.

There is considerable scatter for all driving resistances (especially at the two extremes, namely, very low blow count (less than 10 BPI) and very high blows) at refusal (no set). It also can be noted that the predictions for the small displacement piles present, on average, much better performance than that of the large displacement piles, including the area of low driving resistance.

Figure 74 presents the ratio between the load test results to the Energy Approach predictions (K_{sp}), in the same format as that of figure 73. Considerably less scatter appears in the figure compared to that of figure 73. A large range of K_{sp} (from over-prediction of $K_{sp} \approx 0.4$ to under-prediction of about $K_{sp} \approx 1.7$) appears at the range of small resistance to driving of about 0 to 10 BPI. A few additional observations can be made in relationship to figure 74:

- In the majority of the cases, the Energy Approach over-predicts, however, there is improvement with the increase of driving resistance.
- Most of the significant under-predictions exist in the low-resistance zone.
- Very good performance appears at very high driving resistance, when actually no displacement takes place under each blow.

8.5.4 Dynamic Predictions - Driving Resistance and Time of Driving Graphical Correlations

Additional subdivision of the dynamic analyses prediction ratios vs. driving resistance was conducted based on the time of driving, namely, end of driving (EOD) and beginning of restrike (BOR).

(a) All Piles at EOD

Figure 75 presents the correlation between driving resistance and K_{sw} coefficient for all piles at EOD (AEA) and the results indicate a scatter similar to the results shown in figure 73. A major scatter remains at low driving resistances when the full resistance of the soil is mobilized.

The correlation between the K_{sp} coefficients for all piles in all soil types at EOD (AEA) and driving resistance is presented in figure 76, and the results are similar to those of figure 60. This is consistent with the findings of sections 8.3 and 8.4 for piles at the end of driving, with the emphasis on under-prediction cases at the low-resistance zone. Most of the under-prediction cases observed in figure 74 for the low blow count seem to be a result of the EOD cases as shown in figure 76. These cases are confined, however,

mostly within a zone of blow count between 0 to 6 BPI, which may, as a result, be defined as "easy driving."

(b) All Piles at BOR

Figure 77 represents the relationship of driving resistance and K_{sw} -values for all piles at BOR (ABA). A scatter among the predictions for driving resistances ranging from 0 to 25 blows per inch (0.98 blows per mm) is observed. The scatter appears, however, to be substantially smaller than that observed for EOD in figure 75, with lower under-predictions.

In both cases (EOD and BOR), the office analysis predictions produced a scatter. At the BOR, however, a large concentration of cases appear around the $K_{sw}=1$ and the K_{sw} -values are lower cases than those observed in figure 75.

Figure 78 presents the relationship of driving resistance and K_{sp} -values for all piles at BOR (ABA). A major scatter, mostly to the over-prediction side, appears in figure 78. When comparing figures 76 and 78 to figure 74, it appears that:

- The Energy Approach tends to over-predict at the low driving resistance for BOR cases and under-predict at the EOD cases. It should be emphasized that both under-prediction and over-prediction at the low-resistance zone appears in both EOD and BOR. The extreme over-predictions, however, exist only at the BOR and the extreme under-predictions exist only at the EOD.
- On the average, the performance of the Energy Approach at EOD is better than that at BOR, especially for piles with driving resistances greater than 6 BPI (0.24 blows per mm).

8.5.5 Dynamic Predictions - Driving Resistance and Pile-Type Graphical Correlations

Section 8.5.2 examined the relationship between the dynamic predictions and the pile area ratio and concluded that small displacement piles can be referred to as piles with $A_R > 350$. Section 8.5.3 examined the relationship between the dynamic predictions and the driving resistance and determined the effect of the driving resistance on the accuracy of the predictions of both dynamic analyses.

The subdivision of the dynamic predictions vs. driving resistance to small and large displacement, based on the pile area ratio definition, is presented in this section.

(a) Small Displacement Piles

The relationship between K_{sw} and the driving resistance for small displacement piles with $A_R > 350$ is presented in figure 79. The office analysis, in general, appears to perform better for small displacement piles than for the large displacement piles. When

comparing the data in figure 79 to that of 69 and 70, a relatively good agreement exists between the predicted and observed capacity with the exception of very low and very high driving resistances. This agreement suggests that the relatively high under-predictions of the office methods for the small displacement piles are associated with either very low driving resistances (which result in high inertia of the soil mass) of less than 6 BPI (0.24 blows per mm), or a very high driving resistance (which results in a lack of full-capacity mobilization). In relationship to figure 79 and the following figures, it should be clear that the criteria for distinguishing between small and large displacement piles is the area ratio of $A_R=350$. As such, the open symbols in those figures refer to piles that, by observation, would be considered as large displacement piles (e.g., square concrete pile), however, their area ratio of $A_R>350$ would categorize them as small displacement piles as explained in section 4.4 and concluded in section 8.5.2.

Figure 80 presents the relationship between driving resistance and K_{sp} for piles with $A_R>350$. Excellent agreement exists between the predictions of the Energy Approach and the observed static capacity for all driving resistances. Two major conclusions can be made regarding the data in figure 80:

- The influence of the pile type on the performance of the dynamic methods is evident. The mean K_{sp} for figure 80 is 0.938 with a standard deviation of 0.239, which indicates an excellent performance.
- The highest scatter and over- and under-predictions occur at the lower resistance zone of less than 6 BPI (0.24 blows per mm).

In reference to figures 79 and 80, it should be noted that with the new definition of small/large displacement piles based on the pile area ratio of 350, the piles that were previously considered as large displacement (i.e., open symbols) fit well into the general trend of the small displacement piles.

(b) Large Displacement Piles

Figures 81 and 82 present the relationships between K_{sw} and K_{sp} to the driving resistance for large displacement (pile area ratio <350), respectively. The data in figure 81 indicates that substantial scatter appears in the predictions of the office method. Over-prediction takes place especially for the low blow count (figure 79) and under-predictions appear to exist for all driving resistances. When compared to predictions of the small displacement piles (figure 79), the existing scatter and under-prediction seem to be much more significant.

Figure 82 indicates that much larger scatter and inaccuracy in prediction exists for the large displacement piles when compared to the small displacement piles (figure 80). The inaccuracy is, however, highly related to the driving resistance with a decrease in scatter (mainly due to the decrease in the under-prediction) and an increase in accuracy with

the increase in the driving resistance. The predictions above approximately 10 BPI (0.39 blows per mm) seem to be much better than those below that resistance.

8.5.6 The Effect of the Combined Major Controlling Parameters on the Accuracy of the Dynamic Predictions

(a) Breakdown of Combinations

The previous correlations that were presented throughout chapter 8 indicated the following factors as the major controlling parameters:

- Pile type, according to the pile area ratio, distinguishing between large displacement piles with $A_R < 350$ and small displacement piles with $A_R > 350$.
- Time of driving, distinguishing between end of driving (EOD) records to analyses on records obtained at some time later at the beginning of restrike (BOR).
- Driving resistance, distinguishing between easy driving of less than 6 BPI (0.24 blows per mm) to intermediate driving resistance between 6 and 12 BPI (0.24 and 0.47 blows per mm) with high driving resistance above 12 BPI (0.47 blows per mm).
- Type of soil, distinguishing between predictions of piles predominately in clay vs. those driven in granular materials.

Different combinations of these factors are presented in the following sections with a summary of their statistical data presented in table 9.

(b) Combinations of Pile Type and Driving Resistance

The previously mentioned criteria for pile type and driving resistance assisted in establishing the following combinations:

- (1) Small displacement piles with easy driving; $A_R > 350$ and blow count < 6 BPI (0.24 blows per mm) shown in figures 83 and 84 for K_{sw} and K_{sp} , respectively.
- (2) Small displacement piles with hard driving; $A_R > 350$ and blow count > 6 BPI (0.24 blows per mm) shown in figures 85 and 86 for K_{sw} and K_{sp} , respectively.
- (3) Large displacement piles with easy driving; $A_R < 350$ and blow count < 6 BPI (0.24 blows per mm) shown in figures 87 and 88 for K_{sw} and K_{sp} , respectively.

Table 9. Statistical analysis of the area ratio, resistance, and time of driving combination.

Pile Area Ratio	Driving Resistance	Time of Driving	Ksw			Ksp		
			No.	Mean	Standard Deviation	No.	Mean	Standard Deviation
<350	all piles	anytime	144	1.427	0.543	146	0.920	0.317
<350	0-6 BPI	anytime	64	1.374	0.512	64	0.962	0.347
<350	> 6 BPI	anytime	80	1.469	0.567	82	0.887	0.288
<350	all piles	EOD	56	1.643	0.654	57	1.068	0.345
<350	0-6 BPI	EOD	36	1.545	0.569	36	1.102	0.349
<350	> 6 BPI	EOD	20	1.820	0.769	21	1.026	0.340
<350	all piles	BOR	88	1.290	0.407	89	0.825	0.257
<350	0-6 BPI	BOR	28	1.155	0.319	28	0.783	0.254
<350	> 6 BPI	BOR	60	1.352	0.430	61	0.844	0.258
>350	all piles	anytime	57	1.247	0.502	57	0.938	0.239
>350	0-6 BPI	anytime	16	1.542	0.595	16	1.031	0.259
>350	> 6 BPI	anytime	41	1.133	0.414	41	0.902	0.224
>350	all piles	EOD	39	1.151	0.408	39	0.902	0.240
>350	0-6 BPI	EOD	12	1.476	0.492	12	1.021	0.291
>350	> 6 BPI	EOD	27	1.161	0.473	27	0.928	0.214
>350	all piles	BOR	18	1.225	0.530	18	0.897	0.240
>350	0-6 BPI	BOR	4	1.740	0.901	4	1.062	0.154
>350	> 6 BPI	BOR	14	1.078	0.274	14	0.850	0.243

1 BPI = 0.039 blows per mm

Pile-case legend:

- <350 - pile area ratio definition of large displacement piles.
- >350 - pile area ratio definition of small displacement piles.
- 0-6 BPI - low driving resistance, resulting in full mobilization of the soil resistance.
- > 6 BPI - intermediate (6 to 12 BPI) and high driving resistance of more than 12 BPI.

- (4) Large displacement piles with hard driving; $A_R < 350$ and blow count > 6 BPI (0.24 blows per mm) shown in figures 89 and 90 for K_{sw} and K_{sp} , respectively.

The above four combinations clearly suggest (with the limitation of the small number of pile-cases for some combinations):

- Small displacement piles with high driving resistance present very good prediction conditions for the dynamic methods.
- These conditions are followed by the predictions for small displacement piles with easy driving resistance (especially for the Energy Approach).
- Less favorable conditions result from the predictions of large displacement piles with high resistance (especially for the office methods).
- The worst conditions are presented for the large displacement piles with easy driving where both dynamic methods predict poorly with a high scatter.

(c) Combinations of Pile Type, Driving Resistance, and Time of Driving

The above combinations were further investigated, incorporating the time of driving into the above criteria as follows:

- (I) Small displacement piles with easy driving at the end of driving; $A_R > 350$ and blow count < 6 BPI (0.24 blows per mm) shown in figures 91 and 92 for K_{sw} and K_{sp} , respectively.
- (II) Small displacement piles with hard driving at the end of driving; $A_R > 350$ and blow count > 6 BPI (0.24 blows per mm) shown in figures 93 and 94 for K_{sw} and K_{sp} , respectively.
- (III) Large displacement piles with easy driving at the end of driving; $A_R < 350$ and blow count < 6 BPI (0.24 blows per mm) shown in figures 95 and 96 for K_{sw} and K_{sp} , respectively.
- (IV) Large displacement piles with hard driving at the end of driving; $A_R < 350$ and blow count > 6 BPI (0.24 blows per mm) shown in figures 97 and 98 for K_{sw} and K_{sp} , respectively.
- (V) Small displacement piles at the beginning of restrrike for all driving resistances; $A_R > 350$ shown in figures 99 and 100 for K_{sw} and K_{sp} , respectively.

- (VI) Large displacement piles at the beginning of restrike for all driving resistances; $A_R < 350$ shown in figures 101 and 102 for K_{sw} and K_{sp} respectively.

These combinations again suggest the following trends (with the limitation of the small number of pile-cases for some combinations):

- Small displacement piles at the end of driving (EOD) with high driving resistance present very good prediction conditions for the office methods and even better conditions for the predictions of the Energy Approach.
- The office methods present a considerable scatter for large displacement piles at the end of driving, especially in the cases with high driving resistance. The Energy Approach presents very good predictions under these conditions as can be observed for the 20 pile-cases shown in figure 98.
- The prediction conditions for small displacement piles at EOD with low driving resistance presented difficulties for the office methods, while good predictions were obtained by the Energy Approach. Again, this conclusion may be affected by the limited number of pile-cases for this combination.
- The least favorable prediction conditions for the end of driving state for the office methods occur for large displacement piles with high driving resistance.
- The prediction conditions for small displacement piles at BOR with all driving resistances yield good results for the Energy Approach and a moderate scatter for the office predictions. This conclusion should once again be subjected to the limited number of pile-cases for this combination.
- Small variation was observed between easy and hard driving resistances that may have been the result of the scatter produced in both methods.

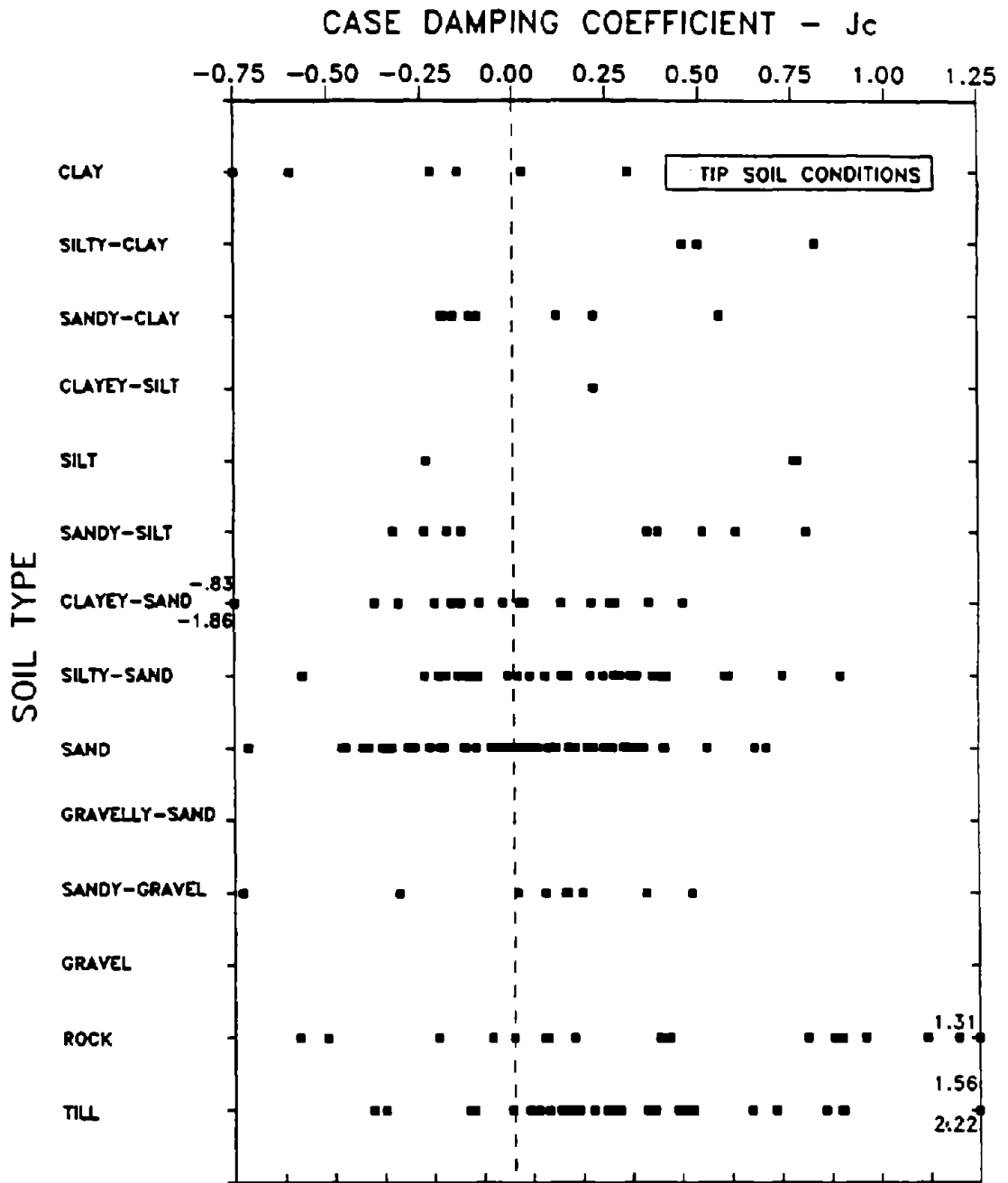


Figure 21. Tip soil conditions vs. calculated case damping coefficient (J_c) based on static load test results for 208 PD/LT pile-cases.

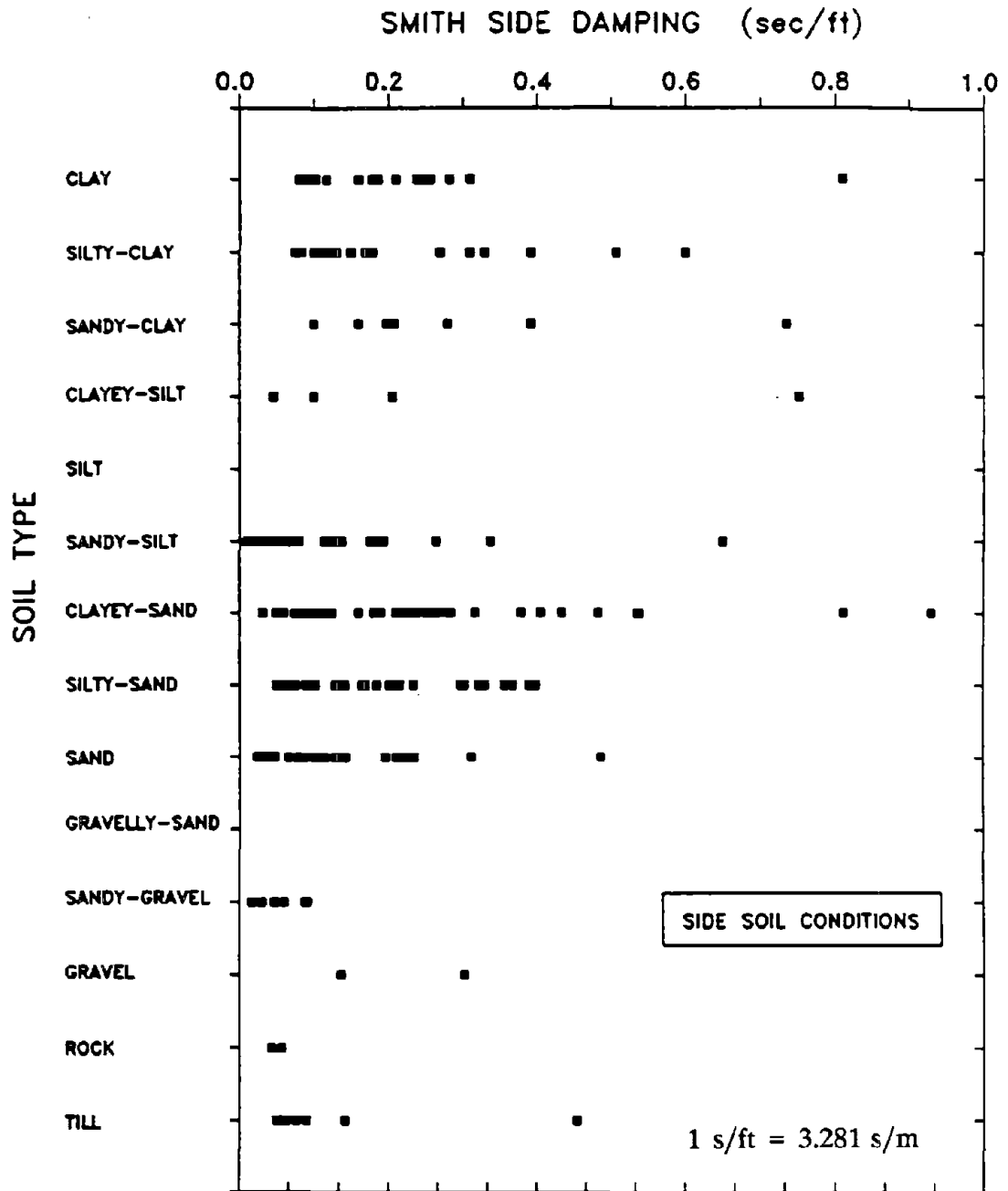


Figure 22. Side soil conditions vs. Smith side damping coefficient based on CAPWAP/TEPWAP results.

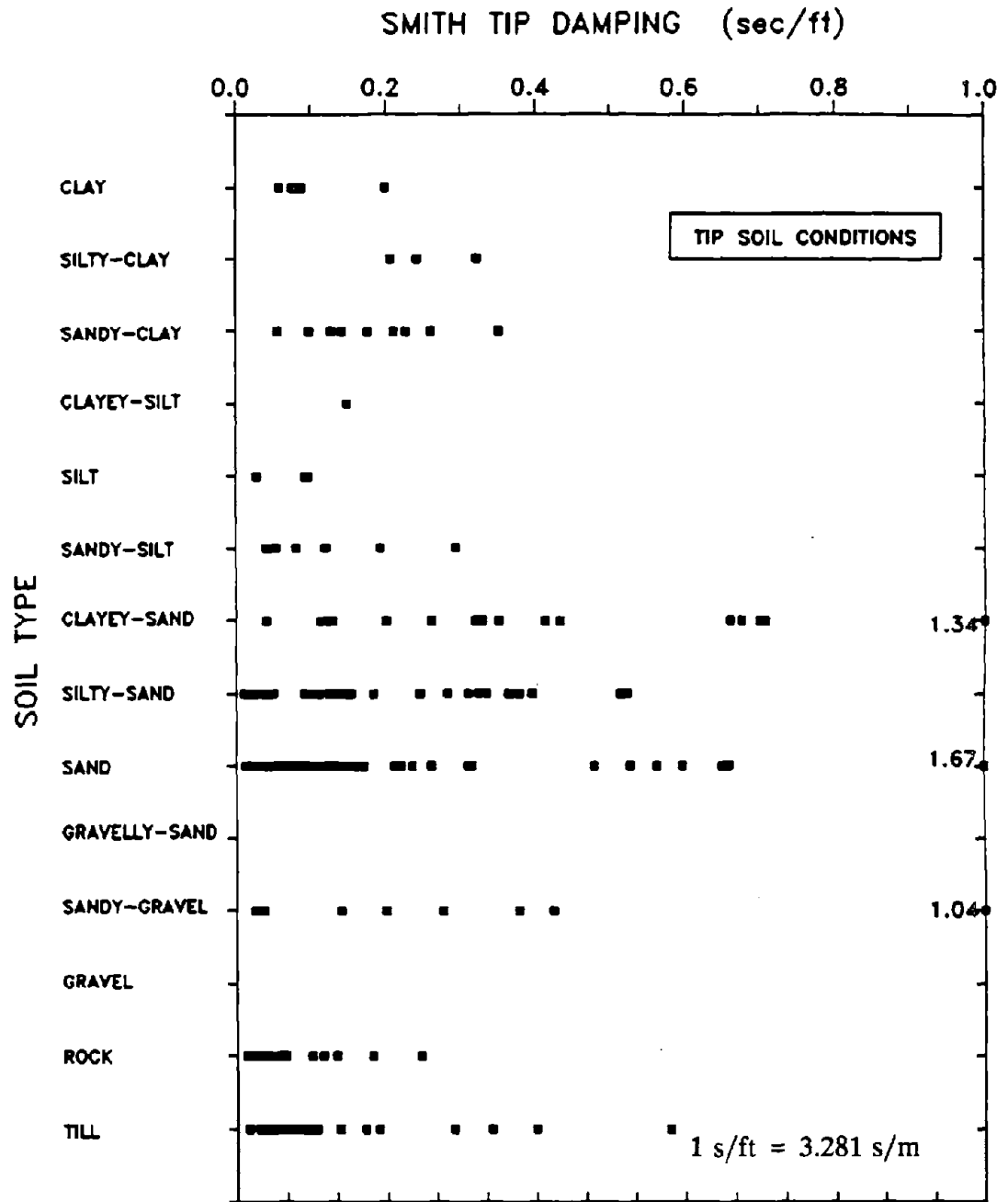


Figure 23. Tip soil conditions vs. Smith tip damping coefficient based on CAPWAP/TEPWAP results.

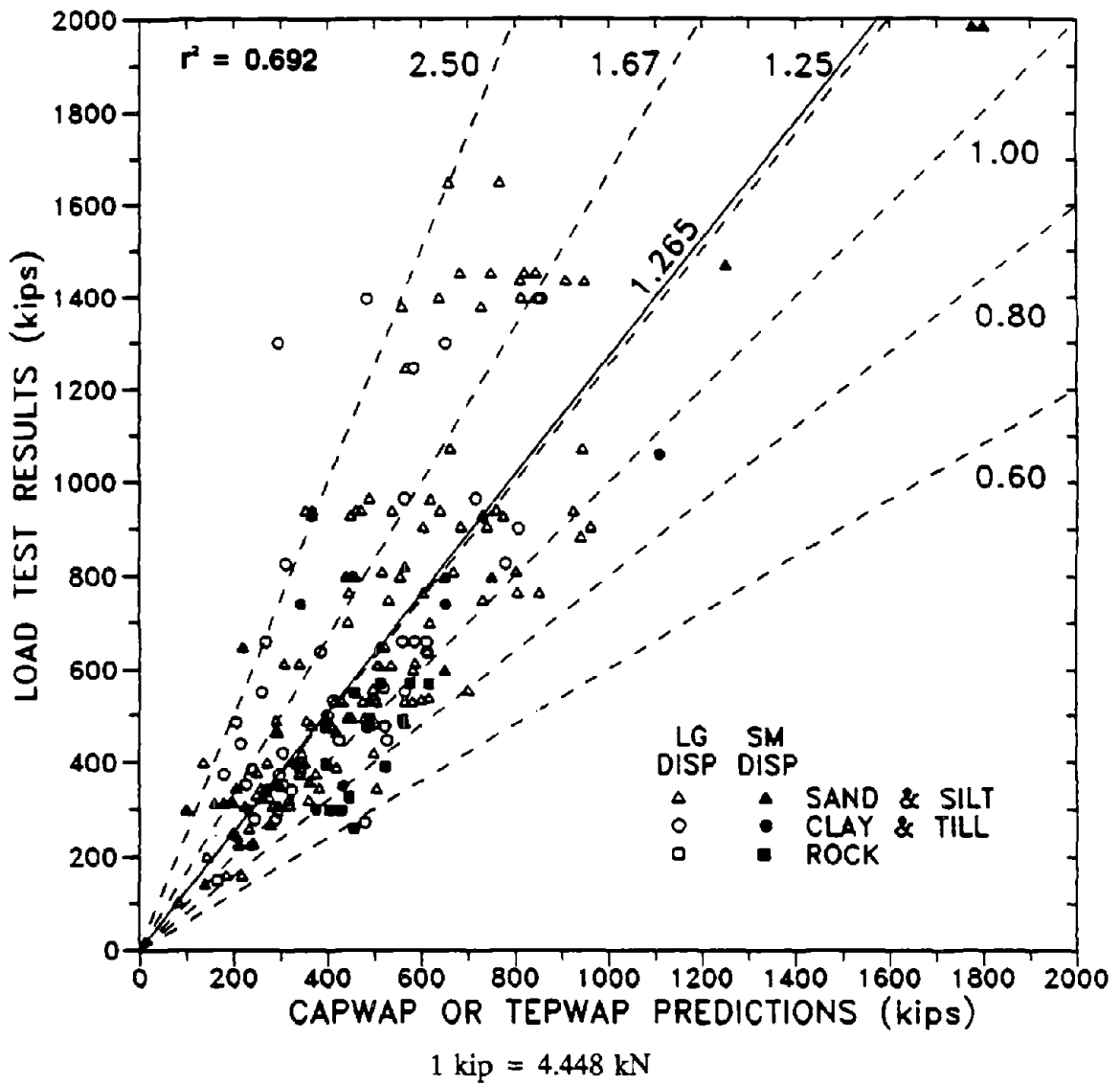


Figure 24. Static load test results vs. CAPWAP or TEPWAP predictions for 204 PD/LT pile-cases in all types of soil (AAA).

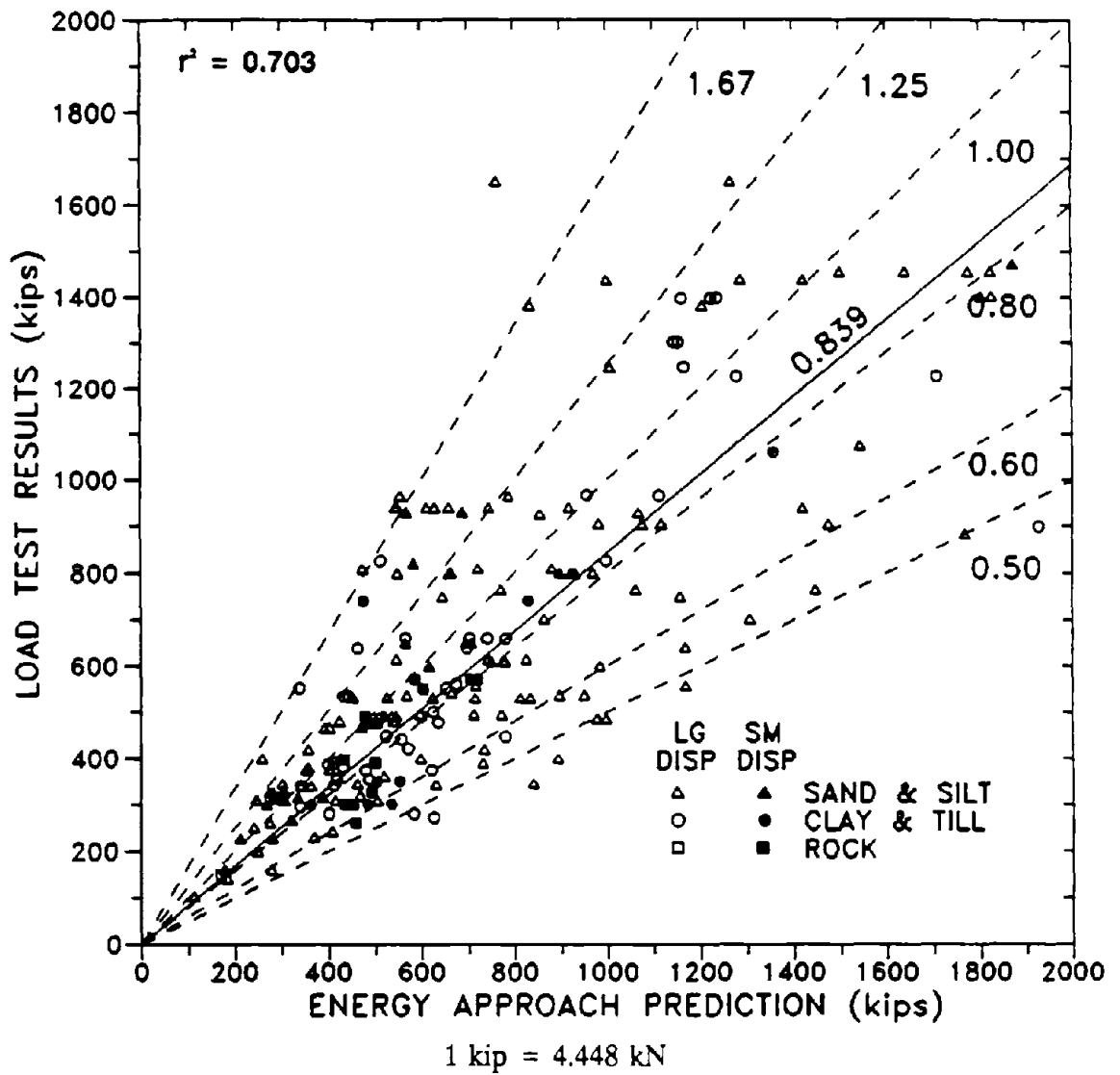


Figure 25. Static load test results vs. Energy Approach predictions for 202 PD/LT pile-cases in all types of soil (AAA).

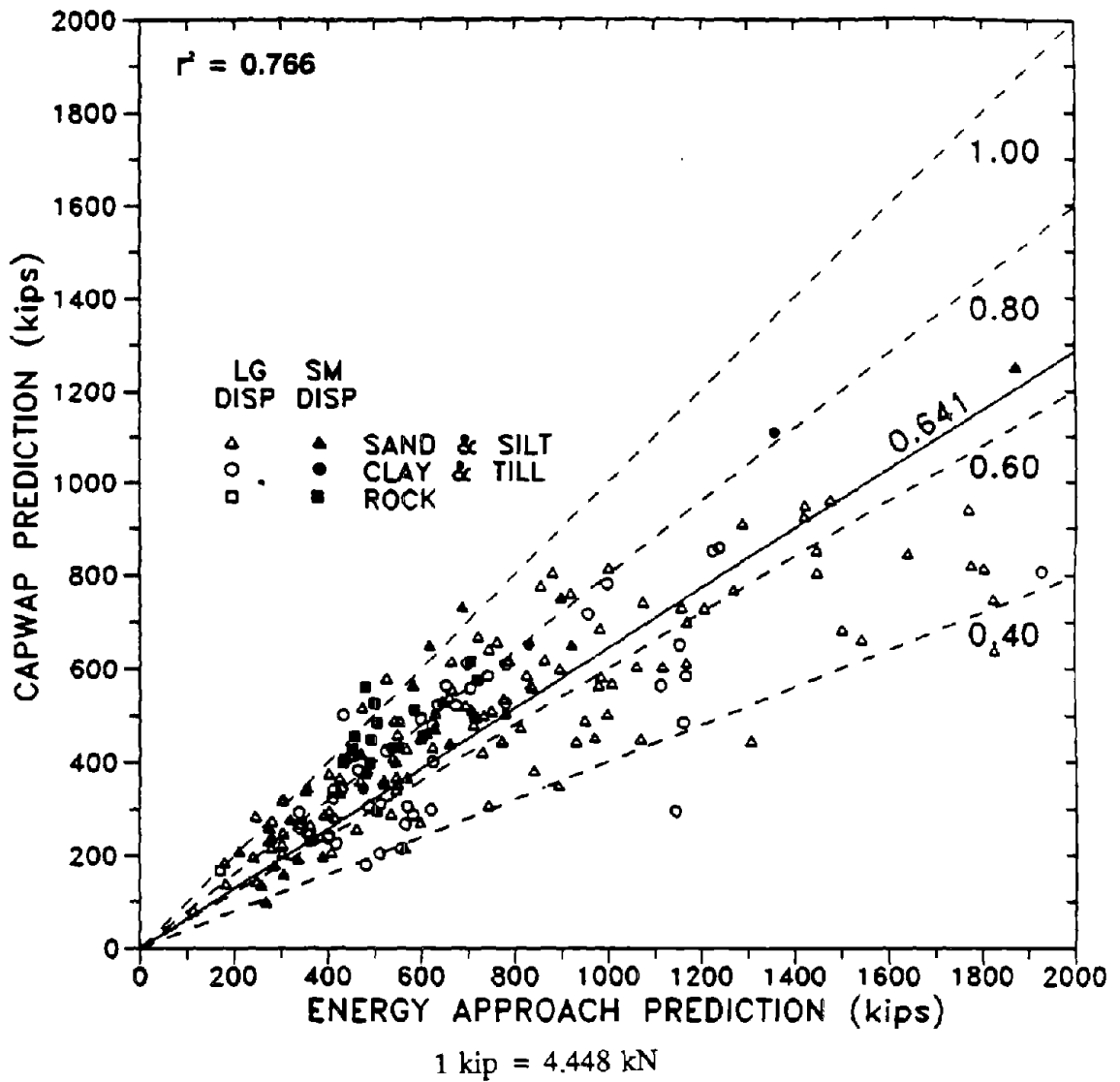


Figure 26. CAPWAP or TEPWAP predictions vs. Energy Approach predictions for 201 PD/LT pile-cases in all types of soil (AAA).

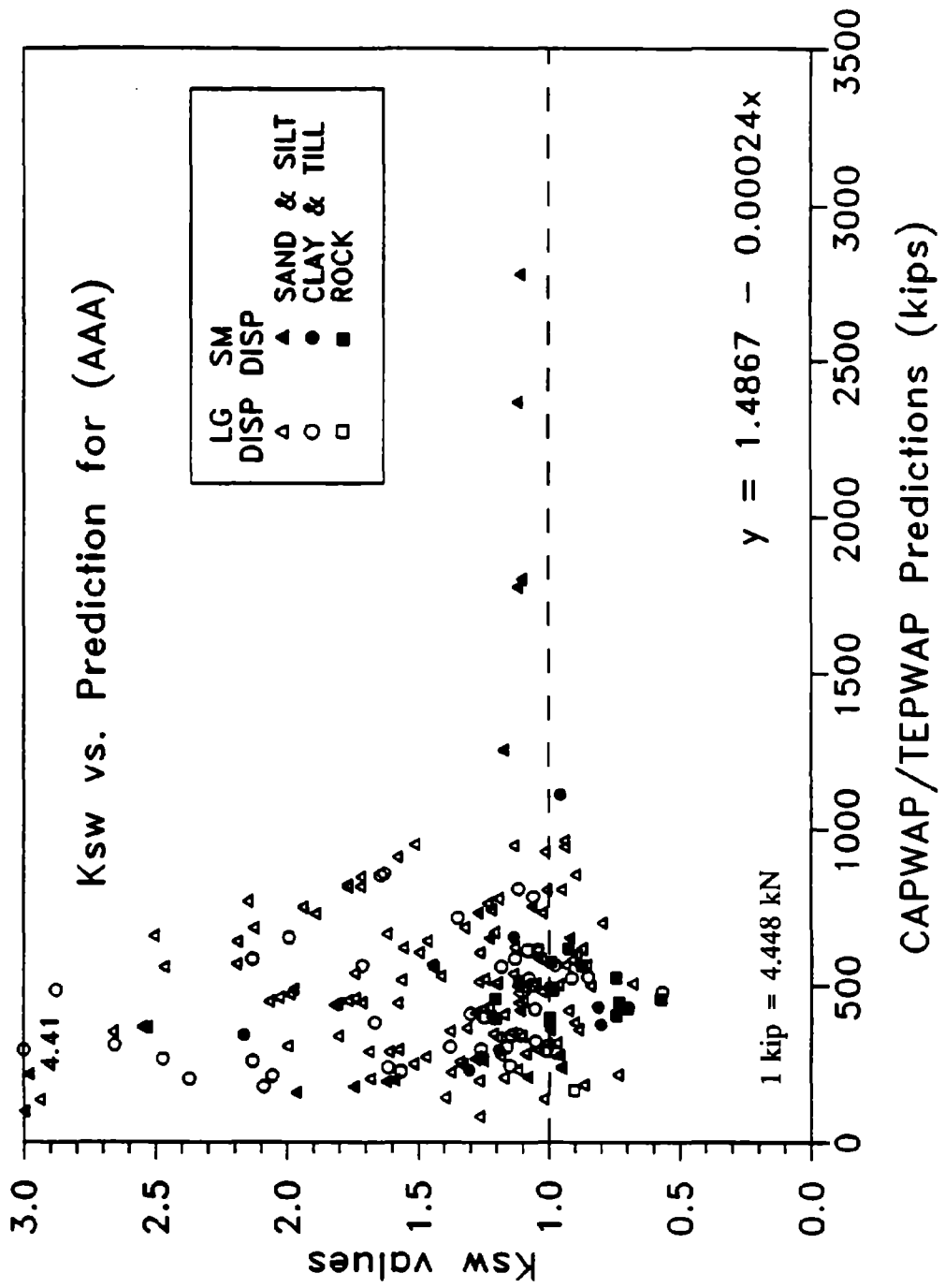


Figure 27. K_{sw} vs. CAPWAP/TEPWAP predictions for 206 PD/LT pile-cases in all types of soil (AAA).

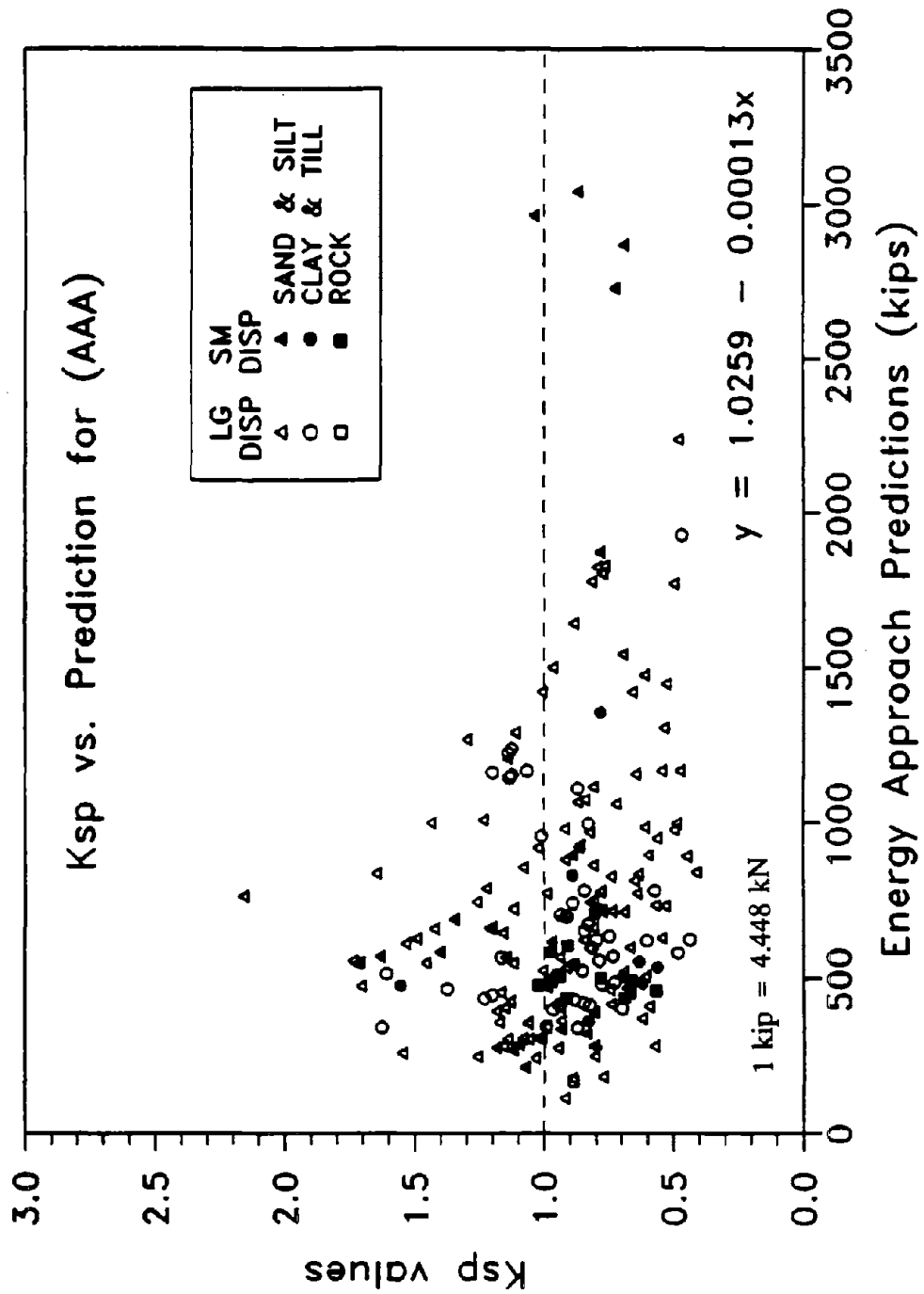


Figure 28. K_{sp} vs. Energy Approach predictions for 208 PD/LT pile-cases in all types of soil (AAA).

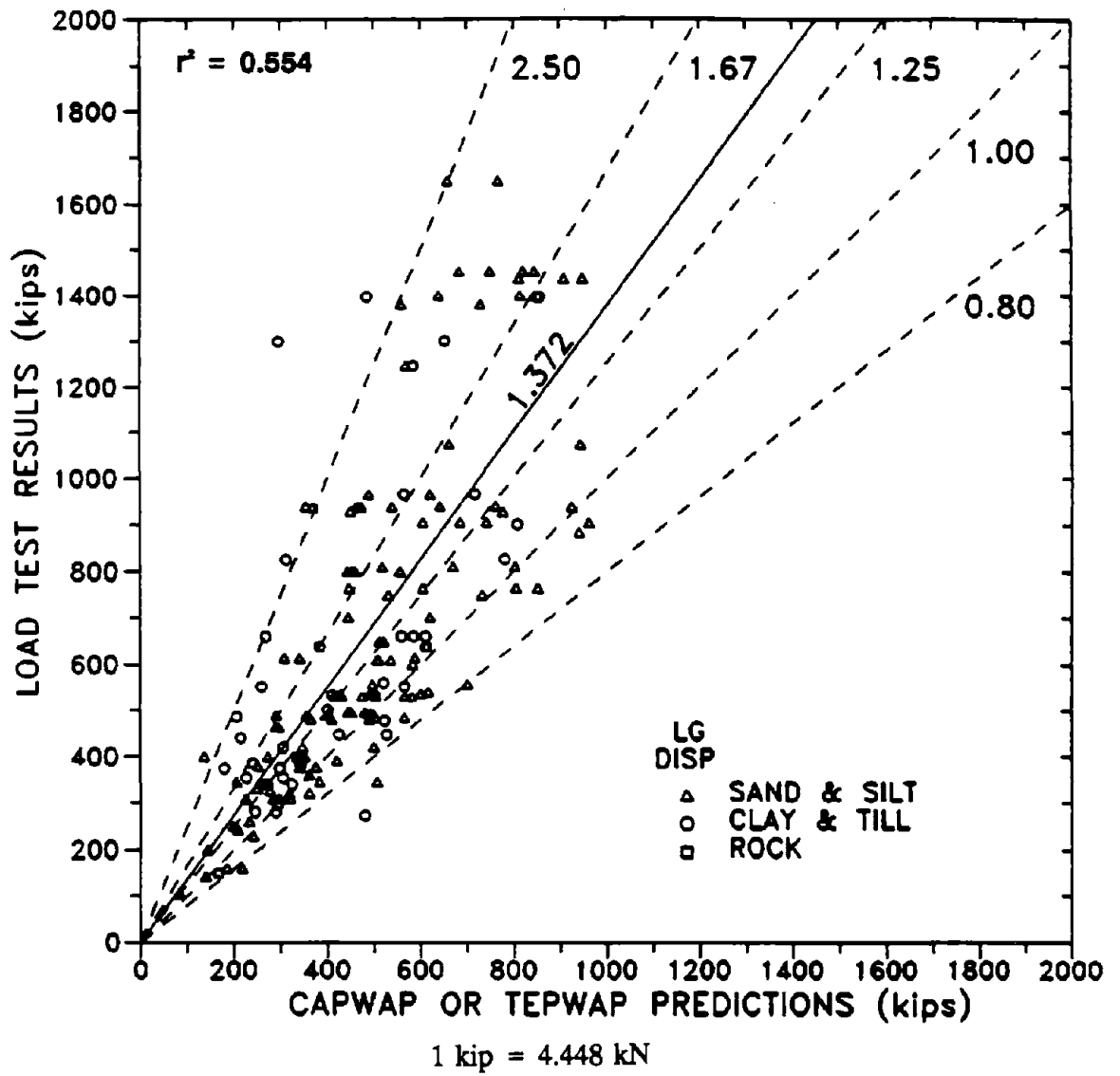
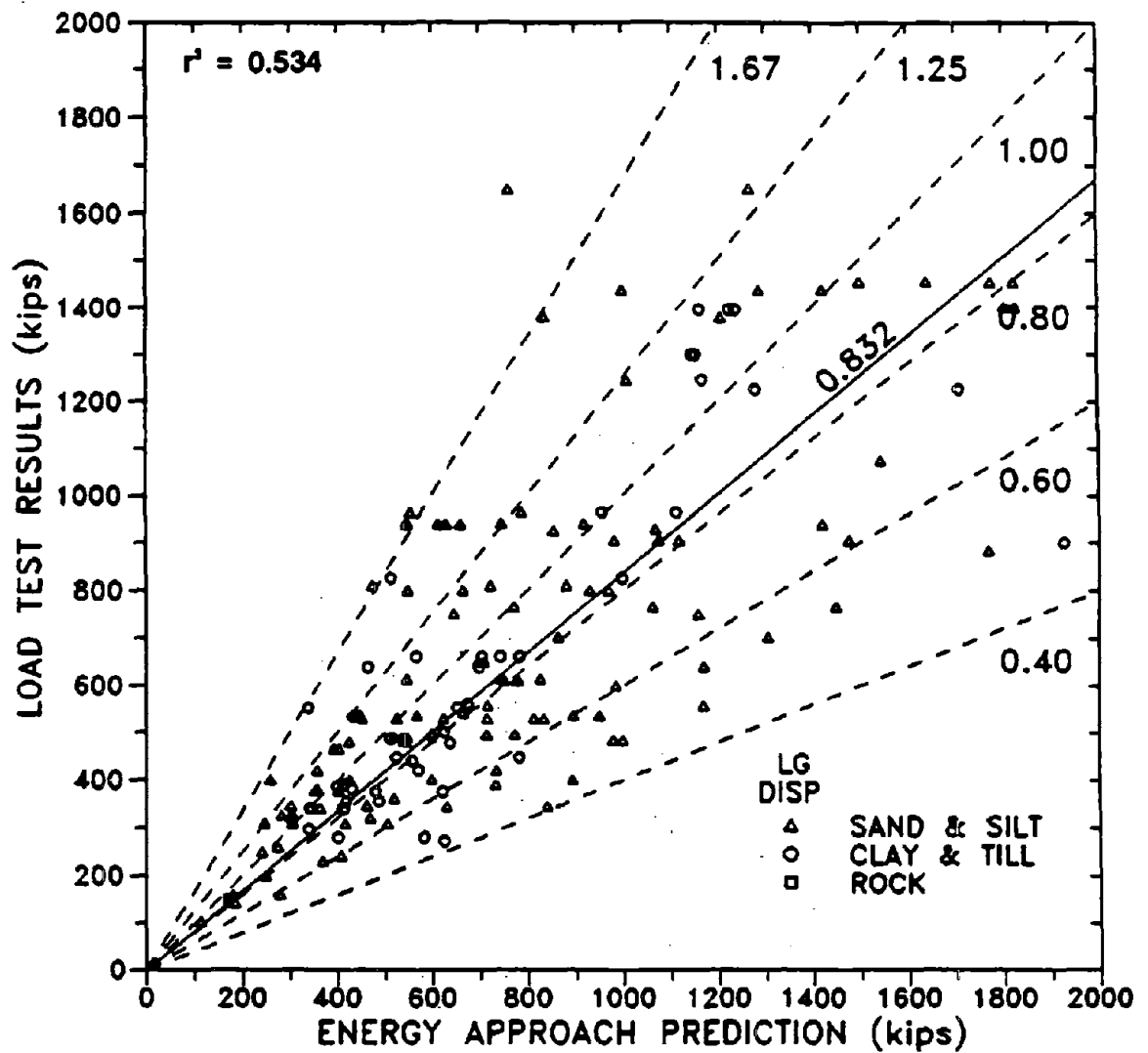
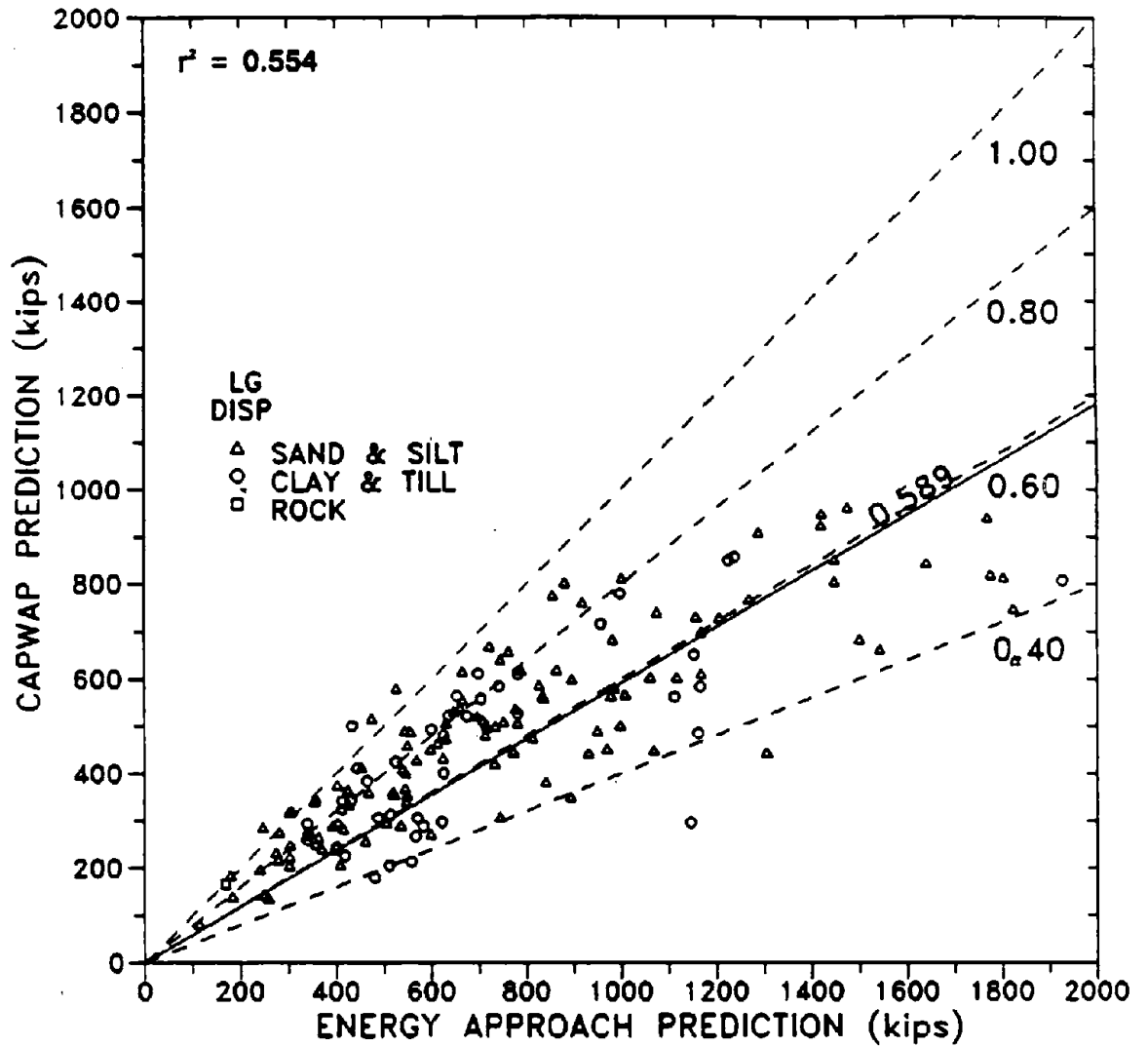


Figure 29. Static load test results vs. CAPWAP or TEPWAP predictions for 162 large displacement PD/LT pile-cases in all types of soil (LAA).



1 kip = 4.448 kN

Figure 30. Static load test results vs. Energy Approach predictions for 163 large displacement PD/LT pile-cases in all types of soil (LAA).



1 kip = 4.448 kN

Figure 31. CAPWAP or TEPWAP predictions vs. Energy Approach predictions for 161 large displacement PD/LT pile-cases in all types of soil (LAA).

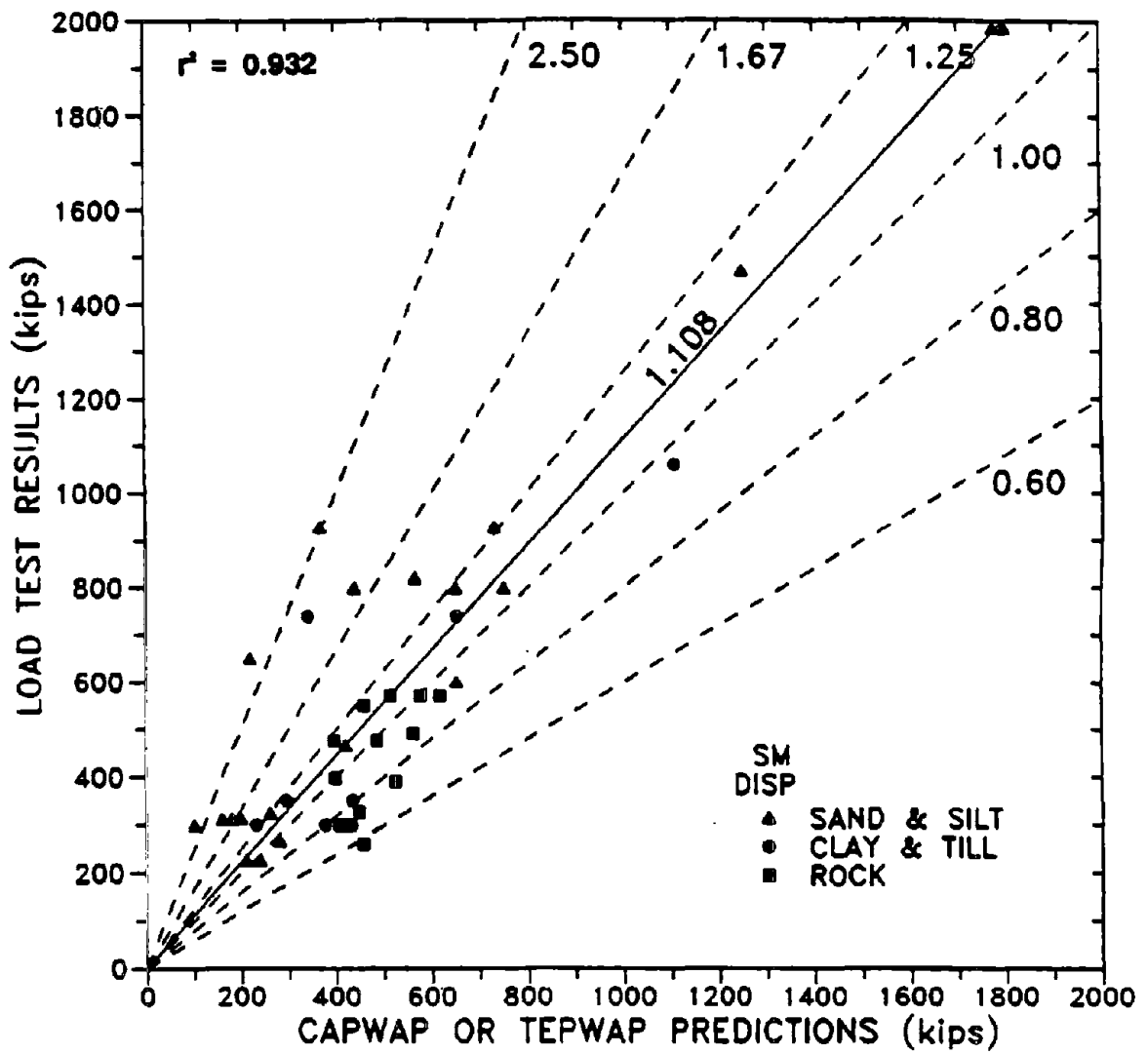
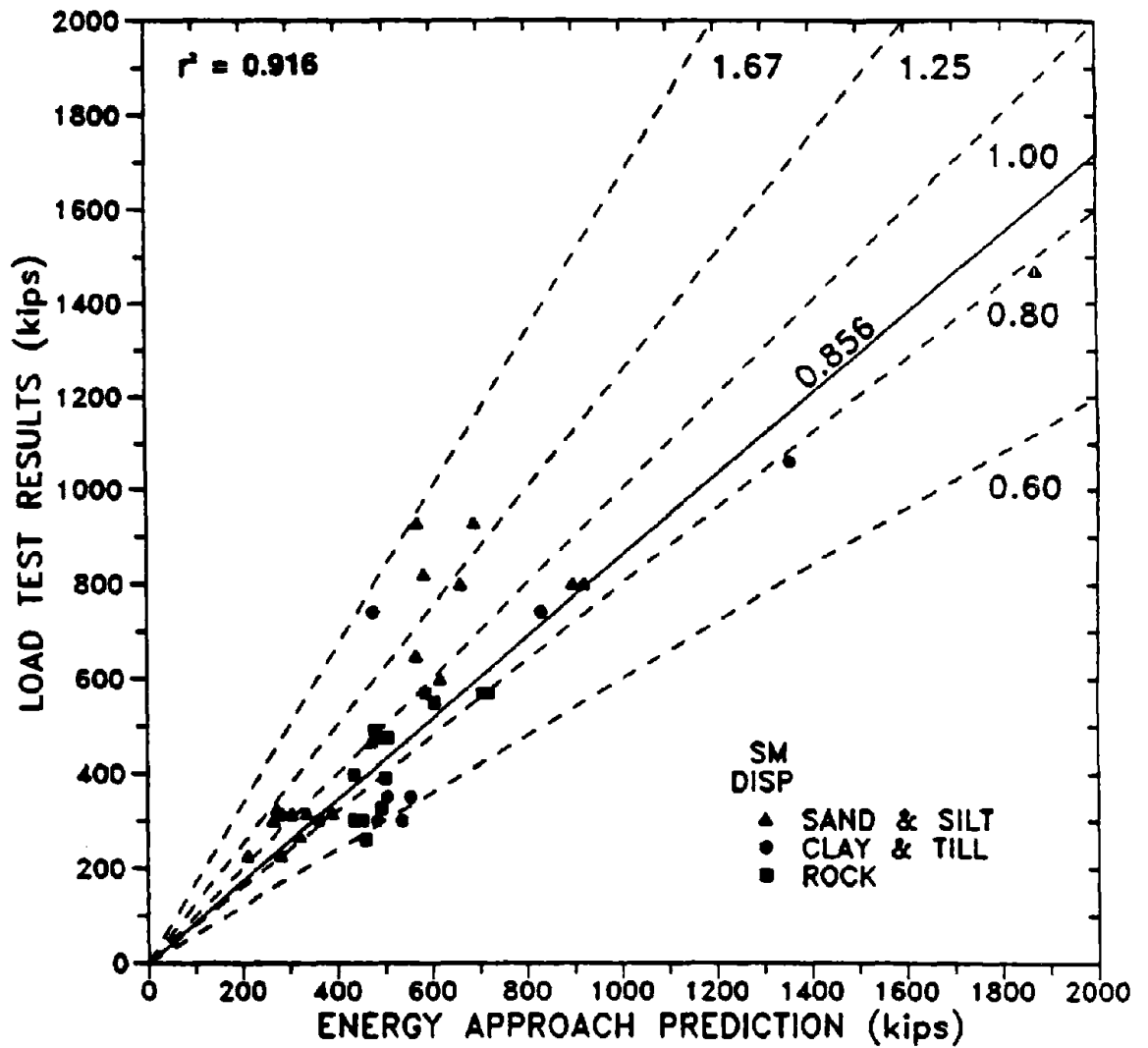
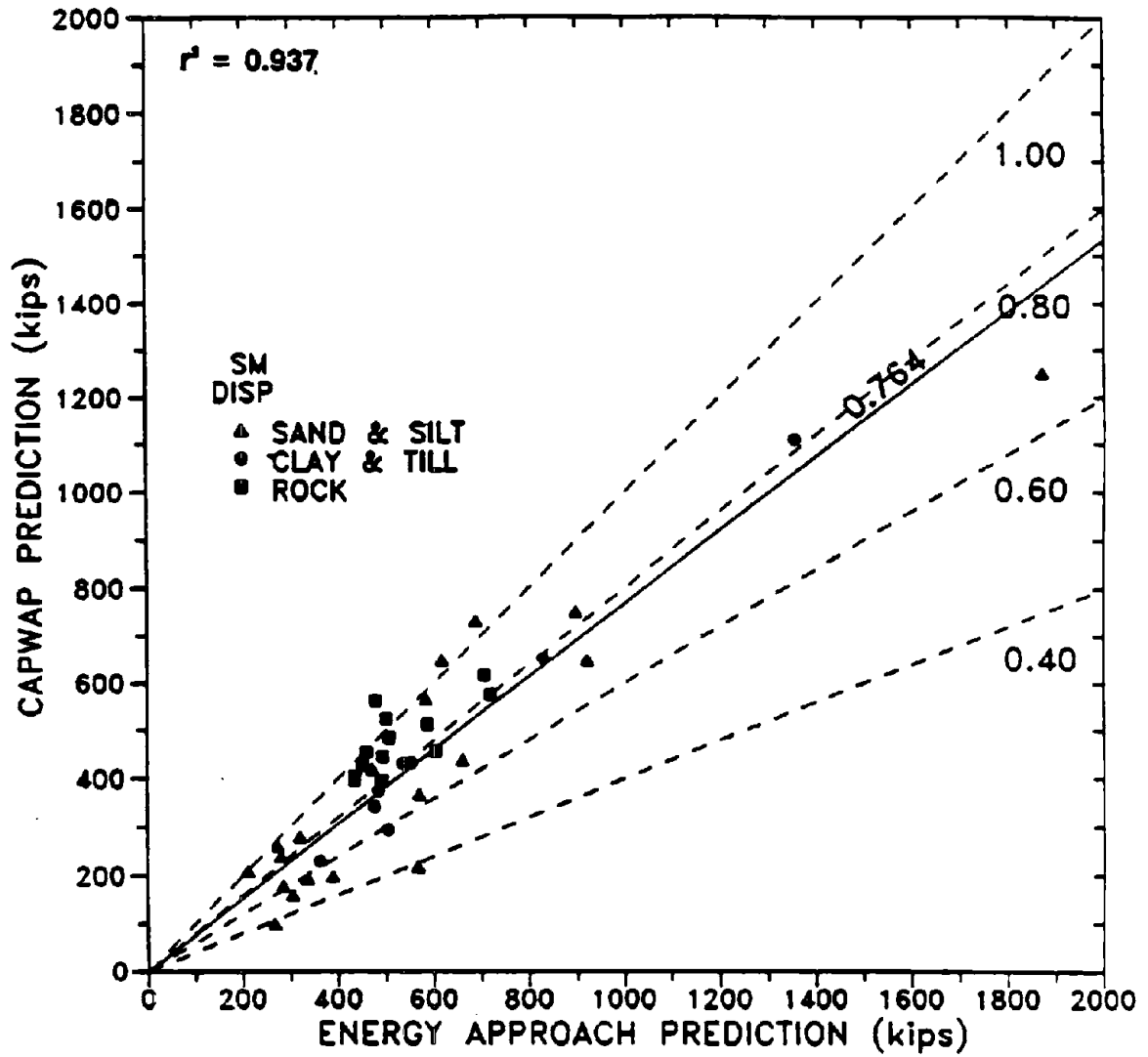


Figure 32. Static load test results vs. CAPWAP or TEPWAP predictions for 42 small displacement PD/LT pile-cases in all types of soil (SAA).



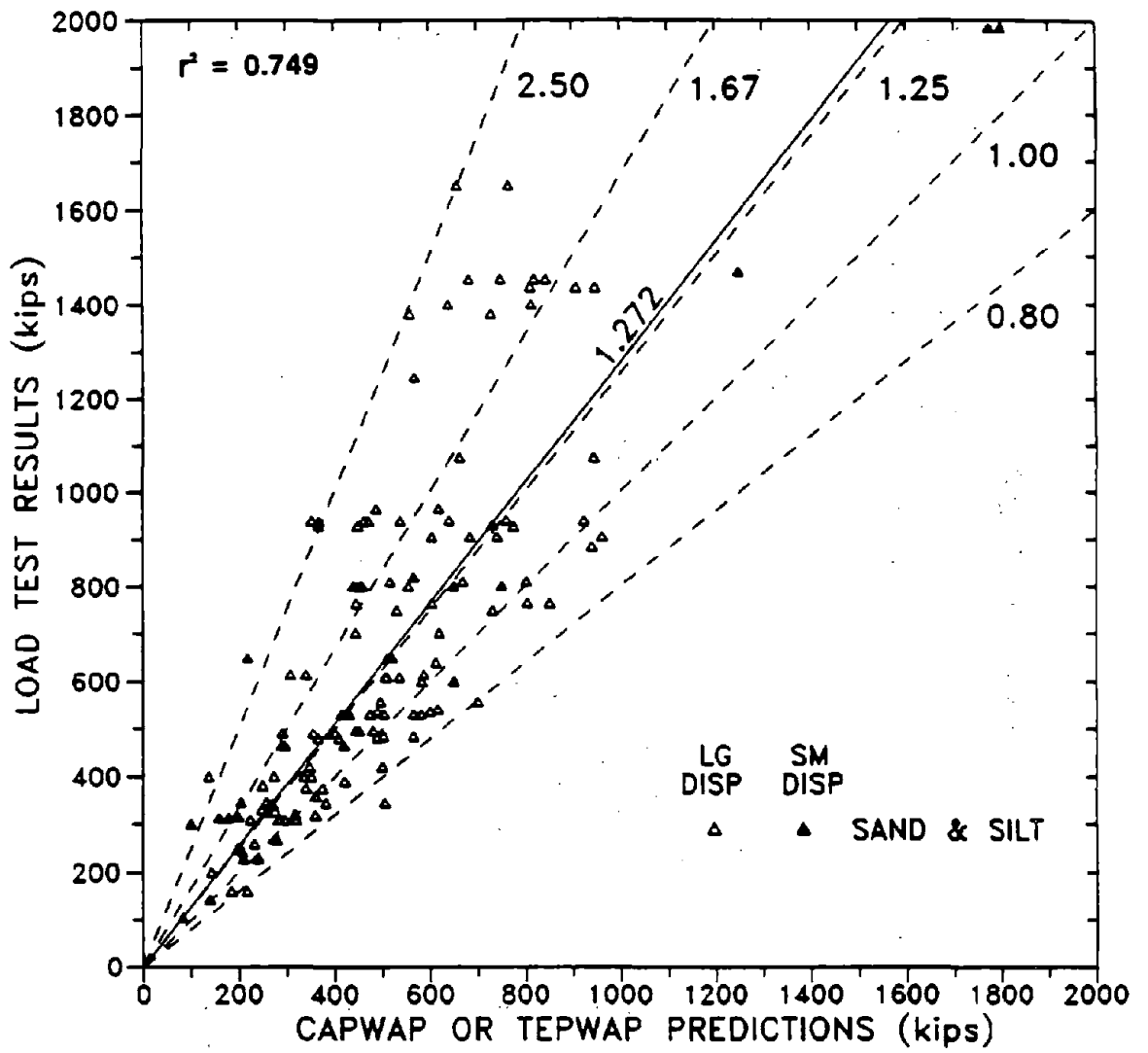
1 kip = 4.448 kN

Figure 33. Static load test results vs. Energy Approach predictions for 40 small displacement PD/LT pile-cases in all types of soil (SAA).



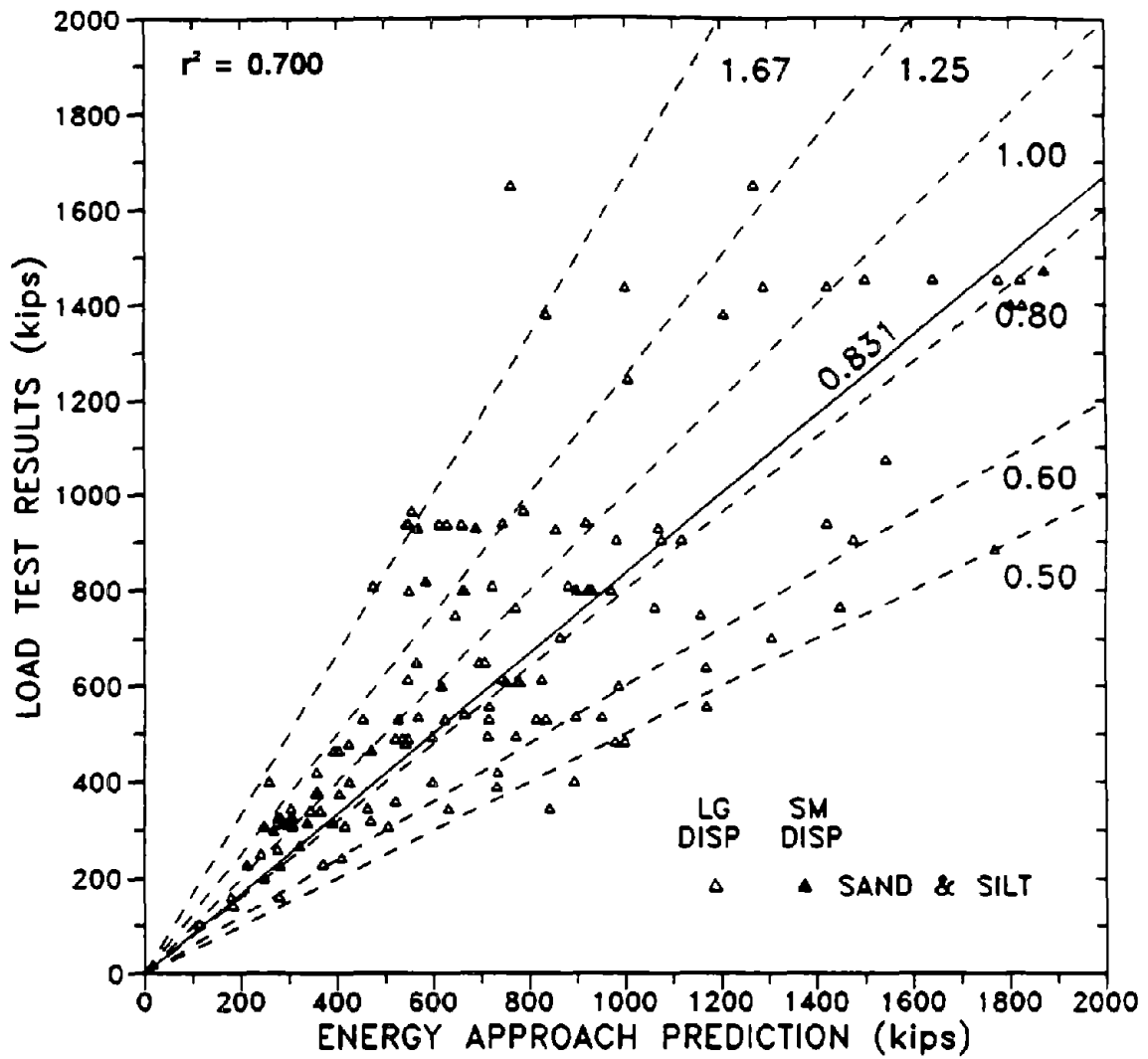
1 kip = 4.448 kN

Figure 34. CAPWAP or TEPWAP predictions vs. Energy Approach predictions for 38 small displacement PD/LT pile-cases in all types of soil (SAA).



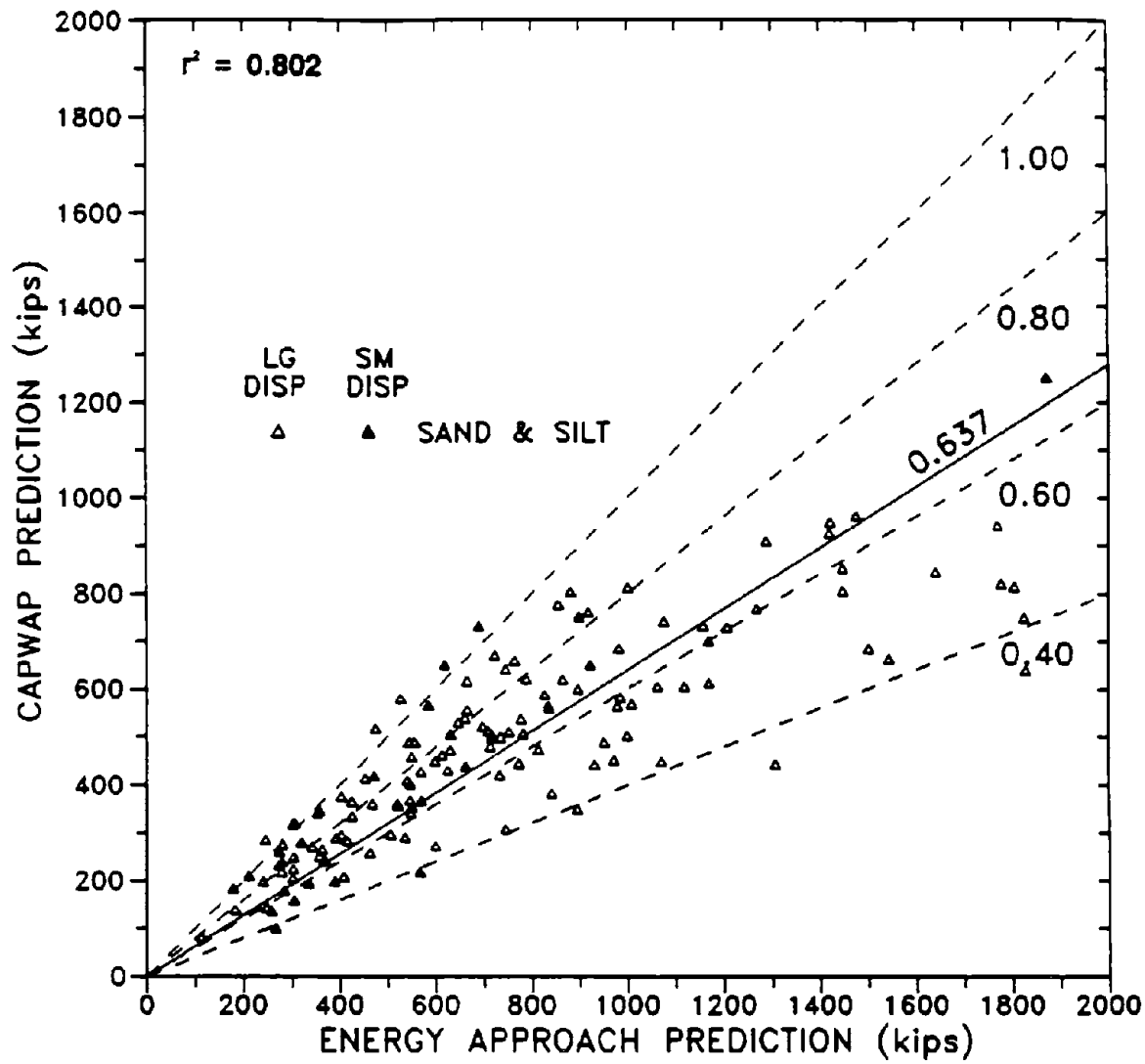
1 kip = 4.448 kN

Figure 35. Static load test results vs. CAPWAP or TEPWAP predictions for 139 PD/LT pile-cases in sand and silt (AAS).



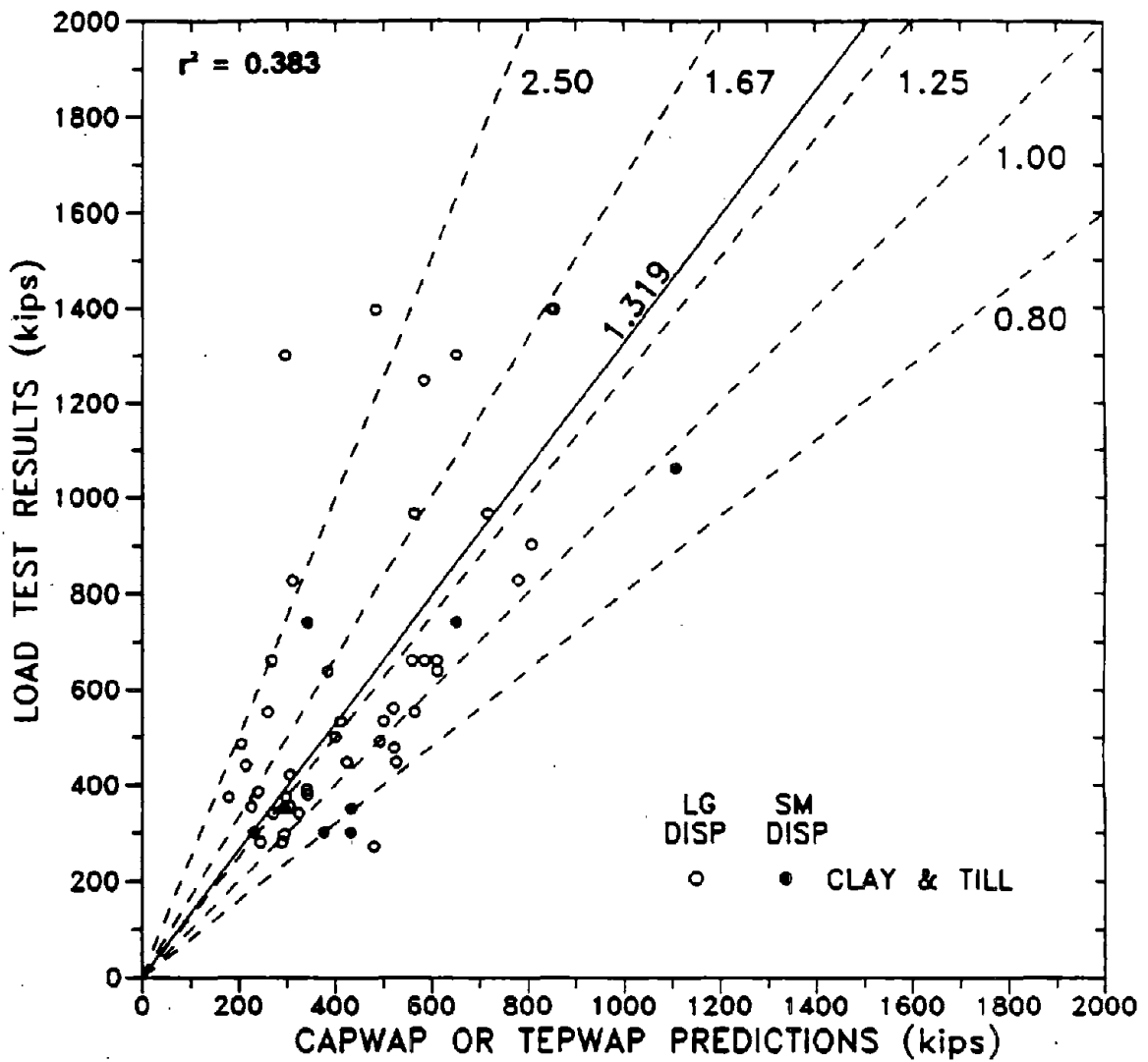
1 kip = 4.448 kN

Figure 36. Static load test results vs. Energy Approach predictions for 136 PD/LT pile-cases in sand and silt (AAS).



1 kip = 4.448 kN

Figure 37. CAPWAP or TEPWAP predictions vs. Energy Approach predictions for 136 PD/LT pile-cases in sand and silt (AAS).



1 kip = 4.448 kN

Figure 38. Static load test results vs. CAPWAP or TEPWAP predictions for 51 PD/LT pile-cases in clay and till (AAC).

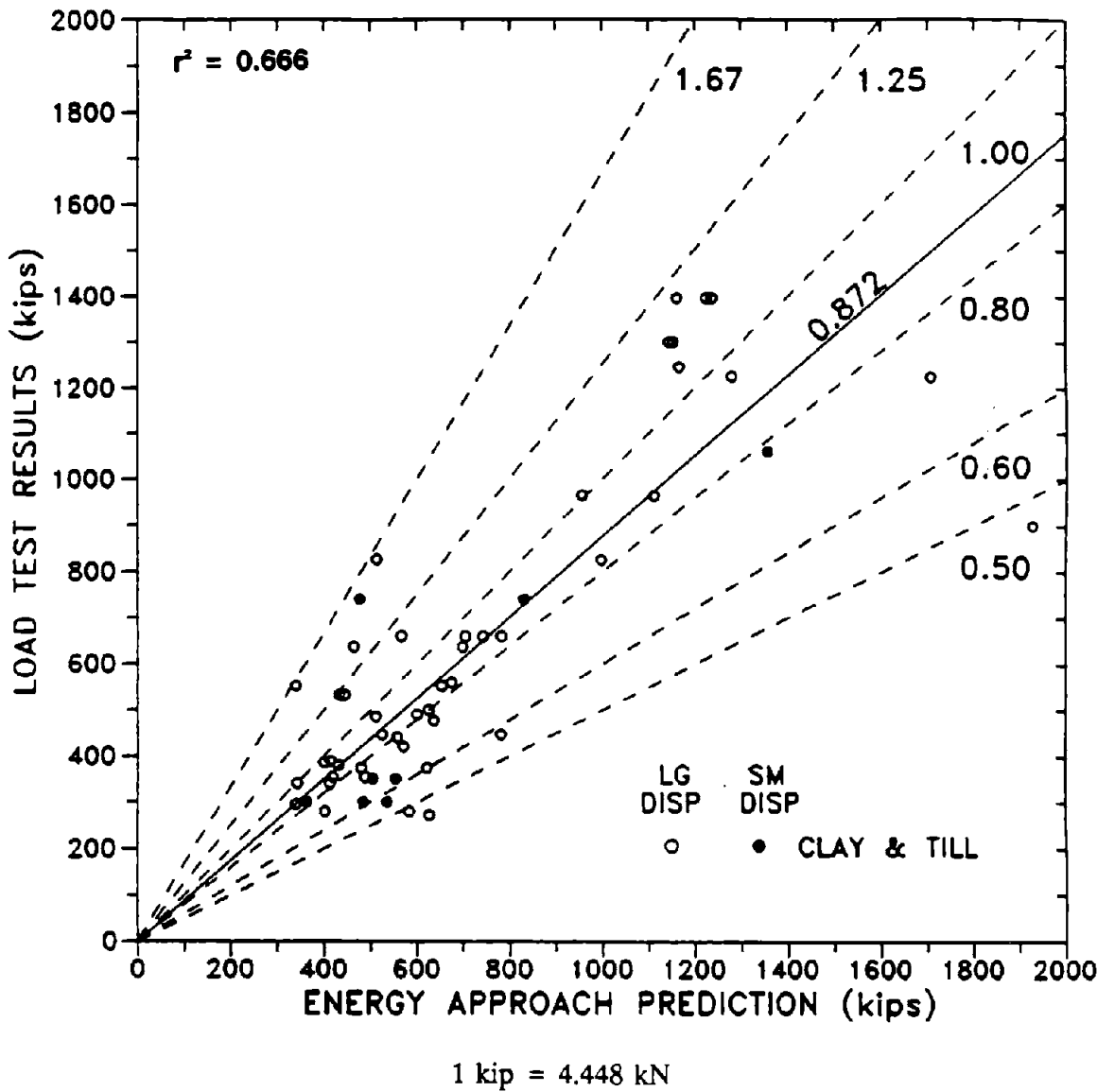
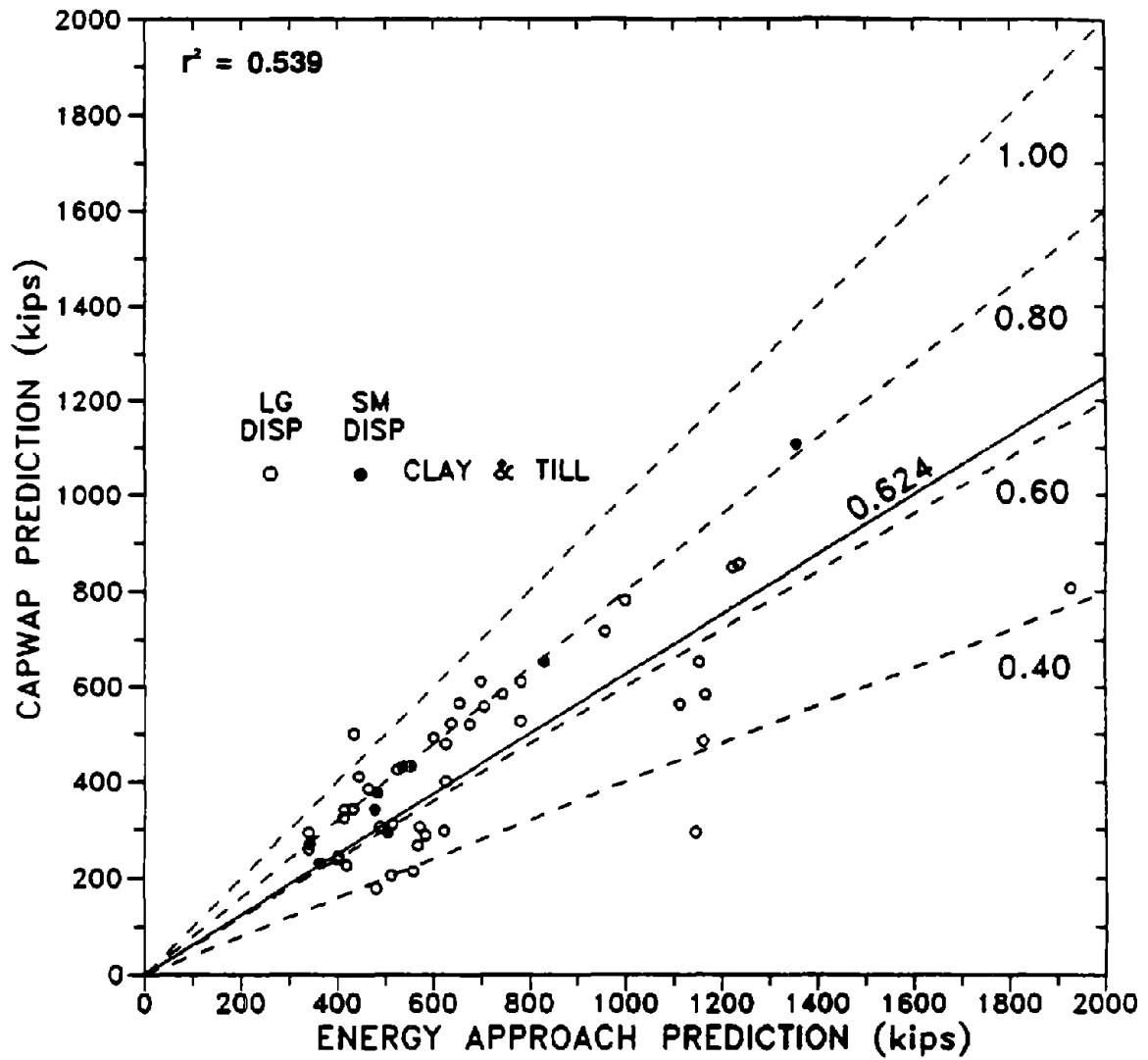


Figure 39. Static load test results vs. Energy Approach predictions for 53 PD/LT pile-cases in clay and till (AAC).



1 kip = 4.448 kN

Figure 40. CAPWAP or TEPWAP predictions vs. Energy Approach predictions for 51 PD/LT pile-cases in clay and till (AAC).

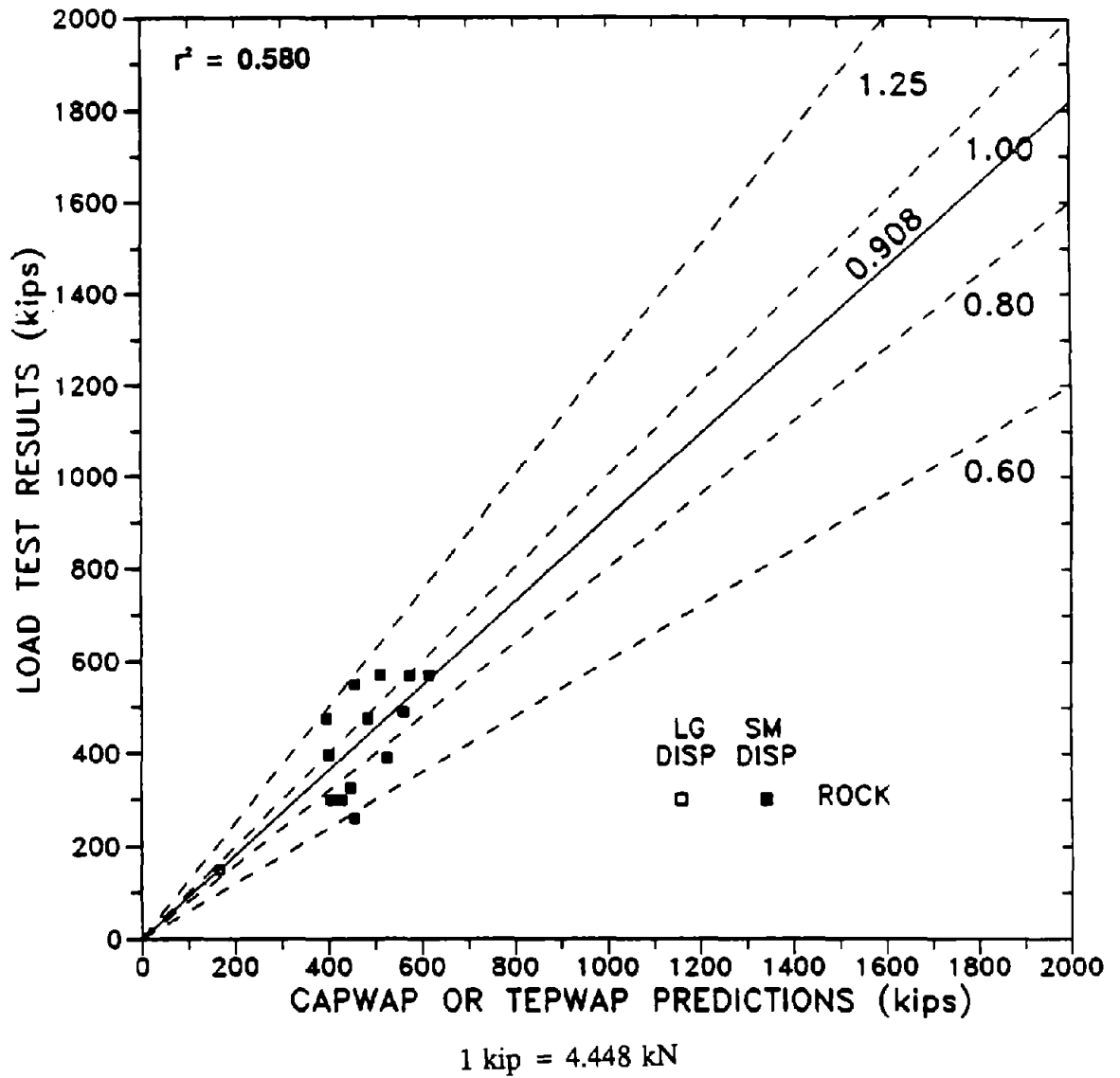
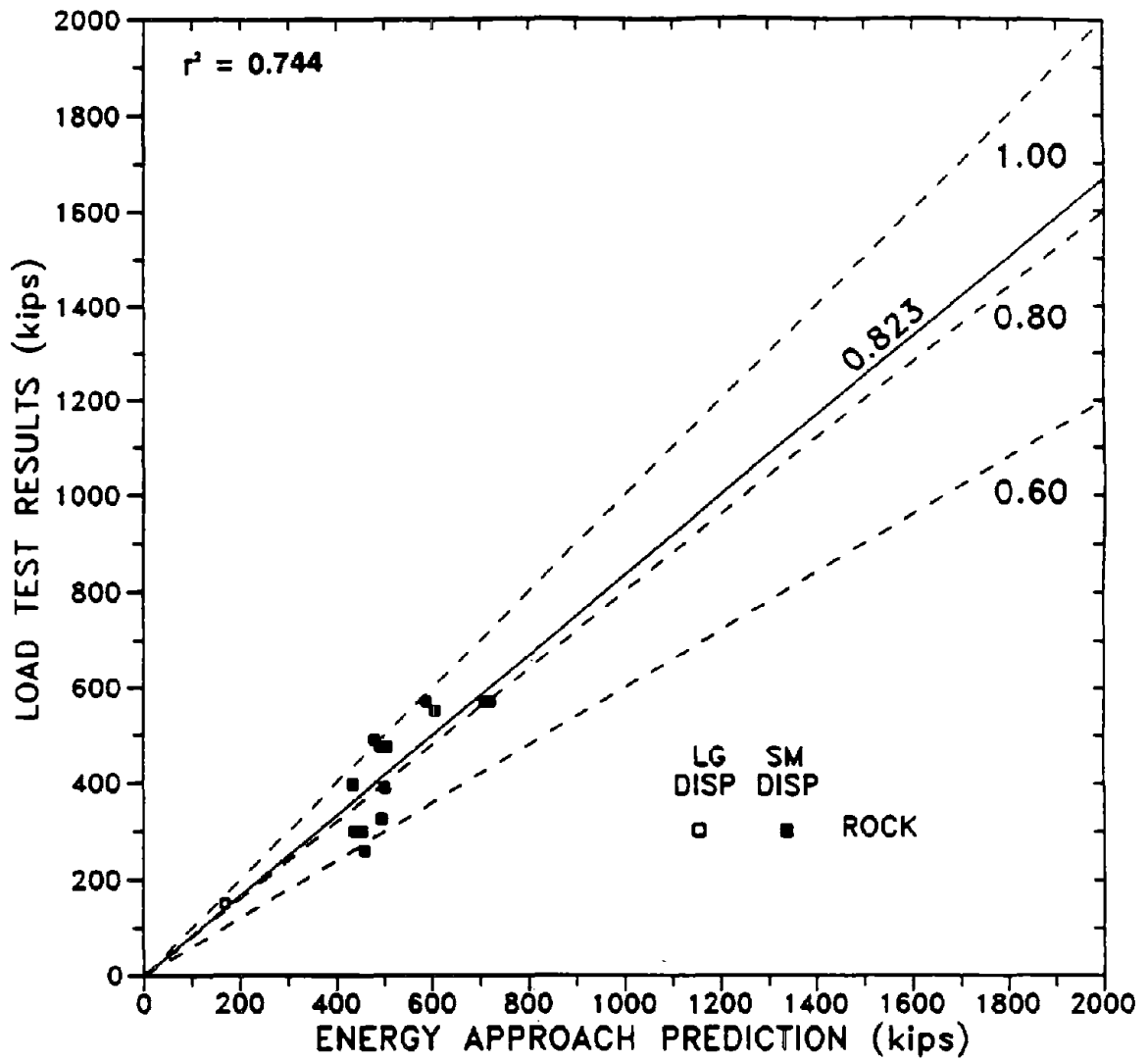
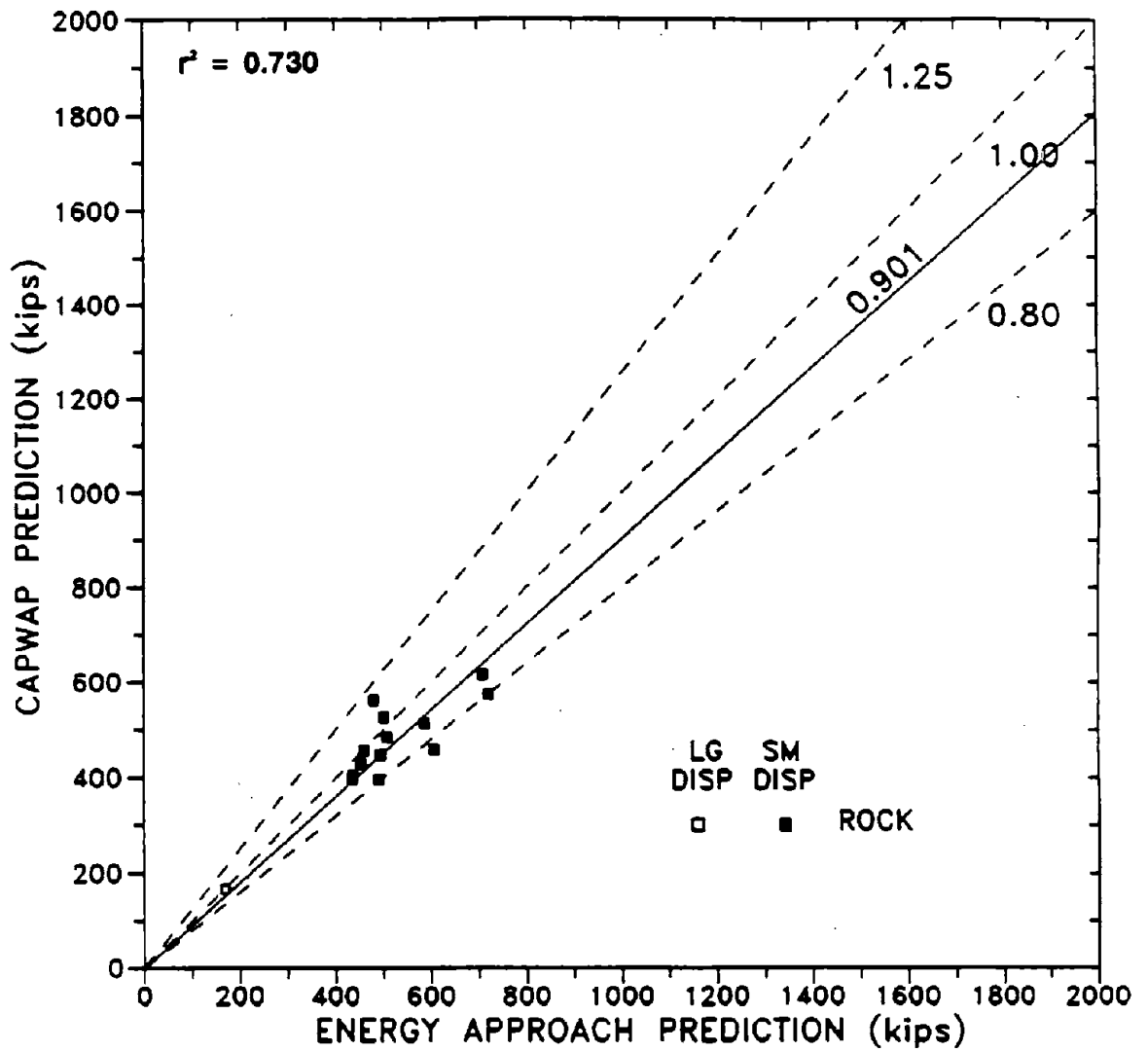


Figure 41. Static load test results vs. CAPWAP or TEPWAP predictions for 14 PD/LT pile-cases in rock (AAR).



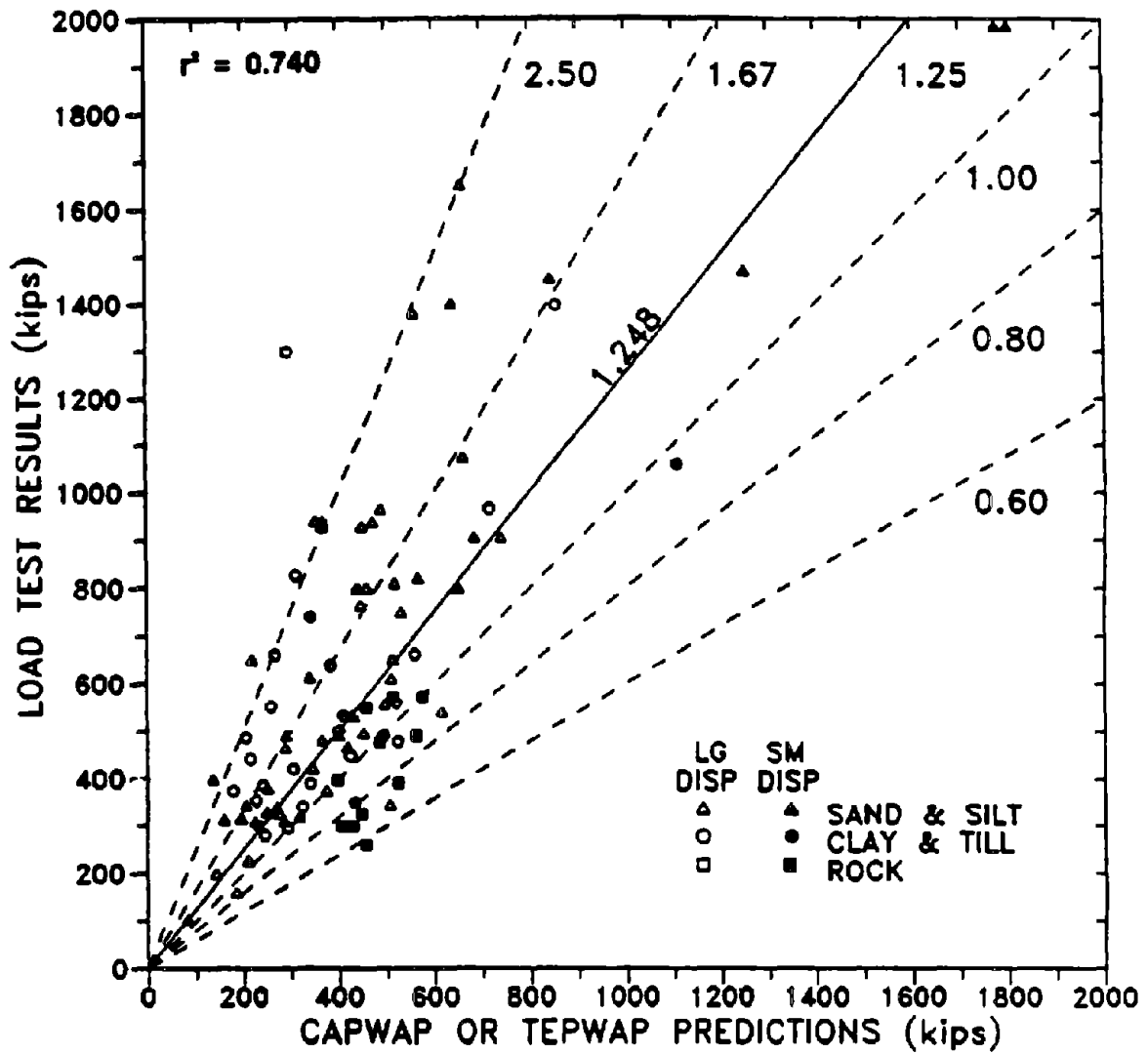
1 kip = 4.448 kN

Figure 42. Static load test results vs. Energy Approach predictions for 14 PD/LT pile-cases in rock (AAR).



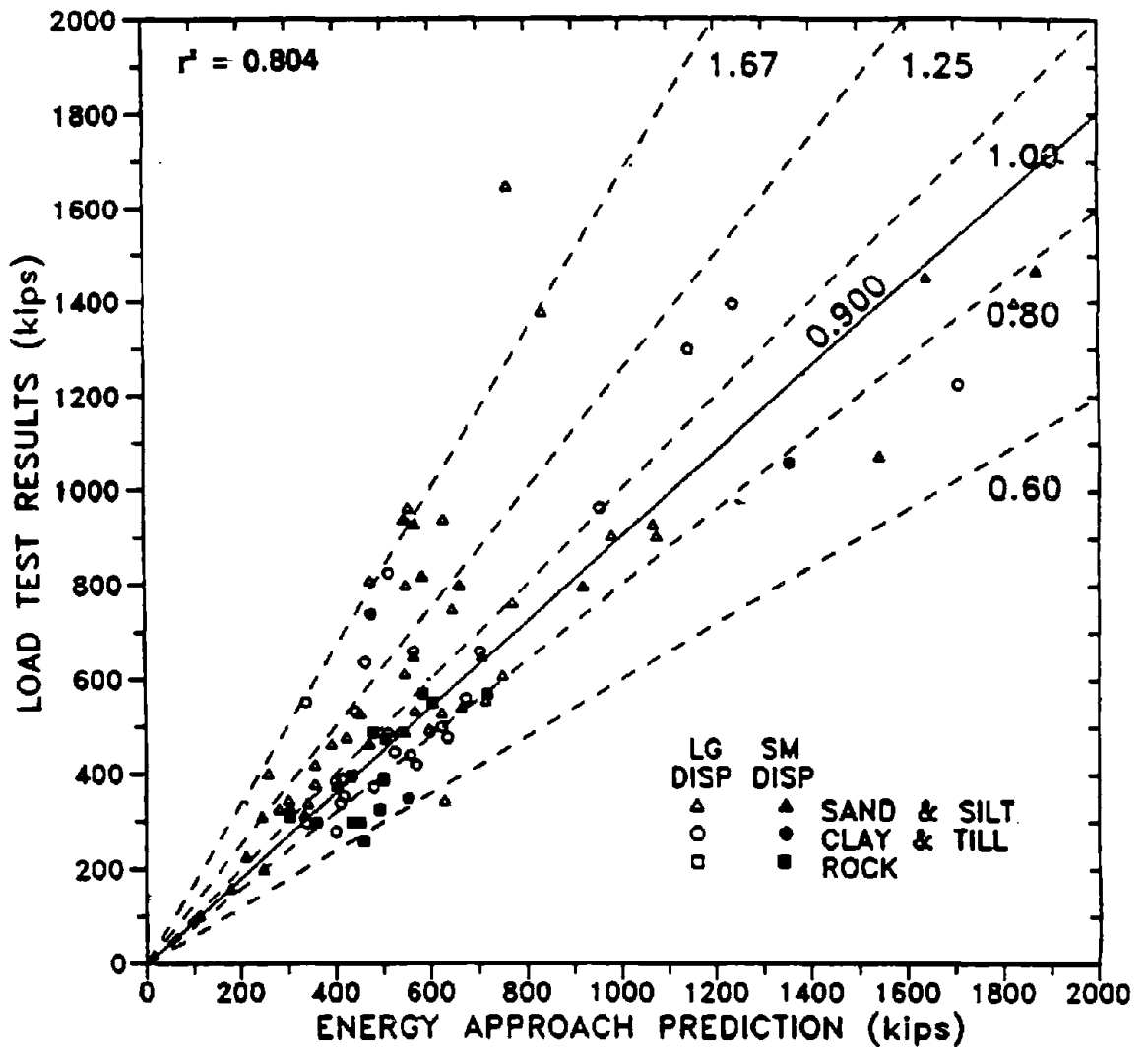
1 kip = 4.448 kN

Figure 43. CAPWAP or TEPWAP predictions vs. Energy Approach predictions. for 14 PD/LT pile-cases in rock (AAR).



1 kip = 4.448 kN

Figure 44. Static load test results vs. CAPWAP or TEPWAP predictions for 96 PD/LT pile-cases in all types of soil at EOD (AEA).



1 kip = 4.448 kN

Figure 45. Static load test results vs. Energy Approach predictions for 94 PD/LT pile-cases in all types of soil at EOD (AEA).

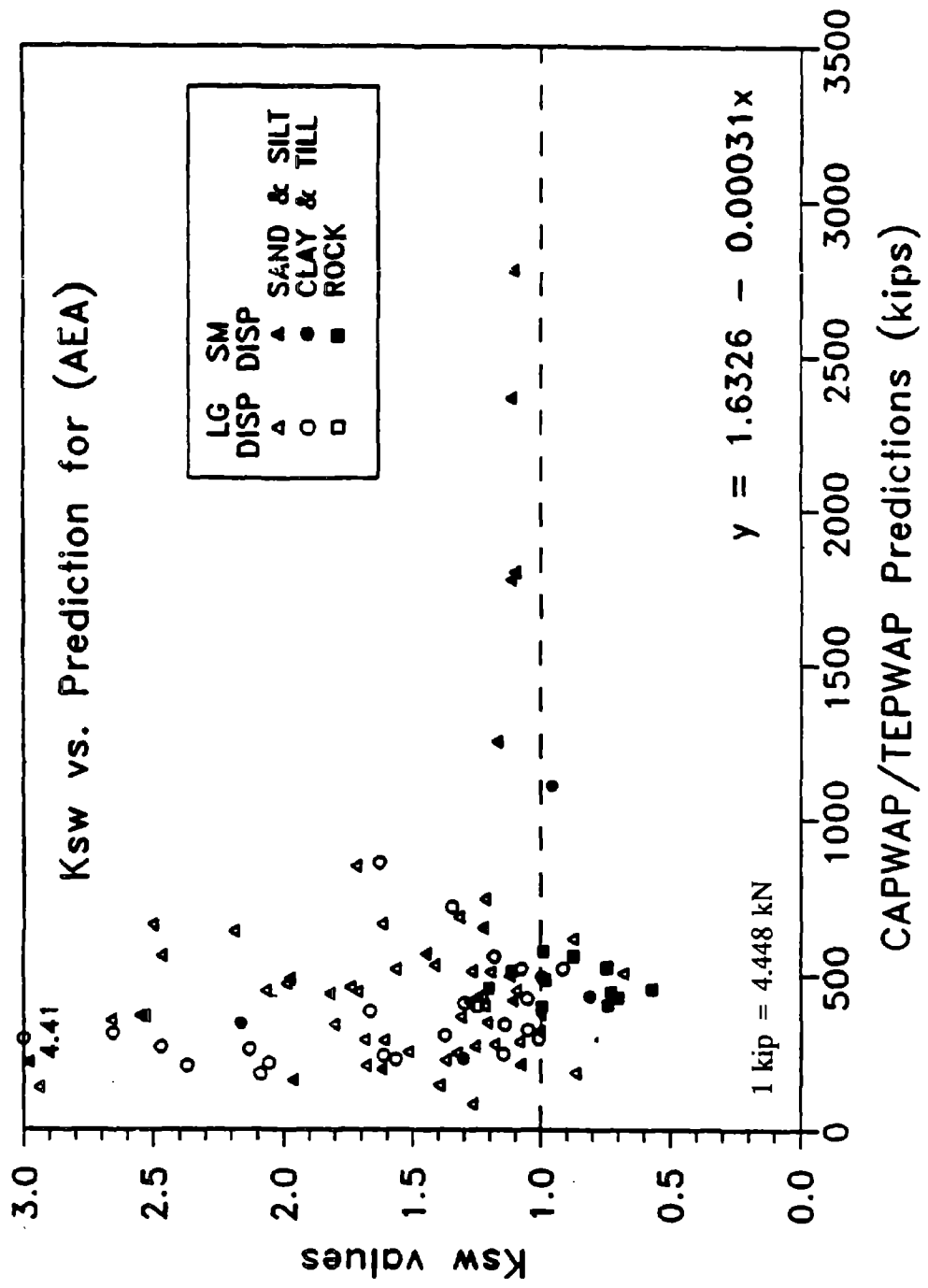


Figure 46. K_{sw} vs. CAPWAP/TEPWAP predictions for 97 PD/LT pile-cases at EOD in all types of soil (AEA).

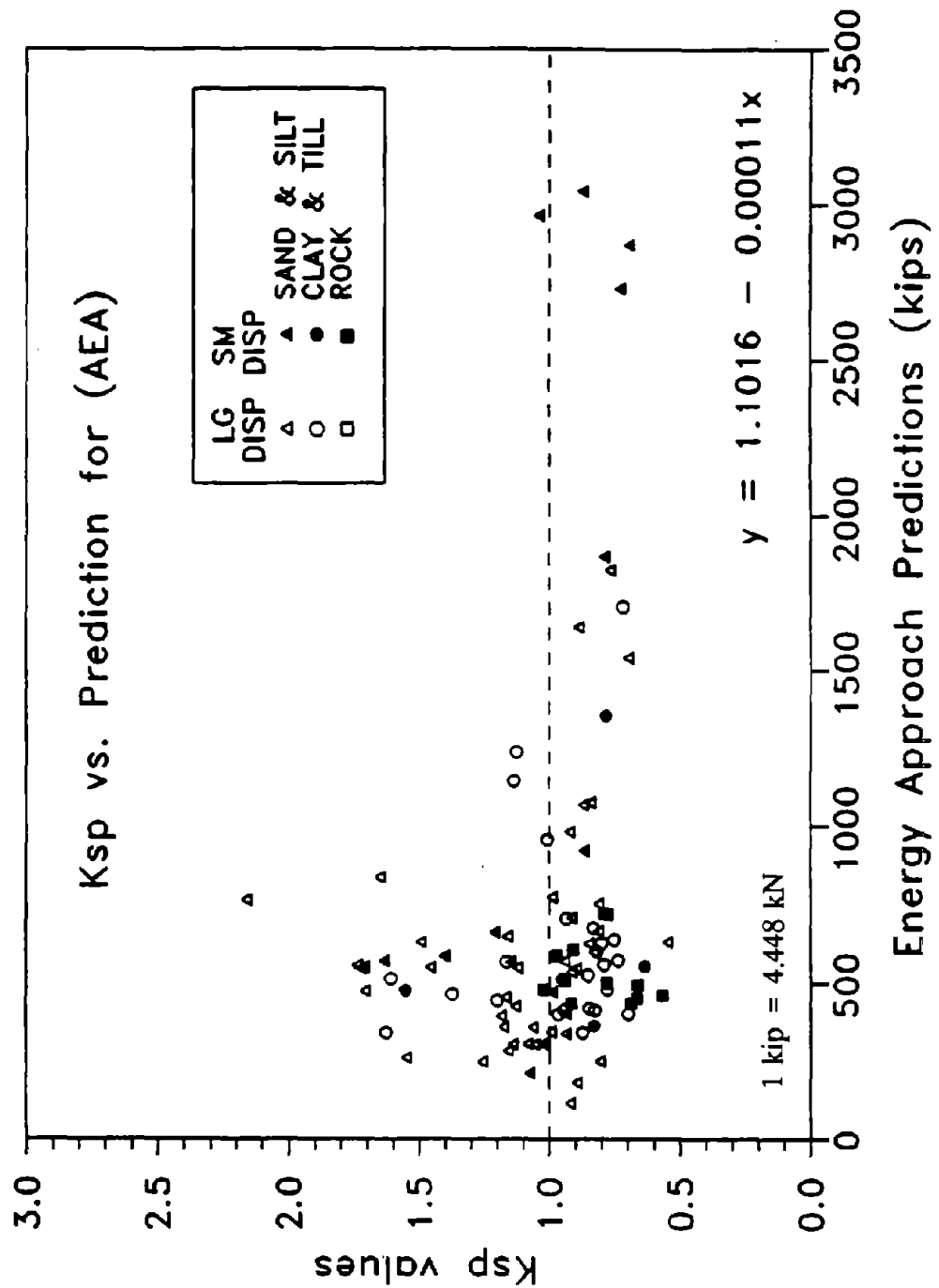
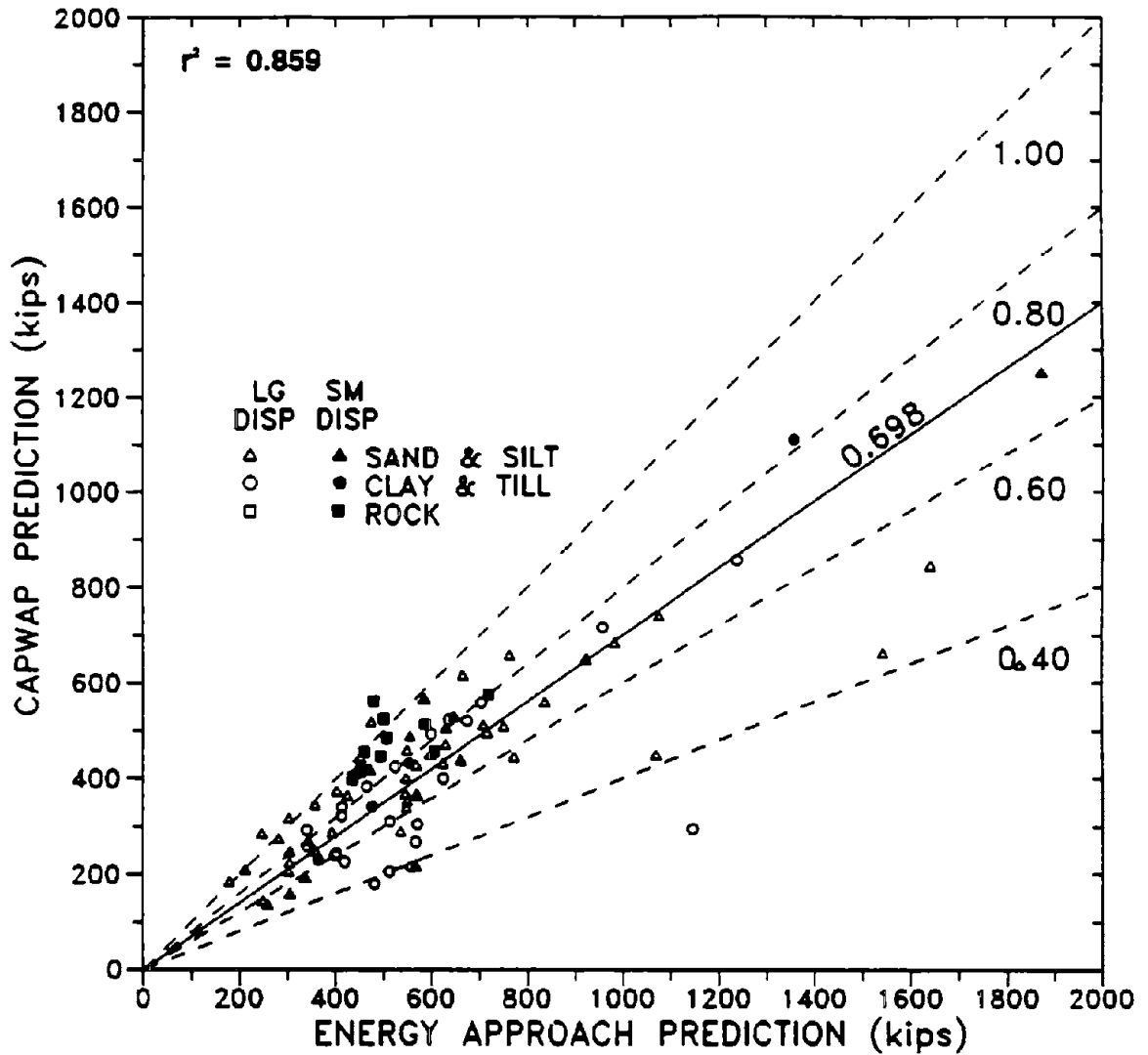
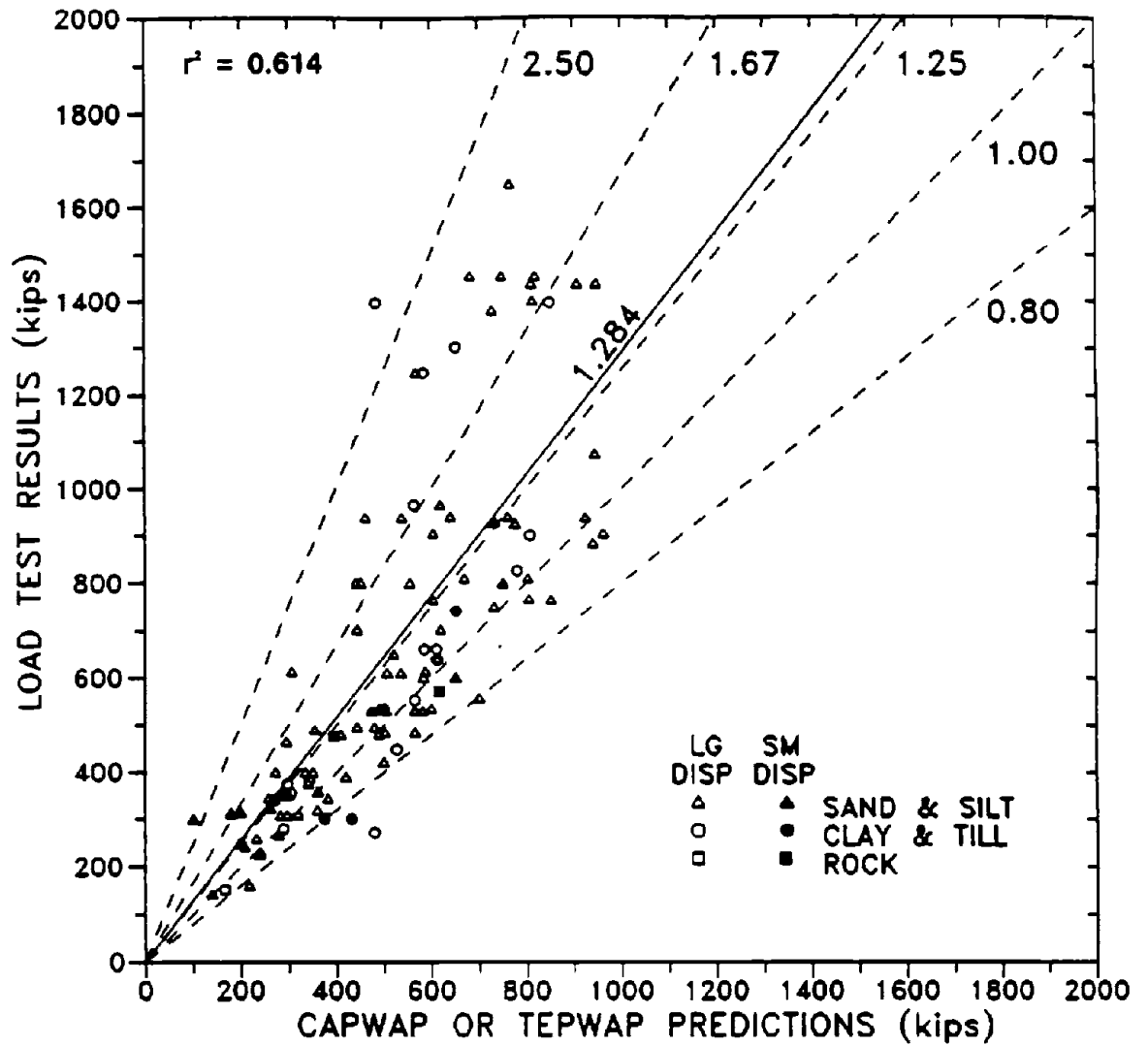


Figure 47. K_{sp} vs. Energy Approach predictions for 98 PD/LT pile-cases at EOD in all types of soil (AEA).



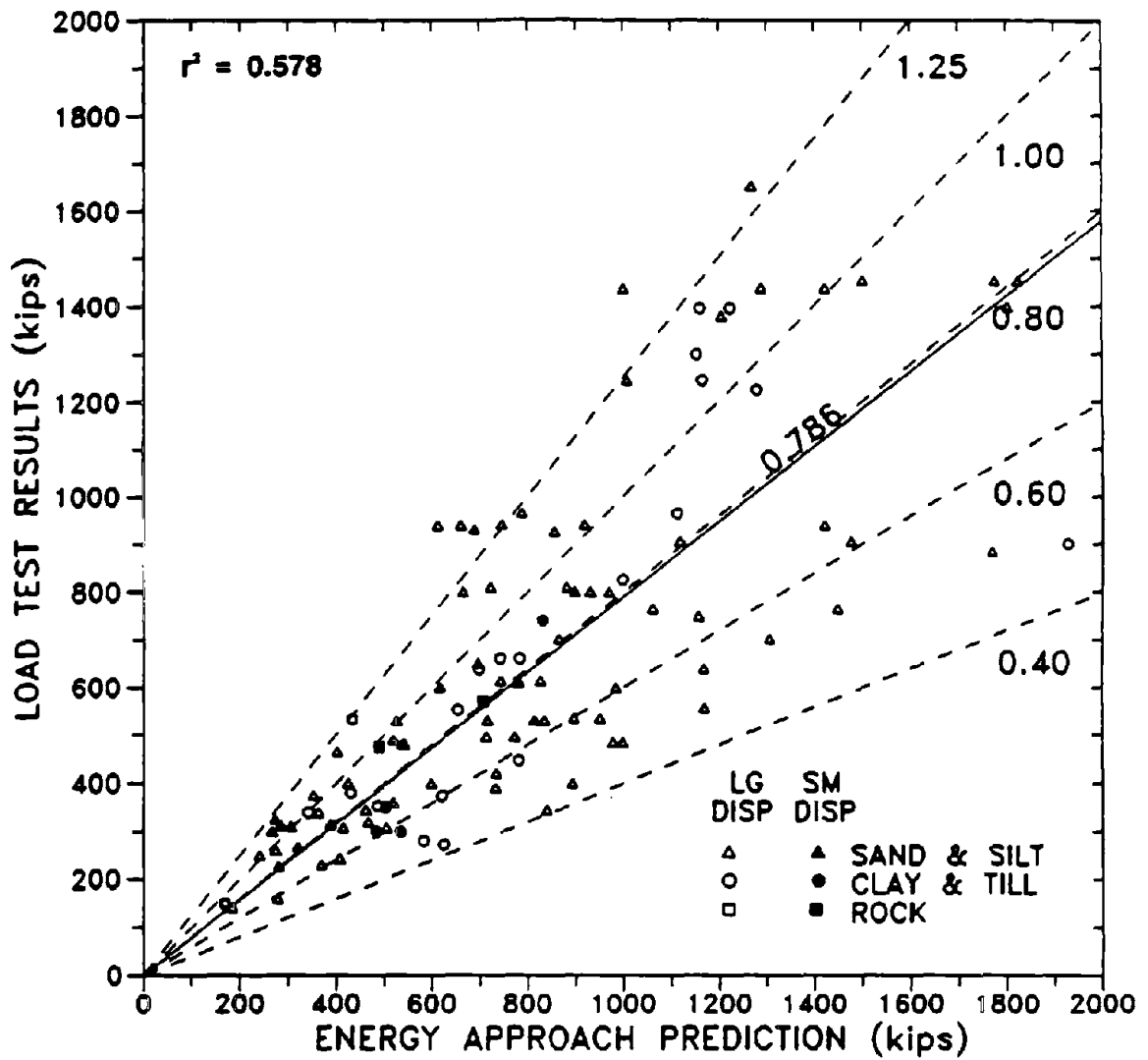
1 kip = 4.448 kN

Figure 48. CAPWAP or TEPWAP predictions vs. Energy Approach predictions for 94 PD/LT pile-cases in all types of soil at EOD (AEA).



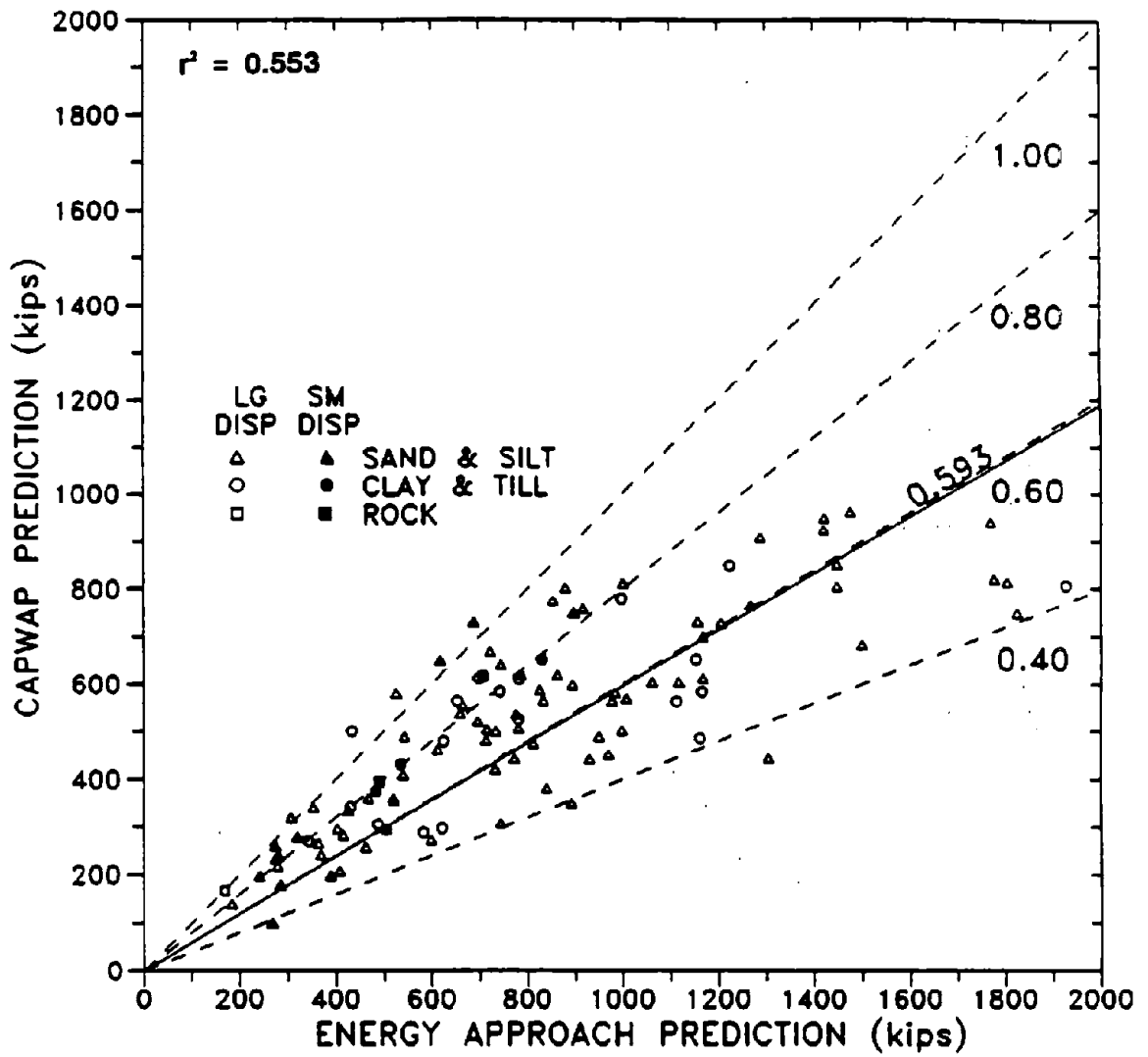
1 kip = 4.448 kN

Figure 49. Static load test results vs. CAPWAP or TEPWAP predictions for 108 PD/LT pile-cases in all types of soil at BOR (ABA).



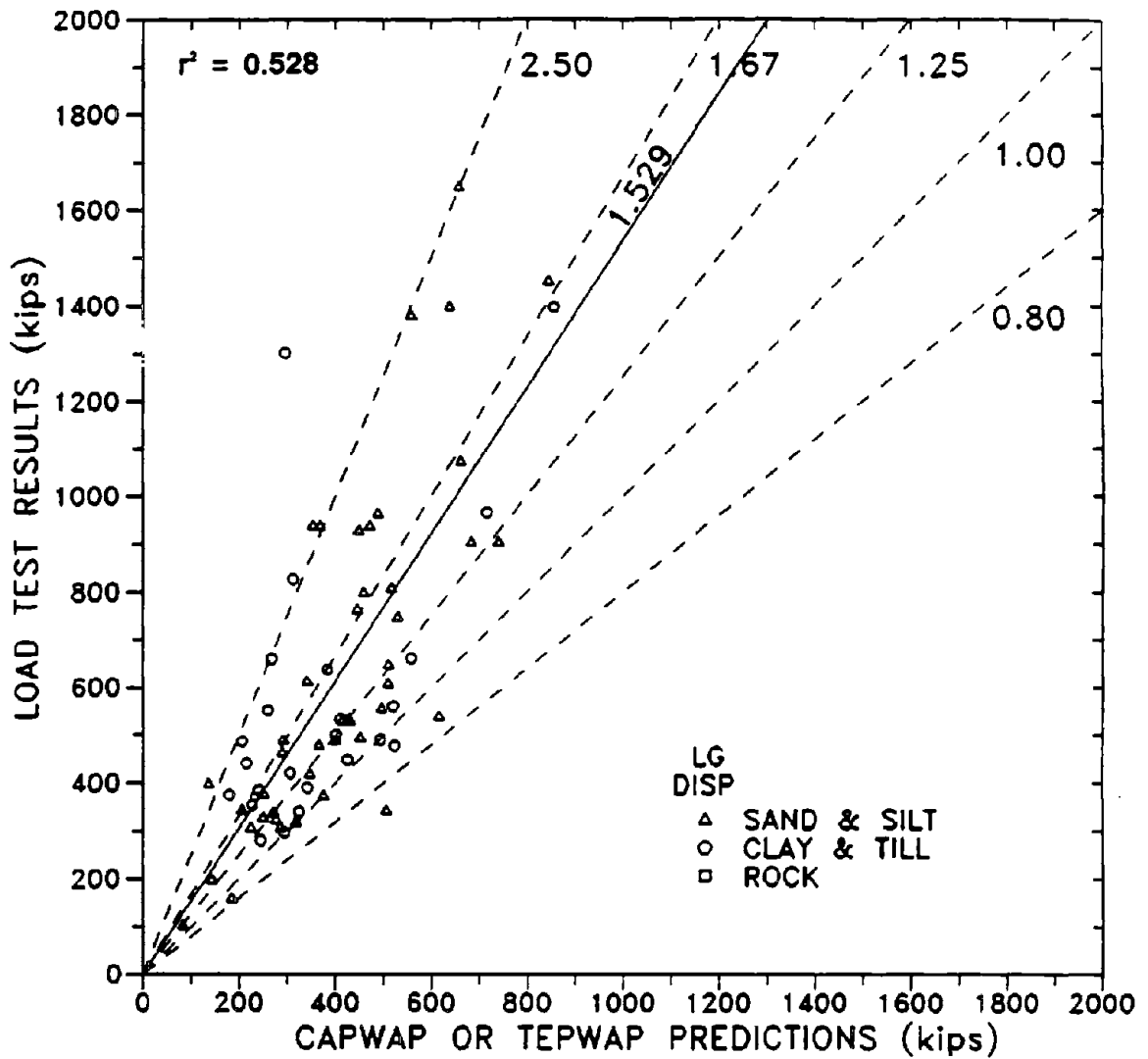
1 kip = 4.448 kN

Figure 50. Static load test results vs. Energy Approach predictions for 108 PD/LT pile-cases in all types of soil at BOR (ABA).



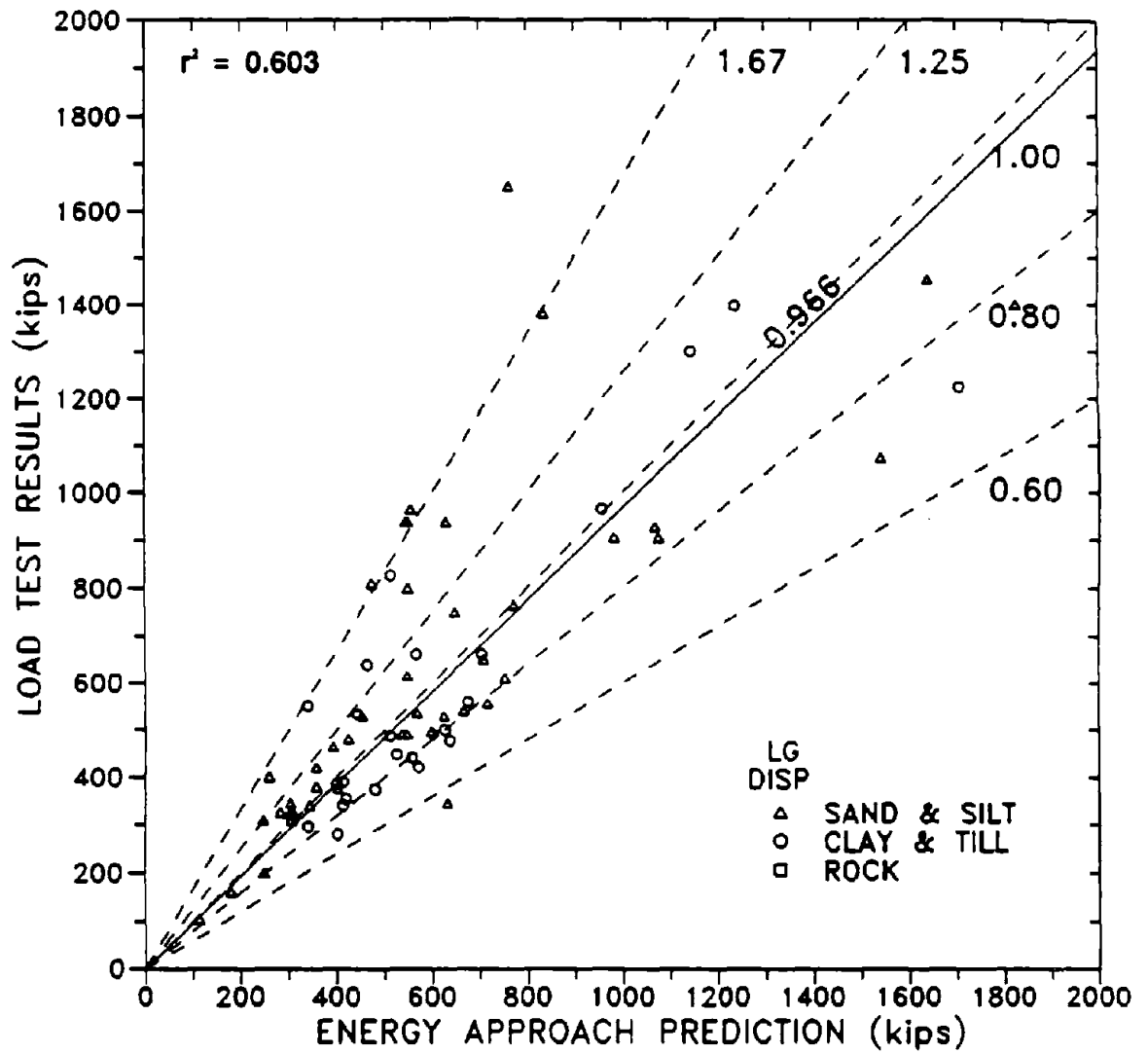
1 kip = 4.448 kN

Figure 51. CAPWAP or TEPWAP predictions vs. Energy Approach predictions for 108 PD/LT pile-cases in all types of soil at BOR (ABA).



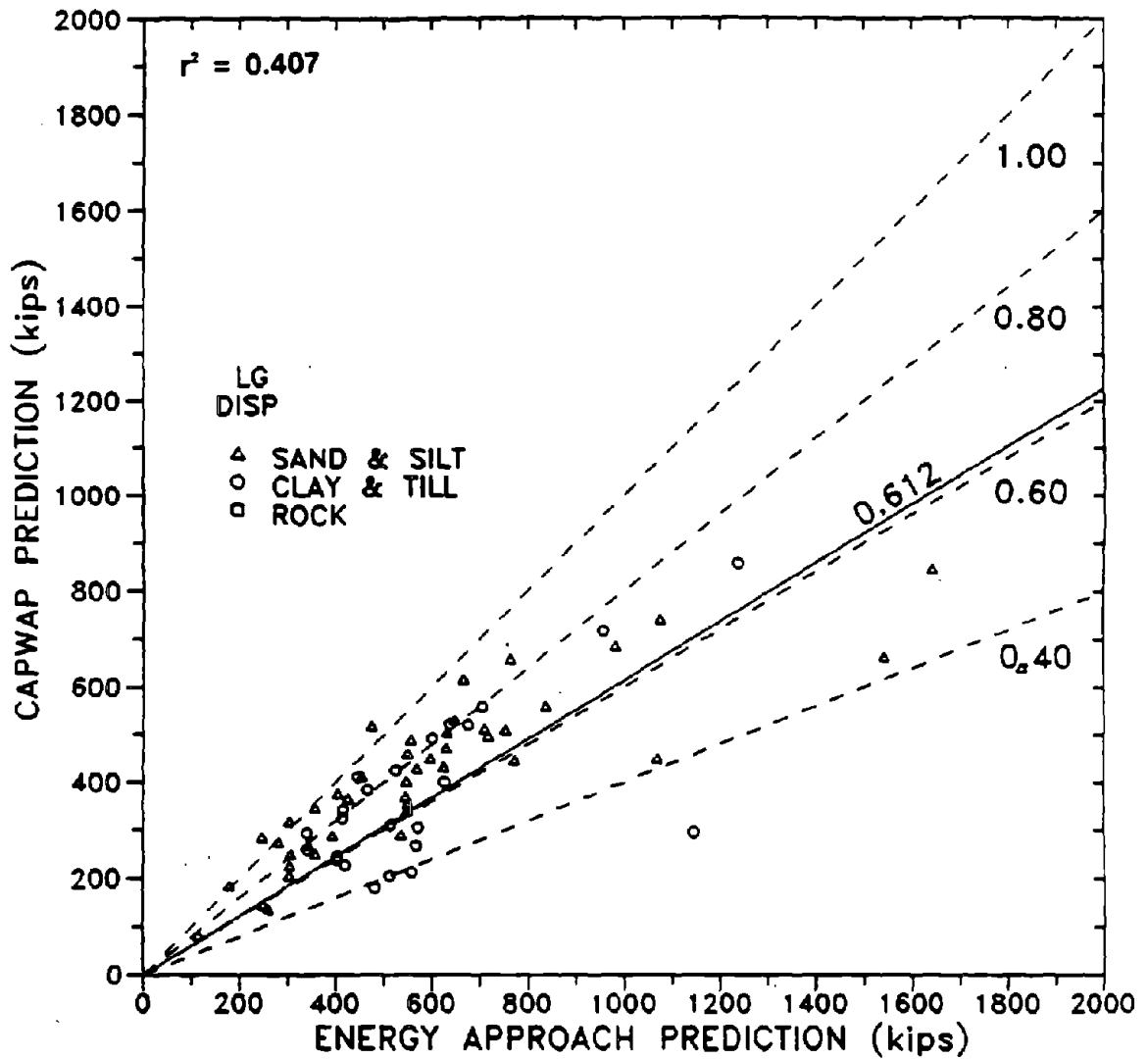
1 kip = 4.448 kN

Figure 52. Static load test results vs. CAPWAP or TEPWAP predictions for 68 large displacement PD/LT pile-cases in all types of soil at EOD (LEA).



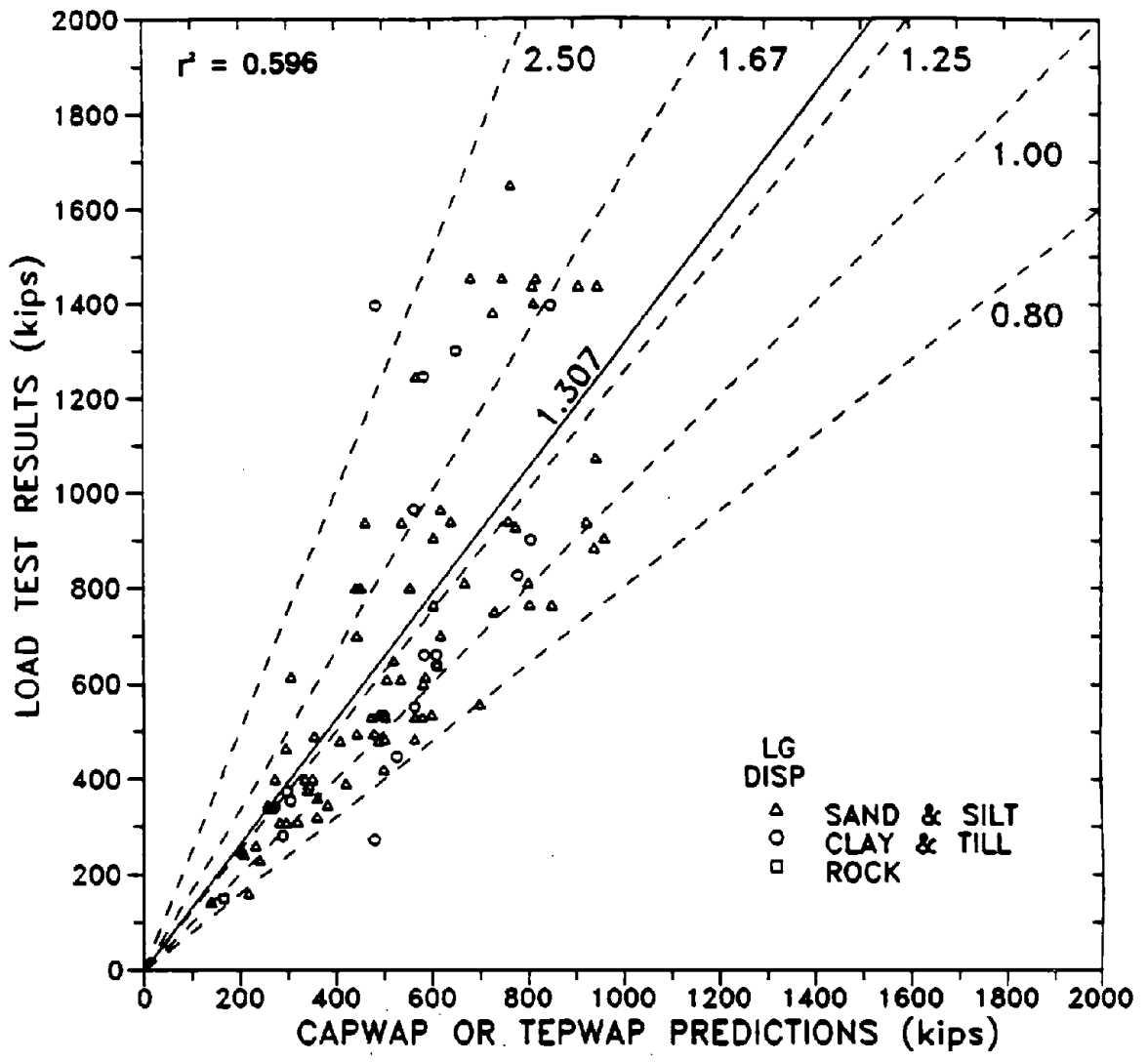
1 kip = 4.448 kN

Figure 53. Static load test results vs. Energy Approach predictions for 69 large displacement PD/LT pile-cases in all types of soil at EOD (LEA).



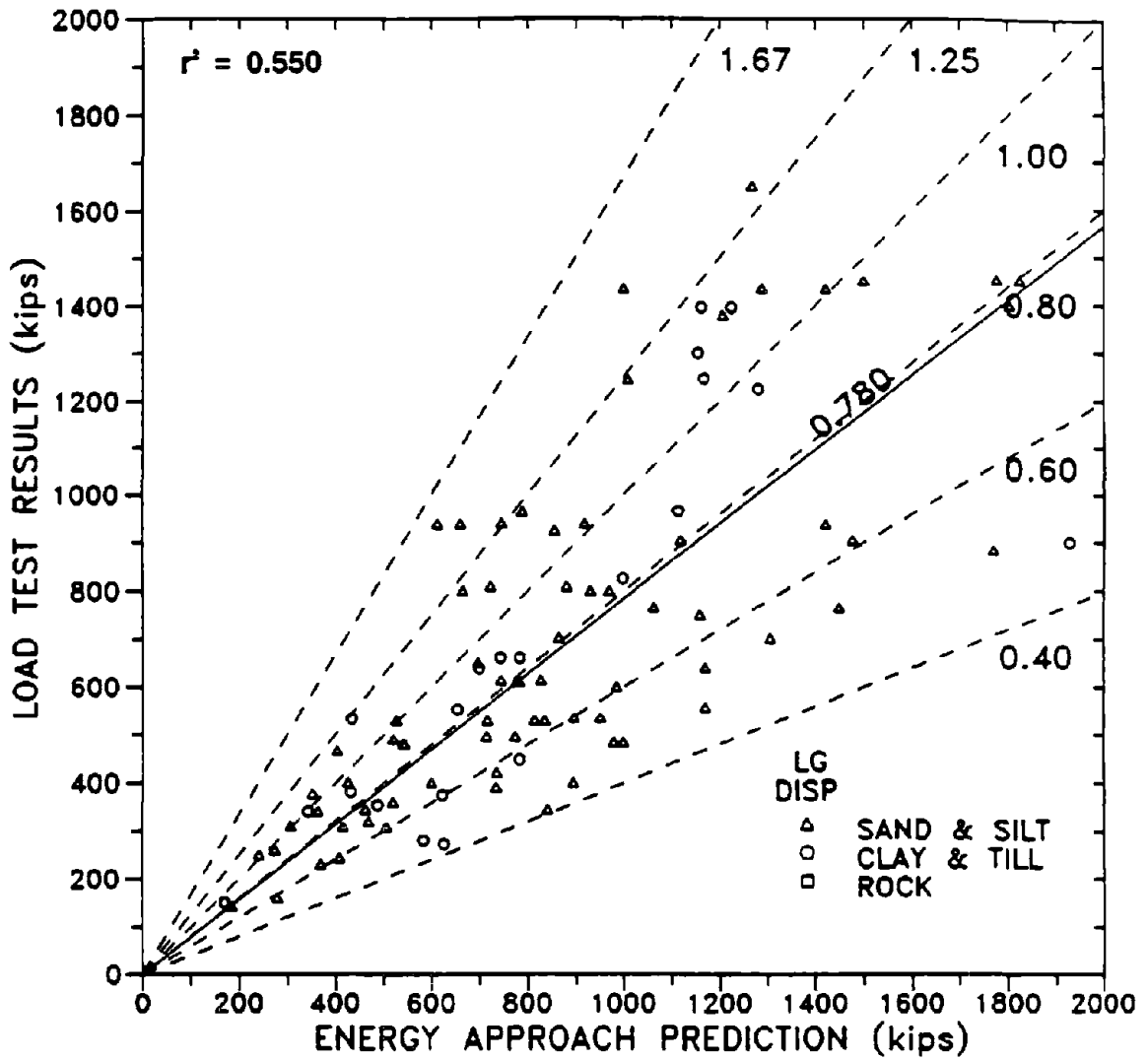
1 kip = 4.448 kN

Figure 54. CAPWAP or TEPWAP predictions vs. Energy Approach predictions for 68 large displacement PD/LT pile-cases in all types of soil at EOD (LEA).



1 kip = 4.448 kN

Figure 55. Static load test results vs. CAPWAP or TEPWAP predictions for 94 large displacement PD/LT pile-cases in all types of soil at BOR (LBA).



1 kip = 4.448 kN

Figure 56. Static load test results vs. Energy Approach predictions for 94 large displacement PD/LT pile-cases in all types of soil at BOR (LBA).

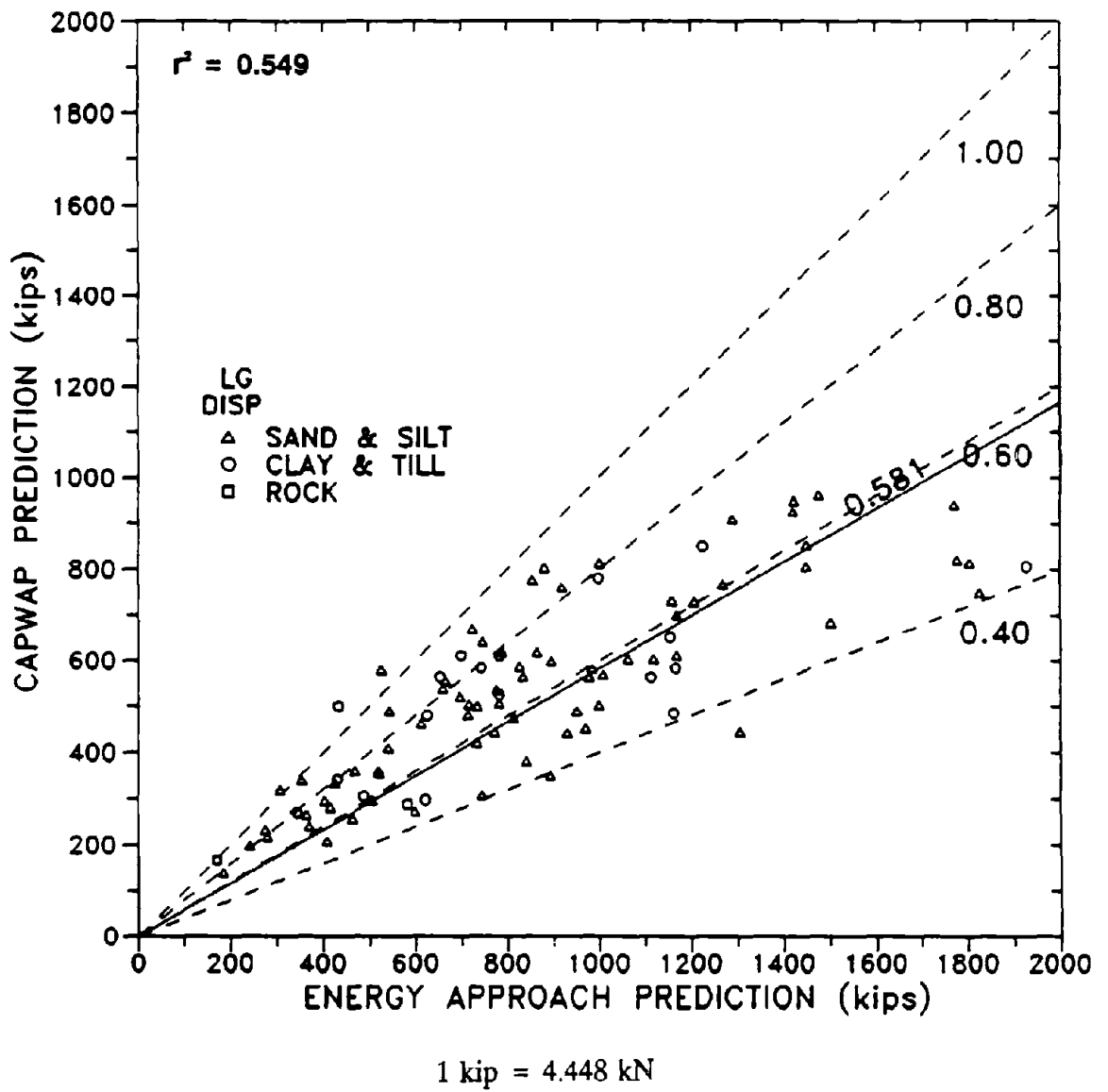
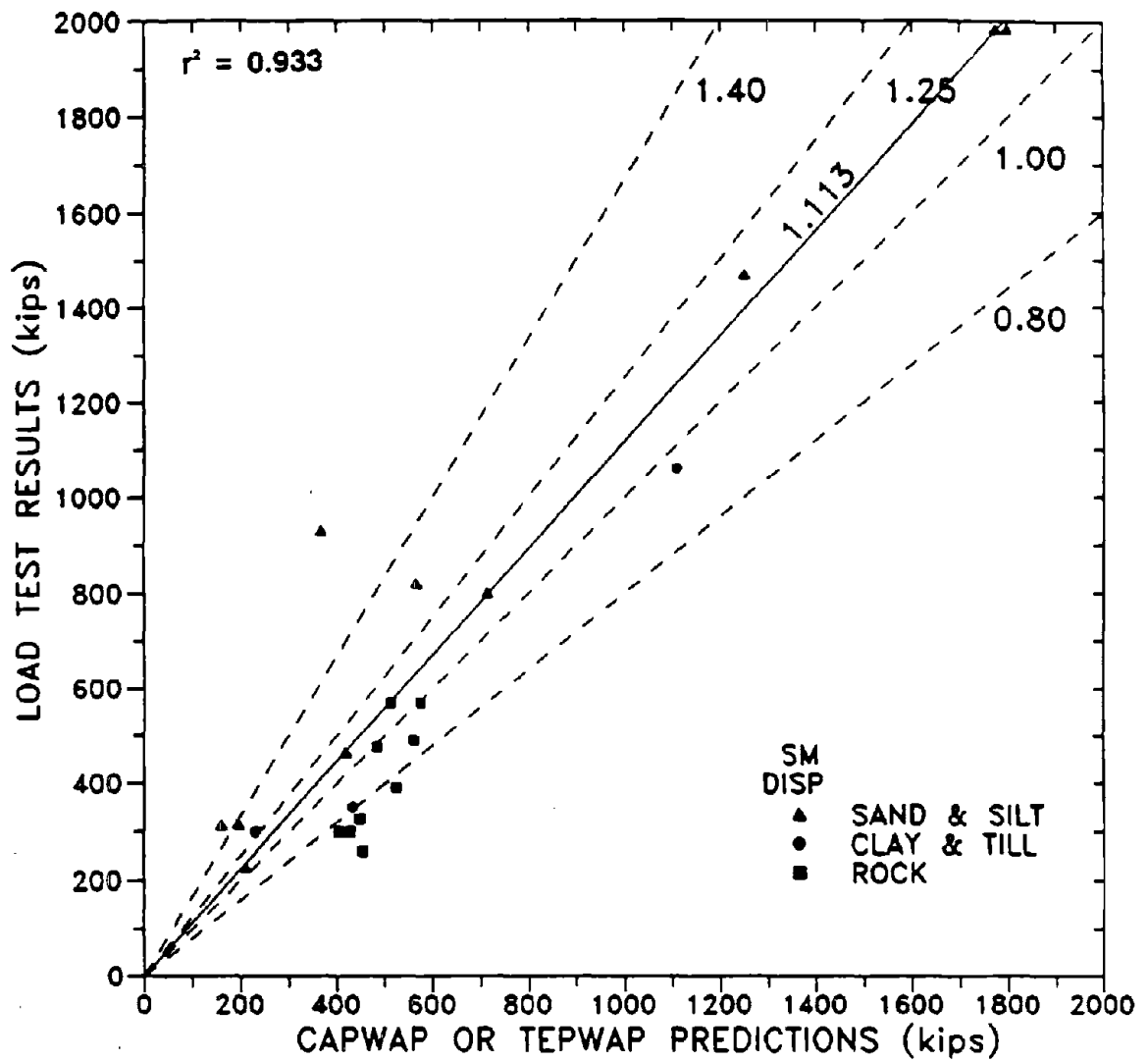
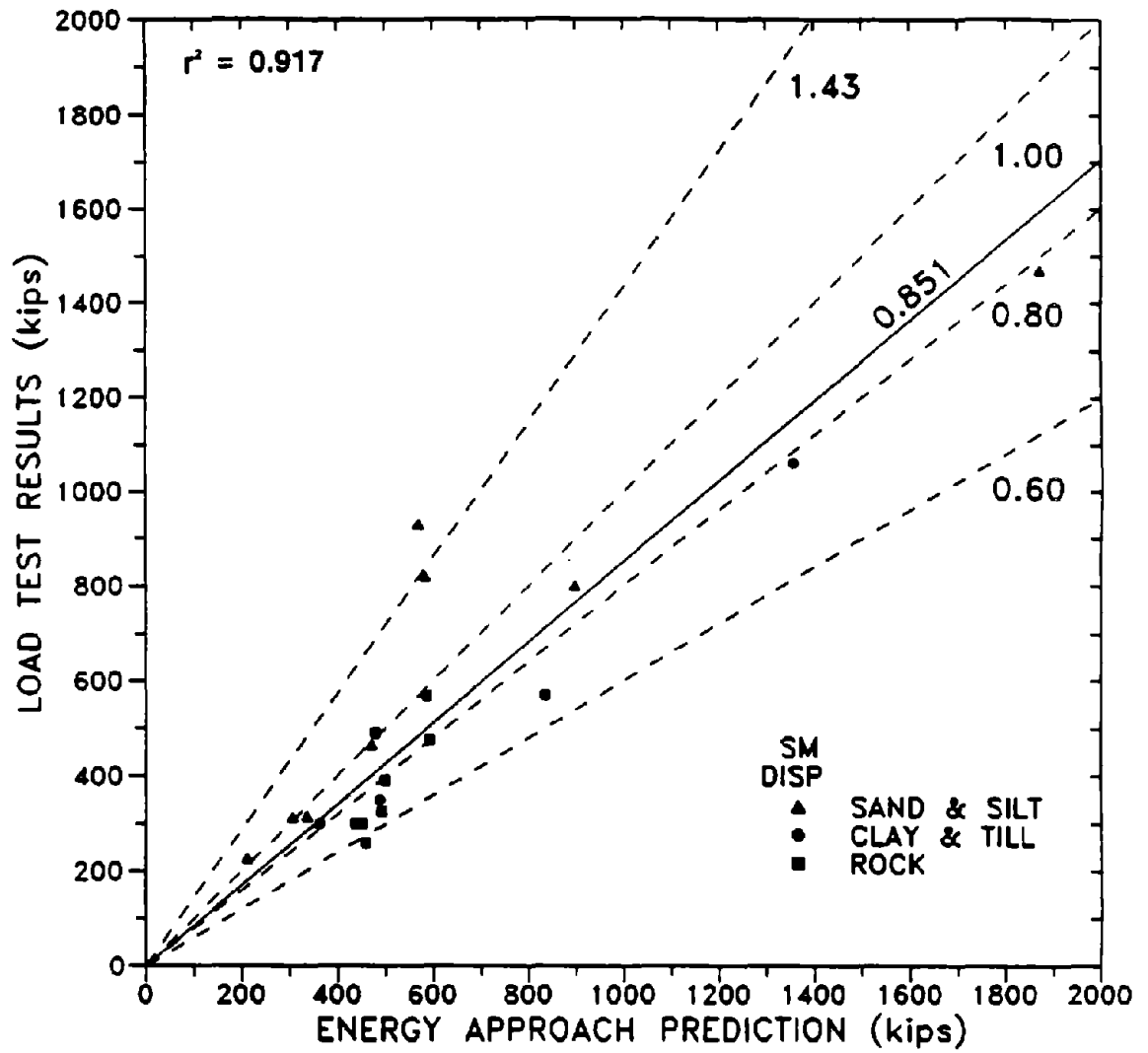


Figure 57. CAPWAP or TEPWAP predictions vs. Energy Approach predictions for 93 large displacement PD/LT pile-cases in all types of soil at BOR (LBA).



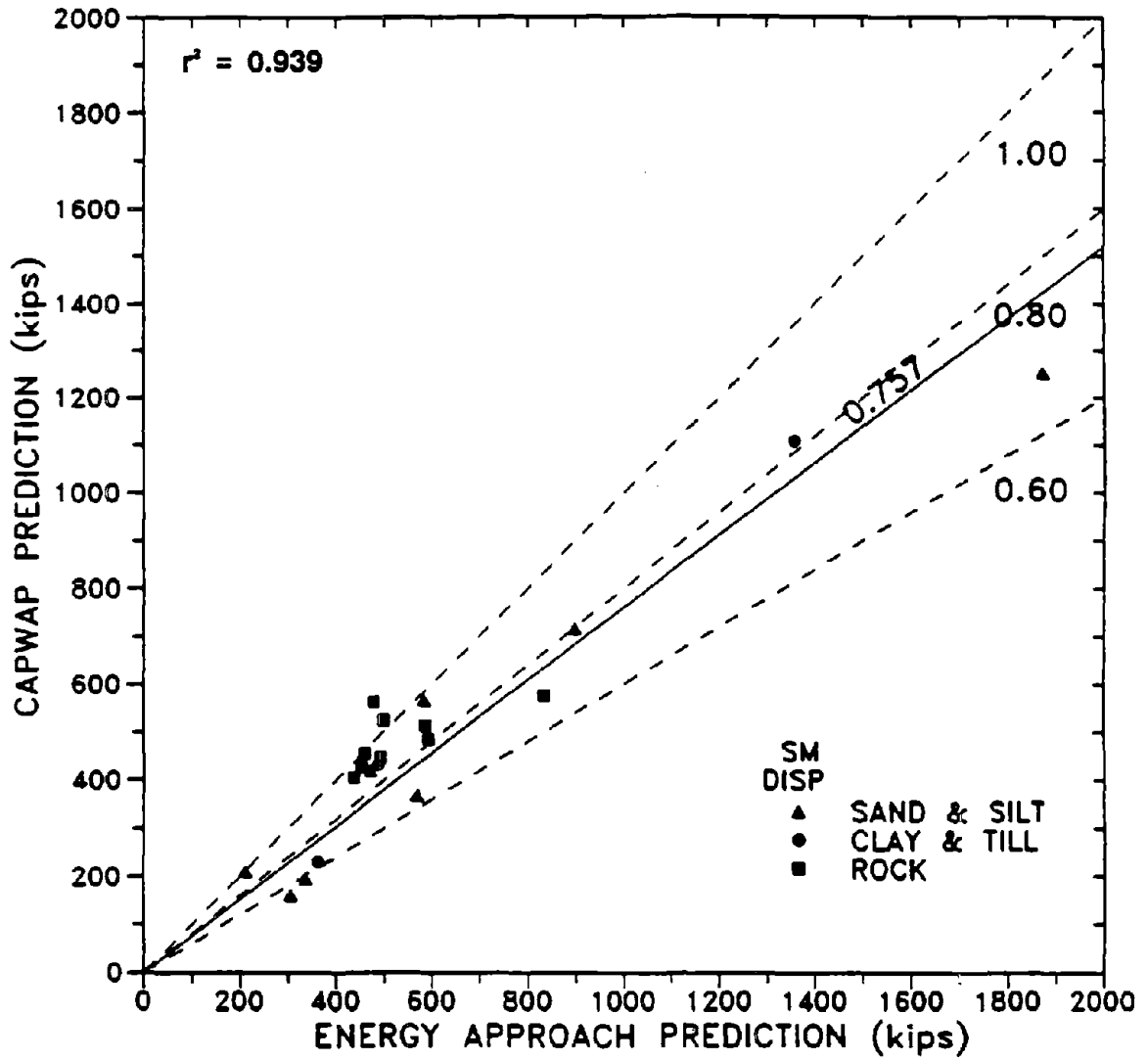
1 kip = 4.448 kN

Figure 58. Static load test results vs. CAPWAP or TEPWAP predictions for 22 small displacement PD/LT pile-cases in all types of soil at EOD (SEA).



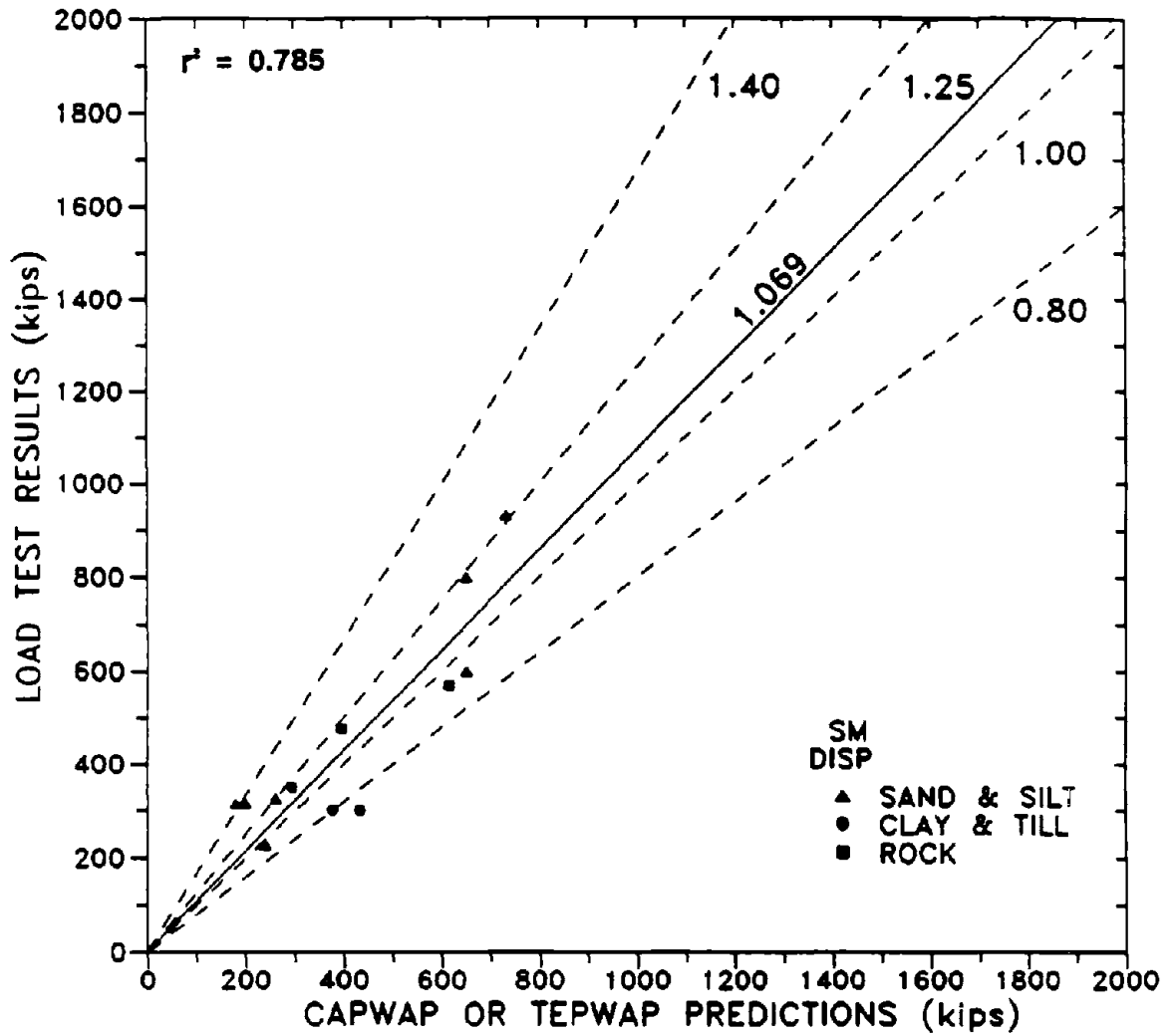
1 kip = 4.448 kN

Figure 59. Static load test results vs. Energy Approach predictions for 20 small displacement PD/LT pile-cases in all types of soil at EOD (SEA).



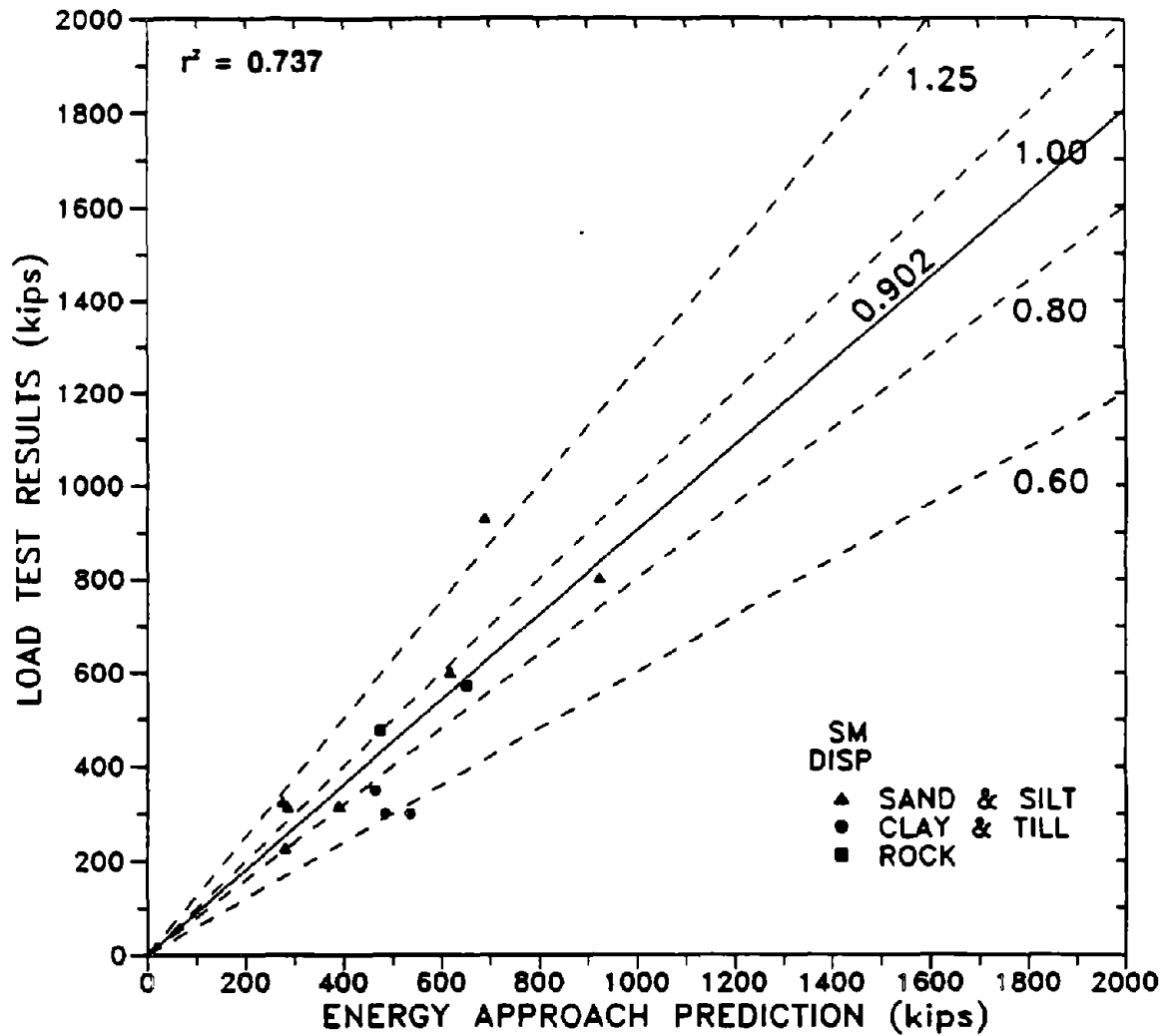
1 kip = 4.448 kN

Figure 60. CAPWAP or TEPWAP predictions vs. Energy Approach predictions for 20 small displacement PD/LT pile-cases in all types of soil at EOD (SEA).



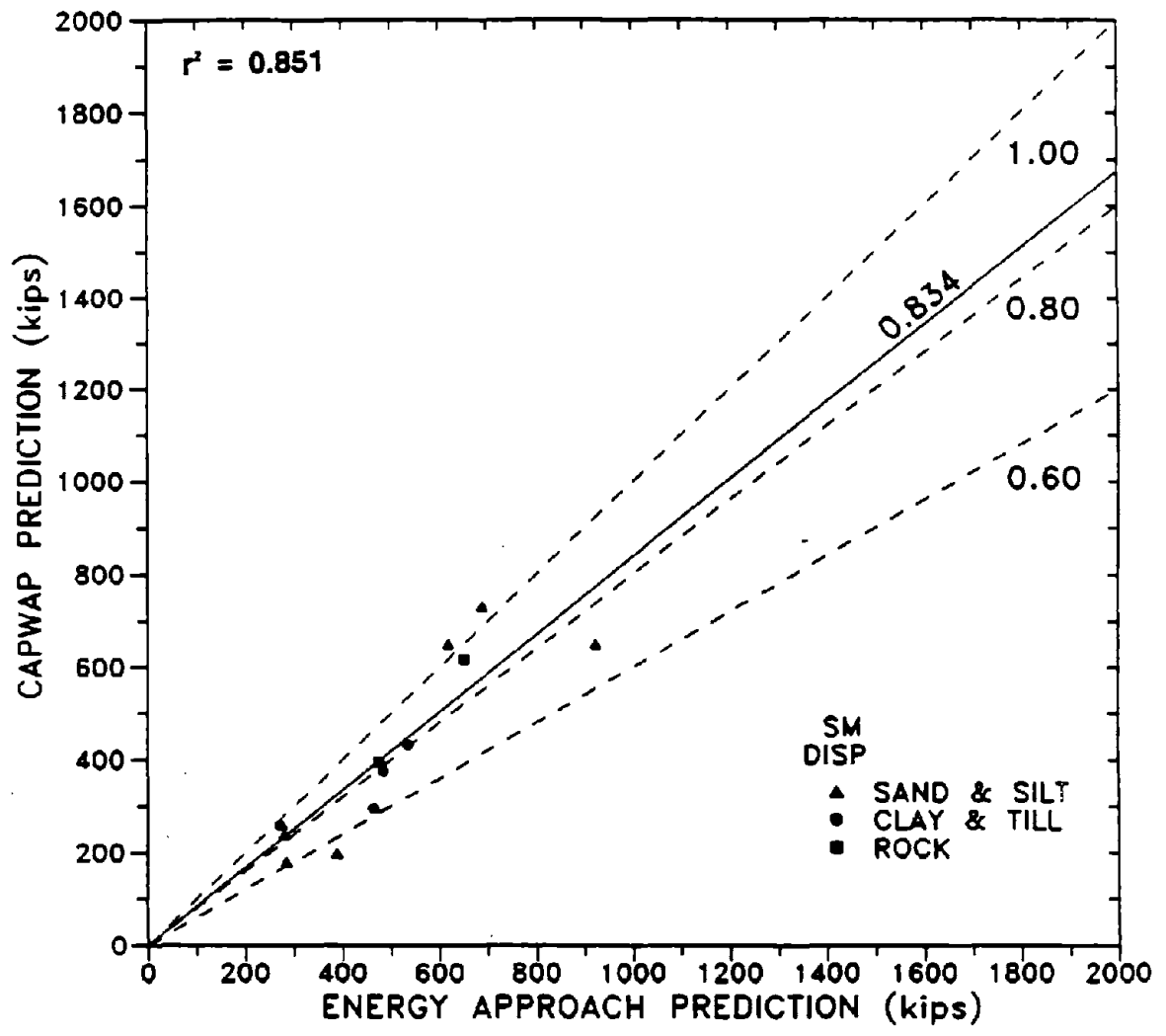
1 kip = 4.448 kN

Figure 61. Static load test results vs. CAPWAP or TEPWAP predictions for 12 small displacement PD/LT pile-cases in all types of soil at BOR (SBA).



1 kip = 4.448 kN

Figure 62. Static load test results vs. Energy Approach predictions for 12 small displacement PD/LT pile-cases in all types of soil at BOR (SBA).



1 kip = 4.448 kN

Figure 63. CAPWAP or TEPWAP predictions vs. Energy Approach predictions for 12 small displacement PD/LT pile-cases in all types of soil at BOR (SBA).

**Ksw histogram and frequency distribution
for 206 PD/LT pile-cases (AAA)**

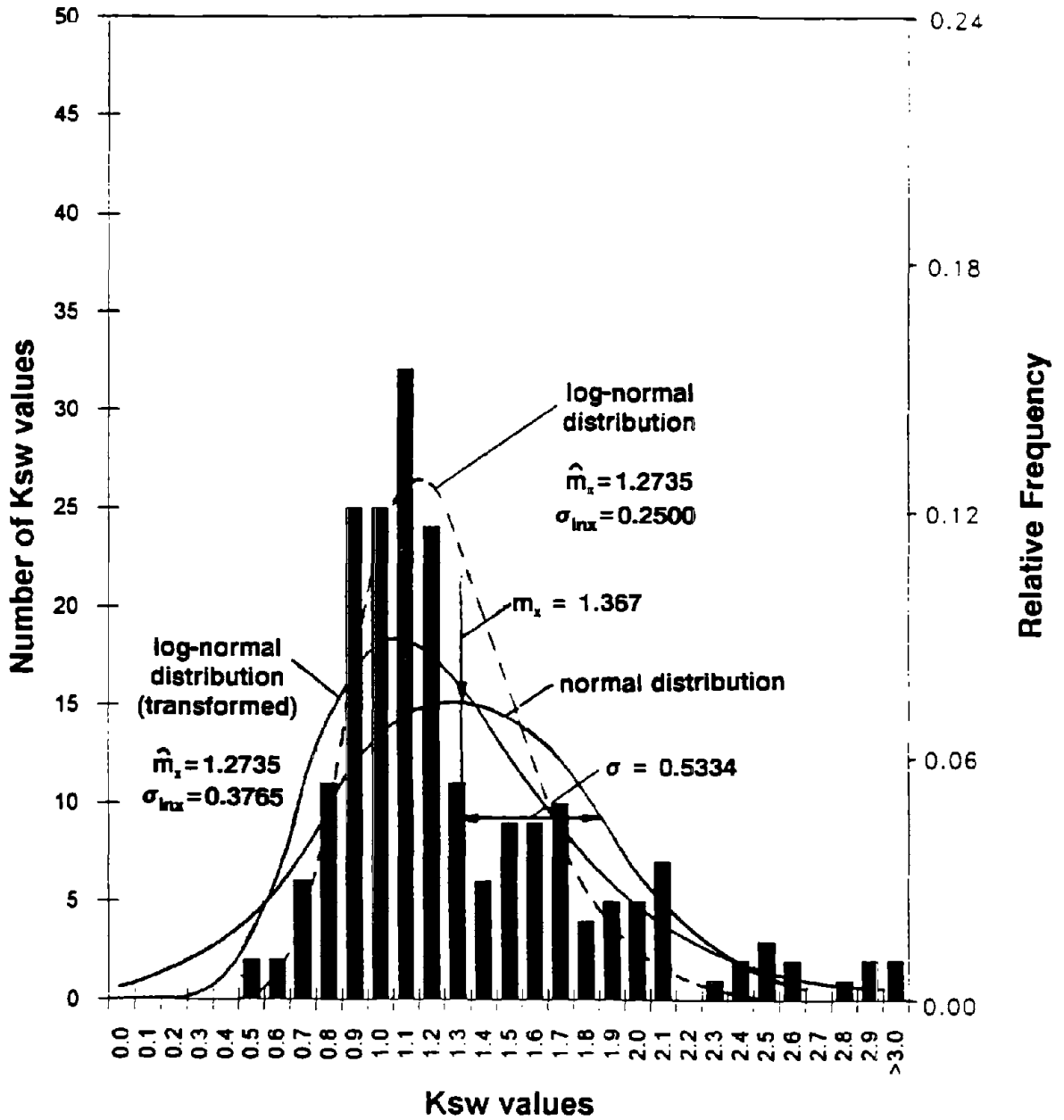


Figure 64. Histogram and frequency distributions of K_{sw} for 206 PD/LT pile-cases in all types of soil (AAA).

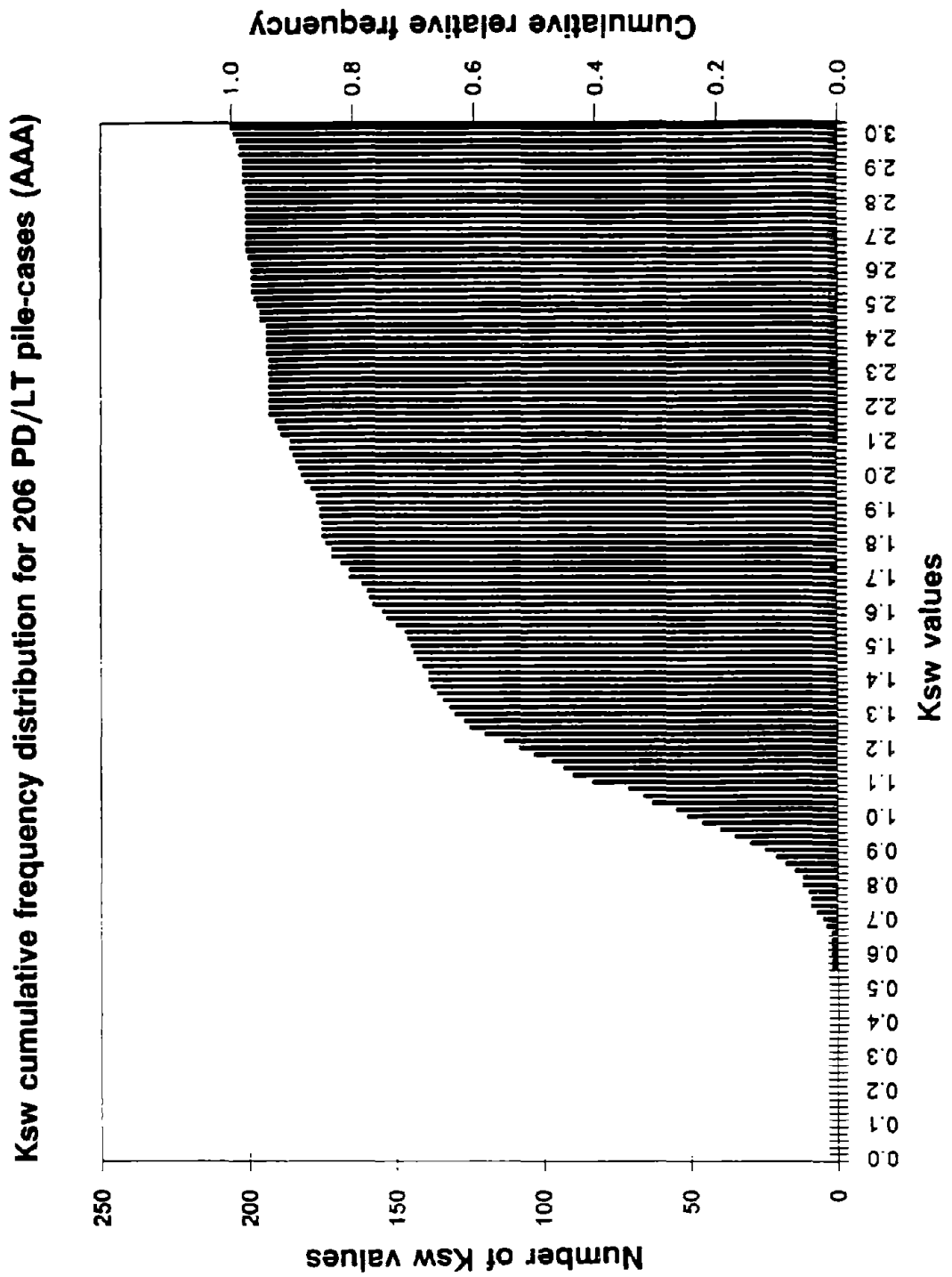


Figure 65. Cumulative frequency distribution of K_w for 206 PD/LT pile-cases in all types of soil (AAA).

**Ksp histogram and frequency distribution
for 208 PD/LT pile-cases (AAA)**

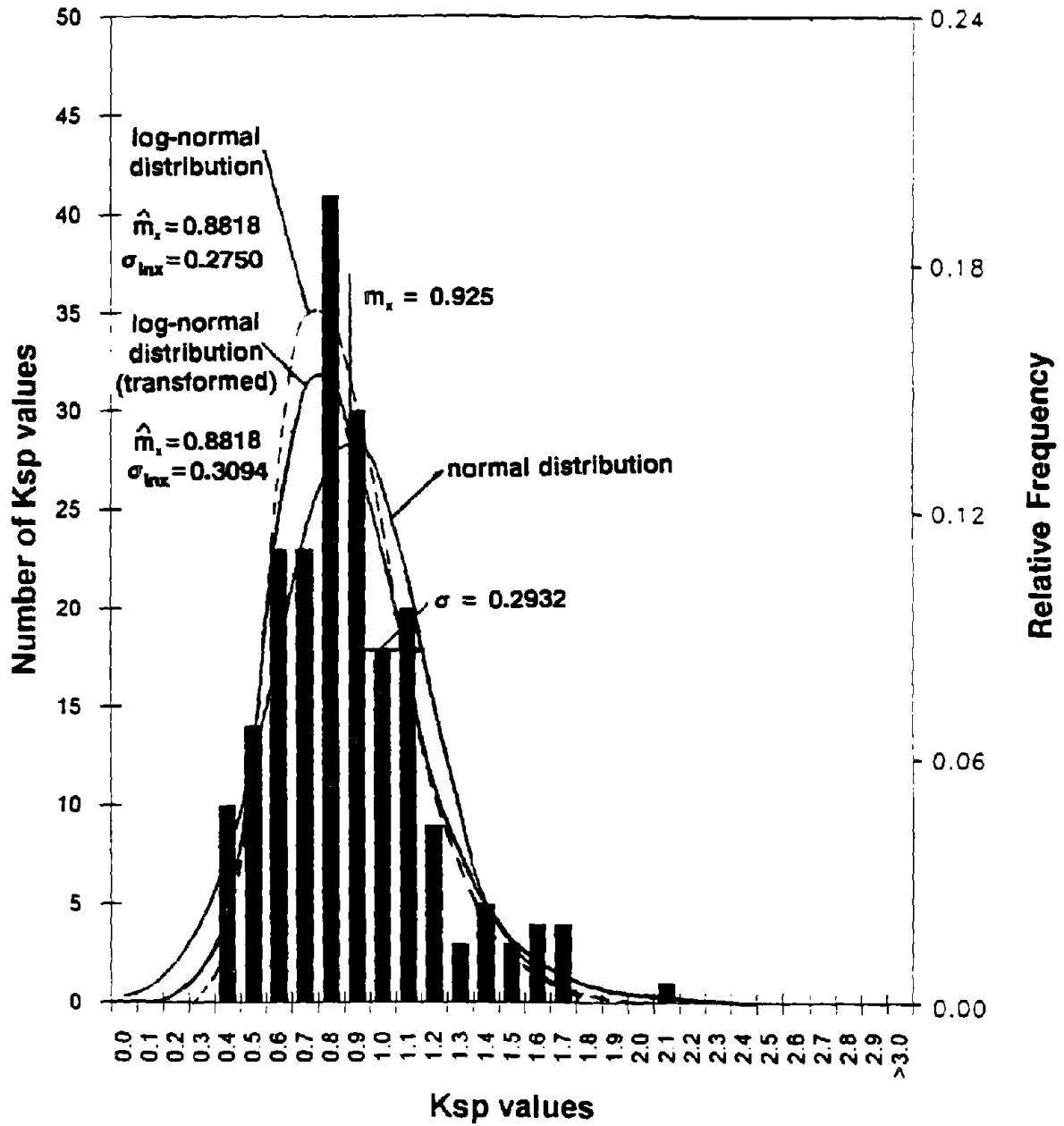


Figure 66. Histogram and frequency distributions of K_{sp} for 208 PD/LT pile-cases in all types of soil (AAA).

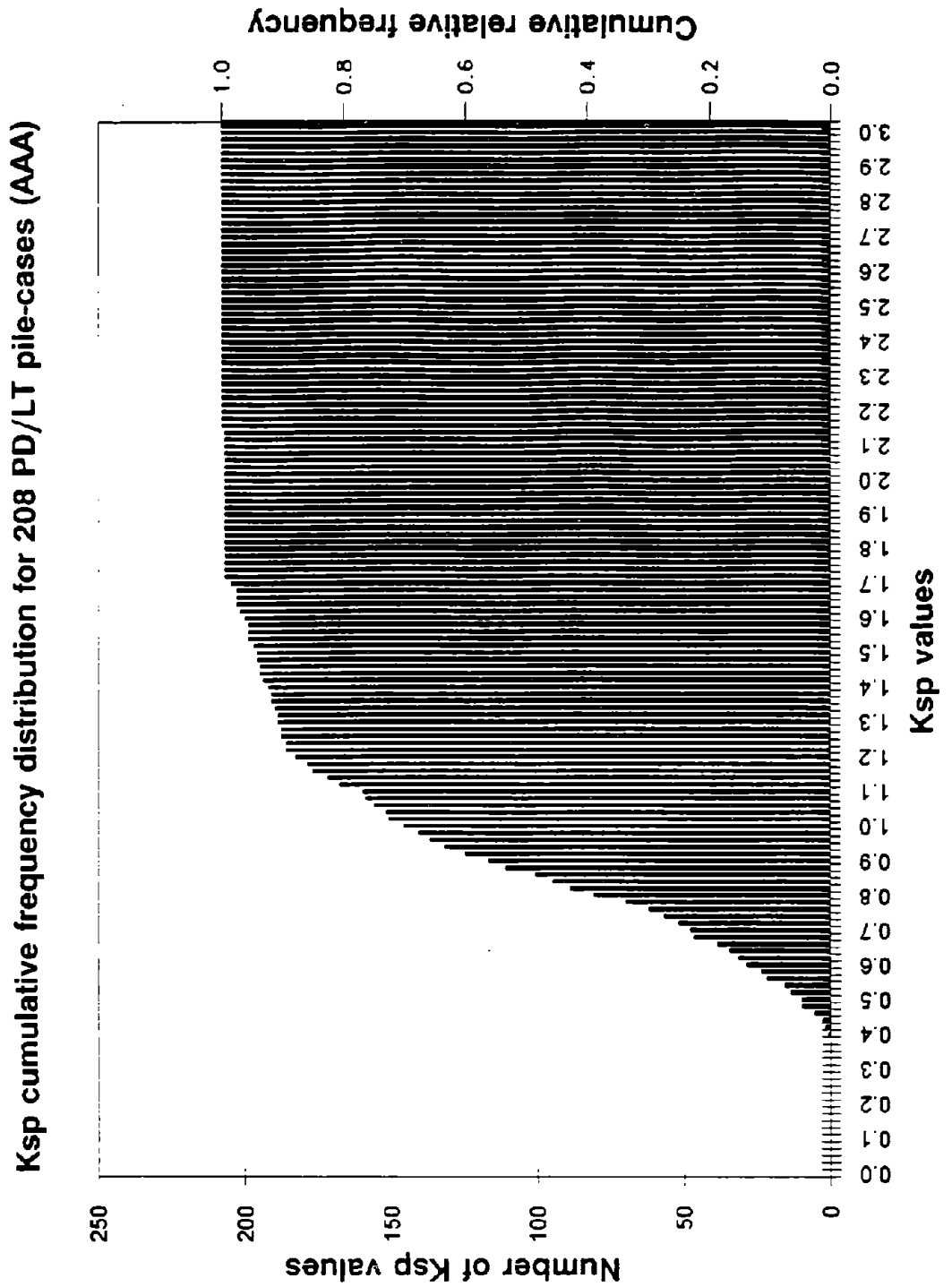


Figure 67. Cumulative frequency distribution of K_{sp} for 208 PD/LT pile-cases in all types of soil (AAA).

**Kew histogram and frequency distribution
for 206 PD/LT pile-cases (AAA)**

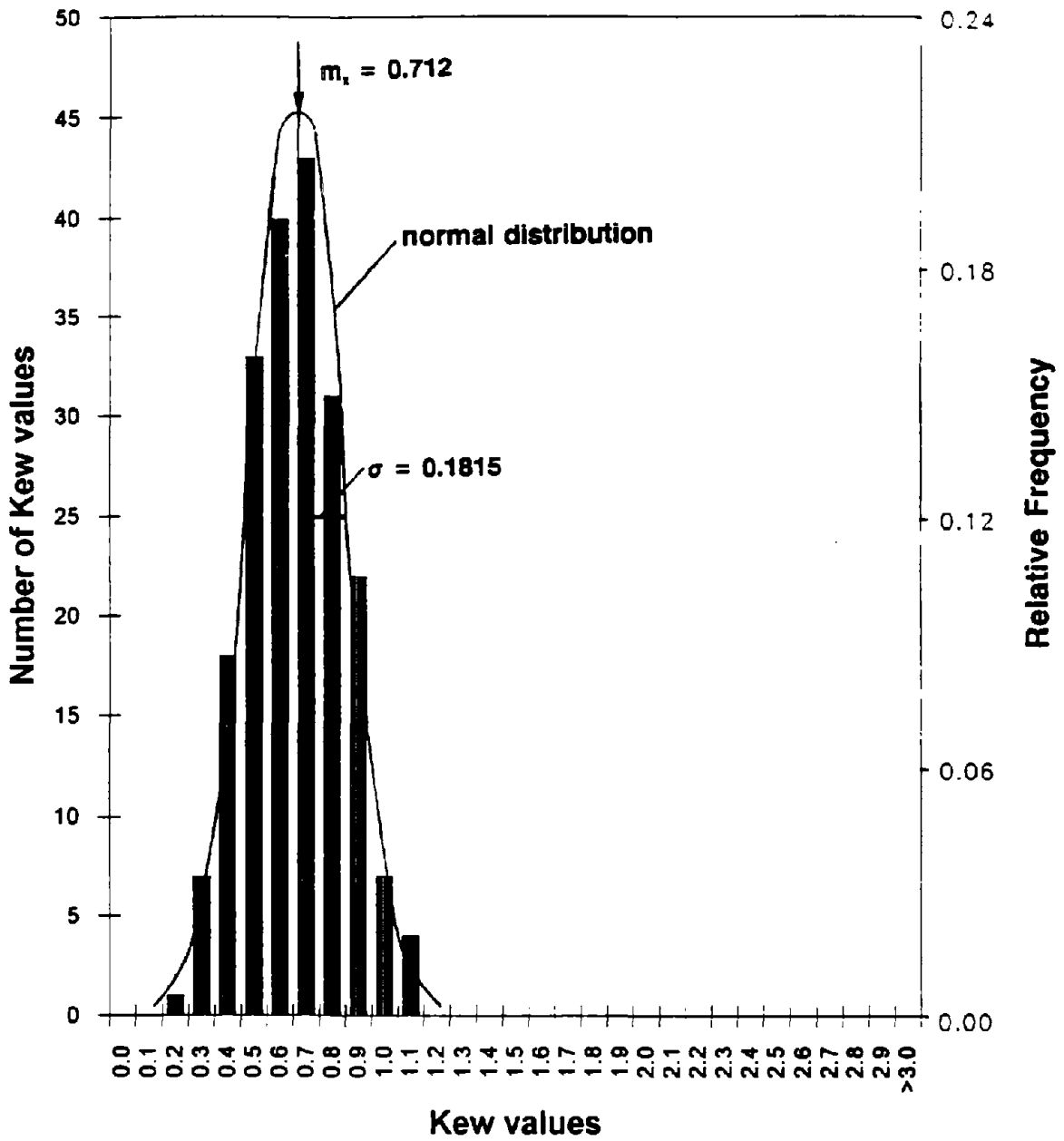


Figure 68. Histogram and frequency distribution of K_{cw} for 206 PD/LT pile-cases in all types of soil (AAA).

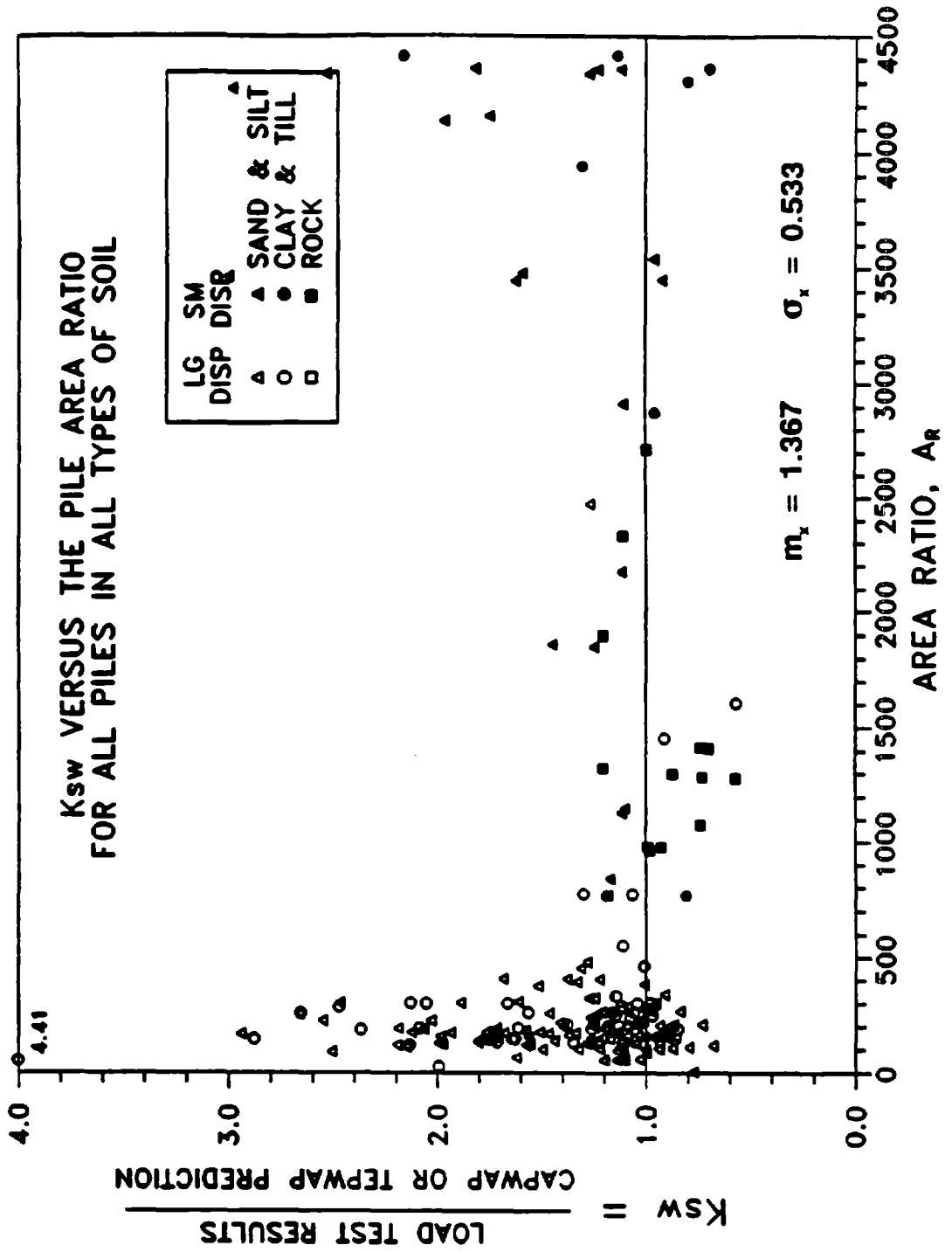


Figure 69. K_{sw} vs. the pile area ratio (A_r) for 201 PD/LT pile-cases in all types of soil.

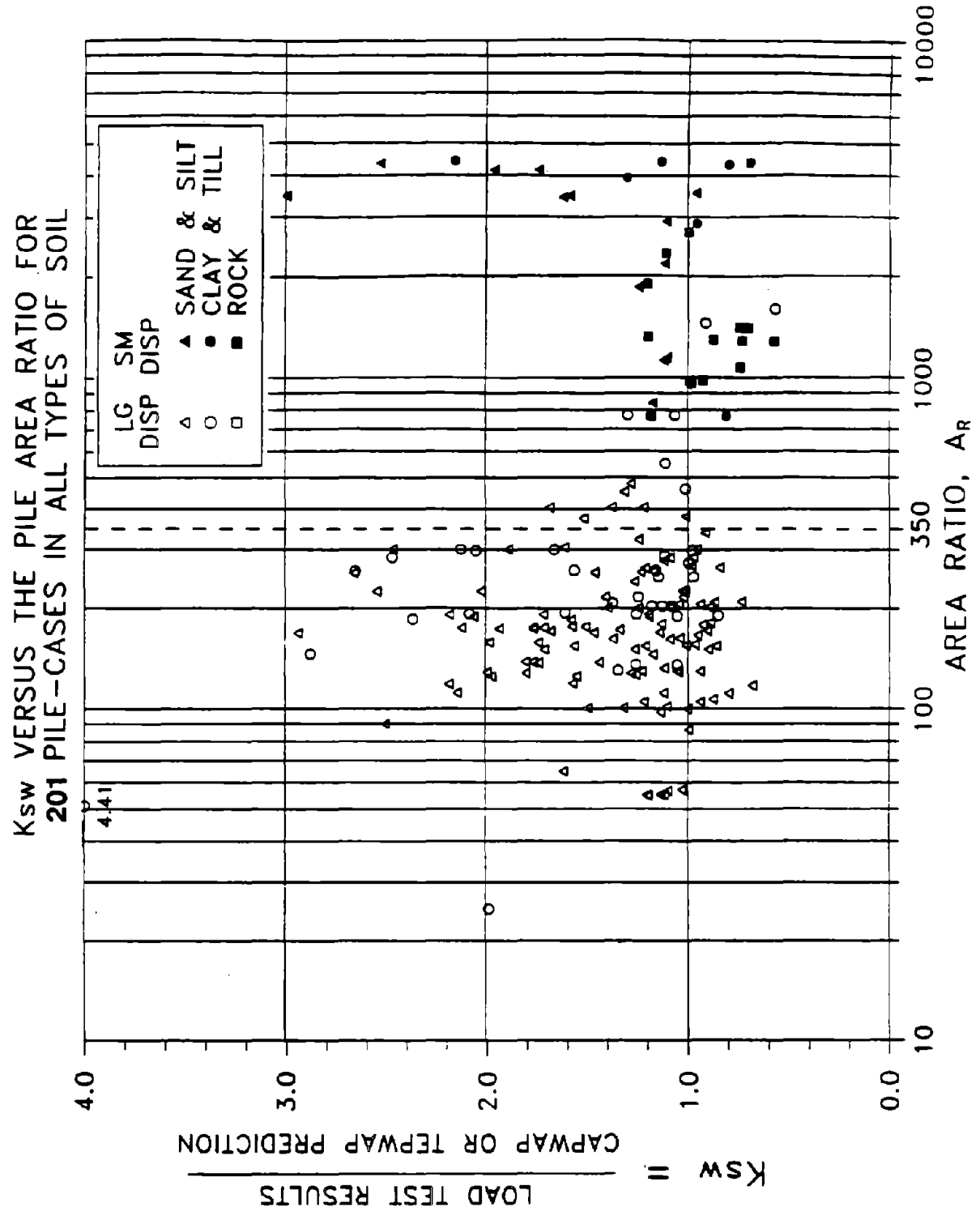


Figure 70. K_{sw} vs. the pile area ratio (A_R) for 201 PD/LT pile-cases in all types of soil (logarithmic scale).

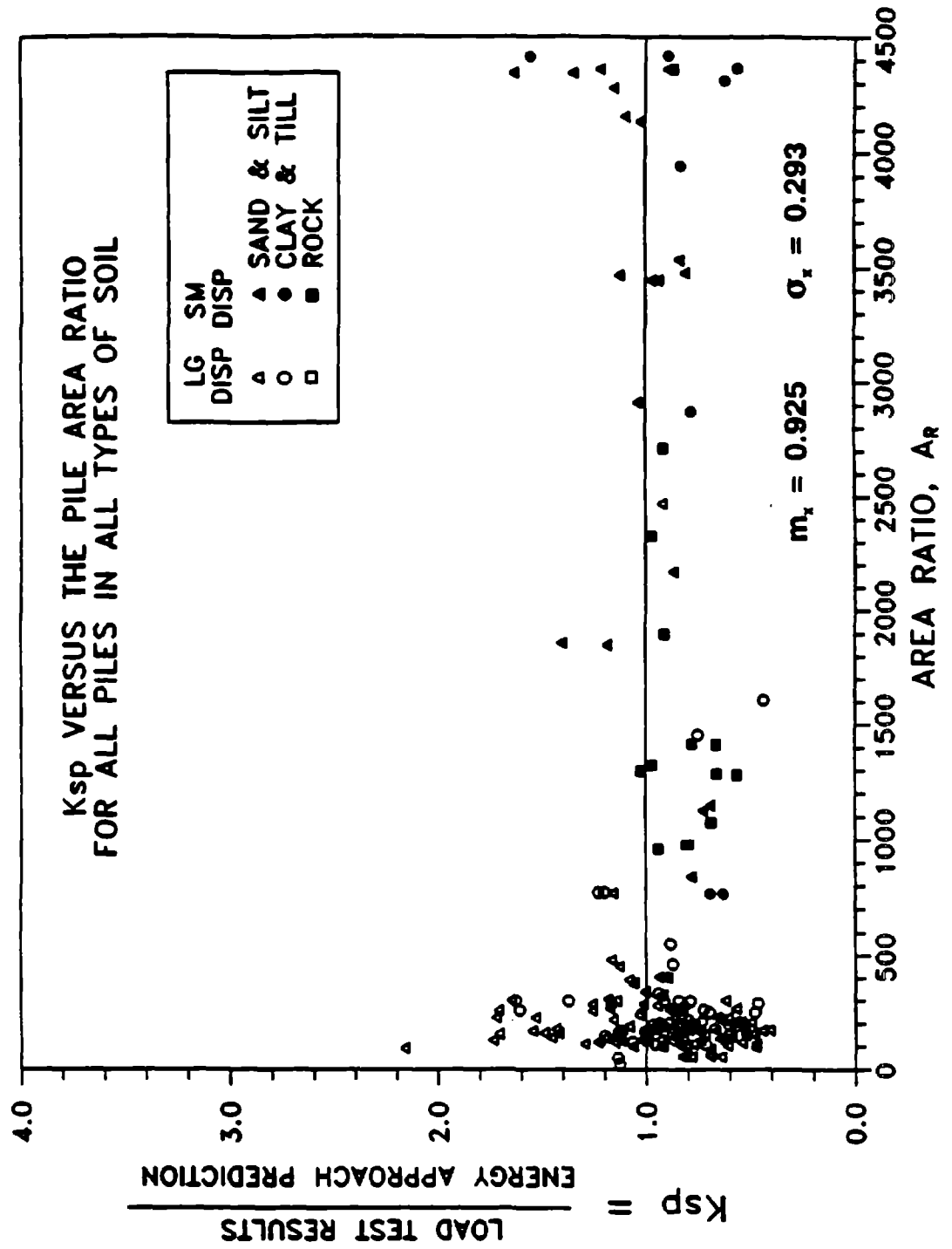


Figure 71. K_{sp} vs. the pile area ratio (A_R) for 203 PD/LT pile-cases in all types of soil.

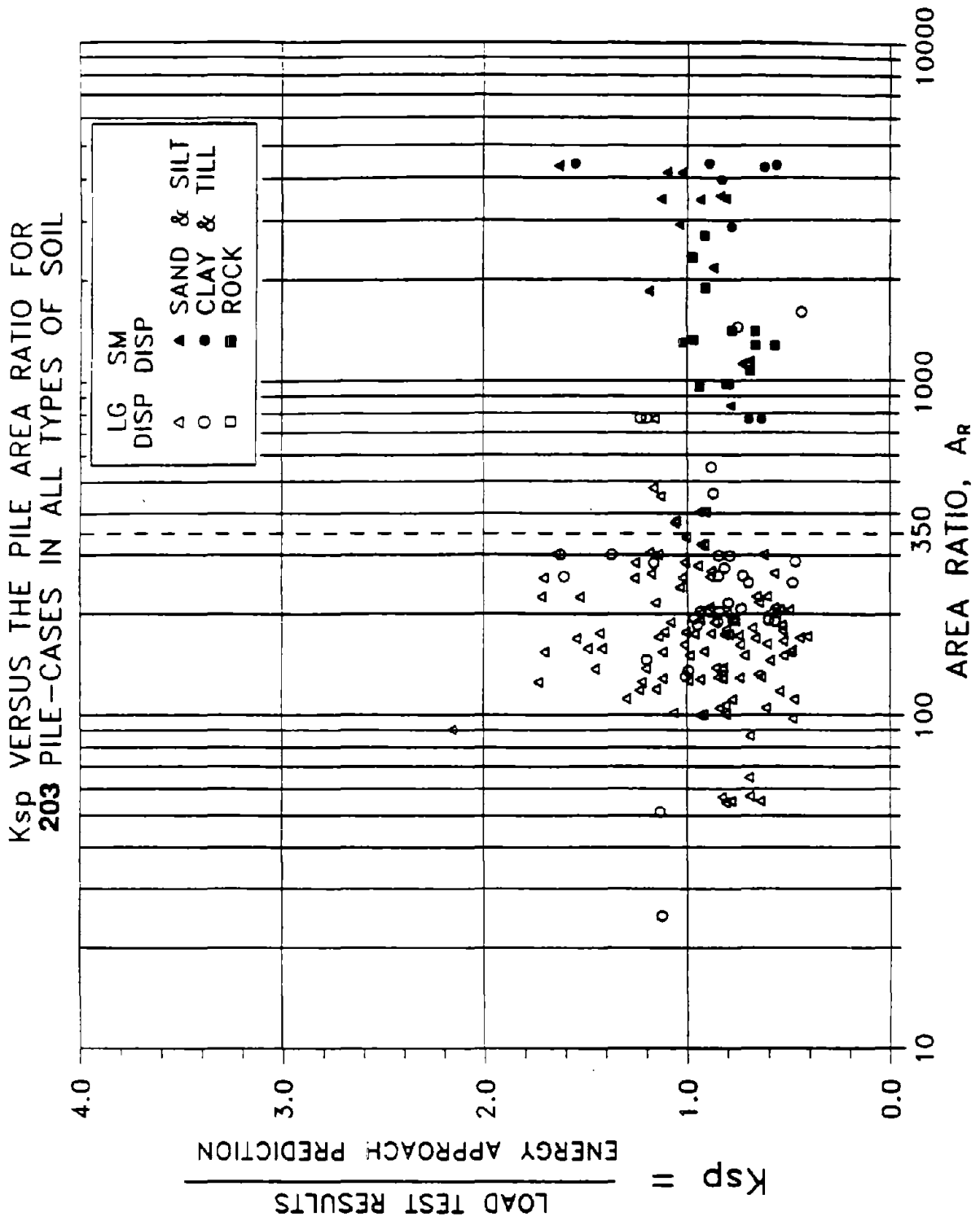


Figure 72. K_{sp} vs. the pile area ratio (A_p) for 203 PD/LT pile-cases in all types of soil (logarithmic scale).

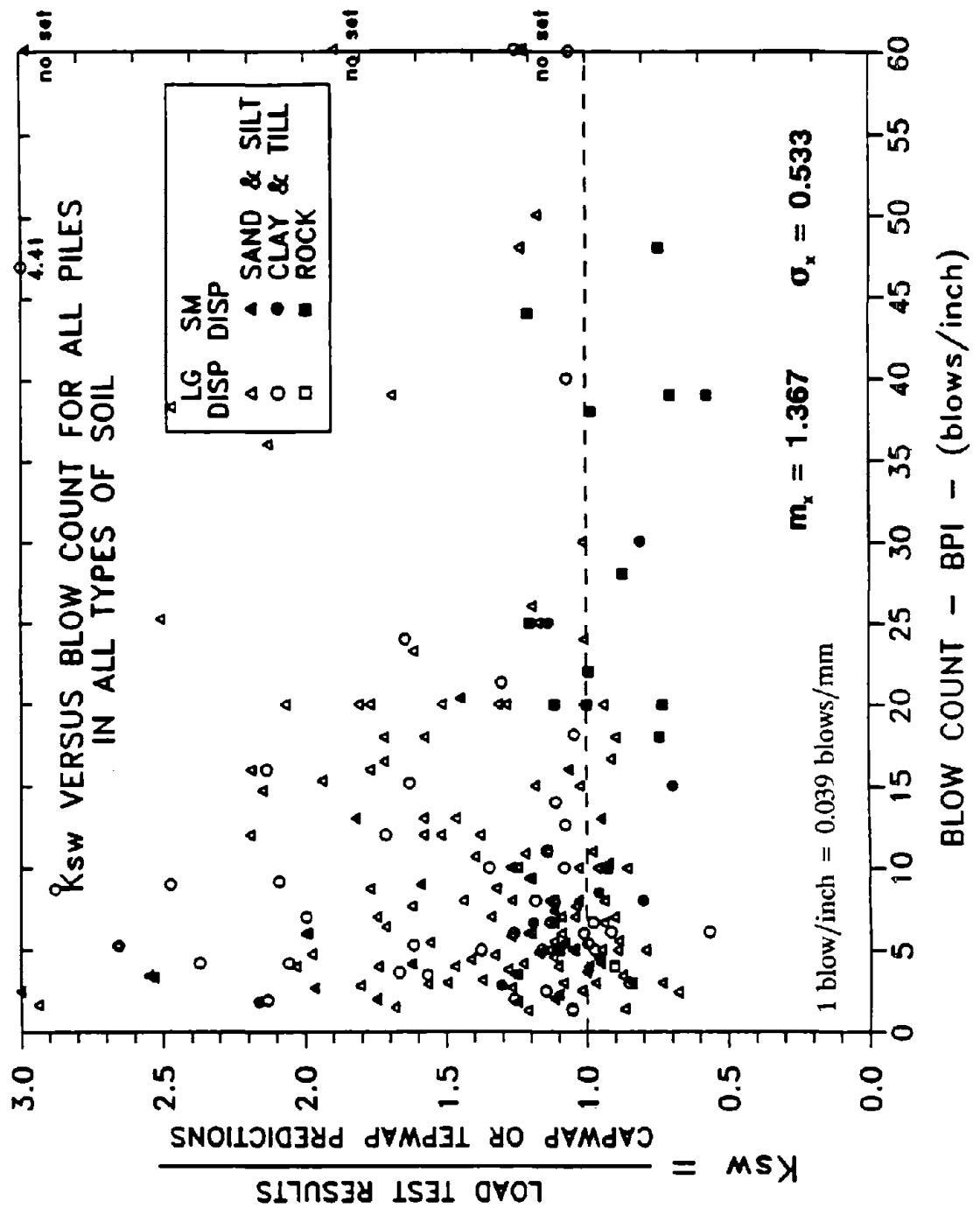


Figure 73. K_{sw} vs. blow count (BPI) for 206 PD/LT pile-cases in all types of soil (AAA).

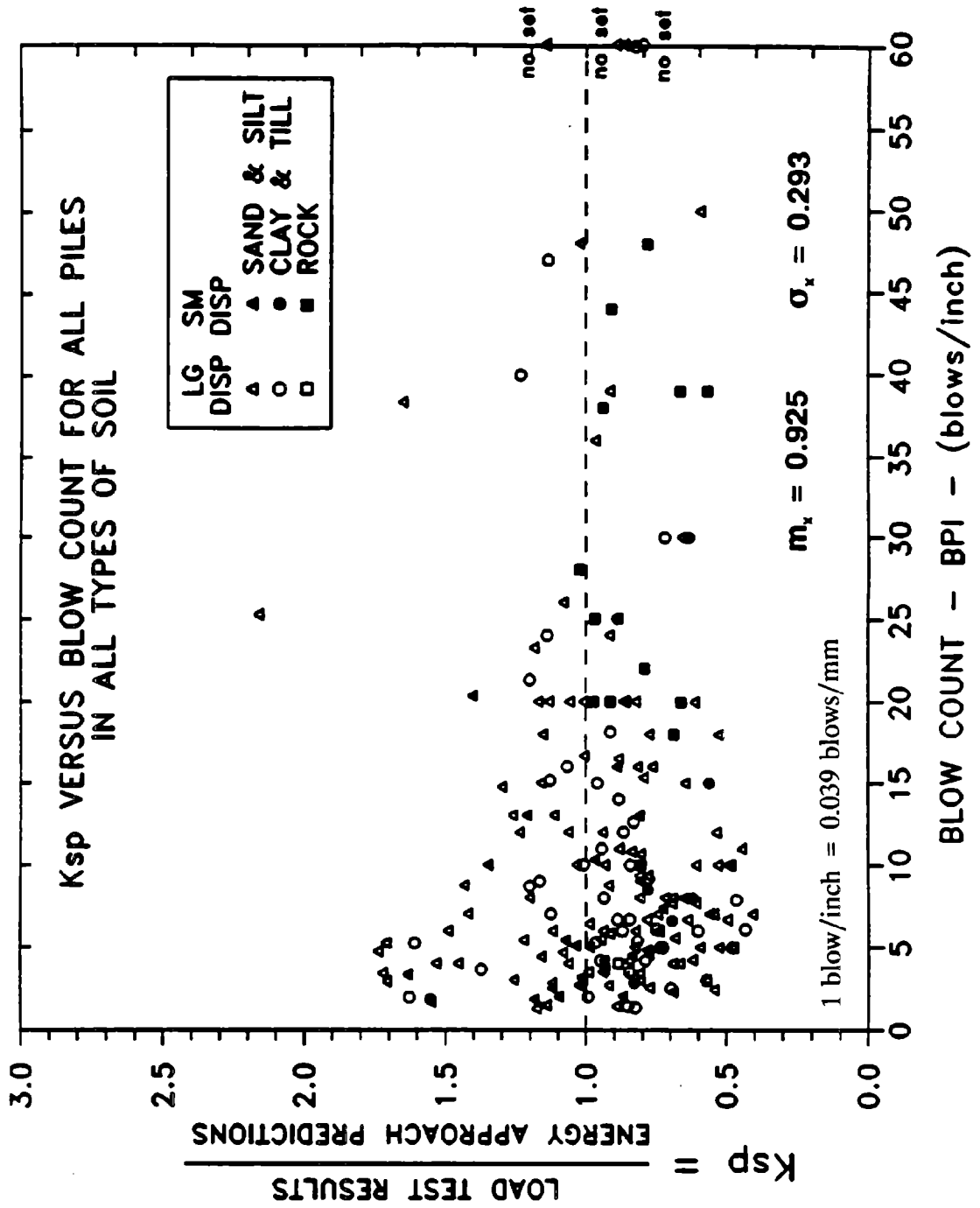


Figure 74. K_{sp} vs. blow count (BPI) for 208 PD/LT pile-cases in all types of soil (AAA).

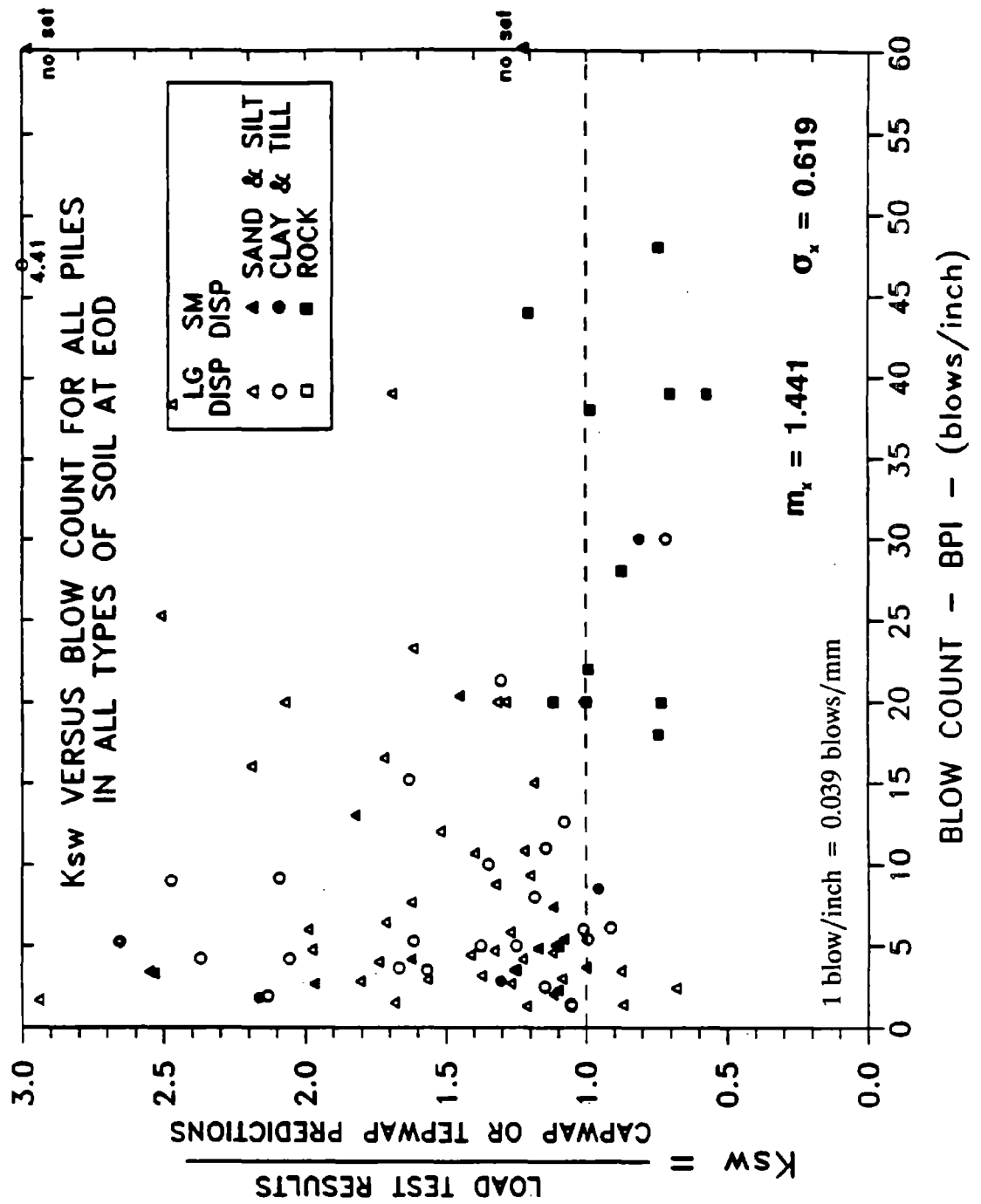


Figure 75. K_{sw} vs. blow count (BPI) for 95 PD/LT pile-cases in all types of soil at EOD (AEA).

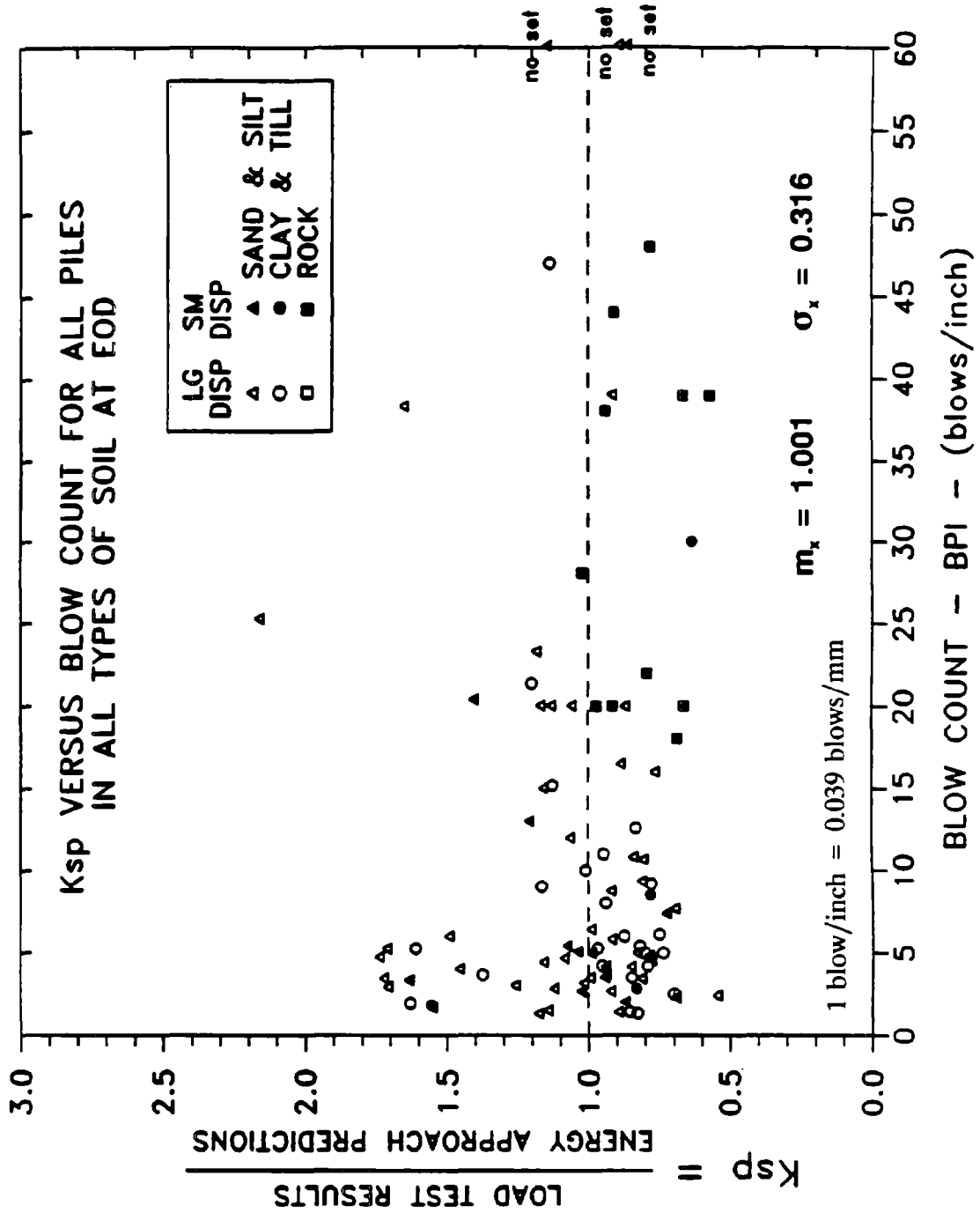


Figure 76. K_{sp} vs. blow count (BPI) for 96 PD/LT pile-cases in all types of soil at EOD (AEA).

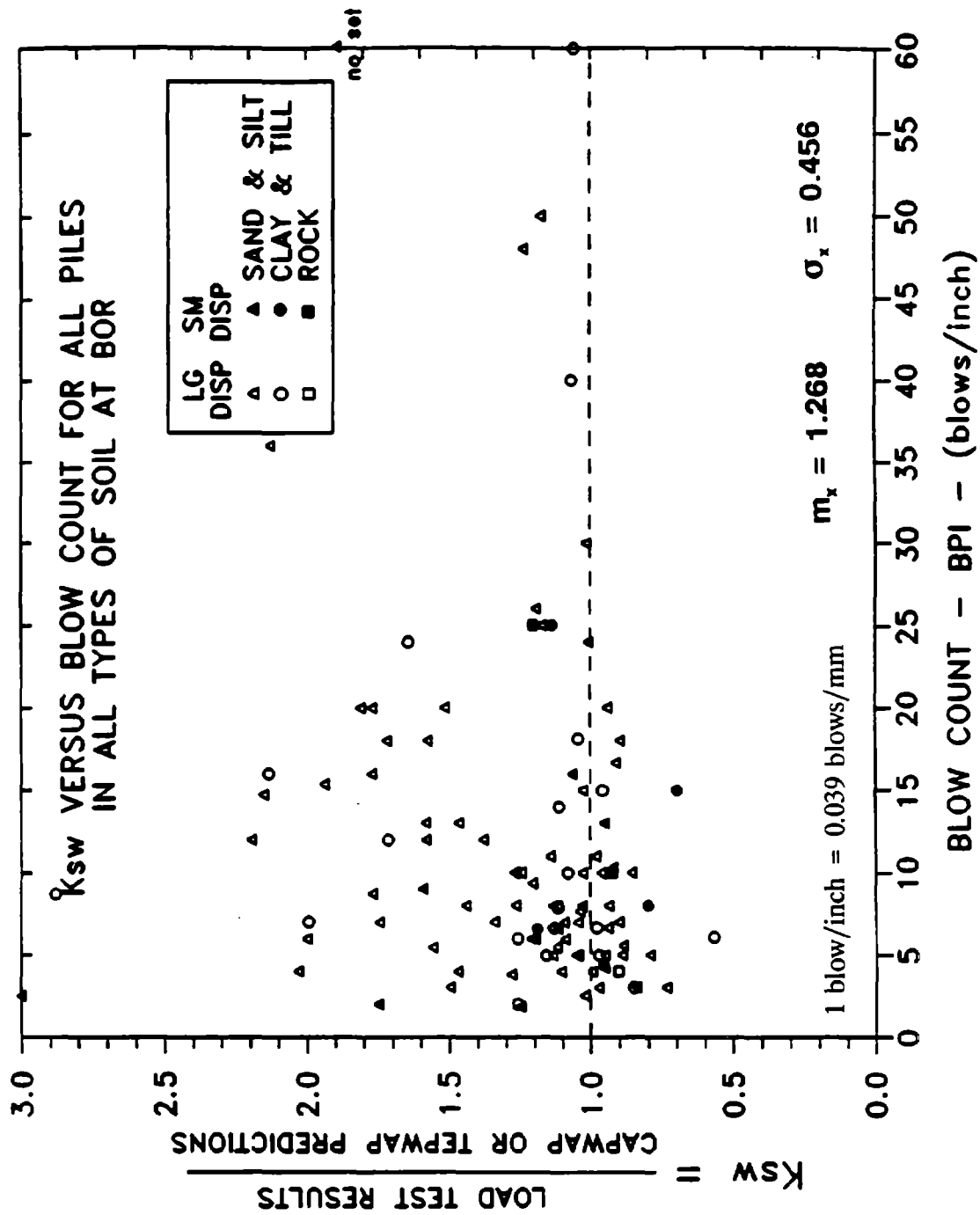


Figure 77. K_{sw} vs. blow count (BPI) for 109 PD/LT pile-cases in all types of soil at BOR (ABA).

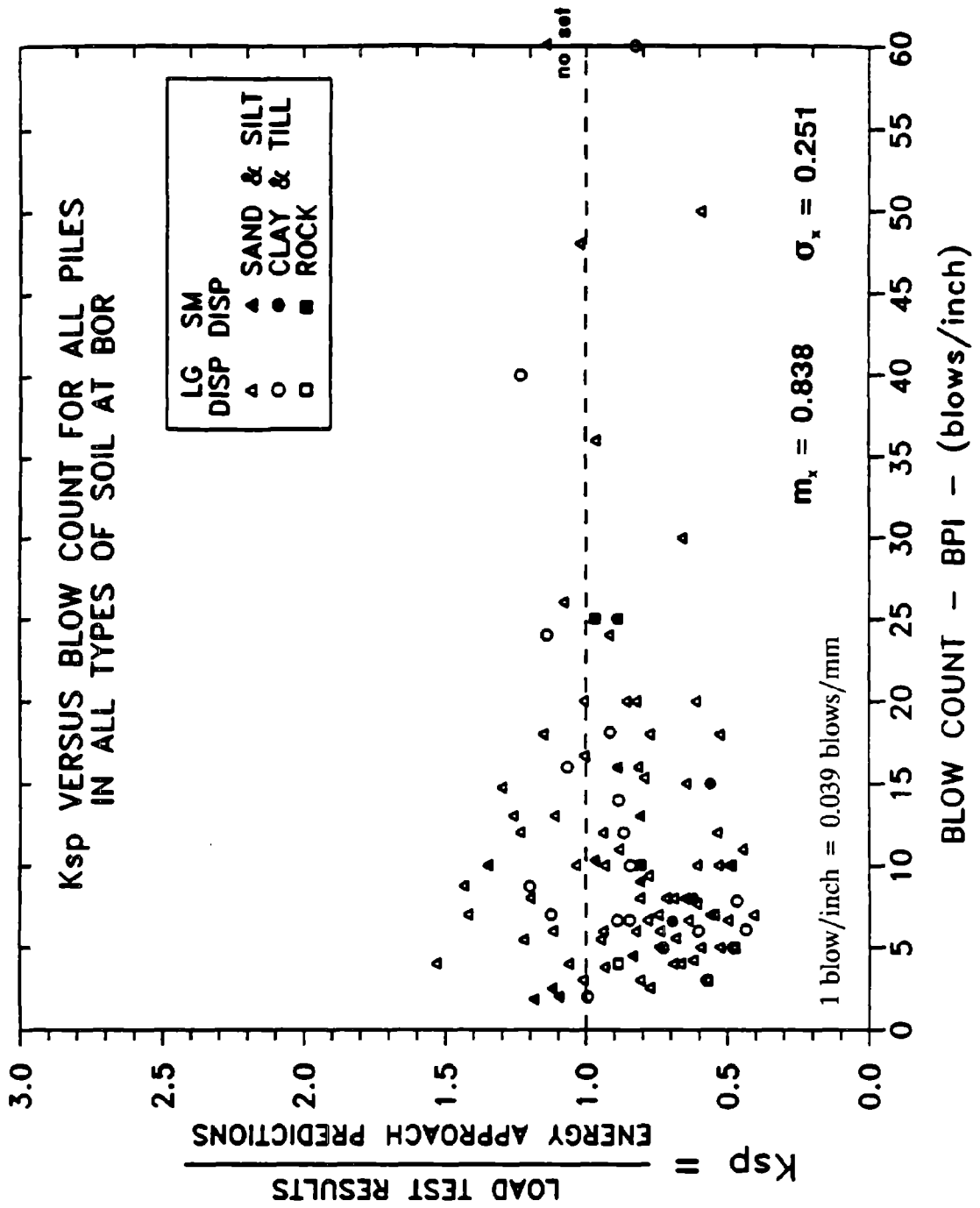


Figure 78. K_{sp} vs. blow count (BPI) for 110 PD/LT pile-cases in all types of soil at BOR (ABA).

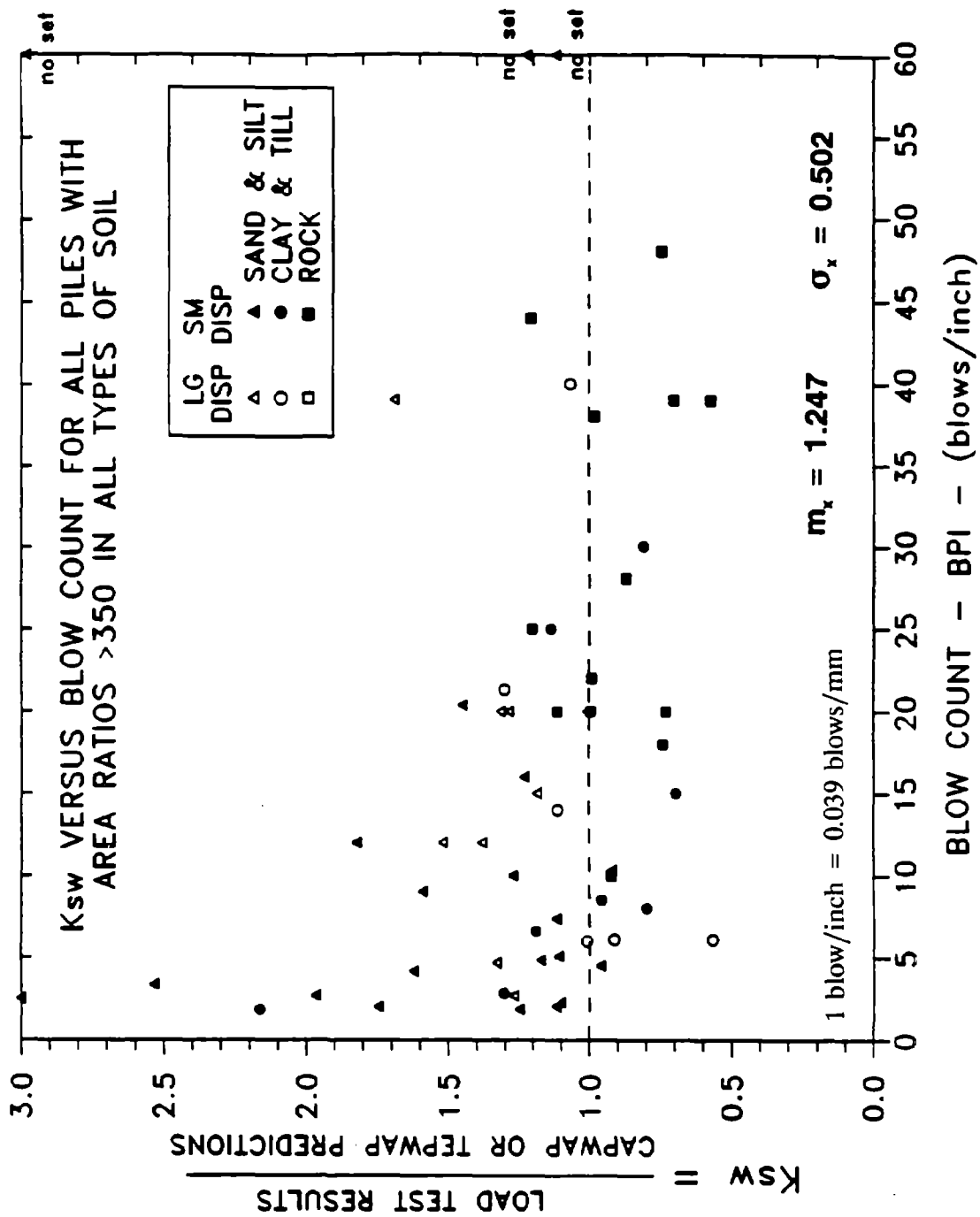


Figure 79. K_{sw} vs. blow count (BPI) for 57 PD/LT pile-cases with pile area ratios >350 in all types of soil.

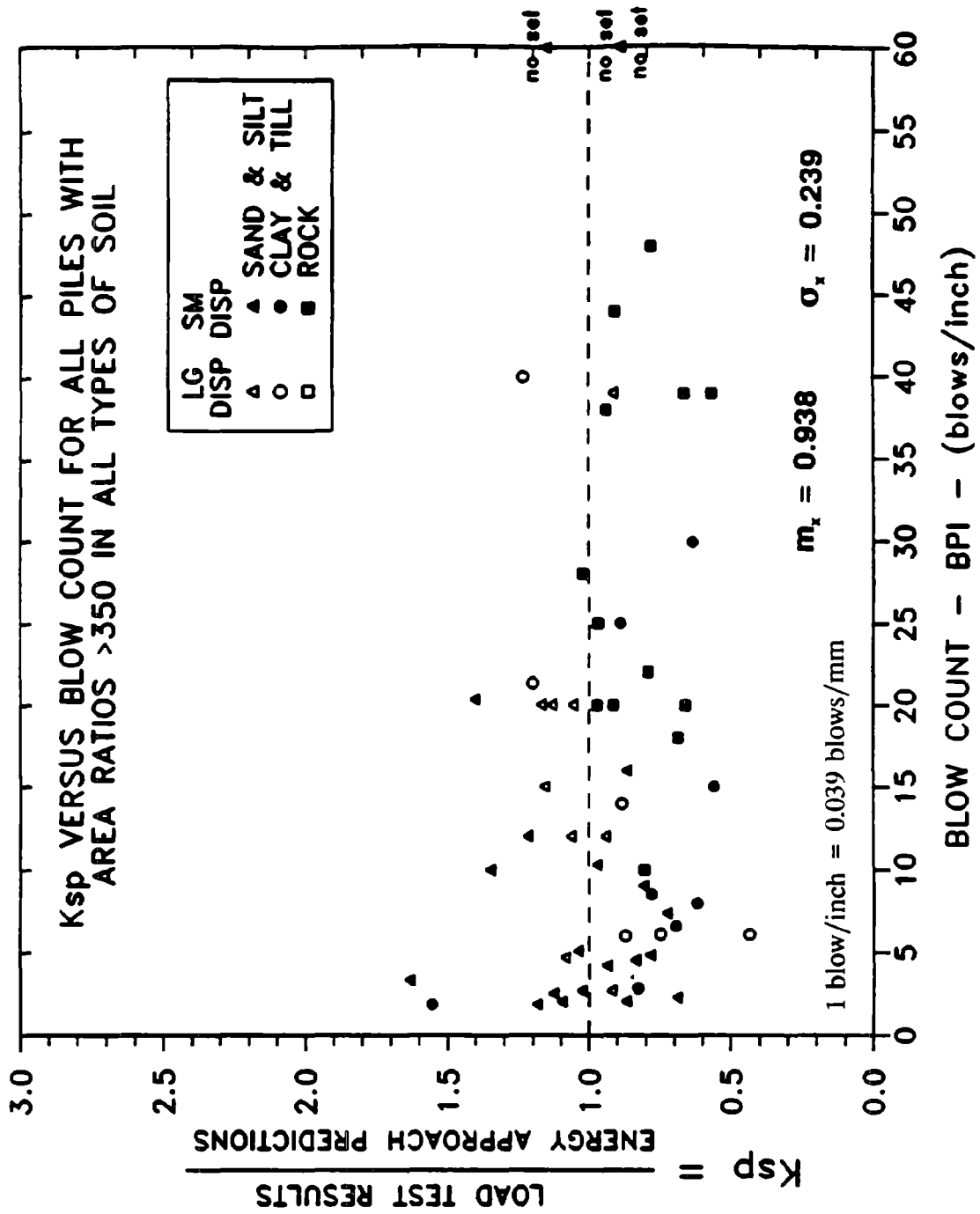


Figure 80. K_{sp} vs. blow count (BPI) for 57 PD/LT pile-cases with pile area ratios >350 in all types of soil.

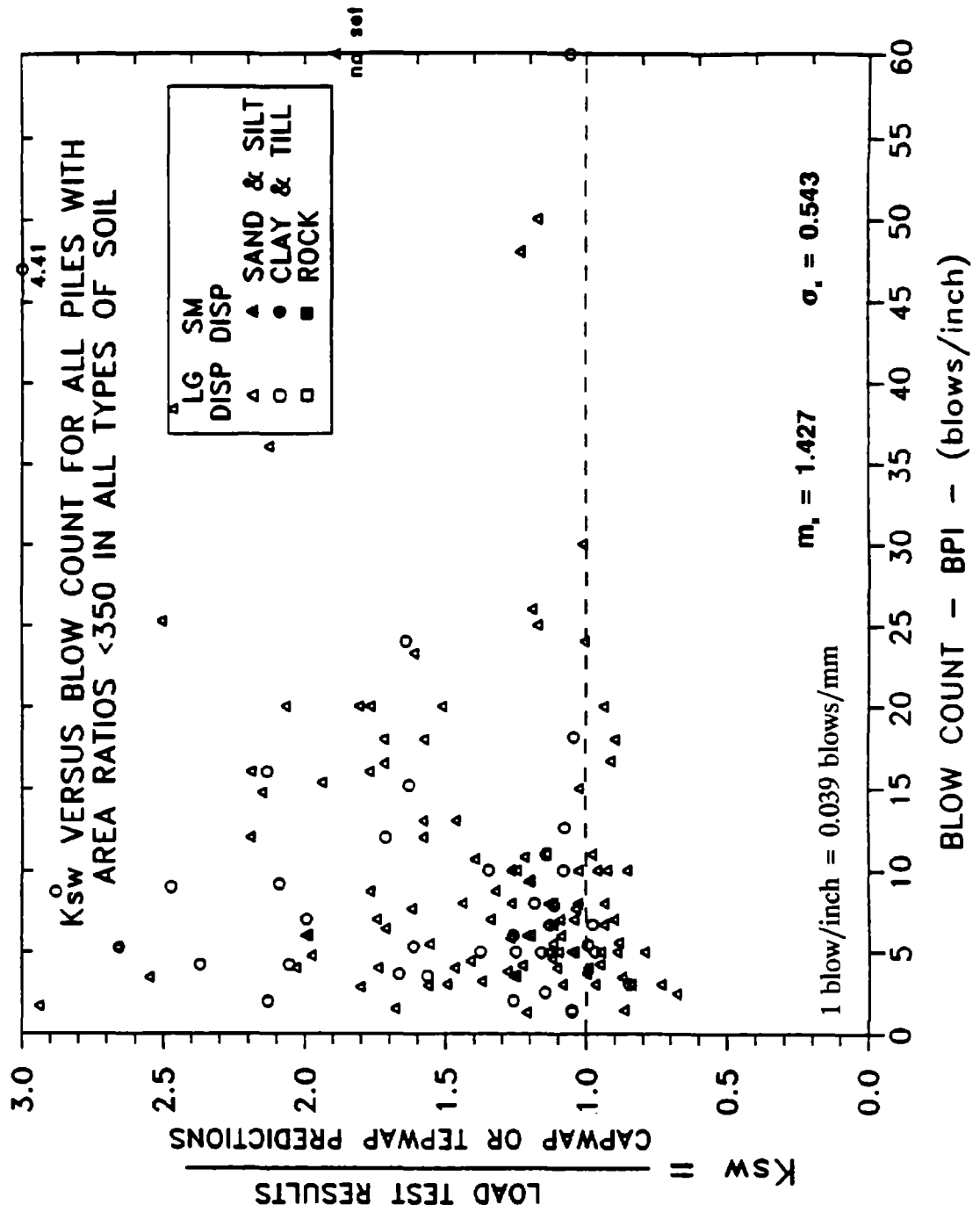


Figure 81. K_{sw} vs. blow count (BPI) for 144 PD/LT pile-cases with pile area ratios <350 in all types of soil.

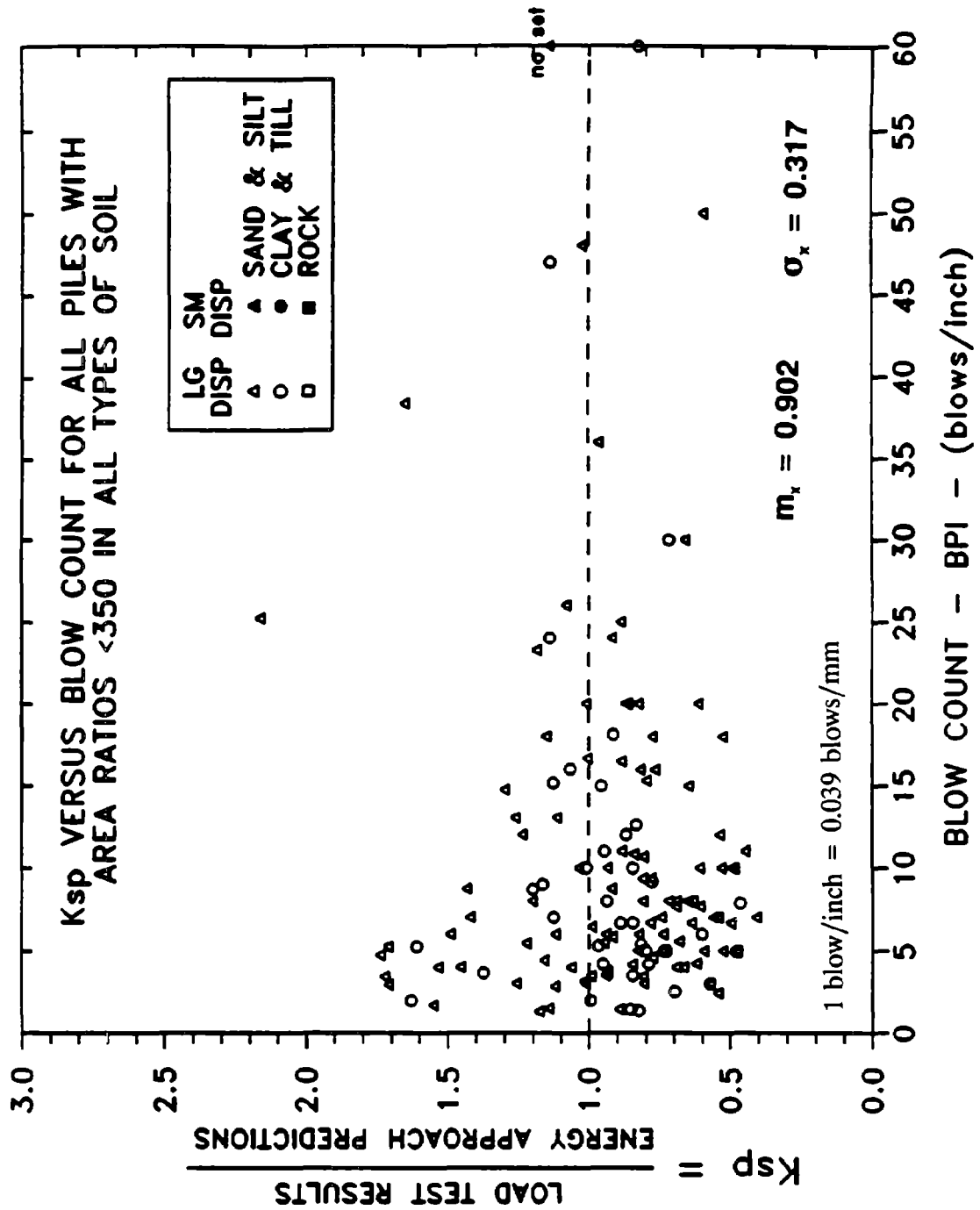


Figure 82. K_{sp} vs. blow count (BPI) for 146 PD/LT pile-cases with pile area ratios <350 in all types of soil.

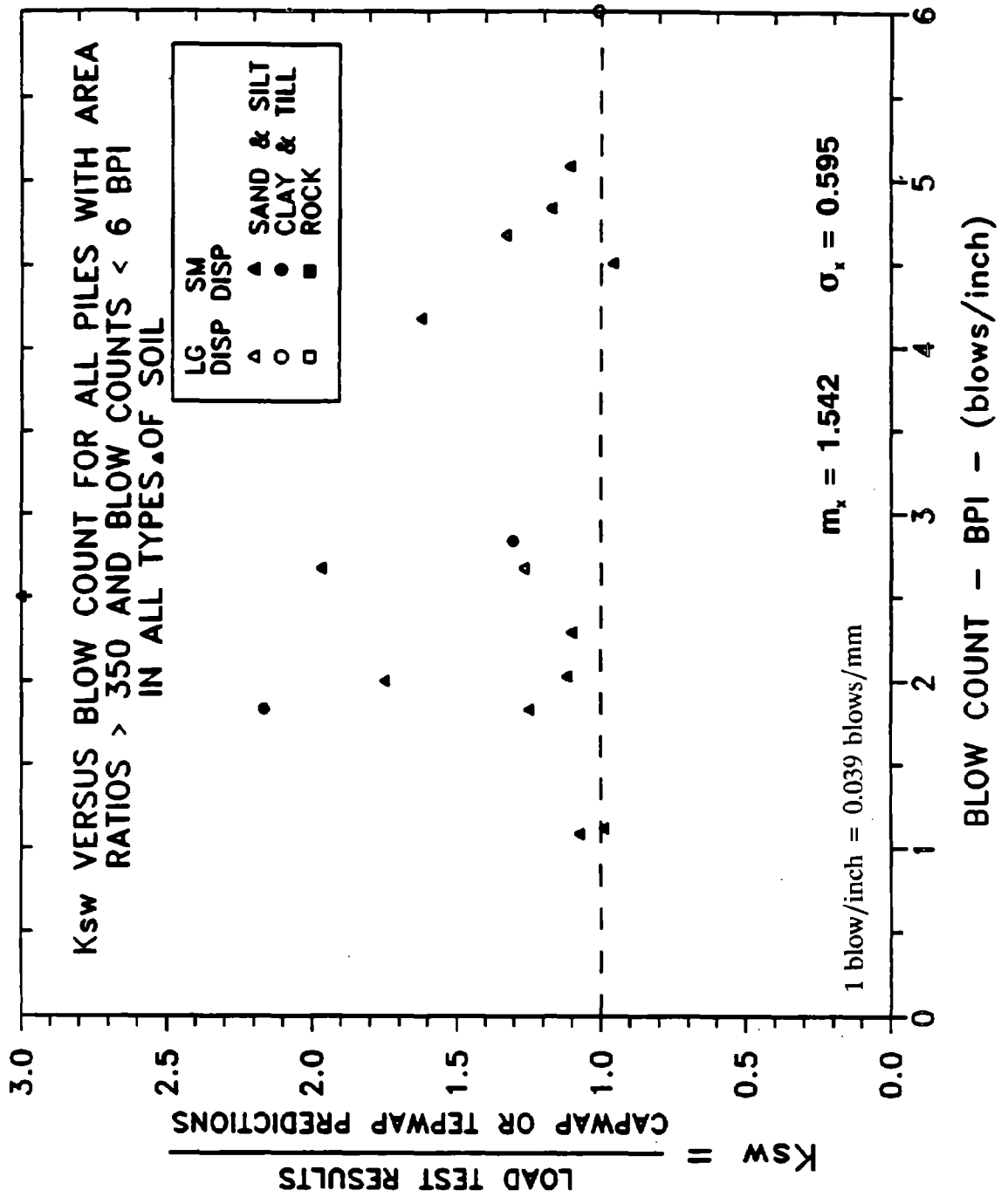


Figure 83. K_{sw} vs. blow count (BPI) for 16 PD/LT pile-cases with pile area ratios >350 and blow counts <6 BPI (0.24 blows/mm) in all types of soil.

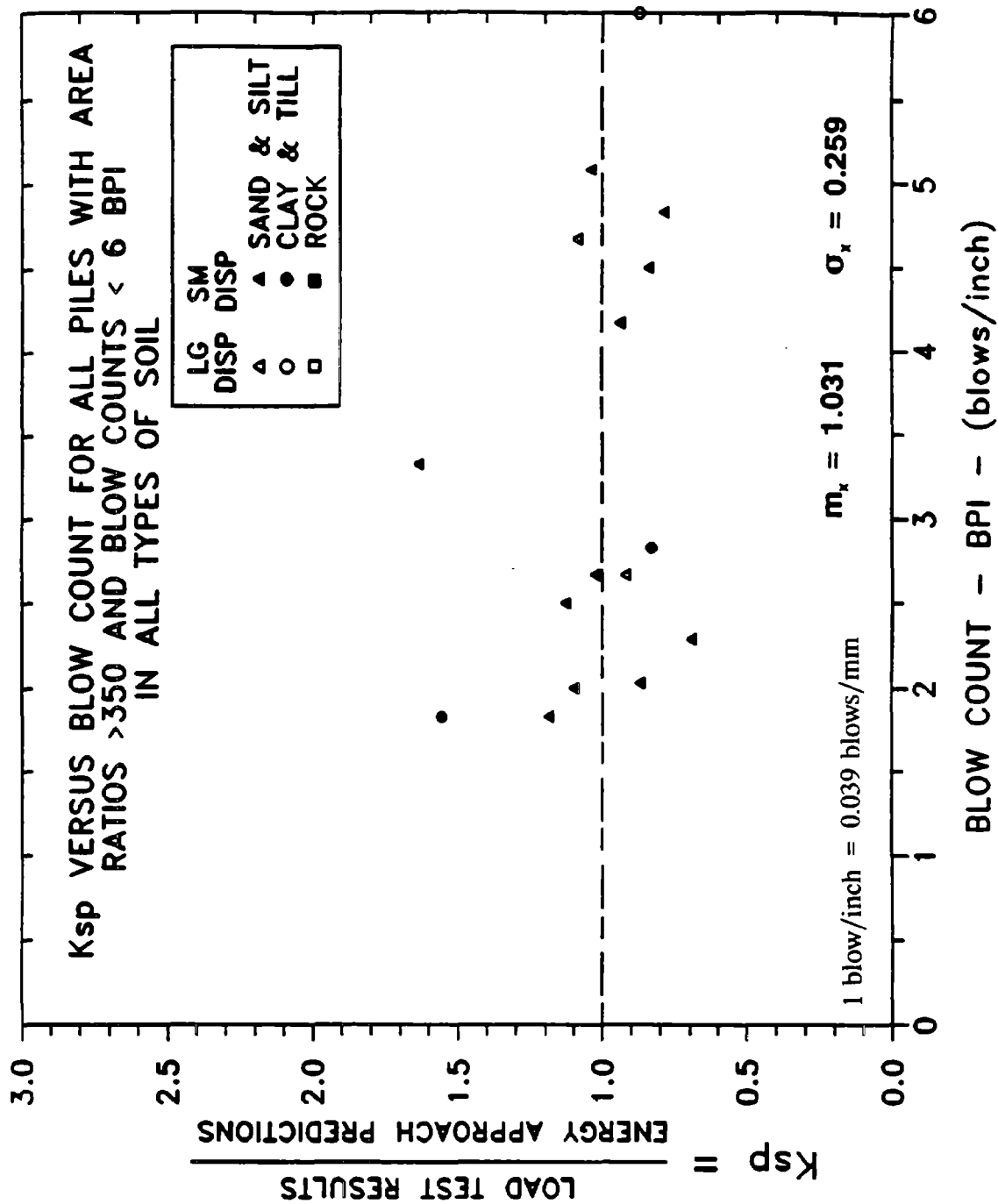


Figure 84. K_{sp} vs. blow count (BPI) for 16 PD/LT pile-cases with pile area ratios >350 and blow counts <6 BPI (0.24 blows/mm) in all types of soil.

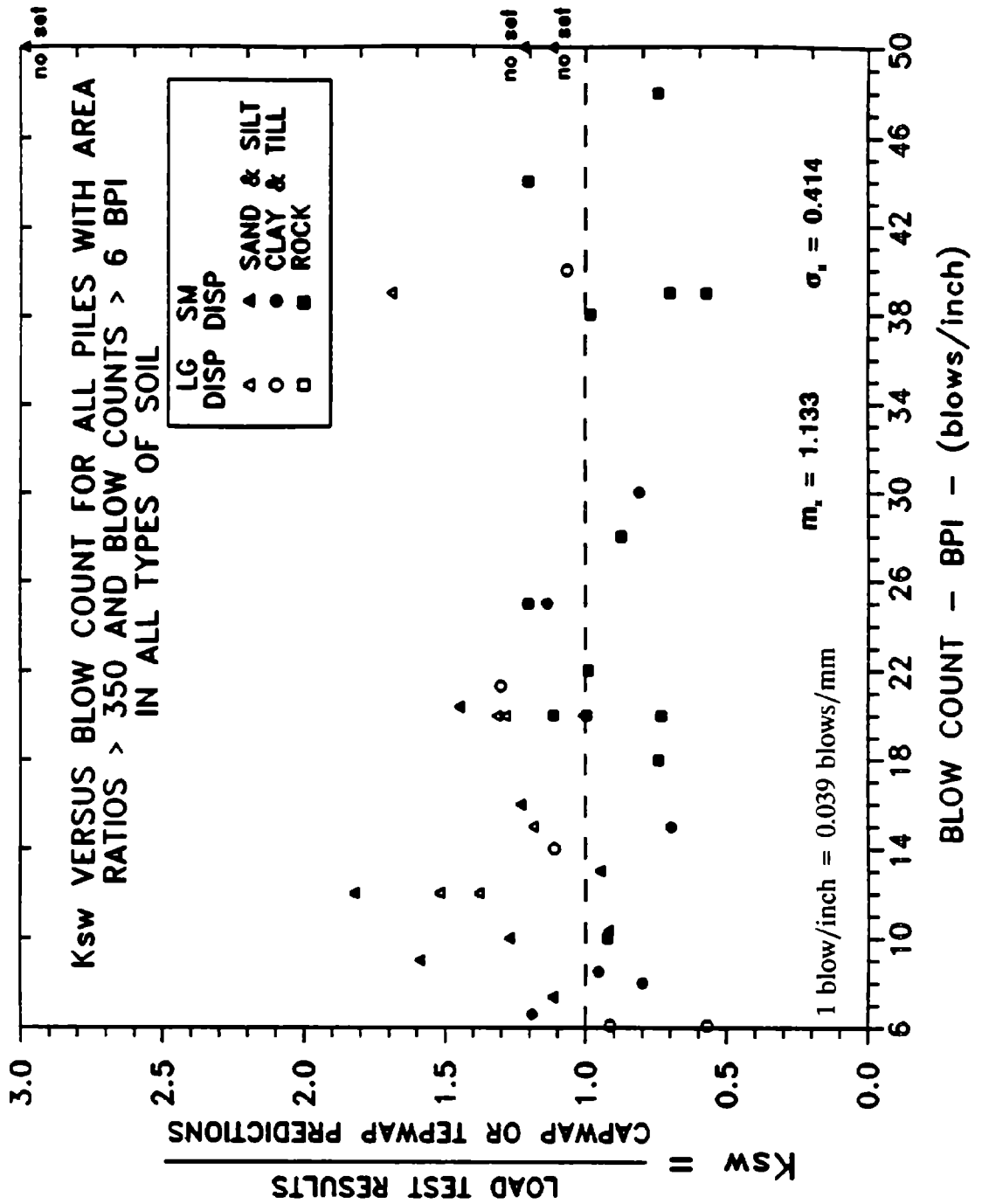


Figure 85. K_{sw} vs. blow count (BPI) for 41 PD/LT pile-cases with pile area ratios > 350 and blow counts > 6 BPI (0.24 blows/mm) in all types of soil.

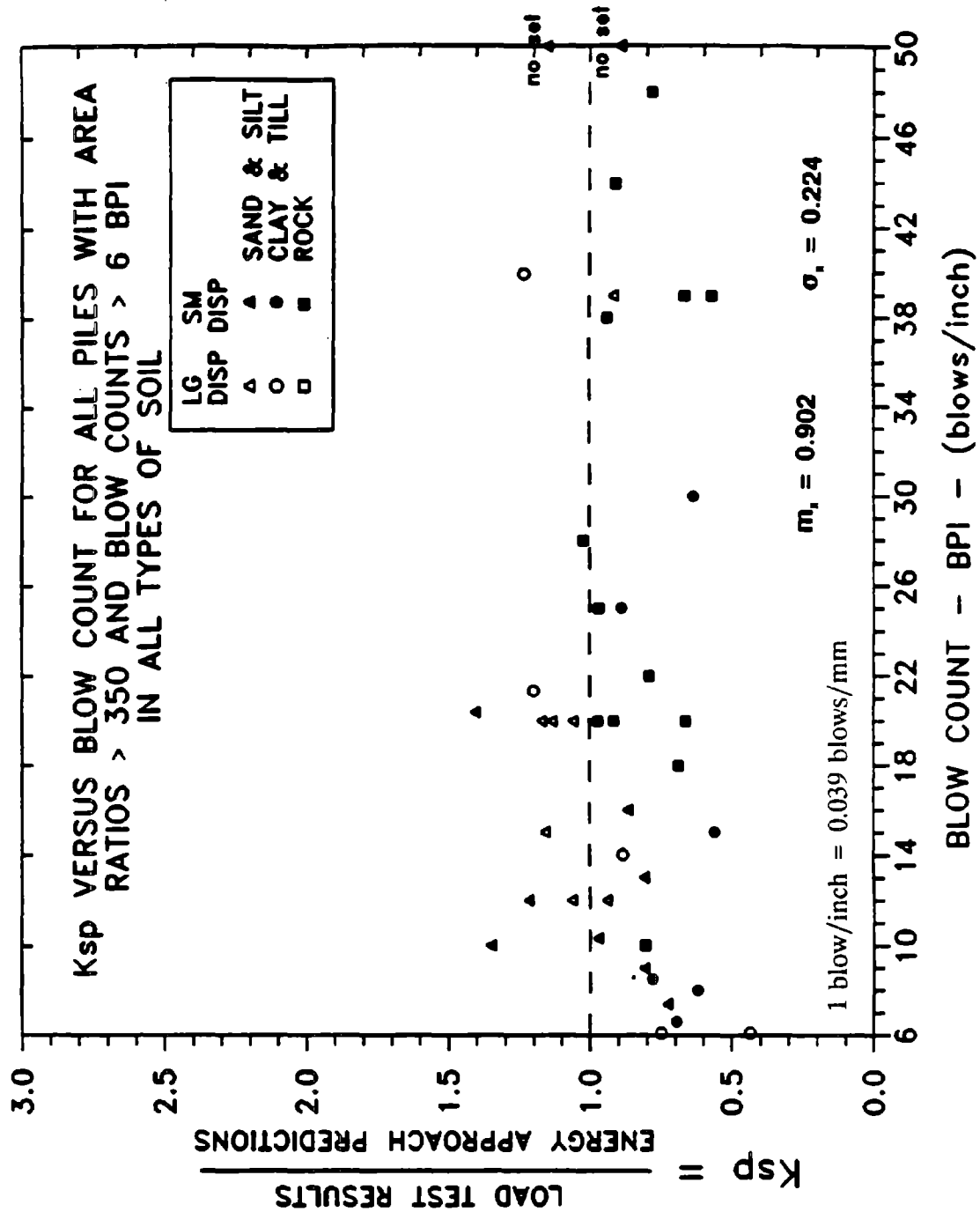


Figure 86. K_{sp} vs. blow count (BPI) for 41 PD/LT pile-cases with pile area ratios >350 and blow counts >6 BPI (0.24 blows/mm) in all types of soil.

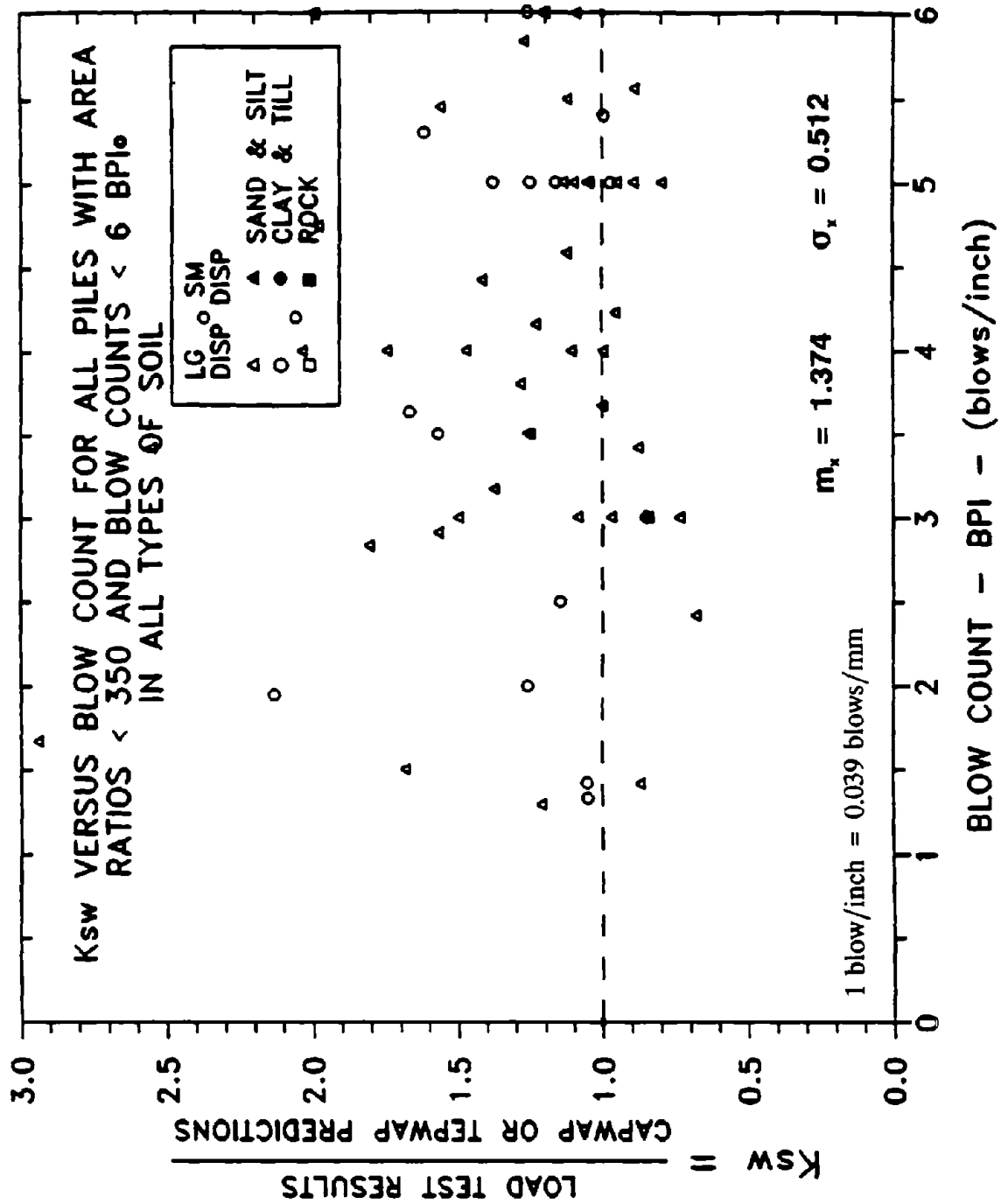


Figure 87. K_{sw} vs. blow count (BPI) for 64 PD/LT pile-cases with pile area ratios < 350 and blow counts < 6 BPI (0.24 blows/mm) in all types of soil.

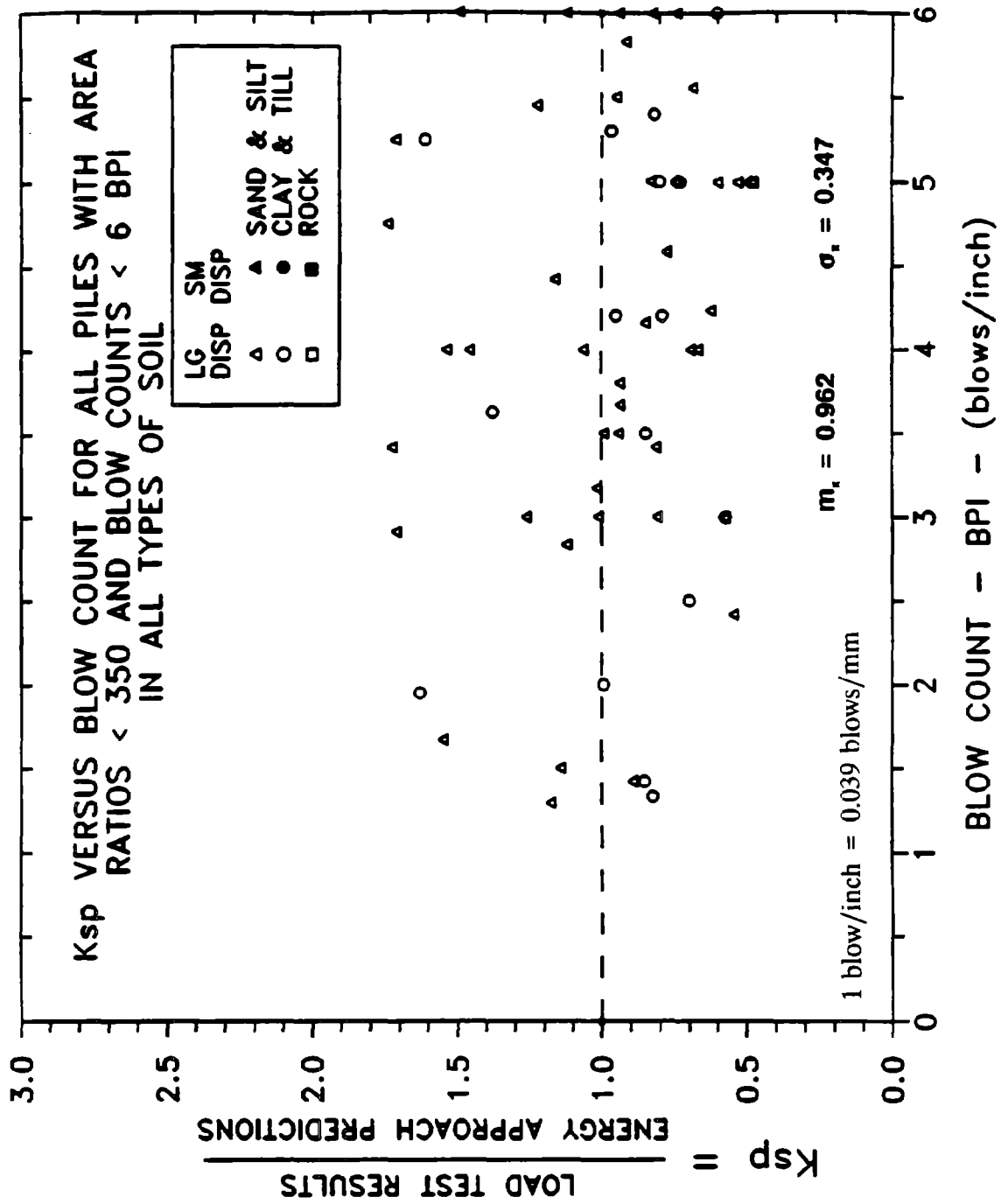


Figure 88. K_{sp} vs. blow count (BPI) for 64 PD/LT pile-cases with pile area ratios < 350 and blow counts < 6 BPI (0.24 blows/mm) in all types of soil.

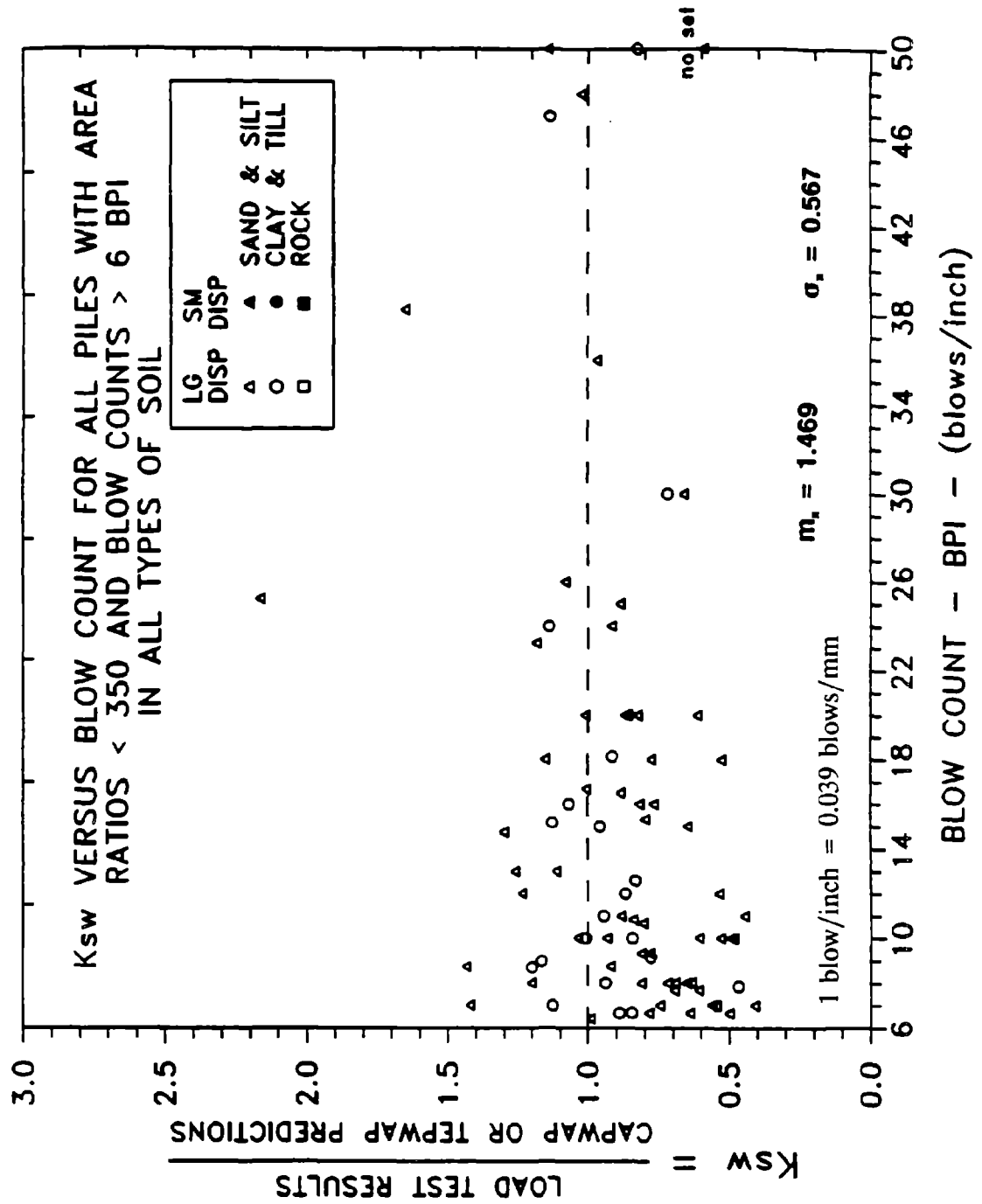


Figure 89. K_{sw} vs. blow count (BPI) for 80 PD/LT pile-cases with pile area ratios < 350 and blow counts > 6 BPI (0.24 blows/mm) in all types of soil.

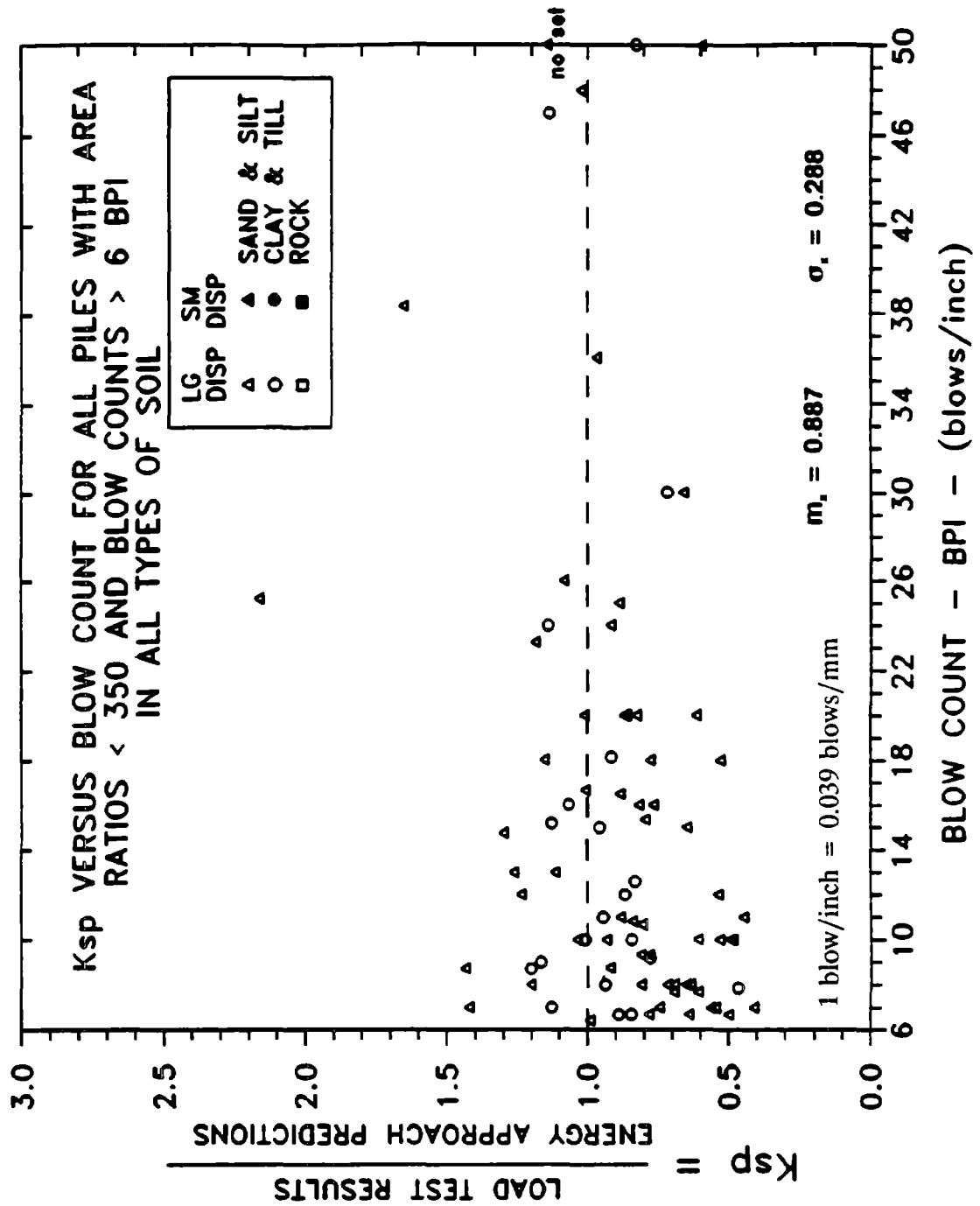


Figure 90. K_{sp} vs. blow count (BPI) for 82 PD/LT pile-cases with pile area ratios < 350 and blow counts > 6 BPI (0.24 blows/mm) in all types of soil.

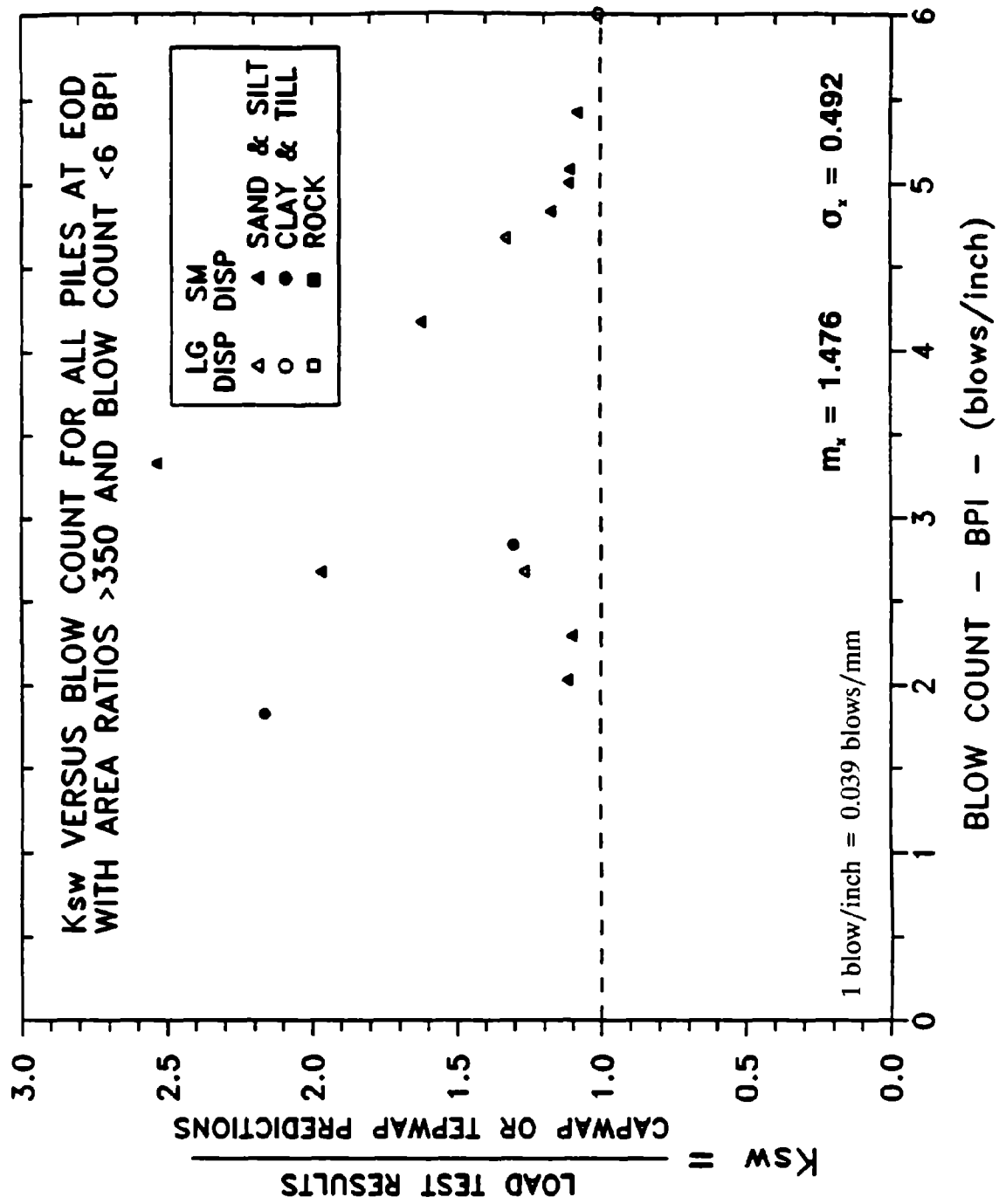


Figure 91. K_{sw} vs. blow count (BPI) for 12 PD/LT pile-cases at EOD with pile area ratios >350 and blow counts <6 BPI (0.24 blows/mm).

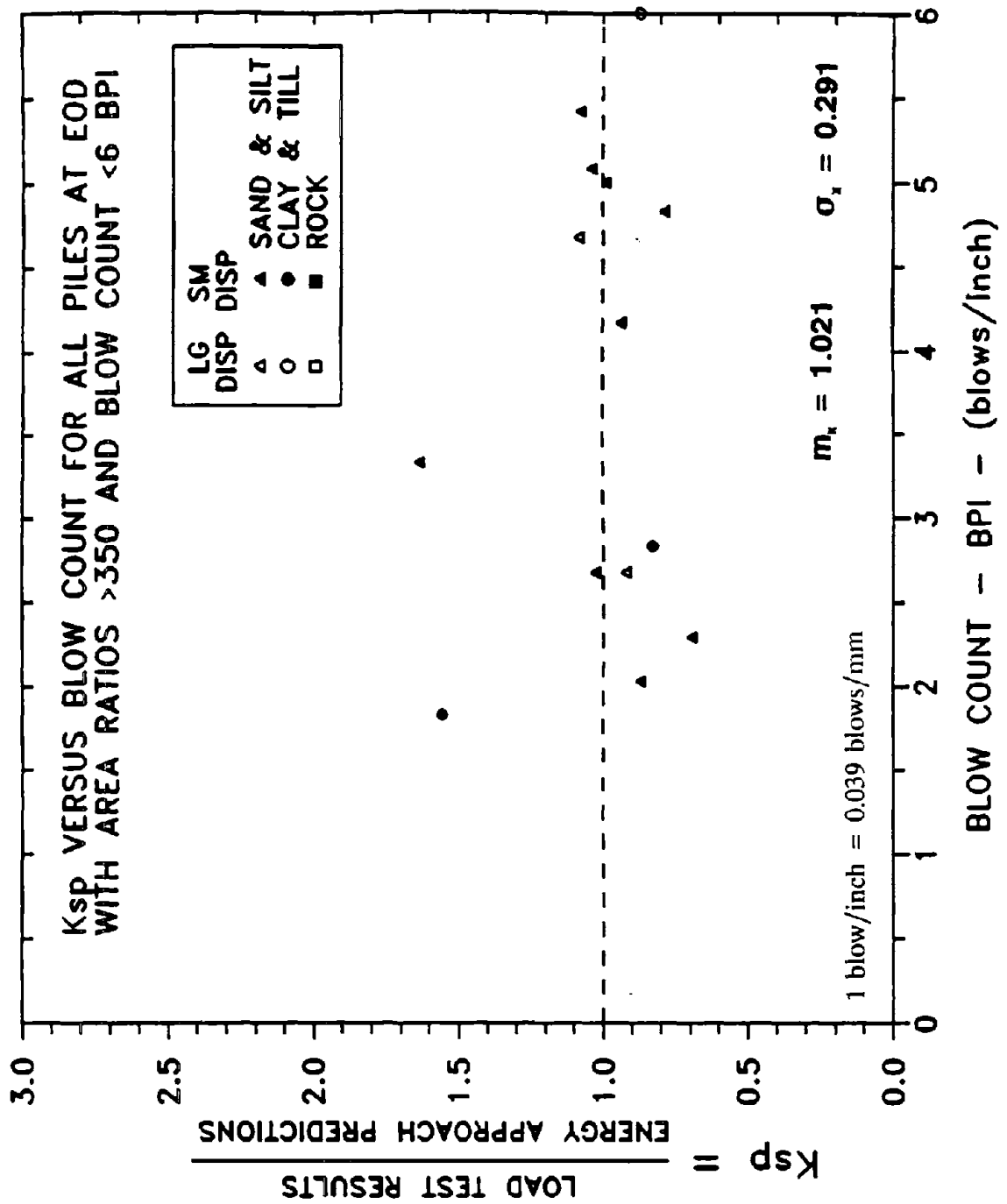


Figure 92. K_{sp} vs. blow count (BPI) for 12 PD/LT pile-cases at EOD with pile area ratios >350 and blow counts <6 BPI (0.24 blows/mm).

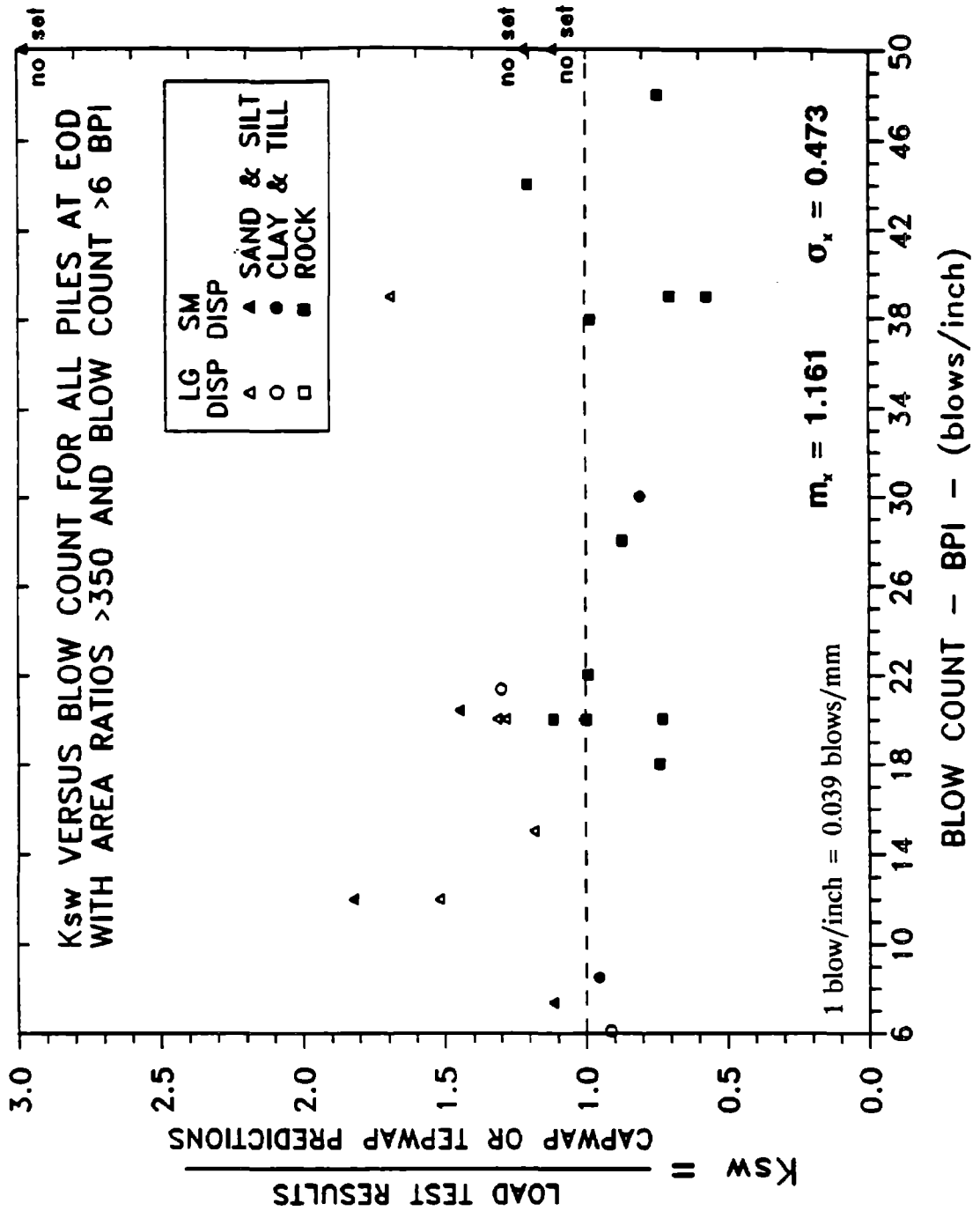


Figure 93. K_{sw} vs. blow count (BPI) for 27 PD/LT pile-cases at EOD with pile area ratios >350 and blow counts >6 BPI (0.24 blows/mm).

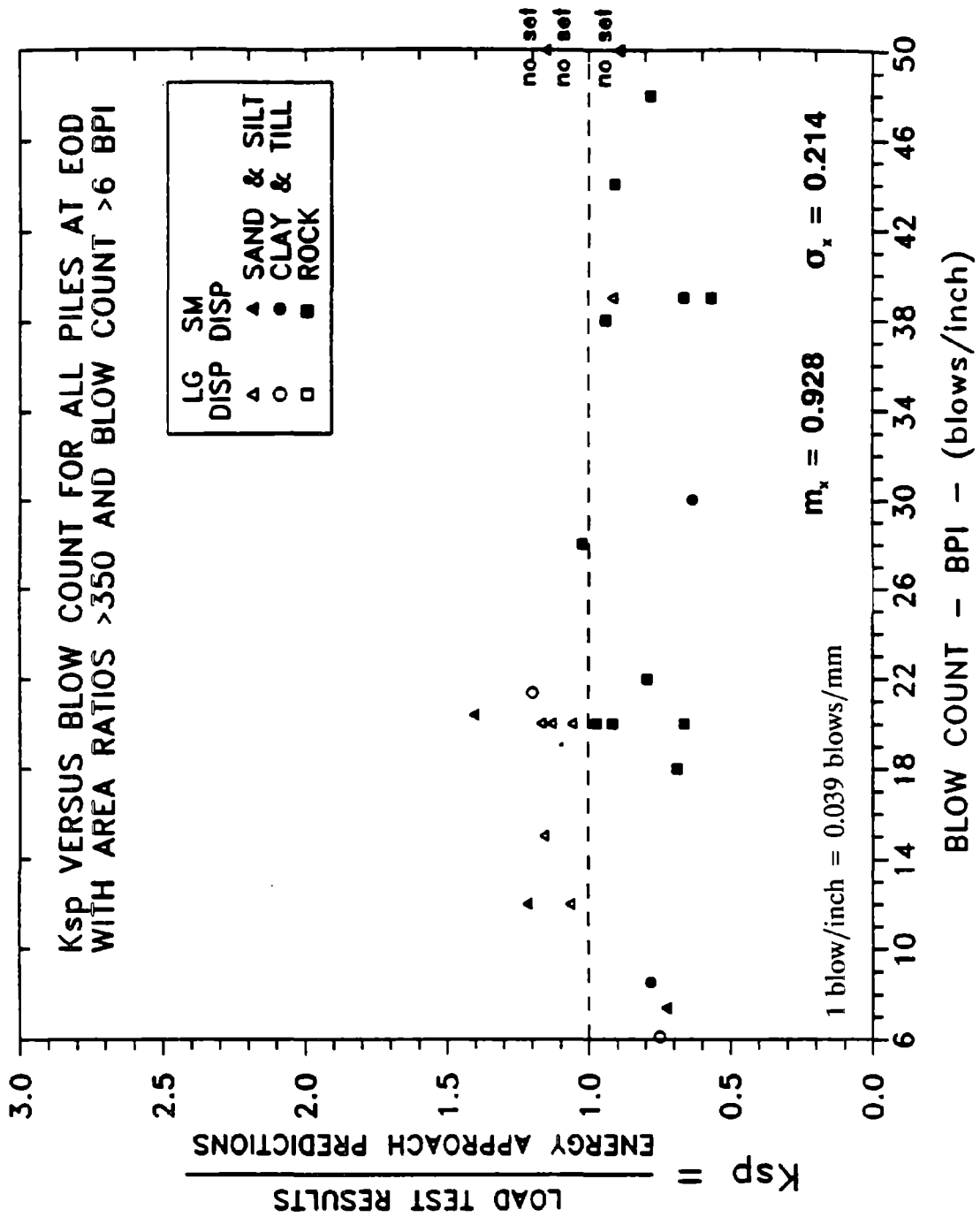


Figure 94. K_{sp} vs. blow count (BPI) for 27 PD/LT pile-cases at EOD with pile area ratios >350 and blow counts >6 BPI (0.24 blows/mm).

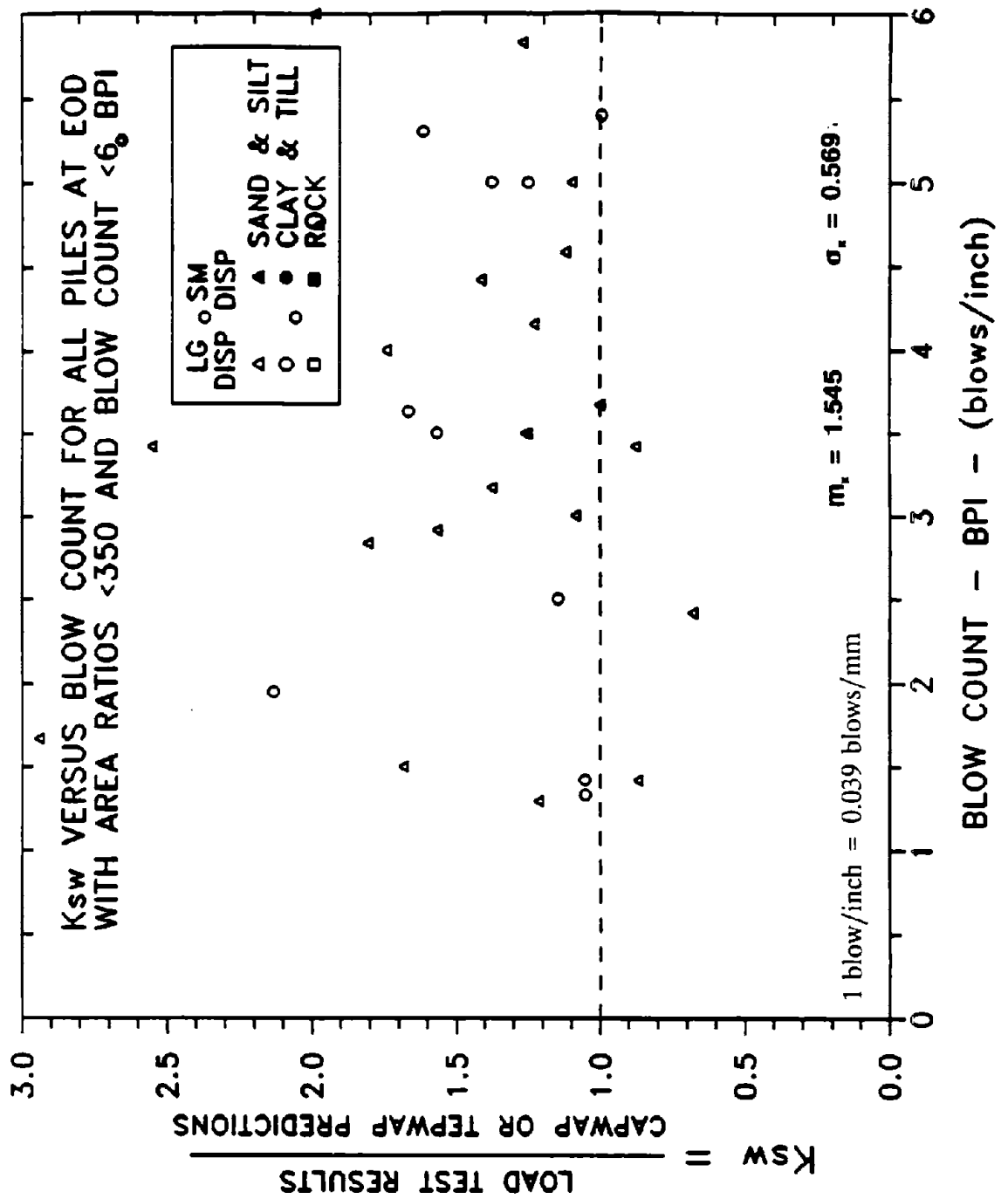


Figure 95. K_{sw} vs. blow count (BPI) for 36 PD/LT pile-cases at EOD with pile area ratios <350 and blow counts <6 BPI (0.24 blows/mm).

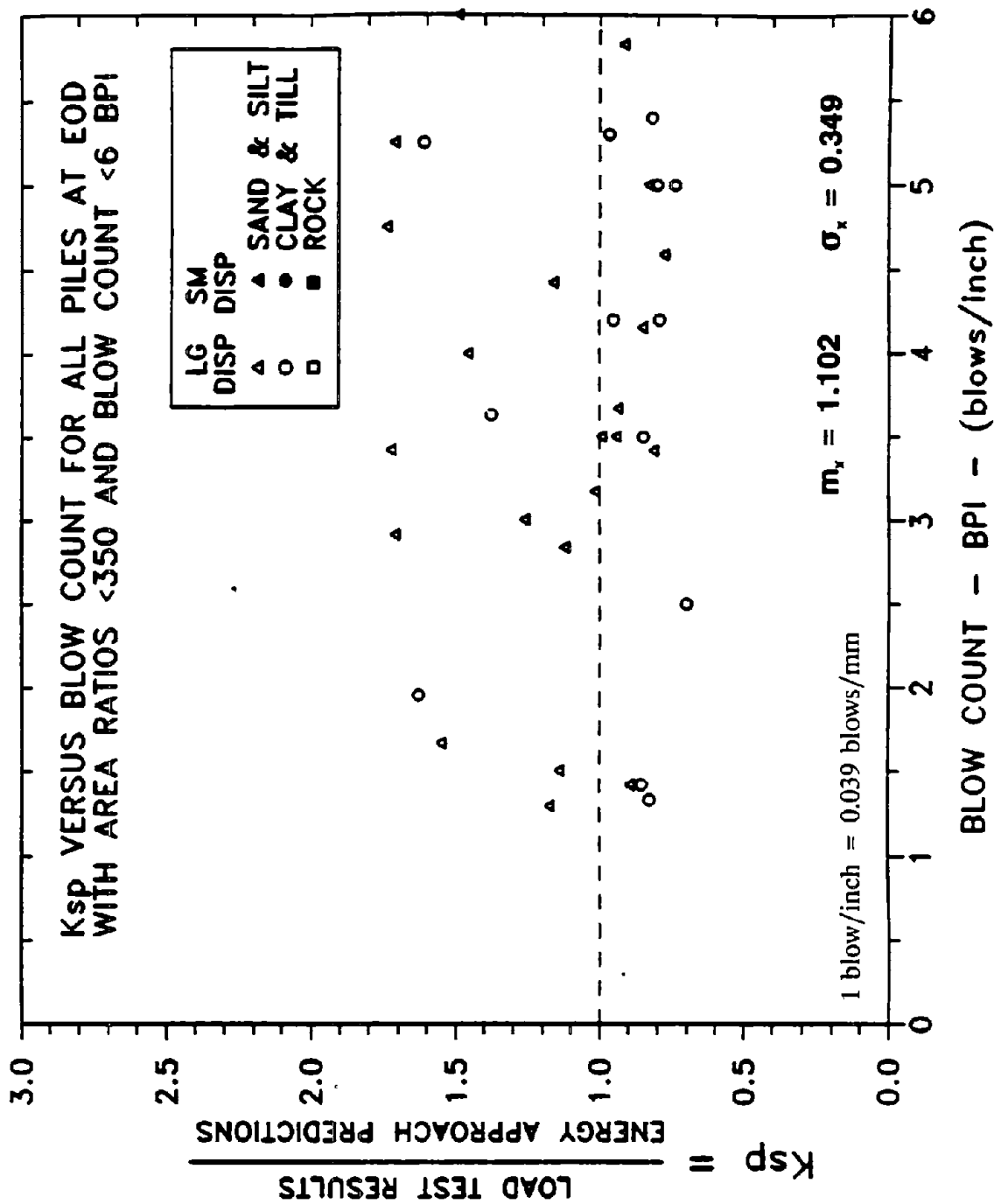


Figure 96. K_{sp} vs. blow count (BPI) for 36 PD/LT pile-cases at EOD with pile area ratios <350 and blow counts <6 BPI (0.24 blows/mm).

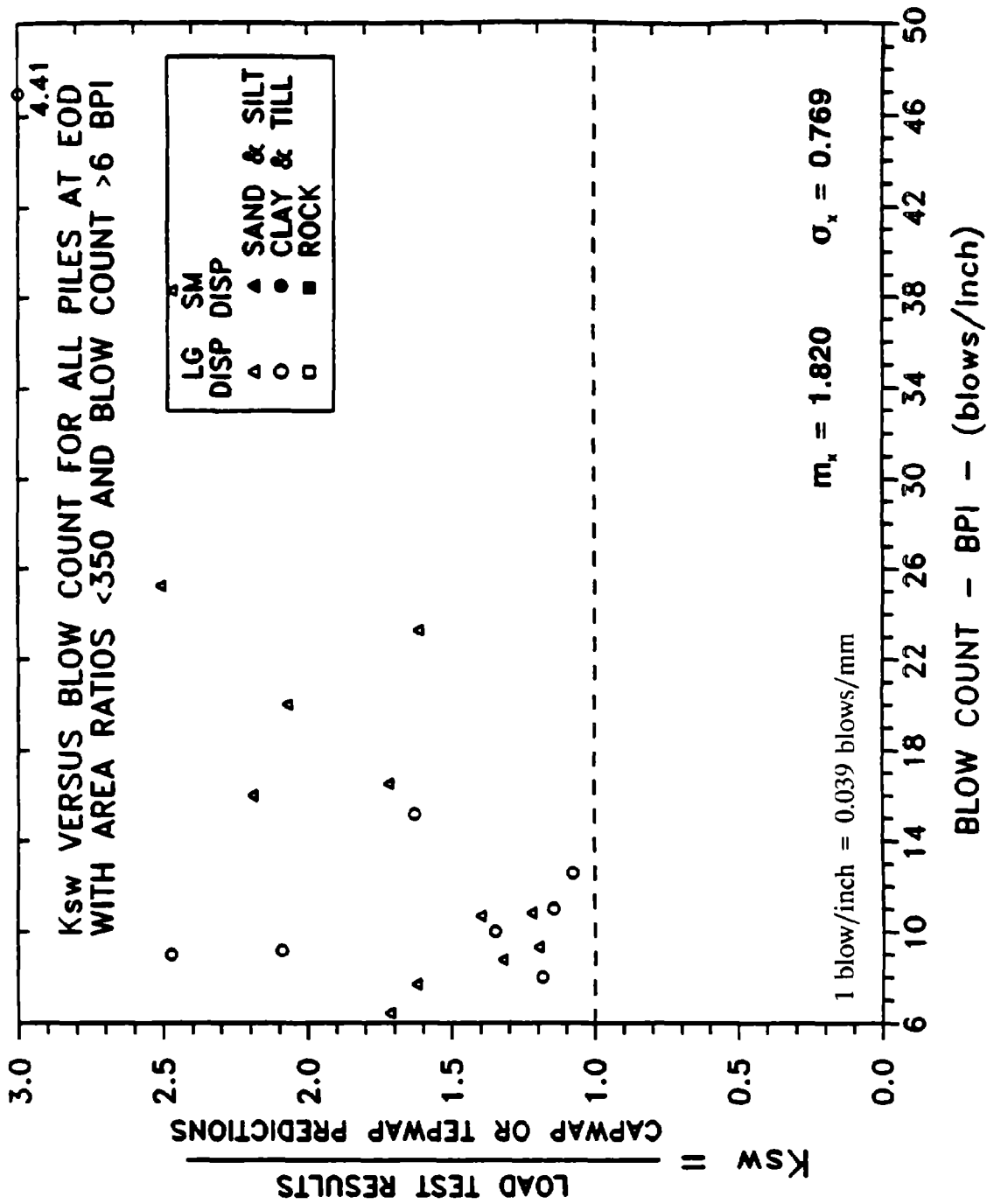


Figure 97. K_{sw} vs. blow count (BPI) for 20 PD/LT pile-cases at EOD with pile area ratios <350 and blow counts >6 BPI (0.24 blows/mm).

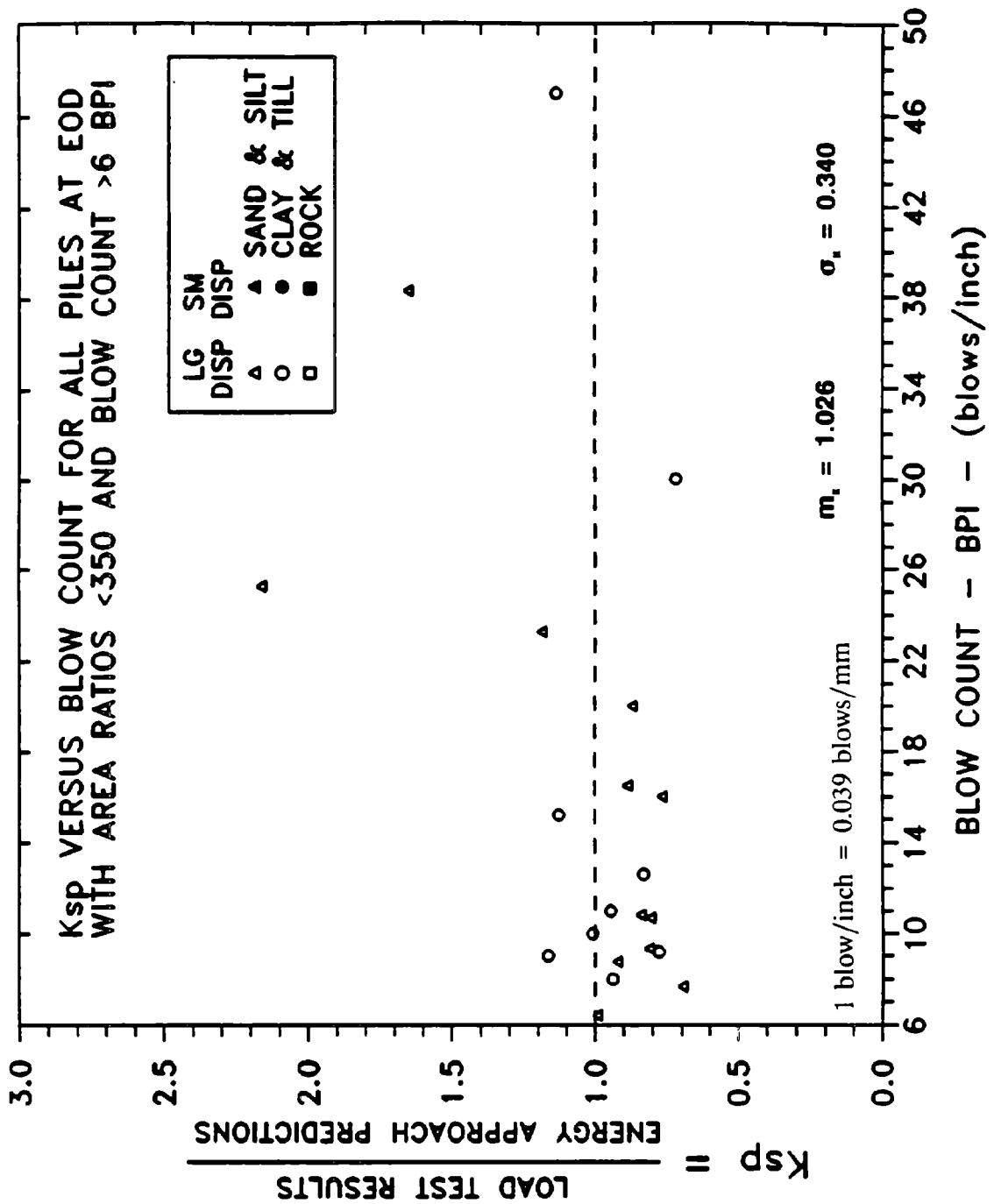


Figure 98. K_{sp} vs. blow count (BPI) for 21 PD/LT pile-cases at EOD with pile area ratios <350 and blow counts >6 BPI (0.24 blows/mm).

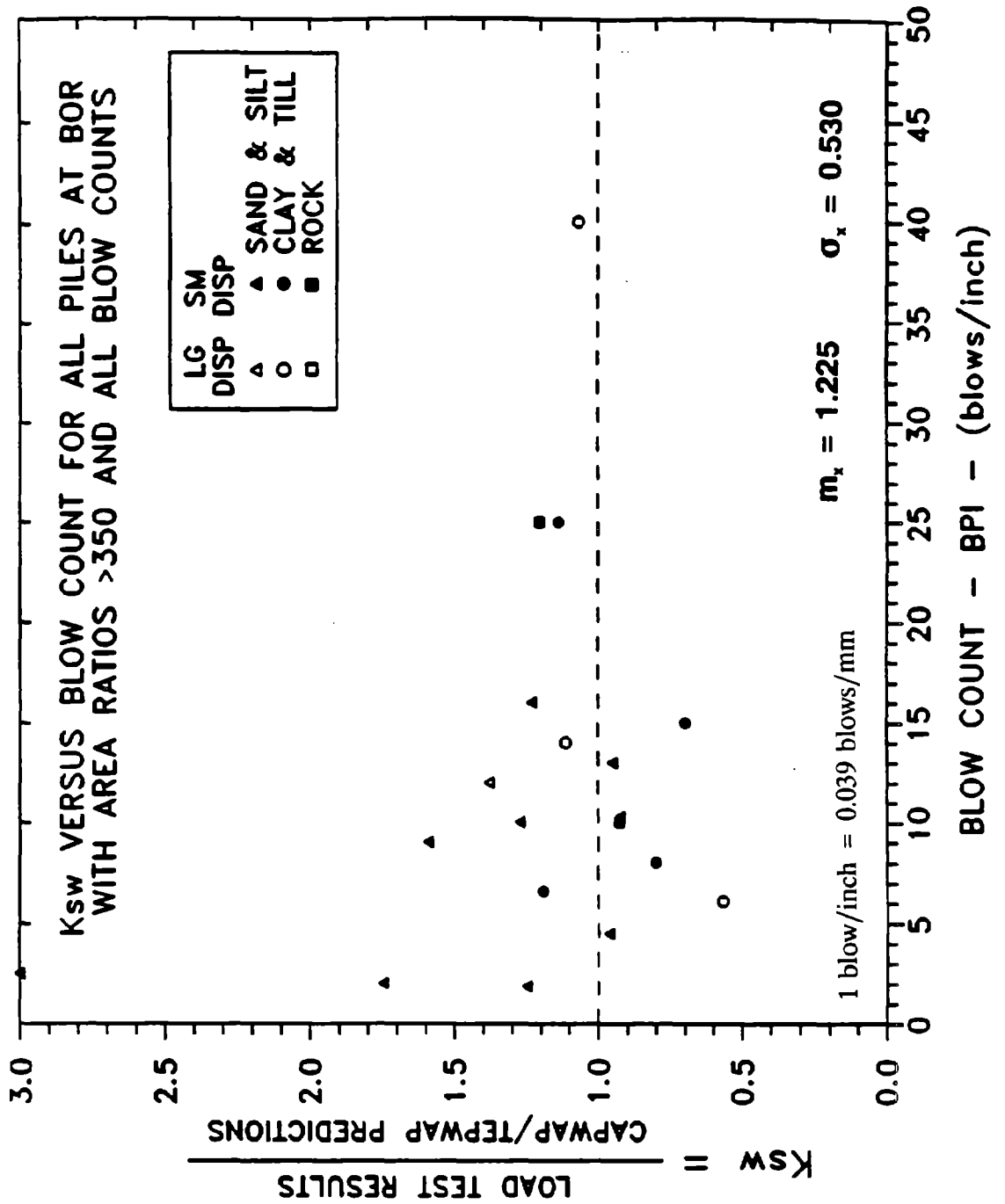


Figure 99. K_{sw} vs. blow count (BPI) for 18 PD/LT pile-cases at BOR with pile area ratios >350 and all blow counts.

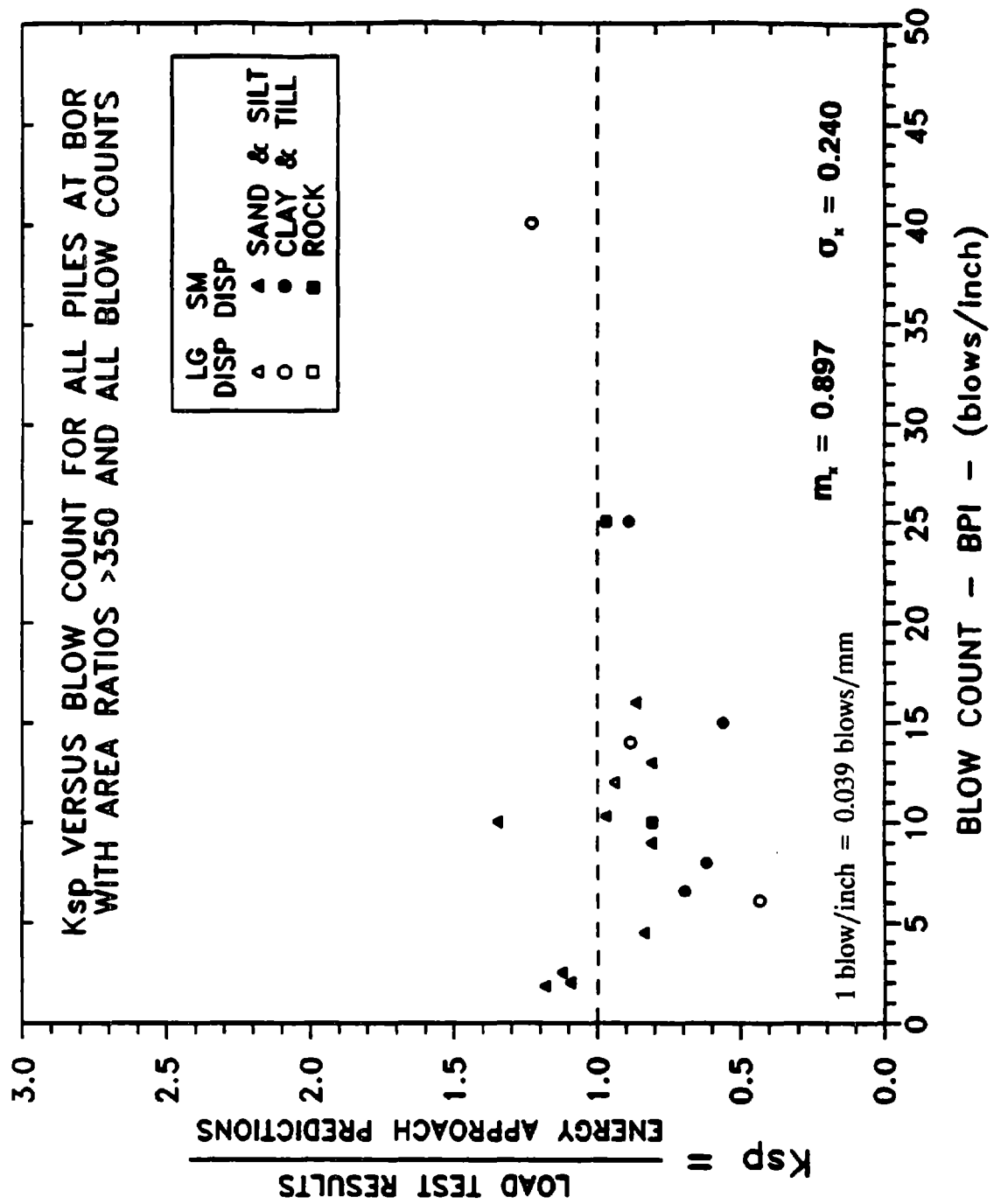


Figure 100. K_{sp} vs. blow count (BPI) for 18 PD/LT pile-cases at BOR with pile area ratios >350 and all blow counts.

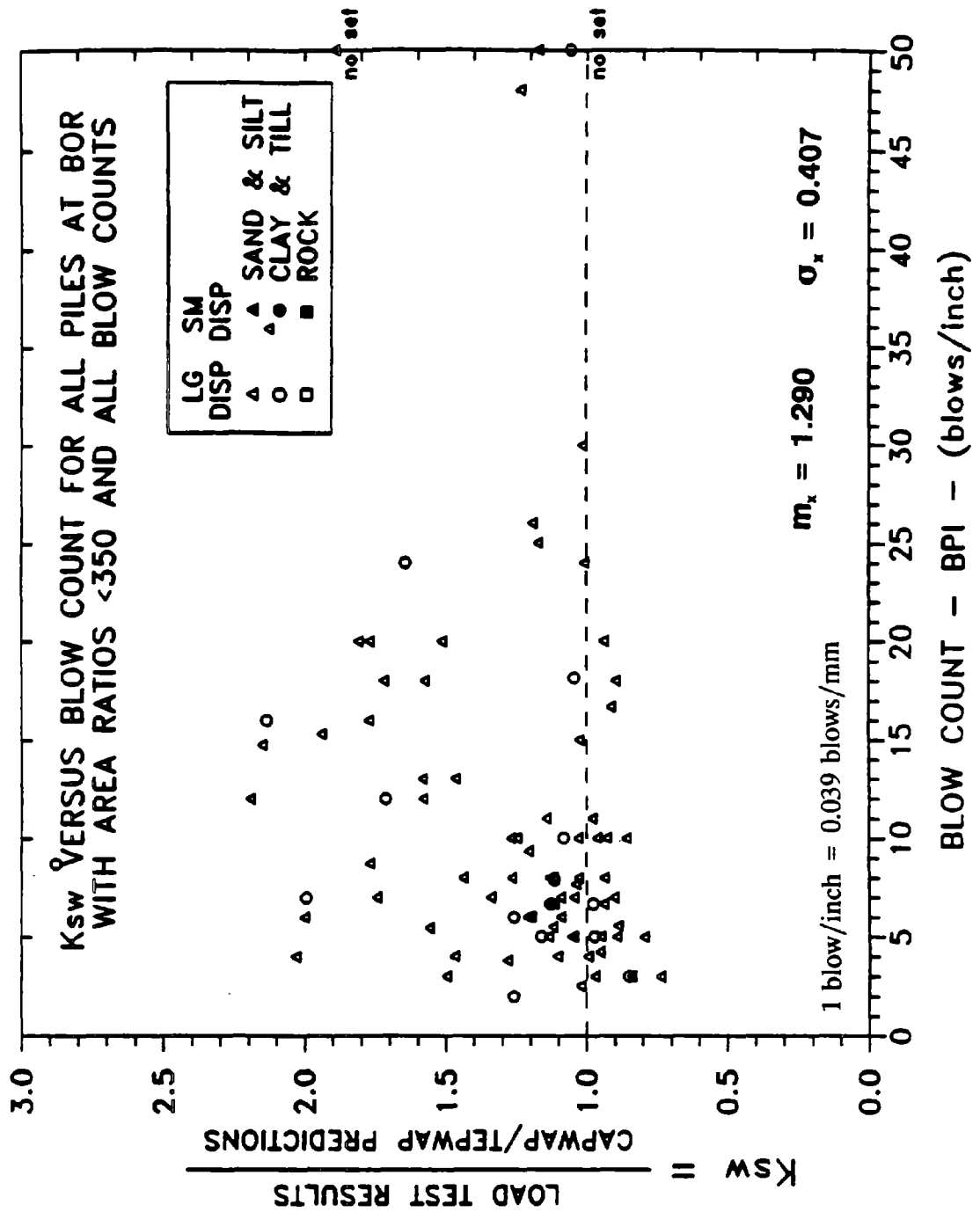


Figure 101. K_{sw} vs. blow count (BPI) for 88 PD/LT pile-cases at BOR with pile area ratios <350 and all blow counts.

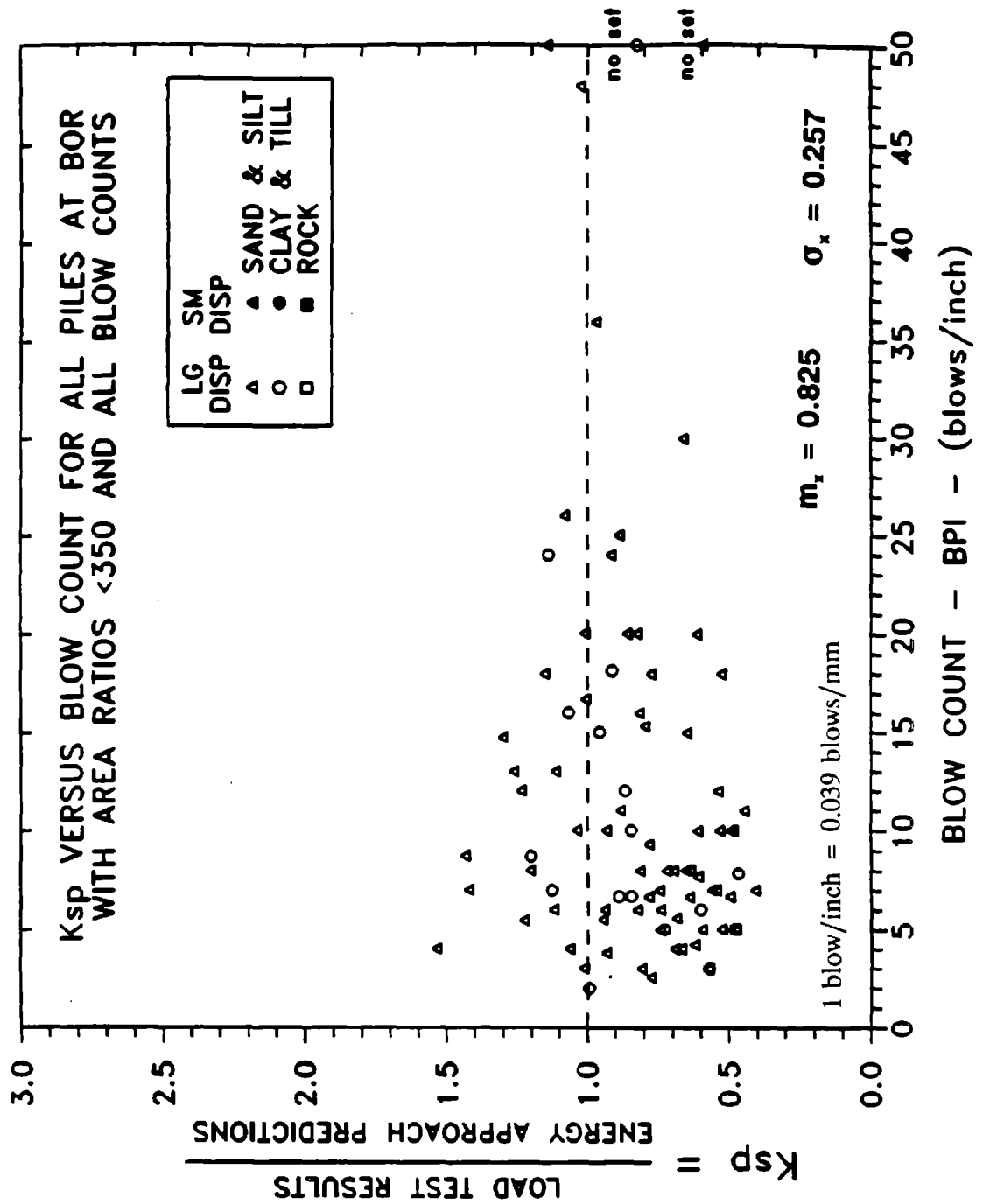


Figure 102. K_{sp} vs. blow count (BPI) for 89 PD/LT pile-cases at BOR with pile area ratios <350 and all blow counts.

CHAPTER 9 - ANALYSIS OF DATA SET PD

9.1 INTRODUCTION

9.1.1 Purpose

This chapter presents the graphical and statistical analysis of the pile-cases of data set PD. Graphical relationships in the form of scattergrams considering pile type and soil type are presented. A statistical analysis was performed in combination with the graphical relationships in an effort to correlate the results of chapter 8 with pile-cases that were not load tested to failure.

9.1.2 Overview

Two different types of correlations were examined for the pile-cases of data set PD. These can be summarized as follows:

(a) Damping Parameters - Soil-Type Correlations

Smith damping parameters (side and tip) obtained from CAPWAP results were correlated to the soil type at the side and tip of the pile, respectively. These graphical relationships are presented in section 9.2.

(b) Office Method - Field Method Predictions

The relationship between the office analysis predictions and the Energy Approach predictions of data set PD were obtained. These relationships can be compared to the correlations of data set PD/LT that were presented in the form of the coefficient K_{ew} , the ratio of CAPWAP or TEPWAP predictions over the Energy Approach predictions. Strong correlations between the two prediction methods may prove beneficial where load test data is not available. This approach can be especially useful since piles are dynamically monitored far more often than they are load tested to failure; hence, large data sets can be accumulated. The subgrouping of these correlations is consistent with table 3.

9.2 SMITH DAMPING PARAMETERS AND SOIL-TYPE CORRELATIONS

Figure 103 presents the relationship between Smith side damping parameters and the soil conditions along the pile shaft for 378 pile-cases analyzed by CAPWAP. The parameters shown are those obtained directly from the CAPWAP analyses performed on the pile-cases of data set PD. No corrections were performed on these parameters. A

substantial scatter exists in figure 103 with no clear correlation between the damping and the soil type at the pile shaft.

The information in figure 104, presenting the relationship between Smith tip damping parameters and tip soil conditions, indicates that no specific correlation can be made. These results are similar to those obtained in figures 22 and 23 for data set PD/LT.

9.3 CAPWAP AND THE ENERGY APPROACH CORRELATIONS

The following graphs compare CAPWAP and Energy Approach predictions based on pile type and soil type at the pile tip. The pile-type subgrouping includes large and small displacement piles, as well as miscellaneous piles (see table 3). The indicated slopes of the lines are identical to the parameter K_{ew} , which is the ratio of CAPWAP predictions to the Energy Approach predictions.

9.3.1 All Piles - All Soils

The relationship between the predicted capacities of CAPWAP and the Energy Approach for 398 PD pile-cases is shown in figure 105. The information indicates a good agreement between the two types of analyses, with the majority of data points in the ratio range of 1.00 to 0.60. The best-fit line through zero yields a ratio of $K_{ew} = 0.695$ (CAPWAP over Energy Approach) with a coefficient of determination $r^2 = 0.699$. It can be seen that the small displacement piles (solid symbols) are concentrated in a narrow band, indicating a very good correlation of the two prediction methods for these pile-cases.

9.3.2 Large Displacement Piles

The following graphs compare the CAPWAP results to that of the Energy Approach predictions for large displacement piles.

(a) All Cases

Figure 106 presents all 238 large displacement pile-cases in all types of soil. The data points range from approximately 1.10 to 0.20. Overall, good agreement is presented with the best-fit line through zero at 0.676 (CAPWAP over Energy Approach) and a general trend between 1.00 and 0.60. The coefficient of determination is $r^2 = 0.650$.

(b) Sand and Silt

The information in figure 107 indicates excellent correlation between CAPWAP predictions and Energy Approach predictions for cases of large displacement piles in sand and silt. Most of the data points lie within the range of 1.00 to 0.60. The best-fit line is at 0.669 with $r^2 = 0.812$.

(c) Clay and Till

Figure 108 shows the correlation of CAPWAP and Energy Approach predictions for 50 large displacement pile-cases in clay and till. The majority of data points fall on or near the 0.80 line, with other cases reaching 0.40 and slightly below. The best-fit line through zero is at $K_{ew} = 0.600$ with $r^2 = 0.404$.

(d) Rock

The relationship between CAPWAP and the Energy Approach for 78 cases of large displacement piles found in rock is shown in figure 109. The information indicated a general scatter with the majority of data points falling between 1.00 and 0.60. The best-fit line through zero yielded $K_{ew} = 0.652$ with $r^2 = 0.572$.

(e) Unknown Soil Type

The correlation of the prediction methods for the 22 cases of large displacement piles in unknown soil types is presented in figure 110. It can be seen that regardless of soil type, good agreement is generally observed in these cases between the CAPWAP and Energy Approach predictions. The obtained best-fit line through zero is $K_{ew} = 0.844$ with $r^2 = 0.589$.

(f) Intermediate Conclusions

- Generally good agreement exists between the predictions of CAPWAP to those of the Energy Approach for large displacement piles. The obtained relationship for all large displacement piles, at all times and in all types of soil (242 cases), is similar to that obtained for the corresponding cases in data set PD/LT.
- The breakdown of the piles to the different soil types shows that the highest correlation between the methods exists for piles driven in sand and silt. The worst correlation is obtained for piles driven in clay and till.
- No subdivision was made regarding the time of driving. The analysis of data set PD is, therefore, equivalent to all time of driving cases in data set PD/LT.

9.3.3 Small Displacement Piles

The correlations of the two dynamic analysis predictions for small displacement piles in all soil types are presented in figures 111 through 114.

(a) All Cases

The information in figure 111 indicates an outstanding correlation between the CAPWAP and Energy Approach predictions for 76 small displacement pile-cases in all

soil types. The data points are almost exclusively within the range of 1.00 and 0.60 with the best-fit line at $K_{ew} = 0.800$ and $r^2 = 0.826$.

(b) Sand and Silt

The correlation for 26 small displacement pile-cases in sand and silt is shown in figure 112. A very well-defined relationship is observed with all data points within the range of 1.00 and 0.60. The best-fit line forced through zero is shown with a ratio of $K_{ew} = 0.807$ and $r^2 = 0.922$.

(c) Clay and Till

Figure 113 presents the correlation between CAPWAP and Energy Approach predictions for 21 small displacement pile-cases in clay and till. These data points are also indicating a relatively good correlation with the best-fit line at $K_{ew} = 0.723$ and $r^2 = 0.736$. The data points are within the range of 1.00 and 0.60, however, there is a larger scatter than that observed in sand and silt. This is also indicated by the reduction in the value of the calculated coefficient of determination.

(d) Rock

Figure 114 presents the comparison of the dynamic prediction methods for 29 small displacement pile-cases on rock. The relationship yields similar results to those of figures 111 through 113, with an excellent correlation between the prediction methods. The best-fit ratio is equal to $K_{ew} = 0.838$ with $r^2 = 0.797$.

(e) Intermediate Conclusions

- A better agreement with better correlation was found between the office method and the Energy Approach for small displacement piles when compared to large displacement piles. As both data sets contained a large number of cases (242 large displacement and 76 small displacement pile-cases for all soil types at all driving times), the findings reflect the importance of pile type in the accuracy of the predictions.
- The predictions for small displacement piles in sand were found to match and correlate better than those in clay. In both cases, a better fit was found when compared to the large displacement pile-cases with the respective soil type. These results indicate that the soil type is secondary to the pile type as factors shaping the prediction results.

9.3.4 Miscellaneous Piles

The relationships of CAPWAP and Energy Approach predictions for miscellaneous piles for different soil conditions are presented in figures 115 through 119.

(a) All Cases

The correlation between the two prediction methods is presented in figure 115 for 85 miscellaneous pile-cases in all soil types. It is shown that there is excellent agreement between these predictions, with the majority of data points falling in the range of 1.00 to 0.60. The best-fit ratio is $K_{ew} = 0.763$ (CAPWAP over Energy Approach) with $r^2 = 0.873$.

(b) Sand and Silt

Figure 116 shows similar agreement between the two prediction methods for 40 miscellaneous pile-cases in sand and silt. The best-fit ratio equals 0.787 and most of the data points are within ± 20 percent of the 0.80 line with $r^2 = 0.857$.

(c) Clay and Till

The correlation of the predictions for 21 miscellaneous pile-cases in clay and till are shown in figure 117. Very good correlations are obtained with a best-fit ratio of $K_{ew} = 0.735$. The majority of data points lie within the 1.00 to 0.60 range, with a coefficient of determination of $r^2 = 0.783$.

(d) Rock

The information of figure 118 indicates a very good agreement between the CAPWAP and Energy Approach predictions for 19 pile-cases of piles found in rock. The best-fit ratio is 0.742 with $r^2 = 0.899$.

(e) Unknown Soil Type

Figure 119 presents the correlation results for five cases of miscellaneous piles driven in unknown soils. Good correlation is obtained from this small and non-specific data set.

9.4 STATISTICAL ANALYSIS OF DATA SET PD

In order to quantify the correlations obtained from the graphical relationships of section 9.3, a statistical analysis was performed as follows:

- (1) Determination of the first-order best-fit lines (forced through zero and y-intercept) by linear regression along with the sample coefficient of determination (r^2) to measure the quality of the best-fit line.
- (2) Determination of the mean and standard deviation of the K_{ew} ratio (CAPWAP over Energy Approach) as a measure of the accuracy (through the mean) and precision (through the standard deviation) of the calculated ratio distribution.

Table 10. Linear regression analysis of K_{ew} for PD pile-cases.

Kew = CAPWAP predictions / Energy Approach predictions						
Pile-Case Group	Linear Regression					
	Number	Best Fit			Forced through Zero	
		X-coefficient	y-intercept	r-squared	X-coefficient	r-squared
AA	403	0.603	75.4	0.723	0.695	0.699
LA	242	0.593	77.0	0.667	0.676	0.650
LS	92	0.580	81.8	0.841	0.669	0.812
LC	50	0.407	142.4	0.570	0.600	0.404
LR	78	0.563	89.7	0.591	0.652	0.572
LN	22	0.814	31.5	0.590	0.844	0.589
SA	76	0.751	22.7	0.830	0.800	0.826
SS	26	0.774	13.0	0.924	0.807	0.922
SC	21	0.651	32.2	0.747	0.723	0.736
SR	29	0.728	56.3	0.817	0.838	0.797
MA	85	0.678	51.8	0.892	0.763	0.873
MS	40	0.705	42.5	0.871	0.787	0.857
MC	21	0.640	46.6	0.807	0.735	0.783
MR	19	0.652	76.8	0.924	0.742	0.899
MN	5	0.816	61.3	0.933	0.955	0.898

Pile-case legend:

XX

- first letter denotes pile type: A = all piles, L=large displacement, S=small displacement, and M=miscellaneous piles.
- second letter denotes soil type: A=all soils, S=sand and silt, C=clay and till, R=rock, and N=not available.

9.4.1 Linear Regression Analysis

The results of the linear regression analysis performed on the subgroups of data set PD are presented in table 10. The first two columns of table 10 report the pile-case subgroups and the total number of pile-cases included in the analysis, respectively. This analysis is similar to that which was performed in section 8.4.1 for data set PD/LT. The results of the best-fit linear regression performed for each subgroup are listed in columns 3, 4, and 5. Column 3 shows the first-order best-fit ratio, and the corresponding intercept is presented in column 4. Column 5 shows the sample coefficient of determination (r^2) for each subgroup. The coefficients for the best-fit ratio forced through zero are listed in columns 6 and 7. Column 6 presents the first-order best-fit sample coefficient and column 7 presents the corresponding coefficient of determination.

Table 10 indicates a relatively consistent best-fit ratio (forced through zero) for all pile types and soil types. It can be seen that pile type is the controlling factor in the resulting best-fit ratio as very little change is seen for large or small displacement piles in different soils. For example, considering small displacement piles, the most extreme best-fit ratios range from 0.723 for piles found in clay and till to 0.838 for piles found in rock. Similarly, for large displacement piles in sand, clay, and rock, the best-fit ratios range from 0.676 to 0.600. Excellent coefficients of determination are reported for all small displacement piles ($r^2 = 0.826$) and, in particular, in sand ($r^2 = 0.922$). This is in comparison to all large displacement piles ($r^2 = 0.600$) that improve in sand only to $r^2 = 0.812$, compared to clay with $r^2 = 0.404$.

9.4.2 Mean and Standard Deviation Analysis

Table 11 presents the results of the statistical analysis, evaluating the mean and standard deviation of the PD subgroups outlined in table 3. The first two columns are consistent with table 10 and they report the pile-case subgroup and the total number of pile-cases included in each analysis, respectively. The mean of all cases was found to be 0.774 with mean values obtained for the subgroups in the range of 0.701 to 0.863 (with the exception of miscellaneous piles in unknown soil types, which represent a subgroup of only five piles). Overall, the values obtained are very consistent with very good standard deviations compared to those obtained for the relationships between the predictions and the actual capacity. This suggests that the prediction methods may be similar in their analysis and, based on the mean values, it appears that soil type has a lesser effect on the correlation between CAPWAP and the Energy Approach predictions.

9.5 SUMMARY AND CONCLUSIONS

Data set PD contains information that allows capacity predictions to be conducted on 403 pile-cases, based on dynamic measurements. As no comparison can be made to the actual static resistance, the results serve two purposes:

Table 11. Statistical analysis of K_{ew} for PD pile-cases.

Pile-Case Group	Kew = CAPWAP/ Energy Approach		
	Number	Mean	Standard Deviation
AA	403	0.774	0.2099
LA	242	0.742	0.2359
LS	92	0.754	0.1753
LC	50	0.701	0.2093
LR	78	0.722	0.2202
LN	22	0.860	0.4528
SA	76	0.813	0.1255
SS	26	0.815	0.0862
SC	21	0.741	0.1396
SR	29	0.863	0.1229
MA	85	0.827	0.1734
MS	40	0.861	0.1410
MC	21	0.806	0.2297
MR	19	0.821	0.1544
MN	5	1.022	0.1233

Pile-case legend:

- XX** - first letter denotes pile type: A=all piles, L=large displacement, S=small displacement, and M=miscellaneous piles.
 - second letter denotes soil type: A=all soils, S=sand and silt, C=clay and till, R=rock, and N=not available.

- They can be compared to the pile-cases of data set PD/LT to allow assessment of trends found in that data set.
- They indirectly serve as an excellent indicator for the controlling parameters through the conditions in which the different prediction methods are close to each other or different from each other.

The following conclusions are based on the scattergrams presented in figures 103 through 119:

1. No correlations seem to exist between soil type and damping parameters for either Smith damping at the pile side or the pile tip.
2. General comparisons between the best-fit linear regression of the different subgroups in data set PD/LT (tables 5 through 7) and in data set PD (table 10) indicate a reasonably good agreement between the two independent data sets. Some of the major parameters are summarized in table 12 below.

Table 12. Linear regression summary of selected PD/LT and PD subgroups.

Pile-Case Group	K_{ew} Coefficient					
	PD/LT			PD		
	number	x-coefficient	r^2	number	x-coefficient	r^2
AAA	206	0.641	0.766	403	0.695	0.699
LAA	162	0.589	0.554	242	0.676	0.650
LAS	118	0.571	0.586	92	0.669	0.812
LAC	43	0.446	0.600	50	0.600	0.404
SAA	44	0.764	0.937	76	0.800	0.826
SAS	23	0.750	0.942	26	0.807	0.922
SAC	8	0.779	0.971	21	0.723	0.736

For many of these cases, r^2 can serve as a good indicator of the agreement as mentioned above. The assigned x-coefficient refers to the slope of the best-fit line forced through zero. A more realistic comparison may be obtained through the slope of the natural best-fit line.

3. General comparisons between the parameters of the normal distribution of the different subgroups in data set PD/LT (table 8) indicate a reasonably good agreement between the two independent data sets. Some of the major parameters are summarized in table 13.
4. Based on the data, it seems that both methods predict fairly similarly in the case of small displacement piles and, in particular, in sand. The small displacement piles present higher mean values, higher x-coefficients, higher coefficients of determination, and smaller standard deviation ratios. This conclusion verifies the fact that when small soil inertia and soil damping exist, both methods give similar results.
5. The cases related to the large displacement piles exhibit lower x-coefficients, lower coefficients of determination, and lower mean values, while having higher standard deviation values. This indicates that, in the case of large displacement piles, the dynamic methods differ from each other as the damping modeling has an active role in the CAPWAP analysis of these cases.
6. The consistent pattern of better agreement in the predictions for piles in sand compared to those in clay indicates the relative importance of the soil type. This, however, is secondary to the importance of pile type.

Table 13. Statistical analysis summary of selected PD/LT and PD subgroups.

Pile Case Group	Kew Coefficient					
	PD/LT			PD		
	number	mean	standard deviation	number	mean	standard deviation
AAA	206	0.712	0.182	403	0.774	0.210
LAA	162	0.689	0.176	242	0.742	0.236
LAS	118	0.693	0.171	92	0.754	0.175
LAC	43	0.670	0.184	50	0.701	0.209
SAA	44	0.796	0.180	76	0.813	0.126
SAS	23	0.746	0.203	26	0.815	0.086
SAC	8	0.738	0.085	21	0.741	0.140

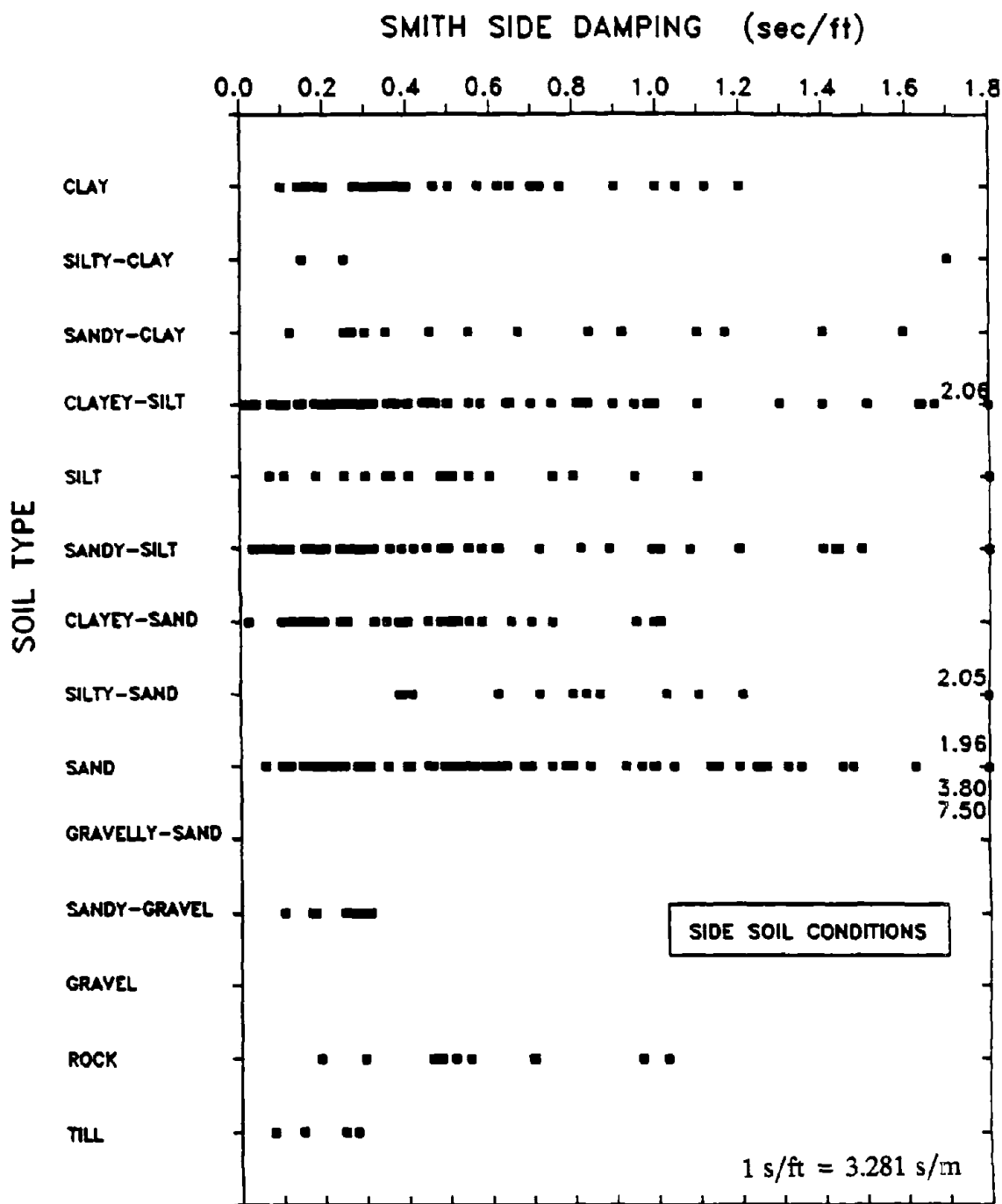


Figure 103. Side soil conditions vs. Smith side damping based on CAPWAP results for 372 PD pile-cases.

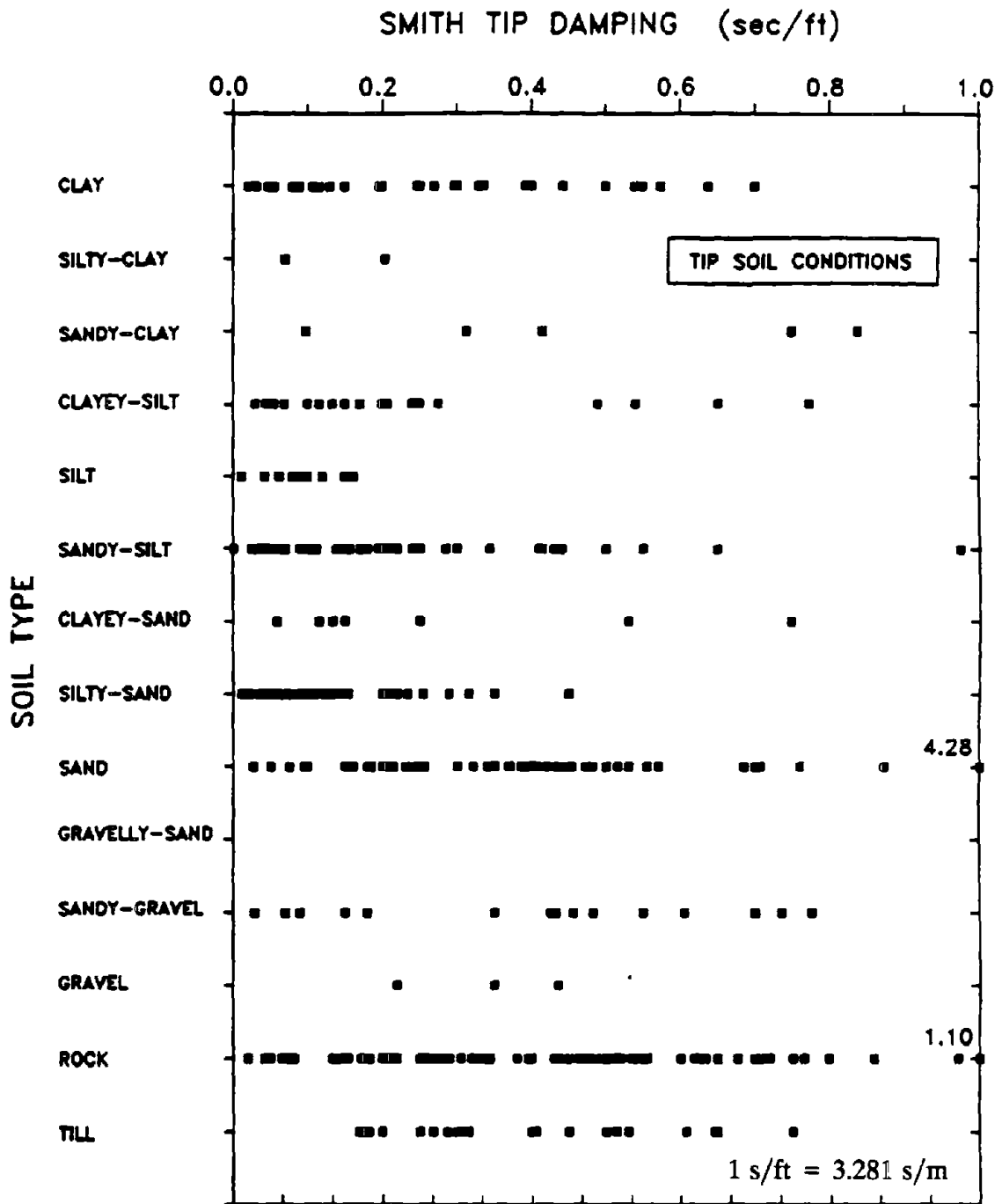
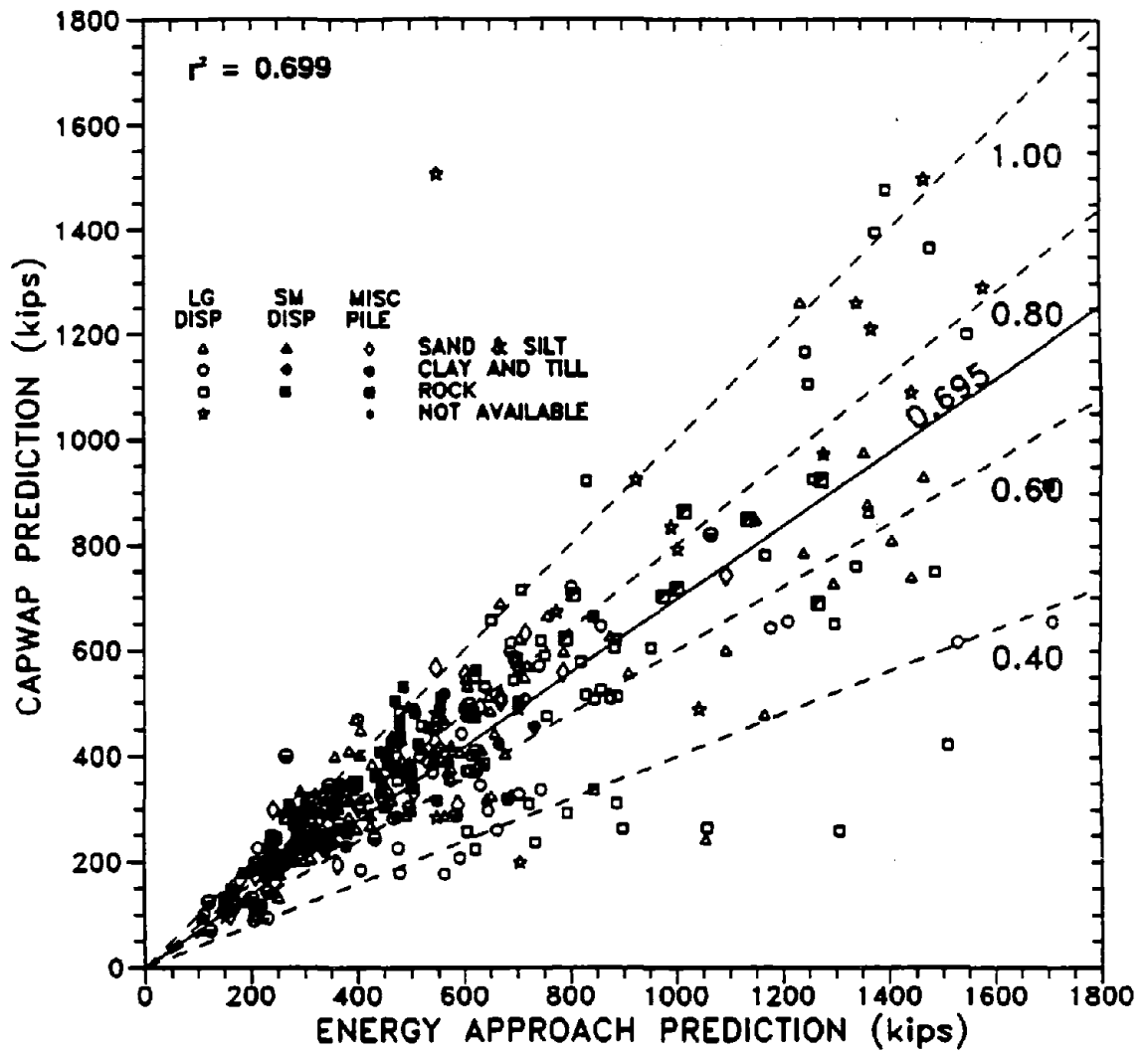
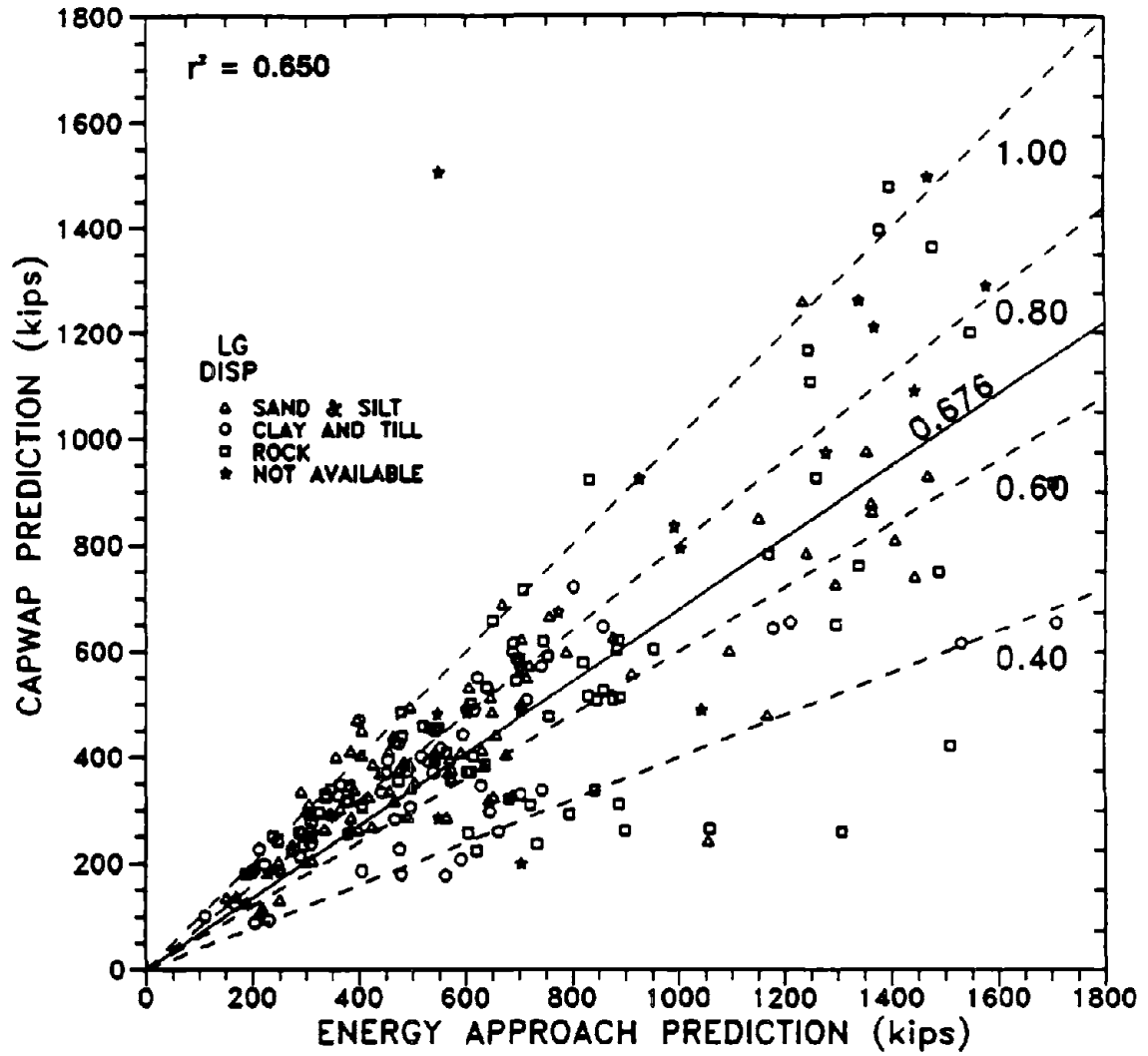


Figure 104. Tip soil conditions vs. Smith tip damping based on CAPWAP results for 377 PD pile-cases.



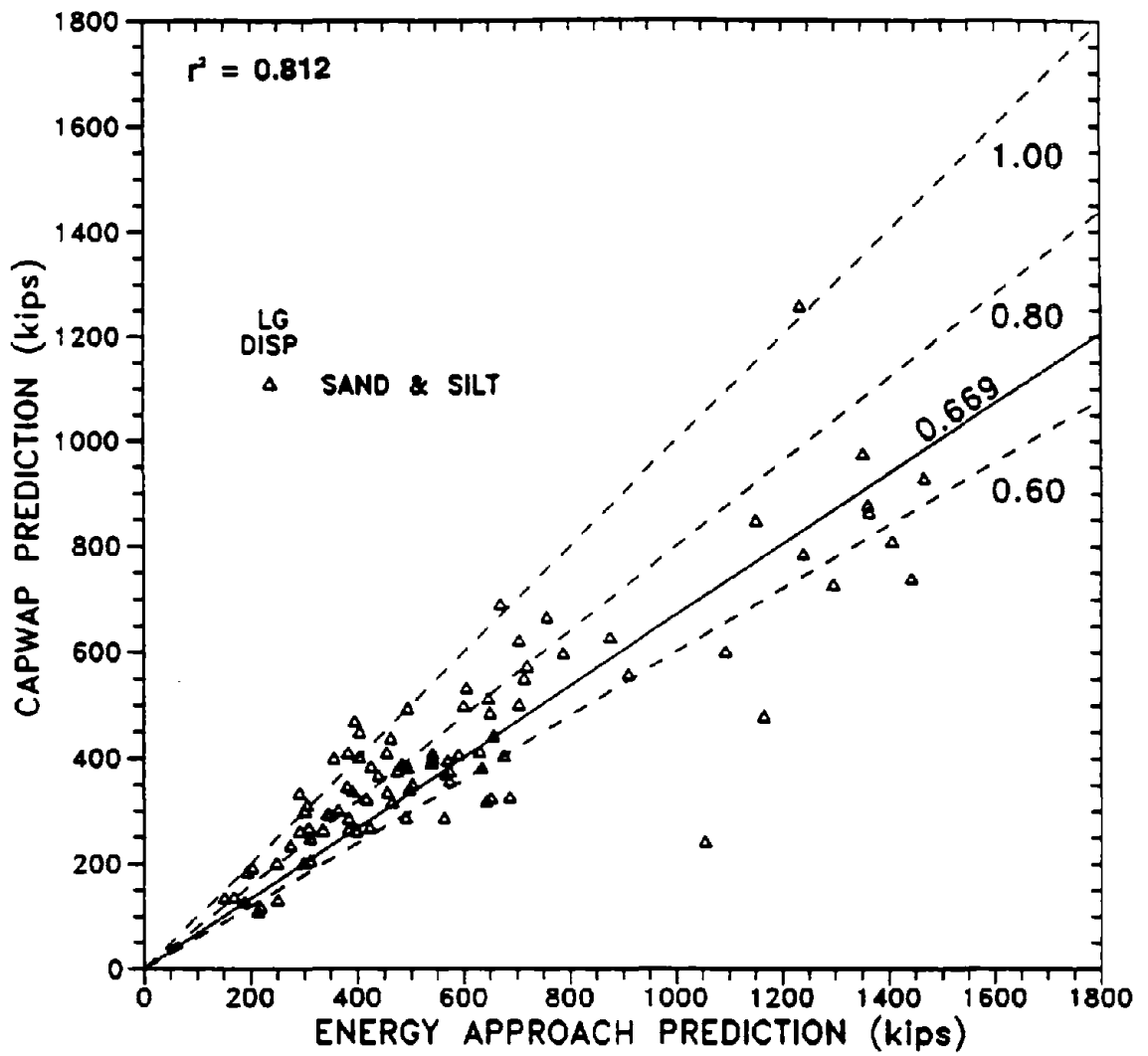
1 kip = 4.448 kN

Figure 105. CAPWAP predictions vs. Energy Approach predictions for 398 PD pile-cases in all types of soil.



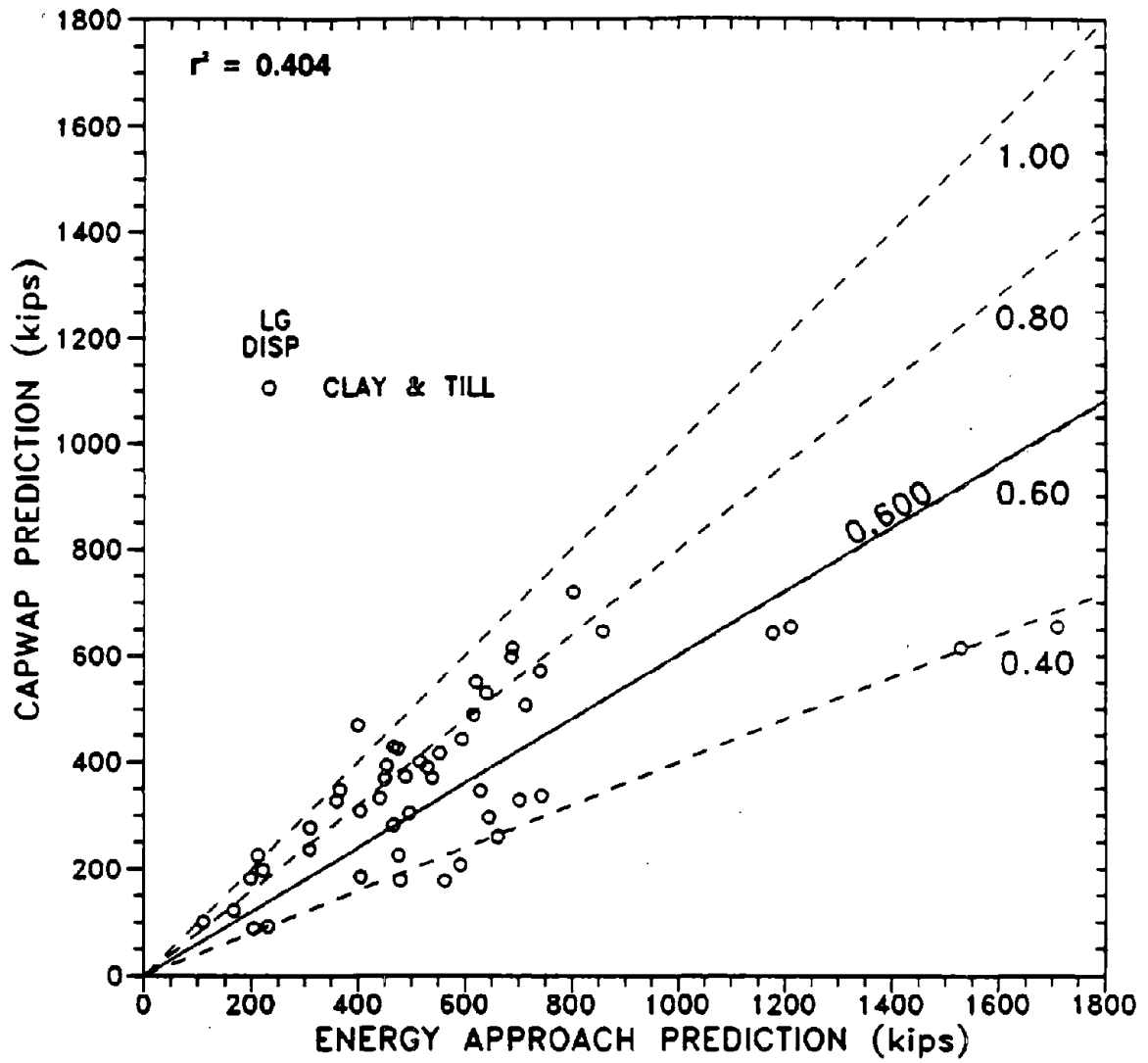
1 kip = 4.448 kN

Figure 106. CAPWAP predictions vs. Energy Approach predictions for 238 large displacement PD pile-cases in all types of soil.



1 kip = 4.448 kN

Figure 107. CAPWAP predictions vs. Energy Approach predictions for 89 large displacement PD pile-cases in sand and silt.



1 kip = 4.448 kN

Figure 108. CAPWAP predictions vs. Energy Approach predictions for 50 large displacement PD pile-cases in clay and till.

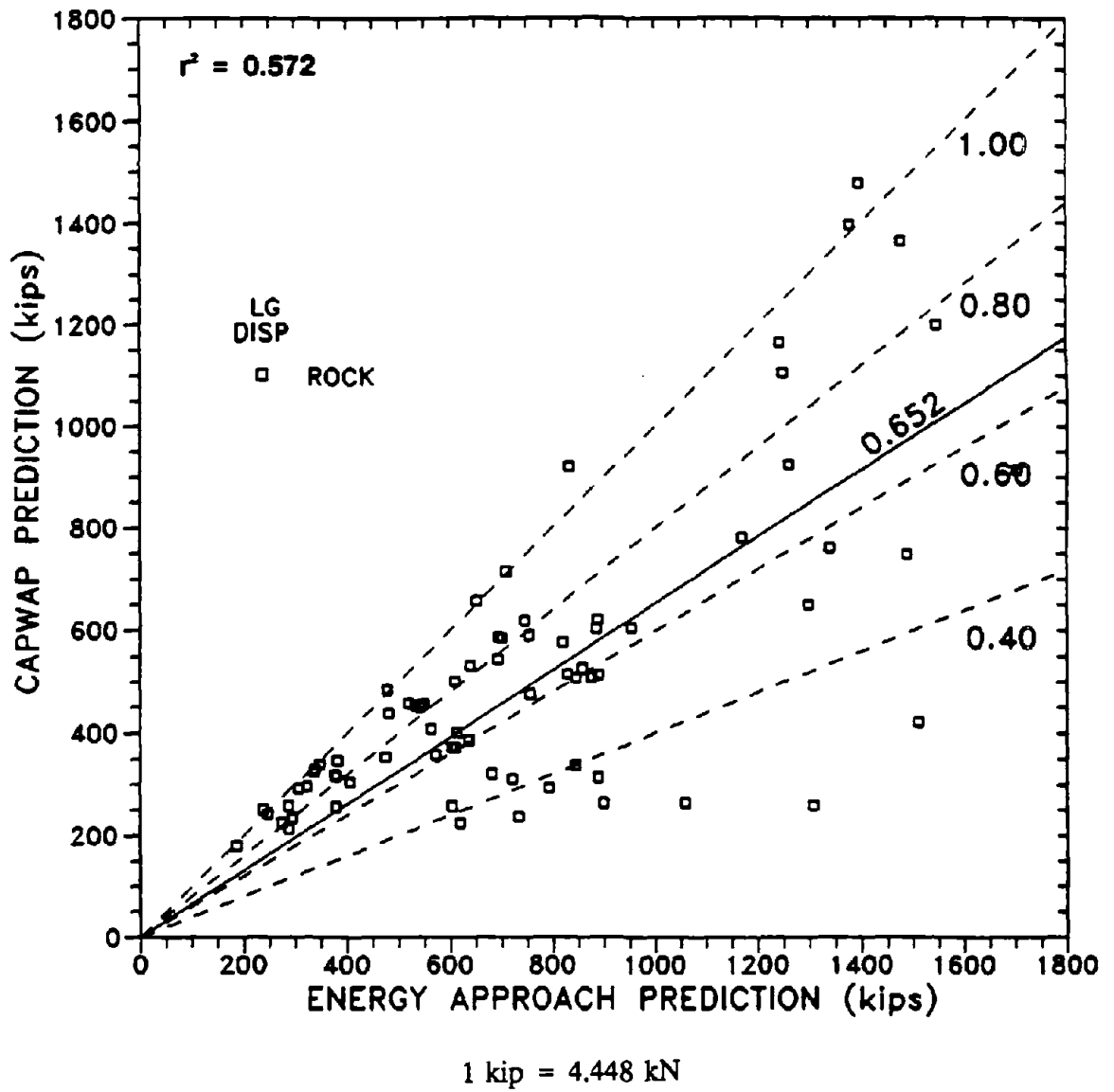
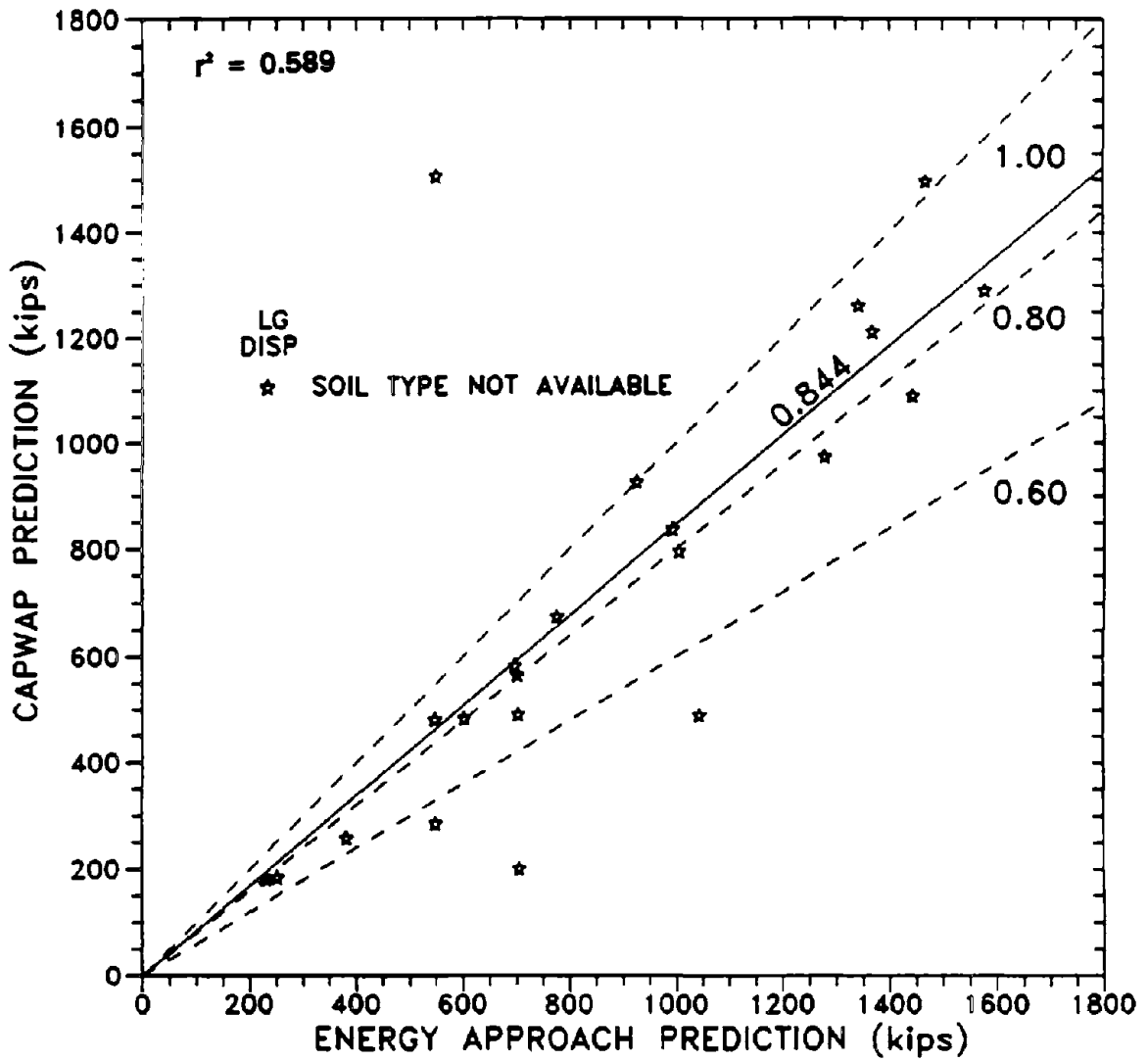
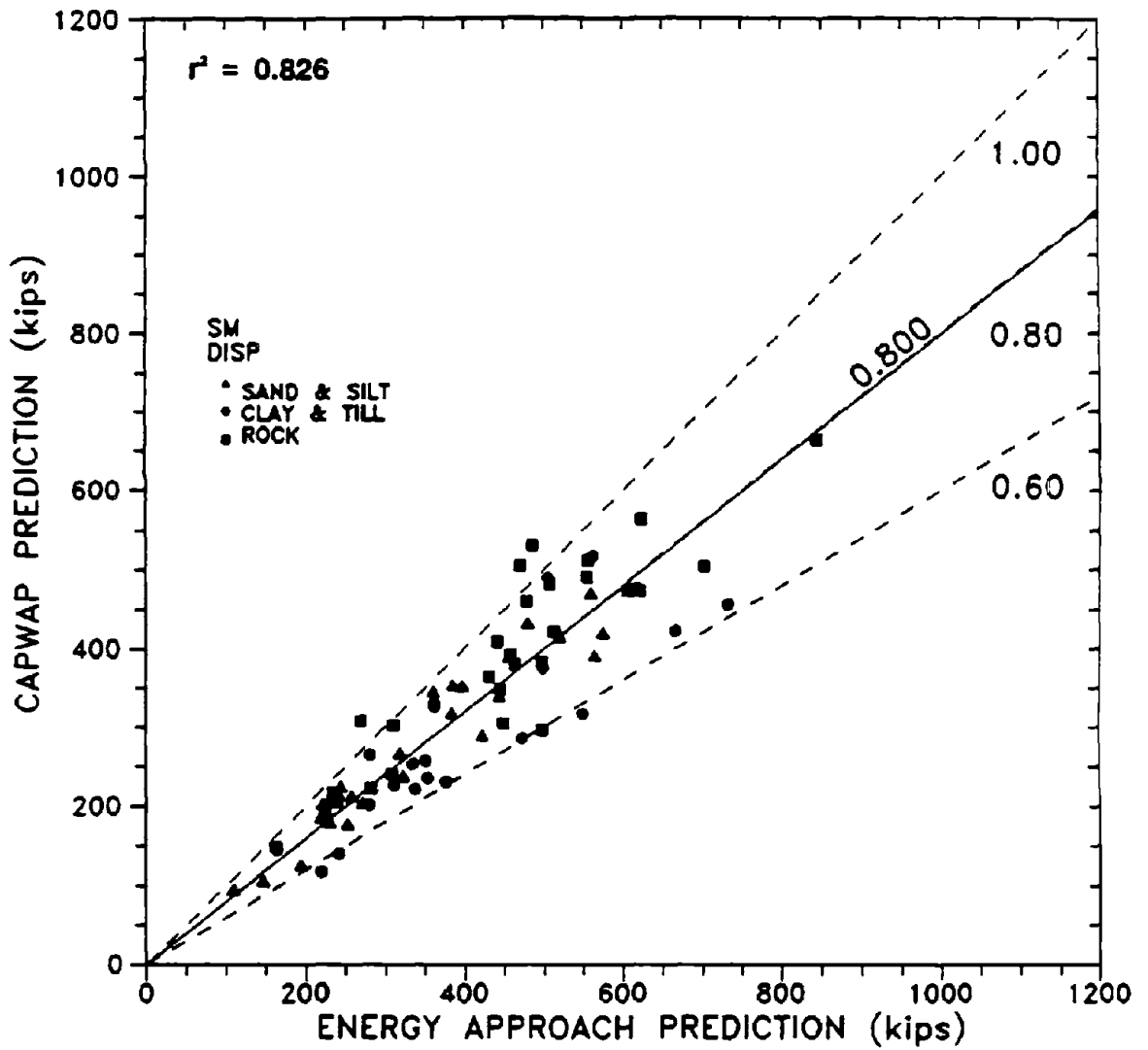


Figure 109. CAPWAP predictions vs. Energy Approach predictions for 76 large displacement PD pile-cases in rock.



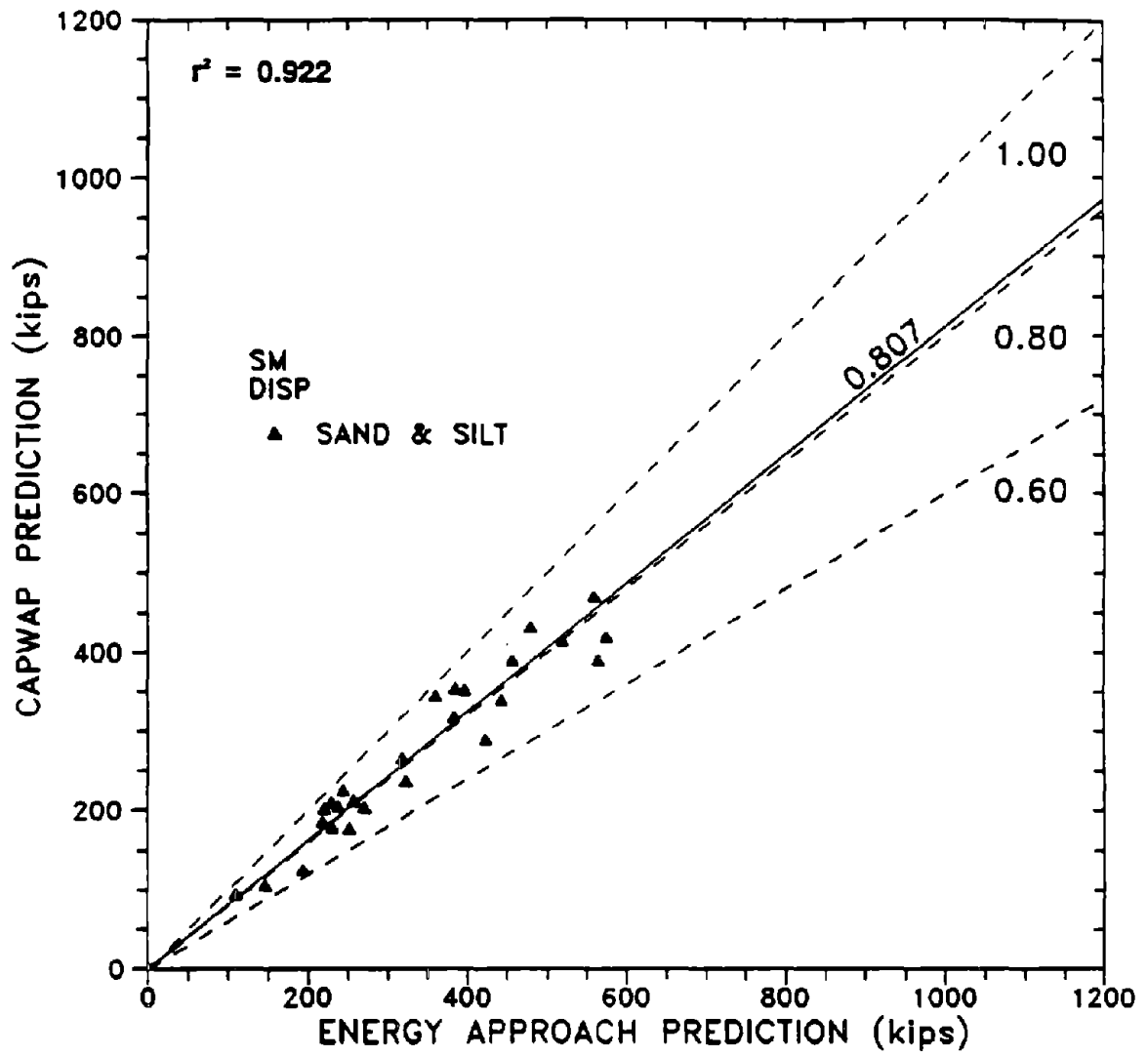
1 kip = 4.448 kN

Figure 110. CAPWAP predictions vs. Energy Approach predictions for 22 large displacement PD pile-cases in unknown soil types.



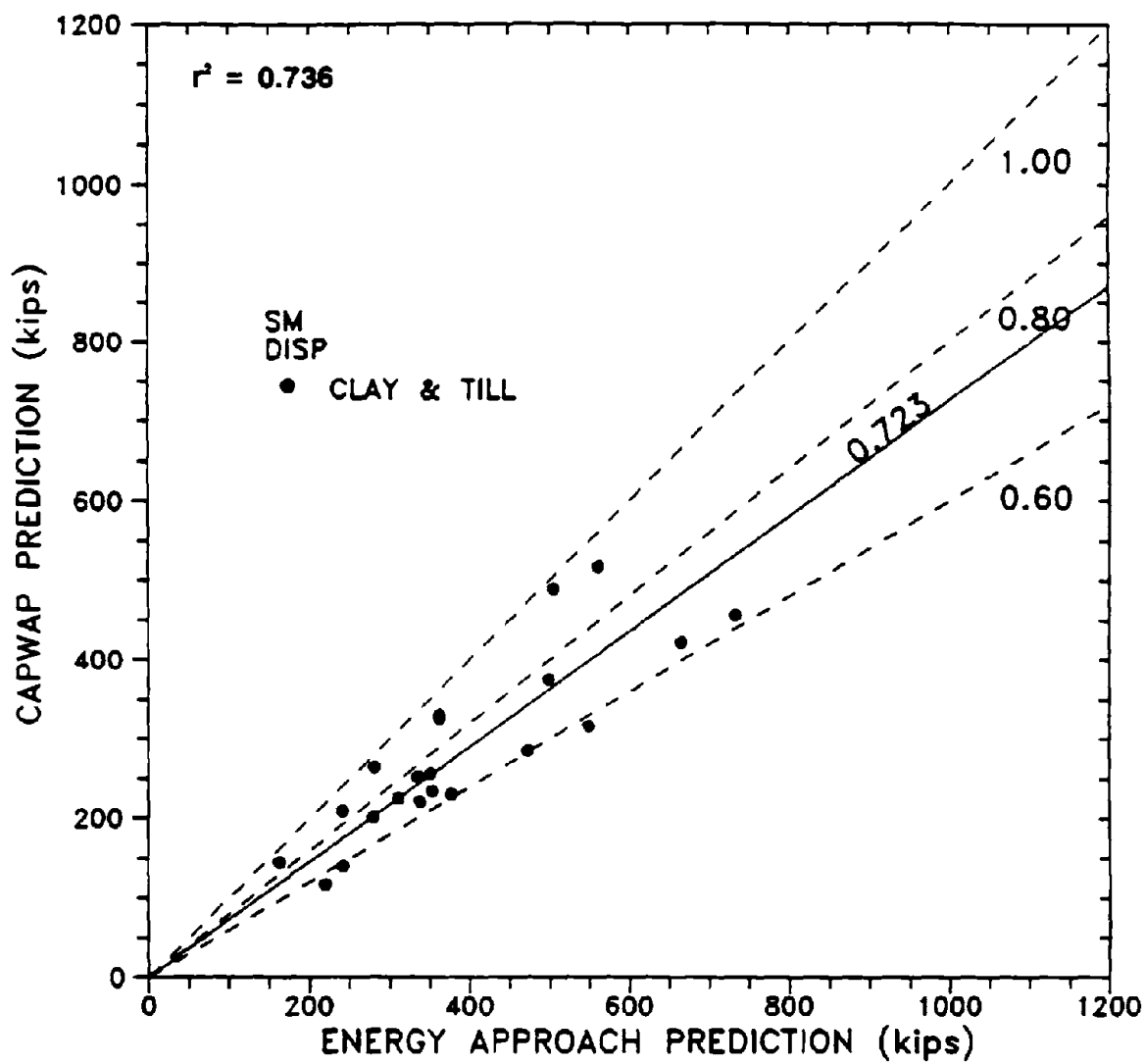
1 kip = 4.448 kN

Figure 111. CAPWAP predictions vs. Energy Approach predictions for 76 small displacement PD pile-cases in all types of soil.



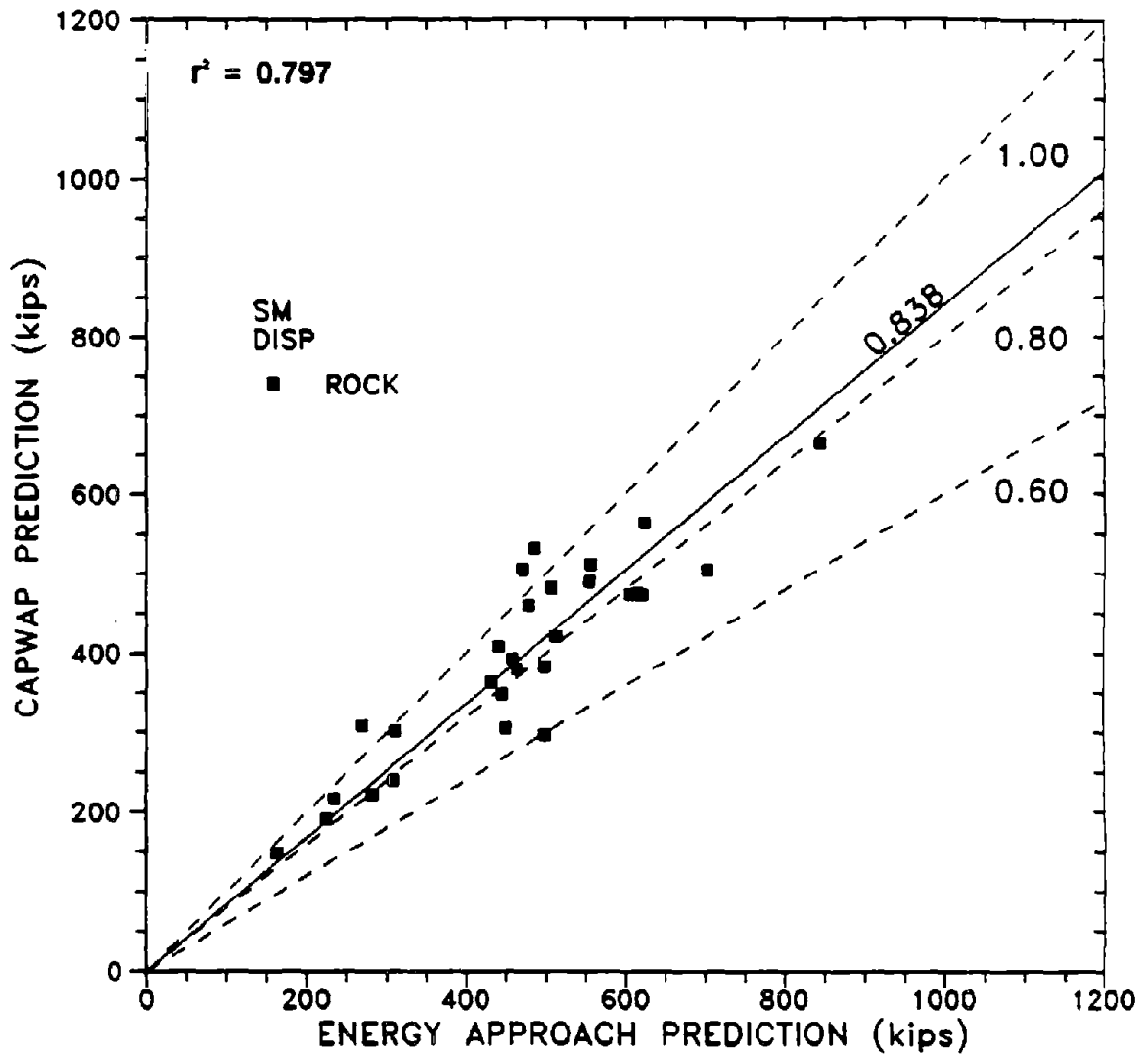
1 kip = 4.448 kN

Figure 112. CAPWAP predictions vs. Energy Approach predictions for 26 small displacement PD pile-cases in sand and silt.



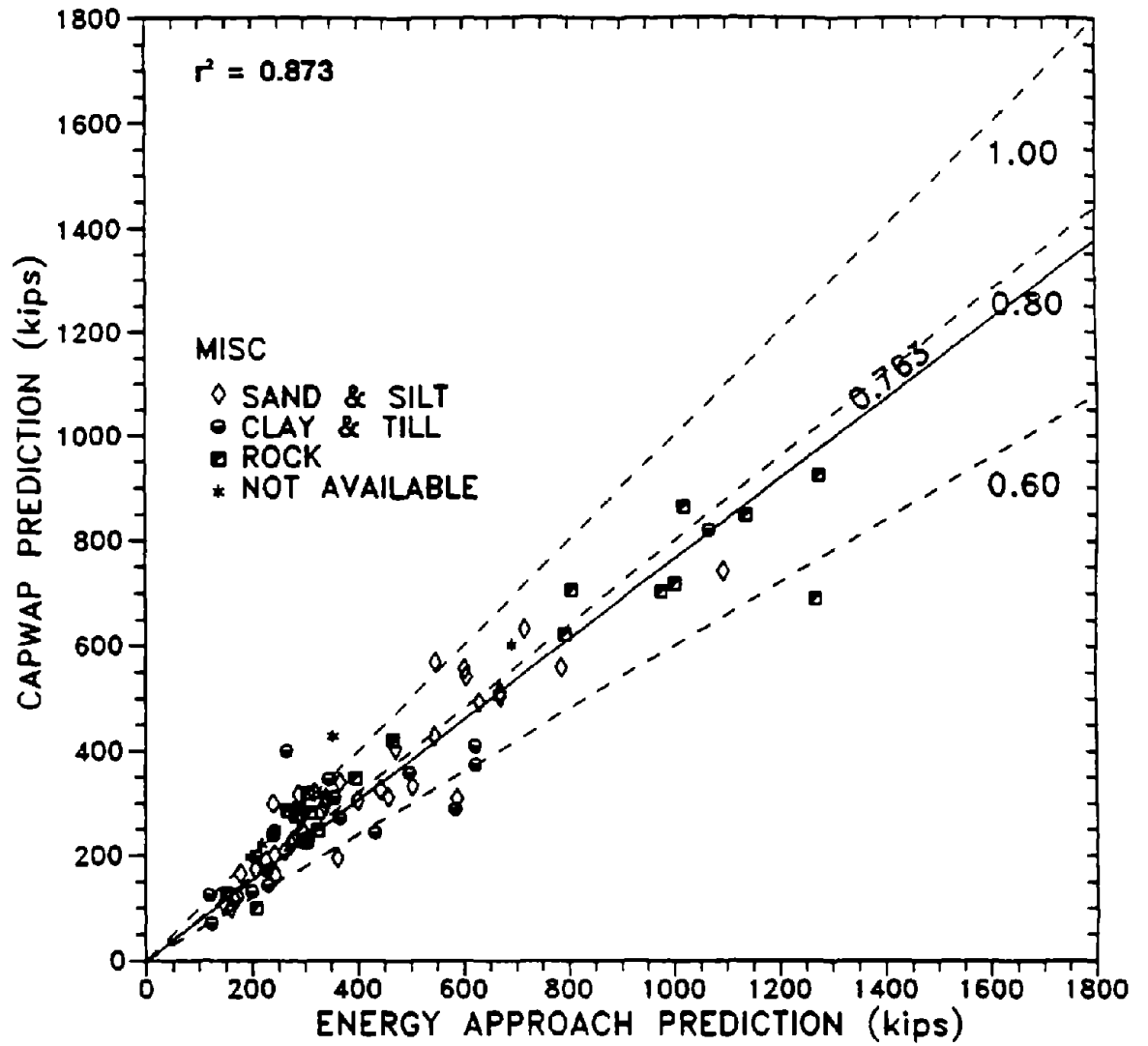
1 kip = 4.448 kN

Figure 113. CAPWAP predictions vs. Energy Approach predictions for 21 small displacement PD pile-cases in clay and till.



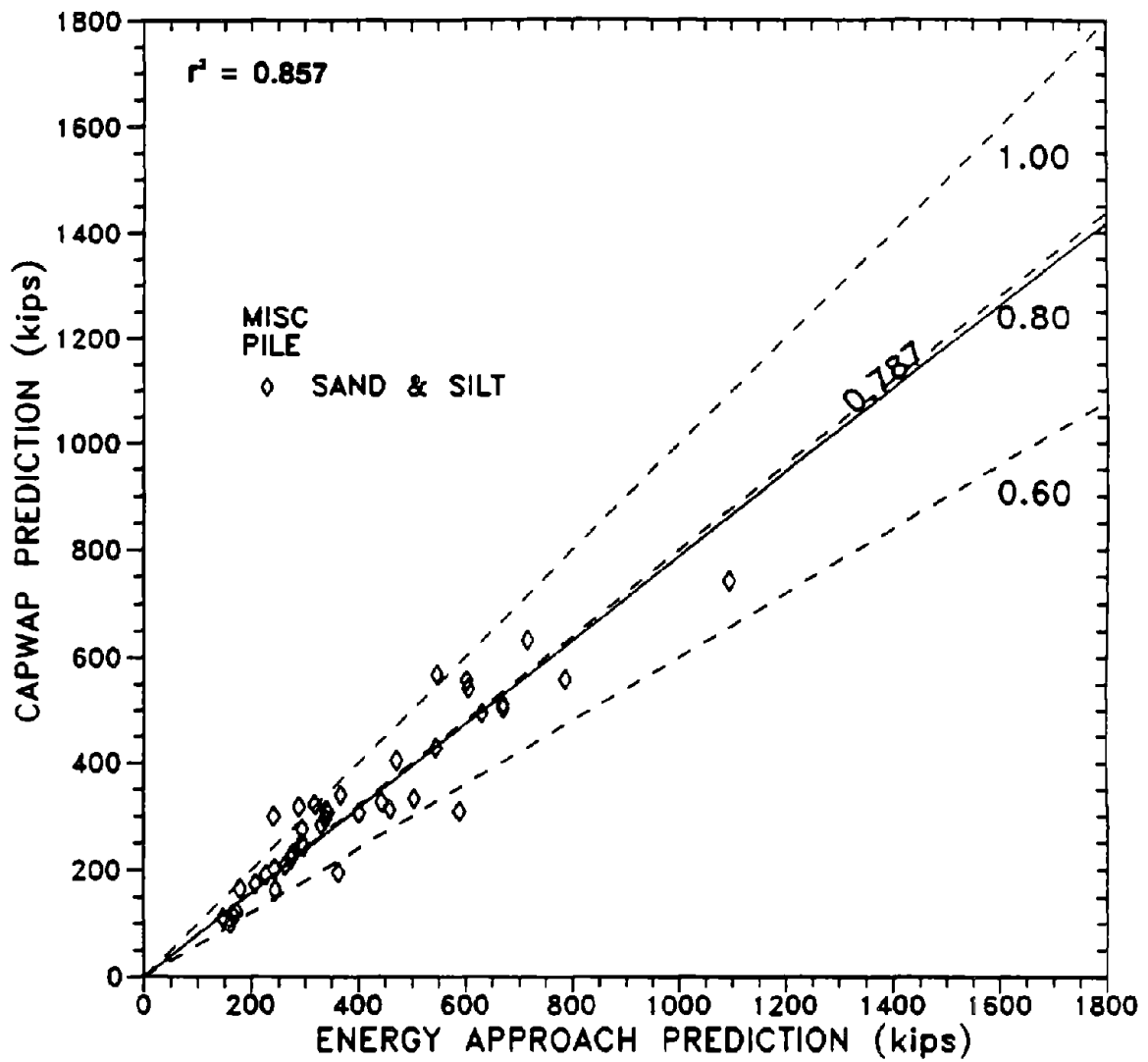
1 kip = 4.448 kN

Figure 114. CAPWAP predictions vs. Energy Approach predictions for 29 small displacement PD pile-cases in rock.



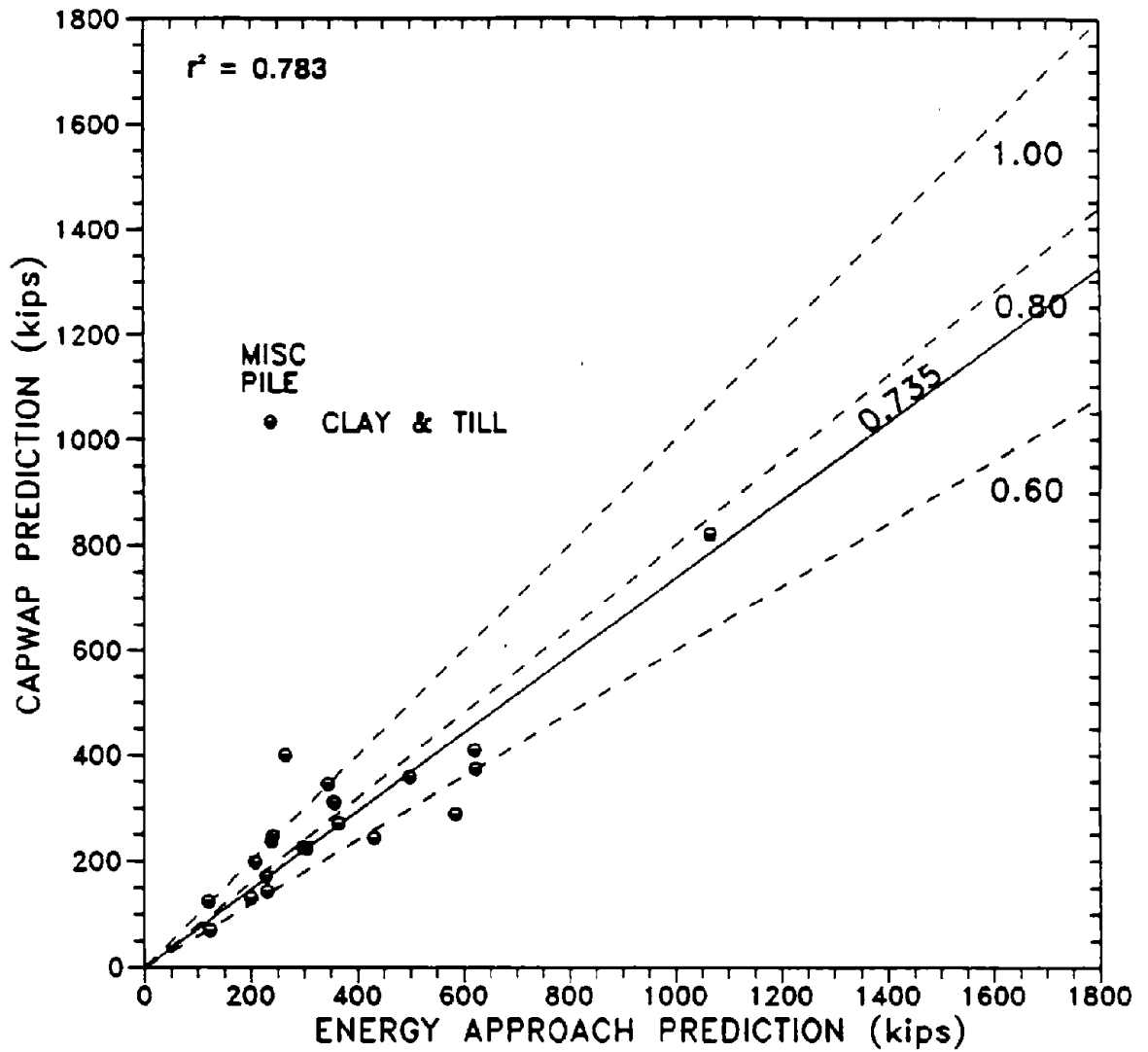
1 kip = 4.448 kN

Figure 115. CAPWAP predictions vs. Energy Approach predictions for 85 miscellaneous PD pile-cases in all types of soil.



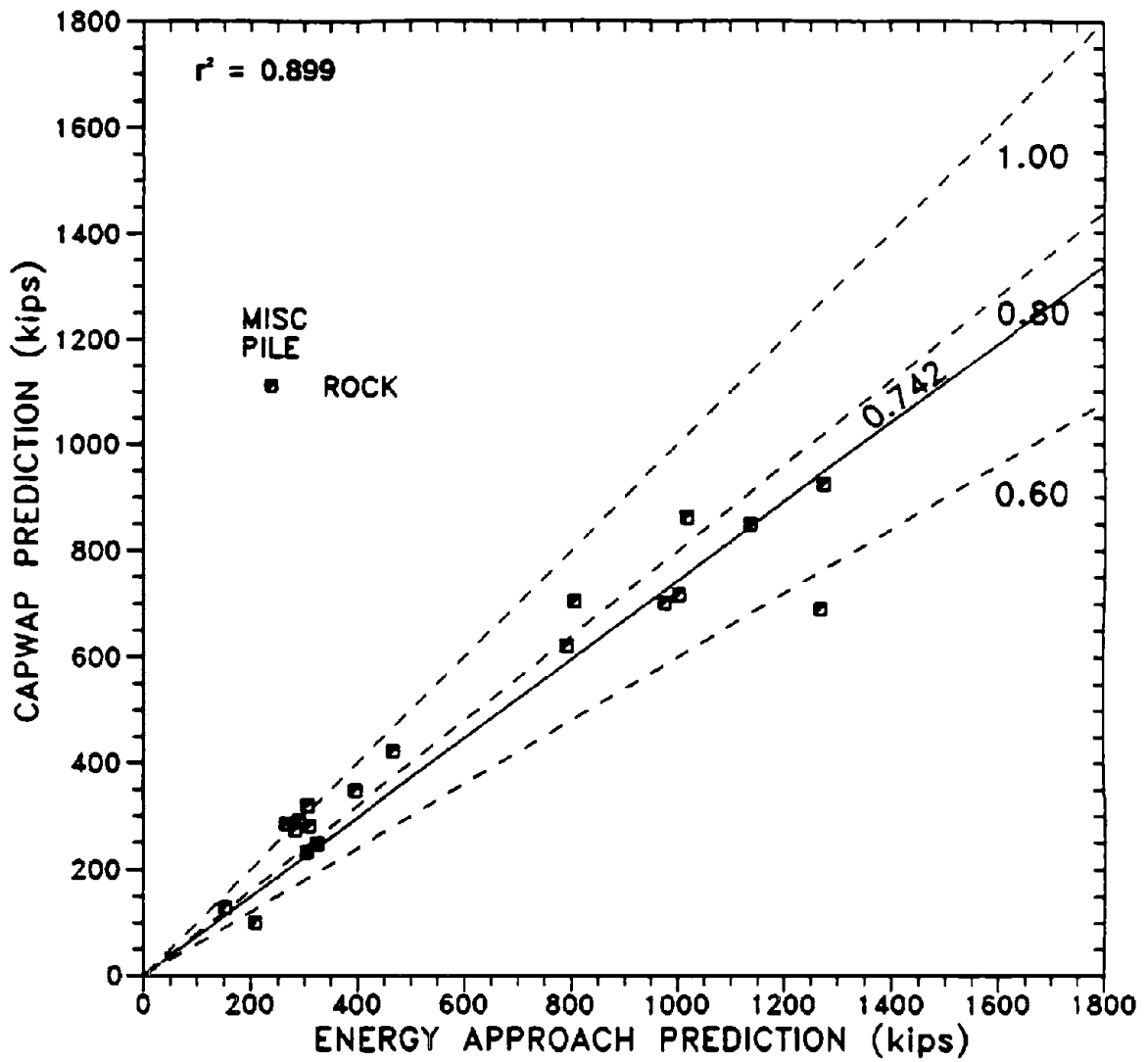
1 kip = 4.448 kN

Figure 116. CAPWAP predictions vs. Energy Approach predictions for 40 miscellaneous PD pile-cases in sand and silt.



1 kip = 4.448 kN

Figure 117. CAPWAP predictions vs. Energy Approach predictions for 21 miscellaneous PD pile-cases in clay and till.



1 kip = 4.448 kN

Figure 118. CAPWAP predictions vs. Energy Approach predictions for 19 miscellaneous PD pile-cases in rock.

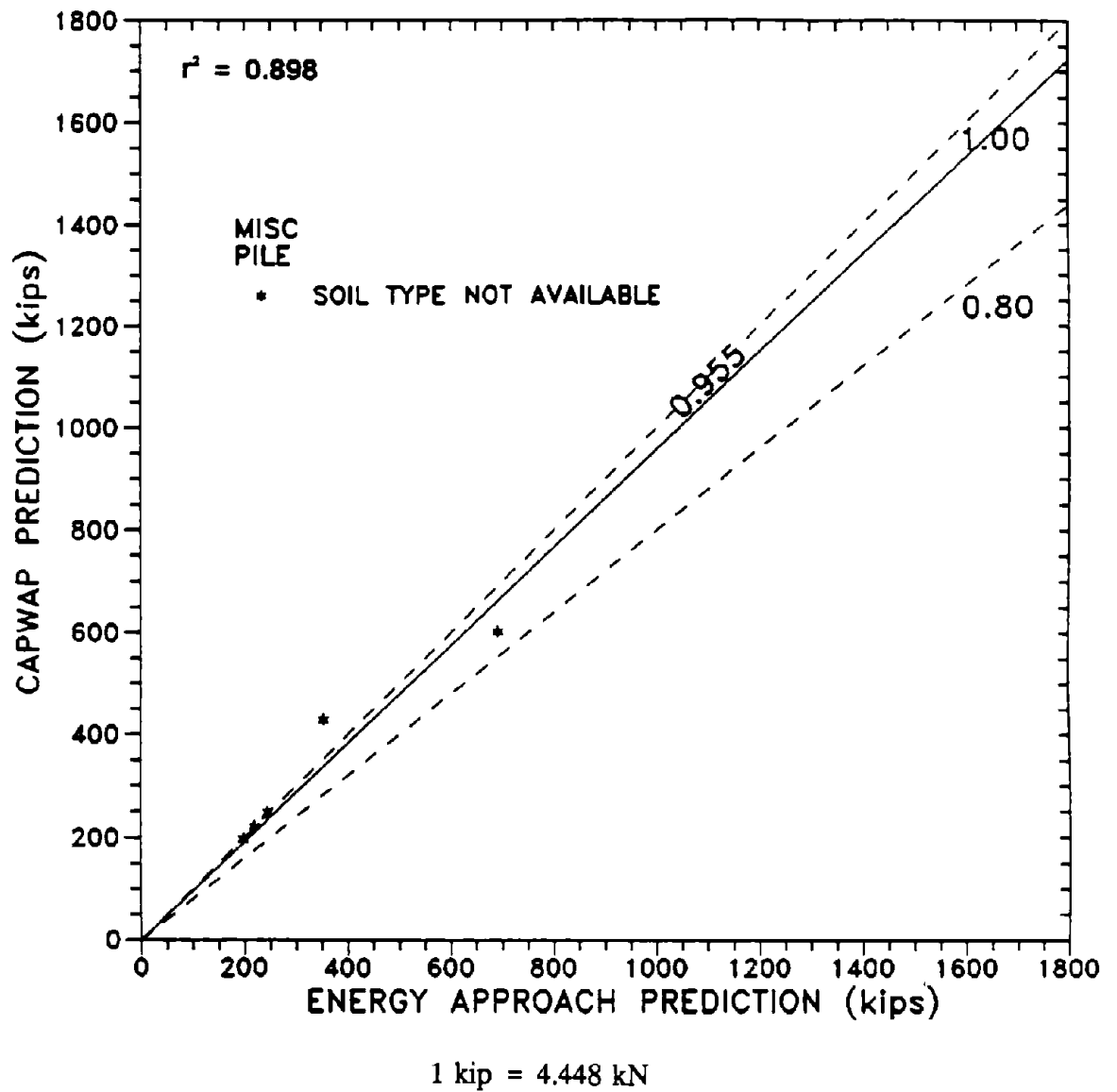


Figure 119. CAPWAP predictions vs. Energy Approach predictions for five miscellaneous PD pile-cases in unknown soil types.

CHAPTER 10 - SUMMARY, CONCLUSIONS, AND RECOMMENDATIONS

10.1 SUMMARY

Two methods are currently employed for the analysis of dynamic measurements obtained during pile driving. Both methods are based on the solution of the one-dimensional wave equation for the stress wave traveling through the pile following the hammer's impact. The first method, an office analysis, utilizes a numerical solution of a mathematical model for the pile-soil system under measured boundary conditions (e.g., the computer codes CAPWAP or TEPWAP). The other method, a field analysis known as the Case Method, which is based on a simplified closed-form solution and empirical correlations, provides an instantaneous evaluation of the pile capacity following each hammer blow.

Substantial experience suggests the existence of major limitations in the field method. In addition, no large-scale evaluation has been carried out for the office methods since their development.

A simplified method, based on the energy balance between the total energy delivered to the pile and the work done by the pile/soil systems, is proposed as an alternative field method. This method, entitled the Energy Approach, assumes elasto-plastic load displacement pile-soil relations. Calculated transferred energy and maximum pile displacement from the measured data together with the field blow count are used as input parameters for the Energy Approach. The method does not consider the propagation process and is aimed at providing a real-time pile capacity prediction in the field. The Energy Approach simplified analysis considers the energy loss from elastic soil/pile deformations and the work done by the static resistance due to plastic soil deformation.

The stress-wave-based solutions represent the external forces acting on the penetrating pile as a stationary soil resistance. Traditionally, this resistance consists of static and dynamic components. The static component is usually considered to be elasto-plastic and the dynamic component is represented by viscous damping.

It was presented and argued (in this research) that this type of formulation does not correctly represent the physical phenomena associated with pile driving. The dynamic resistance component needs to stand for phenomena such as soil inertia, wave radiation, and true damping. These factors are determined by the pile shape, penetration depth, acceleration at the pile toe, and the surrounding soil and, hence, cannot be correlated through viscous damping parameters to soil type alone.

The energy loss due to various combined factors associated with the pile penetration, such as damping radiation and inertia, are not considered directly by the Energy Approach. As such, the method serves as an excellent indicator for pointing out the physical phenomena that should account for dynamic energy losses during driving.

Two large data sets were gathered at the University of Massachusetts at Lowell. One, PD/LT, contains 208 dynamic measurement cases on 120 piles monitored during driving, followed by a static load test to failure. The data were obtained from various sources and reflect varying combinations of soil-pile-driving systems. The other, PD, contains data on 403 piles monitored during driving and was provided by Pile Dynamics, Inc. of Cleveland, Ohio. All cases were examined and analyzed.

Data set PD/LT was analyzed for the static resistance, dynamic measurements, office analysis predictions, Case damping coefficient, and the Energy Approach predictions. Data set PD was analyzed for CAPWAP analysis and the Energy Approach predictions.

The results of this study invalidate the concept of a unique recommended correlation between the viscous damping parameters and soil type in both wave-based analyses. It is shown that energy losses should be attributed more to soil inertia rather than soil damping. As such, energy losses are mostly pile-shape-dependent, in addition to the soil type and driving resistance influences.

A pile-shape parameter denoted as area ratio (A_R) was introduced as a quantitative measurement for the pile shape. The area ratio allows one to distinguish between large and small displacement piles on the basis of their soil mobilization at the pile tip relative to their skin-friction contact area.

The accuracy of the dynamic methods, when compared to the actual static capacity, and the relations between the predictions themselves, provided insight into the controlling mechanisms and the preferable conditions for these methods. It was found that best results are obtained for small displacement piles (with area ratio $A_R > 350$). The worst analysis conditions are for large displacement piles in clay under low driving resistance (< 6 BPI [0.24 blows per mm]).

The Energy Approach method was found to provide excellent evaluations of pile capacity under all conditions. The method is, therefore, proposed to be used in the field for instantaneous capacity determination. The predictions of this method were found, on the average, to provide more accurate evaluations than the sophisticated office methods, especially for records obtained at the end of initial driving. The Energy Approach is, therefore, also proposed to be used as an independent tool to evaluate the office methods.

10.2 CONCLUSIONS

The research investigated four general correlations:

- (1) Damping parameters vs. soil type.
- (2) Load test results vs. office methods (CAPWAP/TEPWAP) predictions using the parameter K_{sw} = load test capacity/office method prediction.
- (3) Load test results vs. Energy Approach predictions using the parameter K_{sp} = load test capacity/Energy Approach prediction.
- (4) CAPWAP/TEPWAP vs. Energy Approach using the parameter K_{cw} = office method prediction/Energy Approach prediction that is also equivalent to $K_{cw} = K_{sp}/K_{sw}$.

The conclusions based on the graphical and statistical analyses presented in the preceding chapters are summarized as follows:

1. Viscous damping does not truly represent the physical phenomena through which energy is lost and, hence, cannot be viewed as intrinsic to soil type.

Figure 21 presents the relationship between the back-calculated case-damping parameter, J_c (which was required to provide the actual measured static resistance), to the soil type at the tip. No correlation can be observed in this figure. Moreover, in many cases, the obtained damping parameters are negative, which has no physical meaning.

Figures 120 and 121 present the relationship between soil conditions and Smith side and tip damping for all PD/LT and PD pile-cases combined (581 cases combining figures 22 and 104, 23 and 105, respectively). Figures 120 and 121 present the damping parameters that were used in the analyses in order to obtain the best signal match between the calculated and measured signals. No correlation was found between the damping parameter used in these analyses and soil type.

2. The capacity predictions for small displacement piles resulted in higher accuracy and substantially lower scatter for both dynamic methods when compared to the predictions and the scatter obtained for large displacement piles. (See, for example, figures 29 and 30 compared to figures 32 and 33).

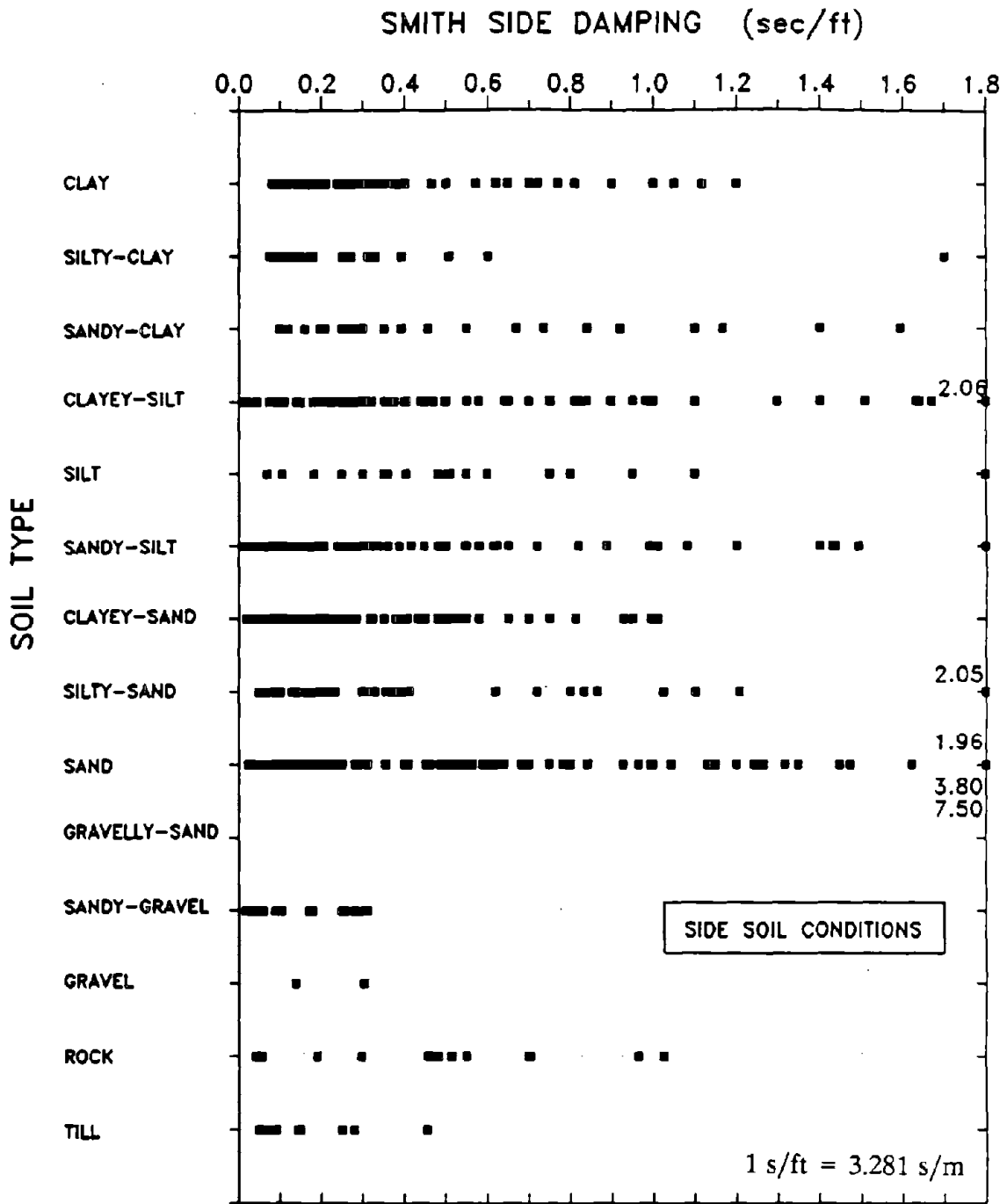


Figure 120. Side soil conditions vs. Smith side damping based on CAPWAP/TEPWAP results for 581 pile-cases.

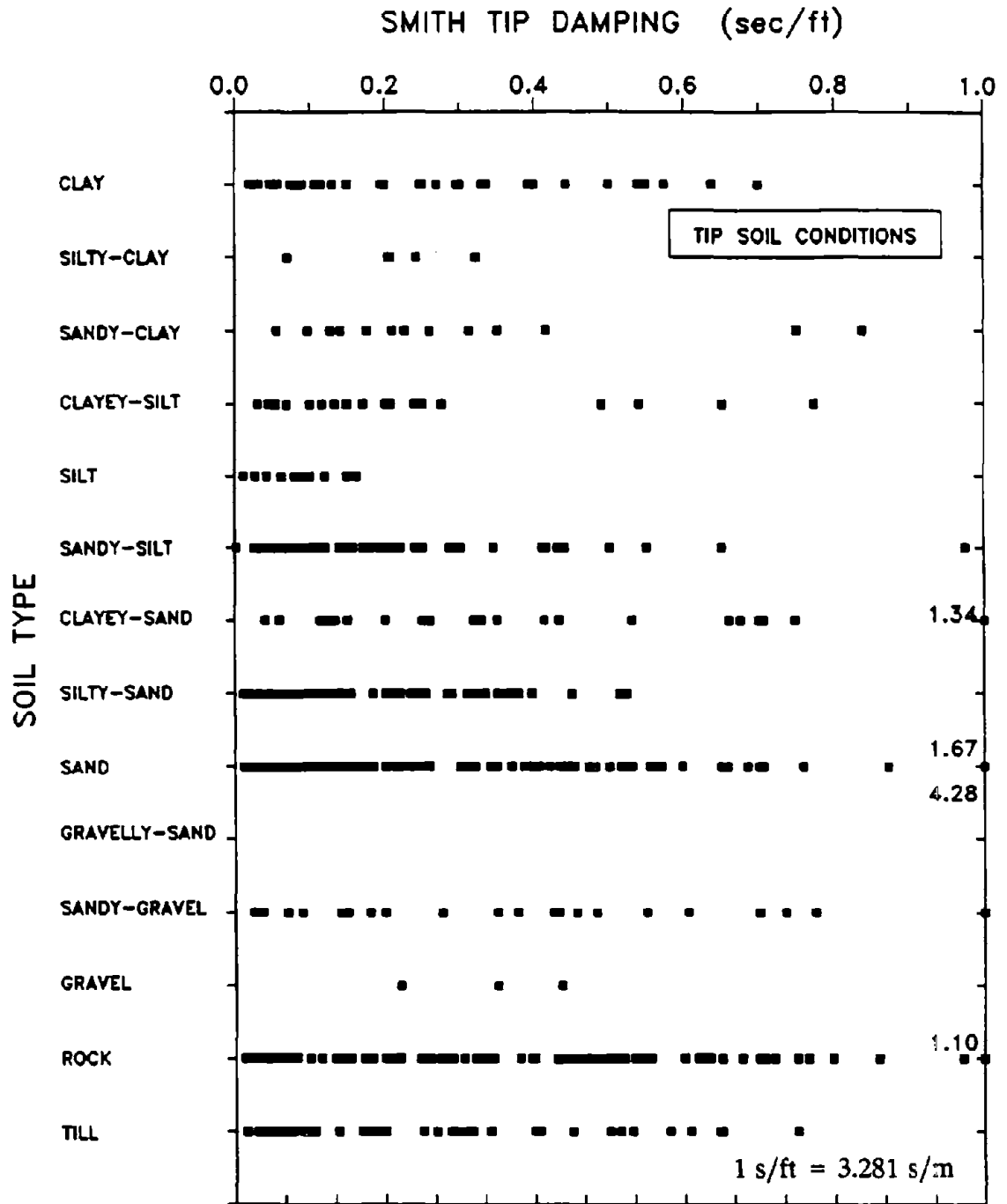


Figure 121. Tip soil conditions vs. Smith tip damping based on CAPWAP/TEPWAP results for 581 pile-cases.

Small and large displacement piles can be defined according to area ratio ($A_R > 350$ for small displacement piles and $A_R < 350$ for large displacement), as presented and discussed in sections 4.4 and 8.5.4 (see figures 70 and 72).

3. The above conclusion is reinforced by the excellent correlations that were obtained between the prediction methods for the small displacement pile cases (see tables 12 and 16). These observations show that energy is lost mainly due to soil inertia as a result of the mobilization of the soil mass at the pile tip. The correlations of section 8.3 (see tables 5 and 8) indicate that soil type has very little effect on the accuracy of the Energy Approach predictions. As such, correlations were examined based on pile type, driving resistance, and time of driving (see section 8.5).
4. Correlations between driving resistance and dynamic predictions do not lead to definitive conclusions (see table 9). Figures 73 through 102 and reanalysis of the prediction coefficients on the basis of blow counts between 0 to 10 BPI (0.39 blows per mm) and over 10 BPI indicate the following trends:
 - Small displacement piles with high driving resistance will result in a small loss of energy due to soil inertia and, therefore, more accurate predictions, as the actual pile resistance is similar to the maximum resistance during driving. The results of both methods of analysis performed well for that category. For example, the mean and standard deviation for 25 small displacement piles ($A_R > 350$) driven in the range of 0 to 10 BPI (0.39 blows per mm) is $K_{sw} = 1.360$, $\sigma_x = 0.5581$ and $K_{sp} = 0.939$, $\sigma_x = 0.2788$, compared to the 32 pile-cases driven under resistances higher than 10 BPI (0.39 blows per mm) that resulted in $K_{sw} = 1.159$, $\sigma_x = 0.4422$ and $K_{sp} = 0.929$, $\sigma_x = 0.2185$.
 - Large displacement piles with low driving resistance will result in a large loss of energy due to soil inertia and less accurate predictions, as the actual pile resistance is the difference between the maximum pile resistance during driving and the large energy loss. (For this category, the Energy Approach predicts well for EOD and over-predicts for BOR while the office methods seem to under-predict for EOD and improve with time.) For example, the mean and standard deviation for 101 large displacement pile cases ($A_R < 350$) driven at the range of 0 to 10 BPI (0.39 blows per mm) is $K_{sw} = 1.353$, $\sigma_x = 0.4879$ and $K_{sp} = 0.906$, $\sigma_x = 0.3257$, compared to the 43 pile-cases driven in resistances higher than 10 BPI (0.39 blows per mm), which resulted in $K_{sw} = 1.601$, $\sigma_x = 0.6279$ and $K_{sp} = 0.951$, $\sigma_x = 0.2961$.

5. The End of Driving (EOD) condition is of special interest as it represents the ability of the methods to predict the capacity during driving and to evaluate for the most common state. The predictions for EOD were examined, in particular, in figures 44 (and 46), 45 (and 47), 75, 76, and tables 5, 6, 8, and 9. The data clearly indicate very good predictions and correlations of the Energy Approach under all categories with better performance for small displacement piles. For example, 97 piles at EOD resulted in $K_{sw} = 1.478$, $\sigma_x = 0.6167$ and $K_{sp} = 1.023$, $\sigma_x = 0.3073$. These numbers improved for the subgroup of 29 small displacement piles showing $K_{sw} = 1.252$, $\sigma_x = 0.5616$, and $K_{sp} = 0.935$, $\sigma_x = 0.2616$. The large mean and standard deviation ratios for the K_{sw} -coefficient suggest limitations of the office analysis methods for all piles at the end of driving, but, in particular, for large displacement piles.

10.3 RECOMMENDATIONS

10.3.1 General

The recommendations are comprised of three parts. One part (sections 10.3.2, 10.3.3, and 10.3.4) describes the major prediction parameters and their statistical evaluation for the different pile-cases. The statistical evaluation is shown in the form of:

- Determination of the first-order best-fit line forced through zero (x-coefficient) and the measure of its accuracy through the coefficient of determination (r^2). Section 8.4.1 reviewed these parameters, mainly indicating that good correlation exists for $r^2 \geq 0.8$ and that $0.6 \leq r^2 < 0.8$ indicates a moderate correlation only.
- Mean and standard deviation of the normal distribution. The mean represents the accuracy of the prediction (the ability to predict the measured ultimate static capacity) and the precision of the method refers to the scatter, which is represented by the standard deviation (the smaller the scatter, the lower the standard deviation).

In examining a certain pile-case category, it is advised to check both the x-coefficient and the mean as measures of the prediction accuracy and check the coefficient of determination and the standard deviation as measures of the scatter. It is also advised to look at the actual data presented in the scattergram associated with the particular case.

The second part of the recommendations refers to a discussion regarding the factors of safety that are associated with the predictions of the office methods and the Energy Approach. The third part lists several recommendations for the implementation of the methods and potential future improvements.

10.3.2 The Performance of the Office Methods (CAPWAP/TEPWAP)

Table 14 summarizes the major numerical parameters obtained through the analysis of data set PD/LT, concerning the performance of the office analyses. Only the pile-cases that contained a significant number of cases and/or could indicate an important influence were included. Table 14 indicates the following:

- For all piles at any time of driving in all soils, the office method under-predicts the actual static capacity by about 30 percent with a relatively large scatter. The scatter is mostly due to low accuracy in the prediction of cases involving large displacement piles (see LAA compared to SAA) and driving in clay (see AAC compared to AAS). It must be emphasized that a separate observation (not presented in this study) shows a clear improvement of the office method predictions with time. The accuracy of the method when analyzing records close to the time of load testing is, therefore, not evident in the data.
- The major single parameter controlling the accuracy of the method is the pile type. The accuracy of the method and its scatter reduces substantially for small displacement piles at any time of driving in all soils. It is further evident with the accuracy of the small displacement piles at the end of driving for which the office method presented excellent results with a mean and x-coefficient close to 1 and $r^2=0.95$.

10.3.3 The Performance of the Energy Approach

Table 15 summarizes the major numerical parameters obtained through the analysis of data set PD/LT concerning the performance of the Energy Approach. Only the pile groups that contained a significant number of pile-cases and/or could indicate an important influence were included. The Energy Approach was proposed as the field method and, hence, the performance at the end-of-driving condition is emphasized. Table 15 indicates the following:

- For all piles at any time of driving in all soils, the Energy Approach over-predicts the actual static capacity by about 8 percent with a noticeable scatter that is, however, significantly smaller than that of the office method. As in the prediction of the office methods, the scatter is mostly due to lower accuracy in the prediction of cases involving large displacement piles (see LAA compared to SAA) and driving in clay (see AAC compared to AAS).

- Good correlation exists for predictions related to end of driving and small displacement piles. This is evident through the high coefficients of determination (r^2) and small standard deviations for these cases.
- The mean prediction ratio for all cases at the end of driving (AEA) is 1.0. Higher accuracy is obtained for small displacement piles (SEA) compared to large displacement piles (LEA).

10.3.4 The Correlation Between the Office Methods and the Energy Approach

Tables 16 and 17 summarize the correlations obtained between the two methods under the different pile cases. Table 16 has a similar format to that of tables 14 and 15 and is based on the PD/LT data set. The parameters in table 16 referring to the end-of-driving conditions present excellent correlations between the methods, except for predicting large displacement piles for which each of the methods encountered its own difficulties.

Table 17 is based on the data combined in both data sets (PD and PD/LT) and, hence, refers to 609 pile-cases. The low correlations were again obtained for large displacement piles (LAA), especially when driven in clay (LAC).

The obtained relationships of tables 16 and 17 can perform as excellent guidelines when comparing the results of the office methods to that of the Energy Approach.

10.3.5 Factors of Safety and Risk Analysis

(a) General

Factor of safety in the current common use is the factor that we apply to our prediction in order to come up with an allowed capacity for which we would feel freedom from meaningful risk.

Risk is defined (see, for example, Briaud and Tucker, 1988) as the probability (P) that the predicted ultimate capacity (Q_p) divided by the factor of safety (F.S.) exceeds the measured ultimate load (Q_m):

$$R = P\left[\left(\frac{Q_p}{F.S.}\right) > Q_m\right] \quad (41)$$

The calculated K-values (K_{sw} and K_{sp}) as presented throughout this research study are the ratio of $K = Q_m/Q_p$, using the above notation. The risk can therefore be rewritten in the following format:

$$R = P[K \cdot F.S. < 1] \quad (42)$$

where $K = K_{sw}$ or K_{sp} .

As the construction cost is directly related to the factor of safety, we are interested in several forms of that factor:

- What is the minimum factor of safety that will allow us absolute safety?
- What is the risk associated with any factor of safety?
- What is the actual factor of safety when considering the inaccuracy of the prediction method?

These aspects are discussed in the following section.

(b) Absolute Safety Based on Data Set PD/LT

The data sets were searched for the worst over-prediction ratio. The absolute factor of safety was defined as the one that should have been used in this case in order to make certain that the allowed capacity would not exceed the ultimate capacity. The results of the analysis based on this approach are summarized in table 18 in the following manner:

Columns 1 through 3 detail the method of analysis, pile-case category, and number of cases related to that category.

Column 4 indicates the minimum K-factor (K_{sw} or K_{sp}) in the related data set. The K_{min} -value is associated with the maximum over-prediction ratio.

Column 5 is the inverse ratio of K_{min} , indicating the absolute factor of safety that would have been needed in this case in order to guarantee that the allowed capacity would not exceed the ultimate static capacity.

Column 6 takes into consideration the average built-in risk or safety that exists in each of the methods. The office methods under-predict on the average, such that the mean K_{sw} for the AAA category is 1.367. Using, in addition, a factor of safety of 1.75 means that the actual mean factor of safety is 1.367×1.75 , which results in 2.40. The Energy Approach is over-predicting on the average. The mean K_{sp} for the AAA category is 0.925, which means that when employing a factor of safety of 2.44, the actual mean factor of safety is $0.925 \times 2.44 = 2.26$.

Column 6 indicates that although the Energy Approach requires somewhat higher factors of safety in order to cover the worst over-prediction case, the actual factor of safety that is used when considering the accuracy of the method is smaller than that of the office

Table 14. Linear regression and statistical analysis of Ksw for selected PD/LT pile-cases.

Pile-Case Group	Number of Cases	Ar Area Ratio	Ksw = Load Test/CAPWAP or TEPWAP			
			Linear Best Fit through Zero		Normal Distribution	
			x-coefficient	r-squared	mean	standard deviation
AAA	206	all	1.265	0.692	1.367	0.5334
AAS	141	all	1.272	0.749	1.385	0.4758
AAC	51	all	1.319	0.383	1.443	0.676
SAA	60	>350	1.108 (44)	0.932	1.237	0.4916
LAA	144	<350	1.372 (102)	0.554	1.427	0.5433
AEA	97	all	1.248	0.740	1.478	0.6167
SEA	41	>350	1.113 (29)	0.933	1.250	0.4838
LEA	56	<350	1.529 (68)	0.528	1.643	0.6544

Pile-case legend: XXX - first letter denotes pile type: A=all piles, L=large displacement, and S=small displacement.
 - second letter denotes time of measurement: A=anytime, E=end of driving, and B=beginning of restrike.
 - third letter denotes soil type: A=all soils, S=sand and silt, C=clay and till, and R=rock.

Table 15. Linear regression and statistical analysis of Ksp for selected PD/LT pile-cases.

Pile-Case Group	Number of Cases	Ar Area Ratio	Ksp = Load Test/Energy Approach			
			Linear Best Fit through Zero		Normal Distribution	
			x-coefficient	r-squared	mean	standard deviation
AAA	206	all	0.839	0.703	0.925	0.2932
AAS	141	all	0.831	0.700	0.942	0.3127
AAC	53	all	0.872	0.666	0.906	0.2689
SAA	41	>350	0.856 (44)	0.416	0.960	0.2347
LAA	144	<350	0.832 (164)	0.534	0.920	0.3165
AEA	98	all	0.900	0.804	1.023	0.3073
SEA	41	>350	0.851 (29)	0.917	0.960	0.2347
LEA	57	<350	0.966 (69)	0.603	1.068	0.3453

Pile-case legend: XXX - first letter denotes pile type: A=all piles, L=large displacement, and S=small displacement.
 - second letter denotes time of measurement: A=anytime, E=end of driving, and B=beginning of restrike.
 - third letter denotes soil type: A=all soils, S=sand and silt, C=clay and till, and R=rock.

Table 16. Linear regression and statistical analysis of Kew for selected PD/LT and PD pile-cases.

Pile-Case Group	Number of Cases	Kew = CAPWAP or TEPWAP/Energy Approach				
		Linear Best Fit through Zero		Normal Distribution		
		x-coefficient	r-squared	mean	standard deviation	
AAA	609	0.670	0.727	0.753	0.203	
LAA	404	0.638	0.609	0.721	0.215	
LAS	210	0.617	0.690	0.720	0.175	
LAC	93	0.600	0.447	0.687	0.198	
SAA	120	0.772	0.937	0.807	0.147	
SAS	49	0.754	0.950	0.783	0.155	
SAC	29	0.752	0.914	0.740	0.126	

Pile-case legend: XXX

- first letter denotes pile type: A=all piles, L=large displacement, and S=small displacement.
- second letter denotes time of measurement: A=anytime E=end of driving, and B=beginning of restrike.
- third letter denotes soil type: A=all soils, S=sand and silt, C=clay and till, and R=rock.

Table 17. Linear regression and statistical analysis of Kew for selected PD/LT pile-cases.

Pile-Case Group	Number of Cases	Ar Area Ratio	Kew = CAPWAP or TEPWAP/Energy Approach			
			Linear Best Fit through Zero		Normal Distribution	
			x-coefficient	r-squared	mean	standard deviation
AEA	95	all	0.699	0.861	0.743	0.179
SEA	39	>350	0.762	0.947	0.813	0.147
LEA	56	<350	0.598	0.398	0.695	0.184

Pile-case legend: XXX - first letter denotes pile type: A=all piles, L=large displacement, and S=small displacement.
 - second letter denotes time of measurement: A=anytime, E=end of driving, and B=beginning of restrike.
 - third letter denotes soil type: A=all soils, S=sand and silt, C=clay and till, and R=rock.

methods. This situation is especially clear for the end-of-driving cases where a factor of safety of 2.0 actually means an average factor of safety of 2.0 for all cases.

Column 7 examines the maximum factor of safety that will be employed for the worst under-prediction ratio, using this approach. Since the maximum under-prediction ratio for the office method is $K_{sw_{max}} = 4.42$, the maximum actual factor of safety that will result from using an F.S. of 1.75 is $1.75 \times 4.42 = 7.74$.

The small scatter for the Energy Approach is again demonstrated for all the end-of-driving predictions where the use of a factor of safety of 2.0 will result in a maximum conservative factor of safety of only 4.24.

Table 18. Absolute factor of safety based on data set PD/LT.

Method of Analysis	Pile-Case Group	No. of Cases	K_{min}	Factor of Safety (F.S.)	F.S. x mean K	F.S. x K_{max}
CAPWAP/TEPWAP	AAA	206	0.57	1.75	2.40	7.74
CAPWAP/TEPWAP	AEA	97	0.57	1.75	2.59	7.74
Energy Approach	AAA	208	0.41	2.44	2.26	5.28
Energy Approach	AEA	98	0.51	1.96	2.01	4.24

(c) Factor of Safety and the Associated Risk Based on the Actual Data

The PD/LT data set was used to prepare the relationships between the applied factor of safety and its associated risk as defined earlier. The procedure was described by Briaud and Tucker (1988) and contains the following steps:

1. Select an arbitrary F.S. (factor of safety).
2. Calculate the risk of failure as the ratio between the number of piles in the data set for which $Q_p/Q_m > F.S.$ over the total number of piles in that data base.
3. Repeat steps 1 and 2 for different F.S. values.
4. Plot the obtained relations between the applied factor of safety and the associated risk.

This analysis was carried out for three pile group cases (AAA, AEA, and SEA) for each of the two prediction methods. Figures 122, 124, and 126 are related to the office

method predictions and figures 123, 125, and 127 are related to the Energy Approach predictions. An accurate prediction occurs when the predicted value is equal to the failure value and, hence, associated with a risk of 100 percent for a factor of safety of 1. A smaller risk with F.S. = 1 reflects on under-prediction. For example, according to figure 122, 77.7 percent of the piles (AAA cases) will be safe using CAPWAP and F.S. = 1 as the method under-predicts in most cases. In order to include the bias of the prediction method itself, the relationships between the applied factor of safety and the mean over-prediction ratio (or the mean actual factor of safety) were added in each chart. For example, figure 122 indicates that using a factor of safety of 1.2 for all cases of the office method, will result in a risk of 5.8 percent. This factor of safety, however, is actually equivalent to a factor of safety of 1.64 when considering the mean of $K_{sw} = 1.367$ for the AAA pile-case group.

Table 19 summarizes numerically, based on figures 122 through 127, a few representative factors of safety and their associated risks. The numerical values show the accuracy and reliability of the Energy Approach, especially for the end-of-driving analysis. The use of a factor of safety of 1.6, for example, will be associated with an actual F.S. of 1.6 and a risk of 2.1 percent for the Energy Approach, while the same factor of safety means an actual F.S. of 2.3 and risk of 1.1 percent for the office method.

(d) Factor of Safety and the Associated Risk Based on the Probability Distribution Function

The risk associated with the factor of safety can also be evaluated based on the probabilistic models. The models associated with the distribution of the predictions were presented in section 8.4.

The use of these evaluations can be done in the following way:

$$R = P[K \times F.S. < 1] = P\left[K < \frac{1}{F.S.}\right] \quad (43)$$

using $x = 1/F.S.$

for a normal distribution

$$P[K < x] = P\left[U \leq \left(\frac{x - m_x}{\sigma_x}\right)\right] = F_u\left(\frac{x - m_x}{\sigma_x}\right) = F_u(u) \quad (44)$$

for a log-normal distribution

$$P[K < x] = P[\ln K \leq \ln x] = F_u\left(\frac{\ln(x/m_x)}{\sigma_{\ln x}}\right) \quad (45)$$

where F_u is obtained directly from the standard tables of the normal distribution function.

For example, using the log-normal distribution for K_{sp} for AAA pile-cases (see figure 66):

$$m_x = 0.8818, \sigma_{\ln x} = 0.3094$$

F.S.	1/F.S.	U	F_u	R = P[K < 1/F.S.]	R (table 19)
1.0	1	0.4066	0.6591	65.9%	67.8%
1.6	0.625	-1.2517	1-0.8944	10.6%	14.4%
1.8	0.556	-1.4932	1-0.93189	6.8%	7.7%
2.0	0.500	-1.8337	1-0.96712	3.3%	4.8%
2.5	0.400	-2.5549	1-0.996	0.4%	0%

These numbers fit very well with the risk presented in figure 123 and table 19.

10.3.6 Recommendations for Implementation

- I. The simplicity of the Energy Approach formulation together with its high accuracy at the end of driving makes it an ideal method of analysis to be used in the field and as a check for the office methods.

The following factors of safety are recommended to be used with the Energy Approach predictions:

- F.S. = 2.50 for all piles in all cases (AAA, mean K_{sp} = 0.93).
- F.S. = 2.00 for all end-of-driving cases (AEA, mean K_{sp} = 1.00).
- F.S. = 2.00 for all small displacement piles ($A_R > 350$) in all cases (SAA, mean K_{sp} = 0.94).

The following recommendations are made for improving the use of the Energy Approach method:

1. Implement the Energy Approach as part of the Pile-Driving Analyzer (PDA) routine analysis. This will ensure more accurate field predictions that may be further enhanced by using K_{sp} correction factors based on the pile group cases as shown in the previous section.

2. The limited accuracy of the displacements obtained from acceleration measurements brought the use of the blow count for set evaluation. It was found that, in many cases, blows are counted along a distance of a foot rather than an inch, even during the final penetration. Whenever records of blows per foot were replaced by measurements along 1 in (25.4 mm), a significant improvement was obtained for the estimated set and, as a result, in the accuracy of the Energy Approach predictions. It is proposed to remediate the problem by measuring blows along 1 in (25.4 mm) of penetration together with the following recommendations.
 3. The Energy Approach can be improved by analysis based on average blows per inch, average E_{MAX} , average D_{MAX} , and average capacity for the last inch during driving rather than for a single blow.
- II. Both methods of analysis, the simple Energy Approach and the stress-wave-based formulation, require the recording of the pile displacement with time. Currently, we either double integrate the acceleration measurements to obtain displacement with time, or integrate once, using the velocity in the numerical solution of the wave equation. Direct and accurate displacement measurements can be currently obtained, instead of using accelerometers. Such measurements based, for example, on laser devices will enhance substantially the accuracy of all dynamic methods.

Table 19. Factor of safety and associated risk.

Prediction method	CAPWAP/TEPWAP			Energy Approach		
	AAA	AEA	SEA	AAA	AEA	SEA
Pile Case						
No. of Cases	206	95	39	208	96	39
F.S.	1.00	1.00	1.00	1.00	1.00	1.00
Actual F.S.*	1.37	1.44	1.15	0.92	1.00	0.90
Risk (%)	22.3	16.8	41.0	67.8	60.4	41.0
F.S.	1.20	1.20	1.20	1.20	1.20	1.20
Actual F.S.*	1.64	1.73	1.38	1.11	1.20	1.08
Risk (%)	5.8	7.4	25.6	42.3	31.3	25.6
F.S.	1.40	1.40	1.40	1.40	1.40	1.40
Actual F.S.*	1.91	2.02	1.61	1.30	1.40	1.26
Risk (%)	2.4	3.2	5.1	22.6	9.4	5.1
F.S.	1.60	1.60	1.60	1.60	1.60	1.60
Actual F.S.*	2.19	2.31	1.84	1.48	1.60	1.44
Risk (%)	1.0	1.1	2.6	14.4	2.1	2.6
F.S.	1.80	1.80	1.80	1.80	1.80	1.80
Actual F.S.*	2.46	2.59	2.07	1.67	1.80	1.62
Risk (%)	0	0	0	7.7	1.0	0
F.S.	2.00	2.00	2.00	2.00	2.00	2.00
Actual F.S.*	2.74	2.88	2.30	1.84	2.00	1.80
Risk (%)	0	0	0	4.8	0	0
F.S.	2.5	2.5	2.5	2.5	2.5	2.5
Actual F.S.*	3.43	3.60	2.88	2.30	2.50	2.25
Risk (%)	0	0	0	0	0	0

Actual F.S. = F.S. x mean OPR
 mean OPR = mean Over-Prediction Ratio

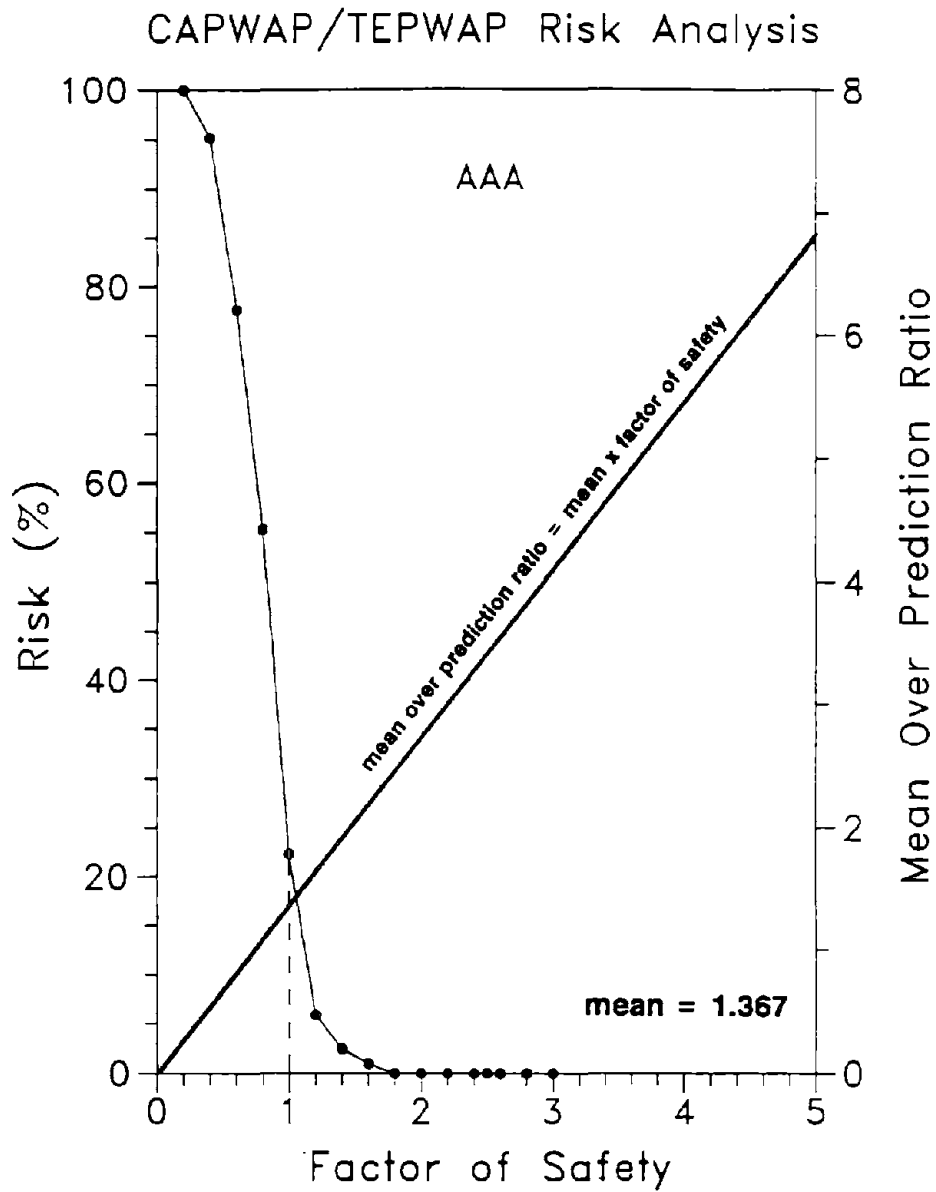


Figure 122. Risk analysis of CAPWAP/TEPWAP predictions for 206 PD/LT pile-cases in all types of soil.

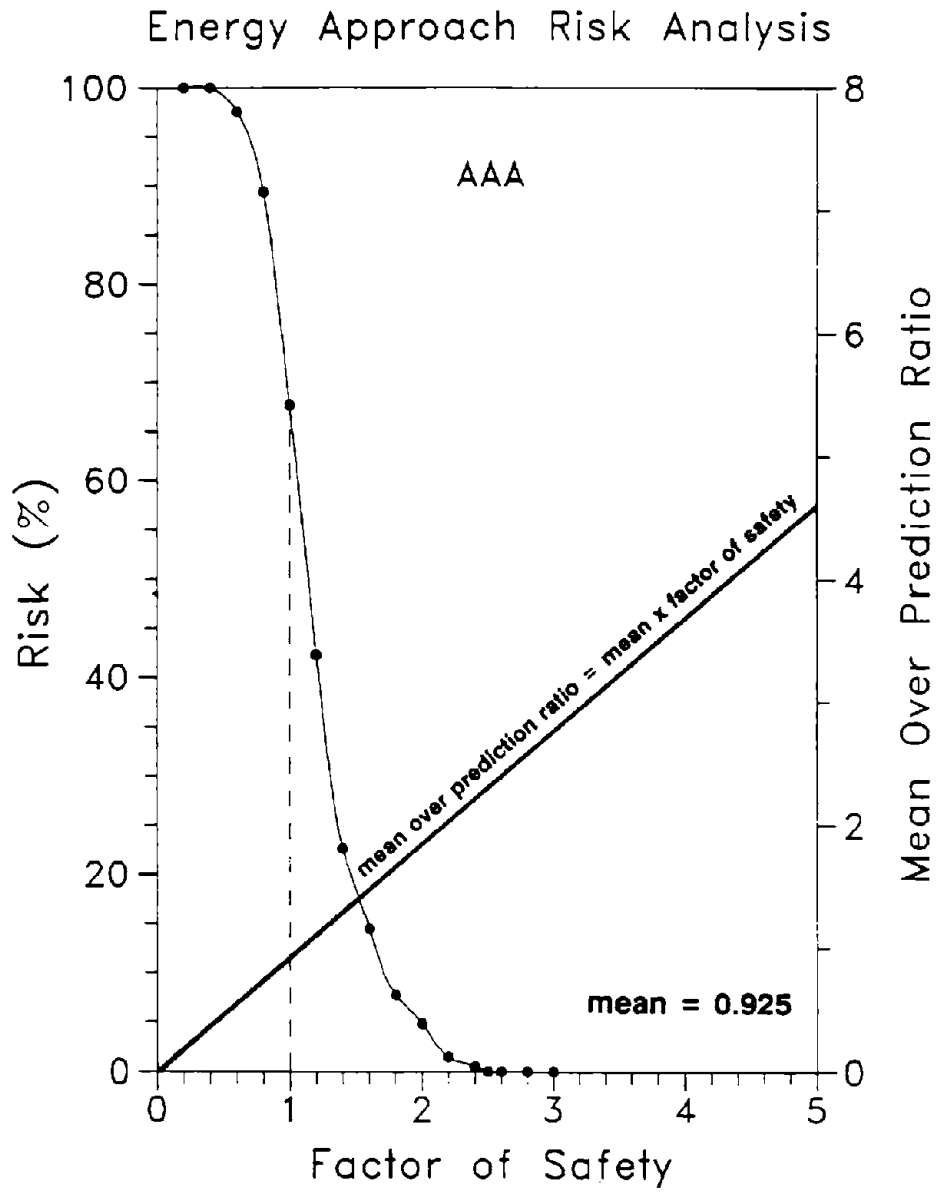


Figure 123. Risk analysis of Energy Approach predictions for 208 PD/LT pile-cases in all types of soil.

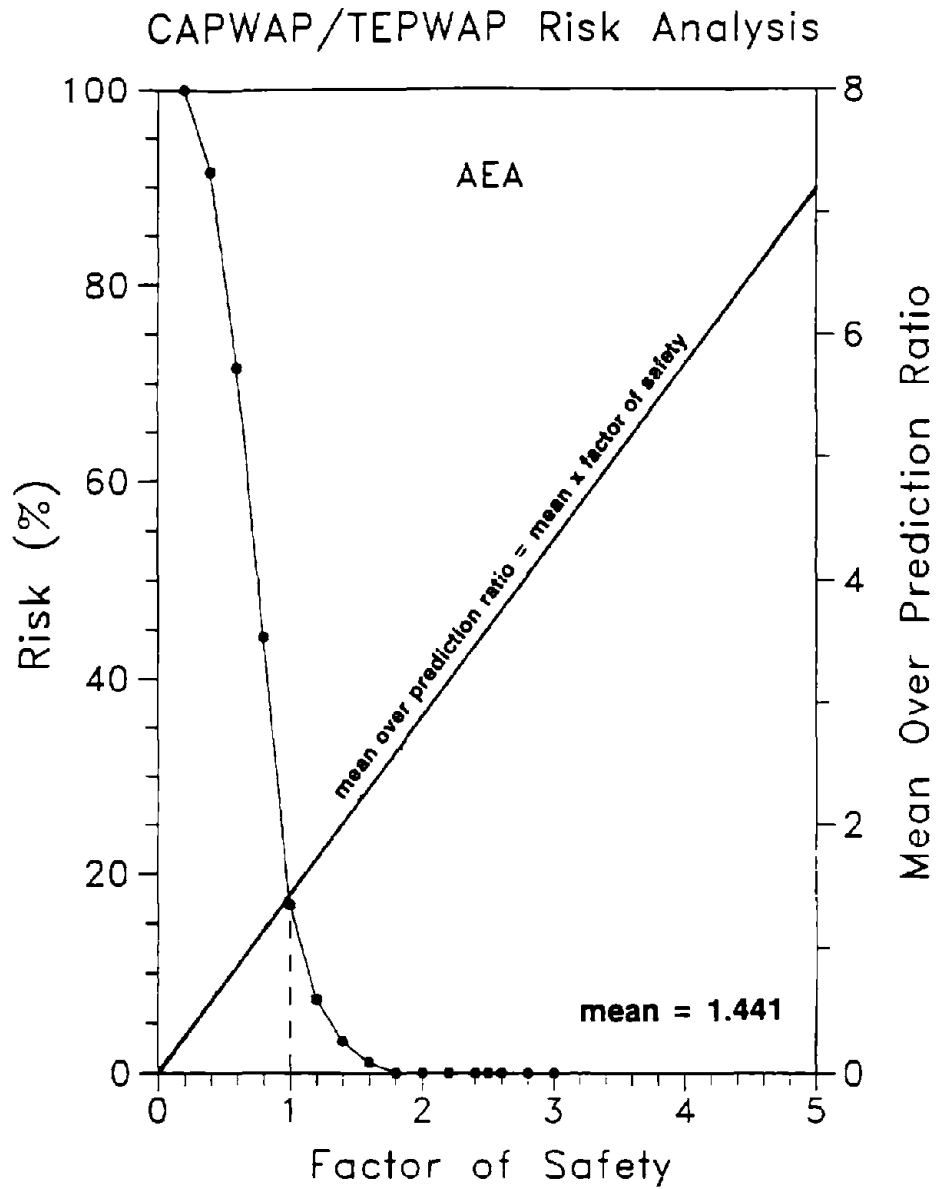


Figure 124. Risk analysis of CAPWAP/TEPWAP predictions for 95 PD/LT pile-cases in all types of soil at EOD.

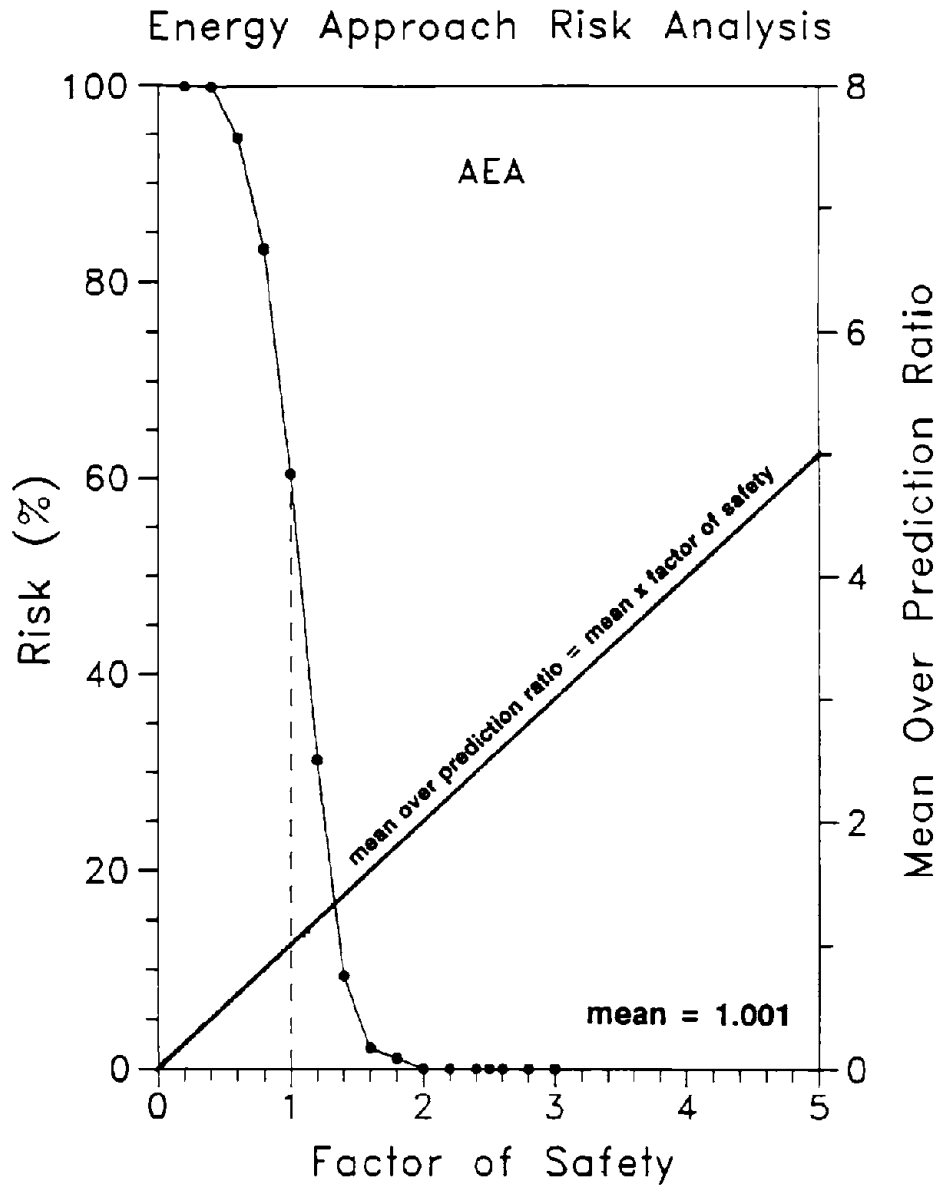


Figure 125. Risk analysis of Energy Approach predictions for 96 PD/LT pile-cases in all types of soil at EOD.

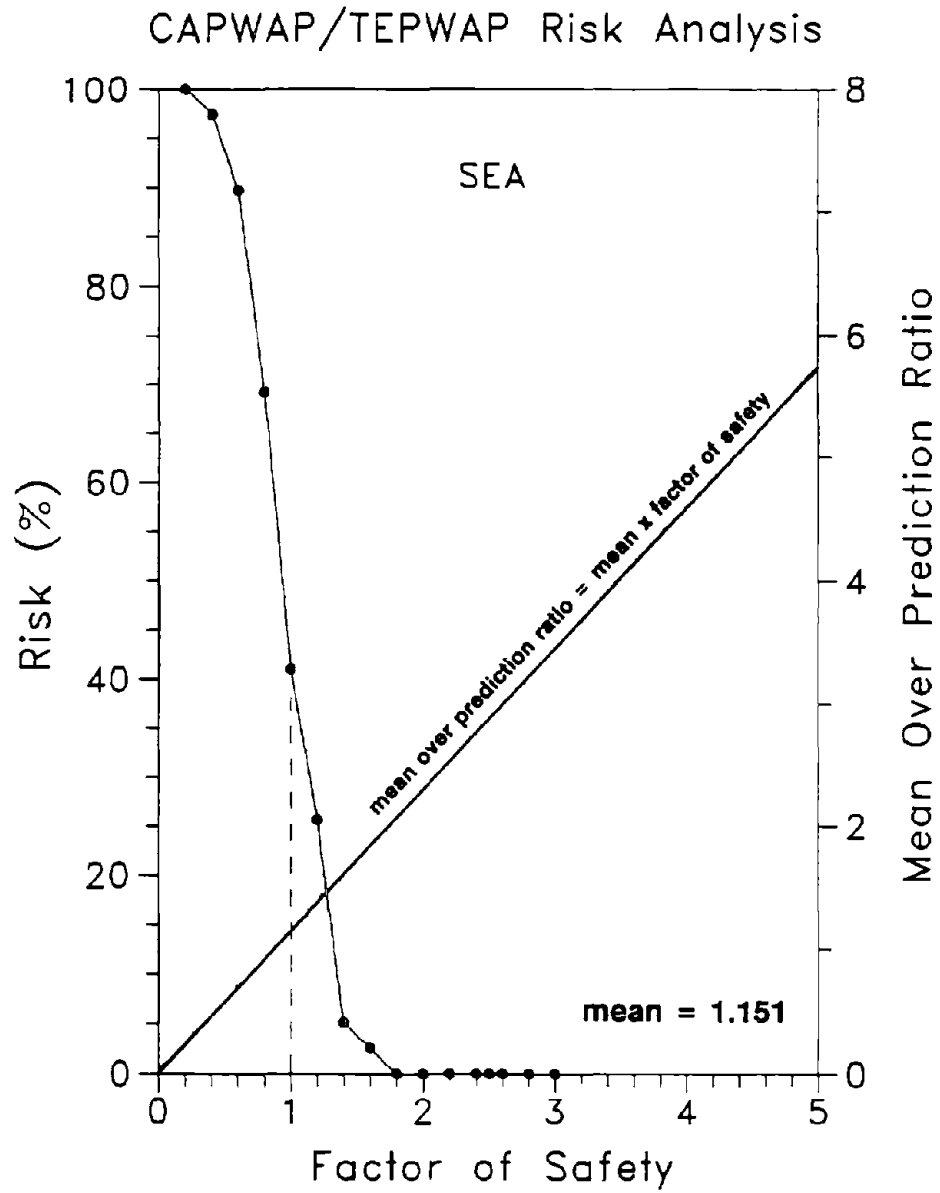


Figure 126. Risk analysis of CAPWAP/TEPWAP predictions for 39 small displacement ($A_R > 350$) PD/LT pile-cases in all types of soil at EOD.

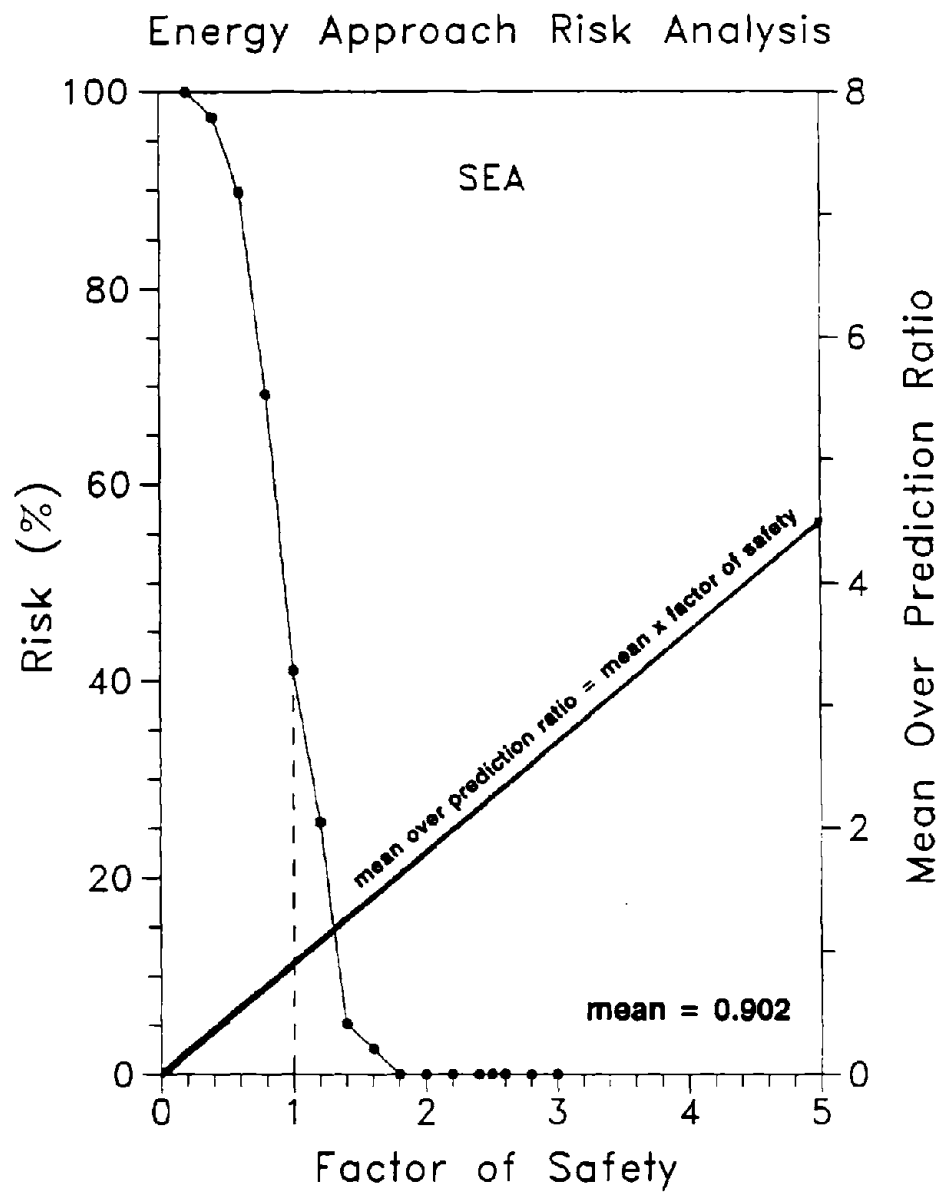


Figure 127. Risk analysis of Energy Approach predictions for 39 small displacement ($A_R > 350$) PD/LT pile-cases in all types of soil at EOD.

APPENDIX A - DATA SET PD/LT

Table 20. Site and pile information for PD/LT.

No.	Pile-Case Number	Refer. No.	Location	Pile Type	Pile Area (in ²)	Length Below Gauges (ft)	Penetr Depth (ft)	Soil Type	
								Side	Tip
1	FN1-EOD	I-480	Omaha NE	HP10x42	12.40	72.0	72.0	silty clay	III
2	FN1-BOR1	I-480	Omaha NE	HP10x42	12.40	72.0	72.1	silty clay	III
3	FN1-BOR2	I-480	Omaha NE	HP10x42	12.40	72.0	73.0	silty clay	III
4	FN2-EOD	I-480	Omaha NE	PSC12"sq	144.00	62.0	65.0	silty clay	III
5	FN2-BOR	I-480	Omaha NE	PSC12"sq	144.00	62.0	65.0	silty clay	III
6	FN3-EOD	I-480	Omaha NE	PSC14"sq	196.00	62.0	56.0	silty clay	III
7	FN3-BOR	I-480	Omaha NE	PSC14"sq	196.00	62.0	56.0	silty clay	III
8	FN4-EOD	I-480	Omaha NE	CEP12.75'	19.20	66.0	66.0	silty clay	III
9	FN4-BOR	I-480	Omaha NE	CEP12.75'	19.20	66.0	66.0	silty clay	III
10	FA-EOD	Site 1	Iowa	HP14x89	26.10	117.5	114.1	clayey sand	sand
11	FA-BOR	Site 1	Iowa	HP14x89	26.10	117.5	114.1	clayey sand	sand
12	FIB-EOD	Site 1	Iowa	CEP 14"	21.20	97.5	94.1	clayey sand	sand
13	FIB-BOR	Site 1	Iowa	CEP 14"	21.20	97.5	94.1	clayey sand	sand
14	FO1-EOD	Cim S-1	Oklahoma	CEP 26"	67.70	60.3	60.2	silty sand	silty sand
15	FO1-BOR	Cim S-1	Oklahoma	CEP 26"	67.70	60.3	60.2	silty sand	silty sand
16	FO2-EOD	Cim S-1	Oklahoma	PSC24"oct	470.90	61.5	63.0	silty sand	silty sand
17	FO2-BOR	Cim S-1	Oklahoma	PSC24"oct	470.90	61.5	63.1	silty sand	silty sand
18	FO3-EOD	Cim S-2	Oklahoma	HP14x117	34.40	110.0	63.7	sa-sl-clay	clayey sand
19	FO4-EOD	Cim S-2	Oklahoma	RC24"sq	576.00	60.3	45.0	sa-sl-clay	clayey sand
20	FO4-BOR	Cim S-2	Oklahoma	RC24"sq	576.00	60.3	55.8	sa-sl-clay	clayey sand
21	FOR1-EOD	Aleas	Oregon	PSC20"sq	393.00	131.0	125.5	sand & silt	siltstone
22	FOR1-BOR	Aleas	Oregon	PSC20"sq	393.00	131.0	125.6	sand & silt	siltstone
23	FM5-EOD	Site A	Maine	CEP 18"	27.50	117.3	99.0	clay & sand	sand
24	FM5-BOR	Site A	Maine	CEP 18"	27.50	101.0	99.1	clay & sand	sand
25	FM17-EOD	Site B	Maine	CEP 18"	27.50	77.8	71.1	III	III
26	FM17-BOR	Site B	Maine	CEP 18"	27.50	77.8	71.3	III	III
27	FM23-EOD	Site B	Maine	CEP 18"	27.50	56.8	50.7	III	III
28	FM23-BOR	Site B	Maine	CEP 18"	27.50	56.8	50.8	III	III
29	FC1-EOD	Crook	Colorado	CEP12.75'	9.82	33.5	33.5	sand	sand
30	FC1-BOR	Crook	Colorado	CEP12.75'	9.82	33.5	33.9	sand	sand
31	FC2-EOD	Crook	Colorado	CEP12.75'	9.82	27.5	26.5	sand	sand

Table 20. Site and pile information for PD/LT (continued).

No.	Pile-Case Number	Refer. No.	Location	Pile Type	Pile Area (in ²)	Length Below Gauges (ft)	Penetr Depth (ft)	Soil Type	
								Side	Tip
32	FC2-BOR	Crook	Colorado	CEP12.75"	9.82	27.5	26.9	sand	sand
33	FM11-EOD	Rt. 115	Missouri	CEP 14"	16.10	83.0	83.0	sand-gravel	sand
34	FM11-BOR	Rt. 115	Missouri	CEP 14"	16.10	83.0	83.1	sand-gravel	sand
35	FM12-EOD	Rt. 115	Missouri	CEP 14"	16.10	81.5	81.0	sand-gravel	sand
36	FM12-BOR	Rt. 115	Missouri	CEP 14"	16.10	81.5	81.0	sand-gravel	sand
37	FWA-EOD	3 rd lake	Washingtn	CEP 48"	111.3	152.0	24.8	fill-gravel	till
38	FWA-BOR	3 rd lake	Washingtn	CEP 48"	111.3	152.0	24.9	fill-gravel	till
39	FWB-EOD	3 rd lake	Washingtn	CEP 48"	111.3	140.0	109.0	fill-gravel	till
40	FWB-BOR	3 rd lake	Washingtn	CEP 48"	111.3	140.0	109.3	fill-gravel	till
41	FA1-EOD	I-165	Alabama	PSC 18"sq	324.00	63.0	64.0	silty sand	silty sand
42	FA1-BOR1	I-165	Alabama	PSC 18"sq	324.00	63.0	64.5	silty sand	silty sand
43	FA1-BOR2	I-165	Alabama	PSC 18"sq	324.00	63.0	64.8	silty sand	silty sand
44	FA2-EOD	I-165	Alabama	PSC 18"sq	324.00	73.0	75.0	silty sand	silty sand
45	FA2-BOR1	I-165	Alabama	PSC 18"sq	324.00	73.0	75.3	silty sand	silty sand
46	FA2-BOR2	I-165	Alabama	PSC 18"sq	324.00	73.0	75.5	silty sand	silty sand
47	FA3-EOD	I-165	Alabama	PSC 24"sq	489.00	63.0	64.0	silty sand	silty sand
48	FA3-BOR1	I-165	Alabama	PSC 24"sq	489.00	63.0	64.1	silty sand	silty sand
49	FA3-BOR2	I-165	Alabama	PSC 24"sq	489.00	63.0	64.5	silty sand	silty sand
50	FA4-EOD	I-165	Alabama	PSC 24"sq	489.00	73.0	75.0	silty sand	silty sand
51	FA4-BOR1	I-165	Alabama	PSC 24"sq	489.00	73.0	75.1	silty sand	silty sand
52	FA4-BOR2	I-165	Alabama	PSC 24"sq	489.00	73.0	75.2	silty sand	silty sand
53	FA5-EOD	I-165	Alabama	PSC 36"sq	898.00	70.0	73.0	silty sand	silty sand
54	FA5-BOR	I-165	Alabama	PSC 36"sq	898.00	70.0	73.1	silty sand	silty sand
55	FV15-EOD	WRJ	Vermont	HP14x73	21.40	92.0	75.0	silt-cl.sand	sand gravel
56	FV15-BOR	WRJ	Vermont	HP14x73	21.40	92.0	75.8	silt-cl.sand	sand gravel
57	FV10-EOD	WRJ	Vermont	HP14x73	21.40	92.0	90.0	silt-cl.sand	sand gravel
58	FV10-BOR	WRJ	Vermont	HP14x73	21.40	92.0	90.4	silt-cl.sand	sand gravel
59	FMN2-EOD	Rt. 18	Minnesota	HP14x73	21.4	97.0	96.0	sa-sl-clay	fat clay
60	FMN2-BOR	Rt. 18	Minnesota	HP14x73	21.4	97.0	96.1	sa-sl-clay	fat clay
61	FPS-EOD	Tioga	Penn.	Monotube	7.00	34.5	23.8	sandy grvl	sandy grvl
62	FPS-BOR	Tioga	Penn.	Monotube	7.00	34.5	23.8	sandy grvl	sandy grvl

Table 20. Site and pile information for PD/LT (continued).

No.	Pile-Case Number	Refer. No.	Location	Pile Type	Pile Area (in ²)	Length Below Gauges (ft)	Penetr Depth (ft)	Soil Type	
								Side	Tip
63	FKG-EOD	RL27	Kentucky	PSC14"sq	196.00	72.0	34.7	soft clay	dense
64	FKG-BOR	RL27	Kentucky	PSC14"sq	196.00	72.0	34.7	soft clay	dense
65	FL3-EOD	RL415	Louisiana	PSC24"sq	463.00	100.0	84.3	silty clay	silty sand
66	FL3-BOR1	RL415	Louisiana	PSC24"sq	463.00	100.0	84.3	silty clay	silty sand
67	FL3-BOR2	RL415	Louisiana	PSC24"sq	463.00	100.0	84.3	silty clay	silty sand
68	CA1-EOD	Site C-L	O.S. Ont	CEP 9.6"	15.42	172.0	154.3	sl-sa-clay	sl-sa-silt
69	CA1-BOR	Site C-L	O.S. Ont	CEP 9.6"	15.42	172.0	154.3	sl-sa-clay	sl-sa-silt
70	CA2-BOR	Site C-L	O.S. Ont	CEP 9.6"	15.42	112.5	110.1	sl-sa-clay	sl-sa-clay
71	CA5-BOR1	Site A	N.Y. Ont	CEP11.73"	11.98	67.0	63.2	fill-sand	sand
72	CA5-BOR2	Site A	N.Y. Ont	CEP11.73"	11.98	67.0	65.6	fill-sand	sand
73	CA3/8-BOR	Marina	Bar. Ont	CEP10.24"	8.74	73.6	64.4	sand-silt	silt
74	CA24-BOR	Site D	Tor. Ont	CEP12.75"	14.54	38.6	38.6	sand	sand
75	CA6-BOR1	Site E	Ham. Ont	CEP12.75"	14.54	60.2	54.0	sa-sl-silt	silt-silt
76	CA6-BOR2	Site E	Ham. Ont	CEP12.75"	14.54	60.2	54.0	sa-sl-silt	silt-silt
77	CA6-EOR	Site E	Ham. Ont	CEP12.75"	13.55	60.2	54.0	sa-sl-silt	silt-silt
78	WC3-EOD	White	Florida	PSC24"sq	576.00	48.4	27.3	ls.-d.sand	dense
79	WC3-BOR1	White	Florida	PSC24"sq	576.00	48.4	27.5	ls.-d.sand	dense
80	WC3-BOR2	White	Florida	PSC24"sq	576.00	37.5	27.5	ls.-d.sand	dense
81	WC6-EOD	White	Florida	PSC24"sq	576.00	39.5	28.3	ls.-d.sand	dense
82	WC6-BOR1	White	Florida	PSC24"sq	576.00	39.5	28.5	ls.-d.sand	dense
83	WC6-BOR2	White	Florida	PSC24"sq	576.00	28.0	27.5	ls.-d.sand	dense
84	WB9-BOR	West	Florida	PSC30"sq	645.50	130.0	128.5	clayey sand	clayey
85	WB15-BOR	West	Florida	PSC30"sq	645.50	105.0	103.6	sand	silt-clay
86	T1/A-EOD	offshore	Israel	OEP 60"	212.00	138.5	52.8	clcr sand	sand
87	T1/A-ALT	offshore	Israel	OEP 60"	212.00	173.9	53.8	clcr sand	sand
88	T1/B-EOD	offshore	Israel	OEP 60"	212.00	216.2	101.7	clcr sand	sand
89	T2/A-EOD	offshore	Israel	OEP 48"	111.33	117.1	52.5	clcr sand	sand
90	T2/B-EOD	offshore	Israel	OEP 48"	111.33	260.5	182.1	clcr sand	sand
91	35-1-BOR	C.N.R.	Toronto	HP12x74	21.80	60.1	48.5	cl-sa-silt	silty sand
92	35-4-BOR	C.N.R.	Toronto	CEP12.75"	9.80	52.2	48.2	cl-sa-silt	silty sand
93	35-5-BOR	C.N.R.	Toronto	HP12x74	21.80	100.2	90.5	cl-sa-silt	silty sand

Table 20. Site and pile information for PD/LT (continued).

No.	Pile-Case Number	Refer. No.	Location	Pile Type	Pile Area (m ²)	Length Below Gauges (m)	Penetr Depth (m)	Soil Type	
								Side	Tip
94	35-8-BOR	C.N.R.	Toronto	CEP12.75'	9.80	105.4	90.0	cl-sa-silt	silty sand
95	35-7-BOR	C.N.R.	Toronto	T. Timber	157.00	44.4	41.6	cl-sa-silt	silty sand
96	35-10-BOR	C.N.R.	Toronto	PSC 12'sq	144.00	50.0	46.0	cl-sa-silt	silty sand
97	E2-BOR	DFI	Raleigh	PSC 12'sq	144.00	43.5	44.5	cl-sa-silt	cl-sa-silt
98	63S-BOR	Mahonig	Penn.	HP12x53	15.50	68.8	66.0	sand-silt	silt
99	LB21-BOR	Site A	NA	PSC 20'sq	400.00	38.0	38.0	silt-sand	silt-sand
100	LB20-BOR	Site B	NA	PSC 20'sq	400.00	51.0	55.0	sand	sand
101	LC3-BOR	Site C	NA	PSC 20'sq	400.00	115.0	86.0	cl-sa-silt	cl-sa-silt
102	LIN18-BOR	Site D	NA	PSC 20'sq	400.00	155.0	94.0	cl-sa-silt	cl-sa-silt
103	LE37-BOR	Site E	NA	PSC 10'sq	100.00	60.0	50.0	cl-sa-silt	limestone
104	LE64-BOR	Site F	NA	PSC 10'sq	100.00	60.0	58.0	cl-sa-silt	sa-cl-silt
105	ST1-EOD	Site H	Florida	PSC 18'sq	324.00	68.0	44.0	-	carb sand
106	ST2-EOD	Site P	Florida	PSC 18'sq	324.00	62.0	40.0	-	carb sand
107	ST9-BOR	I-664	Virginia	PSC 54'sq	770.00	131.0	109.0	-	silt-clay
108	ST46-EOD	Castletn	New York	CEP 10'	5.80	40.0	38.0	silt-sand	silt-sand
109	GZA3-EOD	Cvic	Prov. RI	CEP13.38'	20.30	143.0	125.5	silt-sand	gr-sa-silt
110	GZA5-EOD	Cvic	Prov. RI	CEP 8.75'	15.50	138.0	93.8	silt-sand	till-shale
111	GZA6-EOD	Cvic	Prov. RI	CEP 8.75'	15.50	171.0	156.0	silt-sand	gr-sa-silt
112	GZB8C-EOD	Cvic	Prov. RI	CEP 10'	18.40	116.0	89.5	silt-sand	silt
113	GZB92-EOD	Cvic	Prov. RI	CEP13.38'	20.30	143.7	106.0	silt-sand	gr-sa-silt
114	GZ68-EOD	Cvic	Prov. RI	CEP13.38'	20.30	97.0	82.3	silt-sand	sl-sa-till
115	GZZ5-EOD	Deer Is.	Boston MA	CEP 14'	21.20	87.0	87.0	till-clay	till
116	GZ05-EOD	Deer Is.	Boston MA	CEP 14'	21.20	87.0	54.0	till-clay	till
117	GZCC5-EOD	Deer Is.	Boston MA	CEP 14'	21.20	117.0	80.0	till-clay	till
118	GZL2-EOD	Deer Is.	Boston MA	CEP 14'	21.20	117.0	83.0	till-clay	till
119	GZP14-EOD	Deer Is.	Boston MA	CEP 14'	21.20	105.0	60.5	till-clay	till
120	GZP11-EOD	Deer Is.	Boston MA	CEP 14'	21.20	106.0	56.5	till-clay	till
121	GZP12-EOD	Deer Is.	Boston MA	CEP 14'	21.20	115.5	69.0	till-clay	till
122	GZB22-EOD	NWS	Coll Neck	OEP 36'	54.00	138.0	118.0	sand-clay	silt-clay
123	GZW1-EOR	Water	Vermont	CP12.75'	14.60	126.0	99.5	silty sand	sand
124	A54-EOD	HICC	Australia	RC10.8'sq	117.22	67.9	67.6	silty clay	clay

Table 20. Site and pile information for PD/LT (continued).

No.	Pile-Case Number	Refer. No.	Location	Pile Type	Pile Area (in ²)	Length Below Gauges (ft)	Penetr Depth (ft)	Soil Type	
								Side	Tip
125	A54-BOR	HICC	Australia	RC10.8"sq	117.22	67.9	67.6	silty clay	clay
126	A147-EOD	HICC	Australia	RC10.8"sq	117.22	67.9	67.6	silty clay	clay
127	A147-BOR	HICC	Australia	RC10.8"sq	117.22	67.9	67.6	silty clay	clay
128	GF19-EOD	Site 1	Pgh. PA	HP10x42	12.30	58.5	48.5	grvl-snd-silt	shale
129	GF110-EOD	Site 1	Pgh. PA	HP12x74	21.70	57.0	49.7	grvl-snd-silt	shale
130	GF222-EOD	Site 2	Pgh. PA	HP12x74	21.70	67.0	61.1	grvl-snd-silt	shale
131	GF224-EOD	Site 2	Pgh. PA	Monotube	9.70	53.0	29.6	grvl-snd-silt	grvl-snd-silt
132	GF312-EOD	Site 3	Pgh. PA	HP12x74	21.70	33.0	28.2	snd-grvl-shl	shale
133	GF313-EOD	Site 3	Pgh. PA	HP10x57	18.70	35.0	31.5	snd-grvl-shl	claystone
134	GF412-EOD	Site 4	Pgh. PA	HP12x74	21.70	48.5	33.8	grvl-snd-silt	claystone
135	GF413-EOD	Site 4	Pgh. PA	HP10x57	18.70	34.2	34.8	grvl-snd-silt	claystone
136	GF414-EOD	Site 4	Pgh. PA	HP10x57	18.70	47.5	34.7	grvl-snd-silt	claystone
137	GF415-EOD	Site 4	Pgh. PA	HP12x74	21.70	47.5	34.1	grvl-snd-silt	claystone
138	EF82-EOD	Ottawa	Canada	CP 8.625"	15.54	-	62.3	sl-sa-cl	till
139	EF167-BOR	Ottawa	Canada	CP 8.625"	15.54	-	68.9	sl-sa-cl	till
140	A3-EOD1	Apalach	Florida	VC 24"sq	462.90	94.0	63.4	clayey sand	sand
141	A3-BOR1	Apalach	Florida	VC 24"sq	462.90	94.0	63.4	clayey sand	sand
142	A3-EOD2	Apalach	Florida	VC 24"sq	462.90	94.0	90.3	clayey sand	sand
143	A3-BOR2	Apalach	Florida	VC 24"sq	462.90	94.0	90.4	clayey sand	sand
144	A3-BOR3	Apalach	Florida	VC 24"sq	462.90	89.3	90.6	clayey sand	clayey sand
145	A14-DD1	Apalach	Florida	VC 24"sq	462.90	107.0	45.0	sandy clay	sand
146	A14-DD2	Apalach	Florida	VC 24"sq	462.90	107.0	47.0	sandy clay	sand
147	A14-BOR1	Apalach	Florida	VC 24"sq	462.90	107.0	58.5	clayey sand	sand
148	A14-BOR2	Apalach	Florida	VC 24"sq	462.90	75.0	58.8	clayey sand	sand
149	A25-EOD	Apalach	Florida	VC 24"sq	462.90	106.0	55.1	clayey sand	sand
150	A25-BOR1	Apalach	Florida	VC 24"sq	462.90	106.0	55.2	clayey sand	sand
151	A25-BOR2	Apalach	Florida	VC 24"sq	462.90	59.3	55.4	clayey sand	sand
152	A25-BOR3	Apalach	Florida	VC 24"sq	462.90	59.3	55.5	clayey sand	sand
153	A18-EOD	Apalach	Florida	PSC18"sq	324.00	65.0	60.6	sandy clay	sand
154	A18-BOR1	Apalach	Florida	PSC18"sq	324.00	65.0	60.6	sandy clay	sand
155	A18-BOR2	Apalach	Florida	PSC18"sq	324.00	62.2	61.0	sandy clay	sand

Table 20. Site and pile information for PD/LT (continued).

No.	Pile-Case Number	Refer. No.	Location	Pile Type	Pile Area (in ²)	Length Below Gauges (ft)	Penetr Depth (ft)	Soil Type	
								Side	Tip
156	A41-EOD	Apalach	Florida	VC 24"sq	462.90	91.0	52.0	clay	sand
157	A41-BOR1	Apalach	Florida	VC 24"sq	462.90	91.0	52.0	clay	sand
158	A41-BOR2	Apalach	Florida	VC 24"sq	462.90	81.5	52.8	clay	sand
159	A101-EOD	Apalach	Florida	VC 24"sq	462.90	88.0	61.8	clay	clayey sand
160	A101-BOR1	Apalach	Florida	VC 24"sq	462.90	88.0	61.8	clay	clayey sand
161	A101-BOR2	Apalach	Florida	VC 24"sq	462.90	71.5	62.1	clay	clayey sand
162	A133-EOD	Apalach	Florida	VC 24"sq	462.90	130.0	103.9	clayey sand	sandy clay
163	A133-BOR	Apalach	Florida	VC 24"sq	462.90	115.7	104.9	clayey sand	sandy clay
164	A145-EOD	Apalach	Florida	VC 24"sq	462.90	132.0	102.9	clayey sand	sand
165	A145-BOR1	Apalach	Florida	VC 24"sq	462.90	132.0	102.9	clayey sand	sand
166	A145-BOR2	Apalach	Florida	VC 24"sq	462.90	115.1	103.0	clayey sand	sand
167	CB3-BOR	Choctw	Florida	PSC24"sq	576.00	77.9	77.0	clayey sand	sand
168	CB3-BORL	Choctw	Florida	PSC24"sq	576.00	79.9	77.8	clayey sand	sand
169	CB5-BOR	Choctw	Florida	VC 30"sq	645.53	87.0	53.1	clayey sand	sand
170	CB5-BORL	Choctw	Florida	VC 30"sq	645.53	61.1	54.0	clayey sand	sandy clay
171	CB11-BORL	Choctw	Florida	VC 30"sq	645.53	97.6	85.7	clayey sand	clayey sand
172	CB11-EORL	Choctw	Florida	VC 30"sq	645.53	97.6	85.8	clayey sand	clayey sand
173	CB17-BOR1	Choctw	Florida	VC 30"sq	645.53	97.0	77.7	clayey sand	clayey sand
174	CB17-BOR2	Choctw	Florida	VC 30"sq	645.53	97.0	77.8	clayey sand	clayey sand
175	CB17-BORL	Choctw	Florida	VC 30"sq	645.53	90.0	77.9	clayey sand	clayey sand
176	CB17-DRL	Choctw	Florida	VC 30"sq	645.53	90.0	78.2	clayey sand	clayey sand
177	CB23-BOR	Choctw	Florida	VC 30"sq	645.53	96.0	80.3	clayey sand	sand
178	CB23-BORL	Choctw	Florida	VC 30"sq	645.53	96.0	82.7	clayey sand	sand
179	CB29-BORL	Choctw	Florida	VC 30"sq	645.53	95.1	84.5	clayey sand	clayey sand
180	CB29-EORL	Choctw	Florida	VC 30"sq	645.53	95.1	84.5	clayey sand	clayey sand
181	CB35-BOR1	Choctw	Florida	VC 30"sq	645.53	97.1	78.5	clayey sand	clayey sand
182	CB35-BOR2	Choctw	Florida	VC 30"sq	645.53	97.1	78.9	clayey sand	clayey sand
183	CB35-BORL	Choctw	Florida	VC 30"sq	645.53	89.1	79.1	clayey sand	clayey sand
184	CB41-EOR	Choctw	Florida	VC 30"sq	645.53	102.3	64.7	sandy clay	sandy clay
185	CB41-BOR	Choctw	Florida	VC 30"sq	645.53	101.3	64.7	sandy clay	sandy clay
186	CB41-BORL	Choctw	Florida	VC 30"sq	645.53	79.0	65.4	sandy clay	sandy clay

Table 20. Site and pile information for PD/LT (continued).

No.	Pile-Case Number	Refer. No.	Location	Pile Type	Pile Area (in ²)	Length Below Gauges (ft)	Penetr Depth (ft)	Soil Type	
								Side	Tip
187	CB26-EOD	Choctw	Florida	PSC24"sq	576.00	80.1	62.5	clayey sand	sand
188	CB26-BOR	Choctw	Florida	PSC24"sq	576.00	80.1	62.8	clayey sand	sand
189	CB26-EOR	Choctw	Florida	PSC24"sq	576.00	80.1	64.8	clayey sand	sandy clay
190	CB26-BOR2	Choctw	Florida	PSC24"sq	576.00	65.0	65.0	sandy clay	sandy clay
191	33P1-EOD	Site P	Ontario	HP 12x74	21.80	120.9	114.4	cl-sa-silt	silty sand
192	33P1-BOR	Site P	Ontario	HP 12x74	21.80	120.9	114.4	cl-sa-silt	silty sand
193	33P1-EOR	Site P	Ontario	HP 12x74	21.80	120.9	114.4	cl-sa-silt	silty sand
194	33P2-EOD	Site P	Ontario	CP 12.75'	9.80	149.8	107.2	cl-sa-silt	silty sand
195	33P2-BOR	Site P	Ontario	CP 12.75'	9.80	111.0	107.2	cl-sa-silt	silty sand
196	33P2-EOR	Site P	Ontario	CP 12.75'	9.80	111.0	107.2	cl-sa-silt	silty sand
197	33P4-EOD	Site P	Ontario	PSC 12"sq	144.00	65.0	54.2	cl-sa-silt	cl-silt-till
198	33P5-EOD	Site P	Ontario	#14 Timber	144.9	43.0	28.4	cl-sa-silt	cl-silt-till
199	TRD22-EOD	Site R	Ontario	HP 12x74	21.80	22.5	20.1	sand	till
200	TRD22-BOR	Site R	Ontario	HP 12x74	21.80	22.5	20.1	sand	till
201	TRE22-EOD	Site R	Ontario	HP 12x74	21.80	30.0	25.7	sand	rock
202	TRE22-BOR	Site R	Ontario	HP 12x74	21.80	30.0	25.7	sand	rock
203	TRP5X-EOD	Site R	Ontario	HP 12x53	15.80	25.0	25.2	sand	rock
204	TRP5X-BOR	Site R	Ontario	HP 12x53	15.80	25.0	25.2	sand	rock
205	TR131-BOR	Site R	Ontario	CP 7.063'	7.80	28.8	NA	sand	rock
206	TRAH-EOR	Site S	Brunswick	HP 12x89	26.50	138.0	126.0	clayey silt	sandy gravel
207	TRBH-BOR	Site S	Brunswick	HP 12x89	26.50	114.3	102.1	clayey silt	sandy gravel
208	TRBP-EOR	Site S	Brunswick	CP 12.75'	12.40	110.0	104.0	clayey silt	sandy gravel

1 in = 25.4 mm
 1 in² = 645.2 mm²
 1 ft = 0.305 m

Table 21. Pile driving and dynamic measurements for PD/LT.

No.	Pile-Case Number	Hammer Type	Rated Hammer Energy (kip-ft)	Delivered Energy (kip-ft)	Blow Count (BPI)	Impedance EA/C (kips/ft/s)	V _{imp} (ft/s)	F _{imp} (kips)	VEA/C F	D _{max} (in)
1	FN1-EOD	D-30	54.2	17.30	2.83	22.13	13.24	322.4	0.909	.793
2	FN1-BOR1	D-30	54.2	18.42	8.00	22.13	13.24	315.2	0.930	.813
3	FN1-BOR2	D-30	54.2	20.15	15.00	22.13	13.04	308.9	0.934	.837
4	FN2-EOD	D-30	54.2	12.70	3.50	60.49	7.35	462.0	0.963	.444
5	FN2-BOR	D-30	54.2	12.35	5.00	60.49	8.36	508.9	0.994	.409
6	FN3-EOD	D-30	54.2	9.90	8.17	85.89	6.14	558.0	0.943	.386
7	FN3-BOR	D-30	54.2	18.20	8.00	85.89	7.88	691.1	0.979	.459
8	FN4-EOD	D-30	54.2	15.55	2.50	34.26	12.97	478.5	0.929	.531
9	FN4-BOR	D-30	54.2	17.40	5.00	34.26	13.23	475.8	0.953	.517
10	FIA-EOD	K-25	51.5	23.38	3.33	46.60	14.90	667.8	1.039	.686
11	FIA-BOR	K-25	51.5	18.88	1.83	46.60	15.00	657.6	1.062	.556
12	FIB-EOD	K-25	51.5	25.40	5.83	37.80	15.10	555.3	1.027	.689
13	FIB-BOR	K-25	51.5	22.47	2.50	37.80	15.30	548.2	1.054	.675
14	FO1-EOD	DE110	93.5	18.06	5.67	120.80	5.40	788.7	0.827	.413
15	FO1-BOR	DE110	93.5	37.47	5.00	120.80	8.90	1223.6	0.873	.541
16	FO2-EOD	DE110	93.5	18.28	5.08	199.10	3.90	805.9	0.963	.453
17	FO2-BOR	DE110	93.5	31.37	12.00	199.10	5.70	1114.0	1.018	.450
18	FO3-EOD	DE110	93.5	16.40	18.87	81.40	6.90	489.5	0.828	.625
19	FO4-EOD	DE110	93.5	9.81	11.87	214.60	2.50	675.3	0.933	.269
20	FO4-BOR	DE110	93.5	22.73	1.00	214.60	4.70	1011.7	0.997	.362
21	FOR1-EOD	D-46-23	105	30.11	9.17	159.00	6.10	946.0	1.025	.838
22	FOR1-BOR	D-46-23	105	23.77	77.33	159.00	5.80	918.1	1.004	.462
23	FMS-EOD	K-45	92.8	27.00	1.29	49.08	10.73	550.5	0.957	1.033
24	FMS-BOR1	K-45	92.8	40.20	3.00	49.08	13.30	658.2	0.992	.981
25	FM17-EOD	K-45	92.8	39.50	1.42	49.08	11.14	590.8	0.926	1.105
26	FM17-BOR	K-45	92.8	36.50	3.00	49.08	13.17	697.7	0.926	.788
27	FM23-EOD	K-45	92.8	33.30	1.33 [*]	49.08	11.37	559.0	0.998	1.180
28	FM23-BOR	K-45	92.8	31.00	2.00	49.08	10.57	508.1	1.021	1.247
29	FC1-EOD	KC-25	51.5	15.47	3.50 [*]	17.54	13.40	272.8	0.862	.799
30	FC1-BOR	KC-25	51.5	16.19	3.80 [*]	17.54	13.40	276.2	0.851	.806
31	FC2-EOD	KC-25	51.5	18.07	3.87 [*]	17.54	14.90	290.0	0.901	.806

* - Denotes blow count (BPI) based on blows per foot.

Table 21. Pile driving and dynamic measurements for PD/LT (continued).

No.	Pile-Case Number	Hammer Type	Rated Hammer Energy (kip-ft)	Delivered Energy (kip-ft)	Blow Count (BPI)	Impedance EA/C (kips/ft/s)	V _{imp} (ft/s)	F _{imp} (kips)	VEA/C F	D _{max} (in)
32	FC2-BOR	KC-25	51.5	13.86	4.00*	17.54	13.10	298.1	0.857	.680
33	FMI1-EOD	ICE-640	40.0	11.00	3.00*	28.73	8.10	250.3	0.919	.738
34	FMI1-BOR	ICE-640	40.0	12.00	3.00	28.73	8.80	304.5	0.830	.632
35	FM2-EOD	ICE-640	40.0	11.66	1.42*	28.73	7.10	230.1	0.688	.861
36	FM2-BOR	ICE-640	40.0	13.58	3.00	28.73	9.00	285.7	0.905	.834
37	FWA-EOD	Con300	90.0	44.90	47.00	198.62	9.80	1925.	1.011	.920
38	FWA-BOR	Con300	90.0	33.30	7.00	198.62	8.80	1708.	1.023	.550
39	FWB-EOD	Con300	90.0	47.20	30.00	198.62	8.50	1715.	0.990	.630
40	FWB-BOR	Con300	90.0	39.30	15.00	198.62	7.60	1516.	0.996	.670
41	FA1-EOD	K-45	92.8	17.53	1.50*	145.72	4.37	628.7	1.013	.727
42	FA1-BOR1	K-45	92.8	9.19	7.00	145.72	3.60	547.9	0.957	.335
43	FA1-BOR2	K-45	92.8	21.84	7.00	145.72	7.30	1074.	0.990	.481
44	FA2-EOD	K-45	92.8	21.22	3.50*	145.72	3.98	639.0	0.908	.611
45	FA2-BOR1	K-45	92.8	22.87	7.00	140.52	6.90	1024.	0.948	.430
46	FA2-BOR2	K-45	92.8	20.80	5.00	145.72	6.70	1025.	0.952	.357
47	FA3-EOD	K-45	92.8	22.79	2.83*	221.53	3.31	729.1	1.006	.646
48	FA3-BOR1	K-45	92.8	15.22	8.00	219.99	3.41	782.4	0.959	.324
49	FA3-BOR2	K-45	92.8	16.31	5.00	221.53	5.30	1199.	0.979	.274
50	FA4-EOD	K-45	92.8	19.06	6.42*	221.53	3.56	782.4	1.007	.437
51	FA4-BOR1	K-45	92.8	16.82	8.00	219.93	5.19	1108.	1.030	.255
52	FA4-BOR2	K-45	92.8	20.42	18.00	219.93	6.78	1488.	1.013	.283
53	FA5-EOD	D-62-22	153.2	37.06	7.67*	403.88	5.10	2106.	0.978	.446
54	FA5-BOR	D-62-22	153.2	45.51	5.00	403.88	7.40	3016.	0.991	.288
55	FV15-EOD	MKT-35B	22.0	10.00	4.17*	38.19	10.40	403.2	0.985	.475
56	FV15-BOR	MKT-35B	22.0	12.23	9.00	38.19	14.20	522.8	1.037	.643
57	FV10-EOD	MKT-35B	22.0	10.98	2.87*	38.19	10.70	417.8	0.978	.490
58	FV10-BOR	MKT-35B	22.0	13.98	2.00	38.19	16.30	609.1	1.022	.675
59	FMN2-EOD	ICE-90S	90.0	28.29	1.83*	38.19	15.00	627.6	0.913	.878
60	FMN2-BOR	ICE-90S	90.0	29.14	25.00	38.19	18.50	675.6	0.932	.802
61	FP5-EOD	D-12	22.0	7.56	5.42*	12.49	13.80	177.4	0.972	.877
62	FP5-BOR	D-12	22.0	7.55	13.00	12.49	14.90	192.5	0.967	.570

* - Denotes blow count (BPI) based on blows per foot.

Table 21. Pile driving and dynamic measurements for PD/LT (continued).

No.	Pile-Case Number	Hammer Type	Rated Hammer Energy (kip-ft)	Delivered Energy (kip-ft)	Blow Count (BPI)	Impedance EA/C (kips/ft/s)	V _{imp} (ft/s)	F _{imp} (kips)	VEA/C F	D _{max} (ft)
63	FKG-EOD	LB-520	31.0	8.31	23.25*	80.23	4.28	353.5	0.971	.468
64	FKG-BOR	LB-520	31.0	7.78	18.00	80.23	4.55	373.3	0.978	.407
65	FL3-EOD	VUH-020	60.0	14.60	1.67*	203.74	3.28	678.3	0.985	.757
66	FL3-BOR1	VUH-020	60.0	17.03	4.00	203.74	3.70	811.4	0.929	.433
67	FL3-BOR2	VUH-020	60.0	14.43	11.00	203.74	3.70	795.4	0.946	.297
68	CA1-EOD	B-400	46.0	20.32	21.33	27.87	15.75	432.2	1.016	1.061
69	CA1-BOR	B-400	46.0	18.98	40.00	27.87	14.44	427.9	0.941	1.025
70	CA2-BOR	B-400	46.0	16.74	14.00	27.87	15.08	424.1	0.992	.863
71	CA5-BOR1	35kdrop	38.7min	30.48	25.00	21.38	15.08	341.8	0.944	1.312
72	CA5-BOR2	49kdrop	54.2min	31.44	11.00	21.38	13.45	307.3	0.936	1.298
73	CA3/B-BOR	ICE 40S	40.0	19.03	4.23	15.60	15.42	275.6	0.873	1.001
74	CA24-BOR	D-12	24.0	8.83	50.00	13.44	14.11	215.7	0.878	.500
75	CA6-BOR1	D-30-13	66.0	41.23	10.00	25.93	17.33	494.4	0.909	1.185
76	CA6-BOR2	D-30-13	66.0	42.68	6.67	25.93	17.91	502.7	0.924	1.230
77	CA6-EOR	D-30-13	66.0	37.60	8.00	25.93	16.83	417.7	1.045	1.156
78	WC3-EOD	Delmag	106.0	17.50	9.33	268.75	4.23	1122.6	1.013	.452
79	WC3-BOR1	Delmag	106.0	18.90	9.33	268.75	4.25	1179.6	0.968	.412
80	WC3-BOR2	Delmag	106.0	17.89	6.67	268.75	3.47	1042.4	0.895	.403
81	WC6-EOD	Delmag	105.0	17.60	5.00	265.88	4.47	1191.0	0.998	.508
82	WC6-BOR1	Delmag	105.0	18.24	8.00	265.88	4.50	1224.8	0.977	.489
83	WC6-BOR2	Delmag	105.0	26.28	6.67	265.88	5.04	1330.1	1.007	.667
84	WB9-BOR	Con300	90.0	39.87	6.67	271.52	6.42	1748.2	0.997	.383
85	WB15-BOR	Con300	90.0	34.70	5.00	269.50	5.84	1533.7	1.025	.375
86	T1/A-EOD	D-55	125.0	44.99	7.37	378.57	8.01	2967	1.022	.260
87	T1/A-ALT	D-55	125.0	151.50	2.29	378.57	12.50	4423	1.070	.830
88	T1/B-EOD	M-2500	NA	172.73	2.03	378.57	12.70	4787	1.004	.870
89	T2/A-EOD	D-55	125.0	80.62	4.83	198.75	9.40	1891	0.968	.570
90	T2/B-EOD	M-2500	NA	168.68	5.08	198.75	13.60	2814	0.961	1.169
91	35-1-BOR	B-400	46.0	13.10	1.83	38.93	10.20	423.0	0.939	.600
92	35-4-BOR	B-400	46.0	23.20	5.56*	17.50	17.94	377.0	0.833	1.010
93	35-5-BOR	B-400	46.0	17.70	10.31*	38.93	14.50	584.0	0.967	.590

* - Denotes blow count (BPI) based on blows per foot.

Table 21. Pile driving and dynamic measurements for PD/LT (continued).

No.	Pile-Case Number	Hammer Type	Rated Hammer Energy (kip-ft)	Delivered Energy (kip-ft)	Blow Count (BPI)	Impedance EA/C (kips/ft/s)	V _{imp} (ft/s)	F _{imp} (kips)	VEA/C F	D _{max} (ln)
94	35-6-BOR	B-400	48.0	26.10	16.87*	17.50	18.60	372.0	0.875	1.130
95	35-7-BOR	B-225	29.0	9.90	2.53*	18.97	10.70	217.0	0.935	.810
96	35-10-BOR	B-400	48.0	11.10	6.00	60.56	9.10	522.0	1.055	.460
97	E2-BOR	Com65	26.5	15.01	10.00	64.20	7.96	527.7	0.966	.392
98	63S-BOR	ICE-640	40.0	12.13	4.50	30.34	10.85	327.1	1.006	.597
99	LB21-BOR	VUL-510	50.0	13.47	4.00*	169.40	4.60	821.7	0.948	.373
100	LB20-BOR	VUL-510	50.0	14.77	6.00	161.80	5.90	966.0	0.986	.311
101	LC3-BOR	D-48-23	107.0	39.40	7.00	161.90	8.30	1437.0	0.935	.666
102	LN16-BOR	D-48-23	107.0	28.00	10.00*	161.90	5.90	1087.0	0.878	.579
103	LE37-BOR	VUL-01	15.0	5.40	10.00	38.80	5.74	226.3	0.977	.434
104	LE64-BOR	VUL-01	15.0	6.90	5.50	38.80	6.10	247.2	0.957	.422
105	ST1-EOD	D-36-13	84.0	33.13	2.42*	123.00	8.30	1035.4	0.986	.848
106	ST2-EOD	D-36-13	84.0	33.03	3.42*	132.20	8.33	861.1	0.973	.899
107	ST9-BOR	CN5300	150.0	45.70	7.86*	339.10	6.10	2076.0	0.996	.442
108	ST48-EOD	VUL-1	15.0	5.50	2.67*	10.35	10.00	102.5	1.010	.790
109	GZA3-EOD	ICE-640	40.0	16.12	20.00	36.20	10.60	362.1	1.079	.864
110	GZA5-EOD	ICE-640	40.0	17.36	6.00	27.80	10.20	300.9	0.942	1.062
111	GZA6-EOD	ICE-640	40.0	13.40	15.00	27.70	8.10	219.8	1.021	1.076
112	GZB8C-EOD	ICE-640	40.0	17.67	20.00	37.80	8.90	362.2	0.929	.886
113	GZBP2-EOD	ICE-640	40.0	9.57	20.00	36.20	6.80	258.7	0.952	.710
114	GZB6-EOD	ICE-640	40.0	15.91	11.00	27.70	10.90	344.5	0.876	.834
115	GZZ5-EOD	ICE1070	72.6	28.73	4.20	37.80	13.30	533.8	0.942	1.000
116	GZ06-EOD	ICE1070	72.6	23.71	4.20	37.80	14.20	566.1	0.945	.876
117	GZCC5-EOD	ICE1070	72.6	34.05	5.40	37.80	14.60	590.6	0.934	1.180
118	GZL2-EOD	ICE1070	72.6	25.81	9.00	37.80	12.90	500.8	0.974	.984
118	GZP14-EOD	ICE1070	72.6	25.68	5.00	37.80	11.40	502.3	0.858	.882
120	GZP11-EOD	ICE1070	72.6	16.13	5.30	37.80	11.20	471.5	0.896	.782
121	GZP12-EOD	ICE1070	72.6	34.64	12.60	37.80	12.70	499.5	0.961	1.155
122	GZB22-EOD	MH72B	135.0	55.17	8.50	111.00	11.80	1326.1	0.971	.859
123	GZW1-EOR	K-25	47.0	12.79	12.00	26.10	12.21	339.3	0.939	.776
124	AS4-EOD	Banul-6	34.72	21.05	3.63	50.82	8.73	407.0	1.090	.862

* - Denotes blow count (BPI) based on blows per foot.

Table 21. Pile driving and dynamic measurements for PD/LT (continued).

No.	Pile-Case Number	Hammer Type	Rated Hammer Energy (kip-ft)	Delivered Energy (kip-ft)	Blow Count (BPI)	Impedance EA/C (kips/ft/s)	V _{imp} (ft/s)	F _{imp} (kips)	VEA/C F	D _{max} (in)
125	A54-BOR	Banut	34.72	25.87	18.14*	50.82	10.40	491.0	1.077	.827
126	A147-EOD	Banut	34.72	19.69	1.95*	48.44	8.14	404.2	0.978	.880
127	A147-BOR	Banut	34.72	25.30	6.68*	47.20	9.14	437.3	0.987	.780
128	GF19-EOD	LB-520	NA	9.40	20.00	29.80	10.55	342.8	0.918	.470
129	GF110-EOD	LB-520	NA	10.16	20.00	38.73	10.43	449.0	0.900	.380
130	GF222-EOD	ICE-640	NA	16.60	20.00	38.73	12.59	503.0	0.969	.590
131	GF224-EOD	ICE-640	NA	21.00	5.00	17.31	15.70	258.9	1.050	.900
132	GF312-EOD	LB-520	NA	6.86	18.00	38.73	9.16	396.1	0.889	.285
133	GF313-EOD	LB-520	NA	10.05	20.00	29.80	10.81	352.1	0.915	.403
134	GF412-EOD	LB-520	NA	8.49	39.00	38.73	9.81	408.8	0.911	.359
135	GF413-EOD	LB-520	NA	9.07	39.00	29.80	10.74	360.4	0.888	.418
136	GF414-EOD	ICE-640	NA	16.47	48.00	29.80	11.32	372.0	0.907	.807
137	GF415-EOD	ICE-640	NA	12.25	28.00	38.73	10.39	442.8	0.908	.455
138	EF82-EOD	D30-32	52.0	27.29	6.10	27.95	17.01	532.8	0.886	.868
139	EF167-BOR	D30-32	52.0	25.81	6.10	27.99	15.29	478.8	0.892	.827
140	A3-EOD1	Vul-020	60.0	18.74	6.00	209.66	3.52	743.8	0.992	.548
141	A3-BOR1	Vul-020	60.0	17.38	7.00	209.66	2.87	622.5	0.967	.488
142	A3-EOD2	Vul-020	60.0	18.85	3.42	209.66	3.40	788.8	0.904	.538
143	A3-BOR2	Vul-020	60.0	16.87	4.00	209.66	3.09	870.8	0.966	.412
144	A3-BOR3	Vul-020	60.0	21.93	30.00	209.66	3.63	753.4	1.010	.337
145	A14-DD1	Con-300	90.0	29.81	8.75	291.07	3.52	1028.3	0.996	.614
146	A14-DD2	Con-300	90.0	30.91	10.83	291.07	4.33	1218.8	1.034	.597
147	A14-BOR1	Con-300	90.0	40.87	3.00	291.07	6.26	1679.8	1.085	.544
148	A14-BOR2	Con-300	90.0	22.63	20.00	291.07	3.16	962.9	0.955	.318
149	A25-EOD	Vul-020	60.0	22.52	4.00	207.40	3.61	728.3	1.031	.735
150	A25-BOR1	Vul-020	60.0	19.06	8.00	207.40	3.12	651.2	0.994	.563
151	A25-BOR2	Vul-020	60.0	22.20	20.00	207.40	3.62	767.2	1.033	.499
152	A25-BOR3	Vul-020	60.0	22.13	20.00	207.40	3.78	753.8	1.040	.521
153	A18-EOD	Vul-010	32.5	11.52	3.17	150.55	3.98	571.0	1.049	.598
154	A18-BOR1	Vul-010	32.5	10.78	6.00	150.55	3.80	534.0	1.015	.457
155	A18-BOR2	Vul-010	32.5	9.04	7.67	150.55	3.18	457.0	1.051	.299

* - Denotes blow count (BPI) based on blows per foot.

Table 21. Pile driving and dynamic measurements for PD/LT (continued).

No.	File-Case Number	Hammer Type	Rated Hammer Energy (kip-ft)	Delivered Energy (kip-ft)	Blow Count (BPI)	Impedance EA/C (kips/ft/s)	V _{imp} (ft/s)	F _{imp} (kips)	VEA/C F	D _{max} (in)
156	A41-EOD	Vul-002	60.0	21.94	4.16 ^a	205.97	3.74	788.6	0.977	.604
157	A41-BOR1	Vul-020	60.0	25.41	5.00	205.97	4.31	828.1	1.072	.653
158	A41-BOR2	Vul-020	60.0	21.62	6.00	205.97	4.22	865.8	1.004	.497
159	A101-EOD	Vul-020	60.0	20.95	2.91 ^a	208.34	3.68	704.4	1.088	.718
160	A101-BOR1	Vul-020	60.0	21.20	6.00	208.34	3.89	744.3	1.089	.538
161	A101-BOR2	Vul-020	60.0	14.74	24.00	208.34	3.08	643.9	0.997	.360
162	A133-EOD	Vul-020	60.0	18.04	5.25	212.62	4.29	832.0	1.096	.654
163	A133-BOR	Vul-020	60.0	15.42	60.00	212.62	3.47	756.1	0.978	.354
164	A145-EOD	Vul-020	60.0	18.67	5.25	212.71	3.72	771.0	1.026	.626
165	A145-BOR1	Vul-020	60.0	17.50	13.00	212.71	3.01	652.0	0.962	.487
166	A145-BOR2	Vul-020	60.0	16.52	48.00	212.71	3.59	748.6	1.020	.411
167	CB3-BOR	Vul-020	60.0	16.55	10.00	255.08	3.08	766.8	1.025	.308
168	CB3-BORL	Vul-020	60.0	15.85	10.00	255.08	3.37	808.4	1.063	.261
169	CB5-BOR	ICE200S	100.0	15.34	12.00	291.95	3.31	897.6	1.077	.282
170	CB5-BORL	ICE200S	100.0	24.97	18.00	291.95	4.25	1289.2	0.962	.451
171	CB11-BORL	ICE200S	100.0	28.36	18.00	318.10	5.10	1634.8	0.992	.322
172	CB11-EORL	ICE200S	100.0	29.12	16.00	318.10	5.07	1630.5	0.989	.320
173	CB17-BOR1	ICE200S	100.0	29.19	16.00	297.16	4.95	1483.6	0.991	.332
174	CB17-BOR2	ICE200S	100.0	36.58	15.33	297.16	6.15	1822.5	1.003	.416
175	CB17-BORL	ICE200S	100.0	20.50	36.00	297.16	4.21	1256.9	0.995	.300
176	CB17-DRL	ICE200S	100.0	26.85	16.50	297.16	4.64	1518.1	0.908	.332
177	CB23-BOR	ICE200S	100.0	14.07	8.00	309.73	2.64	642.0	0.971	.266
178	CB23-BORL	ICE200S	100.0	22.68	12.00	309.73	4.45	1407.5	0.979	.337
179	CB29-BORL	ICE200S	100.0	8.89	26.00	268.26	2.11	639.3	0.961	.211
180	CB29-EORL	ICE200S	100.0	16.92	20.00	268.26	3.51	1018.4	0.994	.330
181	CB35-BOR1	ICE200S	100.0	31.33	8.73 ^a	293.99	5.14	1394.6	1.084	.637
182	CB35-BOR2	ICE200S	100.0	22.70	20.00	293.99	4.78	1340.4	1.048	.333
183	CB35-BORL	ICE200S	100.0	19.60	13.00	293.99	4.19	1232.9	0.999	.288
184	CB41-EOR	ICE200S	100.0	32.18	15.17	302.20	5.03	1503.8	1.011	.558
185	CB41-BOR	ICE200S	100.0	27.09	24.00	302.20	5.23	1555.1	1.016	.489
186	CB41-BORL	ICE200S	100.0	21.50	8.70	302.20	4.62	1450.5	0.963	.329

^a - Denotes blow count (BPI) based on blows per foot.

Table 21. Pile driving and dynamic measurements for PD/LT (continued).

No.	Pile-Case Number	Hammer Type	Rated Hammer Energy (kip-ft)	Delivered Energy (kip-ft)	Blow Count (BPI)	Impedance EA/C (Kips/ft/s)	V_{imp} (ft/s)	F_{imp} (kips)	$\frac{VEA/C}{F}$	D_{max} (in)
187	CB26-EOD	Vul-020	60.0	15.53	4.75	261.84	2.87	754.2	0.996	.461
188	CB26-BOR	Vul-020	60.0	22.67	5.45	261.84	3.62	847.4	1.001	.507
189	CB26-EOR	Vul-020	60.0	25.40	10.00	261.84	3.83	1034.1	0.970	.537
190	CB26-BOR2	Vul-020	60.0	20.93	12.00	261.84	3.50	937.9	0.977	.368
191	33P1-EOD	B-400	46.0	32.67	12.00	38.90	15.38	615.4	0.972	1.110
192	33P1-BOR	B-400	46.0	31.80	16.00	38.90	15.78	637.4	0.963	.787
193	33P1-EOR	B-400	46.0	32.50	no set	38.90	16.60	656.0	0.984	.845
194	33P2-EOD	B-400	46.0	32.84	39.00	17.54	16.44	281.3	1.025	1.859
195	33P2-BOR	B-400	46.0	30.97	76.00	17.54	16.66	317.0	0.922	1.418
196	33P2-EOR	B-400	46.0	31.24	no set	17.54	17.28	337.8	0.885	1.374
197	33P4-EOD	B-400	46.0	24.47	5.00	65.68	10.92	789.3	0.964	.665
198	33P5-EOD	B-225	29.0	8.41	10.67	24.56	8.75	240.9	0.892	.527
199	TRD22-EOD	D-12	22.5	9.76	30.00	38.70	10.50	394.7	1.005	.391
200	TRD22-BOR	D-12	22.5	7.83	20.00	38.70	9.62	410.3	0.886	.323
201	TRE22-EOD	D-22	40.0	15.18	22.00	38.70	13.33	502.5	1.003	.461
202	TRE22-BOR	D-22	40.0	15.18	10.00	38.70	14.28	801.7	0.896	.415
203	TRP5X-EOD	D-12	22.5	9.17	38.00	27.80	12.99	376.1	0.960	.409
204	TRP5X-BOR	D-12	22.5	9.70	25.00	27.80	12.13	361.5	0.933	.435
205	TR131-BOR	D-12	22.5	7.10 [*]	4.00	14.10	11.10	158.0	0.991	.759
206	TRAH-EOR	B-225	29.0	9.50	no set	46.70	10.30	489.0	0.990	.404
207	TRBH-BOR	B-225	29.0	12.50	2.50	46.80	11.10	532.0	0.874	.727
208	TRBP-EOR	B-225	29.0	8.60	4.87	21.80	12.90	306.0	0.918	.468

* - Denote blow count (BPI) based on blows per foot.

1 kip-ft = 1.36 kN-m
 1 BPI = 0.039 blows per mm
 1 kip/ft/s = 14.59 kN/m/s
 1 ft/s = 0.305 m/s
 1 kip = 4.448 kN
 1 in = 25.4 mm

Table 22. Parameters of dynamic analysis for PD/LT.

No.	Pile-Case Number	Case J_c	EA/C (Kips/s/ft)	2L/C (ms)	Tip Quake (In)	Side Quake (In)	Tip Damping (s/ft)	Side Damping (s/ft)
1	FN1-EOD	0.884	22.13	8.57	.200	.100	.070	.170
2	FN1-BOR1	1.564	22.13	8.57	.100	.100	.400	.130
3	FN1-BOR2	2.217	22.13	8.57	.100	.100	.580	.110
4	FN2-EOD	0.356	60.49	9.55	.200	.220	.050	.270
5	FN2-BOR	0.837	60.49	9.55	.080	.150	.100	.330
6	FN3-EOD	0.066	85.89	9.55	.120	.060	.290	.800
7	FN3-BOR	0.283	85.89	9.55	.210	.070	.340	.310
8	FN4-EOD	0.377	34.26	7.85	.150	.120	.050	.150
9	FN4-BOR	0.703	34.26	7.85	.100	.110	.050	.180
10	FIA-EOD	-0.454	46.60	13.98	.300	.170	.479	.049
11	FIA-BOR	-0.453	46.60	13.98	.050	.100	.597	.055
12	FIB-EOD	0.147	37.80	11.59	.200	.150	.086	.059
13	FIB-BOR	-0.025	37.80	11.59	.150	.100	.129	.068
14	FO1-EOD	0.133	120.80	7.17	.280	.100	.139	.136
15	FO1-BOR	0.720	120.80	7.17	.280	.100	.092	.092
16	FO2-EOD	-0.150	199.10	9.41	.230	.100	.049	.185
17	FO2-BOR	0.285	199.10	9.41	.250	.100	.039	.166
18	FO3-EOD	-0.828	61.40	13.08	.050	.080	.675	.082
19	FO4-EOD	-1.855	214.80	10.48	.130	.100	.115	.127
20	FO4-BOR	-0.570	214.80	10.48	.200	.120	.244	.193
21	FOR1-EOD	-0.578	159.00	20.96	.380	.250	.060	.179
22	FOR1-BOR	-0.503	159.00	20.96	.220	.220	.246	.185
23	FMS-EOD	0.022	49.08	13.96	.320	.100	.041	.086
24	FMS-BOR	0.877	49.08	12.02	.390	.100	.097	.074
25	FM17-EOD	0.438	49.08	9.26	.530	.090	.077	.078
26	FM17-BOR	0.877	49.08	9.26	.200	.100	.050	.142
27	FM23-EOD	0.259	49.08	6.75	.400	.080	.041	.454
28	FM23-BOR	0.146	49.08	6.75	1.000	.210	.045	.090
29	FC1-EOD	-0.226	17.54	3.98	.300	.157	.038	.038
30	FC1-BOR	-0.278	17.54	3.98	.330	.140	.030	.032
31	FC2-EOD	-0.229	17.54	3.27	.330	.148	.041	.026

* - Determined from TEPWAP analysis.

Table 22. Parameters of dynamic analysis for PD/LT (continued).

No.	Pile-Case Number	Case J_c	EA/C (kips/s/ft)	2L/C (ms)	Tip Quake (in)	Side Quake (in)	Tip Damping (s/ft)	Side Damping (s/ft)
32	FC2-BOR	-0.393	17.54	3.14	.330	.150	.029	.024
33	FMI1-EOD	-0.010	28.73	9.87	.100	.100	.051	.047
34	FMI1-BOR	0.113	28.73	9.87	.150	.100	.086	.017
35	FM2-EOD	0.198	28.73	7.32	.140	.100	.030	.080
36	FM2-BOR	0.348	28.73	7.32	.150	.100	.055	.030
37	FWA-EOD	0.125	198.82	18.08	.500	.260	.095	.303
38	FWA-BOR	0.213	198.82	18.08	.301	.251	.188	.137
39	FWB-EOD	0.272	198.82	16.66	-	-	-	-
40	FWB-BOR	0.141	198.82	16.66	-	-	-	-
41	FA1-EOD	0.043	145.72	8.40	.100	.100	.123	.234
42	FA1-BOR1	0.241	145.72	9.07	.200	.080	.368	.387
43	FA1-BOR2	0.373	145.72	9.07	.250	.100	.363	.322
44	FA2-EOD	-0.108	145.72	10.51	.420	.100	.098	.215
45	FA2-BOR1	0.207	140.52	10.90	.250	.100	.282	.205
46	FA2-BOR2	0.577	145.72	10.51	.170	.130	.323	.327
47	FA3-EOD	-0.199	221.53	9.18	.350	.100	.183	.329
48	FA3-BOR1	0.085	219.99	9.06	.200	.070	.513	.336
49	FA3-BOR2	0.313	221.53	9.00	.205	.080	.309	.395
50	FA4-EOD	-0.204	221.53	10.43	.250	.100	.153	.297
51	FA4-BOR1	0.331	219.93	10.51	.120	.080	.334	.380
52	FA4-BOR2	0.587	219.93	10.51	.150	.100	.282	.358
53	FA5-EOD	0.133	403.88	10.07	.330	.120	.395	.302
54	FA5-BOR	0.414	403.88	10.45	.240	.070	.398	.395
55	FV15-EOD	0.085	38.19	10.95	.300	.100	.140	.102
56	FV15-BOR	0.009	38.19	10.95	.300	.100	.424	.089
57	FV10-EOD	0.478	38.19	10.95	.300	.100	.377	.202
58	FV10-BOR	0.143	38.19	10.95	.340	.125	.276	.164
59	FMN2-EOD	-0.223	38.19	11.19	.500	.180	.079	.104
60	FMN2-BOR	0.025	38.19	11.19	.150	.152	.085	.114
61	FP5-EOD	0.183	12.49	4.10	.200	.040	.037	.091
62	FP5-BOR	0.358	12.49	4.10	.190	.045	.030	.068

* - Determined from TEPWAP analysis.

Table 22. Parameters of dynamic analysis for PD/LT (continued).

No.	Pile-Case Number	Case J_c	EA/C (kips/s/ft)	2L/C (ms)	Tip Quake (in)	Side Quake (in)	Tip Damping (s/ft)	Side Damping (s/ft)
63	FKG-EOD	-0.268	80.23	11.39	.250	.090	.104	.258
64	FKG-BOR	-0.189	80.23	11.39	.140	.060	.113	.282
65	FL3-EOD	-0.119	203.74	15.04	.400	.100	.246	.269
66	FL3-BOR1	0.149	203.74	15.04	.250	.150	.378	.392
67	FL3-BOR2	0.394	203.74	15.04	.250	.124	.523	.507
68	CA1-EOD	-0.120	27.87	20.47	.140	.140	.089	.083
69	CA1-BOR	-0.108	27.87	20.47	.130	.130	.089	.075
70	CA2-BOR	0.558	27.87	13.39	.100	.100	.097	.105
71	CA5-BOR1	-0.354	21.58	7.97	.362	.100	.012	.088
72	CA5-BOR2	-0.408	21.58	7.97	.327	.217	.035	.024
73	CA3/8-BOR	0.785	15.80	8.78	.374	.278	.098	.118
74	CA24-BOR	0.295	13.44	4.59	.177	.118	.113	.077
75	CA6-BOR1	0.040	25.93	7.18	.354	.278	.048	.050
76	CA6-BOR2	-0.006	25.93	7.18	.394	.258	.047	.052
77	CA6-EOR	-0.347	25.93	7.18	.335	.258	.037	.062
78	WC3-EOD	-0.063	268.75	6.80	.400	.100	.168	.068
79	WC3-BOR1	-0.056	268.75	6.80	.350	.130	.038	.198
80	WC3-BOR2	-0.042	268.75	5.38	.320	.080	.087	.137
81	WC8-EOD	-0.038	265.88	5.54	.420	.100	.118	.143
82	WC8-BOR1	-0.044	265.88	5.54	.471	.080	.127	.212
83	WC8-BOR2	-0.005	265.88	3.93	.610	.100	.048	.311
84	WB9-BOR	0.455	271.52	20.00	.260	.050	.433	.251
85	WB15-BOR	0.457	269.50	16.28	.225	.060	.242	.488
86	T1/A-EOD	0.265	378.57	16.49	.150	.050	.070	.115
87	T1/A-ALT	0.257	378.57	20.70	.200	.100	.157	.079
88	T1/B-EOD	0.153	378.57	25.74	.060	.060	.021	.047
89	T2/A-EOD	0.348	198.75	13.94	.150	.040	.235	.087
90	T2/B-EOD	0.057	198.75	31.01	.070	.070	.154	.033
91	35-1-BOR	0.068	38.93	7.15	.250	.100	.114	.043
92	35-4-BOR	0.315	17.50	6.21	.300	.100	.024	.033
93	35-5-BOR	0.382	38.93	11.93	.040	.040	.042	.063

* - Determined from TEPWAP analysis.

Table 22. Parameters of dynamic analysis for PD/LT (continued).

No.	File-Case Number	Case J_c	EA/C (Kips/s/ft)	2L/C (ms)	Tip Quake (in)	Side Quake (in)	Tip Damping (s/ft)	Side Damping (s/ft)
94	35-6-BOR	0.266	17.50	12.55	.100	.060	.001	.093
95	35-7-BOR	0.007	18.97	8.88	.200	.100	.040	.047
96	35-10-BOR	-0.182	80.58	7.89	.250	.040	.019	.083
97	E2-BOR	0.599	84.20	6.31	.260	.100	.120	.175
98	639-BOR	0.756	30.34	8.19	.280	.100	.027	.264
99	LB21-BOR	0.129	189.40	5.50	.310	.100	.128	.189
100	LB20-BOR	0.184	181.80	7.91	.230	.120	.211	.211
101	LC3-BOR	0.389	161.80	20.31	.350	.250	.192	.137
102	LIN16-BOR	0.787	161.10	24.50	.220	.120	.293	.337
103	LE37-BOR	0.082	38.80	10.00	.140	.080	.181	.650
104	LE64-BOR	0.218	38.80	10.00	.105	.070	.148	.132
105	ST1-EOD	0.242	123.0	11.52	.300	.080	.054	.061
106	ST2-EOD	-0.102	132.3	9.98	.600	.080	.017	.020
107	ST9-BOR	0.500	339.1	24.19	.220	.100	.322	.148
108	ST46-EOD	0.010	10.35	4.52	.400	.150	.033	.042
109	GZA3-EOD	-0.240	36.20	17.00	.330	.150	.053	.050
110	GZA6-EOD	0.000	27.80	18.50	.320	.150	.030	.050
111	GZA6-EOD	-0.180	27.70	20.37	.250	.125	.118	.053
112	GZB8CEOD	-0.234	37.80	13.79	.058	.050	.091	.075
113	GZBP2EOD	0.361	36.20	17.08	.040	.050	.051	.129
114	GZB6-EOD	0.174	27.70	11.56	.240	.120	.061	.064
115	GZZ5-EOD	0.281	37.80	10.34	.450	.350	.171	.238
116	GZ06-EOD	0.481	37.80	10.34	.580	.100	.059	.810
117	GZCC5EOD	0.471	37.80	13.91	.430	.220	.029	.117
118	GZL2-EOD	-0.038	37.80	13.91	.530	.320	.137	.244
119	GZP14-EOD	0.457	37.80	12.48	.450	.100	.077	.102
120	GZP11-EOD	0.268	37.80	12.48	.100	.100	.063	.178
121	GZP12-EOD	0.247	37.80	13.73	.110	.170	.038	.188
122	GZB22-EOD	0.812	111.0	18.71	.065	.065	.207	.126
123	GZW1-EOR	0.094	26.10	15.02	.170	.100	.118	.142
124	A54-EOD	-0.785	50.82	12.07	.138	.099	.189	.101

* - Determined from TEPWAP analysis.

Table 22. Parameters of dynamic analysis for PD/LT (continued).

No.	File-Case Number	Case J_c	EA/C (kips/s/ft)	2L/C (ms)	Tip Ousake (In)	Side Ousake (In)	Tip Damping (s/ft)	Side Damping (s/ft)
125	A54-BOR	-0.149	50.82	12.07	.100	.343	.088	.109
126	A147-EOD	-0.599	48.44	11.18	.669	.100	.068	.112
127	A147-BOR	0.310	47.20	10.89	.219	.100	.075	.100
128	GF19-EOD	0.280	29.80	9.45	.110	.100	.035	.082
129	GF110-EOD	-0.117	38.73	6.79	.160	.110	.034	.117
130	GF222-EOD	0.221	38.73	7.97	.140	.130	.065	.078
131	GF224-EOD	0.008	17.31	8.30	.080	.030	.048	.023
132	GF312-EOD	0.830	38.73	3.93	.120	.080	.115	.057
133	GF313-EOD	1.124	29.80	4.18	.150	.080	.133	.043
134	GF412-EOD	1.355	38.73	5.78	.120	.120	.058	.026
136	GF413-EOD	1.056	29.80	4.07	.100	.120	.064	.029
138	GF414-EOD	1.390	29.80	5.85	.120	.110	.043	.012
137	GF415-EOD	0.622	38.73	5.88	.130	.100	.058	.027
138	EF82-EOD	0.083	27.85	-	-	-	-	-
139	EF167-BOR	0.835	27.99	-	-	-	-	-
140	A3-EOD1	-0.392	209.68	13.43	.330	.120	.110	.230
141	A3-BOR1	-0.714	209.68	13.43	.270	.100	.130	.160
142	A3-EOD2	-0.329	209.68	13.43	.250	.150	.160	.180
143	A3-BOR2	-0.464	209.68	13.43	.020	.080	.150	.260
144	A3-BOR3	0.209	209.68	12.76	.170	.100	.260	.220
145	A14-DD1	-0.130	291.07	15.35	.390	.100	.130	.280
146	A14-DD2	-0.008	291.07	15.35	.370	.140	.110	.280
147	A14-BOR1	0.213	291.07	15.35	.100	.120	.220	.220
148	A14-BOR2	0.402	291.07	10.76	.200	.150	.120	.230
149	A25-EOD	-0.287	207.40	15.31	.350	.120	.080	.120
150	A25-BOR1	-0.188	207.40	15.31	.320	.100	.100	.110
151	A25-BOR2	0.010	207.40	15.31	.380	.270	.310	.100
152	A25-BOR3	-0.008	207.40	15.31	.380	.250	.260	.190
153	A16-EOD	0.064	150.55	9.05	.230	.100	.150	.100
154	A16-BOR1	0.103	150.55	9.05	.330	.100	.160	.100
155	A16-BOR2	0.332	150.55	8.68	.240	.080	.650	.180

* - Determined from TEPWAP analysis.

Table 22. Parameters of dynamic analysis for PD/LT (continued).

No.	Pile-Case Number	Case J_c	EA/C (kips/s/ft)	2L/C (ms)	Tip Quake (in)	Side Quake (in)	Tip Damping (s/ft)	Side Damping (s/ft)
156	A41-EOD	-0.027	205.97	13.24	.290	.080	.150	.080
157	A41-BOR1	0.034	205.97	13.24	.370	.090	.140	.090
158	A41-BOR2	0.090	205.97	8.95	.350	.100	.130	.100
159	A101-EOD	-0.375	208.34	12.65	.400	.120	.040	.310
160	A101-BOR1	-0.142	208.34	12.65	.120	.080	.120	.160
161	A101-BOR2	0.273	208.34	10.28	.100	.090	.200	.210
162	A133-EOD	-0.195	212.62	18.31	.360	.180	.260	.210
163	A133-BOR	0.217	212.62	16.30	.130	.130	.210	.190
164	A145-EOD	-0.454	212.71	18.59	.190	.090	.150	.240
165	A145-BOR1	-0.338	212.71	18.59	.170	.170	.170	.270
166	A145-BOR2	-0.019	212.71	16.21	.160	.140	.210	.210
167	CB3-BOR	0.647	255.08	11.98	.190	.100	.563	.317
168	CB3-BORL	0.520	255.08	11.67	.190	.110	.527	.378
169	CB5-BOR	-0.395	291.95	12.45	.140	.100	.314	.929
170	CB5-BORL	-0.188	291.95	8.74	.300	.100	.227	.405
171	CB11-BORL	0.363	318.10	12.81	.140	.180	1.335	.249
172	CB11-EORL	0.259	318.10	12.81	.120	.170	.660	.538
173	CB17-BOR1	0.029	297.18	13.63	.130	.210	.413	.258
174	CB17-BOR2	0.128	297.18	13.63	.250	.160	.318	.277
175	CB17-BORL	-0.092	297.18	12.65	.220	.030	.350	.125
176	CB17-DRL	0.024	297.18	12.65	.250	.010	.328	.031
177	CB23-BOR	0.312	309.73	12.95	.140	.130	.858	.284
178	CB23-BORL	0.408	309.73	12.95	.050	.170	1.674	.535
179	CB29-BORL	-0.213	288.28	13.78	.090	.100	.707	.483
180	CB29-EORL	0.017	288.28	13.78	.200	.100	.129	.812
181	CB35-BOR1	-0.311	293.99	13.79	.240	.100	.113	.095
182	CB35-BOR2	-0.167	293.99	13.79	.180	.100	.113	.433
183	CB35-BORL	-0.029	293.99	12.66	.090	.170	.700	.228
184	CB41-EOR	-0.161	302.20	14.14	.260	.100	.141	.209
185	CB41-BOR	0.118	302.20	14.00	.260	.110	.127	.198
186	CB41-BORL	-0.117	302.20	10.82	.140	.130	.351	.392

¹ - Determined from TEPWAP analysis.

Table 22. Parameters of dynamic analysis for PD/LT (continued).

No.	File-Case Number	Case J_c	EA/C (kips/s/ft)	2L/C (ms)	Tip Quake (in)	Side Quake (in)	Tip Damping (s/ft)	Side Damping (s/ft)
187	CB26-EOD	-0.408	261.84	11.40	.210	.120	.078	.105
188	CB26-BOR	-0.137	261.84	11.40	.270	.110	.099	.059
189	CB26-EOR	-0.098	261.84	11.40	.330	.090	.056	.056
190	CB26-BOR2	-0.164	261.84	9.25	.230	.100	.176	.736
191	33P1-EOD	-0.141	38.90	14.39	.150*	.300*	.080*	.010*
192	33P1-BOR	-0.017	38.90	14.39	.080	.040	.030	.038
193	33P1-EOR	-0.240	38.90	14.39	.100	.100	.012	.028
194	33P2-EOD	-0.182	17.54	17.81	.400*	.200*	.150*	.020*
195	33P2-BOR	-0.125	17.54	13.21	.300	.300	.048	.048
196	33P2-EOR	-0.096	17.54	13.21	.300	.300	.010	.033
197	33P4-EOD	0.152	67.30	10.45	.100*	.025*	.100*	.050*
198	33P5-EOD	0.509	21.21	6.94	.090*	.100*	.040*	.040*
199	TRD22-EOD	0.371	38.70	2.68	.150	.100	.015	.224
200	TRD22-BOR	0.157	38.70	2.68	.180	.100	.108	.216
201	TRE22-EOD	0.661	38.70	3.53	.100*	.100*	.100*	.100*
202	TRE22-BOR	0.411	38.70	3.53	.250	.100	.018	.136
203	TRP5X-EOD	0.418	27.80	2.94	.150	.100	.020	.111
204	TRP5X-BOR	-0.059	27.80	2.94	.150	.100	.013	.128
205	PR131-BOR	0.162	14.10	3.15	.300	.300	.034	.235
206	TRAH-EOR	-0.310	46.70	16.24	.200	.100	.025	.753
207	TRBH-BOR	0.138	46.80	13.40	.050	.050	1.040	.206
208	TRBP-EOR	-0.730	21.80	12.94	.025*	.100*	.200*	.100*

* - Determined from TEPWAP analysis.

1 kip/s/ft = 14.6 kN/s/m

1 in = 25.4 mm

1 s/ft = 3.281 s/m

Table 23. Pile capacity based on static load test and dynamic analysis for PD/LT.

No	Pile-Case Number	Load Test Type	Davison's Criteria (kips)	Shape of Curve (kips)	$\Delta = 1'$ (kips)	$\Delta = 0.1B$ (kips)	DeBeer (kips)	Static Resist R_u (kips)	CAPWAP TEPWAP (kips)	Energy Appr. R_u (kips)	$K_{sp} \frac{E_p}{R_u}$
1	FN1-EOD	Q	304	300	304	304	300	300	230	382	0.829
2	FN1-BOR1	Q	304	300	304	304	300	300	375	484	0.820
3	FN1-BOR2	Q	304	300	304	304	300	300	431	535	0.581
4	FN2-EOD	Q	358	354	362	368	358	354	228	418	0.847
5	FN2-BOR	Q	358	354	362	368	358	354	305	487	0.727
6	FN3-EOD	Q	378	370	382	383	388	374	178	480	0.779
7	FN3-BOR	Q	378	370	382	383	388	374	297	621	0.602
8	FN4-EOD	Q	284	280	288	292	282	280	244	401	0.698
9	FN4-BOR	Q	284	280	288	292	282	280	268	582	0.481
10	FIA-EOD	Q	928	934	772	910	920	930	367	589	1.634
11	FIA-BOR	Q	928	934	772	910	920	930	731	689	1.349
12	FIB-EOD	Q	650	480-640	650	NA	648	650	511	708	0.918
13	FIB-BOR	Q	650	480-640	650	NA	648	650	521	696	0.934
14	FO1-EOD	Q	598	500-560	672	NA	544	557	498	718	0.811
15	FO1-BOR	Q	598	500-560	672	NA	544	557	700	1169	0.478
16	FO2-EOD	Q	780	750	780	800	754	750	530	646	1.181
17	FO2-BOR	Q	780	750	780	800	754	750	731	1158	0.848
18	FO3-EOD	Q	778	700-850	816	862	820	820	566	584	1.404
19	FO4-EOD	Q	1700	1400	1716	1800	1664	1650	658	763	2.163
20	FO4-BOR	Q	1700	1400	1716	1800	1664	1850	787	1268	1.300
21	FOR1-EOD	Q	1360	1350	1188	1600	1400	1380	558	839	1.651
22	FOR1-BOR	Q	1360	1350	1188	1600	1400	1380	729	1207	1.143
23	FM5-EOD	Q	440	360-440	528	NA	461	420	348	357	1.178
24	FM5-BOR	Q	440	360-440	528	NA	461	420	499	734	0.572
25	FM17-EOD	Q	408	375-440	541	NA	430	447	424	524	0.853
26	FM17-BOR	Q	408	375-440	541	NA	430	447	526	781	0.572
27	FM23-EOD	Q	342	290-330	378	NA	358	340	323	412	0.825
28	FM23-BOR	Q	342	290-330	378	NA	358	340	340	426	0.798
29	FC1-EOD	Q	318	320-380	370	372	358	340	270	342	0.994
30	FC1-BOR	Q	318	320-380	370	372	358	340	265	363	0.937
31	FC2-EOD	Q	368	350-400	442	NA	338	378	375	402	0.935

* - Determined from TEPWAP analysis.

Table 23. Pile capacity based on static load test and dynamic analysis for PD/LT (continued).

No	Pile-Case Number	Load Test Type	Davison's Criteria (kips)	Shape of Curve (kips)	$\Delta = 1'$ (kips)	$\Delta = 0.1B$ (kips)	DeBeer (kips)	Static Resist R_s (kips)	CAPWAP TEPWAP (kips)	Energy Appr. R_U (kips)	$K_{up} \frac{B_u}{R_U}$
32	FC2-BOR	Q	368	350-400	442	NA	336	376	340	353	1.066
33	FM11-EOD	Q	330	288-317	333	NA	320	310	285	246	1.260
34	FM11-BOR	Q	330	288-317	333	NA	320	310	319	306	1.013
35	FM12-EOD	Q	208	180	NA	NA	126	160	184	179	0.894
36	FM12-BOR	Q	208	180	NA	NA	126	160	217	279	0.573
37	FWA-EOD	SM	1300	1300	1300	NA	1150	1300	285	1145	1.135
38	FWA-BOR	SM	1300	1300	1300	NA	1150	1300	652	1154	1.127
39	FWB-EOD	SM	1000	1200	1000	NA	1497	1225	plug	1708	0.717
40	FWB-BOR	SM	1000	1200	1000	NA	1497	1225	plug	1280	0.957
41	FA1-EOD	S	370	325-350	419	NA	334	345	205	302	1.142
42	FA1-BOR1	S	370	325-350	419	NA	334	345	257	462	0.747
43	FA1-BOR2	S	370	325-350	419	NA	334	345	382	840	0.411
44	FA2-EOD	S	550	480-550	588	NA	541	535	428	568	0.942
45	FA2-BOR1	S	550	480-550	588	NA	541	535	486	850	0.563
46	FA2-BOR2	S	550	480-550	588	NA	541	535	599	896	0.597
47	FA3-EOD	S	625	500-640	679	NA	648	614	340	547	1.122
48	FA3-BOR1	S	625	500-640	679	NA	648	614	307	744	0.825
49	FA3-BOR2	S	625	500-640	679	NA	648	614	587	826	0.743
50	FA4-EOD	S	817	685-825	887	NA	748	773	446	772	1.001
51	FA4-BOR1	S	817	685-825	887	NA	748	773	604	1062	0.728
52	FA4-BOR2	S	817	685-825	887	NA	748	773	852	1448	0.534
53	FA5-EOD	S	1140	1050	1188	NA	939	1074	662	1543	0.696
54	FA5-BOR	S	1140	1050	1188	NA	939	1074	845	2238	0.480
55	FV15-EOD	Q	315	300-350	372	440	246	315	194	336	0.838
56	FV15-BOR	Q	315	300-350	372	440	246	315	198	369	0.810
57	FV10-EOD	Q	345	230-300	400	484	240	313	158	305	1.026
58	FV10-BOR	Q	345	230-300	400	484	240	313	179	285	1.096
59	FMN2EOD	Q	765	720-740	722	752	724	740	342	476	1.555
60	FMN2BOR	Q	765	720-740	722	752	724	740	652	831	0.890
61	FPS-EOD	Q	243	220-235	NA	NA	211	227	210	211	1.076
62	FPS-BOR	Q	243	220-235	NA	NA	211	227	239	280	0.811

* - Determined from TEPWAP analysis.

Table 23. Pile capacity based on static load test and dynamic analysis for PD/LT (continued).

No	File-Case Number	Load Test Type	Davison's Criteria (kips)	Shape of Curve (kips)	$\Delta = 1''$ (kips)	$\Delta = 0.18$ (kips)	DeBeer (kips)	Static Resist R_s (kips)	CAPWAP TEPWAP (kips)	Energy Appr. R_u (kips)	$K_{sp} \frac{R_u}{R_s}$
63	FKG-EOD	Q	368	480-520	530	NA	475	465	288	392	1.188
64	FKG-BOR	Q	368	480-520	530	NA	475	465	295	403	1.154
65	FL3-EOD	LLT	400	400	NA	NA	400	400	136	258	1.550
66	FL3-BOR1	LLT	400	400	NA	NA	400	400	272	568	0.669
67	FL3-BOR2	LLT	400	400	NA	NA	400	400	350	893	0.448
68	CA1-EOD	S	540	500-560	390	390	530	533	410	444	1.200
69	CA1-BOR	S	540	500-560	390	390	530	533	500	433	1.231
70	CA2-BOR	S	368	320-400	370	370	355	380	342	430	0.884
71	CA5-BOR1	S	488	480-500	500	NA	460	480	409	540	0.888
72	CA5-BOR2	S	488	480-500	500	NA	480	480	489	543	0.883
73	CA38-BOR	Q	189	200-230	271	271	227	230	241	369	0.623
74	CA24-BOR	S	242	220-260	NA	NA	248	243	207	403	0.595
75	CA8-BOR1	S	680	620-660	590	650	640	660	610	782	0.844
76	CA8-BOR2	S	680	620-660	590	650	640	660	584	742	0.889
77	CA8-EOR	S	680	620-660	590	650	640	660	558	704	0.938
78	WC3-EOD	FQ	610	550-650	NA	NA	620	610	509	751	0.812
79	WC3BOR1	FQ	610	550-650	NA	NA	620	610	506	781	0.781
80	WC3BOR2	FQ	610	550-650	NA	NA	620	610	536	777	0.785
81	WC8EOD	FQ	453	445-545	NA	NA	537	495	450	597	0.829
82	WC8BOR1	FQ	453	445-545	NA	NA	537	495	480	713	0.694
83	WC8BOR2	FQ	453	445-545	NA	NA	537	495	443	772	0.841
84	WB9-BOR	FQ	900	830-880	925	NA	855	884	941	1789	0.500
85	WB15BOR	FQ	820	740-790	833	NA	767	766	805	1448	0.529
86	T1/A-EOD	SM	1984	1984	1984	NA	1808	1984	1775	2729	0.726
87	T1/A-ALT	SM	1984	1984	1984	NA	1808	1984	1800	2870	0.690
88	T1/B-EOD	SM	2868 ^a	2425	NA	NA	1852	2648	2368	3042	0.871
89	T2/A-EOD	SM	1345	1323	NA	NA	1554	1470	1252	1872	0.785
90	T2/B-EOD	SM	3285	> 2204	NA	NA	NA	3080 ^b	2778	2964	1.040
91	35-1-BOR	S	322	320-350	354	366	318	325	260	274	1.164
92	35-4-BOR	S	330	300-330	334	342	314	320	360	465	0.684
93	35-5-BOR	S	612	580-620	600	608	600	600	650	616	0.971

^a - Davison's reduced for creep.

^b - Extrapolated. (Load taken to 2200 kips.)

Table 23. Pile capacity based on static load test and dynamic analysis for PD/LT
(continued).

No	Pile-Case Number	Load Test Type	Davison's Criteria (kips)	Shape of Curve (kips)	$\Delta = 1^*$ (kips)	$\Delta = 0.1B$ (kips)	DeBeer (kips)	Static Resist R_s (kips)	CAPWAP TEPWAP (kips)	Energy Appr. R_U (kips)	K_{wp} $\frac{R_s}{R_U}$
94	35-6-BOR	S	900	500-550	530	548	526	530	580	526	1.007
95	35-7-BOR	S	122	120-170	152	146	144	142	139	183	0.776
96	35-10-BOR	S	402	370-420	432	444	378	400	334	425	0.941
97	E2-BOR	Q	415	375-395	NA	NA	369	390	420	732	0.533
98	63S-BOR	CRP	264	250-272	292	NA	258	268	279	320	0.838
99	LB21-BOR	S	380	380	NA	484	280	380	381	519	0.694
100	LB20-BOR	S	580	480	NA	NA	480	530	474	813	0.652
101	LC3-BOR	S	620	600	680	NA	560	640	612	1169	0.547
102	LIN18-BOR	S	600	600	600	NA	600	600	562	985	0.609
103	LE37-BOR	S	250	240	270	NA	230	250	197	241	1.037
104	LE84-BOR	S	270	240	NA	NA	220	260	232	274	0.949
105	ST1-EOD	S	344	280-320	NA	NA	300	344	505	630	0.546
106	ST2-EOD	S	510	540	NA	NA	500	540	618	865	0.812
107	ST9-BOR	S	920	720-840	920	NA	800	900	807	1927	0.487
108	ST48-EOD	S	NA	104	NA	NA	104	104	82	113	0.920
109	GZA3-EOD	Q	440	500	460	520	480	480	365	424	1.132
110	GZA5-EOD	Q	256	180-210	320	314	270	298	293	339	0.873
111	GZA8-EOD	Q	188	350	316	308	350	326	275	281	1.180
112	GZBBCEOD	Q	440	500-560	500	590	560	530	413	453	1.169
113	GZBP2EOD	Q	280	340	340	324	290	320	317	302	1.059
114	GZB6-EOD	Q	380	420	456	530	360	380	341	413	0.944
115	GZZ5-EOD	Q	464	420-470	540	NA	410	440	214	557	0.790
116	GZ05-EOD	Q	480	440-480	600	NA	490	486	205	511	0.951
117	GZCC5EOD	Q	450	480-520	520	750	NA	490	482	599	0.818
118	GZL2-EOD	Q	640	600-660	690	780	530	660	267	566	1.187
119	GZP14-EOD	Q	390	360-400	440	500	480	420	305	570	0.737
120	GZP11-EOD	Q	250	340-420	380	440	430	386	239	399	0.967
121	GZP12-EOD	Q	500	600	630	NA	NA	560	520	674	0.831
122	GZB22-EOD	Q	1120	1120	1040	NA	840	1060	1109	1357	0.781
123	GZW1-EOR	Q	360	335-400	404	416	353	380	250	357	1.064
124	A54-EOD	CRP	652	630-652	618	638	639	638	383	464	1.437

* - Determined from TEPWAP analysis.

Table 23. Pile capacity based on static load test and dynamic analysis for PD/LT
(continued).

No	Pile-Case Number	Load Test Type	Davison's Criteria (kips)	Shape of Curve (kips)	$\Delta = 1'$ (kips)	$\Delta = 0.1B$ (kips)	DeBeer (kips)	Static Resist R_s (kips)	CAPWAP TEPWAP (kips)	Energy Appr. R_u (kips)	K_{sp} $\frac{R_u}{R_s}$
125	A54-BOR	CRP	652	630-652	618	636	639	638	611	696	0.914
126	A147-EOD	CRP	558	547	555	560	540	552	259	339	1.628
127	A147-BOR	CRP	558	547	555	560	540	552	564	653	0.845
128	GF19-EOD	Q	330	400-460	380	380	325	397	398	434	0.915
129	GF110-EOD	Q	500	500-600	560	560	450	550	457	605	0.909
130	GF222-EOD	Q	580	540-600	590	590	540	570	512	623	0.916
131	GF224-EOD	Q	NA	450-470	NA	NA	465	463	419	458	1.011
132	GF312-EOD	Q	340	300-310	NA	NA	280	310	405	483	0.642
133	GF313-EOD	Q	334	320-330	NA	NA	334	330	448	532	0.820
134	GF412-EOD	Q	240	240-280	294	294	200	272	455	530	0.513
135	GF413-EOD	Q	300	280-320	350	350	270	300	428	491	0.611
136	GF414-EOD	Q	360	360-420	420	420	320	390	524	630	0.619
137	GF415-EOD	Q	460	460-520	540	540	440	500	561	599	0.835
138	EF82-EOD	Q	502	440-510	486	456	480	477	522	636	0.750
139	EF167-BOR	Q	271	267	279	277	267	272	479	625	0.436
140	A3-EOD1	FQ	958	850-940	960	NA	958	939	472	629	1.493
141	A3-BOR1	FQ	958	850-940	960	NA	958	939	538	660	1.423
142	A3-EOD2	FQ	958	850-940	960	NA	958	939	368	545	1.723
143	A3-BOR2	FQ	958	850-940	960	NA	958	939	462	612	1.534
144	A3-BOR3	FQ	958	850-940	960	NA	958	939	825	1421	0.661
145	A14-DD1	FQ	NA	860-945	NA	NA	908	905	684	982	0.922
146	A14-DD2	FQ	NA	860-945	NA	NA	908	905	741	1076	0.841
147	A14-BOR1	FQ	NA	860-945	NA	NA	908	905	604	1118	0.809
148	A14-BOR2	FQ	NA	860-945	NA	NA	908	905	962	1476	0.613
149	A25-EOD	FQ	715	750-840	840	NA	845	800	459	549	1.457
150	A25-BOR1	FQ	715	750-840	840	NA	845	800	555	695	1.203
151	A25-BOR2	FQ	715	750-840	840	NA	845	800	452	970	0.825
152	A25-BOR3	FQ	715	750-840	840	NA	845	800	442	930	0.860
153	A16-EOD	FQ	315	275-315	350	NA	272	308	224	303	1.017
154	A16-BOR1	FQ	315	275-315	350	NA	272	308	282	415	0.742
155	A16-BOR2	FQ	315	275-315	350	NA	272	308	296	505	0.610

* - Determined from TEPWAP analysis.

Table 23. Pile capacity based on static load test and dynamic analysis for PD/LT
(continued).

No	Pile-Case Number	Load Test Type	Davissan's Criteria (kpa)	Shape of Curve (kpa)	$\Delta = 1'$ (kpa)	$\Delta = 0.1B$ (kpa)	DeBeer (kpa)	Static Resist R_s (kpa)	CAPWAP TEPWAP (kpa)	Energy Appr. R_U (kpa)	K_{sp} $\frac{R_U}{R_s}$
156	A41-EOD	FQ	524	500-525	540	NA	536	530	431	624	0.849
157	A41-BOR1	FQ	524	500-525	540	NA	536	530	503	715	0.741
158	A41-BOR2	FQ	524	500-525	540	NA	536	530	565	834	0.835
159	A101-EOD	FQ	812	800-840	NA	NA	800	810	517	474	1.709
160	A101-BOR1	FQ	812	800-840	NA	NA	800	810	669	722	1.122
161	A101-BOR2	FQ	812	800-840	NA	NA	800	810	803	881	0.919
162	A133-EOD	FQ	808	780-860	810	NA	866	826	311	513	1.610
163	A133-BOR	FQ	808	780-860	810	NA	866	826	780	998	0.828
164	A145-EOD	FQ	976	860-950	975	NA	913	940	353	549	1.712
165	A145-BOR1	FQ	976	860-950	975	NA	913	940	641	745	1.262
166	A145-BOR2	FQ	976	860-950	975	NA	913	940	761	918	1.024
167	CB3-BOR	FQ	500	488-500	470	NA	472	484	564	978	0.485
168	CB3-BORL	FQ	500	488-500	470	NA	472	484	502	998	0.485
169	CB5-BOR	FQ	1250	1240	1325	NA	1170	1246	588	1008	1.236
170	CB5-BORL	FQ	1250	1240	1325	NA	1170	1246	584	1167	1.068
171	CB11-BORL	FQ	1435	1370	1430	NA	1364	1400	814	1803	0.776
172	CB11-EORL	FQ	1435	1370	1430	NA	1364	1400	939	1827	0.768
173	CB17-BOR1	FQ	1515	1400	1500	NA	1400	1453	820	1776	0.818
174	CB17-BOR2	FQ	1515	1400	1500	NA	1400	1453	749	1824	0.797
175	CB17-BORL	FQ	1515	1400	1500	NA	1400	1453	683	1501	0.968
176	CB17-DRL	FQ	1515	1400	1500	NA	1400	1453	845	1641	0.885
177	CB23-BOR	FQ	843	840-810	732	NA	758	702	819	864	0.813
178	CB23-BORL	FQ	843	840-810	732	NA	758	702	444	1308	0.538
179	CB29-BORL	FQ	917	870-960	960	NA	910	926	778	855	1.083
180	CB29-EORL	FQ	917	870-960	960	NA	910	926	449	1069	0.868
181	CB35-BOR1	FQ	1463	1400	1490	NA	1400	1437	812	1001	1.436
182	CB35-BOR2	FQ	1463	1400	1490	NA	1400	1437	949	1422	1.011
183	CB35-BORL	FQ	1463	1400	1490	NA	1400	1437	909	1288	1.115
184	CB41-EOR	FQ	1410	1380	1435	NA	1357	1398	857	1238	1.128
185	CB41-BOR	FQ	1410	1380	1435	NA	1357	1398	850	1225	1.140
186	CB41-BORL	FQ	1410	1380	1435	NA	1357	1398	485	1182	1.201

* - Determined from TEPWAP analysis.

Table 23. Pile capacity based on static load test and dynamic analysis for PD/LT (continued).

No	Pile-Case Number	Load Test Type	Deviason's Criteria (kips)	Shape of Curve (kips)	$\Delta = 1'$ (kips)	$\Delta = 0.1B$ (kips)	DeBeer (kips)	Static Resist R_s (kips)	CAPWAP TEPWAP (kips)	Energy Appr. R_U (kips)	$K_{sp} \frac{R_s}{R_U}$
187	CB28-EOD	FQ	960	850-950	1000	NA	1000	965	488	555	1.739
188	CB28-BOR	FQ	960	850-950	1000	NA	1000	965	619	788	1.225
189	CB28-EOR	FQ	960	850-950	1000	NA	1000	965	716	957	1.008
190	CB28-BOR2	FQ	960	850-950	1000	NA	1000	965	563	1113	0.887
191	33P1-EOD	S	>800	800	520	600	800	800	439	657	1.218
192	33P1-BOR	S	>800	800	520	600	800	800	715	898	0.891
193	33P1-EOR	S	>800	800	520	600	800	800	650	923	0.887
194	33P2-EOD	S	490	450-500	450	490	460	490	290*	418	1.172
195	33P2-BOR	S	490	450-500	450	490	460	490	356	520	0.942
196	33P2-EOR	S	490	450-500	450	490	460	490	401	546	0.897
197	33P4-EOD	S	468	350-500	558	592	470	500	400*	625	0.800
198	33P5-EOD	S	164	160-200	244	284	200	200	143*	248	0.808
199	TRD22-EOD	S	354	350	NA	NA	356	350	432	553	0.633
200	TRD22-BOR	S	354	350	NA	NA	356	350	294	504	0.694
201	TRE22-EOD	S	568	570	NA	NA	570	570	575*	720	0.792
202	TRE22-BOR	S	568	570	NA	NA	570	570	618	707	0.808
203	TRP5X-EOD	S	410	500-550	510	560	400	475	484	506	0.939
204	TRP5X-BOR	S	410	500-550	510	560	400	475	395	490	0.968
205	TR131-BOR	S	140	160-200	210	200	200	150	168	169	0.888
206	TRAH-EOR	S	730	650-700	600	650	640	650	218	564	1.152
207	TRBH-BOR	S	325	275-300	337	352	304	300	100	268	1.128
208	TRBP-EOR	S	340	>300	340	340	325	330	248*	308	1.078

* - Determined from TEPWAP analysis.

1 kip = 4.448 kN
1 in = 25.4 mm

APPENDIX B - DATA SET PD

Table 24. Pile/soil and dynamic measurements of data set PD.

REF. NO.	PILE NAME	SKIN SOIL	TOE SOIL	PILE TYPE	LEN. FT	AREA IN2	E MOD KSI	HAMMER	FMX KIPS	EMX K-FT	VMX FT/S	DMX IN	BLOWS/INCH	CAPWAP RUIT KIPS	ENERGY APPROACH KIPS
362	BOR TP1	CLSA	CL	PSC 18	67.0	324.0	6097.2	D46-32	1581.0	41.61	10.10	0.453	5.00	616	1529
321	83E 2 RE	CL	CL	PSC 18	32.5	324.0	5651.5	D 46 T3	1156.3	24.33	8.47	0.824	2.00	333	441
319	S4PC N20	CL	CL	PSC 30	63.0	900.0	5122.0	C5300	1684.1	40.19	4.64	0.632	1.50	337	743
70	DD TP2	ALLUV	CL	CEP12x0.18	37.0	7.0	30000.0	D12	161.0	7.93	11.70	0.848	3.42	123	167
155	BOR T2	CLSI	CL	PSC 12	67.0	144.0	5452.0	D30	541.0	12.56	8.60	0.409	5.00	305	495
69	BOR TP3	ALLUV	CL	CEP12x0.18	38.0	7.0	30000.0	D12	184.0	4.81	10.30	0.438	7.00	183	199
162	EOD T3	CLSI	CL	PSC 14	62.0	196.0	5934.0	D30	558.0	9.86	6.10	0.386	9.17	179	478
156	BOR T3	CLSI	CL	PSC 14	62.0	196.0	5934.0	D30	717.0	16.16	8.10	0.459	7.00	297	644
328	EOD TP1799	SASI	CL	PSC	70.0	96.5	6190.0	MKT DE33	223.0	5.22	4.00	0.587	1.83	101	111
161	EOD T2	CLSI	CL	PSC 12	62.0	144.0	5452.0	D30	476.0	12.74	7.40	0.444	5.00	226	475
329	RES TP1799	SASI	CL	PSC	73.0	96.5	6190.0	MKT DE33	192.0	2.66	3.10	0.232	14.42	226	212
363	BOR TP2	CLSA	CL	PSC 24	77.0	576.0	6500.0	D46-32	1049.0	17.08	3.80	0.257	11.00	643	1178
366	BOR TP5	CLSA	CL	PSC 24	76.0	576.0	6609.2	D46-32	1922.0	37.34	6.60	0.453	14.00	655	1709
365	BOR TP4	CLSA	CL	PSC 18	71.0	324.0	6790.0	D46-32	1279.0	28.96	7.60	0.374	5.00	655	1211
409	EOD PN7	CL SA	CL SA	CEPPE24	60.3	54.8	30000.0	K35	854.2	17.09	9.03	0.501	13.50	507	714
235	BOR L-8	SUCL	CL SI	PSC 12	66.8	144.0	4644.0	ICE 640	480.3	11.83	8.20	0.513	15.00	373	489
410	BOR PN7	CL SI	CL SI	CEPPE24	60.3	54.8	30000.0	K35	854.2	17.09	9.03	0.501	13.50	507	714
252	DD J31	CL TIL	CL TIL	CEPIPE 1	91.0	31.2	30000.0	K35	761.1	40.79	13.41	1.326	2.25	416	553
191	BOR TP1235	SA	CLSA	PSC 14	97.0	196.0	6120.0	VUL 512	636.0	22.47	7.20	0.590	26.00	646	858
276	BOR PN420	CLSA	CLSA	PSC 12	58.0	144.0	5120.0	VUL 06	472.0	11.16	7.90	0.463	5.00	185	404
277	EOD PN420	CLSA	CLSA	PSC 12	58.0	144.0	5120.0	VUL 06	426.0	11.59	8.20	0.862	2.00	89	204
275	BOR PNF2	CLSA	CLSA	PSC 12	58.0	144.0	5120.0	VUL 06	286.0	5.86	4.10	0.409	5.00	93	231
192	BOR TP1259	SA	CLSA	PSC 14	97.0	196.0	6120.0	VUL 512	542.0	18.74	5.00	0.618	28.00	598	688
224	BOR PN111	SACL	CLSI	PSC 16	35.0	256.0	5057.0	CON 65	435.0	4.56	3.30	0.150	166.67	329	702
226	EOD PN111	SACL	CLSI	PSC 16	35.0	256.0	5057.0	CON 65	248.0	1.83	1.90	0.120	44.67	237	308
225	EOD PN110	SACL	CLSI	PSC 16	35.0	256.0	5220.0	CON 65	424.0	4.16	2.90	0.175	25.33	282	466
58	DD TP15	CLSI	CLSI	PSC 18	84.0	324.0	5177.5	CON 160	551.0	16.13	4.30	0.594	2.67	469	400
223	BOR PN110	SACL	CLSI	PSC 16	35.0	256.0	5220.0	CON 65	451.0	4.30	3.60	0.145	52.33	346	629
57	DD TP15	CLSI	CLSI	PSC 18	84.0	324.0	5037.6	CON 160	664.0	19.16	5.50	0.693	5.75	390	530
59	DD TP16	CLSI	CLSI	PSC 14	77.0	196.0	4658.0	CON 160	397.0	19.72	4.50	0.814	2.08	348	366
61	DD TP16	CLSI	CLSI	PSC 14	77.0	196.0	4658.0	CON 160	482.0	23.62	6.20	0.711	9.00	615	690
11	EOD TP6	SASI	CLSI	PSC 12	53.0	144.0	6116.0	VUL 01	385.0	6.18	5.90	0.317	100.00	393	454
10	BORTP6	SASI	CLSI	PSC 12	53.0	144.0	6116.0	VUL 01	219.0	3.02	3.20	0.233	833.33	277	309
60	DD TP16	CLSI	CLSI	PSC 14	77.0	196.0	4658.0	CON 160	460.0	22.20	5.70	0.747	2.67	425	475
62	RES TP15	CLSI	CLSI	PSC 18	84.0	324.0	4658.0	CON 160	604.0	18.08	4.70	0.469	14.00	720	803
258	EOD 258	ALLUV	TIL ALL	CEPIPE 1	98.5	12.1	30000.0	VUL 508	330.3	21.71	14.93	1.112	5.58	308	404

Table 24. Pile/soil and dynamic measurements of data set PD (continued).

REF. NO.	PILE NAME	SKIN SOIL	TOE SOIL	PILE TYPE	LEN. FT	AREA IN2	E MOD KSI	HAMMER	FMX KIPS	EMX K-FT	VMX FT/S	DMX IN	BLOWS/ INCH	CAPWAP Ruff KIPS	ENERGY APPROACH KIPS
52	EOD PIT6NW	CL	TILL	PSC 14	145.0	196.0	4355.0	ICE 660	544.0	30.53	7.70	1.079	10.00	550	621
355	X PNA3	CLSA	TILL	CEP 14x0.5	84.0	21.2	30000.0	D16-32	596.0	27.83	16.20	0.931	5.00	208	591
360	EOD PN126	CL	TILL	PSC 14	70.0	196.0	4000.0	VUL 140C	520.0	19.73	6.70	0.649	11.00	530	640
56	RES PN50	CL	TILL	PSC 14	137.0	196.0	4974.0	ICE 640	324.0	9.58	4.20	0.486	40.00	369	450
51	EOD B611	CL	TILL	PSC 16	145.0	256.0	4355.0	ICE 660	635.0	26.13	6.40	0.783	16.00	571	742
356	X PNB5	CLSA	TILL	CEP 14x0.5	87.0	21.2	30000.0	D16-32	590.0	25.18	15.50	0.810	3.75	178	561
358	BOR PN126	CL	TILL	PSC 14	70.0	196.0	4000.0	VUL 140C	434.0	11.84	5.80	0.430	21.00	442	595
55	RES PN20	CL	TILL	PSC 14	137.0	196.0	4974.0	ICE 640	352.0	10.21	4.60	0.512	80.00	428	467
361	EOD PN177	CL	TILL	PSC 14	70.0	196.0	3920.0	VUL 140C	476.0	19.22	6.10	0.665	12.00	489	616
54	RES PN9	CL	TILL	PSC 14	128.0	196.0	4974.0	ICE 640	407.0	15.23	5.50	0.668	25.00	400	516
359	BOR PN177	CL	TILL	PSC 14	72.0	196.0	4000.0	VUL 140C	413.0	11.51	5.60	0.446	15.00	370	539
53	EOD PN10	CL	TILL	PSC 14	130.0	196.0	4974.0	ICE 640	339.0	11.29	4.50	0.670	12.00	328	360
357	X PNC3	CLSA	TILL	CEP 14x0.5	88.0	21.2	30000.0	D16-32	637.0	29.32	16.80	0.865	5.00	260	661
36	EOD PN1	CL	TILL	CEP 10.75	39.0	5.9	30000.0	CON 65	213.0	9.57	13.20	0.849	5.33	198	222
LARGE DISPLACEMENT PILES SOIL TYPE UNKNOWN															
378	BOR 174	ALLUV	ALLUV	PSC 12	42.0	144.0	6230.0	VUL 508	583.5	12.52	8.35	0.403	10.42	483	601
259	X PN29K	NA	NA	CEP 20x0.5	97.5	12.1	30000.0	MKT DE70	305.6	16.93	14.56	0.928	7.00	257	380
333	X PN25BK	NA	NA	CEP 20x0.5	77.0	30.6	30000.0	MKT DE70	897.0	24.07	14.80	0.513	16.00	794	1004
332	EOD PN7E3	NA	NA	PSC 30	125.0	900.0	5554.1	CON 300	1652.0	29.81	4.20	0.371	17.00	674	774
7	EOD PN210	NA	NA	CEP 12.75	80.0	14.6	30000.0	VUL 50C	224.0	5.93	8.56	0.465	7.50	181	230
334	X PN30K	NA	NA	CEP 20x0.5	70.0	30.6	30000.0	MKT DE70	815.0	21.67	13.40	0.537	40.00	925	925
39	EOR PN30	NA	NA	PSC 30	63.0	900.0	5344.2	CON 300	1746.0	34.10	4.50	0.474	6.00	974	1277
133	EOD PN7	NA	NA	PSC NU	165.0	900.0	4976.0	CON 300	1477.0	27.96	4.20	0.400	17.50	1497	1468
305	RES PN7-61	NA	NA	PSC 18 NU	54.0	324.0	5540.0	CON 5125	1377.0	34.51	9.20	0.606	5.33	490	1044
278	BOR KS21C2	NA	NA	PSC 14	88.0	196.0	4720.0	VUL 506	530.0	13.58	6.80	0.425	23.33	582	697
279	BOR M27A1	NA	NA	PSC 14	93.0	196.0	5122.0	VUL 506	517.0	15.11	7.80	0.483	29.50	565	702
22	EOD PN1	NA	NA	PSC 24 NU	99.0	576.0	5055.0	VUL 506	1210.0	23.54	5.40	0.487	3.17	200	704
280	BOR M29C3	NA	NA	PSC 14	98.0	196.0	4759.4	VUL 506	395.0	11.21	4.40	0.419	0.00	481	547
304	RES PN2	NA	NA	PSC 18	48.0	324.0	5540.0	CON 5125	763.0	17.12	4.20	0.501	0.00	285	547
132	EOD PN6	NA	NA	PSC	134.0	900.0	5057.0	CON 300	1463.0	34.77	3.90	0.490	0.00	1211	1368
399	BOR 20W6	NA	NA	PSC24	92.0	576.0	5888.5	CON E5-2	929.8	21.65	4.19	0.374	0.00	836	992
95	BOR PNPE28	NA	NA	PSC 30	125.0	900.0	5440.5	CON 300	1757.0	33.05	4.30	0.352	0.00	1507	550
38	EOD PN25	NA	NA	PSC 30 NU	162.0	900.0	5300.0	CON 300	1159.0	18.38	2.60	0.299	0.00	1261	1341
281	BOR M29C3	NA	NA	PSC 14	98.0	196.0	4768.6	VUL 506	592.0	17.91	7.20	0.539	13.67	490	702
37	DD PN25	NA	NA	PSC 30 NU	162.0	900.0	5290.0	CON 300	1586.0	26.76	4.20	0.332	13.33	1290	1578

Table 24. Pile/soil and dynamic measurements of data set PD (continued).

REF. NO.	PILE NAME	SKIN SOIL	TOE SOIL	PILE TYPE	LEN. FT	AREA INZ	E MOD KSI	HAMMER	FMX KIPS	EMX K-FT	VMAX FT/S	DMX IN	BLOWS/ INCH	CAPWAP RUII KIPS	ENERGY APPROACH KIPS
6	EOD PN165	NA	NA	CEP 12.75	77.0	14.6	30000.0	VUL 50C	261.0	6.73	10.06	0.504	7.17	185	251
LARGE DISPLACEMENT PILES IN ROCK															
21	BOR TN	AGDITE	AGDITE	PSC 16	38.0	256.0	4280.3	ICE 660	587.0	12.79	5.50	0.371	300.00	578	820
19	RES TN12	AGDITE	AGDITE	PSC 16	65.0	256.0	4278.0	ICE 660	439.0	10.77	4.60	0.403	833.33	532	639
20	BOR CT	AGDITE	AGDITE	PSC 16	65.0	256.0	4278.0	ICE 660	493.0	11.41	4.80	0.384	404.00	715	709
327	X PN213E2	SASI	COOPMAR	PSC 18	38.0	324.0	5500.0	D46-13	908.0	23.51	6.70	0.916	1.08	291	307
125	BOR ET2	CLSI	COOPMAR	PSC 24	91.0	478.0	5302.7	D46-23	1048.0	22.81	5.20	0.524	8.00	337	844
68	BOR PN225	CLSI	COOPMAR	PSC 18 NU	113.0	294.0	30000.0	ICE 1070	694.0	18.93	5.40	0.436	6.00	590	754
66	BOR PN121R9	SI	COOPMAR	PSC 24	76.0	478.0	6060.0	D46-23	1123.0	23.07	5.10	0.643	4.00	224	620
288	BOR PN234A3	SASI	COOPMAR	PSC 18	42.0	324.0	5542.6	D46-13	554.0	11.92	3.40	0.538	2.17	257	286
65	BOR PN120R9	SI	COOPMAR	PSC 24	82.0	478.0	6060.0	D46-23	937.0	16.19	4.20	0.477	6.00	257	604
129	BOR ET3	CLSI	COOPMAR	PSC	91.0	477.0	5469.7	D46-23	1194.0	27.69	5.70	0.392	8.33	651	1298
324	X PN201E2	SASI	COOPMAR	PSC 18	35.0	324.0	5500.0	D46-13	846.0	22.40	6.20	1.105	1.17	224	274
208	BOR21B12	COOPMAR	COOPMAR	OCT24	76.0	477.0	5898.5	D46-23	1225.3	27.75	5.93	0.539	11.08	264	1058
131	RES PN120	CLSI	COOPMAR	PSC	82.0	477.0	5898.5	D46-23	935.0	15.82	4.10	0.393	8.00	236	733
204	PN8B43B0	COOPMAR	COOPMAR	OCT.18	117.0	268.4	5898.5	ICE 1070	624.6	18.07	6.06	0.641	2.33	304	405
199	C-41 BOR	COOPMAR	COOPMAR	PSC 18	103.0	324.0	5469.7	CON 125E	732.1	16.85	4.44	0.414	24.00	621	887
326	X PN209E3	SASI	COOPMAR	PSC 18	36.0	324.0	5500.0	D46-13	932.0	22.89	6.70	0.810	1.58	346	381
385	BOR B43P	COOPMAR	COOPMAR	OCT.18	117.0	268.0	5898.5	ICE 1070	852.1	23.91	6.60	0.477	8.00	605	953
325	X PN205E3	SASI	COOPMAR	PSC 18	36.0	324.0	5500.0	D46-13	806.0	19.03	5.90	0.749	1.75	339	346
106	BOR PN123	SI	COOPMAR	PSC 24	73.0	478.0	5600.5	D46-23	1054.0	23.68	5.70	0.764	1.33	318	375
63	RES PN119R24	SI	COOPMAR	PSC 24	82.0	478.0	6062.0	D16-23	1214.0	22.48	5.40	0.449	3.33	310	720
206	BOR 14B1	COOPMAR	COOPMAR	OCT24	82.0	477.0	5898.0	D46-23	1119.9	24.89	5.55	0.465	5.00	263	898
64	RES PN122B23	SI	COOPMAR	PSC 24	73.0	478.0	6062.0	D16-23	1874.0	36.04	8.20	0.675	3.33	312	887
107	BOR PN123R7	SI	COOPMAR	OCT.24	82.0	477.0	5898.5	DEL46-23	1136.0	27.14	5.42	0.376	18.17	422	1511
254	B1P26BOR	SA	LIMESTN	PSC18"SQ	82.0	324.0	4660.6	DEL D36	983.5	20.58	7.12	0.560	4.00	372	610
425	F20.5 MI	SI	LIMESTN	PSC24	71.0	576.0	5224.4	D4623	1353.5	21.84	5.39	0.371	22.00	925	1259
366	BOR B12P	SA/SI	LIMESTN	PSC18"	77.0	324.0	5057.0	DEL D36	664.1	12.49	4.27	0.349	83.33	921	832
167	BOR PN898B	SA	LIMESTN	PSC 14	97.0	496.0	4896.5	D30	497.0	12.38	5.80	0.447	8.00	458	519
407	B.2P.16B	SA CL	LIMESTN	PSC24	79.0	576.0	5611.1	D46-32	1640.4	28.45	6.41	0.527	3.00	293	794
253	BORPN290	SA/SI	LIMESTN	PSC14	48.1	196.0	5158.2	LINK520	420.4	6.26	4.23	0.296	6.67	324	336
120	BOR PN115	CLSA	LIMESTN	PSC 12	52.0	196.0	6074.6	ICE 520	550.0	10.39	5.70	0.335	21.00	658	652
144	BOR PN5E25	SA	LIMESTN	PSC 30	104.0	900.0	5469.7	CON 300	1333.0	24.69	3.30	0.307	5.00	782	1169
398	BOR-E64	CL	LIMESTN	PSC16"SQ	58.0	256.0	4660.6	V06	632.7	17.63	6.14	0.472	5.50	585	701
143	BOR PN5E22	SA	LIMESTN	PSC 30	120.0	900.0	5469.7	CON 300	1362.0	27.15	3.60	0.333	20.00	915	1701

Table 24. Pile/soil and dynamic measurements of data set PD (continued).

REF. NO.	PILE NAME	SKIN SOIL	TOE SOIL	PILE TYPE	LEN. FT	AREA IN ²	E MOD KSI	HAMMER	FMX KIPS	EMX K-FT	VMX FT/S	DMX IN	BLOWS/ INCH	CAPWAP RUII KIPS	ENERGY APPROACH KIPS
142	BOR PNB5E19	SA	LIMESTN	PSC 30	116.0	900.0	5469.7	CON 300	1487.0	30.13	3.50	0.322	30.00	913	2035
256	EODP 26	SASTONE	LIMESTN	PSC18"SQ	82.0	324.0	4722.7	DEL D36	1093.4	33.26	8.11	0.817	3.00	587	694
422	PN B EOD	SA	LIMESTN	PSC24	71.0	576.0	5469.7	CON 300	1318.1	31.57	5.19	0.473	13.00	1396	1378
285	EOD TP3	CLSA	LIMESTN	PSC 10 NU	58.0	100.0	5120.0	ICE 520	375.0	14.98	8.60	0.768	5.50	256	379
284	BOR PNA4W	CLSA	LIMESTN	PSC 14	32.0	196.0	5122.0	ICE 520	380.0	5.18	4.00	0.241	56.67	438	481
255	B11P50B0	SA	LIMESTN	PSC18"SQ	77.0	324.0	4660.6	DEL D36	841.3	21.75	6.61	0.617	12.00	619	745
393	EOD-15-3	SA SI	LIMESTN	PSC10	58.0	100.0	4658.0	VUL1	248.7	5.32	6.09	0.397	8.33	242	247
257	B13P48B0	SA	LIMESTN	PSC18"SQ	77.0	324.0	4660.6	DEL D36	841.3	21.75	6.61	0.617	12.00	619	745
415	EOD PN1	SA	LIMESTN	PSC18	52.4	324.0	4976.4	D16-32	626.1	11.36	4.73	0.369	7.00	454	533
387	EORPN20	SA	LIMESTN	PSC18"SQ	75.0	324.0	4660.6	DEL D36	419.9	6.47	3.16	0.284	5.67	330	337
119	BOR PN11	CLSA	LIMESTN	PSC 12	53.0	144.0	6343.5	ICE 520	466.0	11.10	6.20	0.430	18.00	455	549
388	EODPN23	SA	LIMESTN	PSC18"SQ	75.0	324.0	4660.6	DEL D36	419.9	6.47	3.16	0.284	5.67	330	337
196	X TP3	CLSA	LIMESTN	CEP	74.0	9.6	30000.0	LB 440	247.0	7.75	9.50	0.733	20.00	250	238
236	BOR 36	CLAY	LIMESTN	PSC	52.0	196.0	6199.4	MKT DE 4	556.6	6.82	6.17	0.221	20.00	372	603
207	PN9B BOR	MARK	MARK	OCT 24	75.0	477.0	5898.5	DEL 46-2	1329.7	29.60	5.91	0.464	12.50	258	1306
411	BOR 13B6	OVERBURD	MARL	OCT 24	115.0	26.0	30000.0	D46-23	1378.9	31.86	6.19	0.485	35.00	749	1489
417	BOR2/59	MARL	MARL	OCT18	115.0	261.0	5898.5	ICE1070	847.2	24.17	6.70	0.494	5.50	526	858
418	BOR4/58	MARL	MARL	OCT18	115.0	261.0	5898.5	ICE1070	882.4	26.51	6.84	0.534	5.50	513	889
412	BOR 5B.5	MARL	MARL	OCT 18	116.0	268.0	5898.5	ICE1070	819.3	21.29	6.65	0.458	8.00	508	877
169	EOD PNB4	TILL	ROCK	CEP 18	69.0	27.5	30000.0	ICE 1070	592.0	19.35	10.90	0.690	6.00	450	542
282	DD SD91	CLSA	ROCK	PSC 10 NU	47.0	100.0	4950.0	VUL 50C	211.0	4.63	5.20	0.353	30.00	213	288
283	EOD A8345	CLSA	ROCK	PSC 10	47.0	100.0	4430.0	VUL NO.1	166.0	3.71	4.40	0.352	8.00	180	187
126	EOD TP1	SASI	ROCK	PSC 12	57.0	144.0	5138.3	CON 65E5	548.0	15.24	9.30	0.496	10.00	401	614
168	EOD PNB1	TILL	ROCK	CEP 18	69.0	27.5	30000.0	ICE 1070	570.0	17.32	10.30	0.647	4.50	484	478
127	EOD TP2	SASI	ROCK	PSC 12	57.0	144.0	5057.0	CON 65E5	601.0	17.16	10.30	0.580	15.00	386	637
139	BOR PNB7N6	SA	SASTONE	PSC 30	100.0	900.0	5469.7	CON 300	1181.0	21.35	2.90	0.300	15.00	1477	1397
312	BOR TP8	SA	SASTONE	PSC 14	77.0	196.0	4720.0	ICE 640	765.0	19.72	6.20	0.488	14.00	507	846
138	BOR PNB7E	SA	SASTONE	PSC 30	116.0	900.0	5288.2	CON 300	1319.0	28.41	3.50	0.374	15.00	1200	1547
306	BOR TP1	SA	SASTONE	PSC 14	77.0	196.0	4720.0	ICE 640	517.0	10.98	5.70	0.352	36.00	544	694
311	BOR TP7	SA	SASTONE	PSC 14	77.0	196.0	4720.0	ICE 640	487.0	11.22	5.20	0.378	10.00	407	563
307	BOR TP10	SA	SASTONE	PSC 14	77.0	196.0	4720.0	ICE 640	661.0	14.21	6.40	0.359	37.50	604	884
309	BOR TP5	SA	SASTONE	PSC 14	77.0	196.0	4720.0	ICE 640	316.0	7.22	3.80	0.371	11.50	316	378
141	EOD PNB5E18	SA	SASTONE	PSC 30 NU	155.0	900.0	6243.1	CON 300	2231.0	41.64	5.20	0.423	25.00	1492	2158
316	EOD TP8	SA	SASTONE	PSC 14	77.0	196.0	4720.0	ICE 640	509.0	13.57	5.50	0.521	6.00	354	474
146	EOD PN4	SA	SASTONE	PSC 30	134.0	900.0	5385.8	CON 300	1211.0	28.71	4.10	0.432	8.33	1106	1248
308	BOR TP3	SA	SASTONE	PSC 18	77.0	324.0	4767.2	ICE 640	608.0	8.76	4.40	0.243	28.50	476	755
145	BOR PN5	SA	SASTONE	PSC 30	105.0	900.0	5329.8	CON 300	1868.0	35.56	5.10	0.437	5.00	761	1340
140	EOD PNB6E25	SA	SASTONE	PSC 30 NU	155.0	900.0	6163.6	CON 300	1512.0	28.53	3.60	0.433	33.33	1364	1479

Table 24. Pile/soil and dynamic measurements of data set PD (continued).

REF NO.	PILE NAME	SKIN SOIL	TOE SOIL	PILE TYPE	LEN. FT	AREA IN ²	E MOD KSI	HAMMER	FMX KIPS	EMX K-FT	VMX FT/S	DMX IN	BLOWS/ INCH	CAPWAP RAIL KIPS	ENERGY APPROACH KIPS
313	BOR TP9	SA	SASTONE	PSC 14	77.0	196.0	4720.0	ICE 640	614.0	14.46	7.40	0.393	39.00	515	829
314	EOD TP1	SA	SASTONE	PSC 14	77.0	196.0	4720.0	ICE 640	494.0	13.56	5.50	0.705	2.50	234	295
315	EOD TP3	SA	SASTONE	PSC 18	77.0	324.0	4720.0	ICE 640	665.0	10.92	4.70	0.382	13.00	357	571
123	EOD PN225E	SA	SASTONE	PSC 30	132.0	900.0	5500.0	CON 300	1127.0	26.85	2.80	0.398	8.33	1167	1244
310	BOR TP6	SA	SASTONE	PSC 18	77.0	324.0	4814.4	ICE 640	740.0	13.42	5.50	0.362	9.00	320	681
74	EOD PNE17	SI	SHALE	CEP 11x0.4	41.0	12.2	30000.0	LB 640	531.0	23.70	15.40	0.913	50.00	500	610
LARGE DISPLACEMENT PILES IN SAND															
212	EOD PN316	CLSI	SA	PSC 12	52.0	144.0	5875.4	CON 65	391.0	10.12	6.30	0.483	7.58	470	395
213	EOD PN332	CLSI	SA	PSC 12	62.0	144.0	5652.1	CON 65	411.0	11.65	6.80	0.712	2.42	203	248
197	BOR PN14	SASI	SA	PSC 14	92.0	196.0	5496.7	VUL 010	628.0	16.64	6.70	0.397	5.00	690	669
81	BOR TP11	SASI	SA	PSC 36	47.0	487.0	6720.0	CON 300E	1287.0	31.80	5.50	0.464	10.00	976	1353
215	BOR P5	SA CL	SA	PSC 14*	42.5	196.0	5469.7	KOBE 25	495.8	10.07	5.77	0.317	15.00	413	631
209	DD PN69	CLSI	SA	PSC 12	72.0	144.0	6053.5	CON 65	366.0	9.01	5.80	0.512	10.50	400	356
198	BOR PN24	SASI	SA	PSC 14	82.0	196.0	5469.7	VUL 010	551.0	14.90	6.10	0.397	10.00	573	720
337	EOD TP4	SASI	SA	CEP 12/75	57.0	9.8	30000.0	VUL 506	256.0	11.01	11.80	0.807	10.00	262	291
210	EOD PN232	CLSI	SA	PSC 12	68.0	144.0	5690.9	CON 65	490.0	12.94	8.10	0.571	4.17	410	383
270	199EOD	SA/SISA	SA	PSC 12	46.0	144.0	5896.0	D30-23	479.7	13.86	5.63	0.573	2.92	302	363
83	BOR TP21	SASI	SA	PSC 36	63.0	487.0	6782.4	CON 300E	1390.0	33.97	5.60	0.473	8.00	864	1363
364	BOR TP3	CLSA	SA	PSC 18	102.0	324.0	6885.4	D46-32	1724.0	43.89	10.40	0.405	10.00	1264	2086
383	TP8	SA	SA	OCT16.5"	92.0	225.0	6790.0	D36-23	866.4	21.62	7.19	0.412	16.00	601	1095
220	EOD P2	SA CL	SA	PSC 14*	47.5	196.0	6343.5	KOBE 25	600.0	12.19	6.08	0.416	10.00	372	568
216	EOD P7	SA CL	SA	PSC 14*	47.5	196.0	5898.5	KOBE 25	652.3	13.57	7.38	0.442	8.00	359	574
222	EOD P6	SA CL	SA	PSC 14*	47.5	196.0	5469.7	KOBE 25	697.9	11.45	8.09	0.405	6.42	287	490
322	B 70 P 5	CL	SA	PSC24	66.7	576.0	5888.9	V 020	987.4	19.38	3.83	0.353	41.67	1259	1235
271	293BOR	SA/SASI	SA	PSC12	47.0	144.0	5896.0	D30-23	630.9	14.50	6.22	0.368	8.33	550	714
149	BOR PN12	SA	SA	CEP 16	77.0	16.8	30000.0	K25	359.0	14.07	11.10	0.727	70.83	411	456
219	EOD P11	SA CL	SA	PSC 14*	42.5	196.0	6343.5	KOBE 25	604.3	9.66	7.12	0.299	15.00	383	634
5	EOD PA8	NA	SA	PSC 18	114.0	324.0	5787.0	VUL 020	891.0	26.47	6.40	0.686	8.33	598	788
330	X TP1799	SI	SA	PSC	70.0	96.5	6190.0	MKT DE33	251.0	6.84	4.90	0.600	2.67	137	168
181	EOR PN1056	SASI	SA	PSC 14	77.0	196.0	6450.9	VUL 020	793.0	25.23	8.30	0.625	2.50	408	591
73	EOD PN398	CLSI	SA	PSC 20	78.0	400.0	5682.1	D46-32	1611.0	37.17	9.10	0.480	7.25	740	1444
214	EOD TP1	CLSI	SA	PSC 12	52.0	144.0	5655.4	CON 65	358.0	9.86	5.90	0.485	10.00	450	405
91	EOD TP21	SASI	SA	PSC 36	63.0	487.0	6782.4	CON 300E	1081.0	26.87	4.60	0.445	8.67	850	1151
165	BOR PN1056	CLSI	SA	PSC 14	77.0	196.0	5057.0	VUL 512	560.0	32.11	6.40	0.894	5.00	502	704
71	EOD PN392	CLSI	SA	PSC 20	79.0	400.0	5794.2	VUL 512	1252.0	27.85	7.20	0.444	14.00	728	1297
9	PN1	NA	SA	CEP 16	67.0	12.4	30000.0	D16-32	338.0	13.12	14.90	0.742	5.00	265	334

Table 24. Pile/soil and dynamic measurements of data set PD (continued).

REF. NO.	PILE NAME	SKIN SOIL	TOE SOIL	PILE TYPE	LEN. FT	AREA IN2	E MOD KSI	HAMMER	FMX KIPS	EMX K-FT	VMX FT/S	DMX IN	BLOWS/ INCH	CAPWAP Rull KIPS	ENERGY APPROACH KIPS
336	BOR TP4	SASI	SA	CEP 12.75	57.0	9.8	30000.0	VUL 506	264.0	11.95	12.70	0.841	11.00	267	308
377	151-BOR	CL,SC,S	SA	PSC12	42.0	144.0	6230.0	MKT DE40	490.5	10.40	6.69	0.332	19.00	486	650
164	BOR PN1040	CLSI	SA	PSC 14	77.0	196.0	6343.5	VUL 512	621.0	19.18	6.50	0.483	8.00	666	757
211	EOD PN244	CLSI	SA	PSC 12	66.0	144.0	5595.6	CON 65	450.0	12.00	7.30	0.637	3.08	300	300
221	EOD P8	SA CL	SA	PSC 14*	47.5	196.0	6343.5	KOBE 25	699.6	14.23	7.18	0.409	9.00	443	657
286	BOR TP2	CLSA	SA	PSC 14	38.0	196.0	5115.6	VUL 06	310.0	6.66	4.40	0.428	2.50	185	193
190	TP2 BOR	SI/CL	SA	PSC 12*	65.0	144.0	5898.5	VUL 512	561.4	16.42	8.90	0.650	5.00	317	464
287	EOR TP1	CLSA	SA	PSC 14	48.0	196.0	5243.4	VUL 06	345.0	8.09	6.00	0.606	2.83	193	202
217	EOD P7	SA CL	SA	PSC 14*	47.5	196.0	5898.5	KOBE 25	652.3	13.57	7.38	0.442	8.00	377	574
218	EOD P 10	SA CL	SA	PSC 14*	42.5	196.0	6253.2	KOBE 25	530.1	9.82	5.91	0.330	12.00	396	570
72	EOD PN396	CLSI	SA	PSC 20	79.0	400.0	5680.0	D46-32	1597.0	37.29	8.70	0.486	6.67	810	1407
331	151.EOD	CL/SA	SA	PSC12	42.0	144.0	6230.0	MKT DE40	531.7	12.41	7.77	0.402	10.58	499	600
150	EOD PN12	SA	SA	CEP 16	77.0	16.8	30000.0	K25	368.0	15.72	10.90	0.787	36.17	438	463
389	EOD TP1	SA SAT	SA SAT	CEPIPE 1	72.3	12.4	30000.0	D16-32	408.2	15.98	15.76	0.758	6.67	269	422
419	TP2 BOR	SA SI	SA SI	PSC24	96.0	576.0	7040.0	D80-23	1506.4	40.95	4.91	0.410	27.00	1630	2199
397	EOD-TP1	SA SI	SA SI	CEP16*	56.0	12.4	30000.0	D16-32	358.0	13.94	16.79	0.793	20.00	262	397
426	EOD PHAS	SA	SA TILL	CEP18	117.3	27.5	30000.0	K45	550.5	26.98	10.73	1.034	1.50	346	381
368	BOR PN317	SI	SAGR	CEP 14x0.37	124.0	16.1	30000.0	MH 35	523.0	34.18	15.30	1.169	10.00	513	646
369	EOD PN317	SI	SAGR	CEP 14x0.37	125.0	16.1	30000.0	MH 35	465.0	34.61	15.00	1.343	3.00	383	496
367	BOR PN243	SI	SAGR	CEP 14x0.37	130.0	16.1	30000.0	MH 35	539.0	40.98	16.00	1.313	12.00	622	704
8	EOD PN15E	NA	SAGR	CEP 10.75	120.0	10.1	30000.0	VUL 06	209.0	12.27	11.38	0.925	6.67	235	274
335	X PN2031	SASI	SAROCK	PSC 12	57.0	144.0	5169.7	CON 65E5	481.0	15.34	8.90	0.628	9.00	342	498
350	EOD PN13	CLSI	SASI	PSC 12	30.0	144.0	4400.0	D30-23	556.0	19.12	8.60	1.083	1.33	132	250
4	BOR PN24	SASI	SASI	PSC 20	126.0	400.0	5947.0	VUL 020	925.0	23.50	5.60	0.476	7.00	558	911
32	BOR TP26	SASI	SASI	PSC 12	64.0	144.0	4660.6	D30-23	654.0	26.04	10.00	0.660	4.00	328	687
348	BOR PN43	CLSI	SASI	PSC 12	30.0	144.0	4400.0	D30-23	539.0	15.98	7.10	0.480	2.00	338	391
87	EOD PN3	SIGR	SASI	CEP 12x0.6	60.0	14.6	30000.0	ICE 520	296.0	10.00	10.00	0.695	10.67	312	304
82	BOR TP11	SIGR	SASI	PSC 36	47.0	487.0	6720.0	CON 300E	1287.0	32.00	5.50	0.464	10.00	878	1362
3	BOR PA35	SASI	SASI	PSC 20	126.0	400.0	5839.0	VUL 020	928.0	22.95	5.40	0.565	4.00	405	676
354	EOR PN310	CLSI	SASI	PSC 12	32.0	144.0	4400.0	D30-23	368.0	7.00	6.00	0.311	4.00	203	299
342	BOR PN13	CLSI	SASI	PSC 12	30.0	144.0	4400.0	D30-23	574.0	19.60	7.80	0.628	1.67	285	383
303	RES G37	SASI	SASI	PSC 14	83.0	196.0	5331.5	VUL 010	494.0	14.29	5.40	0.501	4.00	336	457
343	BOR PN19	CLSI	SASI	PSC 12	30.0	144.0	4400.0	D30-23	586.0	16.24	7.40	0.524	1.67	292	347
301	RES B58	SASI	SASI	PSC 14	85.0	196.0	5250.0	VUL 010	439.0	11.35	4.90	0.424	12.50	392	540
344	BOR PN218	CLSI	SASI	PSC 12	30.0	144.0	4400.0	D30-23	469.0	13.90	7.50	0.471	2.00	294	344
34	EOD TP26	SASI	SASI	PSC 12	62.0	144.0	4660.0	D30-23	592.0	23.21	10.20	0.995	1.25	206	310
92	EOD TP23	SIGR	SASI	PSC 54	54.0	905.0	7420.0	CON 300E	2220.0	29.60	4.90	0.304	25.17	1182	2067
269	EOD IP3	SASI	SASI	PSC 12	65.0	144.0	5100.0	K25	618.0	19.00	9.90	0.670	5.83	400	542

Table 24. Pile/soil and dynamic measurements of data set PD (continued).

REF. NO.	PILE NAME	SKIN SOIL	TOE SOIL	PILE TYPE	LEN. FT	AREA IN2	E MOD KSI	HAMMER	FMX KIPS	EMX K-FT	VMX FT/S	DMX IN	BLOWS/ INCH	CAPWAP RULI KIPS	ENERGY APPROACH KIPS
351	EOD PN213	CLSI	SASI	PSC 12	32.0	144.0	4400.0	D30-23	477.0	18.34	8.40	1.275	1.33	118	217
302	RES F14	SASI	SASI	PSC 14	91.0	196.0	5200.0	VUL 010	505.0	15.74	5.90	0.519	4.33	352	504
349	BOR PN49	CLSI	SASI	PSC 12	30.0	144.0	4400.0	D30-23	440.0	9.41	5.30	0.316	2.17	335	290
347	BOR PN37	CLSI	SASI	PSC 12	32.0	144.0	4400.0	D30-23	513.0	12.92	6.80	0.369	2.50	402	403
90	EOD TP13	SIGR	SASI	PSC 36	46.0	487.0	7270.0	CON 300E	1109.0	23.51	4.70	0.348	27.33	930	1467
300	EOD TP9	SASI	SASI	PSC 18	56.0	324.0	5057.0	MKT DE70	554.0	9.71	3.90	0.369	4.17	264	383
353	EOD PN49	CLSI	SASI	PSC 12	30.0	144.0	4400.0	D30-23	436.0	16.54	8.00	1.111	1.00	127	188
352	EOD PN26	CLSI	SASI	PSC 12	32.0	144.0	4400.0	D30-23	470.0	20.33	8.70	1.368	1.08	110	213
346	BOR PN31	CLSI	SASI	PSC 12	32.0	144.0	4355.1	D30-23	555.0	14.92	7.30	0.387	2.83	390	484
79	BOR PN3	SIGR	SASI	CEP 12x0.6	60.0	14.6	30000.0	ICE 520	401.0	15.18	12.60	0.714	19.00	376	475
89	EOD TP11	SIGR	SASI	PSC 36	47.0	487.0	6720.0	CON 300E	1068.0	23.99	4.50	0.413	19.58	786	1241
33	EOD TP114	SASI	SASI	PSC 12	64.0	144.0	4583.2	D30-23	591.0	28.02	9.30	1.243	1.08	250	310
268	EOD IP1	SASI	SASI	PSC 12	65.0	144.0	5346.0	K25	543.0	16.39	8.60	0.566	6.25	409	542
345	BOR PN26	CLSI	SASI	PSC 12	32.0	144.0	4400.0	D30-23	504.0	13.69	6.70	0.397	2.67	385	426
30	BOR TP114	SASI	SASI	PSC 12	64.0	144.0	4583.2	D30-23	694.0	34.86	11.80	0.951	3.00	325	651
299	RES PN6	SASI	SASI	PSC 14	107.0	196.0	5171.2	VUL 506	422.0	10.34	4.90	0.418	12.00	495	495
31	BOR TP2	SASI	SASI	PSC 12	64.0	144.0	4583.2	D30-23	670.0	26.07	11.20	0.641	3.00	320	642
318	B9P3BOR	SACY	SACY	PSC 18	41.0	324.0	5120.0	D4602	817.6	13.30	4.26	0.239	8.00	628	876
234	75 ABUT	Sa/Si/Gr	Sa/Si/Gr	CEP 10.75	53.7	8.3	30000.0	VUL 50C	127.2	5.37	8.00	0.656	5.00	135	150
48	RES PN125	SI	SI	PSC 24	82.0	478.0	6062.0	D46-23	1553.0	33.67	7.10	0.516	4.00	243	1055
49	RES PN125	SI	SI	PSC 24	82.0	478.0	6062.0	D62-22	1008.0	26.81	4.90	0.810	3.00	287	563
370	RES TP13	SI	SIGR	CEP 14x0.37	84.0	16.1	29990.9	ICE 422	284.0	6.85	7.60	0.369	40.00	323	417
371	RES TP6	SI	SIGR	CEP 14x0.37	79.0	16.0	29990.9	ICE 422	325.0	7.59	7.60	0.402	78.00	368	439
320	P3 P1R	SI/SA	SI/SA	PSC 18	63.0	324.0	4672.8	D 46-02	757.2	10.75	4.35	0.226	5.00	532	606
323	PIER 7 P	SI/SA	SI/SA	PSC 18	87.5	324.0	5244.5	D4602	1026.9	23.28	6.83	0.354	8.00	480	1166

SMALL DISPLACEMENT PILES IN CLAY

40	BOR D12N	CL	CL	HP 10x42	46.0	12.4	30000.0	MKT 9B3	208.0	2.68	10.20	0.237	34.00	140	241
245	TP4 EOD	CL	CL	HP 14x73	27.0	21.4	30000.0	KOBE 25	398.4	9.43	9.78	0.478	4.00	226	311
152	BOR R1	CLSI	CL	HP 14x73	71.0	21.4	30000.0	D30	548.0	19.48	13.30	0.577	8.00	422	666
153	BOR R10	CLSI	CL	HP 14x73	72.0	21.4	30000.0	D30	583.0	21.44	13.80	0.602	10.00	456	733
246	TP4 BOR	CL	CL	HP 14x73	27.0	21.4	30000.0	KOBE 25	433.8	10.71	10.72	0.493	4.25	235	353
154	BOR T1	CLSI	CL	HP 10x42	72.0	12.4	30000.0	D30	392.0	19.51	14.00	0.813	8.00	375	499
41	EOD D18E	CL	CL	HP 10x42	44.0	12.4	30000.0	MKT 9B3	223.0	2.41	10.50	0.220	23.00	117	220
160	EOD T1	CLSI	CL	HP 10x42	72.0	12.4	30000.0	D30	336.0	17.99	13.20	0.793	2.83	230	377
158	EOD R1	CLSI	CL	HP 14x73	71.0	21.4	30000.0	D30	511.0	16.92	12.40	0.543	3.17	285	473
159	EOD R10	CLSI	CL	HP 14x73	72.0	21.4	30000.0	D30	498.0	14.75	12.00	0.495	6.67	316	549

Table 24. Pile/soil and dynamic measurements of data set PD (continued).

REF. NO.	PILE NAME	SKIN SOIL	TOE SOIL	PILE TYPE	LEN. FT	AREA IN2	E MOD KSI	HAMMER	FMX KIPS	EMX K-FT	VMX FT/S	DMX IN	BLOWS/ INCH	CAPWAP RUIT KIPS	ENERGY APPROACH KIPS
244	TP3 20FT	CL	CL	HP14x73	42.1	21.4	30000.0	KOBZ 25	349.9	7.97	8.67	0.462	3.00	209	241
424	BOR TP2	CL SI	CL SI	HP14x73	42.1	21.4	30000.0	K25	506.3	18.07	13.30	0.768	2.33	331	362
243	EOD TP2	CL SI	CL SI	HP 14X73	42.1	21.4	30000.0	K25	348.4	7.60	8.97	0.444	4.83	264	281
423	EOD TP2	CL SI	CL SI	HP14x73	42.1	21.4	30000.0	K25	506.3	18.07	13.30	0.768	2.33	326	362
185	EOD TP1	CLSA	CLSA	HP 10x42	49.0	12.4	30000.0	FEC 1500	288.0	8.10	11.50	0.624	1.75	145	163
274	BOR TP2	CL-SA	CL-SA	HP14	42.0	21.4	30000.0	K25	465.1	10.80	11.39	0.549	4.42	252	335
43	EOR D112E	CL	TILL	HP 10X42	53.0	12.4	30000.0	MKT 9B3	238.0	2.74	10.90	0.219	60.00	201	279
187	EOD PN40	CL	TILL	HP 12x74	47.0	21.8	30000.0	LB 520	473.0	12.28	11.50	0.486	26.00	517	562
44	EOR D6W	CL	TILL	HP 10x42	59.0	12.4	30000.0	DROP	207.0	7.39	8.70	0.509	60.00	221	337
186	EOD PN38	CL	TILL	HP 12X74	47.0	21.8	30000.0	LB 520	390.0	9.86	9.40	0.430	26.00	489	505
42	EOR D110S	CL	TILL	HP 10x42	55.0	12.4	30000.0	DROP	224.0	7.23	9.30	0.475	50.00	256	351
SMALL DISPLACEMENT PILES IN ROCK															
273	69 EOD	SCORIA	CLAYSTN	HP10x57	43.3	16.7	30000.0	MKTDE50	522.4	24.65	15.66	0.810	6.00	473	606
272	177 EOD	SCORIA	CLAYSTN	HP10x57	43.3	16.7	30000.0	MKTDE50	473.6	17.68	13.67	0.661	6.00	421	513
189	BOR PN224	SASI	COOPMAR	HP 12x53	40.0	15.5	30000.0	K25	374.0	11.72	11.90	0.526	10.00	305	449
427	BOR PN246	CLSA	COOPMAR	HP 14x73	54.0	21.4	30000.0	K25	541.0	14.52	13.20	0.455	9.00	475	616
67	BOR PN280	CLSA	COOPMAR	HP 14x73	48.0	21.4	30000.0	K25	443.0	11.91	10.60	0.431	7.00	383	498
188	BOR PN117	SASI	COOPMAR	HP 14x89	48.0	26.2	30000.0	K25	599.0	12.44	12.00	0.369	18.00	504	703
18	EOD J8	CLSHALE	DOLOM	OEP 9.6	45.0	16.0	30000.0	RAY 50	417.0	22.04	12.50	0.933	55.00	511	556
13	BOR D418	CLSHALE	DOLOM	OEP 9.6	45.0	16.0	30000.0	RAY 150C	468.0	10.13	7.50	0.458	47.00	482	507
16	EOD D418	CLSHALE	DOLOM	OEP 9.6	45.0	16.0	30000.0	RAY 150C	454.0	12.26	9.70	0.519	90.00	490	555
14	BOR J3	CLSHALE	DOLOM	OEP 9.6	113.0	16.0	30000.0	RAY 50	431.0	22.23	13.80	0.826	33.33	563	623
17	EOD J1	CLSHALE	DOLOM	OEP 9.6	162.0	16.0	30000.0	RAY 50	378.0	26.02	12.80	1.266	26.00	460	479
15	EOD D205	CLSHALE	DOLOM	OEP 9.6	77.0	16.0	30000.0	RAY 150C	378.0	14.84	9.90	0.740	36.00	380	464
193	DD PN355E6	SASI	LIMESTN	HP 10x42	24.0	12.0	30000.0	D12	311.0	6.94	12.60	0.448	7.00	222	282
180	EOD PN7	CLSA	LIMESTN	HP 10x57	72.0	16.8	30000.0	LB 520	314.0	10.86	8.80	0.580	41.67	364	432
195	EOD PN375D2	SASI	LIMESTN	HP 10x42	32.0	12.0	30000.0	D12	304.0	6.87	12.60	0.445	6.00	308	270
97	BOR SHD1	CLSA	LIMESTN	HP 12x53	82	15.5	30000.0	ICE 640	271.0	11.92	8.30	0.721	2.00	217	234
233	EOD A-5-	CLAY	LIMESTN	HP10X57	67.0	16.7	30000.0	DEL D16-	453.7	13.61	15.84	0.640	10.00	409	441
99	EOD SHD1	CLSA	LIMESTN	HP 12x53	82.0	15.5	30000.0	ICE 640	224.0	11.27	7.20	0.920	1.33	148	162
194	DD PN375P1	SASI	LIMESTN	HP 10x42	32.0	12.0	30000.0	D12	306.0	7.13	12.90	0.472	12.00	240	308
232	BOR TP13	SA	LIMESTN	HP14X74	38.0	21.6	30000.0	MKT 9B3	394.4	4.72	10.99	0.223	41.67	393	458
428	TP4EOD	SA	ROCK	HP12x74	36.3	21.8	30000.0	D25-32	520.9	19.31	13.42	0.730	5.00	297	498
249	EOD 4 DI	CL	ROCK	HP 12X53	58.0	15.6	30000.0	IHC S35	459.6	16.51	14.92	0.588	20.00	473	621
170	EOD PND10	CLTILL	ROCK	OEP 18	64.0	27.5	30000.0	ICE 1070	601.0	17.90	11.30	0.685	5.00	531	485
248	PN28EOD	CL	ROCK	HP10x57	48.0	16.7	30000.0	KOBE K-1	354.0	8.04	10.27	0.428	166.67	348	445

Table 24. Pile/soil and dynamic measurements of data set PD (continued).

REF. NO.	PILE NAME	SKIN SOIL	TOE SOIL	PILE TYPE	LEN. FT	AREA IN ²	E MOD KSI	HAMMER	FMX KIPS	EMX K-FT	VMX FT/S	DMX IN	BLOWS/ INCH	CAPWAP RUII KIPS	ENERGY APPROACH KIPS
229	PILE 6 B	CU/SI	ROCK	HP14X117	97.0	34.4	30000.0	VUL 016	589.6	25.16	9.12	0.685	33.33	664	844
50	EOD PN12	CL	ROCK	HP 10X57	57.0	16.8	30000.0	VUL 08	505.0	9.74	11.20	0.496	833.33	505	470
405	PN8 EOD	SA	SHALE	HP10x57	37.0	16.8	30000.0	V 06	275.6	5.62	6.83	0.389	22.33	302	311
408	EOD TP2	NA	SHALE	HP10x57	37.3	16.8	30000.0	V06	168.8	4.09	5.03	0.371	15.00	191	224
406	PN7 EOD	SA	SHALE	HP10x57	37.0	16.8	30000.0	V 06	275.6	5.62	6.83	0.389	22.33	302	311
SMALL DISPLACEMENT PILES IN SAND															
184	RES TP3	SI	GR	HP 10x12	88.0	12.4	30000.0	ICE 440	202.0	6.94	9.30	0.624	10.00	179	230
109	BOR TP1	SA	SA	HP 14x73	87.0	21.4	30000.0	VUL 06	316.0	9.88	8.20	0.725	2.00	126	194
121	EOD TP2	SASI	SA	HP 12x179	38.0	6.7	30000.0	FEC 1500	204.0	11.07	13.80	0.888	5.00	225	244
151	EOD PN3	SASI	SA	HP 12x74	63.0	21.8	30000.0	VUL 010	511.0	21.64	13.50	0.832	6.00	415	520
420	TP1 EOD	SA CL	SA CL	HP14x73	60.3	21.4	30000.0	K25	464.4	12.97	12.11	0.584	5.00	353	397
421	BOR TP1	SA CL	SA CL	HP14x73	60.3	21.4	30000.0	K25	434.9	12.87	10.69	0.551	8.00	390	457
395	BOR-TP4	SA SI	SA SI	HP14x11	117.0	26.1	30000.0	K-45	591.5	25.61	11.09	0.903	1.00	238	323
46	EOD E18	CLSI	SASI	OEP 12	33.0	8.1	30000.0	VUL 06	146.0	9.30	9.90	1.244	1.25	95	109
80	BOR PN4	SIGR	SASI	OEP 12x0.6	60.0	14.6	30000.0	ICE 520	339.0	11.88	11.80	0.677	15.00	318	383
88	EOD PN4	SIGR	SASI	OEP 12x0.6	60.0	14.6	30000.0	ICE 520	340.0	12.86	12.00	0.730	7.92	345	360
23	BOR PN9	SASI	SASI	HP 12x74	42.0	21.8	30000.0	VUL 01	274.0	4.27	6.30	0.230	833.33	340	443
24	DD PN83	SASI	SASI	HP 12x53	58.0	15.6	30000.0	K13	422.0	11.30	13.70	0.553	1.92	177	252
26	X PN71	SASI	SASI	HP 12x53	112.0	15.6	30000.0	K13	343.0	9.24	11.80	0.540	3.58	204	271
25	DD PN83	SASI	SASI	HP 12x53	104.0	15.6	30000.0	K13	336.0	8.62	11.20	0.524	3.58	212	258
45	BOR A213	CLSI	SASI	OEP 12	86.0	8.1	30000.0	VUL 06	190.0	10.24	10.50	0.911	8.33	205	238
28	X PN80	SASI	SASI	HP 12x53	58.0	15.6	30000.0	K13	383.0	9.87	12.50	0.458	3.50	266	319
47	EOD J210	CLSI	SASI	OEP 12	67.0	8.1	30000.0	VUL 06	166.0	10.54	10.60	1.128	1.67	106	146
86	EOD PN2	SIGR	SASI	HP 10x42	56.0	12.4	30000.0	ICE 520	208.0	11.49	7.80	0.933	3.17	202	221
27	X PN80	SASI	SASI	HP 12x53	58.0	15.6	30000.0	K13	340.0	7.97	11.20	0.475	2.50	186	219
85	EOD PN2	SIGR	SASI	HP 10x42	56.0	12.4	30000.0	ICE 520	214.0	12.03	8.30	0.934	3.08	210	229
84	EOD PN1	SIGR	SASI	HP 12x74	56.0	21.7	30000.0	ICE 520	399.0	12.01	9.70	0.564	5.42	354	385
227	EOR PN12	SA	SA/COBBL	HP14x89	66.4	26.1	30000.0	K25	623.6	13.48	10.69	0.440	7.25	471	560
228	EOD PN2	SA	SA/COBBL	HP14X89	103.1	26.1	30000.0	K25	494.5	12.10	9.97	0.505	10.00	432	480
230	K7EOD	SA/SI	SA/SI	HP14X73	154.5	21.4	30000.0	VUL010	508.6	21.04	13.32	0.832	16.00	391	564
384	BOR TP1	SI	SI	HP305MMX	68.8	17.0	30000.0	16T X 3M	391.2	14.67	10.82	0.582	4.00	290	423
231	K2BOR	SI/SA	SI/SA	HP14X73	171.5	21.4	30000.0	VUL010	540.5	21.21	14.35	0.838	20.83	420	575
MISCELLANEOUS PILE TYPES IN CLAY															
396	BOR-PN43	SA	CL	MONO 11"	38.0	4.4	30000.0	D16-32	406.7	13.81	14.97	0.603	16.00	358	498

Table 24. Pile/soil and dynamic measurements of data set PD (continued).

REF. NO.	PILE NAME	SKIN SOIL	TOE SOIL	PILE TYPE	LEN. FT	AREA IN2	E MOD KSI	HAMMER	FMX KIPS	EMX K-FT	VMX FT/S	DMX IN	BLOWS/INCH	CAPWAP R/ft KIPS	ENERGY APPROACH KIPS
297	RES PN5	SA	CL	MONO 12	56.0	9.0	30000.0	ICE 520	309.0	9.62	7.00	0.622	40.00	310	357
373	RES TP2	SA	CL	PIPE 12	88.0	6.9	30000.0	MKT DE30	162.0	7.55	14.00	0.743	20.00	172	228
292	BOR TP1	SA	CL	MONO 12	62.0	9.0	30000.0	ICE 520	350.0	12.64	11.50	0.703	2.25	400	264
414	BOR PN3	CL	CL	PIPE24	85.1	54.8	30000.0	K35	969.8	19.38	10.00	0.659	11.00	409	620
241	EZ BOR	CL	CL	TIMBER	47.0	50.0	1602.0	MKT 10B3	183.8	3.93	11.74	0.343	15.00	143	230
372	RES TP1	SA	CL	PIPE 12	90.0	7.0	30000.0	MKT DE30	148.0	7.94	13.00	0.830	11.67	198	208
379	A4-21-EO	CL	CL	PIPE26	888.0	78.5	297000.0	D62	1597.6	35.71	11.56	0.564	4.17	821	1066
298	RES PN6	SA	CL	MONO 12	51.0	9.0	30000.0	ICE 520	293.0	7.29	7.60	0.485	130.00	312	355
375	RES TP4	SA	CL	PIPE 12	78.0	7.0	30000.0	MKT DE30	161.0	5.42	10.40	0.641	100.00	131	200
240	AZ EOID	CL	CL	TIMBER	42.0	50.0	1300.0	MKT 10B3	172.9	6.19	11.56	0.711	2.00	71	123
374	RES TP3	SA	CL	PIPE 11 NU	92.0	16.1	30000.0	MKT DE30	276.0	9.93	9.20	0.868	7.67	238	239
413	BOR PN3	CL	CL	PIPE24	85.1	54.8	30000.0	K35	943.9	25.74	10.24	0.882	9.00	374	622
296	RES PN4	SA	CL	MONO 12	52.0	9.0	30000.0	ICE 520	320.0	9.75	9.20	0.602	13.00	346	345
157	BOR T4	CLSI	CL	PIPE 12.75	66.0	19.2	30000.0	D30	502.0	17.43	13.50	0.517	5.00	288	583
163	EOD T4	CLSI	CL	PIPE 12.75	66.0	19.2	30000.0	D30	514.0	16.72	13.00	0.531	2.50	244	431
2	RES PN6	SA	CLSI	MONO 11	38.0	8.1	30000.0	D22-02	316.0	20.56	12.80	1.037	3.17	271	365
108	EOD TP23	SA	CLSI	MONO14 NU	42.0	8.1	30000.0	D22	143.0	7.47	11.30	0.895	1.67	124	120
111	BOR TP24	SA	CLSI	MONO14 NU	42.0	8.1	30000.0	D22	262.0	15.91	12.70	0.899	2.83	224	305
12	EOD TP12	SA	CLSI	MONO	44.0	8.1	30000.0	D16-32	282.0	11.45	14.30	0.741	2.50	246	241
110	BOR TP23	SA	CLSI	MONO14 NU	42.0	8.1	30000.0	D22	278.0	14.96	12.50	0.852	2.83	226	298
MISCELLANEOUS PILE TYPES SOIL TYPE UNKNOWN															
171	EOD B12	NA	NA	PIPE 14	101.0	21.3	30000.0	D30-32	633.0	30.32	16.10	1.005	20.83	602	691
172	EOD B24	NA	NA	PIPE 14	97.0	21.3	30000.0	D30-32	650.0	28.73	16.20	0.958	1.00	428	352
96	EOD TP4	NA	NA	PIPE 10.75	38.0	7.3	30000.0	FEC 1200	195.0	8.56	14.00	0.756	3.50	197	197
203	X PND161.1	NA	NA	PIPE 12.75	39.0	9.8	30000.0	CON 65	229.0	6.72	7.90	0.655	12.00	221	218
202	X PNB141	NA	NA	PIPE 12.75	39.0	9.8	30000.0	CON 65	254.0	6.71	7.70	0.581	12.50	247	244
MISCELLANEOUS PILE TYPES IN ROCK															
201	X PN2	CLSI	COOPMAR	PSC/HP	118.0	478.0	5469.7	D46-23	1483.0	39.61	6.50	0.696	20.00	924	1274
128	BOR PN11B1	CLSA	COOPMAR	HP/PSC NU	142.0	477.0	6064.1	D46-23	882.0	17.66	3.70	0.361	83.33	850	1136
200	RES PN810	CLSA	COOPMAR	PSC/HP	112.0	478.0	5467.0	D46-23	1243.0	31.64	6.30	0.549	20.00	690	1268
179	BOR PNH218	SI	COOPMAR	HP/PSC	123.0	268.0	5055.0	ICE 1070	682.0	17.94	5.80	0.460	12.00	622	792
130	BOR ET4	CLSI	COOPMAR	HP/PSC	119.0	477.0	5467.0	D46-23	1275.0	31.40	5.80	0.641	10.00	864	1017
124	BOR ET2	CLSI	COOPMAR	HP/PSC24	119.0	478.0	5470.0	D46-23	1070.0	26.15	5.10	0.608	56.00	718	1003
381	EOD PN3x011	CLSI	LIMESTN	PIPE	62.0	14.3	30111.2	LB 520	318.0	10.37	10.90	0.604	40.00	348	396

Table 24. Pile/soil and dynamic measurements of data set PD (continued).

REF. NO.	PILE NAME	SKIN SOIL	TOE SOIL	PILE TYPE	LEN. FT	AREA IN2	E MOD KSI	HAMMER	FMX KIPS	EMX K-FT	VMX FT/S	DMX IN	BLOWS/ INCH	CAPWAP R/ft KIPS	ENERGY APPROACH KIPS
100	EOD ST1	CLSA	LIMESTN	PIPE 14	83.0	16.1	30000.0	ICE 640	286.0	12.55	8.10	0.738	2.50	285	265
102	EOR ST1	CLSA	LIMESTN	PIPE 14	83.0	16.1	30000.0	ICE 640	312.0	12.30	8.80	0.632	3.00	319	306
166	BOR PN856A	SA	LIMESTN	PIPE 9.6	81.0	11.5	30000.0	D30	253.0	6.93	13.60	0.673	8.00	100	208
382	EOD TP	CLSI	LIMESTN	PIPE	64.0	14.3	29839.9	LB 520	374.0	16.06	13.70	0.802	40.00	421	466
105	EOD P4T1	SASI	ROCK	PIPE 12.75	37.0	14.6	30000.0	VUL 06	289.0	10.19	11.60	0.605	5.00	232	304
251	BOR J31	CL/SI	ROCK	PIPE 14"	91.0	31.2	30000.0	KOBE K-3	860.7	27.18	15.17	0.651	58.33	703	976
103	BOR PST1	SASI	ROCK	PIPE 12.75	75.0	14.6	30000.0	VUL 06	276.0	9.09	10.30	0.554	8.33	248	324
104	EOD P3T1	SASI	ROCK	PIPE 12.75	75.0	14.6	30000.0	VUL 06	331.0	12.13	12.50	0.741	5.00	281	309
250	EOD J31	CL/SI	ROCK	PIPE 14"	91.0	31.2	30000.0	KOBE K-3	681.7	35.24	11.65	0.999	20.00	705	806
263	EOD PN10.375	CLSI	SHALE	PIPE 7	42.0	10.5	30000.0	D25-32	267.0	15.94	12.50	1.310	0.83	128	152
261	DD PN10	CLSI	SHALE	PIPE 7	65.0	10.5	30000.0	D25-32	336.0	20.15	13.60	1.001	1.50	291	290
262	DD PN16	CLSI	SHALE	PIPE 7	64.0	10.5	30000.0	D25-32	358.0	18.35	14.00	0.932	1.58	274	282
MISCELLANEOUS PILE TYPES IN SAND															
183	RES TP2	SI	GR	PIPE 12	88.0	8.1	30000.0	ICE 440	164.0	8.04	9.40	0.802	20.00	190	226
182	EOD TP5	SI	GR	PIPE 12	108.0	8.1	30000.0	ICE 440	157.0	8.90	8.80	0.981	20.00	174	207
237	BOR TP2	CL	SA	TIM. 12.	42.5	62.2	2400.0	LB 440	157.3	3.39	7.94	0.352	5.00	109	147
391	BORPN50	SA/SI	SA	PIPE 12.75"	76.8	15.7	30000.0	V06	223.2	6.57	6.08	0.540	166.67	316	289
295	RES PN3	SA	SA	MONO 12	45.0	9.0	30000.0	ICE 520	371.0	11.33	9.10	0.541	19.00	311	458
416	BOR TP4	SA	SA	PIPE 12	105.2	13.7	30000.0	D-22	443.8	18.46	15.81	0.857	4.00	304	400
114	BOR PN795	CLSA	SA	PIPE/PSC14	87.0	153.9	5565.4	VUL 010	590.0	22.10	13.70	0.837	22.92	555	787
178	X.PNA17.5	SA	SA	PIPE 16	75.0	20.8	30000.0	K25	519.0	22.10	8.50	0.519	10.58	558	602
294	RES PN2	SA	SA	MONO 12	43.0	9.0	30000.0	ICE 520	304.0	7.27	10.00	0.454	18.00	306	342
115	BOR PN833	CLSA	SA	PIPE/PSC14	88.0	153.9	5043.4	VUL 010	480.0	18.79	8.40	0.588	7.83	492	630
376	G-16-1 B	CL/SA	SA	PIPE, 10	63.4	6.7	30000.0	VUL 01	165.3	6.37	6.69	0.688	6.00	165	179
173	X TP7	SA	SA	MONO	47.0	8.1	30000.0	D16-32	328.0	16.83	17.90	0.840	2.58	283	329
117	BOR PN835	CLSA	SA	PIPE/PSC14	88.0	153.9	5067.0	VUL 010	439.0	15.29	7.20	0.536	83.33	502	670
112	BOR PN608	CLSA	SA	PIPE/PSC14	85.0	153.9	5773.7	VUL 010	605.0	21.69	8.60	0.607	8.33	632	716
118	BOR PN836	CLSA	SA	PIPE/PSC14	89.0	153.9	5565.4	VUL 010	370.0	13.19	5.40	0.517	16.08	567	547
113	BOR PN705	CLSA	SA	PIPE/PSC14	80.0	153.9	5461.5	VUL 010	498.0	16.25	8.20	0.524	8.33	540	606
293	RES PN1	SA	SA	MONO 12	46.0	9.0	30000.0	ICE 520	320.0	9.17	8.40	0.580	50.00	339	367
116	BOR PN834	CLSA	SA	PIPE/PSC14	88.0	153.9	5220.1	VUL 010	533.0	20.73	8.30	0.583	6.25	511	670
239	TP2 BOR	SA	SA	TIMB. 12.	42.5	62.2	2400.0	LINK 440	163.7	3.88	8.38	0.365	5.00	118	165
317	B15T EOD	SA/CY	SA	MONOTUBE	48.0	5.2	30000.0	K13	277.0	10.24	10.27	0.674	6.08	248	293
238	BOR TP2	SA CL	SA CL	TIMBER	42.5	62.2	2400.0	LB440	169.9	3.61	7.76	0.341	5.00	99	160
401	EOR D27	SA CL	SA CL	PIPE 14"	101.3	31.2	30000.0	K25	693.9	27.58	12.29	0.882	3.00	427	545
390	BOR TP1	SA SAT	SA SAT	EICEPIPE	72.3	12.4	30000.0	D16-32	413.7	15.02	15.37	0.640	13.33	332	504

Table 24. Pile/soil and dynamic measurements of data set PD (continued).

REF. NO.	PILE NAME	SKIN SOIL	TOE SOIL	PILE TYPE	LEN. FT	AREA IN2	E MOD KSI	HAMMER	FMX KIPS	EMX K-FT	VMX FT/S	DMX IN	BLOWS/ INCH	CAPWAP Ruit KIPS	ENERGY APPROACH KIPS
400	1R B 120	SA SI	SA SI	COMPOSIT	122.5	26.0	30000.0	D46-23	1140.7	35.13	5.64	0.728	24.00	742	1096
136	BOR PN17	CLSI	SAGR	PIPE 14	51.0	10.8	30000.0	HERA1500	306.0	10.69	15.00	0.567	4.17	320	318
260	BOR PN1	CLSI	SAGR	PIPE 12.75	52.0	9.8	30000.0	D25-32	429.0	29.58	18.70	1.173	3.00	404	471
137	BOR PN26	CLSI	SAGR	PIPE 14	44.0	10.8	30000.0	HERA1500	374.0	11.36	16.20	0.563	4.17	310	340
134	EOD PN16	CLSI	SAGR	PIPE 14	57.0	10.8	30000.0	HERA1500	265.0	7.03	12.90	0.500	5.25	162	244
135	RES TP2	CLSI	SAGR	PIPE 12	38.0	7.6	30000.0	HERA1500	289.0	12.26	14.60	0.692	3.33	243	297
122	BOR PN2	SI	SASI	HP/PSC24	119.0	478.0	5896.0	D46	1196.0	30.80	5.50	0.659	1.67	308	587
29	BOR TB1	SASI	SASI	TIMBER	45.0	168.0	1857.1	D30-23	374.0	29.36	12.00	1.448	2.00	194	362
242	PN#2 EOD	SA	SA/GR	TIM 14"	18.0	89.0	1708.9	FEC 1500	197.2	7.49	11.65	0.638	2.50	121	173
176	EOD TP5	SA	SI	MONO	47.0	8.1	30000.0	D16-32	297.0	13.02	14.70	0.730	3.00	274	294
148	EOD TP27	SA	SI	MONO NU	38.0	8.1	30000.0	D16-32	274.0	15.65	15.20	0.948	1.67	200	243
174	EOD TP12	SA	SI	MONO	42.0	8.1	30000.0	D15	253.0	5.84	10.00	0.447	7.33	298	240
147	EOD TP26	SA	SI	MONO NU	38.0	8.1	30000.0	D16-32	302.0	17.88	15.80	0.963	1.67	220	275
175	EOD TP2	SA	SI	MONO	42.0	8.1	30000.0	D16-32	325.0	13.98	15.60	0.710	3.50	294	337
177	EOD PN2	SA	SI	MONO	43.0	8.1	30000.0	D16-32	284.0	13.97	14.10	0.784	2.33	229	277
1	EOD PN6	SA	SI/CL	MONO 11	38.0	8.1	30000.0	D22-02	244.0	11.54	10.50	0.754	3.33	208	263
247	TP22 BOR	SI/CL	SI/CL	MONO	43.0	4.4	30000.0	DEL 16.3	345.3	13.10	15.03	0.635	13.33	325	443

1 ft = 0.305 m
 1 in² = 645.2 mm²
 1 kip/in² = 6895.1 kPa
 1 kip = 4.448 kN
 1 k-ft = 1.356 kN-m
 1 in = 25.4 mm
 1 blow/in = 0.039 blows/mm

Table 25. Side/tip quake and damping parameters of data set PD.

REF NO.	PILE NAME	SKIN SOIL	TOE SOIL	PILE TYPE	SIDE QUAKE (in)	TIP QUAKE (in)	SIDE DAMPING (s/ft)	TIP DAMPING (s/ft)
1	EOD PN6	SA	SICL	MONO 11	0.100	0.390	0.490	0.070
2	RES PN6	SA	CLSI	MONO 11	0.100	0.530	0.600	0.100
3	BOR PA35	SASI	SASI	PSC 20	0.100	0.300	0.200	0.170
4	BOR PM24	SASI	SASI	PSC 20	0.100	0.200	0.616	0.249
5	EOD PA8	NA	SA	PSC 18	0.100	0.280	0.040	0.340
6	EOD PN165	NA	NA	CEP 12.75	0.105	0.265	0.394	0.175
7	EOD PN210	NA	NA	CEP 12.75	0.110	0.230	0.270	0.200
8	EOD PN15E	NA	SAGR	CEP 10.75	0.090	0.180	0.299	0.350
9	PN1	NA	SA	CEP 16	0.100	0.420	0.350	0.473
10	BOR TP6	SASI	CLSI	PSC 12	0.070	0.070	0.091	0.773
11	EOD TP6	SASI	CLSI	PSC 12	0.100	0.133	0.037	0.651
12	EOD TP12	SA	CLSI	MONO	0.080	0.080	1.200	0.050
13	BOR D416	CLSHALE	DOLOMITE	OEP 9.6	0.080	0.050	0.458	0.473
14	BOR J3	CLSHALE	DOLOMITE	OEP 9.6	0.100	0.080	0.550	0.600
15	EOD D205	CLSHALE	DOLOMITE	OEP 9.6	0.100	0.080	1.025	0.555
16	EOD D418	CLSHALE	DOLOMITE	OEP 9.6	0.100	0.080	0.514	0.971
17	EOD J1	CLSHALE	DOLOMITE	OEP 9.6	0.100	0.100	0.700	0.550
18	EOD J8	CLSHALE	DOLOMITE	OEP 9.6	0.100	0.120	0.481	0.510
19	RES TN12	AGDITE	AGDITE	PCC 16	0.140	0.170	0.513	0.470
20	BOR CT	AGDITE	AGDITE	PCC 16	0.110	0.110	0.486	0.345
21	BOR TN	AGDITE	AGDITE	PCC 16	0.160	0.190	0.296	0.500
22	EOD PN1	NA	NA	PSC 24 NU	0.100	0.350	0.338	0.225
23	BOR PN9	SASI	SASI	HP 12x74	0.096	0.080	1.439	0.194
24	DD PN83	SASI	SASI	HP 12x53	0.050	0.150	0.620	0.051
25	DD PN83	SASI	SASI	HP 12x53	0.040	0.040	0.486	0.042
26	X PN71	SASI	SASI	HP 12x53	0.050	0.050	0.447	0.035
27	X PN80	SASI	SASI	HP 12x53	0.040	0.150	0.270	0.101
28	X PN80	SASI	SASI	HP 12x53	0.060	0.060	1.201	0.052
29	BOR TB1	SASI	SASI	TIMBER	0.100	0.860	0.500	0.030
30	BOR TP114	SASI	SASI	PSC 12	0.100	0.600	0.547	0.065
31	BOR TP2	SASI	SASI	PSC 12	0.130	0.150	0.991	0.210
32	BOR TP28	SASI	SASI	PSC 12	0.100	0.350	0.887	0.109
33	EOD TP114	SASI	SASI	PSC 12	0.100	0.370	0.159	0.039
34	EOD TP28	SASI	SASI	PSC 12	0.100	0.200	0.250	0.037
35	EOD PN1	CL	TILL	CEP 10.75	0.080	0.300	0.400	0.300
36	DD PN25	NA	NA	PSC 30 NU	0.100	0.200	0.150	0.300
37	EOD PN25	NA	NA	PSC 30 NU	0.080	0.120	0.256	0.282
38	EOR PN30	NA	NA	PSC 30	0.143	0.255	0.011	0.354
39	BOR D12N	CL	CL	HP 10x42	0.100	0.115	0.571	0.638
40	EOD D18E	CL	CL	HP 10x42	0.100	0.130	0.292	0.574
41	EOR D110S	CL	TILL	HP 10x42	0.140	0.140	0.770	0.750
42	EOR D112E	CL	TILL	HP 10x42	0.100	0.120	0.722	0.646
43	EOR D6W	CL	TILL	HP 10x42	0.130	0.200	0.164	0.607
44	BOR A213	CLSI	SASI	OEP 12	0.100	0.150	0.439	0.112
45	EOD E18	CLSI	SASI	OEP 12	0.100	0.950	0.103	0.064
46	EOD J210	CLSI	SASI	OEP 12	0.100	0.520	0.252	0.053
47	RES PN125	SI	SI	PSC 24	0.060	0.450	0.481	0.162
48	RES PN125	SI	SI	PSC 24	0.091	0.400	0.182	0.011

Table 25. Side/tip quake and damping parameters of data set PD (continued).

REF NO.	PILE NAME	SKIN SOIL	TOE SOIL	PILE TYPE	SIDE QUAKE (in)	TIP QUAKE (in)	SIDE DAMPING (s/ft)	TIP DAMPING (s/ft)
49	EOD PN12	CL	ROCK	HP 10X57	0.060	0.050	0.300	1.100
50	EOD B611	CL	TILL	PSC 16	0.130	0.400	0.385	0.169
51	EOD PIT6NW	CL	TILL	PSC 14	0.120	0.460	0.295	0.306
52	EOD PN10	CL	TILL	PCC 14	0.120	0.320	0.140	0.250
53	RES PN9	CL	TILL	PCC 14	0.120	0.320	0.272	0.181
54	RES PN20	CL	TILL	PCC 14	0.153	0.199	0.150	0.287
55	RES PN50	CL	TILL	PCC 14	0.167	0.211	0.500	0.268
56	DD TP15	CLSI	CLSI	PSC 18	0.100	0.420	0.150	0.100
57	DD TP15	CLSI	CLSI	PSC 18	0.100	0.350	0.150	0.100
58	DD TP16	CLSI	CLSI	PSC 14	0.060	0.200	0.140	0.030
59	DD TP16	CLSI	CLSI	PSC 14	0.070	0.220	0.500	0.054
60	DD TP16	CLSI	CLSI	PSC 14	0.100	0.150	0.650	0.200
61	RES TP15	CLSI	CLSI	PSC 18	0.080	0.090	0.641	0.133
62	RES PN119R24	SI	COOPERMARL	PSC 24	0.070	0.100	0.510	0.040
63	RES PN122B23	SI	COOPERMARL	PSC 24	0.120	0.500	0.404	0.061
64	BOR PN120R9	SI	COOPERMARL	PSC 24	0.100	0.450	0.350	0.050
65	BOR PN121R9	SI	COOPERMARL	PSC 24	0.100	0.450	0.360	0.060
66	BOR PN280	CLSA	COOPERMARL	HP 14x73	0.080	0.090	0.995	0.134
67	BOR PN225	CLSI	COOPERMARL	PSC 18 NU	0.100	0.120	0.820	0.141
68	BOR TP3	ALLUVIAL	CL	CEP 12x0.18	0.100	0.180	0.696	0.550
69	DD TP2	ALLUVIAL	CL	CEP 12x0.18	0.091	0.650	0.355	0.300
70	EOD PN392	CLSI	SA	PSC 20	0.090	0.300	0.111	0.433
71	EOD PN396	CLSI	SA	PSC 20	0.160	0.330	0.320	0.250
72	EOD PN398	CLSI	SA	PSC 20	0.120	0.300	0.212	0.390
73	EOD PNE17	SI	SHALE	CEP 11x0.4	0.100	0.320	0.359	0.859
74	BOR PN3	SIGR	SASI	CEP 12x0.6	0.150	0.300	0.254	0.198
75	BOR PN4	SIGR	SASI	OEP 12x0.6	0.100	0.170	0.250	0.500
76	BOR TP11	SASI	SA	PSC 36	0.160	0.330	0.277	0.370
77	BOR TP11	SIGR	SASI	PSC 36	0.140	0.330	0.280	0.344
78	BOR TP21	SASI	SA	PSC 36	0.125	0.300	0.388	0.300
79	EOD PN1	SIGR	SASI	HP 12x74	0.100	0.150	0.250	0.300
80	EOD PN2	SIGR	SASI	HP 10x42	0.100	0.520	0.257	0.250
81	EOD PN2	SIGR	SASI	HP 10x42	0.100	0.550	0.180	0.180
82	EOD PN3	SIGR	SASI	CEP 12x0.8	0.150	0.250	0.170	0.220
83	EOD PN4	SIGR	SASI	OEP 12x0.6	0.120	0.230	0.250	0.300
84	EOD TP11	SIGR	SASI	PSC 36	0.130	0.250	0.312	0.415
85	EOD TP13	SIGR	SASI	PSC 36	0.150	0.230	0.300	0.430
86	EOD TP21	SASI	SA	PSC 36	0.170	0.300	0.360	0.321
87	EOD TP23	SIGR	SASI	PSC 54	0.150	0.200	0.300	0.650
88	EOD PN7E3	NA	NA	PSC 30	0.108	0.254	0.030	0.311
89	BOR PNPE28	NA	NA	PSC 30	0.073	0.143	0.572	0.500
90	EOD TP4	NA	NA	PIPE 10.75	0.100	0.410	0.300	0.451
91	BOR SHD1	CLSA	LIMESTONE	HP 12x53	0.100	0.300	0.319	0.042
92	EOD SHD1	CLSA	LIMESTONE	HP 12x53	0.080	0.450	0.323	0.067
93	EOD ST1	CLSA	LIMESTONE	PIPE 14	0.100	0.250	0.323	0.154
94	EOR ST1	CLSA	LIMESTONE	PIPE 14	0.100	0.250	0.178	0.076
95	BOR PST1	SASI	ROCK	PIPE 12.75	0.080	0.080	0.200	0.500
96	EOD P3T1	SASI	ROCK	PIPE 12.75	0.080	0.200	0.120	0.400

Table 25. Side/tip quake and damping parameters of data set PD (continued).

REF NO.	PILE NAME	SKIN SOIL	TOE SOIL	PILE TYPE	SIDE QUAKE (in)	TIP QUAKE (in)	SIDE DAMPING (s/ft)	TIP DAMPING (s/ft)
97	EOD P4T1	SASI	ROCK	PIPE 12 75	0.100	0.250	0.030	0.330
98	BOR PN123	SI	COOPERMARL	PSC 24	0.050	0.700	0.070	0.099
99	BOR PN123R7	SI	COOPERMARL	PSC 24	0.050	0.500	0.106	0.012
100	EOD TP23	SA	CLSI	MONO 14 NU	0.150	0.500	0.300	0.250
101	BOR TP1	SA	SA	HP 14x73	0.100	0.330	0.250	0.050
102	BOR TP23	SA	CLSI	MONO 14 NU	0.110	0.300	0.637	0.044
103	BOR TP24	SA	CLSI	MONO 14 NU	0.130	0.400	0.589	0.069
104	BOR PN608	CLSA	SA	PIPE/PSC14	0.098	0.244	0.250	0.350
105	BOR PN705	CLSA	SA	PIPE/PSC14	0.100	0.220	0.196	0.480
106	BOR PN795	CLSA	SA	PIPE/PSC14	0.100	0.260	0.200	0.530
107	BOR PN833	CLSA	SA	PIPE/PSC14	0.100	0.110	0.146	0.400
108	BOR PN834	CLSA	SA	PIPE/PSC14	0.100	0.120	0.156	0.500
109	BOR PN835	CLSA	SA	PIPE/PSC14	0.080	0.100	0.200	0.400
110	BOR PN836	CLSA	SA	PIPE/PSC14	0.080	0.080	0.350	0.500
111	BOR PN11	CLSA	LIMESTONE	PSC 12	0.100	0.220	0.100	0.520
112	BOR PN115	CLSA	LIMESTONE	PSC 12	0.100	0.150	0.125	0.700
113	EOD TP2	SASI	SA	HP 12x179	0.112	0.391	0.040	0.240
114	BOR PN2	SI	SASI	HP/PSC24	0.120	0.080	0.504	0.001
115	EOD PN22SE	SA	SANDSTONE	PSC 30	0.090	0.250	0.172	0.250
116	BOR ET2	CLSI	COOPERMARL	HP/PSC24	0.092	0.043	0.230	0.100
117	BOR ET2	CLSI	COOPERMARL	PSC 24	0.082	0.425	0.362	0.148
118	EOD TP1	SASI	ROCK	PSC 12	0.470	0.240	0.200	0.540
119	EOD TP2	SASI	ROCK	PSC 12	0.050	0.290	0.120	0.650
120	BOR PN11B1	CLSA	COOPERMARL	HP/PSC NU	0.128	0.120	0.480	0.021
121	BOR ET3	CLSI	COOPERMARL	PSC	0.096	0.350	0.150	0.350
122	BOR ET4	CLSI	COOPERMARL	HP/PSC	0.091	0.080	0.250	0.150
123	RES PN120	CLSI	COOPERMARL	PSC	0.080	0.360	0.497	0.057
124	EOD PN6	NA	NA	PSC	0.100	0.280	0.180	0.180
125	EOD PN7	NA	NA	PSC NU	0.070	0.100	0.100	0.130
126	EOD PN16	CLSI	SAGR	PIPE 14	0.060	0.300	0.400	0.550
127	RES TP2	CLSI	SAGR	PIPE 12	0.080	0.310	1.100	0.070
128	BOR PN17	CLSI	SAGR	PIPE 14	0.071	0.160	0.810	0.605
129	BOR PN28	CLSI	SAGR	PIPE 14	0.050	0.100	0.749	0.425
130	BOR PN7E	SA	SASTONE	PSC 30	0.090	0.080	0.200	0.628
131	BOR PN7N6	SA	SASTONE	PSC 30	0.078	0.070	0.507	0.625
132	EOD PN6E25	SA	SASTONE	PSC 30 NU	0.100	0.240	0.175	0.200
133	EOD PN5E18	SA	SASTONE	PSC 30 NU	0.100	0.270	0.160	0.220
134	BOR PN5E19	SA	LIMESTONE	PSC 30	0.060	0.190	0.681	0.336
135	BOR PN5E22	SA	LIMESTONE	PSC 30	0.070	0.170	0.800	0.320
136	BOR PN5E25	SA	LIMESTONE	PSC 30	0.060	0.100	0.527	0.253
137	BOR PN5	SA	SASTONE	PSC 30	0.053	0.260	0.181	0.305
138	EOD PN4	SA	SASTONE	PSC 30	0.100	0.250	0.060	0.260
139	EOD TP28	SA	SI	MONO NU	0.100	0.600	0.410	0.062
140	EOD TP27	SA	SI	MONO NU	0.090	0.700	0.451	0.042
141	BOR PN12	SA	SA	CEP 16	0.060	0.100	0.462	0.759
142	EOD PN12	SA	SA	CEP 16	0.060	0.160	0.620	0.348
143	EOD PN3	SASI	SA	HP 12x74	0.170	0.250	0.120	0.420
144	BOR R1	CLSI	CL	HP 14x73	0.110	0.110	1.644	0.198

Table 25. Side/tip quake and damping parameters of data set PD (continued).

REF NO.	PILE NAME	SKIN SOIL	TOE SOIL	PILE TYPE	SIDE QUAKE (in)	TIP QUAKE (in)	SIDE DAMPING (s/ft)	TIP DAMPING (s/ft)
145	BOR R10	CLSI	CL	HP 14x73	0.150	0.100	1.669	0.050
146	BOR T1	CLSI	CL	HP 10x42	0.086	0.100	2.058	0.301
147	BOR T2	CLSI	CL	PSC 12	0.150	0.200	1.400	0.080
148	BOR T3	CLSI	CL	PSC 14	0.069	0.360	0.700	0.400
149	BOR T4	CLSI	CL	PIPE 12.75	0.110	0.100	1.298	0.055
150	EOD R1	CLSI	CL	HP 14x73	0.140	0.120	0.898	0.196
151	EOD R10	CLSI	CL	HP 14x73	0.160	0.100	1.508	0.052
152	EOD T1	CLSI	CL	HP 10x42	0.100	0.270	1.631	0.047
153	EOD T2	CLSI	CL	PSC 12	0.220	0.200	0.838	0.032
154	EOD T3	CLSI	CL	PSC 14	0.060	0.310	0.750	0.247
155	EOD T4	CLSI	CL	PIPE 12.75	0.120	0.180	0.950	0.025
156	BOR PN1040	CLSI	SA	PSC 14	0.060	0.100	0.404	0.231
157	BOR PN1056	CLSI	SA	PSC 14	0.100	0.360	0.311	0.400
158	BOR PN896A	SA	LIMESTONE	PIPE 9.6	0.200	0.310	0.220	0.634
159	BOR PN898B	SA	LIMESTONE	PSC 14	0.050	0.050	1.347	0.213
160	EOD PNB1	TILL	ROCK	CEP 18	0.100	0.280	0.250	0.200
161	EOD PNB4	TILL	ROCK	CEP 18	0.100	0.320	0.080	0.701
162	EOD PND10	CLTILL	ROCK	OEP 18	0.100	0.320	0.279	0.492
163	EOD B12	NA	NA	PIPE 14	0.250	0.330	0.349	0.319
164	EOD B24	NA	NA	PIPE 14	0.140	0.380	1.300	0.283
165	X TP7	SA	SA	MONO	0.050	0.120	0.993	0.027
166	EOD TP12	SA	SI	MONO	0.040	0.040	1.200	0.150
167	EOD TP2	SA	SI	MONO	0.050	0.050	0.800	0.120
168	EOD TP5	SA	SI	MONO	0.050	0.050	0.749	0.093
169	EOD PN2	SA	SI	MONO	0.050	0.170	0.800	0.080
170	X PNA17.5	SA	SA	PIPE 16	0.060	0.230	0.150	0.453
171	BOR PNH218	SI	COOPERMARL	HP/PSC	0.150	0.150	0.300	0.450
172	EOD PN7	CLSA	LIMESTONE	HP 10x57	0.106	0.090	0.350	0.534
173	EOR PN1058	SASI	SA	PSC 14	0.080	0.250	0.313	0.095
174	EOD TP5	SI	GR	PIPE 12	0.150	0.220	0.600	0.350
175	RES TP2	SI	GR	PIPE 12	0.150	0.170	0.751	0.436
176	RES TP3	SI	GR	HP 10x12	0.100	0.165	0.600	0.220
177	EOD TP1	CLSA	CLSA	HP 10x42	0.098	0.200	0.250	0.150
178	EOD PN38	CL	TILL	HP 12x74	0.128	0.100	0.900	0.450
179	EOD PN40	CL	TILL	HP 12x74	0.130	0.100	1.000	0.500
180	BOR PN117	SASI	COOPERMARL	HP 14x89	0.089	0.100	1.494	0.254
181	BOR PN224	SASI	COOPERMARL	HP 12x53	0.090	0.250	1.010	0.154
182	TP2 BOR	SI/CL	SA	PSC 12	0.120	0.250	0.250	0.210
183	BOR TP1235	SA	CLSA	PSC 14	0.100	0.150	0.355	0.748
184	BOR TP1259	SA	CLSA	PSC 14	0.100	0.160	0.514	0.530
185	DD PN355E8	SASI	LIMESTONE	HP 10x42	0.100	0.210	0.320	0.430
186	DD PN375P1	SASI	LIMESTONE	HP 10x42	0.100	0.210	0.297	0.492
187	EOD PN375D2	SASI	LIMESTONE	HP 10x42	0.100	0.160	0.320	0.618
188	X TP3	CLSA	LIMESTONE	CEP	0.099	0.070	0.450	0.630
189	BOR PN14	SASI	SA	PSC 14	0.070	0.050	1.009	0.211
190	BOR PN24	SASI	SA	PSC 14	0.070	0.050	0.820	0.100
191	C-41 BOR	COOP.MAR	COOP.MAR	PSC 18	0.059	0.150	1.026	0.289
192	RES PN810	CLSA	COOPERMARL	PSC/HP	0.338	0.349	0.250	0.200

Table 25. Side/tip quake and damping parameters of data set PD (continued).

REF NO.	PILE NAME	SKIN SOIL	TOE SOIL	PILE TYPE	SIDE QUAKE (in)	TIP QUAKE (in)	SIDE DAMPING (s/ft)	TIP DAMPING (s/ft)
193	X PN2	CLSI	COOPERMARL	PSC/HP	0.157	0.186	0.264	0.042
194	X PNB141	NA	NA	PIPE 12.75	0.100	0.200	0.010	0.400
195	X PND181.1	NA	NA	PIPE 12.75	0.100	0.260	0.008	0.582
196	PN8B43B0	COOP MAR	COOP MAR	18"OCT.	0.160	0.400	0.390	0.050
197	PN25BOR	COOP MAR	COOP MAR	24 OCT.	0.275	0.340	0.833	0.211
198	BOR 14B1	COOP MAR	COOP MAR	PPC24OCT	0.250	0.300	0.620	0.140
199	PN9B BOR	MARK	MARK	24 OCT.	0.250	0.400	0.720	0.122
200	BOR21B12	COOP MAR	COOP MAR	PPC24OCT	0.320	0.370	0.414	0.148
201	DD PN69	CLSI	SA	PSC 12	0.100	0.200	0.020	0.554
202	EOD PN232	CLSI	SA	PSC 12	0.100	0.250	0.105	0.368
203	EOD PN244	CLSI	SA	PSC 12	0.100	0.340	0.012	0.256
204	EOD PN318	CLSI	SA	PSC 12	0.100	0.190	0.086	0.516
205	EOD PN332	CLSI	SA	PSC 12	0.100	0.460	0.075	0.185
206	EOD TP1	CLSI	SA	PSC 12	0.096	0.190	0.040	0.398
207	BOR P5	SA CL	SA	PPC 14	0.098	0.150	0.120	0.407
208	EOD P7	SA CL	SA	PPC 14	0.060	0.310	0.250	0.340
209	EOD P7	SA CL	SA	PPC 14	0.060	0.270	0.250	0.340
210	EOD P 10	SA CL	SA	PPC 14	0.080	0.180	0.255	0.400
211	EOD P11	SA CL	SA	PPC 14	0.100	0.100	0.670	0.200
212	EOD P9	SA CL	SA	PPC 14	0.100	0.255	0.300	0.150
213	EOD P8	SA CL	SA	PPC 14	0.080	0.200	0.300	0.200
214	EOID P8	SA CL	SA	PPC 14	0.060	0.110	0.350	0.250
215	BOR PN110	SACL	CLSI	PSC 16	0.080	0.090	0.920	0.540
216	BOR PN111	SACL	CLSI	PSC 16	0.100	0.110	1.100	0.100
217	EOD PN110	SACL	CLSI	PSC 16	0.070	0.140	0.550	0.150
218	EOD PN111	SACL	CLSI	PSC 16	0.044	0.072	0.840	0.170
219	EOR PN12	SA	SA/COBBL	HP14x89	0.100	0.145	0.782	0.483
220	EOD PN2	SA	SA/COBBL	HP14x89	0.125	0.200	0.563	0.433
221	PILE 6 B	CL/SI	ROCK	HP14x117	0.100	0.100	0.700	0.150
222	K7EOD	SA/SI	SA/SI	HP14x73	0.050	0.250	1.400	0.200
223	K2BOR	SI/SA	SI/SA	HP14x73	0.047	0.100	1.800	0.220
224	BOR TP13	SA	LIMESTON	HP14x74	0.060	0.055	0.218	0.650
225	EOD A-5-	CLAY	LIMESTON	HP10x57	0.060	0.060	0.700	0.720
226	7S.ABUT	SA/SI/GR	SA/SI/GR	CEP 10.7	0.100	0.250	0.105	0.456
227	BOR L-8	SI/CL	CL SI	PPC 12	0.140	0.210	0.150	0.490
228	BOR 36	CLAY	LIMESTON	PPC	0.140	0.150	1.050	0.550
229	BOR TP2	CL	SA	TIM. 12	0.040	0.040	1.117	0.350
230	BOR TP2	SA CL	SA CL	TIMBER	0.040	0.040	1.400	0.416
231	TP2 BOR	SA	SA	TIMB.12.	0.050	0.100	1.043	0.215
232	A2 EOID	CL	CL	TIMBER	0.200	0.200	0.620	0.021
233	E2 BOR	CL	CL	TIMBER	0.045	0.130	1.200	0.200
234	PN#2 EOD	SA	SA/GR	TIM 14	0.100	0.350	0.680	0.029
235	EOD TP3	CL SI	CL SI	HP 14x73	0.060	0.170	0.374	0.240
236	TP3 20FT	CL	CL	HP14x73	0.050	0.250	0.340	0.200
237	TP4 EOD	CL	CL	HP 14x73	0.060	0.200	0.330	0.090
238	TP4 BOR	CL	CL	HP 14x73	0.050	0.350	0.400	0.150
239	TP22 BOR	SI/CL	SI/CL	MONO	0.070	0.100	1.700	0.204
240	PN28EOD	CL	ROCK	HP10x57	0.095	0.060	0.310	1.050

Table 25. Side/tip quake and damping parameters of data set PD (continued).

REF NO.	PILE NAME	SKIN SOIL	TOE SOIL	PILE TYPE	SIDE QUAKE (in)	TIP QUAKE (in)	SIDE DAMPING (s/ft)	TIP DAMPING (s/ft)
241	EOD 4 DI	CL	ROCK	HP 12x53	0.080	0.060	0.648	0.765
242	EOD J31	CL/SI	ROCK	PP14	0.090	0.385	0.359	0.081
243	BOR J31	CL/SI	ROCK	PP14	0.078	0.229	0.550	0.250
244	DD J31	CLAY TIL	CLAY TIL	CEPIPE 1	0.100	0.550	0.150	0.316
245	BOR PN20	SA/SI	LIMESTON	PSC 14	0.050	0.130	0.240	0.280
246	B1P26BOR	SA	LIMESTON	PSC18"SQ	0.145	0.215	0.193	0.215
247	B11P50BO	SA	LIMESTON	PSC18"SQ	0.044	0.246	0.120	0.320
248	EODP.26	SANDSTON	LIMESTON	PSC18"SQ	0.080	0.130	0.190	0.360
249	B13P48BO	SA	LIMESTON	PSC18"SQ	0.044	0.246	0.120	0.320
250	EOD 258	ALLUVIUM	TILL ALL	CEPIPE 1	0.185	0.300	0.531	0.406
251	BOR 174	ALLUVIAL	ALLUVIAL	CEPIPE 1	0.114	0.100	0.800	0.570
252	BOR PN1	CLSI	SAGR	PIPE 12.75	0.100	0.220	0.578	0.775
253	DD PN10	CLSI	SHALE	PIPE 7	0.080	0.120	0.550	0.150
254	DD PN18	CLSI	SHALE	PIPE 7	0.080	0.100	0.982	0.050
255	EOD PN10.375	CLSI	SHALE	PIPE 7	0.080	0.800	0.284	0.020
256	EOD IP1	SASI	SASI	PSC 12	0.100	0.242	0.550	0.240
257	EOD IP3	SASI	SASI	PSC 12	0.094	0.364	0.416	0.156
258	199.EOD	SA/SISA	SA	12"PSPC	0.055	0.320	0.382	0.075
259	293.BOR	SA/SASI	SA	12"PSPC	0.083	0.141	1.849	0.161
260	177.EOD	SCORIA	CLAYSTON	HP10x57	0.090	0.207	0.964	0.265
261	69.EOD	SCORIA	CLAYSTON	HP10x57	0.090	0.303	0.705	0.261
262	BOR TP2	CL-SA	CL-SA	HP14	0.070	0.230	0.350	0.250
263	BOR PNF2	CLSA	CLSA	PSC 12	0.100	0.350	0.522	0.134
264	BOR PNH20	CLSA	CLSA	PSC 12	0.150	0.160	0.509	0.115
265	EOD PNH20	CLSA	CLSA	PSC 12	0.500	0.620	0.258	0.059
266	BOR K521C2	NA	NA	PSC 14	0.110	0.110	1.084	0.381
267	BOR M27A1	NA	NA	PSC 14	0.100	0.150	1.065	0.237
268	BOR M29C3	NA	NA	PSC 14	0.170	0.160	1.164	0.105
269	BOR M29C3	NA	NA	PSC 14	0.080	0.275	0.532	0.275
270	DD SD91	CLSA	ROCK	PSC 10 NU	0.080	0.100	0.400	1.000
271	EOD AB345	CLSA	ROCK	PSC 10	0.060	0.100	0.173	0.273
272	BOR PNA4W	CLSA	LIMESTONE	PSC 14	0.090	0.090	0.184	0.438
273	EOD TP3	CLSA	LIMESTONE	PSC 10 NU	0.100	0.110	0.202	0.750
274	BOR TP2	CLSA	SA	PSC 14	0.058	0.350	0.120	0.200
275	EOR TP1	CLSA	SA	PSC 14	0.088	0.450	0.020	0.180
276	BOR PN234A3	SASI	COOPERMARL	PSC 18	0.100	0.500	0.106	0.062
277	BOR TP1	SA	CL	MONO 12	0.078	0.050	1.316	0.107
278	RES PN1	SA	SA	MONO 12	0.119	0.080	1.962	4.277
279	RES PN2	SA	SA	MONO 12	0.038	0.020	1.250	0.250
280	RES PN3	SA	SA	MONO 12	0.105	0.172	1.130	0.242
281	RES PN4	SA	CL	MONO 12	0.090	0.060	1.801	0.297
282	RES PN5	SA	CL	MONO 12	0.047	0.025	7.500	0.393
283	RES PN6	SA	CL	MONO 12	0.056	0.030	1.241	0.443
284	RES PN6	SASI	SASI	PSC 14	0.060	0.060	1.430	0.138
285	EOD TP9	SASI	SASI	PSC 18	0.080	0.240	0.294	0.177
286	RES B58	SASI	SASI	PSC 14	0.090	0.165	1.082	0.410
287	RES F14	SASI	SASI	PSC 14	0.090	0.240	0.823	0.147
288	RES G37	SASI	SASI	PSC 14	0.110	0.300	0.482	0.105

Table 25. Side/tip quake and damping parameters of data set PD (continued).

REF NO.	PILE NAME	SKIN SOIL	TOE SOIL	PILE TYPE	SIDE QUAKE (in)	TIP QUAKE (in)	SIDE DAMPING (s/ft)	TIP DAMPING (s/ft)
289	RES PN2	NA	NA	PCC 18	0.100	0.240	0.287	0.115
290	RES PN7-61	NA	NA	PCC 18 NU	0.164	0.300	0.367	0.022
291	BOR TP1	SA	SANDSTONE	PSC 14	0.120	0.100	1.621	0.049
292	BOR TP10	SA	SANDSTONE	PSC 14	0.100	0.116	1.473	0.138
293	BOR TP3	SA	SANDSTONE	PSC 18	0.134	0.118	0.965	0.172
294	BOR TP5	SA	SANDSTONE	PSC 14	0.186	0.200	0.841	0.183
295	BOR TP6	SA	SANDSTONE	PSC 18	0.130	0.224	0.530	0.250
296	BOR TP7	SA	SANDSTONE	PSC 14	0.140	0.140	0.999	0.143
297	BOR TP8	SA	SANDSTONE	PSC 14	0.150	0.140	0.927	0.208
298	BOR TP9	SA	SANDSTONE	PSC 14	0.080	0.114	1.447	0.450
299	EOD TP1	SA	SANDSTONE	PSC 14	0.100	0.500	0.157	0.065
300	EOD TP3	SA	SANDSTONE	PSC 18	0.100	0.260	0.102	0.254
301	EOD TP8	SA	SANDSTONE	PSC 14	0.100	0.340	0.311	0.135
302	B15T EOD	SA/CY	SA	MONOTUBE	0.100	0.070	1.594	0.684
303	B9P3BOR	SA/CY	SA/CY	18"PCP	0.080	0.125	1.167	0.098
304	S4PC N20	CL	CL	30 PPC	0.110	0.550	0.373	0.023
305	P3 P1.R	SI/SA	SI/SA	18 PPC	0.050	0.100	2.049	0.022
306	83E 2 RE	CL	CL	18 PPC	0.150	0.400	0.156	0.063
307	B 70 P 5	CL	SA	24 PPC	0.110	0.106	0.099	0.454
308	PIER 7 P	SI/SA	SI/SA	18 PPC	0.080	0.220	1.103	0.035
309	X PN201E2	SASI	COOPERMARL	PSC 18	0.150	0.670	0.040	0.040
310	X PN205E3	SASI	COOPERMARL	PSC 18	0.200	0.750	0.080	0.080
311	X PN209E3	SASI	COOPERMARL	PSC 18	0.120	0.700	0.060	0.110
312	X PN213E2	SASI	COOPERMARL	PSC 18	0.200	0.900	0.080	0.090
313	EOD TP1799	SASI	CL	PPC	0.040	0.620	0.250	0.080
314	RES TP1799	SASI	CL	PPC	0.100	0.100	0.580	0.330
315	X TP1799	SI	SA	PPC	0.050	0.450	0.250	0.150
316	151.EOD	CL/SA	SA	12 PPC	0.085	0.179	0.350	0.350
317	X PN25BK	NA	NA	CEP 20x0 5	0.140	0.140	0.600	0.650
318	X PN29K	NA	NA	CEP 20x0 5	0.260	0.210	0.350	0.550
319	X PN30K	NA	NA	CEP 20x0 5	0.200	0.150	0.300	0.350
320	X PN2031	SASI	SAROCK	PSC 12	0.100	0.320	0.207	0.261
321	BOR TP4	SASI	SA	CEP 12 75	0.100	0.250	0.183	0.707
322	EOD TP4	SASI	SA	CEP 12 75	0.060	0.320	0.320	0.481
323	BOR PN13	CLSI	SASI	PSC 12	0.060	0.400	0.470	0.025
324	BOR PN19	CLSI	SASI	PSC 12	0.050	0.330	0.450	0.050
325	BOR PN218	CLSI	SASI	PSC 12	0.210	0.180	0.300	0.220
326	BOR PN28	CLSI	SASI	PSC 12	0.150	0.170	1.000	0.050
327	BOR PN31	CLSI	SASI	PSC 12	0.130	0.300	0.700	0.250
328	BOR PN37	CLSI	SASI	PSC 12	0.180	0.180	0.400	0.440
329	BOR PN43	CLSI	SASI	PSC 12	0.130	0.550	0.550	0.040
330	BOR PN49	CLSI	SASI	PSC 12	0.100	0.100	0.650	0.200
331	EOD PN13	CLSI	SASI	PSC 12	0.080	0.300	0.250	0.030
332	EOD PN213	CLSI	SASI	PSC 12	0.050	0.400	0.150	0.050
333	EOD PN26	CLSI	SASI	PSC 12	0.070	0.300	0.180	0.070
334	EOD PN49	CLSI	SASI	PSC 12	0.150	0.500	0.200	0.030
335	EOR PN310	CLSI	SASI	PSC 12	0.130	0.145	0.250	0.550
336	X PNA3	CLSA	TILL	CEP 14x0 5	0.070	0.070	0.700	0.500

Table 25. Side/tip quake and damping parameters of data set PD (continued).

REF NO.	PILE NAME	SKIN SOIL	TOE SOIL	PILE TYPE	SIDE QUAKE (in)	TIP QUAKE (in)	SIDE DAMPING (s/ft)	TIP DAMPING (s/ft)
337	X PNB5	CLSA	TILL	CEP 14x0.5	0.030	0.050	0.952	0.400
338	X PNG3	CLSA	TILL	CEP 14x0.5	0.200	0.120	0.750	0.200
339	BOR PN128	CL	TILL	PSC 14	0.326	0.218	0.350	0.530
340	BOR PN177	CL	TILL	PSC 14	0.318	0.174	0.320	0.650
341	EOD PN128	CL	TILL	PSC 14	0.366	0.331	0.300	0.514
342	EOD PN177	CL	TILL	PSC 14	0.120	0.340	0.100	0.500
343	BOR TP1	CLSA	CL	PSC 18	0.060	0.170	0.580	0.130
344	BOR TP2	CLSA	CL	PSC 24	0.120	0.180	0.500	0.336
345	BOR TP3	CLSA	SA	PSC 18	0.062	0.090	0.650	0.400
346	BOR TP4	CLSA	CL	PSC 18	0.065	0.200	0.950	0.080
347	BOR TP5	CLSA	CL	PSC 24	0.130	0.369	0.350	0.118
348	BOR PN243	SI	SAGR	CEP 14x0.37	0.144	0.130	0.800	0.700
349	BOR PN317	SI	SAGR	CEP 14x0.37	0.134	0.153	0.800	0.735
350	EOD PN317	SI	SAGR	CEP 14x0.37	0.150	0.430	0.550	0.180
351	RES TP13	SI	SAGR	CEP 14x0.37	0.095	0.060	0.950	0.150
352	RES TP6	SI	SAGR	CEP 14x0.37	0.050	0.050	1.100	0.090
353	RES TP1	SA	CL	PIPE 12	0.120	0.120	1.150	0.500
354	RES TP2	SA	CL	PIPE 12	0.200	0.160	0.700	0.700
355	RES TP3	SA	CL	PIPE 11 NU	0.077	0.069	0.400	0.270
356	RES TP4	SA	CL	PIPE 12	0.150	0.150	1.000	0.539
357	G-18-1.B	CLSA	SA	PIPE 10	0.100	0.152	0.550	0.872
358	151-BOR	CL,SC,S	SA	12 PPC	0.085	0.142	0.380	0.385
359		NA	NA	PPC 12	0.075	0.150	0.380	0.380
360	A4-21-E0	CL	CL	26 PIPE	0.150	0.100	0.700	0.500
361	EOD PN3011	CLSI	LIMESTONE	PIPE	0.187	0.198	0.250	0.400
362	EOD TP	CLSI	LIMESTONE	PIPE	0.140	0.200	0.353	0.677
363	TP8	SA	SA	OCT16.5	0.160	0.225	1.150	0.450
364	BOR TP1	SI	SI	HP305MMX	0.080	0.300	1.800	0.100
365	BOR B43P	COOPERMAR	COOPERMARL	18 OCT.	0.140	0.220	0.865	0.234
366	BOR B12P	SA/SI	LIMESTON	PSC 18	0.035	0.080	0.174	0.798
367	EORPN20	SA	LIMESTON	PSC18"SQ	0.110	0.150	0.400	0.137
368	EODPN23	SA	LIMESTON	PSC18"SQ	0.110	0.150	0.400	0.137
369	EOD TP1	SAND SAT	SAND SAT	CEPIPE 1	0.100	0.250	0.640	0.440
370	BOR TP1	SA SATUR	SA SATUR	ECEPIPE	0.080	0.080	1.265	0.346
371	BORPN50	SA/SI	SA	PP12.75	0.044	0.048	1.800	0.700
372	EOD-15-3	SA SI	LIMESTON	PSC10	0.060	0.100	0.201	0.463
373	BOR-TP4	SA SI	SA SI	HP14x11	0.050	0.060	0.720	0.030
374	BOR-PN43	SA	CL	MONO 11	0.075	0.150	3.800	0.400
375	EOD-TP1	SA SI	SA SI	CEP16	0.090	0.240	0.157	0.974
376	BOR-EB/4	CL	LIMESTON	PSC16"SQ	0.080	0.100	0.465	0.395
377	BOR 20W8	NA	NA	PPC24	0.100	0.160	0.254	0.643
378	1R B.120	SA SI	SA SI	COMPOSIT	0.197	0.180	0.500	0.090
379	EOR D27	SA CL	SA CL	PP14"	0.080	0.450	0.457	0.313
380	B.2P.16B	SA CL	LIMESTON	24"SQ.	0.090	0.300	0.270	0.200
381	EODTP2	NA	SHALE	HP10x57	0.083	0.185	0.330	0.707
382	BOR 13B8	OVERBURD	MARL	24-Oct	0.274	0.200	0.545	0.141
383	BOR 5B.5	MARL	MARL	18 OCT.	0.180	0.180	1.208	0.071
384	F20 S MI	SI	LIMESTON	24 PPC	0.100	0.180	0.058	0.244

Table 25. Side/tip quake and damping parameters of data set PD (continued).

REF NO.	PILE NAME	SKIN SOIL	TOE SOIL	PILE TYPE	SIDE QUAKE (in)	TIP QUAKE (in)	SIDE DAMPING (s/ft)	TIP DAMPING (s/ft)
365	EOD FHA5	SA	SA TILL	CEP18	0.100	0.320	0.250	0.170
366	BOR PN246	CLSA	COOPERMARL	HP 14x73	0.080	0.080	1.010	0.316
367	TP4EOD	SA	ROCK	HP12x74	0.080	0.340	0.100	0.480
368	PN8 EOD	SA	SHALE	HP10x57	0.090	0.127	0.234	0.651
369	PN7 EOD	SA	SHALE	HP10x57	0.090	0.127	0.234	0.651
390	EOD PN7	CL SA	CL SA	CEPIPE24	0.075	0.330	0.240	0.116
391	BOR PN7	CL SI	CL SI	CEPIPE24	0.075	0.330	0.240	0.116
392	BOR PN3	CL	CL	24 PP	0.147	0.672	0.200	0.087
393	BOR PN3	CL	CL	24 PP	0.170	0.340	0.188	0.250
394	EOD PN1	SA	LIMESTON	18 PSC	0.075	0.220	0.281	0.133
395	BOR TP4	SA	SA	12 PP	0.250	0.340	0.550	0.450
396	BOR2/59	MARL	MARL	PPC18OCT	0.110	0.110	0.720	0.102
397	BOR4/58	MARL	MARL	PPC18OCT	0.120	0.200	0.800	0.103
398	TP2 BOR	SA SI	SA SI	24 PSPC	0.140	0.140	1.200	0.285
399	TP1 EOD	SA CL	SA CL	HP14x73	0.080	0.280	0.250	0.750
400	BOR TP1	SA CL	SA CL	HP14x73	0.080	0.170	0.550	0.838
401	PN B EOD	SA	LIMESTON	24 PSC	0.100	0.150	0.250	0.290
402	EOD TP2	CL SI	CL SI	HP14x73	0.090	0.320	0.240	0.208
403	BOR TP2	CL SI	CL SI	HP14x73	0.100	0.320	0.400	0.276

1 in = 25.4 mm
1 s/ft = 3.281 s/m

REFERENCES

- American Society for Testing and Materials, 1992. "Standard Test Method for Piles Under Static Axial Compressive Loads," D-1143-81, Vol. 4.08, Sec. 4, pp. 195-205.
- Abe, S., G. Likins, and C.M. Morgan. 1990. "Three Case Studies on Static and Dynamic Testing of Piles," *Geotechnical News*, December 1990, pp. 26-32.
- Benjamin, J.R. and C.A. Cornell. 1970. *Probability, Statistics, and Decision for Civil Engineers*. McGraw-Hill.
- Bernardes, G.D.P. 1989. *Dynamic and Static Testing of Large Model Piles in Sand*, Eng. Ph.D. Dissertation, Dept. of Civil Engineering, Norwegian Institute of Technology.
- Bowles, J.E. 1988. *Foundation Analysis and Design*. McGraw-Hill, 4th ed.
- Briaud, J.L. and C.M. Tucker. 1988. "Measured and Predicted Axial Response of 98 Piles," *American Society of Civil Engineers Journal of Soil Mechanics and Foundations*, Div. 114(9): 984-1001.
- Bustamante, M.G. and L.P. Weber. 1988. "Dynamic and Static Measurements of Steel H-Pile Capacities," *3rd International Conference of Stress-Wave Theory in Piles*, Ottawa, Canada, pp. 579-589.
- Butler, H.D. and H.E. Hoy. 1977. *Users Manual for the Texas Quick-Load Method for Foundation Load Testing*. Federal Highway Administration, Office of Development, Washington, DC. Report No. FHWA-IP-77-8, 59 pp.
- Chellis, R.D. 1961. *Pile Foundations*. McGraw-Hill, 2nd ed.
- Cheng, S.S.M. and S.A. Ahmad. 1988. "Dynamic Testing Versus Static Loading Test: Five Case Histories," *3rd International Conference of Stress-Wave Theory in Piles*, Ottawa, Canada, pp. 477-489.
- Chernauskas, L.R. 1993. *Dynamic Analysis of Plugged Piles in Clay*, Master of Science Thesis submitted to the Department of Civil Engineering, University of Massachusetts-Lowell, 1993.
- Cummings, A.E. 1940. "Dynamic Pile-Driving Formulas," *Boston Society of Civil Engineers Journal* 1925-1940, January 1940, pp. 392-413.

Davisson, M.T. 1972. "High Capacity Piles," *Proceedings, Soil Mechanics Lecture Series on Innovations in Foundation Construction*, American Society of Civil Engineers, Illinois Section, Chicago, March 22, 1972, pp. 81-112.

DeBeer, E.E. 1970. "Proefondervindelijke bijdrage tot de studie van het grandsdraagvermogen van zand onder funderinger op staal." English version, *Geotechnique*, Vol. 20, No. 4, pp. 387-411.

Dynamic Pile Monitoring and Pile Load Test Report Demonstration Project 66-Proposed Cimarron River Bridge U.S. 64, Buffalo, Oklahoma: FHWA Bridge and Demonstration Projects Divisions, February 1989.

Dynamic Pile Monitoring and Pile Load Test Report Demonstration Project 66- Replacement Bridge State Route 115 over Missouri River, Bridgeton/St. Charles, Missouri: FHWA Bridge and Demonstration Projects Divisions, April 1989.

Dynamic Pile Monitoring and Pile Load Test Report Demonstration Project 66-I-80/480 Interchange, Omaha, Nebraska: FHWA Bridge and Demonstration Projects Divisions, October 1989.

Dynamic Pile Monitoring and Pile Load Test Report Demonstration Project 66-State Highway 77 Fore River Bridge Replacement, Portland-South Portland, Maine: FHWA Bridge and Demonstration Projects Divisions, April 1990.

Dynamic Pile Monitoring and Pile Load Test Report Demonstration Project 66-Mo-Pac Railroad Overpass Route LA, 415, West Baton Rouge, Louisiana: FHWA Bridge and Engineering Applications Divisions, November 1990.

Dynamic Pile Monitoring and Pile Load Test Report Demonstration Project 66-Hartford Bridge BRZ1444, White River Junction, Vermont: FHWA Technology Applications and Bridge Divisions, January 1991.

Dynamic Pile Monitoring and Pile Load Test Report Demonstration Project 66-State Route 15, Section 63M, Tioga County, Pennsylvania: FHWA Technology Applications and Bridge Divisions, December 1991.

DiMaggio, J. 1986. Dynamic Pile Monitoring and Pile Load Test Report-Proposed Relocated U.S. 61 over the Peosta Channel, Dubuque, Iowa: FHWA Bridge Division and Demonstration Projects Division, December 1986.

DiMaggio, J. 1991. Dynamic Pile Monitoring and Pile Load Test Report Demonstration Project 66-County Route 18 over Minnesota River, Bloomington, Minnesota: FHWA Engineering Applications and Bridge Divisions, January 1991.

- Dumas, C. 1993. Dynamic Pile Monitoring and Pile Load Test Report Demonstration Project 66-Central Bridge over the Ohio River-U.S. 27, Campbell County, Kentucky: FHWA Technology Applications and Bridge Divisions, January 1993.
- Edde, R.D. and B.H. Fellenius. 1990 "Static or Dynamic Test - Which to Trust," *Geotechnical News*, December 1990, pp. 28-32.
- Fellenius, H.B. 1989. *Guidelines for the Interpretation and Analysis of the Static Loading Test*, Deep Foundations Institute.
- Fellenius, H.B. 1991. "Pile Foundations," Chapter 13 of *Foundation Engineering Handbook*, edited by Hsai-Yang Fang. Van Nostrand Reinhold. New York, NY. 2nd edition.
- Flaate, K. 1964. *An Investigation of the Validity of Three Pile-Driving Formulae in Cohesionless Material*, Norwegian Geotechnical Institute, Publication 56, Oslo, Norway.
- Fox, E. 1932. "Stress Phenomena Occurring in Pile Driving," *Engineering Journal*, London, England, Vol. 134.
- FPDS-3 Foundation Pile Diagnostic System-3*, TNO Building and Construction Research, Delft, The Netherlands, 1993.
- Graff, K.F. 1975. *Wave Motion in Elastic Solids*, Ohio State University Press, Columbus, Ohio.
- Goble, G.G., G. Likins, and F. Rausche. 1970. *Dynamic Studies on the Bearing Capacity of Piles - Phase III*, Report No. 48, Division of Solid Mechanics, Structures, and Mechanical Design. Case Western Reserve University.
- Goble, G.G., G. Likins, and F. Rausche. 1975. *Bearing Capacity of Piles from Dynamic Measurements*, Final Report, Ohio Dept. of Trans., OHIO DOT-05-75.
- Goble, G.G., R.H. Scanlan, and J.J. Tomko. 1967. *Dynamic Studies on the Bearing Capacity of Piles, Phase II*, Volumes I and II, Case Institute of Technology.
- Goble, G.G., F. Rausche, and G. Likins. 1980. "The Analysis of Pile-Driving: A State of the Art," *Proceedings from the 2nd Conference on the Application of Stress-Wave Theory on Piles*, Stockholm, Sweden, June 1980, pp. 1-34.
- Gravare, C.J., G.G. Goble, F. Rausche, and G. Likins. 1980. "Pile-Driving Construction Control by the Case Method," *Ground Engineering*, pp. 21-24.

- Highway Research Record No. 167. 1967. *Bridges and Structure*, Highway Research Board, Washington, DC.
- Highway Research Record No. 333 1970. *Pile Foundations*, Highway Research Board, Washington, DC.
- Holtz, R.D. and W.D. Kovacs, 1981. *An Introduction to Geotechnical Engineering*. Prentice-Hall, Inc., Englewood Cliffs, New Jersey.
- Housel, W.S. 1965. "Michigan Study of Pile-Driving Hammers," *Proceeding of the ASCE Journal of Soil Mechanics and Foundations*, Volume 91, No. SM5, September 1965, pp. 37-64.
- Housel, W.S. 1970. "Pile Load Capacity: Estimates and Test Results," *Proceeding of the ASCE Journal of Soil Mechanics and Foundations*, Volume 92, No. SM4, July 1966, pp. 1-30.
- Issacs, D. 1931. "Reinforced Concrete Pile Formula," *Transactions of the Institute of Engineers*, Australia, Vol. 12, pp. 312-323.
- Iwanowski, T. 1987. "Stress-Wave Testing of Piles," *Proceedings of the International Conference on Foundations and Tunnels*, University of London, March 1987, pp. 262-266.
- Kazmierowski, T. and M. Devata. 1978. *Pile Load Capacity Evaluation, HWY 404 Structures*, Report EM-20, Ontario Ministry of Transportation and Communications, Engineering Materials Office, Soil Mechanics Section. July 1978.
- Kazmierowski, T. and M. Devata. 1983. *Evaluation of Selected Piles Under Axial and Lateral Loading Conditions - C.N.R./C.P.R. Structures Northwest Metro Arterial*, Ontario Ministry of Transportation and Communications, Engineering Materials Office, Soil Mechanics Section. Feb. 1983.
- Lambe, T.W. and R.V. Whitman, 1969. *Soil Mechanics*. John Wiley and Sons Inc., New York, NY.
- Likins, G., F. Rausche, and M. Hussein, 1990. "Introduction to the Dynamics of Pile Testing," *Geotechnical News*, December 1990, pp. 21-23.
- Lowery, L.L., T.J. Hirsh, T.C. Edwards, H.M. Coyle, and C.H. Samson, 1969. *Pile-Driving Analysis - State of the Art Research Report 33-13 (Final)*, Texas Highway Department, Research Study No. 2-5-62-33.

- McDonnell, J. 1991. *The Energy Approach Method for the Prediction of Pile Capacity*, A Research Project Submitted in Partial Fulfillment of the Requirements for the Degree of Master of Science (Unpublished).
- Michigan State Highway Commission. 1965. *A Performance Investigation of Pile-Driving Hammers and Piles*.
- Middendorp, P. and P.J. van Weel. 1986. "Application of Characteristic Stress-Wave Method in Offshore Practice." *Proceedings of the 3rd International Conference on Numerical Methods in Offshore Piling*.
- Ohio Department of Transportation. 1975. *Bearing Capacity of Piles from Dynamic Measurements*, Research Report OHIO-DOT-05-75, Final Report.
- Olsen, R.E. and K.S. Flaate. 1967. "Pile-Driving Formulas for Friction Piles in Sand," *ASCE Journal of Soil Mechanics and Foundations*. Vol. 92(6): pp. 279-297.
- Olsen, R.E. and N. Dennis. 1982. "Actual Capacity of Driven Pipe Piles in Clay," *Proceedings of the Symposium on State of the Art in Offshore Geotechnical Engineering, American Society of Civil Engineers*.
- Paikowsky, S.G. 1982. *Use of Dynamic Measurements to Predict Pile Capacity Under Local Conditions*, M.Sc. Thesis, Dept. of Civil Engineering Technion-Israel Institute of Technology, July 1982.
- Paikowsky, S.G. 1984. "Use of Dynamic Measurements for Pile Analysis," including PDAP-Pile-Driving Analysis Program, GZA Inc., Newton, Massachusetts, 1984.
- Paikowsky, S.G., R.V. Whitman, and M.M. Baligh. 1989. "A New Look at the Phenomenon of Offshore Pile Plugging," *Marine Geotech.*, 8(3): 213-230.
- Paikowsky, S.G. 1990. *Investigation of Pile Foundation Behavior, Northern Avenue Bridge, Boston, MA*, Consulting/Research Report submitted to GZA, Inc.
- Paikowsky, S.G. and R.V. Whitman. 1990. "The Effects of Plugging on Pile Performance and Design," *Canadian Geotechnical Journal*, Vol. 27, No. 3, August 1990.
- Paikowsky, S.G. and L.R. Chernauskas. 1992. "Energy Approach for Capacity Evaluation of Driven Piles," *4th International Conference on the Application of Stress-Wave Theory to Piles*, The Hague, The Netherlands, pp. 595-601.
- Pile Dynamics Inc. 1990. *Model GCPC Pile-Driving Analyzer*, Manual.

- Poulos, H.G. and E.H. Davis, 1980. *Pile Foundation Analysis and Design*, Robert E. Krieger Publishing Co., 2nd edition.
- Prakash, S. and H.D. Sharma. 1990. *Pile Foundations in Engineering Practice*. John Wiley and Sons Inc., New York, NY.
- Rausche, F., F. Moses, and G.G. Goble. 1972. "Soil Resistance Predictions from Pile Dynamics," *ASCE Journal of Soil Mechanics and Foundations*. Vol. 98, No. SM9, Sept. 1972, pp. 917-937.
- Rausche, F., G.G. Goble, and G.E. Likins, 1985. "Dynamic Determination of Pile Capacity," *Journal of Geotechnical Engineering*, ASCE, Vol. III, No. 3, pp. 367-383.
- Reiding, F.J., P. Middendorp, R.P. Schoenmaker, F.M. Middeldorp, and M.W. Bielefeld. 1988. "FPDS-2, A New Generation of Foundation Pile Diagnostic Equipment," *3rd International Conference on Stress-Wave Theory in Piles*, Ottawa, Canada, pp. 123-134.
- Riker, R.E. and B.H. Fellenius. 1988. "Case Method Capacity Estimates for Piles in Glacial Soils," *3rd International Conference on Stress-Wave Theory in Piles*, Ottawa, Canada, pp. 565-578.
- Ryan, T.P. 1989. "Linear Regression," Chapter 13 of *Handbook of Statistical Methods for Engineers and Scientists*, H.M. Wadsworth, editor. McGraw-Hill.
- Schmertmann, J. 1991. "The Mechanical Aging of Soils," *The 25th Terzaghi Lecture*, *Journal of Geotechnical Engineering*, ASCE, Vol. 117, No. 9, Sept. 1991, pp. 1288-1303.
- Selby, K.G., M.S. Devata, P. Prayer, and D. Dundas, 1989. "Ultimate Capacities Determined by Load Test and Predicted by the Pile Analyzer," *Proceeding of the 12th International Conference on Soil Mechanics and Foundation Engineering*, Rio De Janeiro, August 13-18, 1989, pp. 1179-1182.
- Smith, E.A.L. 1960. "Pile-Driving Analysis by the Wave Equation," *Journal of Soil Mechanics and Foundations*, American Society of Civil Engineers, August 1960, pp. 35-61.
- Stokes, W.L. and D.J. Varnes, 1955. *Glossary of Selected Geologic Terms*, Colorado Scientific Society Proceedings, Volume 16.
- Taylor, Donald W. 1948. *Fundamentals of Soil Mechanics*, John Wiley and Sons, Inc. 12th edition.

- Terzaghi, K. 1942. "Discussions of the Progress Report of the Committee on the Bearing Value of Pile Foundations," *Proceedings ASCE*, Vol. 68:311-323.
- Texas Highway Department. 1973. *Bearing Capacity for Axially Loaded Piles*, Research Report 125-8-F, Sept. 1967-Aug 1973, pp. 134.
- Thompson, C.D. and M. Devata. 1980. "Evaluation of Ultimate Bearing Capacity of Different Piles by Wave Equation Analysis," *Proceedings from the 2nd Conference on the Application of Stress-Wave Theory on Piles*, Stockholm, Sweden, June 1980, pp. 1-33.
- Thompson, C.D. and G.G. Goble. 1988. "High Case Damping Constants in Sand," *3rd International Conference on Stress-Wave Theory in Piles*, Ottawa, Canada, pp. 464-555.
- Trow Report. 1978. Research Project: Dynamic Behavior of Foundation Piles and Driving Equipment, The Trow Group Ltd., Ontario, Canada.
- Vanikar, S.N. 1984. Dynamic Pile Monitoring and Pile Load Test Report-I-90, Third Lake Washington Bridge, Seattle, Washington: FHWA Office of Highway Operations Demonstration Projects Program, April 1984.
- Vanikar, S.N. 1987. Dynamic Pile Monitoring and Pile Load Test Report - Proposed Alsea River Bridge (Oregon Coast Highway 101), Walport, Oregon: FHWA Bridge and Demonstration Projects Divisions, June 1987.
- Vanikar, S.N. 1987. Dynamic Pile Monitoring and Pile Load Test Report - Bridges on Colorado S.H. 55 (BRS 0055(4)), Crook, Colorado: FHWA Bridge and Demonstration Projects Divisions, August 1987.
- Vesic, A.S. 1977. *Design of Pile Foundations*, National Cooperative Highway Research Program. Synthesis of Highway Practice, Publication No. 42.
- Veneziano, D. 1993. Personal Communication.

